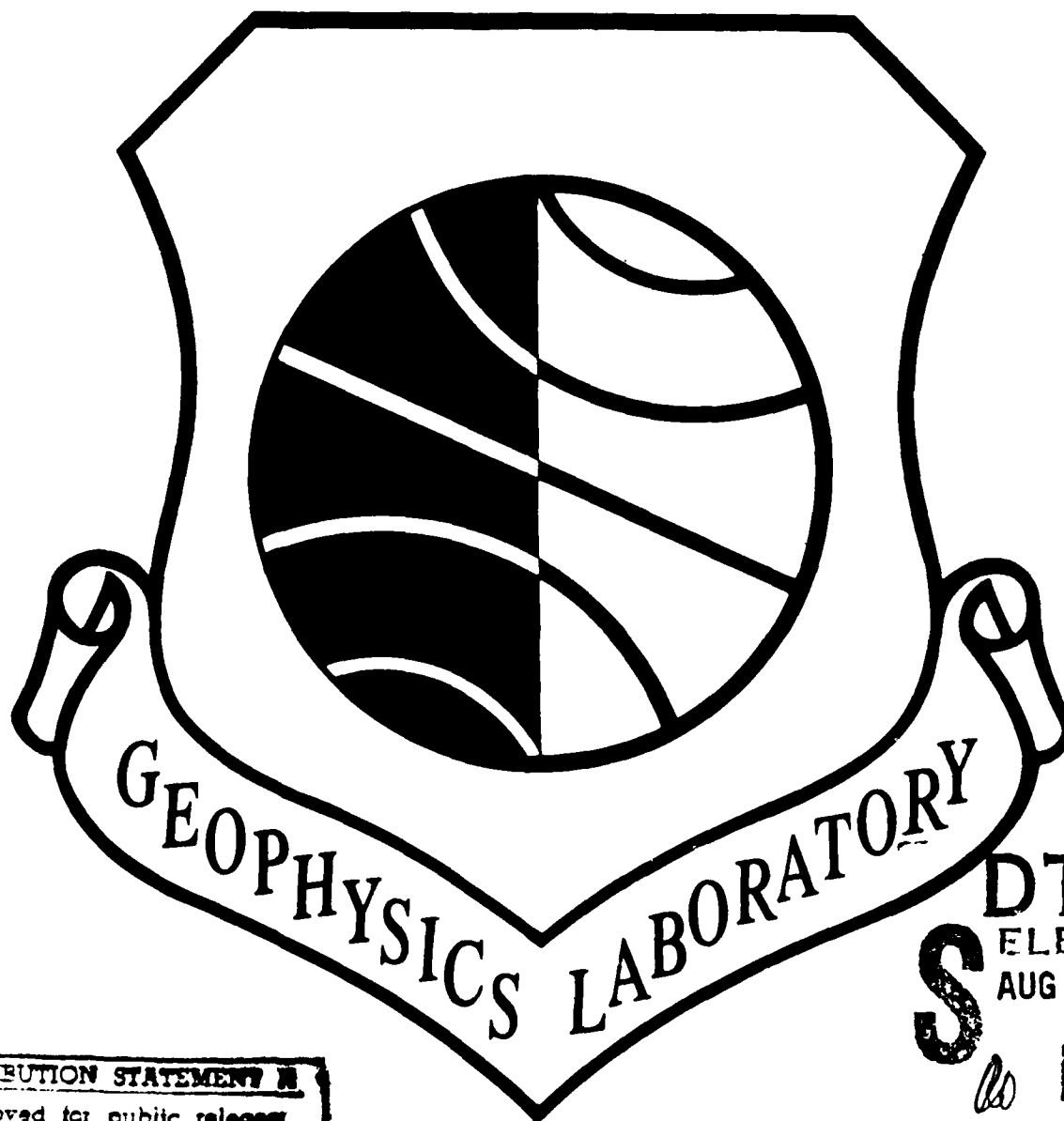


1

DTIC FILE COPY

AD-A225 831



DTIC
ELECTE
AUG 28 1990
S D

DISTRIBUTION STATEMENT A
Approved for public release
Distribution Unlimited

90 08 27 324 REPORT ON RESEARCH
FOR THE PERIOD JANUARY 1987-DECEMBER 1988

REPORT DOCUMENTATION PAGE

1a. REPORT SECURITY CLASSIFICATION UNCLASSIFIED			1b. RESTRICTIVE MARKINGS		
2a. SECURITY CLASSIFICATION AUTHORITY			3. DISTRIBUTION/AVAILABILITY OF REPORT Approved for public release; distribution unlimited		
2b. DECLASSIFICATION/DOWNGRADING SCHEDULE					
4. PERFORMING ORGANIZATION REPORT NUMBER(S) GL-TR-89-0119 SR. NO. 260			5. MONITORING ORGANIZATION REPORT NUMBER(S)		
6a. NAME OF PERFORMING ORGANIZATION Geophysics Laboratory		6b. OFFICE SYMBOL (If applicable) CAP		7a. NAME OF MONITORING ORGANIZATION	
6c. ADDRESS (City, State, and ZIP Code) Hanscom AFB, MA 01731			7b. ADDRESS (City, State, and ZIP Code)		
8a. NAME OF FUNDING/SPONSORING ORGANIZATION		8b. OFFICE SYMBOL (If applicable)		9. PROCUREMENT INSTRUMENT IDENTIFICATION NUMBER	
8c. ADDRESS (City, State, and ZIP Code)			10. SOURCE OF FUNDING NUMBERS		
			PROGRAM ELEMENT NO.	PROJECT NO. 9993	TASK NO. XX
			WORK UNIT ACCESSION NO. XX		
11. TITLE (Include Security Classification) Report on Research					
12. PERSONAL AUTHOR(S) Alice B. McGinty, Editor					
13a. TYPE OF REPORT Scientific Interim		13b. TIME COVERED FROM Jan 87 TO Dec 88		14. DATE OF REPORT (Year, Month, Day) 1989 June	
15. PAGE COUNT 294					
16. SUPPLEMENTARY NOTATION					
17. COSATI CODES			18. SUBJECT TERMS (Continue on reverse if necessary and identify by block number)		
FIELD	GROUP	SUB-GROUP			
			Geokinetics Seismology Balloon Technology		
			Geodesy Meteorology Optical Physics		
			Gravity Solar Radiations Ionospheric Physics		
19. ABSTRACT (Continue on reverse if necessary and identify by block number) This is the fourteenth report on research at the Geophysics Laboratory. It covers a two-year interval. Although written primarily for Air Force and DOD managers of research and development, it is intended to interest an even broader audience. For this audience, the report relates the Laboratory's programs to the larger scientific fields of which they are a part. The work of each of the Laboratory's six scientific divisions is discussed in a separate chapter, followed by a listing of its publications. The report also includes an introductory chapter on GL management and logistic activities related to the reporting period.					
20. DISTRIBUTION/AVAILABILITY OF ABSTRACT <input type="checkbox"/> UNCLASSIFIED/UNLIMITED <input type="checkbox"/> SAME AS RPT <input checked="" type="checkbox"/> DTIC USERS			21. ABSTRACT SECURITY CLASSIFICATION UNCLASSIFIED		
22a. NAME OF RESPONSIBLE INDIVIDUAL Alice B. McGinty			22b. TELEPHONE (Include Area Code) 617 377-3452		22c. OFFICE SYMBOL GL/CAP

GL-TR-89-0119
JUNE 1989

**REPORT
ON
RESEARCH
AT
GL**

JANUARY 1987-DECEMBER 1988

**SURVEY OF PROGRAMS
AND
PROGRESS**

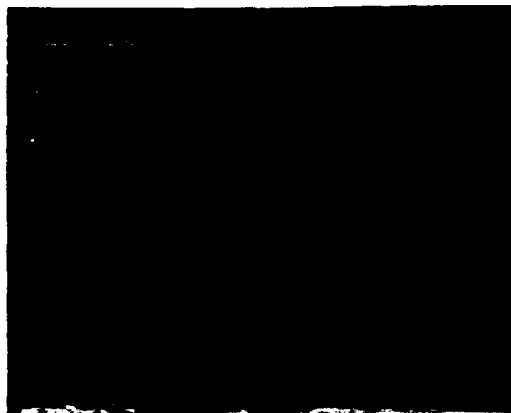
THE GEOPHYSICS LABORATORY

**AFSC
HANSCOM AIR FORCE BASE
MASSACHUSETTS**

JUNE 1989

Accession For	
NTIS CRA&I	<input checked="checked" type="checkbox"/>
DTIC TAB	<input type="checkbox"/>
Unannounced	<input type="checkbox"/>
Justification	
By	
Distribution /	
Availability Codes	
Dist	Avail and/or Special
A-1	

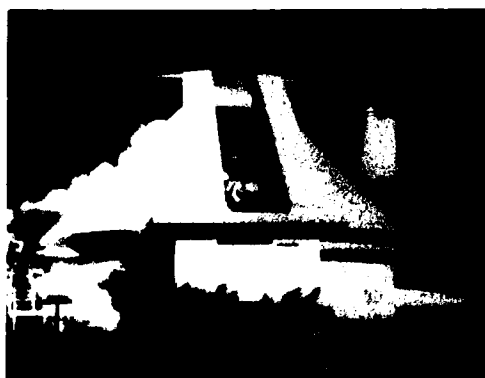
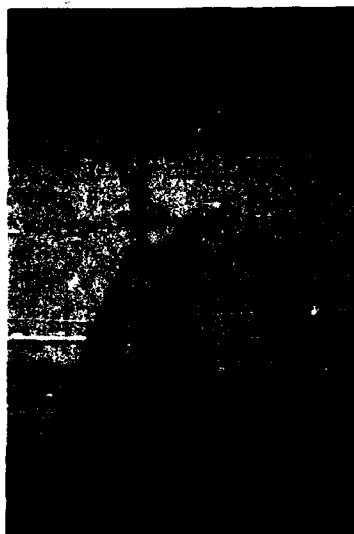




Foreword

This report summarizes the recent achievements and progress of ongoing programs at the Geophysics Laboratory. It is the fourteenth in a series initiated by GL's predecessor, the Air Force Cambridge Research Laboratories (AFCRL). Written primarily for Air Force and DoD managers of research and development, it shows how GL met the needs of Air Force systems and extended the technology base in geophysics during the period from January, 1987, through December, 1988.

JOHN R. KIDD
Colonel, USAF
Commander

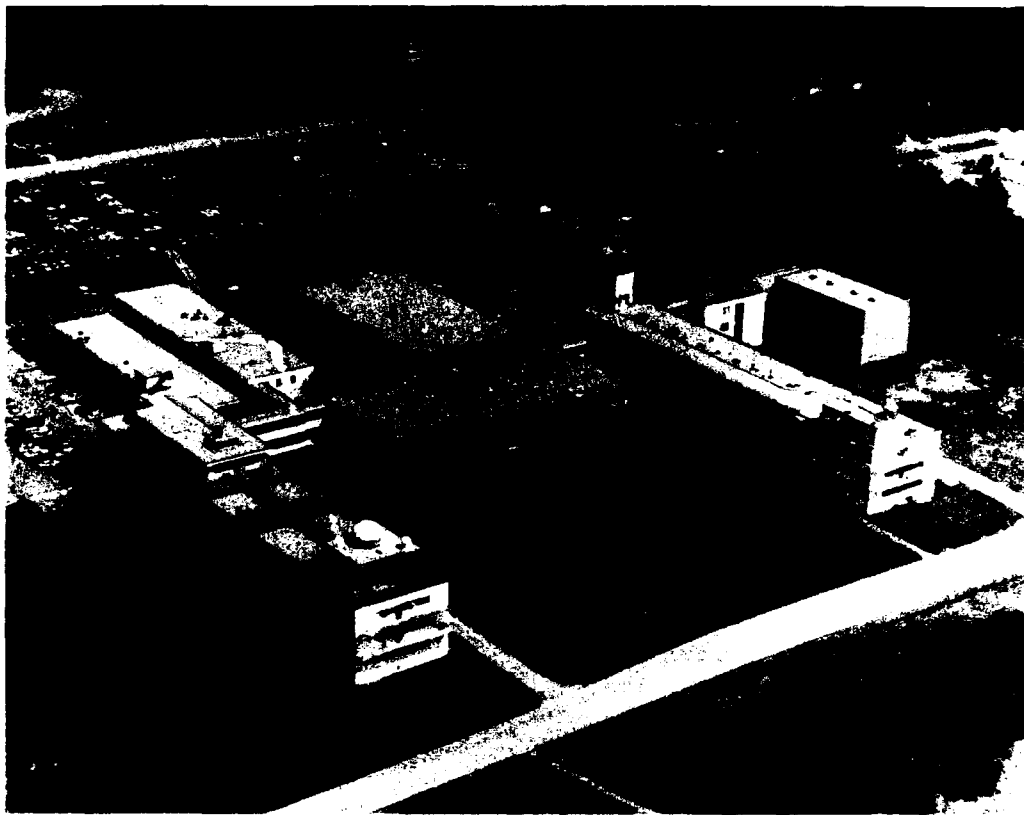


Contents

I. Geophysics Laboratory	1
<i>Technology Transition . . . Scientific Staff . . . Annual Budgets . . . Field Sites . . . Facilities</i>	
II Space Physics Division	12
<i>Solar Research . . . Energetic Particles . . . Space Weather . . . Active Experiments . . . Spacecraft Environmental Interactions . . . Spacecraft Contamination . . . Space Systems Environmental Interactions Technology</i>	
III Ionospheric Physics Division	86
<i>Ionospheric Effects . . . Ionospheric Scintillations . . . Ionospheric Modeling . . . Atmospheric Density and Satellite Drag . . . Ionospheric Interactions . . . Artificial Plasma Technology . . . UV Remote Sensing</i>	
IV Atmospheric Sciences Division	140
<i>Satellite Meteorology . . . Atmospheric Predictions . . . Ground-Based Remote Sensing . . . Atmospheric Characterization . . . Battlefield Weather . . . Cloud Physics . . . Upper Atmosphere Specification</i>	
V Optics and Infrared Technology Division	176
<i>Ground and Airborne Experiments . . . Rocket and Satellite Experiments . . . Laboratory Research . . . Computer Codes and Databases . . . New Instrumentation</i>	
VI Earth Sciences Division	234
<i>Geodesy and Gravity . . . Solid Earth Geophysics</i>	
VII Aerospace Engineering Division	262
<i>Balloon Program . . . Sounding Rockets . . . Space Shuttle Systems . . . Data Systems Analysis</i>	

Appendices

A Service on International Committees by GL Scientists	276
B Service on National Committees by GL Scientists	277
C GL Projects by Program Element	278
D Organization Charts	284



The Geophysics Laboratory is located at Hanscom AFB, 17 miles west of Boston. The GL Research Library is at the upper right beyond the trees. (USAF photo by Patrick J. Windward)

I GEOPHYSICS LABORATORY

The Geophysics Laboratory (GL) advances the operational capabilities of the Air Force by providing technology that enhances the interaction between systems and their environments. The Laboratory maintains itself as a center of excellence by conducting research and development programs in space, atmospheric, and earth environmental sciences important to the Air Force.

Although colocated with the Electronic Systems Division at Hanscom AFB, Massachusetts, GL reports to the Air Force Space Technology Center, Kirtland AFB, New Mexico. The Center is part of the Space Systems Division of Air Force System Command, Los Angeles AFB, California.

In 1987, Colonel Joseph R. Johnson commanded the Laboratory until August 7, when Colonel John R. Kidd succeeded him. Colonel Kidd was formerly Director of Strategic Defense Initiative Programs at the Air Force Space Technology Center. Colonel James K. McDonough served as Vice Commander of the Laboratory until July 3, 1987. Colonel Thomas W. Holycross, formerly Chief of Staff, Armament Division, Eglin AFB, succeeded Colonel McDonough on October 3, 1988. Dr. Richard G. Hendl, Director of the Laboratory's Office of Technical Plans and Programs, became the third Chief Scientist of the

Laboratory on October 9, 1988.

This report describes the achievements and activities of the Geophysics Laboratory from January 1, 1987, through December 31, 1988. During this period, GL conducted research, exploratory, and advanced development programs in space and ionospheric physics, atmospheric sciences, optical and infrared technology, and earth sciences. The products of these programs were transitioned into the Air Force as military design standards, computer-aided design tools, databases of geophysical parameters, tactical decision aids, computer models of the environment and its interaction with Air Force systems, feasibility studies, and prototype hardware and software.

TECHNOLOGY TRANSITION

The Geophysics Laboratory was the first laboratory to sign a Cooperative Research and Development Agreement (CRDA) with industry. On September 1, 1988, GL and ONTAR Corp., a software company in Brookline, Massachusetts, agreed that ONTAR will develop a personal computer version of GL's LOWTRAN7 atmospheric transmission code. ONTAR will supply user-friendly graphics and menus and will market the code. This agreement saves the Air Force the \$200,000 it would have cost GL to develop a PC version of LOWTRAN7.

Three members of GL's Space Physics Division (Dr. Allen G. Rubin, Dr. David L. Cooke, and Mr. Charles P. Pike) received a Special Award for Excellence in Technology Transition from the Federal Laboratory Consortium in 1988. The physicists identified the causes of satellite charging in space, which disrupts vital communication links, and developed computer models of the interactions of satellites with the space environment. They modified their models for use on a



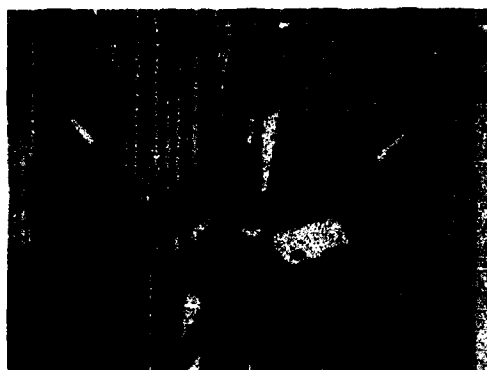
Mr. Charles P. Pike (standing), Dr. David L. Cooke (left), and Dr. Allen G. Rubin (right) with Computer Model of Interaction of Satellites with the Space Environment (They received a Special Award for Excellence in Technology Transition for this effort.)

variety of industrial computer systems, held applications workshops for industrial users, and provided instructional manuals.

SCIENTIFIC STAFF

The excellence of the Laboratory's staff of 299 civilian and military scientists and engineers, 106 of whom have doctor's degrees and 93 master's degrees, is reflected in the awards they received during the reporting period, the fellowships they hold in professional societies, and their service on important professional national and international committees.

Dr. John F. Paulson, research chemist in the Ionospheric Physics Division, won the Harold Brown Award in 1987, the fourth Brown Award to a GL scientist since 1976. Dr. Paulson and his group developed new chemical techniques to reduce the number of free electrons in the wakes of spacecraft during re-entry. The free electrons reflect radio and radar waves, causing radio blackouts and increasing the vulnerability of re-entry vehicles to detection. The Paulson techniques can also generate holes in the



Dr. Harold Brown (left) presents the 1986 award named in his honor to Dr. John F. Paulson, research chemist in the Ionospheric Physics Division. Secretary of the Air Force Mr. Edward C. Aldridge, Jr., looks on.



Assistant Secretary of the Air Force for Acquisition John J. Welch, Jr., presents 1987 USAF Research and Development Award to Lt Col George G. Koenig, chief of optical field activities for the Optical and Infrared Technology Division.

ionosphere.

Lieutenant Colonel George G. Koenig, chief of optical field activities of the Optical and Infrared Technology Division, received the 1987 USAF Research and Development Award for his contributions to the Infrared Search and Track System (IRSTS). This system is under development for operational use with the Advanced Tactical Fighter in

the NATO theatre of operations, where the effect of weather on visibility can be severe. Colonel Koenig produced the first data on the effect of optically thin cirrus clouds on long-path infrared transmittance. Future system designers will have access to this new environmental database.

Solar astronomer Dr. Richard C. Altmann earned Systems Command's Quarterly Science and Engineering Technical Achievement Award for the second quarter of 1987. By studying faint emissions of iron in the corona, or halo, of the sun Dr. Altmann discovered a dual solar cycle of 18 to 22 years, overlapping

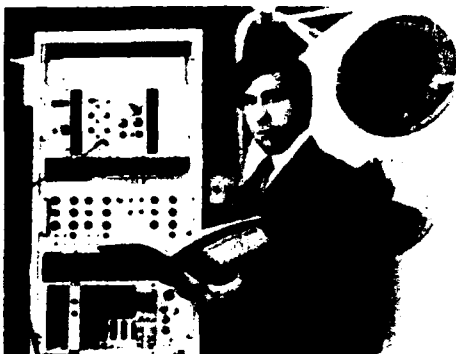


Dr. Richard Altmann, GL solar astronomer at Sacramento Peak Observatory, NM, adjusts the coronagraph through which he observed a dual solar cycle. Systems Command awarded him its Quarterly Science and Engineering Technical Achievement Award for this achievement in the second quarter of FY87.

the familiar 11-year cycle of solar activity. His discovery corroborates similar conclusions at the Mount Wilson Observatory. Together these findings revolutionize how scientists explain the sun's behavior and predict its activity, a subject crucial to the Air Force as it operates farther from Earth.

The American Defense Preparedness Association presented its 1987 Strategic Defense Initiative Laboratory Award to GL for its development of a helium-cooled infrared telescoped interferometer spectrometer (SPIRIT), which obtained infrared emissions from an intense aurora over Northwest Canada. The SPIRIT data will help the Air Force and the Strategic Defense Initiative Organization improve their capabilities to detect targets against highly disturbed backgrounds.

In 1987, Dr. Robert A. McClatchey, Director of the Atmospheric Sciences Division, received the Presidential Rank Award in the Senior Executive Service for his achievements as a technical manager and scientist. He developed satellite meteorological techniques that give global weather coverage at a savings of \$10 million to the Air Force. He also led the



Dr. David A. Hardy, astrophysicist in GL's Space Physics Division, was selected by his peers to receive the 1987 Guenter Loeser Memorial Award for his career achievements in space instrumentation, space particle physics, and auroral research.

development of Tactical Decision Aids, software which predicts the effectiveness of smart weapons under different weather conditions.

Paul I. Tattleman, research meteorologist in the Atmospheric Sciences Division, received the Climatics Award of the Institute of Environmental Sciences



Col Joseph R. Johnson (left) presents the Marcus D. O'Day Award for the best scientific paper published in 1986 to Dr. John R. Jasperse (center), of the Ionospheric Physics Division, and Dr. Bamandas Basu (right), a Laboratory contractor. Their paper, "The Dielectric Function for the Balescu-Lenard-Poisson Kinetic Equations," was published in *The Physics of Fluids*, January, 1986.

for significant contributions to the characterization of climatic conditions through the development of MIL-STD-210C.

Dr. Kenneth S W. Champion, Dr. Donald E. Bedo, and Mr. Frank A. Marcos were cited for their pioneering work in the upper atmosphere in the NASA historical publication "Into the Thermosphere, the Atmosphere Explorers," published in 1988. The fundamental work of Mr. Norman Sissenwine and Dr. Hans Hinteregger, now retired, on the three Atmosphere Explorer satellites launched from 1973-75 was also acknowledged.

Ten scientists have been elected by their peers to be fellows of their profes-



Dr. Larry Thomason (left), Col John R. Kidd, and Mr. Robert d'Entremont (right), satellite meteorologists in GL's Atmospheric Sciences Division, at the Marcus D. O'Day Award luncheon. Thomason and d'Entremont's paper, "Interpreting Meteorological Satellite Images using a Color-Composite Technique," appeared in the *Bulletin of the American Meteorological Society*, July, 1987

sional societies, including two who are fellows of two societies. Dr. Randall E. Murphy, Dr. George A. Vanasse, Dr. Frederic E. Volz, and Lt. Col George G. Koenig are Fellows of the Optical Society of America. Dr. Richard Altrock is a Fellow of the American Society for the Advancement of Science. Dr. Edmond Murad and Dr. Kenneth Champion are Members of the New York Academy of Science. Dr. Robert A. McClatchey and Lt Col George G. Koenig are Fellows of the American Meteorological Society. Dr. John J. Cipar is a Fellow of the Royal Astronomical Society. Dr. Thomas P. Rooney is a Fellow of the Geological Society of America and the Mineralogy Society of America.

Many Laboratory scientists serve on prestigious international committees, such as the Committee on Space Research of the International Council of Scientific Unions, The International Scientific Radio Union (URSI), the International Association of Geomagnetism and Aeronomy (IAGA), and the World Meteorological Organization. (For a complete listing, see

Appendix A.)

Both federal and professional organizations have called GL scientists to serve on committees, such as the Office of Science Technology Policy of the President, OSD Aerospace Vehicle Technology Working Group, AFSC/NASA Spacecraft Environmental Interactions



Mr. Jack R. Griffin, senior engineer in the Aerospace Engineering Division, won the 1987 Commander's Award for his many contributions to GL balloon, rocket, and space programs.

Technology Steering Committee, Tri-Service Clouds Modeling Committee, and the National Academy of Sciences. (A complete listing is given in Appendix B.)

Several GL scientists are editors and associate editors of professional journals such as the *Journal of Geophysical Research*, *Advances in Space Research*, *Radio Science*, and *Physics of Space Plasmas*. Others are members of editorial boards such as the books board of the American Geophysical Union, Geodynamic Series, and the journal of *Planetary and Space Science*.

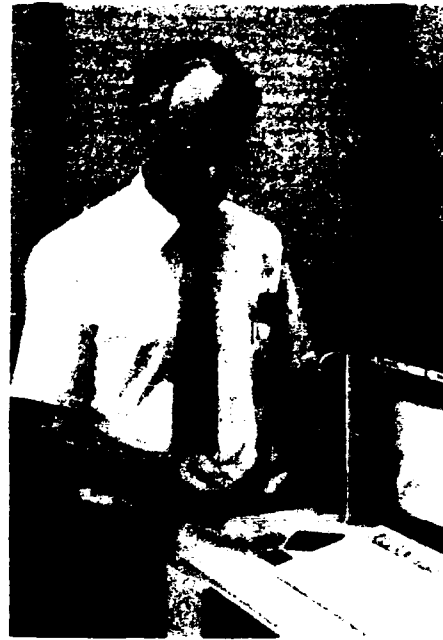
Many GL scientists were invited to give lectures, or chair sessions, at important scientific conferences. Among them were the Meteor Burst Communications in the 1990s, at Farnborough, England; Atmospheric Spectroscopy Applications Workshop, Rutherford Appleton Laboratory, England; invited professor, University of Paris; chair, Ninth Annual



Mr. John W. Armstrong, GL selection and acquisitions librarian, received the 1988 Commander's Award for his outstanding contributions to the Research Library since 1951.

MAXENT Meeting, Cambridge, England; International Conference on Ionospheric Modification, Tromso, Norway; chair, Symposium on Molecular Spectroscopy, Infrared Session; chair, Review of Modeling of the Atmosphere, SPIE; co-chair, Chapman Conference; Tropical Cyclone Conference; Triggered Lightning Workshop; NASA Technology Workshop for Earth Science Geostationary Platform.

The Laboratory also sponsored a series of workshops in which scientists from other services, federal agencies, universities, and private contractors exchanged information and planned future research. They included the Tenth Annual Tri-Service Review Conference on Atmospheric Transmission models, Fifth Tri-Service Clouds Modeling Workshop, SPEAR I (Space Power Experiments Aboard Rockets) Theory



Mr. Brian Sandford, chief of the Airborne Measurements Branch of the Optical and Infrared Technology Division, won the first GL Technology Management Award, established in 1987. He manages the Flying Infrared Signatures Technology Aircraft, which has acquired the largest database of aircraft infrared signatures in the world.

Group, Ionospheric Effects on Space-Based Radars, GL/AFOSR Artificial Plasma Workshop, Tri-Service Workshop on Cloud Impact on DoD Operational Systems, Tenth Annual GL DARPA Seismic Research Symposium, Eighth Annual Workshop on GL FASCODE/LOWTRAN Models. GL cosponsored the Battan Memorial and Fortieth Anniversary Conference on Radar Meteorology and the International Workshop on Remote Sensing Retrieval Methods.

To maintain its excellent technical staff, GL must interest the best young scientists in its mission and its technical programs. To accomplish this objective, the Laboratory has for a number of years participated in programs to attract and encourage young post-doctoral scholars

to continue their research at the Laboratory with internationally recognized experts in their fields.

One such program is the National Research Council Post Doctoral Associateship. Through this program, candidates receive one-year appointments (with an opportunity to renew for one additional year) as regular or senior appointees. Recently, there have been four or five such appointees at GL each year, including both United States and foreign citizens.

The GL Geophysics Scholars Program was initiated in the fall of 1982. This program also awards one-year fellowships which can be renewed for an additional year. It is open only to citizens of the United States and is designed primarily to attract young scientists with newly awarded doctoral degrees and little or no nonuniversity experience. Geophysics Scholars have numbered eleven to thirteen over the past two years and have come from universities across the country. The contributions of these young men and women scientists, along with the ideas and enthusiasm they bring with them, are readily apparent and stand out as examples of the program's success.

Other programs in which the Laboratory participates are the USAF Summer Faculty Program and the Graduate Student Summer Support Program administered by the Air Force Office of Scientific Research. Qualified faculty members from universities across the country work at Air Force laboratories during the summer months. GL has benefited from twelve to fourteen such appointees each summer during the past two years.

ANNUAL BUDGETS

The annual budgets for the two years covered in this report are shown in the accompanying table. The totals include salaries, equipment, travel, supplies,

computer rental, and those funds going into contract research. The largest expenditure is for contract research and development.

Funds received from GL's higher headquarters, the HQ AFSC Director of Science and Technology (XT), and to a lesser extent those received from AFSC organizations other than headquarters, are used to conduct continuing programs.

GL receives support from the Electronic Systems Division, the host organization at Hanscom AFB, in accounting, personnel, procurement, security, civil engineering, and supply. Holloman AFB, New Mexico, provides services to the GL Balloon Detachment. GL supports two divisions of the Rome Air Development Center at Hanscom AFB in the areas of the Research Library, laboratory materials needed for the electronic technology mission, the computer, technical photography, mechanical and electrical engineering, laboratory layouts, electronic instrumentation, and woodworking.

GL contracts are monitored by scientists who are themselves active, participating researchers, and who plan the research, organize the program, interpret the results, and share the workload of the actual research.

TABLE 1
SOURCE OF GL FUNDS
FISCAL YEARS 1987-88

	FY87 (\$M)	FY88 (\$M)
Air Force Systems Command XT	63.8	59.2
Air Force Systems Command-		
Other than XT	8.8	7.8
Defense Nuclear Agency	7.5	5.8
Defense Mapping Agency	1.3	0.2
Defense Advanced Research		
Projects Agency	3.2	4.4
Other Defense Agencies	22.4	24.7
Other Government Agencies	0.1	2.4
	107.1	104.5

FIELD SITES

GL operates several field sites, the largest of which is the Ground-Based Remote Sensing Facility in Sudbury, Massachusetts. Here four meteorological radars and data acquisition and processing equipment, including Perkin-Elmer 3242 and Digital VAX 11/750 computers, support a variety of meteorological investigations.

In New Mexico, GL maintains a detachment of 13 people to launch balloons at Holloman AFB and other locations and supports the Solar Research Branch (seven scientists) of the Space Physics Division at the Sacramento Peak Solar Observatory, Sunspot.

At Goose Bay Station, Labrador, GL's Goose Bay Ionospheric Laboratory provides observations to study subarctic events, including the aurora and polar cap absorption of high-frequency radio waves.

GL carries out field tests at a number of military installations, including Sondrestrom AFB, Greenland, and the White Sands Missile Range, New Mexico. In addition, the Poker Flat Research Range, Alaska, and commercial airports are also used.

GL launched 24 research balloons during 1987-88. Nine of these flights were tethered balloon operations. The most unusual free-balloon mission was the first launch of a large (11.6 million cu ft) stratospheric balloon from Antarctica. It carried GRAD, DARPA's 2000-lb Gamma Ray Advanced Detector, originally designed for the space shuttle. Launch was timed to coincide with the peak intensity of gamma ray emission from Supernova 1987A, the closest supernova to Earth since invention of the telescope. The other launches were from the permanent GL balloon facility at Holloman AFB, NM, and temporary sites on the White Sands Missile Range, NM, and

Roswell, NM.

The Aerospace Engineering Division and Detachment 1 at Holloman AFB conducted balloon missions for the other GL divisions, and for Space Systems Division, the Ballistic Missile Organization, the Electronic System Division, the Defense Advanced Research Projects Agency, the Defense Communications Agency, the United States Army, and several universities.

In 1987-88 four sounding rockets were launched in support of USAF scientists and all were highly successful. Effort began on four new 1500 - 3500 pound payloads on guided sounding rockets. GL also started development of a high performance booster that will increase our maximum performance capability by 40 percent.

Systems integration and test of payloads for free-flying satellites and the shuttle accelerated during 1987-88. Work concentrated on two large programs, CIRRIS 1A and IBSS, scheduled for the same shuttle flight. CIRRIS 1A (Cryogenic Infrared Radiance Instrument for Shuttle) is a 2-axis gimbaled telescope containing a radiometer and interferometer for characterizing atmospheric backgrounds as seen from space. IBSS (Infrared Background Signature Survey) will be flown on a "free flyer" deployed and recovered during a shuttle flight, while the associated CIV (Critical Ionization Velocity) payload remains in the shuttle cargo bay.

Technology-based research included development of a field-portable telemetry ground receiving station with high data-rate capability and high-capacity optical disk data storage. Research was also initiated on a guided parawing recovery system to improve recovery of balloon and rocket payloads, and on a shuttle-qualified optical disk storage system.

FACILITIES

Science Center: New conference facilities were built during the renovation of Building 1106, giving GL an auditorium seating 300 people with state-of-the-art video and audio systems. A new Narcisi Conference Room seating 35 people and a new Holzman Seminar Room seating 75 people were also constructed, with access to a comfortably furnished lobby with cloakroom and telephone facilities.

Fabrication Center: A new Research and

vides a 45 percent larger work area, allowing more room for each operator and work station. A \$100,000 computerized milling machine was installed, which greatly reduces the time required to produce machine parts.

Lidar Facility: GL's laser sounding laboratory has been used routinely since August, 1988, to observe the density and temperature structure of the atmosphere. The transmitter of this facility is a powerful laser that transmits, at each



Workstations in GL's New Research and Development Fabrication Center.

Development Fabrication Center, consolidating formerly separate machine, sheet metal, welding, and carpentry shops, was built in dormant storage space by George Trainer, Chief of R and D Fabrication, and his crew: Robert Vaccaro, Daniel E. Godin, Gerald D. McCarthy, TSgt Thomas Martone, and A1C Jerry Lewis. The new center pro-

sounding, powerful pulses of light at two different frequencies 10 times a second. A large telescope located in the penthouse at GL receives the backscattered signals from the atmosphere along the path of the transmitted pulses. From these data, remote measurements of atmospheric density and temperature profiles are extracted over the range of

15 to 100 km. About 100 soundings per month are collected. The database formed by these routine observations is compared with predictions computed from current models to determine the accuracy of these forecasts.

A mobile lidar sounder is also a part of GL's program. A powerful excimer laser has been added to the trailer to increase the strength of each atmospheric sounding by four times. Daytime capability has also been achieved. Plans have been formulated to move the mobile facility to Wright Patterson AFB to use a large receiving telescope located there. The measurements planned will allow density and temperature soundings to heights never achieved by any other ground-based facility. These results will be an important part of the design of the future generation of hypersonic spacecraft during orbit and re-entry phases.

Computer Facilities: GL is continuing to update its computing facilities. The former Computer Center, which consisted of a large, central-site processing facility, has been augmented with a broadband Local Area Network interconnecting the mainframe computers and intelligent terminals, such as IBM and Zenith personal computers. The mainframe computers are a CDC Cyber 180-860, a VAX 8650, and a VAX-11/780. The fully operational Local Area Network was implemented in December, 1986.

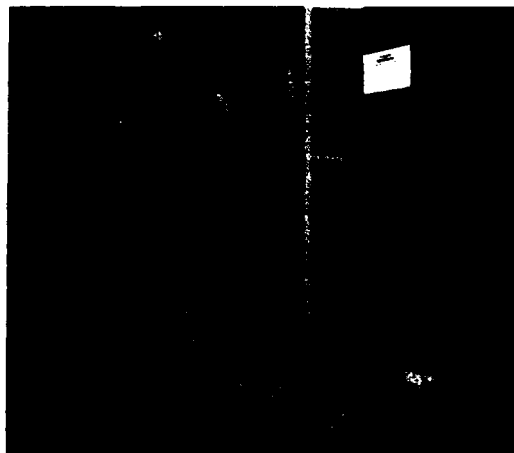
The central site of GL's distributed system will be augmented in 1989 with a central file system which will provide 55 gigabytes of file storage and allow common files to be accessed from any of the three central computer systems. This system will decrease the need for additional disk drives and provide an alternate to tape storage, thus saving considerable hardware dollars in the future.

The distributed network of computers will be integrated completely with the DECNET integration of various DEC-

NET subnets on the GL LAN by mid 1990, allowing high-speed file transfer between computer systems, a virtual disk capability, and a central maintenance capability.

A long-range evolutionary plan completed during FY84 is being carried out to provide a migration toward an advanced, full capability distributed information system. This plan addresses future network enhancements and services, translation of future user needs into information system capabilities, the time-phasing of information systems growth, and the identification and definition of viable alternative information system architectures to meet the stipulated evolutionary needs. A new plan is being developed to further respond to the needs of the GL user community for the next five years.

Research Library: The GL Research Library has the largest and most comprehensive scientific and technical



Mrs. Lee R. McLaughlin, supervisory librarian and chief of acquisitions, was named Air Force Technical Librarian of the year for 1987.

research collection in the United States Air Force. This collection is international in scope and includes extensive holdings

in mathematics, chemistry, physics, astrophysics, electronics, and geophysics. Each year the library adds more than 2,500 new titles to the book collection. The library also subscribes to approximately 1,800 current periodical titles. Of these, approximately 4,000 volumes are bound each year and added to the permanent collection. In-house and contractor technical reports from GL and the Electronic Systems Division are also maintained, both in paper and

microfiche.

In addition to its collection of publications, the library offers computer-aided literature searches of the Defense Technical Information Center's (DTIC) extensive files, as well as many commercially available databases. This service provides the patron with immediate access to millions of citations from journals, books, reports, proceedings, and reviews published throughout the world.

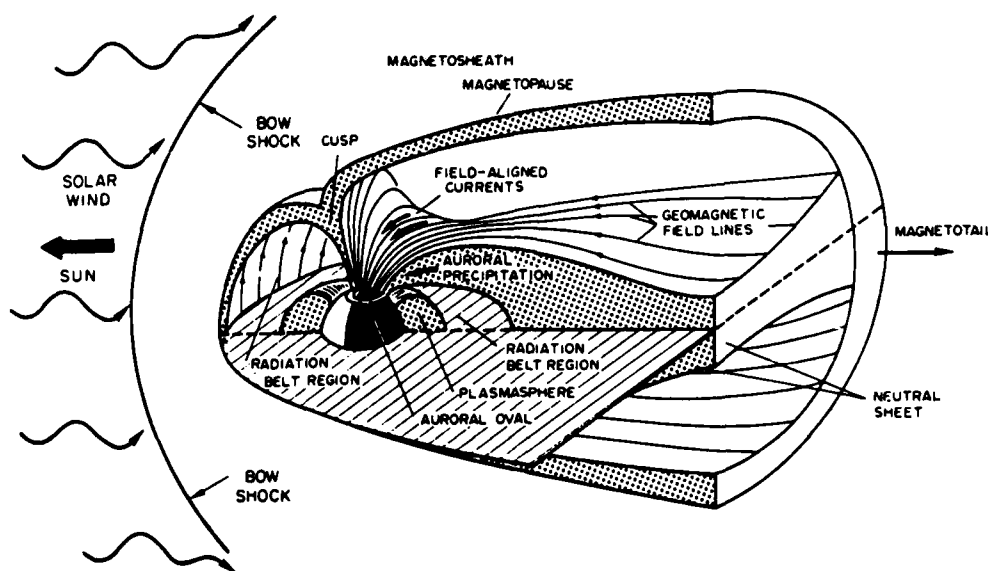


Capt Perry Malcolm aligns a target plate inside a vacuum chamber used for space simulations. When an electron gun fires a 40 kV, 200 mA beam into the chamber, the earth's magnetic field bends the beam just as it would in space. Such vacuum-chamber tests preceded the successful launch of the ECHO-7 payload on February 9, 1988. This resulted in the first picture of an electron beam spiraling around the earth's magnetic field. (USAF photo by Lee Stevens)

II SPACE PHYSICS DIVISION

The Space Physics Division conducts basic research and exploratory and advanced development in the solar-terrestrial system which is required for the next-generation Air Force space systems and rapidly expanding space operations. The results are essential to the design and operation of survivable, autonomous space systems. "Space weather" forecasting tools are developed to optimize performance of command, control, communication, and intelligence systems, to establish launch criteria, and to provide alerts of hazardous space environments.

The sun is the primary source of energy in the solar-terrestrial system. Understanding the physical mechanisms responsible for solar emissions is essential to the success of the Air Force space mission. The Solar Research Branch of the Space Physics Division studies fundamental solar processes, including the emission of electromagnetic radiation, energetic protons, cosmic rays, and the solar wind. Solar particle, plasma, and electromagnetic emissions determine the characteristics of the interplanetary medium; that is, the solar wind and the interplanetary magnetic field. The solar wind, in turn, is a major determinant of the shape and size of the magnetosphere-ionosphere cavity (see the figure), and of the energetic particle content of the magnetosphere. The solar flare is the most striking example of solar distur-



Model of Magnetosphere Showing Major Particle Populations.

bances which can produce catastrophic effects on Air Force space systems. Important new results have been obtained from the solar experiments on the Spacelab II flight, including new understanding of granulation in solar magnetic field regions, the relation between convection and small-scale magnetic field structures, and evidence for a dual solar cycle.

Most Air Force space operations are carried out within the ionosphere-magnetosphere system, as shown in the figure. The outer boundary, the bow shock, is located approximately 10 earth radii upstream from the earth along the sun-earth line. The inner boundary is identified as the base of the ionosphere E-layer at approximately 100 km. Within this system, regions of great importance to Air Force operations are the earth's radiation belts and the high-latitude regions, including the auroral zone and the polar

cap. The performance of Air Force space systems is profoundly affected by energetic particles found in the Earth's magnetosphere. For example, these particles can seriously degrade electronic components or cause single-event upsets (SEU's). They can also cause charging and discharging of materials on both the surface and in the interior of spacecraft which couple to spacecraft electronics. High particle fluxes generate a radiation hazard for manned spaceflight and can interfere with high-frequency radio communications in the polar regions.

To address these problems, the Space Physics Division is studying the processes governing the production, energization, and transport of the energetic particle environment. We begin with the origin of particles in the solar atmosphere, then trace their travel through the interplanetary medium, their acceleration in the Earth's magnetosphere, and finally

their effects on space systems. Recent work has focused on forming an integrated picture of this process, combining the results of solar flare research with solar wind and magnetospheric models to provide complete specification and new analytical representation of the dynamical nature of energetic-particle populations in the space environment. The goal is to develop a capability to model, monitor, and predict the behavior of the entire solar-terrestrial system. Advances in the analytic magnetosphere convection model include incorporation of a realistic magnetic field and effects of particle loss. Studies also have shown that there are three fundamental states of the magnetosphere, rather than the two generally accepted. An important contribution to space-science modeling development was the establishment of a baseline quiet magnetosphere. Major advances were made in the quantitative modeling of geomagnetic substorms.

To carry out these programs, state-of-the-art space flight and ground-based diagnostics must be developed, data analyzed, and phenomenological models of the system derived. During the past year, 18 spaceflight instruments were fully tested, calibrated, and delivered to the SPACERAD/CRRES satellite (Space Radiation/Combined Release and Radiation Effects Satellite). Currently, the instruments are being revalidated in preparation for final systems integration and test by the spacecraft integrator. The satellite is manifested to be launched from an Atlas Centaur into a geosynchronous transfer orbit in June, 1990. A principal goal of this program is to accelerate the transfer of new micro-electronic technologies to Air Force/Department of Defense space systems. It will also obtain data on particles, waves, and fields required to establish the first dynamic radiation-belt models.

Research and development efforts also

address space systems/environmental interaction problems, including spacecraft charging, techniques of charge mitigation, spacecraft contamination, spacecraft and plume signatures, and degradation of surface materials. Computer-aided design guidelines and engineering tools for future space systems are also generated. Measurements of spacecraft particulates and spatial emissions on shuttles provide an essential database for validating contamination codes and for assessing the effects of particulates and optical emissions on space sensor performance. The first phase of the analytic spacecraft charging code SOCRATES was completed. It takes into account scattering of contaminants by the ambient atmosphere and includes excitation of vibrational modes by collisions. A laboratory source of fast, ground-state atomic oxygen was developed which will be used to study the interaction of fast oxygen atoms with orbiting spacecraft. A high-resolution imaging spectrograph was developed to obtain high-resolution and imaging data of space-vehicle optical emissions resulting from shuttle glow and gaseous contamination and to develop an understanding of physical processes which produce radiant emissions on spacecraft and sensor surfaces. Space-system environmental interaction charging codes and large space-structure interaction models have been developed and transitioned to Space Systems Division. The polar charging code successfully explained results obtained on the high space-power rocket test, SPEAR.

The Active Space Experiment program investigates the environment by means of chemical emissions and wave, beam, and high-power rf injections. Theoretical developments during the past decade and advances in diagnostic sensors used to monitor the environmental effects produced by active injection have established the importance of active experi-

ments to advancements in space science. The ECHO-7 rocket electron beam test was successfully conducted. It investigated the long-range propagation of electron beams and determined the effects of beam operations on the host vehicle. Echoes induced by the beam were received after travel to the conjugate hemisphere and the effects of rocket-produced gases on the host payload were found to be an important source of high payload charging.

The Division program is carried out by means of in-house laboratory efforts, an extensive field program, and a broad contractual program. The field programs involve satellite experimentation and rocket, aircraft, and ground-based investigations. The ground-based program includes a large solar research effort at Sunspot, NM. Highlights of the discoveries and advances in solar terrestrial physics resulting from this Space Physics Division program during the past two years are described in the following sections.

SOLAR RESEARCH

Solar activity adversely affects Department of Defense systems and operations in the aerospace environment. Communication disruptions, radar interference, spacecraft charging and microelectronic failures, satellite drag, and radiation hazards to astronauts are among the many effects linked to solar activity. The Space Physics Division has sole responsibility within the Air Force for improving techniques to predict solar activity. To do this, it is necessary to identify and understand the physical mechanisms on the sun that cause the solar flares, high speed wind streams, and coronal mass ejections that produce the geophysical disturbances that disrupt DoD satellite systems and aircraft operating in the aerospace environment.

The three-dimensional structure and

interaction of magnetic fields and hot gas flows in the outer regions of the sun fundamentally drive solar activity. The Air Force solar research program investigates these phenomena at all levels in the solar atmosphere. Program elements include research into: (1) the structure and dynamics of the solar corona; (2) activity processes such as flares, eruptive or disappearing filaments, and coronal mass ejections; (3) the fundamental nature and origins of solar activity; and (4) the development of new instrumentation and techniques, for both ground-based and space-based observations, that will improve the solar database.

Solar Coronal Studies: The solar corona is the million degree outer atmosphere of the sun. It is dominated by intense magnetic forces, which penetrate into it from denser regions of the sun below. The solar source of geophysical disturbances on the magnetosphere, auroral zones,



Computer Enhanced Image of Solar Corona with Calcium II k-Line Image Superimposed to Locations of Active Regions.

upper atmosphere, and ionosphere often either lies in the solar corona or causes visible changes in the corona that can be used to predict such disturbances. Daily observations of the corona are obtained at the GL operating location at Sacramento Peak Observatory (SPO), Sunspot, NM. They are telecopied to USAF space forecasting centers and are used to derive information on coronal processes, with temporal resolutions ranging from a few minutes to periods spanning the 11-year solar activity cycle.

Coronal observations from SPO have recently been published in the form of an atlas. This atlas depicts the intensity of the Fe XIV 5303 Å coronal-emission line in Carrington synoptic chart form. While optimized to display active regions, it may also be used to infer the presence of coronal holes, the vast, low density regions that are the source of the high-speed solar wind streams. A movie of the SPO Emission-Line Coronal Photometer (ELCP) data covering 1975-1986 has also been completed and made available for distribution. It consists of the series of Carrington synoptic maps of Fe XIV intensities at a height of 0.15 solar radius above the solar limb during that period. Such charts display one complete solar rotation plotted as colored contours on a projection similar to a Mercator map. This movie documents the variation of the Fe XIV corona over solar cycle 21 and allows comparison with other solar data.

Observations of the solar corona in the emission from the Fe XIV line have been made daily with the SPO photoelectric photometer since 1973. The observed emission shows temporal variations in a number of characteristics, among the more striking of which is the change in the global integrated flux. This measure is formed by integrating successive limb scans of the corona to approximate the flux emanating from an entire hemisphere of the corona. Previous investiga-

tors found that in solar cycles 18 and 19 (from 1944 to 1965) the Fe XIV flux was double-peaked, with one peak occurring near the maximum of the sunspot number and the second two to three years later. However, the SPO and other data for cycles 20 and 21 (from 1965 to 1986) show a multi-peaked variation with surges of activity every two to three years. Some of the data do not show any clear single maximum. There is evidence that these effects may be due to long-term temperature changes in the corona. In any case, it is now evident that coronal processes provide a rather different picture of solar activity from that of the sunspot number, which is still widely used as a general proxy for all solar-activity processes. The fact that coronal activity looks more like a modulated square wave than the approximately Gaussian distribution of the sunspot number will have to be taken into account in future theoretical models of solar activity.

Coronal observers have variously argued that solar rotation in the Fe XIV line varies from rigid (all solar latitudes rotating at the same angular rate) to semi-rigid to fully differential (the angular rate slowing with increasing latitude, which is the case for photospheric and chromospheric tracers). No consensus has emerged. An autocorrelation study of 12 years of SPO ELCP data in the Fe XIV 5303 Å line shows yet another complex pattern. An average over all years indicates a semirigidly rotating corona similar to that seen in some of the previous studies. This component of the corona probably reflects some large-scale, deep-seated characteristic of global solar structure. In addition, an analysis of individual years shows a fairly strong differential rotation beginning in 1977-1979 and decreasing in 1980 and later years. We infer that this is due to the appearance of high-latitude features in 1977-1979 that rotate at near-chromo-

spheric rates. These distinct features slowly drift toward the equator beginning in 1980. Their eventual disappearance at high latitudes and their merging with faster rotating features at low latitudes result in the semi-rigid rotation rates of the overall Fe XIV corona in 1984-1985. Except for years near solar minimum, during which time the identification of the slow features becomes more difficult, there appears to be a tendency for these features to avoid the location of the coronal activity maxima. A similar effect, known as the Torsional Oscillation (TO) signal, is found in the photosphere and chromosphere. The SPO coronal data may provide the first detection of the TO signal outside the photosphere. If so, this would become a major constraint on theories of solar activity and its prediction.

At the request of Air Force Global Weather Central (WSE), the Solar Research Branch has begun to provide new solar data for use by their forecasters in predicting geomagnetic and other parameters. Specifically, we have provided them with a one-time set of solar training aids (magnetograms, He 10830 filtergrams, and white-light pictures) and new daily data products: (1) a verbal description of solar activity, and copies of (2) a drawing of sunspot locations (with the addition of the location of active regions, prominences, and the like) (3) "raw" uncalibrated coronal scans sent immediately after their acquisition, (4) full-disk coronal maps made from West-limb data (in addition to those made from East-limb data already supplied), and (5) processed calibrated coronal scans.

The new solar data will increase the reliability of the space forecasts with which AFGWC/WSE forecasters are tasked. These products are factored into their daily forecasts of the solar 10.7 cm radio flux (F10) and geomagnetic indices. Specific uses of our data include such

activities as determination of the general level of solar activity; the appearance or disappearance of, or changes in, active regions rotating onto the visible hemisphere of the sun; the location of sources of steady-state high-speed solar wind streams; and the existence of solar active regions having a high probability of unusually energetic flares. The WSE forecasts are in turn provided to a number of customers, who use them to modify operations, understand anomalies of the systems that they control, and the like.

The Solar Research Branch CORONALERT system was instituted during this period. It is currently sent out to 72 space forecasting centers and researchers around the world by electronic mail. It is a system to alert interested parties to unusual activity in the corona. Daily observations at SPO are obtained with the ELCP in Fe XIV, Fe X (6374Å), and Ca XV (5694Å). Most alerts are concerned with Ca XV emission, since this line is associated with regions that have a high potential for energetic flares. Coronal holes as seen in Fe XIV are also reported.

Solar Activity Processes (Flares): Solar flares are one of the principal drivers of solar-induced geophysical disturbances. Flares arise in a highly complex interaction between magnetic fields and plasmas in the solar atmosphere which is totally inaccessible to in-situ sensors but which can be monitored by a variety of telescopic instrumentation. Observationally, the principal interest is to obtain data with which to study the basic processes of flare energy build-up, storage and release, energy transport, and particle acceleration mechanisms. The goal of these studies is to acquire a physical understanding sufficient to develop techniques for predicting the occurrence of flares and their effect on the aerospace environment.

One approach to flare prediction,

which virtually ignores the basic physics, is to use statistical models that relate solar conditions on any given day to flare activity on the next. One such model, known as Multivariate Discriminant Analysis (MVDA), was successfully applied to a large database of daily solar parameters derived largely from the AWS Solar Optical Observing Network (SOON). The results were sufficiently encouraging to prompt AFGWC to request a copy of the program for use on a PC class computer; in response, a PC version of MVDA was written and forwarded to AWS along with documentation, as a Technology Transition effort.

Ultimately, however, the development of highly accurate prediction algorithms depends on understanding the physical mechanisms of flares, thereby allowing forecasts to be based on quantitative models of the solar magnetic field evolution. A growing body of evidence now points to current-carrying, or "sheared," magnetic fields as the principal means by which flare energy is built up and stored. Observations of sheared fields can be obtained directly with a vector magnetograph, although the presence of shear can be inferred also through analysis of solar atmospheric geometry and velocity fields. The following self-consistent picture of the pre-flare process has proven successful: shearing velocity fields (with typical velocities of 0.1 - 0.3 km/sec) in the solar photosphere move the footpoints of closed magnetic field loops (with field strength usually exceeding 1000 gauss). These then respond to the axial electric currents by forming twists (with field vectors inclined in excess of 80 degrees to a potential field vector) that are often observable in atmospheric structures that conform to the magnetic fields. These stressed fields then break and reconnect, forming a more relaxed structure in a lower energy state. The resulting reduction in stored energy (as much as 10^{32} erg) is mani-

festated in the accelerated particles and hot plasmas of the associated flare. Considerable progress has been made in theoretically demonstrating the latter picture by means of time-dependent magnetohydrodynamic (MHD) models, although fundamental questions still remain. The triggering mechanism is elusive, and current efforts are focusing on critical rates and degrees of shear.

Empirical models of shear, based on several easily observed parameters, are being studied in connection with a pre-operations test and evaluation of shear as a flare predictor. The principal observational inputs are derived from low-resolution vector magnetograms and medium-resolution hydrogen-alpha filtergrams. Although this investigation is only beginning, preliminary results indicate that measurements of magnetic shear offer the greatest potential for improved flare predictions using ground-based, medium-resolution observations. Recommendations have already been made to AWS to incorporate a vector magnetograph into the SOON Upgrade scheduled for the mid 1990's. In anticipation of this upgrade, several preliminary design concepts have been briefed to AWS, and development of a new, liquid-crystal tunable filter for this purpose has begun at SPO. In these designs, precise measurements of the solar vector magnetic field are made possible by a rotatable prism analyzer that provides a ten-fold improvement in polarization sensitivity over conventional techniques. A complete design, based on this device, has been thoroughly studied under contract with NASA's Marshall Space Flight Center. A complete prototype vector magnetograph incorporating the essential features of the latter design has now been constructed by the Applied Physics Laboratory of The Johns Hopkins University, under funding by AFOSR's URI program, and will be installed for testing at SPO during FY89.

Energy transport in flares continues to be a focus of research that combines solar atmospheric modeling with optical and x-ray observations. Efforts to distinguish between the effects of heat conduction, irradiation, particle bombardment, and hydrodynamic compression waves in transporting flare energy from the solar corona to the deeper layers of the sun are based on multispectral measurements that determine the flare radiative losses as a function of height in the solar atmosphere. The question of energy transport is fundamental in determining the basic characteristics of the flare energy release process, i. e., in ascertaining the proportion of energy released in the forms of heat, accelerated particles, and mass

motions. Observations obtained with high temporal resolution (<0.2 sec) at several wavelengths in the hydrogen-alpha line provide powerful diagnostics for determining the time scales of excitation, ionization, and atmospheric pressure waves. The latter data, obtained with the Vacuum Tower Telescope (VTT) at Sacramento Peak, are then compared with NASA Solar Maximum Mission (SMM) hard x-ray observations in order to directly monitor the effects of subrelativistic electron beams impinging on the solar chromosphere.

White light flares (flares visible in optical continuum), although relatively rare, are ideally suited to studies of energy transport because their radiative loss-



Large White Light Flare of 00 h UT, April 25, 1984, Photographed at 3610 Å. (This flare, which produced major hf communication outages, occurred in a location where the solar magnetic fields had previously been highly sheared. Analysis of this flare, described in the text, has led to a better understanding of energy transport mechanisms in active regions.)

es are exceptionally large, thereby placing severe constraints upon the transport mechanisms. (White light flares also produce major geophysical effects.) Recently, quantitative measurements of the spectrum and energetics of these events have led to the conclusion that heat conduction, irradiation by soft (1-10Å) x-rays, and protons with energies exceeding 10 MeV are not effective in heating the deep layers of the flare atmosphere. Additional studies of white light flares are now providing spectroscopic evidence of flare structures that are unresolved even by the largest telescopes, as well as new methods for monitoring departures from thermodynamic equilibrium in the flare atmosphere and their variation in space and time. Diagnostic tools such as these are prerequisites in forming a comprehensive picture of the flare, and in leading to an improved basis for understanding flares within the larger context of solar physics.

New perspectives on activity occurring approximately 30 minutes, or less, before the optical brightening in major flares offer the possibility of short-term flare forecasts with high accuracy. The technique in this case is to detect the very early stages of the flare, when irreversible changes in the magnetic field have already begun to occur, but before the flare has produced geophysically significant emissions. Such preflare activity has occasionally been known to produce identifiable signatures in soft x-rays, microwave intensity and polarization, and motions of solar chromospheric structures. The ideal method, however, for monitoring these pre-flare activities is to observe, at high spatial resolution, the solar plasmas in the temperature range (approximately 10^6 K) characteristic of the solar atmosphere at the levels where the magnetic fields actually produce flares. Recently developed thin-film technology has made possible the con-

struction of normal-incidence mirrors that can image solar features in narrow wavelength bands centered on a single emission line in the extreme ultraviolet portion of the spectrum, thereby allowing the hot coronal loop structures to be viewed directly. On June 23, 1988, the Smithsonian Astrophysical Observatory, in cooperation with ground-based observations at SPO, was successful in observing the early stages of a flare at a wavelength of 62.5 Å, using a normal-incidence telescope on a rocket launched from White Sands Missile Range. The results showed loop structures beginning to brighten well before the bright optical and intense x-ray emission of the flare. The design and construction of normal-incidence optics at short wavelengths have been funded through GL for several years as part of a high spatial resolution mission for solar monitoring after 1995.

Solar Activity Processes (Coronal Mass Ejections and Interplanetary Phenomena): SPO observations of the low corona in the Fe XIV emission line show occasional transient events which have many of the characteristics of the more familiar coronal mass ejections (CMEs) seen in white light observations. To the extent that these events do represent CMEs, they may provide constraints on physical conditions within mass ejections and give some clue as to their dynamical evolution. Ongoing studies by the Solar Research Branch of these transient processes have confirmed and extended the earlier results discussed in the 1985-1986 volume of this series. Over a period of 5 years, 511 hours of observations were successfully obtained on 100 days. During this period we recorded 26 emission-line transients associated with hydrogen-alpha activity at the limb as seen in SPO Flare Patrol films, for an average transient rate of 1.2 per 24 h. No transients were recorded in 1985. The solar-cycle variation and production rate of Fe XIV transients is generally similar

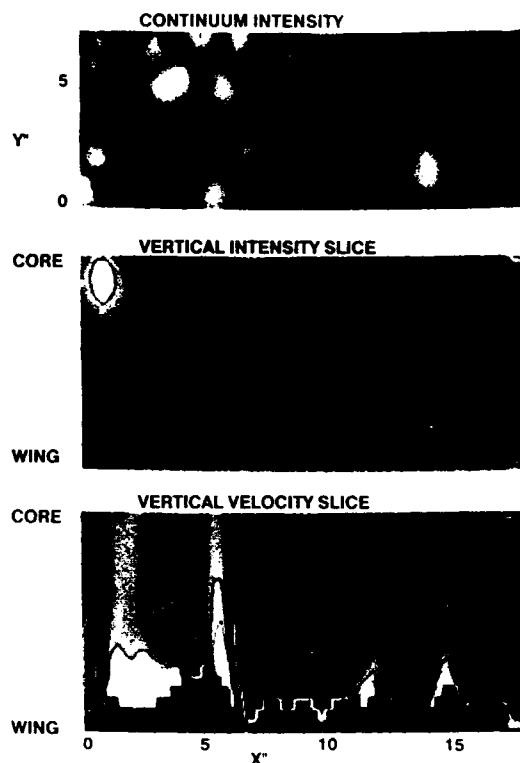
to the data from the High Altitude Observatory's Mark-III K-coronameter and the coronagraphs aboard the SOLWIND and SMM spacecraft. These low coronal transients were associated with surges or eruptive prominences at the limb 88 percent of the time. On only one occasion did we observe a transient associated solely with a flare. We conclude that low-coronal emission-line transients are highly associated with the ejection of chromospheric matter into the corona. This study is expected to help improve USAF capability to predict CME's, which are known to produce effects adverse to USAF systems if they impact on the magnetosphere.

Retrospective work by a Solar Research Branch contractor on observations with white-light photometers on the HELIOS satellites has proven the detectability of (1) coronal mass ejections, (2) coronal streamers, and (3) shock waves in the interplanetary medium. Basic solar wind structures measured and imaged to date include more than fifty solar mass ejections, over ten heliospheric extensions of coronal streamers, and a half dozen shock waves measured in-situ by the spacecraft. In the case of each of these heliospheric structures, it is apparent that Thomson scattering by electrons is adequate to explain the features measured, and that these features can be traced outward to distances of nearly one AU over periods of several days. The ability to image these heliospheric structures in white light allows a remote sensing technique to supplement and enhance our knowledge of features over three-dimensions.

Origins and Nature of Solar Activity: Solar activity originates in the complex interplay between velocity fields, which result from convective, oscillatory, and rotational motions, and the magnetic fields that are embedded in the solar gas. Knowledge of how the magnetic field

responds to these motions is required in order to understand the processes that lead to energy build-up and release in active regions. The interplay between solar dynamics and fields occurs over a broad range of spatial and temporal scales, from small granules (a few hundred kilometers) to scales encompassing the entire sun (about 7×10^5 km) from processes lasting a few milliseconds in flares, to time-scales of the 22 year solar magnetic cycle. A combination of work based on ground-based and space-based solar data, as well as observations of solar-like stars, has yielded several exciting new results that will improve the understanding of how solar activity originates.

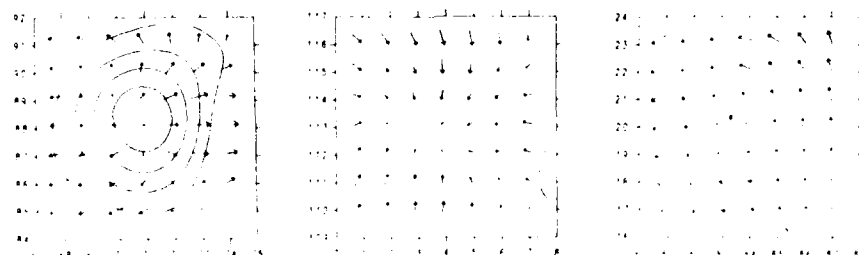
The deepest visible layer of the solar atmosphere is the solar photosphere. Convection, generated below the photosphere, penetrates into the photosphere, giving it a granular appearance of bright and dark cells. The motions associated with these cells, combined with the gas densities of the photosphere, are sufficient to move around magnetic flux tubes, leading to the build-up of stresses in these fields as discussed above. A significant advance in the ability to observe these small-scale flows was made through the development of a very narrow band, tunable filter system. The problem of measuring the properties of flows and structures in the solar atmosphere is one of obtaining good spatial and spectral resolution simultaneously. Spatial resolution is needed to resolve the features while spectral resolution is needed to obtain diagnostics of velocities, temperatures, and other properties of the gas. Spectrographs provide good spectral resolution, but generally give spatial resolution in only one dimension, or trade spatial for temporal resolution in two dimensions. Filter systems generally provide good spatial coverage and resolution, but sacrifice spectral resolu-



Vertical Cross Section Through a Region of the Solar Photosphere Showing Intensity (middle) and Vertical Velocity (bottom). (The location of the cross section with respect to the solar granulation is shown on a continuum intensity image at the top. The cross section passes through a dark pore, usually associated with magnetic flux tubes passing through the atmosphere, at about 5". The velocity cross section varies between 1.5 and -1.5 km/s with a contour interval of 0.33 km/s, where upflow is negative, dark on the figure. The intensity varies from 1.16 times the average photospheric intensity, bright on the figure, to 0.82 times the average with a contour interval of 0.04.)

tion. The development of a very narrow-band filter system gives the ability to do spectroscopy at very high spatial resolution, with acceptable temporal resolution for studying solar convection and many other solar phenomena. Having two-dimensional solar images allows image-enhancement programs to be applied to the data to achieve very high spatial resolution. This system was used to observe the solar granulation and has resulted in the first accurate measurements of the vertical velocity field associated with the granulation in the photosphere. The figure shows an image of the solar granulation brightness field and a vertical cross section through that field in both brightness and velocity. The cross section was chosen to pass through a magnetic feature (dark pore in the brightness image) Fairly strong shears in the velocity field are observed near the edges of the pore. A time sequence of similar data is being studied to follow the interaction of the flow with the flux tube.

The Solar Optical Universal Polarimeter (SOUP) experiment on the Spacelab 2 mission (July-August 1985) provided the best time series ever obtained of solar granulation. Using local correlation-tracking algorithms developed by Solar Research Branch scientists, the SOUP investigators discovered that the surface of the sun is covered by horizontal flow patterns. These data showed that solar granules (1"-3" in diameter)



Mesogranular-sized Source of Diverging Flow, left; Converging Flow into a Sink, center; and Vortex Flow; right. (Coordinates are in units of arcsec.)

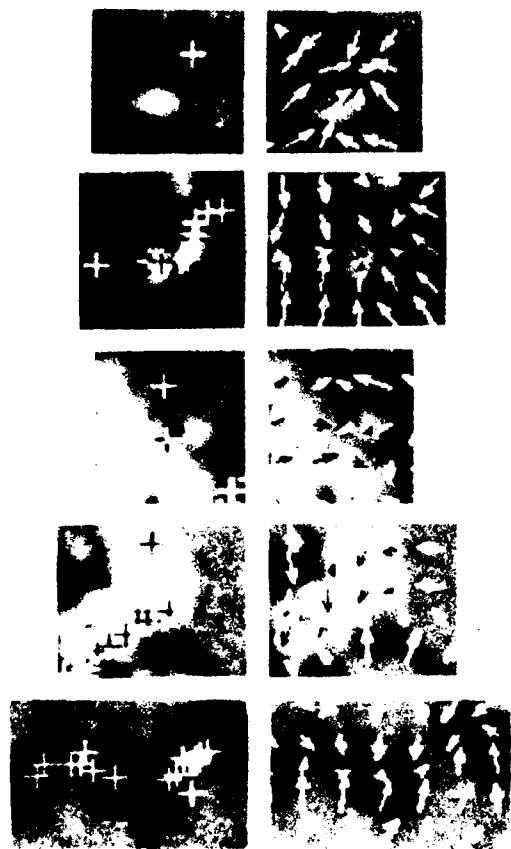
(1" = one arcsec = 720 km) move like test particles ("corks") on top of larger-scale longer-lived flow patterns in the solar atmosphere. These structures are predominantly of mesogranular size (6"-12"), although a few have supergranular (20"-40") scales. For the first time, mesogranules were seen so clearly that remaining skeptics were forced to admit not only the existence of mesogranules, but also to recognize that, indeed, mesogranules are the dominant scale of convection (after granulation) seen at the solar surface. (Solar Research Branch personnel have played a leading role for three decades in understanding solar convection, first discovering supergranulation and the 300s oscillations in 1960, and then mesogranulation in 1980.) These large-scale structures display considerable variability, including outflow from upwellings, convergence into sinks, and often significant vorticity, as seen in the figure. Lifetimes of mesogranular structures range from 2 h to 10 h or more.

While the description and analysis of such motions are fundamental to an understanding of solar convection, the main significance to the Air Force arises from interactions between the motions

and magnetic structures, i. e., magnetoconvection. Significant progress has been made by Solar Research Branch scientists during 1987-1988 in observing and modeling magnetoconvection. By correlating convective flows with simultaneous observations of the solar magnetic field, they found that magnetic flux elements move in patterns which are in almost perfect agreement with those of the granular "corks": Granules and magnetic features are expelled from the centers of mesogranules, moving first to the mesogranular boundaries and ending up at the boundaries (network) of the larger supergranules. The corks then slowly concentrate, over a period of about one day, into small downdrafts (sinks), while the magnetic elements apparently prefer to remain primarily as a network pattern (see the figure). To demonstrate this phenomenon more clearly, five small sections of the preceding figure have been enlarged, and are displayed in the next figure. Each of these examples illustrates the same point: Wherever there is an opposing flow field, the magnetic field becomes concentrated. Except in regions of strongest field (sunspots and pores), the observations indicate that the field apparently does just what the velocity



SOUP Flow Vectors (left) Superposed on a Gray-scale Image of the Flow Divergence (bright areas are sources, dark areas are sinks). (Four prominent sources are labeled.) Positions (center) of Corks 12 h after Starting from a Uniform Distribution Superposed on the Flow Divergence. Superposition of the 12 h Corks (right) and the Magnetic Field Structure Observed Simultaneously at Big Bear Solar Observatory.



Enlargements of Five Small Sections Preceding Figure. (In each case, the velocity vectors point toward a concentration of magnetic field and corks. The five areas shown run from top to bottom. Particularly interesting are a collision, second from top, between outflow from the mesogranule labeled 2 and the sunspot; a collision between outflow from the supergranule labeled 4, third from top, and the sunspot; and convergence to a sink point, bottom. In this last example, the single cork visible is actually a superposition of five corks which have already converged at this site.)

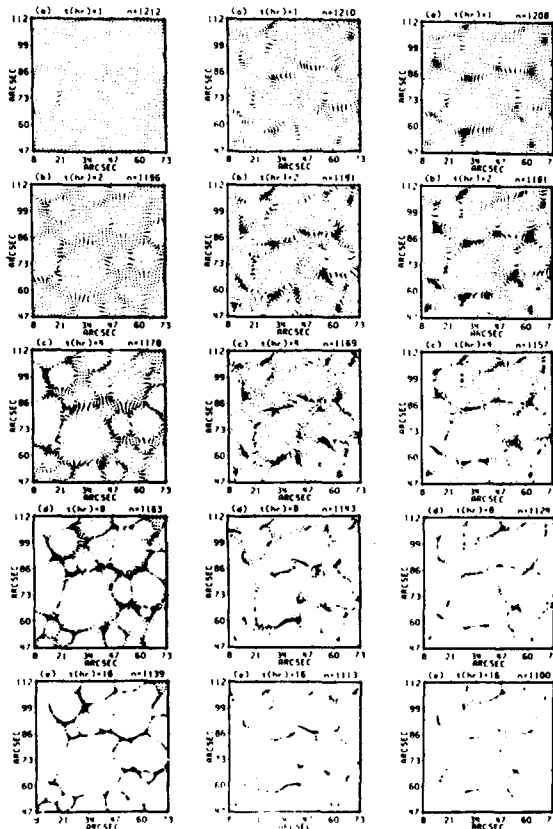
field "dictates."

These observations have important implications for the buildup of magnetic activity on the sun. Since the structure of the magnetic field of the sun's surface closely mimics the motions of granular corks, one can determine where magnetic fields will pile up and undergo stress. In addition, since the observed vorticities

are large enough to twist a magnetic flux tube by a full 360 degrees in less than three hours, it should become possible to pinpoint loci of magnetic mixing and twisting, and thus increase one's ability to predict the occurrence of solar flares, coronal heating, and mass ejections.

Subsequent to the analysis of the Spacelab 2 observations, Solar Research Branch scientists were able to achieve similar results from data obtained at the VTT at SPO, and thus show that it is possible to measure these magnetoconvective phenomena from ground-based observations. Although such data are inherently noisier than those from space, they produced surprisingly excellent results when analyzed by sophisticated crosscorrelation techniques which have been under development by Branch scientists for the last several years. These techniques will permit continuation of this essential research program during the next 6 to 10 years when there will be no relevant solar observations available from spacecraft. Important results have already been obtained here: divergence maps made from the horizontal flows show that the sources are small, 5 to 10 Mm (1 Mm = 1000 km), with a mean size of 6.6Mm. The flow divergence is found to be strictly correlated with concurrent vertical Doppler velocity, thus demonstrating that the divergence source points are the mesogranules. The absence of power in the divergence at the larger supergranular scale shows that supergranulation might be a surface phenomenon without a similar scale of convective up flow. In this case the convection would not be characterized by a discrete "closed cellular" morphology, but rather by a process of convective "fingering" whose resulting horizontal flows add. The larger scale for the horizontal flows would then be the result of a large distribution in the strengths of the individual sources.

Simultaneously with the data analysis from SOUP, Branch scientists began a collaboration to model the observed flows and magnetic structures. Preliminary results were reported two years ago, and



Cork Positions 1, 2, 4, 8, and 16 h after Starting from a Uniform Distribution. (Time increases downward in each column. SOUP data, center; model with sources only, left; model with both sources and sinks, right.)

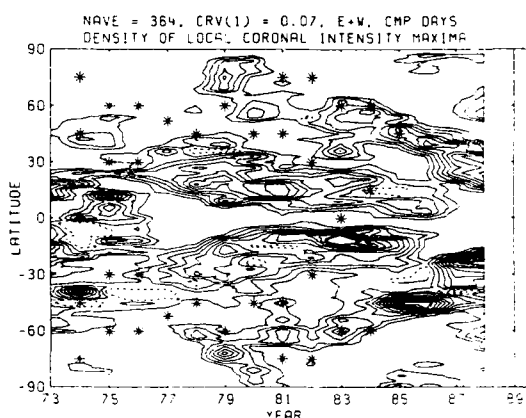
since then a major expansion of this effort has taken place. Two theoretical models of solar flow patterns have been examined, one containing sources only, and one also having sinks. To examine the significance of the differences between the solar data and the two models, a uniformly-spaced grid of test particles ("corks") was placed in the flow field and their motions followed for 16 h. This is illustrated in the figure. It was

observed first that in all three cases the corks are quickly expelled (in less than one hour) from the regions of positive divergence, and then congregate into a network pattern in 1 to 2 h. After that, the SOUP and the source-plus-sink model corks quickly converge to the sinks, while the source-only model corks remain in a network configuration for many hours, much like the actual observed magnetic field.

It is most interesting that the flows appear to end at sink points, in excellent agreement with recent theoretical studies, while the magnetic structure remains as a network structure. This suggests, perhaps, that the magnetic structure depends mainly on larger, longer-lived, deeper-originating convective flows (supergranulation), while the observed surface flows are due to smaller, shorter-lived features (mesogranules). This conclusion regarding the supergranulation appears to conflict with the interpretation above that the supergranulation is probably a surface phenomena and indicates further observational and computation work is required to sort out the scales of solar convections.

The solar activity cycle is traditionally defined in terms of a semi-regular, long-term variation in sunspot numbers, the interval between successive minima currently averaging about 11 years. However, a number of observations now indicate that the activity cycle begins prior to the emergence of the first sunspots of each cycle. The Solar Research Branch, in collaboration with other scientists, has reported results from sunspot cycle 21 concerning ephemeral active regions (ERs), the coronal Fe XIV emission, and the torsional oscillation (large-scale photopheric velocity) signal, which confirm earlier suggestions. For example, they report the appearance of a high-latitude population of ERs in the declining phase of sunspot

cycle 21, with orientations which tend to favor those for cycle 22 rather than 21. Taken together, these data indicate that sunspot activity is simply the major phase of a more extended cycle which begins at high latitudes prior to the maximum of the preceding sunspot cycle and progresses towards the equator during the next 18-22 years, merging with the conventional "butterfly diagram" (the



Contours of Annual Averages of the Density of Local Coronal Intensity Maxima of all Usable Scans from 1973 through 1988. (Note the high-latitude activity zones extending from 1979 through 1988. Asterisks show slow moving zones.)

plot of the latitudes of emerging sunspots against time) as it enters sunspot latitudes. They suggest that this extended cycle may be understood in the perspective of a model of giant convective rolls which generate dynamo waves propagating from pole to equator. As cycle 22 commences, recent observations show the unbroken continuation of this pattern through solar minimum. A pattern of new high latitude emission near the poles began in 1985 and may be indicative of the onset of cycle 23. The figure depicts this "extended" cycle as seen in the SPO coronal observations.

A comprehensive analysis of Ca II H+K (3933 and 3968 Å lines of singly

ionized calcium) emission flux measurements of the sun and similar stars, Mg II h+k (2796 and 2802 Å) fluxes, variability amplitudes, rotation rates, and other data has led to the conclusion that the chromospheric activity of the sun and similar stars comprises two components, one associated with magnetic active regions and the magnetic network, and another that appears to be unrelated to magnetic activity and is therefore possibly non-magnetic (and perhaps acoustic) in origin. This second, or "basal," component appears to cover the entire surface of the least magnetically active stars, stars which are only slightly less active than the sun itself. The basal Ca II H+K flux density for stars similar to the sun equals the average emission observed in the centers of solar supergranulation cells, where the magnetic flux density is small.

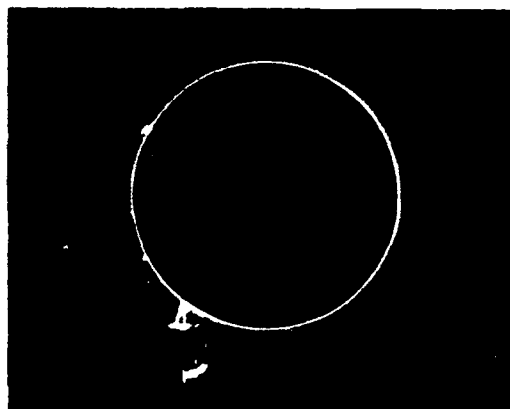
During the past few years, the ACRIM and ERB radiometer experiments aboard the SMM and NIMBUS-7 spacecraft have both detected long-term variations of about 0.1 percent in the total solar irradiance. The irradiance declined from the time of activity maximum (1980) until solar minimum (1986), and has since begun to recover. This discovery implies that bright solar magnetic features (faculae), rather than dark sunspots, are the dominant factor determining solar luminosity variability on the activity cycle time scale, a sharp reversal from the widespread opinion of just a few years ago. Until the recovery was unquestionably detected, the possibility persisted that the observed effects were instrumental. The desire to validate the observed solar variability by stellar analogy and determine its broader stellar context provided the motivation for undertaking an observational program aimed at obtaining long-term measurements of both continuum variability and chromospheric activity for

stars similar to the sun.

Photometric observations in the optical continuum at 4700 and 5500 Å have been made since 1984 for 33 stars, and chromospheric Ca II H+K flux observations for these have been obtained contemporaneously. The data are unique. In particular, the exceptionally high precision of the photometry, sustained over a baseline of several years, sets it apart. Typically, 20-50 observations per season were obtained for each star, enough to ensure well-determined annual mean values for both the brightness and the chromospheric activity level of each star. The annual mean values for photometric brightness and Ca II H+K flux were compared. Variability was frequently detected, even among relatively inactive stars similar to the sun. This suggests that the solar variability detected by SMM/ACRIM and NIMBUS-7/ERB is real. The stellar observations further suggest that the solar variability is typical: old, relatively inactive stars like the sun tend to behave much as the sun does, with brightness variations amounting to a few tenths of a percent, at most, directly correlating with activity changes. On the other hand, the variability of young stars is much more pronounced, by a factor of 10-20, in many cases, and tends to anticorrelate with activity changes. Such stars also do not generally show regular activity cycles as the sun does, but rather more chaotic behavior. This contrasting behavior suggests that the effects of dark spots are, in fact, primarily responsible for the year-to-year luminosity variability of young stars, but become increasingly subordinated to the effects of bright magnetic features as the stars age. Such broader perspectives on solar activity and its stellar analogs will become increasingly important as theoretical models of the operation and evolution of the solar magnetic dynamo are developed and refined.

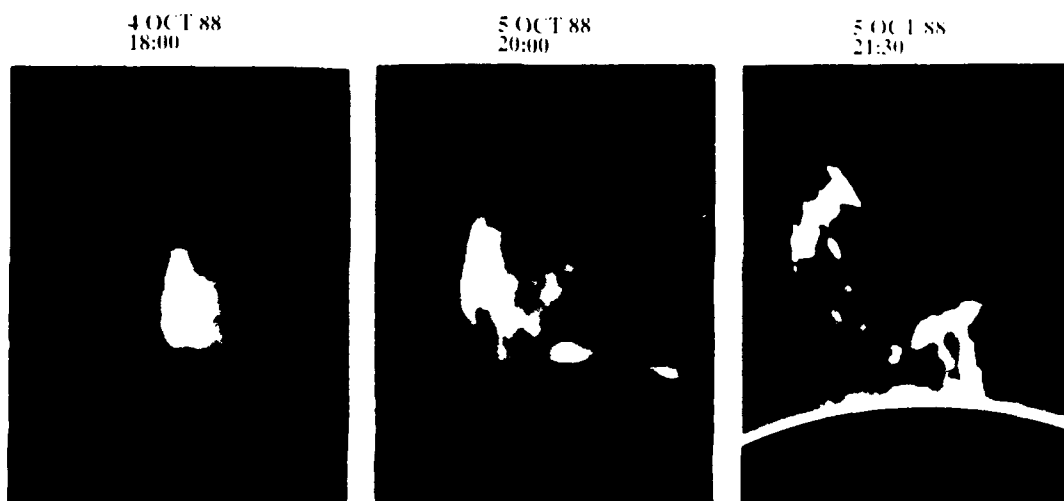
Instrumentation Development: Solar Research Branch personnel have been instrumental in developing, using, and designing reflecting coronagraphs at SPO. The Miniature Advanced Coronagraph (MAC) project was undertaken as a proof-of-concept for building a large-aperture coronagraph using reflecting (mirror) rather than the standard refracting (lens) optics. It was designed to take advantage of recent advances in superpolishing techniques. The MAC incorporates a 5 cm silicon superpolished mirror (effective aperture is 3.9 cm). Although the reflecting coronagraph concept has existed for over 20 years, this is the first successful instrument built for ground-based observations. Images of

LARGE ERUPTIVE PROMINENCE



Full Disk Coronagram Made in Broadband H-alpha (FWHM = 0.6 nm) of a Faint Eruptive Prominence Using the Miniature Mirror Coronagraph, a Silicon Super-Polished Mirror with an Effective Aperture of 3.9 cm, or about 4 arc second Resolution on the Sun. (The three images on the next page are a time sequence leading up to the eruption of the prominence, which resulted in some mass being ejected from the corona into the interplanetary space. The streaks seen in the upper image are caused by dust particles in the Earth's atmosphere. Theoretical calculations show that a larger aperture reflecting coronagraph would be able to see space debris in a similar fashion. Debris can be distinguished from atmospheric dust by both its polarization properties and its speed of transit across the field of view.)

CORONAL MASS EJECTION



the emission corona (Fe XIV) and erupting prominences have been obtained with it using an image tube and CCD camera (see the figure).

A reflecting coronagraph has several advantages over conventional refracting instruments. It is completely achromatic, which implies that reflecting coronagraphs can be used to observe several wavelengths simultaneously, whereas conventional refracting coronagraphs are chromatic and must be refocused every time the observed wavelength is changed. It is polarization-free and thus can be used to study coronal vector magnetic fields. The superpolished mirror produces very low scattered light, allowing faint coronal structures to be observed (as well as other faint objects, such as space debris). The mirror permits observation of a large spectral range from the ultraviolet into the infrared. The success with this instrument indicates it will be possible to develop a larger instrument that could revolutionize ground-based coronal research. Scientific goals of developing a large reflecting coronagraph include: making simultaneous, multi-wavelength coronal studies of oscillations, waves, impulsive events,

mass ejections, and transients in order to develop physical models of these events; studying coronal magnetic fields, coronal heating mechanisms, and loop instabilities that lead to the mass ejections; and making low scattered light measurements of solar features such as critical analysis of sunspot cores and penumbra.

A large reflecting coronagraph will also be capable of observing sub-centimeter space debris, which is now recognized as posing a potentially major hazard for Air Force space operations. The space debris population, especially of small sizes resulting from activities performed in low orbital altitude, is of primary importance for space vehicle design and space activity planning. The testing of space defenses systems by the United States and the Soviet Union is strongly enhancing the need to characterize the rapidly growing population of small fragments.

Work has begun on definition and testing of a proposed space instrument to provide improved imaging of disturbances in the interplanetary medium. The Solar Mass Ejection Imager would operate on a principle similar to that of the HELIOS imaging instrumentation referred to above (the HELIOS probes

are no longer operational). The present instrument would operate with higher spatial and temporal resolution and would have the capability of transferring data in real time to the USAF Space Forecasting Center. Interest at AFGWC/WSE is high, and funding for instrument construction and flight integration is being sought.

High resolution studies of solar phenomena on subarcsecond scales will play an important role in advancing solar physics over the next decade. As described above, many of the basic physical processes in the solar atmosphere occur on spatial scales smaller than one arcsecond, and can be best studied using long time sequences of uniform, high-quality, high-resolution solar images.

Large ground-based solar telescopes such as the VTT at the SPO are theoretically capable of delivering the spatial resolution required by such studies, but generally fall substantially short of this optimum performance. Image degradation occurs primarily as blurring and distortion caused by turbulence in the earth's atmosphere, and gross motion arising from both telescopic effects, such as windshake, and the atmosphere. Fortunately, such effects can be corrected. The successful development of the technology would enhance the resolution of existing ground-based solar instruments by up to a factor of fifteen. Adaptive optics represent the method of choice for compensating solar images, primarily because of the need for a real-time corrected image that can be further analyzed using instruments such as spectrographs, Stokes polarimeters, magnetographs, and tunable filters, that intrinsically require real-time images for input. The long-term objectives of the adaptive optics development at SPO are to provide an integral, user-friendly system at the VTT that is permanently interfaced to the principal focal plane

instrumentation of that facility, and to develop the expertise to adequately support and further develop adaptive optics technology. Recent progress has occurred in the areas of correlation tracking, active mirror design, and wave front sensing.

A correlation tracker, which is a device for removing the gross motion of a telescopic image, has been successfully developed at SPO. This device functions by rapidly and continuously comparing the structure of the presently-observed target with a stored image of the same target and calculating the displacement necessary to move the two into coincidence. The correction is performed by a high-speed movable mirror that is coupled to the target sensor. Because of image blurring and distortion ("seeing"), the match is never perfect. Furthermore, the solar surface, while bright, generally provides only low-contrast targets that evolve with time, namely the granulation pattern. The SPO correlation tracker is robust enough to perform satisfactorily with such constraints. It represents a major breakthrough for high-resolution solar imaging.

A new design for a segmented active mirror has been developed at SPO. The use of triangular Invar segments magnetically coupled to actuators at adjacent corners automatically ensures proper wavefront phasing and also reduces the required number of actuators (and associated electronics) by a factor of three relative to earlier designs. The design also adapts directly to a continuous faceplate. A 13 segment version has been built to explore possible fabrication difficulties and tested to characterize performance. Everything went so well that it has been decided to freeze the concept and proceed to the construction of a 61 actuator system, which will be large enough for use at the VTT.

Since the sun generally does not offer

compact, high contrast targets for wavefront sensing, the routine use of adaptive optics for high-resolution solar imaging requires the development of wavefront sensor systems optimized for the solar targets available. A conventional Hartmann-type wavefront sensor using quadcell detectors provides satisfactory performance using sunspots and pores as targets, but such high-contrast targets are frequently unavailable. The complex, ever-changing, low-contrast granulation pattern is a much more difficult target, especially under poor seeing conditions, and it now seems that more sophisticated approaches to wavefront sensing may be necessary for solar adaptive optics to perform well under arbitrary conditions. One brute force approach that has been considered is the use of parallel correlation trackers, one per mirror segment. Although chips fast enough and inexpensive enough to make this a viable approach may be forthcoming, they are still on the technological horizon. An "analog" version of the correlation tracker, using an LCD TV, is being explored in concept. Other similar concepts have been proposed. Overall, it appears that development of a satisfactory wavefront sensor for solar targets is the single biggest hurdle remaining on the way toward meeting the objectives of this technological program.

The measurement of the polarization transforming properties of the SPO VTT gives the matrix of the system as a function of any telescope pointing angle. Compensation can be effected by the matrix multiplication of a full Stokes measurement or by an active optical compensator. A compensator has been designed and will soon be built based upon liquid crystal technology. Candidate materials are currently being tested at SPO. Modern "self-defining" calibration schemes will be employed to give a precise determination (0.01 per-

cent) of the polarization transformation matrix of liquid crystal materials as a function of voltage and other parameters. The matrix mapping of any incoming polarization state into any outgoing polarization state may be accomplished with a stack of three liquid crystals. The system will be installed near the entrance of the SPO Universal Birefringent Filter and tuned in conjunction with the filter to obtain two concurrent polarization and spectral passband states. The compensator will be regularly calibrated in place using existing polarizers that can be automatically inserted and removed from the optical beam. Such a system will allow high resolution vector magnetometry for the first time and give us the opportunity to pursue observational studies of solar magnetic field morphology and stability, chromospheric heating and atmospheric modeling, flare and active phenomena, and prominence models.

ENERGETIC PARTICLES

The performance of Air Force space systems is profoundly affected by the energetic particles found in the Earth's magnetosphere. For example, these particles can seriously degrade electronic components or cause single-event upsets. They can also cause charging and discharging of materials on both the surface and in the interior of spacecraft, and this couples into the spacecraft electronics. Unusually high particle fluxes generate a radiation hazard for manned space flight and can interfere with high-frequency communications in the Earth's polar regions. To address these problems, the Space Particles Environment Branch of the Space Physics Division is studying the processes governing the energetic-particle environment. They begin with the origins of the particles in the solar atmosphere, continue with their transport through the interplanetary medium

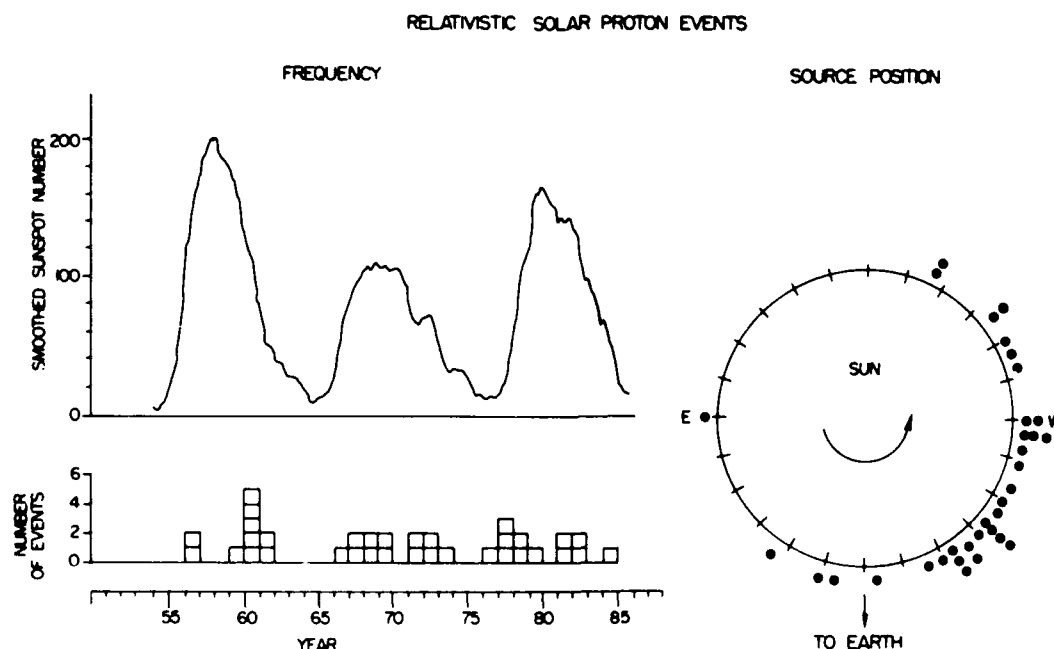
into an acceleration region in the earth's magnetosphere, and finally consider their effects on near-Earth space systems and space-using systems. Much of the recent work has focused on forming an integrated picture of this process, combining the results of solar flare research with solar wind and magnetospheric models to provide a more complete specification of the total space energetic-particle environment.

Solar Event Studies: The Space Particles Environment Branch has begun a major statistical effort to analyze relativistic solar-particle events, since approximately 10 percent of the significant solar-particle events detected at the earth since 1956 have contained protons with energies in excess of 450 MeV. This work entails searching historic data files to obtain the necessary database for the analyses to be conducted. Since this work requires the cooperation of cosmic ray scientists around the world, a stan-

dardized data format has been very important. The figure is a plot of the timing and source location of the relativistic solar-proton events studied.

To complement the statistical study, personnel have conducted extensive case studies of various solar energetic particle events. For example, on February 16, 1984, there occurred the largest relativistic solar-proton event from a flare located on the back side of the sun as seen from the earth. This event, which produced a very hard proton spectrum, did not result in major geomagnetic disturbances. On April 24, 1984, from the eastern hemisphere of the sun, a flare produced a soft proton spectrum but caused a major geomagnetic disturbance. This event was only the second recorded example of ground-level solar neutron detection. Very energetic (>450 MeV) neutrons were detected.

During the initial portions of the December 7-8, 1982, relativistic solar-



Timing and Source Location of the Relativistic Solar-Proton Events Studied.

particle event, high-energy particles were discovered to be highly collimated along the interplanetary magnetic field lines even though the interplanetary magnetic field was highly distorted and was changing very rapidly. In another study, the high-latitude radiation environment at 840 km as measured with a dosimeter on the DMSP/F7 spacecraft showed that solar proton events during solar minimum (December, 1983, through October, 1987) were not significantly different from those reported during the previous solar maximum.

As important as isolated flares are, multiple flares can produce even more dramatic and confusing effects. In mid-1982, a single region on the sun produced a sustained episode of powerful flares. As the sun rotated, these flares led to a heliosphere wide modulation of energetic particles. A whole shell of coronal mass ejections and shocks propagated throughout the solar system. This was observed not only at the earth but also by the Pioneer 10 and 11 spacecraft at 12 and 28 AU (respectively) from the sun. These event studies completed in 1987 and 1988 give us a much better understanding of the radically differing effects flares have on near-Earth space and will lead to improved prediction capabilities of the effects of solar proton events and geomagnetic disturbances on the Earth's magnetosphere.

Cosmic Radiation and the Geomagnetic Field: Changes in the geomagnetic field are known to have an effect on the incoming galactic cosmic radiation as detected on the surface of the earth. Comparing neutron-monitor measurements during various phases of major geomagnetic disturbances has shown an increase in high-latitude cosmic-ray cutoff rigidities during the initial phase of the storm due to the dominating effect caused by the magnetospheric currents. This is then followed by a measurable

decrease in the cosmic-ray cutoff rigidity at the same ground locations. The measurements allow an estimate of the intensity of the ring current and of the magnetopause currents during the initial phase of a magnetic storm based solely on the Dst index and on the cosmic-ray cutoff rigidity changes observed at selected high-latitude neutron monitor locations.

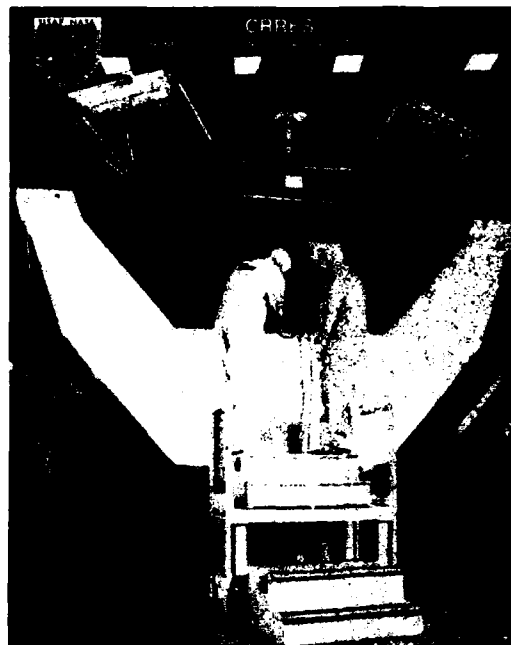
In a related study, the effect of the secular changes in the geomagnetic field on incident galactic cosmic radiation was evaluated. In the period between 1955 and 1980 there has been a significant decrease in the geomagnetic field, which has resulted in lower cosmic-ray cutoff rigidities as calculated for the top of the atmosphere. This lowering of the cutoff rigidities results in a 1.4 percent increase in the galactic solar-minimum cosmic-ray intensity as integrated over the entire earth. However, this effect is not uniformly distributed over the surface of the earth. The effect must be considered in planning long-term manned space missions.

Basic research studies such as those described above have resulted in a new event-oriented solar-proton prediction model which was implemented at the USAF Space Environment forecast facility. This new model generates predicted solar proton time intensity profiles for a number of user-adjustable energy ranges and is also capable of making predictions for the heavy ion flux. The computer program is designed so a forecaster can select inputs based on the data available in near real-time at the forecast center as the solar flare is occurring. The predicted event amplitude is based on the electromagnetic emission parameters of the solar flare (either microwave or soft x-ray emission) and the solar flare position on the sun. The model also has an update capability where the forecaster can normalize the prediction to actual

spacecraft observations of spectral slope and particle flux as the event is occurring in order to more accurately predict the future time-intensity profile of the solar particle flux. Besides containing improvements in the accuracy of the predicted energetic particle-event onset time and magnitude, the new model converts the predicted solar-particle flux into an expected radiation dose that might be experienced by an astronaut during EVA activities or inside the space shuttle.

Radiation Effects: A statistical study of the radiation environment at low altitudes (840 km) was performed using dosimeter data from the DMSP/F7 spacecraft. The dosimeter measures the dose and flux of high energy electrons and ions (>1 MeV and >25 MeV, respectively). The study showed that the standard NASA radiation belt models give orbital dose values which are too high by a factor of four during solar minimum. The discrepancy is due to an overestimate of the electron dose. The conservative NASA models therefore impose more stringent shielding requirements on spacecraft than are necessary.

While more detailed models of the space environment and its effects are being developed, it is important to note that current designs for space microelectronic systems are based on computer models and laboratory testing, but not on in-flight testing of the hardware. The Space Physics Division is preparing to perform this in-flight testing on CRRES (the Combined Release and Radiation Effects Satellite). A picture of the satellite undergoing testing is shown in the figure. This satellite will carry a package of microelectronics which is carefully instrumented to detect radiation-induced anomalies in advanced technology devices. CRRES will also carry a full complement of experiments to measure the particle and field (electric and mag-



CRRES (Combined Release and Radiation Effects Satellite) Undergoing Testing.

netic) environments in which the components are operating. Comparison of these results with laboratory testing and simulations will allow engineers to develop more reliable electronic space systems by improving radiation test procedures.

While radiation damage to electronics is typically caused by particles with energies greater than 1 MeV, lower energy particles (in the kiloelectron volt range) damage spacecraft through the charging and subsequent discharging of spacecraft surfaces. By studying charging effects on the DMSP spacecraft, the electron spectra which create high level charging have been identified. The study also showed that current spacecraft charging models are deficient in their treatment of secondary and backscattered electrons and in handling spacecraft sheath effects.

An upcoming experiment is planned to study spacecraft charging during electrodynamic tethered satellite operations.

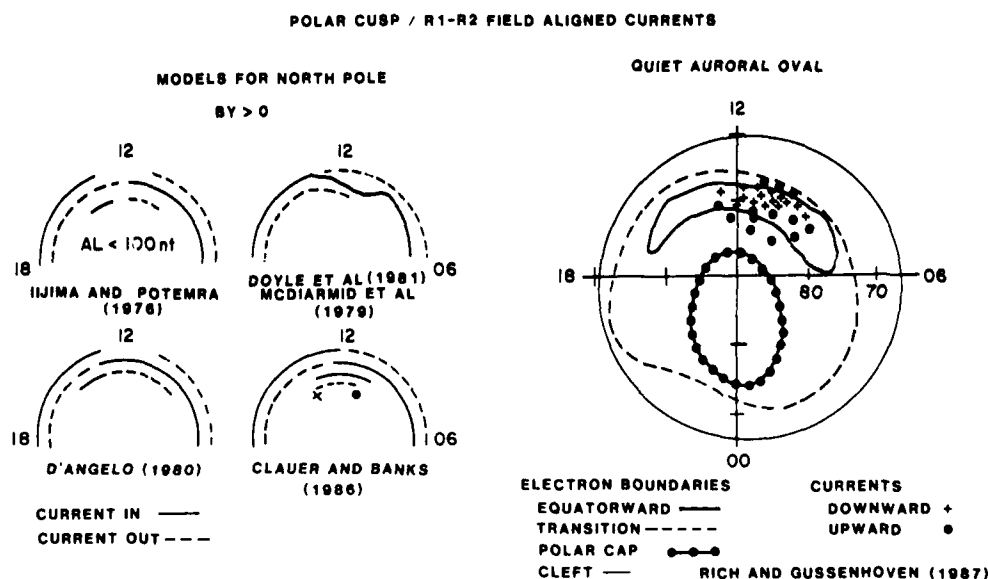
(see SPREE below)

Magnetospheric Research: In the area of magnetospheric dynamics several studies on the energization and transport of auroral particles have been completed. One of the key questions addressed was how the particles from the central plasma sheet are scattered to produce precipitation into the auroral ionosphere. By comparing data from the SCATHA satellite in an equatorial orbit and the P78-1 satellite in a low altitude polar orbit, pitch-angle distributions at low altitudes were found to be isotropic for angles mapping into the SCATHA loss cone. The measured distributions were shown to be inconsistent with current theories for the scattering of electrons by electrostatic waves.

From a global perspective, there are three states of the magnetosphere which may be identified from polar auroral and magnetic activity: the active auroral oval state, the active polar cap state, and the quiet state, defined as that which occurs when the energy transfer from the solar

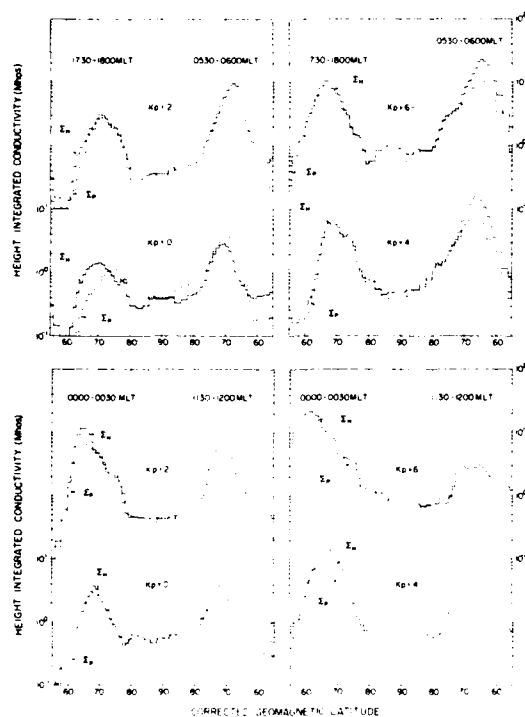
wind has been maintained at a minimum level for several hours. Over the past two years the quiet magnetosphere has been studied extensively since it represents the baseline for the more dynamic conditions. It has been found that the conditions for minimal energy transfer occur for low solar wind velocity and a weak interplanetary magnetic field. During these quiet conditions there is a small but non-zero cross-cap electric field, and therefore low earthward convection velocities. The auroral oval shrinks and the diffuse auroral precipitation is continuous but of lower average energy and number flux. The figure illustrates the important features of the polar cap during these baseline conditions.

For several years GL has provided space environment monitors for the DMSP (Defense Meteorological Satellite Program) spacecraft. One of these instruments, a precipitating particle detector, measures electrons and ions of auroral energy. Data have been provided, resulting in a large database on the auroral



Polar Cap During Quiet Conditions.

and polar regions. From this database GL scientists have developed, and are continuing to upgrade, detailed empirical models of the auroral regions which include the patterns and spectra of precipitating electrons and ions, the patterns of Hall and Pederson conductivities, and a model of Joule heating. The figure shows the model conductivities along several slices through the auroral oval. Two more DMSP spacecraft (F8 and



Model Conductivities of Auroral Region.

F9) were launched in July, 1988, and February, 1989, respectively. Each carried additional GL instruments which will further extend the database and permit development of better and more detailed space environmental models.

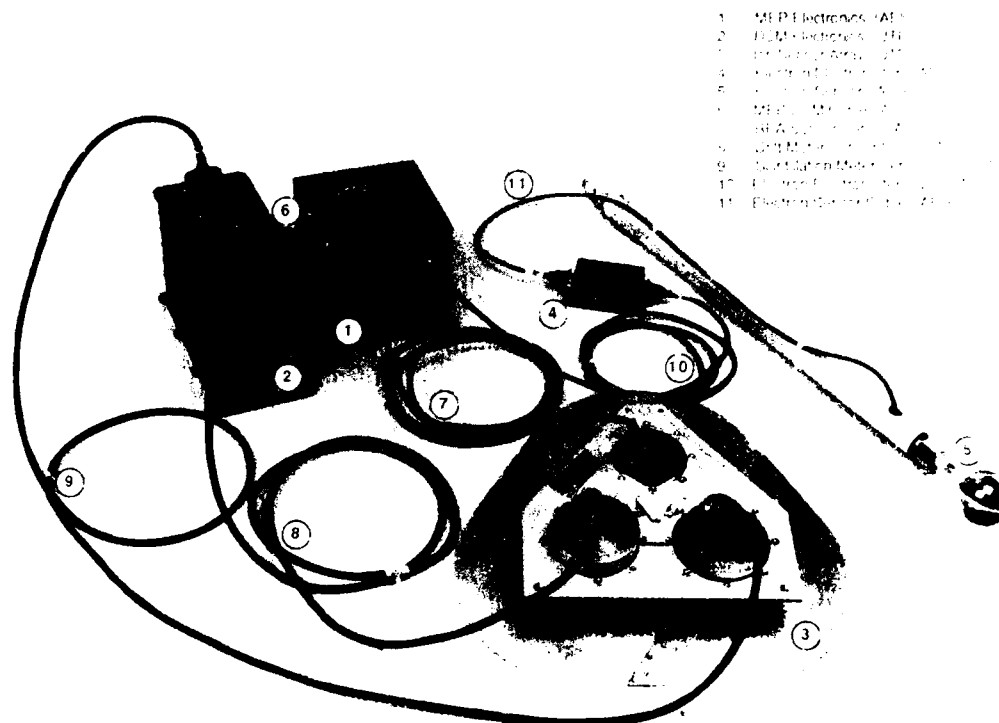
SPACE WEATHER

The space environment is hostile to the survival and operation of Air Force

space-based resources. Just as terrestrial weather changes, space weather varies as magnetic activity increases and decreases under the influence of the sun. Space weather, through the interaction of the environment with spacecraft, can be the cause of operational anomalies resulting from spacecraft charging, single-event-upset increases in satellite drag, and degradation of materials from radiation effects. Satellites at all altitudes are subject to space-weather effects. The thrust of the Space Physics Division effort is to understand, specify, and predict energy coupling and transfer in the space environment and particularly in the magnetosphere.

The vastness of regions, the paucity of data, and the existence of both short-term and long-term variations in the solar driver limit our ability to understand space-weather effects. Research is directed toward greatly expanding the environmental database, developing and testing empirical models of the physical parameters and systems, and developing dynamic analytical models of the coupled solar-wind/magnetosphere/ionosphere system that include time variability of these solar-driven processes. Of particular importance is the understanding of the transfer, storage, and release of energy within the system leading to magnetic storms and substorms.

Magnetospheric Specification: Specification of the environment provides the foundation for empirical and theoretical studies of space-weather processes. Continuous monitoring of the energy inputs from the magnetosphere into the high-latitude regions is underway using the operational DMSP satellites. The first DMSP instruments to monitor ion drift and variations in ion density which cause radio scintillations have been successfully flown (see the figure on next page). Combined with the particle energy inputs, Joule heating can now be deter-



SSIES-2 Plasma Monitor System
Serial No. 001

SSIES Plasma Monitoring System for DMSP. (The combination of sensors monitors plasma drift, from which electric fields can be calculated, electron and ion density and temperature, and the variability of the ion density, which is related to radio scintillations.)

mined on a routine basis. The addition of the magnetometer on future DMSP satellites will complete the set of instruments to continuously monitor the high-latitude electrodynamics and determine magnetospheric energy inputs.

The addition of particle, plasma, and fields data from CRRES, now scheduled for a 1990 launch, will provide a significant impact on our understanding of magnetic substorm dynamics. Instruments are now being designed for the NASA Polar and the ESA Cluster missions, which will be launched in the mid-nineties to measure electric fields in the outer reaches of the magnetosphere, at the magnetopause, and in the solar

wind. Multiple satellites in the Cluster program flying in formation offer the opportunity to determine gradients and separate space/time effects. These missions promise to fill in many of the gaps in our environmental database and provide critical input into future model development.

Magnetospheric Modeling: The Rice University Convection Model (RCM), whose development has been sponsored by GL, provides the framework for large-scale, analytic magnetospheric modeling. The model has been successful in providing a time-dependent description of the inner magnetosphere. A new, more realistic magnetic field model has been incor-

porated into the model, and the effects of particle loss have been accurately introduced in the computation machinery. The model is now capable of computing precipitating particle fluxes along with electric fields and Birkeland currents.

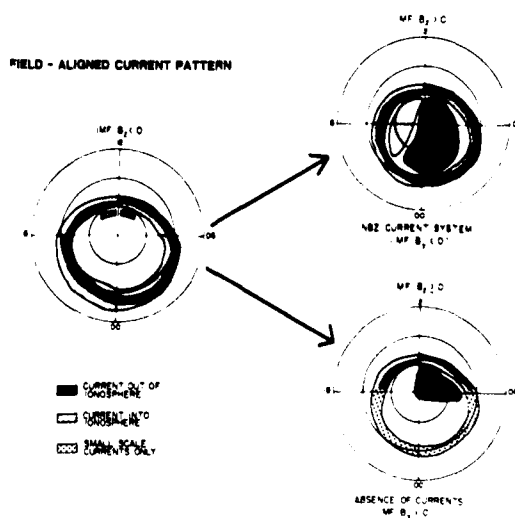
Portions of the RCM research model are being developed into an operational algorithm for use by MAC/Air Weather Service for specification and short-term prediction of the magnetospheric environment at geosynchronous orbit and of the energy input into the high-latitude ionosphere. This first operational Magnetospheric Specification Model will be able to help spacecraft operators mitigate against hazards such as spacecraft charging and single-event upsets.

Energy transfer across the magnetopause boundary is a crucial component of future magnetospheric models. Under GL sponsorship, Dartmouth College has developed a boundary layer model which is coupled with the ionosphere. The model predicts a dawn-dusk asymmetry based on magnetic-field-line distortions from different field-aligned current limitations on the dawn and dusk sides.

Magnetosphere/Ionosphere Energy Coupling: Understanding variations in the magnetosphere resulting from magnetic activity could be easier if the question, "What is the structure of a baseline of a quiet or ground-state magnetosphere and what is its signature?" could be answered. A study to answer this question was carried out at GL by looking at the DMSP/F7 magnetic-field and precipitating-particle data during periods when the standard geomagnetic indices show the environment to be quiet for several hours. The large-scale field-aligned current patterns in the high latitudes tend to fade away. The precipitating particle fluxes and the small-scale field-aligned currents tend to fade much less. The electric field across the polar cap ionosphere, which maps to the electric field

across the magnetosphere, also decreases. A companion study done with NASA/Goddard Space Flight Center showed that a recognizable large-scale pattern in the electric field was three times more probable than in the large scale field-aligned currents.

In the past, it has been assumed that the geomagnetic environment has two fundamental states: an active state for times when the interplanetary magnetic field (IMF) is southward with respect to the earth's magnetic axis, and a quiet state for times when the IMF is northward. Other investigators have found that during some times of northward IMF, the large-scale field-aligned currents exist in a slightly weakened state and that extra largescale field-aligned currents exist in the polar region. This configuration has been named the NBZ current system. The present study does not contradict the finding of the NBZ



Schematic of the Three Configurations of Field-aligned Currents as the Interplanetary Magnetic Field Changes. (The lower right shows the disappearance of the field-aligned current patterns for small positive values of the B_z component.)

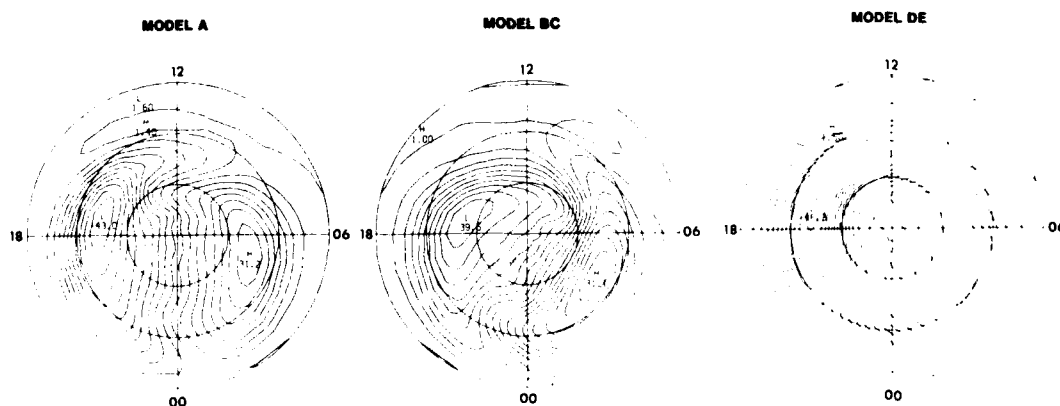
system, but it suggests that there are at least three fundamental states to the magnetospheric configuration: the active state when the solar wind momentum flux is large and the IMF is southward; the NBZ state when the solar-wind momentum flux is large and the IMF is northward; and the quiet state when the solar-wind momentum flux is low and the IMF north/south component is small (see the figure previous page).

Joule heat due to ionospheric currents driven by a magnetospheric generator is second only to the solar ultraviolet in the total heating of the high-latitude ionosphere and atmosphere. Joule heating is an order of magnitude weaker than the solar ultraviolet input in regions where the sun is shining, but dominates in regions of darkness. Since this heat source is variable on time scales of the geomagnetic activity, and since heating can affect the density of the atmosphere at low orbiting satellite and shuttle altitudes, a method of measuring the Joule heat-input on a global scale has great

operational importance for the Air Force. At GL, a method was developed to calculate Joule heating along the path of a DMSP satellite using the precipitating particle and magnetic field data. To verify the method of calculation, Joule heating of the ionosphere has been independently calculated from incoherent radar data from Sondrestromfjord, Greenland, by SRI International. Initial comparisons show both similarities and differences partially explainable by the strengths and weaknesses of each technique. The analysis continues.

The patterns of the high-latitude electrostatic potential developed from the DE-2 satellite (Dynamics Explorer) electric field data by Heppner (NASA/Goddard Space Flight Center) and Maynard (GL) have been converted into analytical functions at GL. These functions can easily be used with a variety of computer modeling programs. Using a simple, two-dimensional static model of the high-latitude ionosphere, we derived analytical functions that

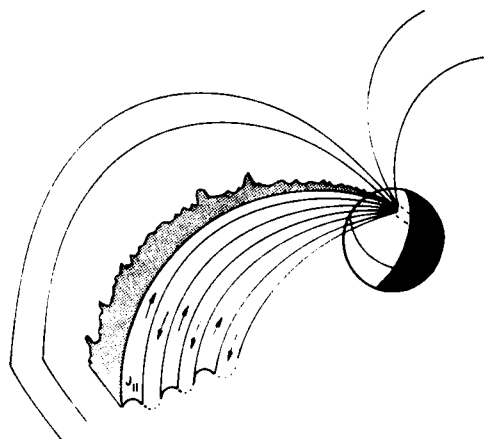
HEPPNER - MAYNARD MODEL



Variation of the Electric Field and Joule Heating Patterns with the Interplanetary Magnetic Field. (With the electric field variation with B_y in the top left and right panels and a conductivity model which includes the particle input in the lower center, the Joule heating variation with IMF B_y was calculated, lower left and right panels. The heating is primarily in the auroral oval as illustrated by the DE - 1 image in the upper center and shows large changes with B_y .)

reproduce configurations for field-aligned currents that are consistent with observations of many investigators for conditions of southward IMF, and produce patterns for Joule heating that vary with the state of the IMF (see the figure on previous page). For northward IMF, the functions do not reproduce the field-aligned current pattern known as the NBZ current system.

By looking at simultaneous electric and magnetic field data from the DE-I and DE-2 satellites when they were on the same field line within a few minutes of each other in the afternoon sector, a study carried out by Regis College found that stationary, spatial field-aligned current oscillations occur sometimes superimposed upon the region 2 auroral current system (see the figure). The oscilla-



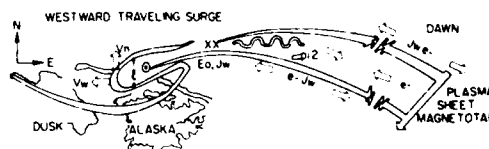
Schematic of the Oscillating Current Sheets in the Dayside of the Magnetosphere Identified from DE -1 and -2 data.

tions can be modeled with simple, steady-state hydromagnetic equations of the magnetosphere ionosphere system. The wavelength of the oscillations is dependent on the ionospheric height-integrated Pedersen conductivity, the magnetic field-aligned conductivity, and

the conductivity of a generator at the magnetospheric equator.

Modeling and Analysis of Substorm Phenomena: The complete understanding and prediction of substorms, a major disturbance in the magnetosphere's particle and field environment which degrades communications, remains an elusive goal. The high-latitude auroral zone is highly dynamic, which makes forecasting in this region very difficult. Two time-dependent models have been developed which address this problem. The first model deals with the large-scale characteristics of the substorm westward traveling surge, while the second model deals with the explosive poleward expansion of individual arc structures during substorm onset.

A comprehensive model of the propagation of the westward traveling surge and the associated generation of Pi 2 pulsations during substorm onset has been developed. The electron temperature anisotropy in the plasma sheet was found to play a major role in determining the direction of surge propagation (see the figure). Narrower surges require greater electron heating parallel to the



Schematic of the Model that Unifies the Explanation of the Westward Traveling Surge with the Generation of Pi -2 Micropulsations. (Model Results: Velocity (V_n) of surge expansion depends on precipitation energy, plasma sheet temperature, and E-W electric field (E_o). Frequency of Pi 2 EM pulsation is a function of V_n and J_w . Pi 2's become tracer of activity away from source. Application: new capability for modeling temporal dynamics of midnight region.)

magnetic field for poleward motion.

The initial pulse shape of the Pi 2 pul-

sations was shown to evolve in time as the decay time for each of the constituent modes was found to be different. After several minutes, a quasimonochromatic wave pulse was predicted. The frequency of this remnant pulse is determined by the north-south extent of the surge region and the poleward expansion speed of the poleward boundary. The model has been successfully verified by comparing its predictions with extensive experimental auroral data taken in Scandinavia.

A major puzzle of magnetospheric physics is the fact that the initial signature of substorms (auroral breakup) usually occurs at a much lower latitude than one would expect. The energy source for the substorm is normally considered to be a near-earth neutral line which is situated at approximately 18 earth radii in the magnetotail, while breakup can be observed in the auroral ionosphere on magnetic field lines that map much closer to the earth. A model has been successfully developed to resolve this paradox, based on the idea that under certain conditions two coupled electrical circuits can form between the ionosphere and the magnetosphere. These quasi-stationary structures can be stable or unstable depending on the background convection electric-field configuration. The unstable case is predicted to be present just south of the Harang discontinuity. Moreover, narrower arcs that form an incipient current system at lower latitudes are found to be more unstable to poleward expansion. These results are presently being compared with experimental data.

One approach to critically evaluate substorm models is to make coordinated observations from numerous spacecraft and ground-based arrays, and to make this data accessible in a single database with an extensive suite of analysis tools. This approach was taken by NASA's National Space Science Data Center (NSSDC) in the eighth Coordinated Data

Analysis Workshop (CDAW8). GL scientists were involved in the workshop and its planning, as well as contributing experimental databases from the GL Magnetometer Network, DMSP satellite, and the Dynamics Explorer satellite, which all played a prominent role at the workshop.

For a few of the CDAW events, auroral images from Dynamics Explorer -1 satellite and magnetometer data from the GL Magnetometer Network have been used to investigate the spatial and temporal relationship between substorm current systems and auroral zone activity. At the beginning of the substorm expansive phase onset, the aurora was found to brighten in the center, or center and western portions of the substorm current wedge as located from ground-based magnetic bay and Pi 2 magnetic pulsation polarization patterns. The location of the initial bright region near the substorm current wedge center and to the west is consistent with our previous work examining DMSP images. In addition to the location of the substorm disturbance in the auroral zone, the GL wave data from the GL Magnetometer Network has been essential for detecting and timing substorm disturbances. These observations have contributed to studies which are important for understanding the near-earth neutral line model of substorms and plasmoid formation. A plasmoid is an enclosed bubble of plasma which is cut off from the plasma sheet during the reconnection process in the tail of the magnetosphere and then propagates down the tail. It is an important signature of, and clue to, understanding substorm dynamics.

Long-duration magnetic pulsations in the Pi 2 band have been observed at mid-latitudes during substorms that occur during very intense geomagnetic activity. The pulsations are not simply damped waves following an initial impulse but

are continuously generated. They decay near the time of the recovery of the plasma sheet in the magnetotail, suggesting that they are signatures of the reconnection process, and continue as long as a near-earth neutral line exists. When reconnection at the neutral line diminishes in strength or the neutral line retreats tailward, the waves also diminish. These long-duration Pi 2 pulsations convey information about their source, and further study may provide us with new insights regarding the reconnection process in the earth's magnetotail.

In the early 90's the Combined Release and Radiation Effects Satellite (CRRES) will return a comprehensive set of fields and particle data from the radiation belts and the inner magnetosphere. In preparation for utilizing that data set for studying ion cyclotron and other wave-particle interactions, we are studying waves observed in the currently available GL Magnetometer Network search-coil data and correlating these observations with in-situ spacecraft measurements in the magnetosphere. This work is being done in collaboration with researchers from Boston University and Dynamics Explorer and GEOS spacecraft experimenters. For one event that was intensely studied, ground-spacecraft correlations have shown that the waves were generated in a relatively small region of magnetospheric space near the spacecraft and calculations were made of the attenuation of the wave through the ionospheric duct to the ground station. Boston University scientists have complemented this observational work with theoretical calculations of the linear growth rate of the ion-cyclotron waves with arbitrary orientation of the wave vector to the magnetic field. Their new results have shown that at large angles to the field the growth rates depend on both the angle and the thermal electron

temperature.

ACTIVE EXPERIMENTS

The Active Experiments Branch of the Space Physics Division carries out experimental and theoretical investigations of controlled perturbations in space. Our main objective is to test understanding of fundamental plasma processes in a laboratory where wall conditions do not affect the results. The two main tools used to produce the perturbations studied in the last two years are energetic electron beams and large amplitude electromagnetic waves.

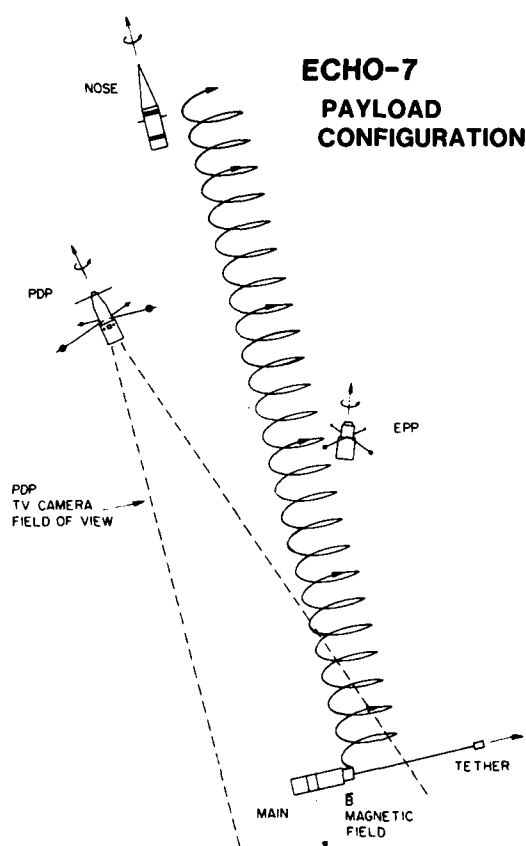
Energetic Electron Beams: The injection of energetic electron beams into space can be used as a tool to understand their long-distance propagation as coherent entities, their interactions with local plasmas, and their interactions with the host vehicle. The two sources of information come from the BERT 1 rocket, which was launched at the White Sands Missile Range in June, 1985, and the ECHO 7 sounding rocket, which was launched from the Poker Flat Research Range in February, 1988.

Prior to the launch of BERT 1, a full-up simulation of the experiment was performed in the large vacuum chamber at NASA's Johnson Space Center. The experiment consisted of a beam-emitting main payload (BERT) and an instrumented, free-flying nosecone (ERNIE). In the laboratory simulation ERNIE was separated from BERT by only 5 m. Here it detected beam-system effects much closer to BERT than it sampled in the space flight. In one of the experiments, the beam current increased from 0.2 to 200 mA and then decreased back to 0.2 mA at beam energies of 500 eV, 1000 eV, and 2000 eV. The potential of the beam-emitting portion of BERT was measured relative to a section from which it was electrically isolated. During the 500 eV emission, the vehicle potential first increased with increasing currents. At a

critical level, the potential difference between the two segments of BERT decreased with increasing current. Simultaneously, intense radio-frequency wave activity appeared at the location of ERNIE. At 1000 eV this phenomenon started only near the highest current level, but at 2000 eV it did not occur at all. These results indicate the formation

These results from BERT have been used to explain seemingly anomalous measurements from the Norwegian MAIMIK sounding rocket, where at high-current emission levels a tethered probe measured potential differences greater than beam energy.

The ECHO 7 sounding rocket experiment was conducted jointly with NASA and the University of Minnesota. As shown in the figure, ECHO consisted of four free-flying payloads: an instrumented nosecone (NOSE) that was ejected up the field line from the beam-emitting payload (MAIN) the Plasma Diagnostic Package (PDP) and Energetic Particle Package (EPP) which were ejected to the south and west of MAIN, respectively. The PDP carried a low-light TV camera



Configuration of the Four Free-flying ECHO 7 Payloads.

of a virtual cathode near ERNIE at low beam energy. In the region of the virtual cathode beam, electrons were slowed and heated. Many of the beam electrons were reflected toward BERT while a few escaped to the distant chamber walls.



Images of a 36 keV Electron Beam Emission Taken by the Low-light Television Camera on the PDP. (The image was taken during re-entry, at an altitude of 100 km from a distance of about 500 m.)

that looked back toward MAIN throughout the flight. It returned the first images from space of an electron beam spiraling along the earth's magnetic field as shown in the figure on the previous page.

Emissions from ECHO 7 were controlled by a 10-second timer, which sent out a repeated sequence at various beam currents, energies, and pitch angles. There were two beam modes, one called "continuous," in which the beam was swept from 40 keV, 250 mA to 8 keV, 30 mA at a repetition rate of 1 kHz, and one called "discrete," in which the beam energy was either 10 keV or 36 keV. The primary objective of the ECHO 7 experiment was accomplished when particle sensors on all four payloads detected electrons after a 200,000 km journey in which they reflected from the southern ionosphere and returned to ECHO.

As the diagnostics payloads moved away from MAIN, they mapped out a region of about 60 m in which ionospheric plasma is heated by the beam. Plasma wave activity measured in this region will allow modeling of the mechanisms by which heating is accomplished in an essentially collisionless region. During "continuous" beam operations when the EPP was outside the heated plasma region, its wave detectors measured signals modulated at harmonics of 1 kHz. This suggests that one day modulated electron beams may be used as virtual antennas in space for specialized communications.

Finally, during 36 keV emissions, a tethered probe ejected from MAIN measured potentials in excess of 5kV. At times of neutral gas releases from MAIN's attitude control system, the potential fell quickly to a near-zero level. This method of vehicle potential control holds promise for the future. There are, however, stressful effects on internal circuitry of rapidly discharging space vehi-

cles that must first be overcome.

Electromagnetic Radiation: The effects of intense electromagnetic radiation on space plasmas has been of active concern since the time of Project Forecast 2. Two general classes of interaction have been investigated: (1) the acceleration of electrons to high energies using waves near the first or second harmonic of the electron cyclotron frequency (ECF) and (2) the acceleration of the precipitation of trapped, energetic particles from the radiation belts using waves from ground transmitters.

Studies of electron cyclotron heating (ECH) have been experimental. The theoretical studies have focused on thresholds of wave amplitudes needed to accelerate with waves near the second ECF harmonic. Solutions to the fully relativistic Lorentz equation were obtained via independent analytical and numerical techniques. Solutions of the Lorentz equation divide into two classes in which the acceleration is that of a particle moving in a potential well and chaotic solutions when the potential wells associated with various ECF harmonics overlap.

The boundary between regular and chaotic solutions is at about 1 W/cm^2 . This is well beyond the 1 mW/cm^2 that characterizes present-day ionospheric heaters. Alternative techniques using the linear conversion of O mode into Z mode radiation in the radio window predict that an amplification of wave power by 10^3 can be gained. An experimental study being carried out by Applied Microwave Plasma Concepts, Inc., using whistler wave injection suggests that a 10^4 increase in wave efficiency can be achieved.

Models have been developed to study the effects of waves from ground stations to control particles in the radiation belts. They have followed and quantified the work of the Soviet physicist Trakhtengerts, who proposed that iono-

spheric heaters modulated at elf or vlf frequencies could efficiently inject and reflect low-frequency waves in the magnetosphere. These waves would extract further energy from free energy contained in the anisotropies of trapped particle distributions. Thus, the waves would grow as in a maser. At large amplitude, the waves would have sufficient energy to diffuse in pitch angle the energetic particle, causing the particles to precipitate into the upper atmosphere. If radiation belt populations can be actively controlled, new satellite orbits for earth resources and military surveillance would be opened for use. Trapped radiation currently limits the use of advanced microelectronics devices on satellites orbiting in the radiation belts.

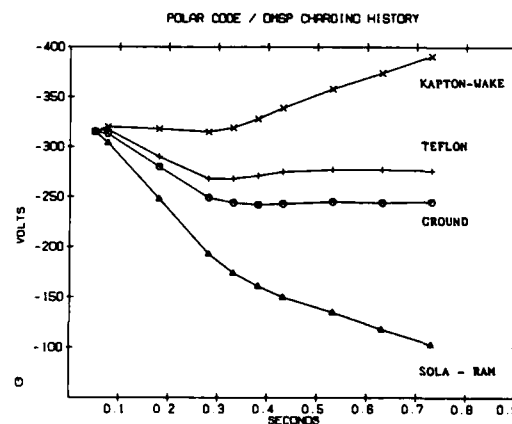
SPACECRAFT ENVIRONMENTAL INTERACTIONS

Spacecraft Charging: Numerical investigations into the phenomenon of spacecraft charging are performed with a variety of computer codes. Most notable are the POLAR (Potentials Of Large objects in the Auroral Region), MACH (Mesothermal Auroral Charging code), and NASCAP (NASA/Air Force Spacecraft Charging Analyzer Program). POLAR and MACH are presently being developed and validated by comparison with space and laboratory experiments.

MACH is a two-dimensional, axisymmetric reverse trajectory code that has been used in a variety of studies. These include: simulation of plasma chamber experiments, where particle sources and sinks dominate the particle kinetics; plasma sheath structure and probe theory, where MACH has helped validate the concept of a sheath edge for charged objects in flowing plasma; and the issue of heating versus filtering of electrons in the wake of satellites.

The POLAR code, intended for transition to the aerospace engineering com-

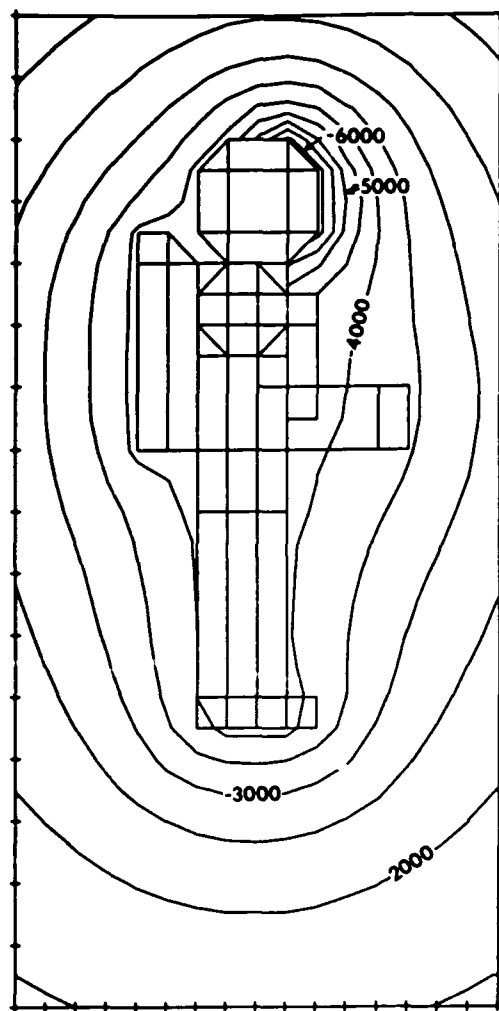
munity, simulates in three dimensions the charging and interaction of space vehicles with space plasmas due to both natural (auroral electrons) and active sources. POLAR models the physical processes of wake generation, ion and electron collection, charging by energetic electrons, secondary electron generation and transport, geomagnetic field effects, and sheath ionization. Potential and particle fields are computed self-consistently with surface potentials that are determined from an equivalent circuit model. POLAR now has an installation base that includes universities and aerospace corporations, on machines ranging from micro to super computers. POLAR has been validated by space shuttle plasma-wake measurements; by accurate prediction of current collection by the SDIO (Strategic Defense Initiative Organization) SPEAR I rocket experiment (Space Power Experiments Aboard Rockets), which exposed 44 kV to the space plasma; and by computing observed levels of



DMSP Charging History Calculated by POLAR for Selected Surfaces Exposed to an Electron Environment Observed by DMSP-F7 on 1 December 1987. (The observed spacecraft potential as deduced from ion spectrographs was -215 volts.)

DMSP spacecraft charging by auroral electrons (see figure).

EVA ASTRONAUT POTENTIAL CONTOURS



SIDE VIEW

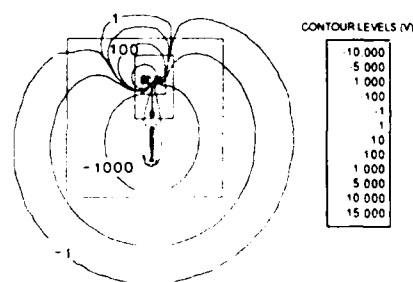
POLAR Code Calculation of Charging Experienced by Astronaut Operating a Manned Maneuvering Unit in Ion Wake.

Interaction theory predicts that auroral charging will be more dramatic for larger objects even in low-altitude orbits, since charging currents will increase in

proportion to surface area, while neutralizing ion currents are collected through sheaths that are, to first order, independent of object size, but do increase with surface voltage. Thus, while a meter-scale satellite such as DMSP charges to hundreds of volts, a 10-meter scale satellite such as the shuttle or other proposed platforms will charge to thousands of volts.

As with the size effect, ion collection is the key to another auroral charging event that occurs when a small subsatellite such as the astronaut's MMU (Manned Maneuvering Unit) is operated in an ion-depleted region such as a wake or sheath. The POLAR code has been used to simulate this charging (see figure) using measured auroral electron fluxes. Since actual space validation of wake charging must await the appropriate platforms and orbits, a laboratory investigation has been initiated to simulate this and other effects in a large vacuum chamber at GL.

Space Power Systems Interactions: SDIO (Strategic Defense Initiative Organization) has considerable interest in the management of power systems in the space plasma environment and, in par-



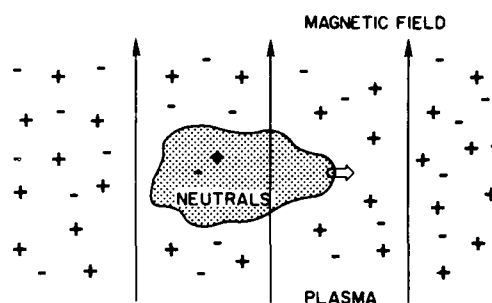
POLAR Code Simulation of the SPEAR I Experiment. (Potential for one probe biased to +38 kV and spacecraft ground at -6 kV are shown along with nested grid boundaries.)

ticular, high-voltage pulsed power where the high weight penalty for full insulation underscores the need to expose components to the plasma and to understand the subsequent interactions. In support of the SDIO-DNA (Defense Nuclear Agency) SPEAR (Space Power Experiments Aboard Rockets) program, GL has used the POLAR code to analyze and accurately predict the collection of electrons across the geomagnetic field by the SPEAR I experiment (see figure previous page).

POLAR code analysis demonstrated that although the electron currents were higher than analytic predictions, they were not "anomalous" and were predictable by accounting for the effect of sheath asymmetries on "classical" electrostatic electron trajectories without invoking plasma turbulence or cross-field electron diffusion. Subsequent SPEAR experiments will involve pulsed power where hundreds of kilovolts will be applied in microseconds. To support this, GL has begun development of a new simulation code DYNAPAC (DYNAMIC Plasma Analysis Code) that will combine features of POLAR with state-of-the-art PIC (Particle In Cell) techniques to provide a simulation capability for SPEAR as well as other plasma dynamic interactions such as arise in spacecraft contamination and critical ionization velocity.

Critical Ionization Velocity (CIV) Theory: The critical ionization velocity (CIV) theory postulates that atoms or molecules are rapidly ionized when their velocity reaches a critical value such that their kinetic and ionization energies are equal. If CIV occurs in space, there would be significant consequences: alteration of the ionization processes in the vicinity of spacecraft, effect on the transport of species in the ionosphere, and optical signatures which are different from normal neutral gas releases in space.

We have advanced the state-of-the-art



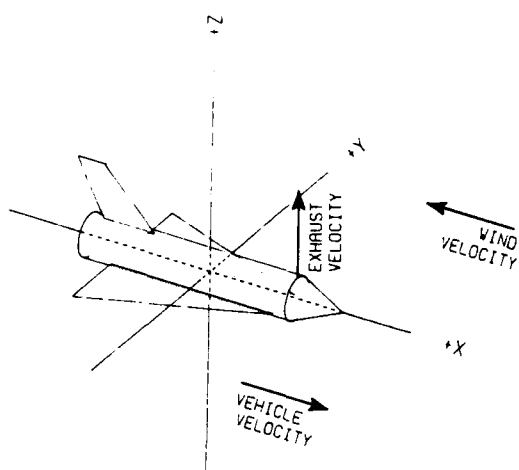
Schematic Diagram of CIV.

of CIV theory by introducing chemical processes into plasma physics. In the preonset stage, metastable states play an important role: they provide an energy pooling mechanism which allows low energy electrons to participate in the ionization processes. Following onset and during the propagation phase, ion-molecule reactions change the temporal chemical composition and may be important in chemical contamination. Dissociative recombination plays an important role in the quenching of CIV; it provides valuable tell-tale signatures in the form of optical and IR radiation. Escape of heated electrons and loss of energy due to recombination, excitation, and radiation may also quench CIV.

SPACECRAFT CONTAMINATION

SOCRATES: Gaseous contaminants emitted in the vicinity of a spacecraft in low earth orbit form a molecular cloud which surrounds the spacecraft. The contaminant cloud arises from a number of sources: desorption and photodesorption from spacecraft surfaces, return fluxes from engine exhaust, and periodic release of gases as needed for the operation of the spacecraft (e.g., the gases released by fuel cells).

The morphology of the contaminant cloud from its origin to its eventual dispersal is determined by altitude, atti-



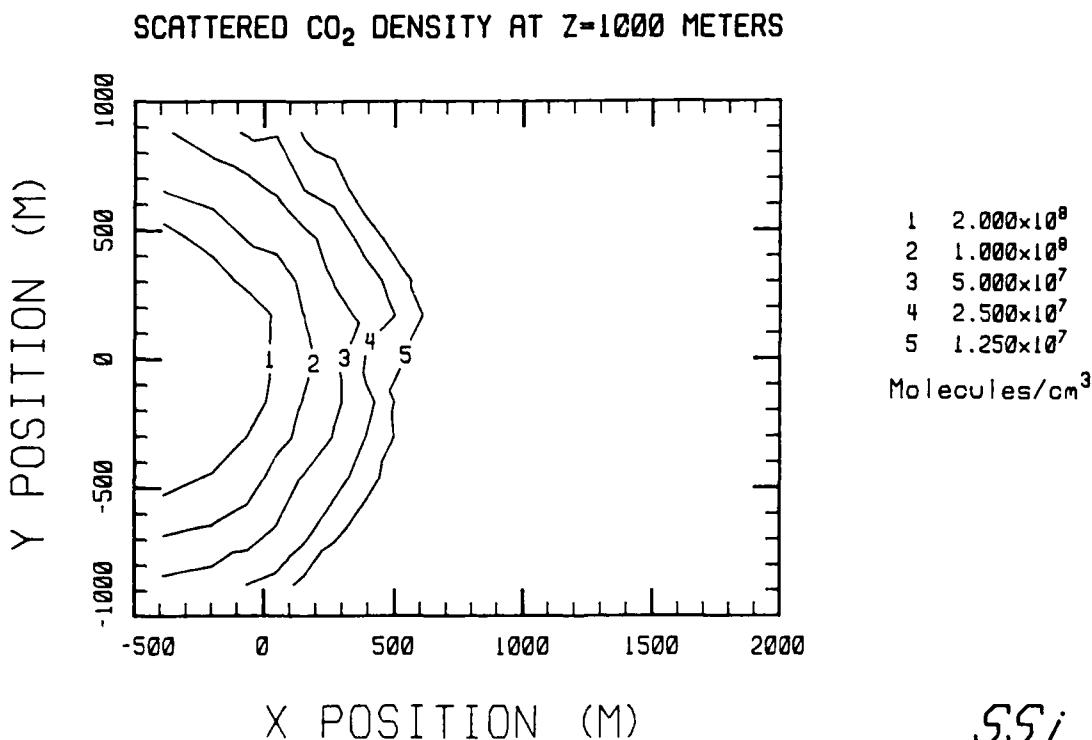
Schematic Diagram of Space Shuttle as Used in Socrates.

tude, and geometry of the spacecraft. The molecular gas cloud is a source of concern because it modifies the environment of a sensor in space. For example, in the case of an optical sensor, the col-

umn length of the molecular cloud may alter the signal observed by the sensor at some wavelength. Since the molecular cloud can undergo ionic reactions as well as neutral reactions, it may lead to a modification of the plasma environment surrounding the spacecraft. This may become important in some space-based radar concepts.

These considerations show that the nature and contour of the contaminant cloud can play an important role in the operation of spacecraft, and for that reason we have undertaken a program for the development of a predictive code. The objective of this Monte Carlo code, SOCRATES, is to provide a user-friendly computer program to predict the optical signatures of the contaminants, their reactions with the (neutral and ionized) ambient atmosphere at orbital velocity, and their eventual dispersal.

During the period of research covered by this report the first module of



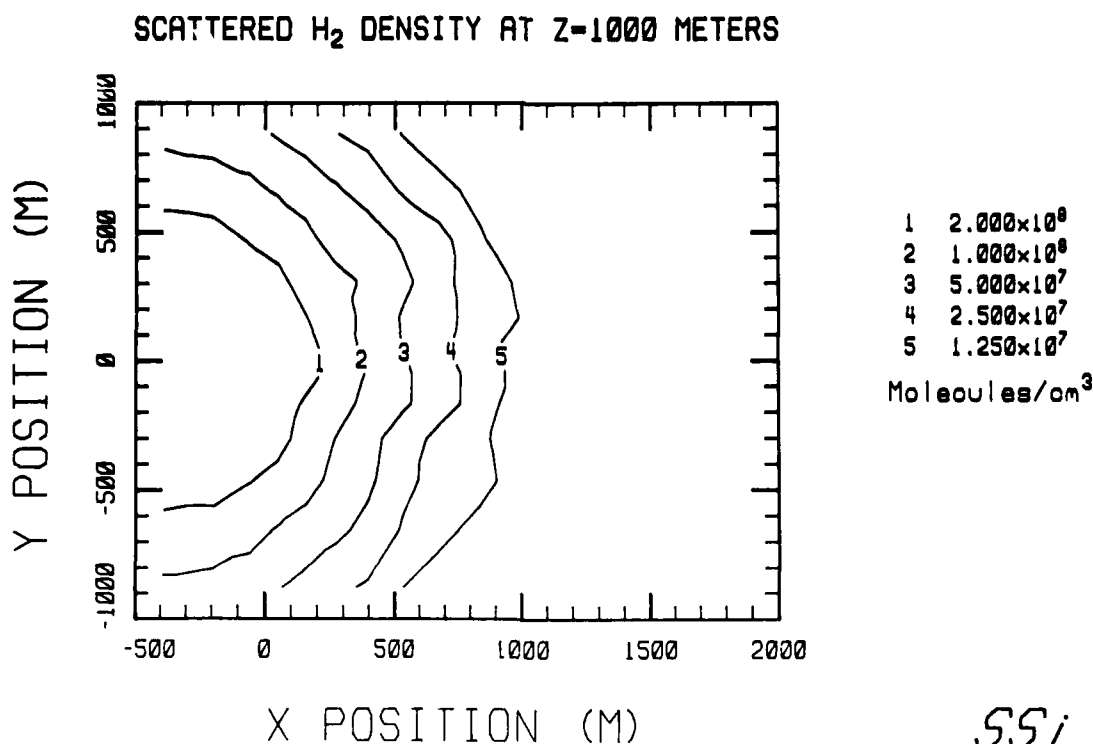
Intensity Contours for CO₂ Emitted by Shuttle Vernier Thrusters.

SOCRATES was finished. This module takes into account the scattering of the contaminants by the ambient atmosphere, and includes excitation of vibrational modes by collisions. Shown in the figures on these pages are two calculations of the predicted contours for the case where a thruster is fired in a direction (z direction) perpendicular to the direction of travel (x direction). Shown on page 48 is the contour diagram of the density of CO_2 as a function of distance at $z = 1$ km. On page 49 is shown a similar diagram for the case of H_2 . The altitude of the shuttle is 200 km. The initial composition of the exhaust gases was taken from the NASA Shuttle Handbook. The code predicts that the gas will travel up to 2 km following the initial expansion before it begins to interact with the atmosphere. Future modules of SOCRATES will include chemical reactions: neutral-neutral reac-

tions, ion neutral reactions, and gas-surface reactions.

Laboratory Studies of Ion-Neutral Chemistry:

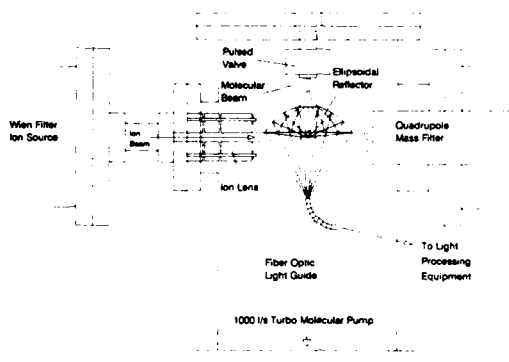
The relatively small ion densities of the low earth-orbit atmosphere can significantly affect the plasma surrounding spacecraft because of the high probabilities and fast rates of ion-neutral reactions. The ambient ions interact with the gas cloud surrounding spacecraft at suprathermal energies given by the orbiting velocities. To this date laboratory experiments have concentrated primarily on ion-neutral chemistry at lower energies, and only a few experiments exist which have addressed the question of excess energy release in these reactions. At energies corresponding to low earth-orbiting velocities, ion-neutral reaction products may be produced in light-emitting states and may therefore be considered to be a potential source of background radiation. Experimental



Intensity Contours for H_2 Emitted by Shuttle Vernier Thrusters.

data from ion-neutral reactions at collision energies between 1 and 10 eV are therefore needed to allow the consideration of these processes in the contamination code SOCRATES being developed for the prediction of these effects.

Current laboratory efforts are centered on determining ion-neutral reaction cross sections with a double mass spectrometer. The instrument in its present state allows the determination of integral cross sections using a static gas cell and kinetic energy release through time-of-flight measurements of ionic reaction



Design of Ion-Neutral Reaction Apparatus Incorporating Optical Diagnosis.

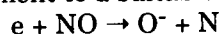
products. A new experiment (see the figure) is being constructed to enable optical studies of ion-neutral reactions. An intense mass and energy selected ion beam is produced with a discharge ion source and a Wien Filter. The static gas cell is replaced with a pulsed supersonic molecular beam. This permits efficient collection of fluorescence from the reaction region. The collection efficiency is maximized with an ellipsoidal reflector

and a fiber optic light guide. The fluorescence may originate either from electronically excited reaction products (chemiluminescence) or from laser-excited products (laser-induced fluorescence). The chemiluminescence is analyzed and recorded with an optical multichannel analyzer. A tunable dye laser is used to laser-excite reaction products. The data obtained will reveal information on the excitation of the various internal modes of reaction products, thus yielding clues to the dynamics of these reactions at suprathermal energies.

Presently experiments are carried out on reactions of ambient ions (e.g. O^+ , N_2^+) with water, an important constituent of the gas cloud surrounding the space shuttle. Preliminary results from time-of-flight studies of the charge transfer reaction $N_2^+ + H_2O \rightarrow N_2 + H_2O^+$ indicate a large degree of internal excitation of the H_2O^+ product. The excited H_2O^+ states allowed by conservation of energy are known to emit.

Atomic Oxygen Studies: Spacecraft in low earth orbit (200-800 km altitude) undergo energetic collisions with the ambient atmosphere because of the high orbital velocity ($\sim 7.7 \text{ km s}^{-1}$). These interactions manifest themselves in a number of observations, e.g. surface glows from spacecraft (the so-called "shuttle glow"), erosion of materials, and contamination of optical surfaces. Since the ambient atmosphere consists mostly of atomic oxygen, it is assumed that these interactions are due to collisions of fast oxygen atoms with surfaces. Indeed, the shuttle glow is thought to be due to the reaction of a fast oncoming oxygen atom and a surface adsorbed NO molecule, leading to the formation of electronically excited NO_2 , which radiates in the visible region of the spectrum. In order to understand

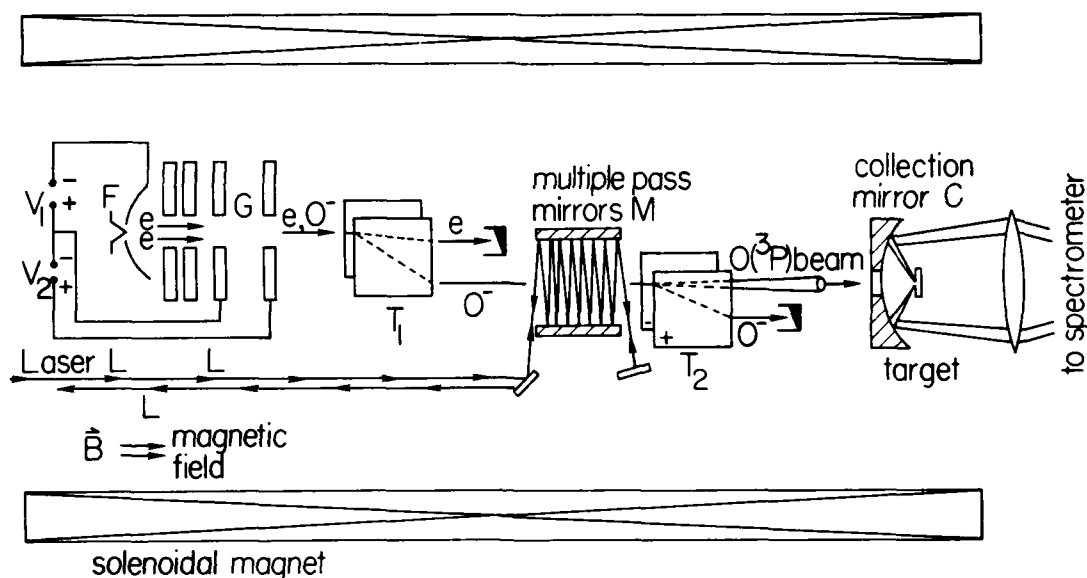
the nature of these interactions under conditions more controlled than those in space, we have undertaken a joint program with The Jet Propulsion Laboratory to develop a laboratory source of fast, ground state atomic oxygen which can then be used to study these phenomena under controlled conditions. The basic idea behind the successful design is to generate O^- by dissociative attachment to a suitable molecule:



O^- is then accelerated to the desired energy, photodetached, and the resulting neutral O atom is then aimed at a sur-

face. Because the background gas contained NO (from the primary source), recombination of fast O atoms with NO was seen. The observed radiation seems to be a pseudo-continuum with two peaks in the wavelength region 400-750 nm. This laboratory glow seems narrower in wavelength span than the shuttle glow.

We are currently building a differentially-pumped chamber in order to study the reactions of fast O atoms with gases, as well as the surface-catalyzed reactions of fast O atoms with a variety of surface-adsorbed molecules. These experiments



Variable Energy, High Flux Atomic Energy Source.

face. A sketch of the apparatus is shown in the figure.

The results of the experiment have shown so far that the technique, dissociative attachment of electrons followed by photodetachment, works. A beam of ground state O atoms, in a flux of about $10^{15} \text{ cm}^{-2} \text{ s}^{-1}$, has been obtained. This beam was made to collide with a magnesium fluoride surface. Optical radiation

will provide cross sections for O atom-gas reactions at high energies for direct input into the Contamination Code SOCRATES. In addition, the gas-surface studies will provide reaction probabilities for off-surface glows observed on spacecraft. The end result of this latter effort will be development of a procedure through which satellite designers can minimize the effects of this phenomenon.

Infrared Background Signature Survey (IBSS) Program: IBSS is a shuttle-based experiment that uses an instrumented Shuttle Pallet Satellite (SPAS) as a space-stabilized platform to make stand-off measurements of infrared (IR), ultra-violet (UV) and visible optical backgrounds and signatures. The SPAS as well as an IR sensor is being built by Messerschmitt Boelkow Blohm (MBB) of West Germany. GL's scientific contribution to the IBSS mission includes two

November, 1990, on shuttle mission STS-39.

The specific objectives of the AIS experiment are to obtain high-resolution spectra and imaging data of space-vehicle optical emissions resulting from shuttle glow, gaseous contamination, and rocket engine products and to understand the physical processes which produce observed radiant emissions. The AIS experiment will characterize the optical emissions observed on the sur-



MEASUREMENT OBJECTIVES:

- PLUMES FROM SHUTTLE
- EARTHLINE
- CHEMICAL RELEASES
- CELESTIAL BACKGROUND
- CONTAMINATION GLOW
- GAS RELEASES

GOAL:

- PROVIDE SENSOR SYSTEM DESIGN DATA FOR "INFORMED DECISIONS" BY SDIO.

Infrared Background Signature Survey (IBSS) Program.

experiments, described in detail below. One of the experiments is an ultraviolet/visible Arizona Imager/Spectrograph (AIS) that will measure engine plumes, earth backgrounds, contamination/glow, and chemical/gas releases. The other is a Critical Ionization Velocity (CIV) experiment that will determine if gas ionization occurs, as predicted by the Critical Ionization Velocity Theory. GL will also be providing two low-light-level cameras for pointing reference and is in charge of the entire IBSS data management effort. The schedule shows a launch in

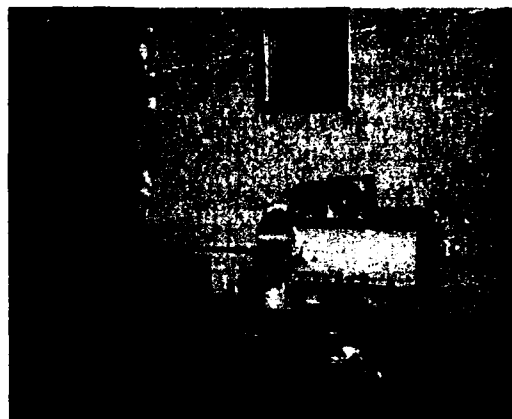
faces of low-altitude spacecraft including the shuttle. The sensor is a seven-channel optical grating spectrometer, bore-sighted with a set of six optical imagers. It will obtain spectra over a broad ultraviolet-visible-near infrared range, 115-1100 nm, and will have a spatial resolution of 0.3 to 1.0 nm. The experiment will determine the dependence between radiant emissions and magnetic field, orbital altitude, vehicle attitude, mission elapsed time, and surface compositions. The first-ever wide-band spectra of engine plumes will also be observed. The

AIS data will validate contamination and glow models. This research data will also be transitioned to Space Systems Division as Computer Aided Design (CAD) tools to be used in future spacecraft design.

The specific objectives of the CIV experiment are to evaluate the conditions under which the CIV phenomenon occurs in space, to gain data on the signature of gaseous species undergoing CIV, and to predict the effect on plume shapes when the components contain ions produced by the CIV phenomenon. The CIV experiment will yield spectra, images, and plasma data when test gases under high pressure are released from special tanks attached to the space shuttle bay. A monitor package placed next to the tanks will contain diagnostic instrumentation consisting of radiometers, a photometer, and a plasma monitor. Additional data will be gathered using sensors located on the SPAS. The CIV data will provide plume spectra and spatial structure needed for acquisition and tracking algorithms for space-based sensors. Current systems rely on modeling codes which do not include ionization. In low earth-orbit CIV may occur and distort plume signatures.

For SDIO and Air Force interests, the resulting SOCRATES contamination and plume models of the AIS and CIV experiments will have broad application to future Air Force space-based surveillance and tracking systems including SSTS, BSTS, and space weapons systems like DEW and KEW.

The Arizona Imaging Spectrograph: In order to obtain both spatial and spectral information on the shuttle glow phenomenon, a system of spectrographs and imagers was constructed to fly on the IBSS mission. The system consists of nine spectrographs with complete spectral coverage between 110 nm and 1100 nm with a spectral resolution of 0.3-1.0 nm. The spectrographs will provide one



Arizona Imaging Spectrograph.

dimension of spatial information along the direction of the spectrographs slit. For more complete spatial coverage of the shuttle glow, there are nine co-aligned imagers which have varying fields of view and spectral band-paths. The imagers, their spectral band paths, and their fields of view are listed in the following table.

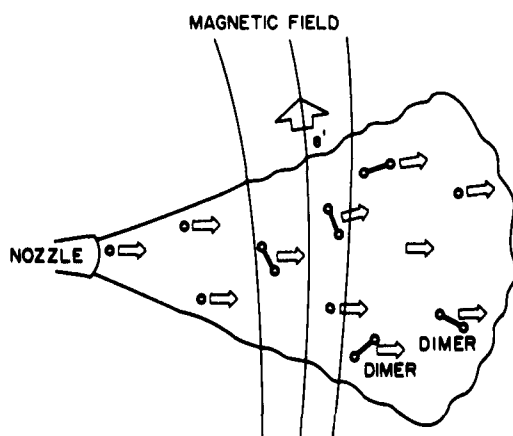
TABLE 2
IMAGER DESCRIPTION, WAVELENGTH,
AND FIELD-OF-VIEW (FOV)

Imager Number	Imager Type	Filter Wavelength peak (HW)	Field of View
1	Nar.-UV	160 (25)nm	2°
2	Nar.-UV	200 (25)nm	2°
3	Nar.-UV	235 (25)nm	2°
4	Nar.-UV	260 (25)nm	2°
5	Wide.-UV	160 (25)nm	25°
6	Wide.-UV	200 (25)nm	25°
7	Wide.-UV	235 (25)nm	25°
8	Wide.-UV	260 (25)nm	25°
9	Med.-Vis	500 (200)nm	5°
10	Med.-Vis	700 (200)nm	5°
11	Wide-IR	900 (400)nm	18°
12	Nar. IR	900 (400)nm	2°

This instrument will provide spectra of the shuttle glow as well as images of specific wavelengths of emitted radiation. The bandpass of the imagers was chosen

to correspond with known or suspected emitting species of the shuttle glow. The instrument's sensitivity and dynamic range will allow data to be taken from both the near field, while the IBSS is in the shuttle bay or on the RMS (Remote Manipulating System), as well as the far field, when the IBSS is 2.5-10 km from the shuttle.

CIV Experiment: As part of the IBSS mission, a CIV experiment is being designed and developed. The purpose of the experiment is to test the conditions under which CIV may occur in space. The experiment involves the sequential releases of four gases from the orbiter space shuttle payload bay and the observation of the resulting gas cloud from the IBSS system and from a CIV monitor subsystem in the payload bay. The four gases proposed are Xe, Ne, NO, and CO₂. One (Ne) of the gas releases will serve as a null test. The gases will be



Gas Release from the Space Shuttle.

released from nozzles. Dimers of the gas molecules are expected to form in the released gas near the nozzle, providing higher neutral masses and kinetic energies while the ionization energies are practically unchanged. We expect that such a combination favors CIV to occur.

Ultraviolet, visible, and infrared radiation will be measured for tell-tale signatures of atomic and molecular processes in CIV. Electron density and temperature, and low frequency plasma waves will be detected by means of Langmuir probes. Plasma densities will also be measured by means of a remote plasma monitor utilizing a low-power radio-frequency transmitter/receiver.

New initiative: The development of an infrared imager for use on low-altitude spacecraft, including the space shuttle, was begun under a design-study contract funded jointly by discretionary funds of GL and the Rome Air Development Center (RADC). The objective is to make quantitative measurements of infrared emissions produced by various interactions of low altitude spacecraft with the residual ambient atmosphere, extending similar measurements at ultraviolet and visible wavelengths. Subjects of interest include the glow surrounding surfaces exposed to the ram direction, interactions of the contaminant gas cloud around the spacecraft with the atmosphere, the effects of thruster firings and other events, and the presence of particulates in the contaminant environment.

The imager depends on recent advances in the technology of large-array detectors based on platinum-silicide and other materials sensitive to shortwave and midwave infrared. RADC has led in this development and has demonstrated a successful laboratory infrared camera that uses a 160-by-240 pixel platinum-silicide array at its focal plane. The instrument has high sensitivity because it is a staring camera (in which all parts of the object are viewed simultaneously), rather than a scanning camera (in which successive elements of the object are scanned by a single detector). Platinum-silicide detectors cover the range of roughly one to six microns; other detector materials currently under develop-

ment would extend coverage to even longer wavelengths. Information on the spectral content is provided by a filter wheel that selects a number of spectral bands in programmed sequence.

The recently completed initial design study addressed the tasks and problems of adapting such a laboratory camera for use on a spacecraft. These include providing suitable refrigeration for cooling the detector to the required temperature of 77 °Kelvin, transmitting and storing the high rate and large volume of quantitative data produced, and devising a pointing system to view in different directions from a platform fixed on the spacecraft. The feasibility of an instrument that can be adapted to a variety of space platforms has been established. The development, through critical design review, of the actual flight instrument is now being started under the Small Business Innovative Research program. Subsequent hardware fabrication of the instrument is expected to permit space flight by 1992.

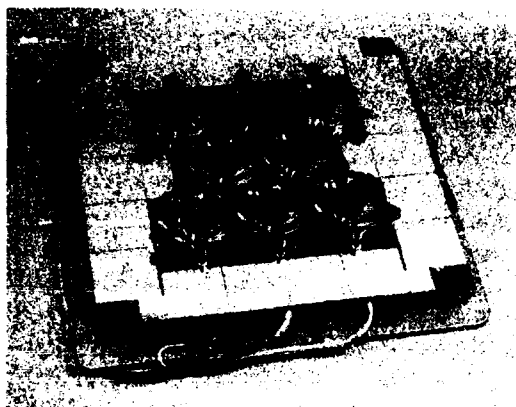
SPACE SYSTEMS ENVIRONMENTAL INTERACTIONS TECHNOLOGY

The Space Systems Environmental Interactions Technology Program addresses the impact of the space environment on large space structures and systems to be designed and built for use in the 1990s and beyond. The program capitalizes on space environment research carried out at GL and other DoD and civilian laboratories. Its purpose is to transition new results about the environmental sensitivities of emerging space technologies. The transition of these results can occur in several ways. They can take the form of design guidelines, military standards and handbooks, and Computer-Aided Engineering (CAE) tools for space systems developers (industry and Space Systems Division). In some cases, techniques may be suffi-

ciently mature to transition directly to DoD space systems operators (AF Space Command and US Space Command). Active methods to avoid, or reduce greatly, mission-threatening space-environmental effects are also developed and demonstrated in space to prove the concept for the systems Project Offices (SPOs). Proposed space systems technologies may have unknown or untested environmental interactions. In these cases, this program supports design, development, ground testing (where possible) and space testing to provide the answers the designers need.

Based upon previous reviews of Air Force and NASA research results on space system environmental interactions, a series of military handbooks and standards is being prepared. The first handbook on spacecraft anomalies has been completed in draft form. A draft of the Space Environment Standard is also finished. After final reviews, both documents will be delivered to the Acquisition Logistics Directorate at Space Systems Division (SD/AL) for publication and distribution as military guidelines and specifications.

IMPS: The Interactions Measurement Payloads (IMPS) project is a series of space experiments under development that will answer specific questions relating to new, planned military technologies, and how these technologies will survive the harsh space environment. For example, the Photovoltaic Array Space Power Plus Diagnostics (PASP Plus) Experiment addresses concerns that the latest designs for hardened, military photovoltaic solar arrays (see the figure) will be subjected to power loss or arc discharges if they are operated at high voltages. Thus, PASP Plus will test these technologies at voltages ranging from -500 volts to +500 volts in the actual space environment. The characteristics of these arrays will be monitored at



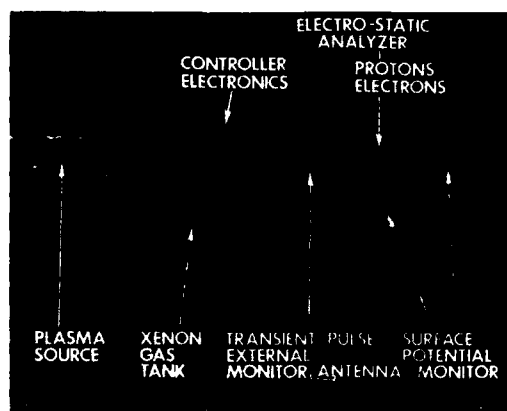
Mini Cassegrainian Concentrator Array for the PASP Plus Experiment.

the same time that the external environment is measured. In this way, analysis of the cause-effect relationship will be established.

SPREE: The IMPS project has several other Environmental Interactions Measurement Investigations (EIMI) underway. One of the larger tasks is SPREE (Shuttle Potential and Return Electron Experiment). This experiment will determine the engineering limitations associated with flying large space structures connected to smaller satellites with a conducting tether. During the tether deployment and operation, the space shuttle voltage will be monitored by the SPREE instrument as current is driven to the shuttle up the tether. This process will involve complex space interactions since the shuttle will be simultaneously operating electron guns and using plasma contactors to maintain charge neutrality. The wealth of information gained in this experiment, due to be launched in FY91, will be used to establish military standards and handbooks for large spacecraft through the Design and Test Standards project discussed above.

Charge Control System: The Charge Control System (CCS) project is based on

results from the Spacecraft Charging at High Altitudes (SCATHA) program. Geosynchronous SCATHA operations demonstrated that satellite surface charge could be actively controlled (dissipated) using a low-energy plasma source. The automatic, advanced technology demonstration CCS has been developed under contract with Hughes Research Laboratories (see the figure). It has three sensors capable of detecting the presence of spacecraft charging/discharging: (1) an electron and proton electrostatic analyzer, (2) a surface potential monitor, and (3) a transient pulse monitor. An advanced,



Assembled Flight Unit for GL Autonomous Charge Control System.

quick-start neutral plasma source has been built which, once turned on, essentially clamps the spacecraft to the back-ground plasma, providing a mechanism to dissipate any differential charge buildup before a potentially harmful discharge can occur.

A breadboard demonstration of this design showed that the CCS is capable of automatically preventing static charge build-up on high altitude satellites. The fabrication of the flight instrument is completed. After the contractor has finished functional and environmental tests of this unit, it will be available for integration on-board a suitable host vehicle.

Several flight configurations are possible, making this experiment an extremely flexible package for the host. Studies are currently underway to determine whether the CCS can be flown on the Geostationary Operational Environmental Satellite (GOES) in FY92.

PUBLICATIONS 1987-1988

AGGSON, T.L. (NASA/Goddard Space Flight Center, Greenbelt, MD); Maynard, N.C. (AFGL); Herrero, F.A., Mayr, H.G., Brace, L.H. (NASA/Goddard Space Flight Center, Greenbelt, MD); Liebrecht, M.C. (Science Applications Research, Lanham, MD)
Geomagnetic Equatorial Anomaly in Zonal Plasma Flow
J.Geophys. Res. 92 (1987)

ALTROCK, R.C.
Coronal Emission-Line Data and Solar Terrestrial Predictions
Proc. Solar-Terr. Predictions Wkshp. (1986)
The Solar Emission-Line Corona: Current and Future Ground-Based Observational Research
Solar and Stellar Coronal Structure and Dynamics Proceedings (July 1988)
ed. R.C. Altrock

ALTROCK, R.C., DEMASTUS, H.L., EVANS, J.W., KEIL, S.L., NEIDIG, D.F., RADICK, R.R., AND SIMON, G.W. 1987, in *Handbook of Geophysics and the Space Environment*. Adolph S. Jursa, ed. (GL), 1-25: Chapter 1: The Sun

ALTROCK, R.C.; GILLIAM, L.B. (Natl. Solar Obs., Sunspot, NM); Sime, D.G., and Fisher, R.R. (High Altitude Obs., Boulder, CO)
The Fe XIV Solar Corona at 5303 Angstroms: An Atlas of Synoptic Charts from the Sacramento Peak Coronal Photometer. May 1973 -December 1985
NCAR Technical Note (1987)

ALTROCK, R.C., KEIL, S.L., NEIDIG, D.F., RADICK, R.R., AND SIMON, G.W. 1987, in the *GL Report on Research for 1985 and 1986*. GL-TR-97-0188:

ALTROCK, R.C. 1988, in *Solar and Stellar Coronal Structure and Dynamics: a Festschrift in Honor of Dr. John W. Evans*.
Proceedings of the Ninth Sacramento Peak Summer Symposium, Sunspot, NM, 17-21 August, 1987. R.C. Altrock, ed., 414-420: Variation of Solar Coronal FE XIV 5303A Emission During Solar Cycle 21

BARRETT, J.L., KOFSKY, I.L. (Photometrics, Inc., Woburn, MA); and Murad, E. (AFGL)
Ultraviolet Glows From Recombination on Spacecraft Surfaces
Proc. SPIE 687 (1988)

BORNMAN, P.L.
Turbulence as a Contributor to Intermediate Energy Storage Mechanisms During Solar Flares
Astrophys. J. 313 (1987)

BURKE, W.J., GINET, G.P. (AFGL); VILLALON, E. (Northeastern Univ., Boston, MA); and Heinemann, M.E. (AFGL)
Electron Acceleration in the Ionosphere by Obliquely Propagating Electromagnetic Waves
J. of Geomagnetism and Geoelectricity 40 (1988)

- CANFIELD, R.C. (Univ. of California, San Diego, CA); BELY-DUBAU, F. (Nice Obs., France); BROWN, J.C. (Univ. of Glasgow, Scotland); DULK, G.A. (Univ. of Colorado, Boulder, CO); EMSLIE, A.G. (Univ. of Alabama in Huntsville, AL); ENOME, S. (Nagoya Univ., Japan); GABRIEL, A.H. (Rutherford Appleton Lab.); KUNDU, M. R. (Univ. of Maryland, Baltimore, MD); MELROSE, D. (Univ. of Sydney, Australia); NEIDIG, D.F. (AFGL); et al
Chapter 3: Impulsive Phase Transport Energetic Phenomena on the Sun
ed. by M. Kundu and B. Woodgate, NASA Conf. Pub. 2401 (1986)
- CLIVER, E.W., DENNIS, B.R., KIPPLINGER, A.L., KANE, S.R., NEIDIG, D.F., SHEELEY, N.R., and KOOMEN, M.J. 1987, *Adv. Space Res.* 6, no. 6, 249-252: *Solar Gradual Hard X-Ray Bursts: Observations and an Interpretation*
- DARA, H.C. (Research Center for Astronomy and Applied Mathematics, Athens, Greece); ALISSANDRAKIS, C.E. (Univ. of Athens, Athens, Greece); and KOUTCHMY, S. (AFGL)
Small Scale Motions Over Concentrated Magnetic Regions of the Quiet Sun
Solar Phys. 109 (1987)
- DENIG, W.F. (AFGL); PARISH, J.L. (Parish Research, Howe, IN); and RAITT, W.J. (Utah State Univ., Logan, UT)
Delay Time for the Onset of Beam Plasma Discharge
Planetary and Space Sci. 35 (1987)
- DENIG, W.F. (AFGL); KENDALL, D.J.W. (Natl. Research Council, Ontario, Canada); MENDE, S.B., SWENSON, G.R., LLEWELLYN, E.J. (Lockheed, Palo Alto, CA); and SLANGER, T.G. (SRI Intl., Menlo Park, CA)
Measurements of Rotational Temperature in the Airglow with a Photometric Imaging Etalon Spectrometer
J. Geophys. Res. 93 (1988)
- DENIG, W.F., MAYNARD, N.C. (AFGL); FRIEDRICH, M. (Tech. Univ., Graz, Austria); MAEHLUM, B.N., TROIM, J. (Norwegian Def. Res. Establishment, Kjeller, Norway); and TORKAR, K.M. (Space Res. Inst., Graz, Austria)
Studies of the Electrical Charging of the Tethered Electron Accelerator Mother-Daughter Rocket Maimik
Geophysical Res. Lett. 15 (1988)
- ENGVOLD, O. (Univ. of Oslo, Norway); and KEIL, S.L. (AFGL)
Vertical Motions in Quiescent Prominences Observed in the He I- 10830Å Line
Coronal and Prominence Plasmas
ed. A. I. Poland, NASA Conf. Pub. 2442 (1986)
- FLUCKIGER, E.O. (Univ. of Bern, Switzerland); SMART, D.F., SHEA, M.A. (AFGL); and GENTILE, L. C. (Emmanuel Coll., Boston, MA)
On the Correlation Between Asymptotic Directions of Cosmic Ray Particles and Cutoff Rigidities in the Evolving Geomagnetic Field
J. Geophys. Res. 92 (1987)
- GELPI, C. (XonTech, Inc., Van Nuys, CA); SINGER, H.J. (AFGL); and HUGHES, J. (Boston Univ., Boston, MA)
A Comparison of Magnetic Signatures and DMSP Auroral Images at Substorm Onset: Three Case Studies
J. Geophys. Res. 92 (1987)
- GOMEZ, M.T. (Capodimonte Obs., Naples, Italy); MARMOLINO, C. (AFGL); ROBERTI, G. (Univ. of Naples, Naples, Italy); and SEVERINO, G. (Capodimonte Obs., Naples, Italy)
Temporal variations of Solar Spectral Line Profiles Induced by the 5 Min Photospheric Oscillation
Astron. Astrophys. 188 (1987)

Broadening and Shift of Fe I Lines Perturbed by Atomic Hydrogen
Solar Phys. 112 (1987)

GREEN, B.D. (Physical Sciences, Inc., Andover, MA); YATES, G.K., AHMADJIAN, M. (AFGL); and MIRANDA, H. (Miranda Labs., Bedford, MA)

The Particulate Environment around the Shuttle as Determined by the PACS Experiment
Proc. SPIE 777 (1987)

GUSSENHOVEN, M.S.
Low Altitude Convection, Precipitation and Current Patterns in the Baseline Magnetosphere
Rev. Geophys. and Space Phys. 26 (1988)

GUSSENHOVEN, M.S., MULLEN, E.G., AND HARDY, D.A.
Artificial Charging of Spacecraft Due to Electron Beam Emission
IEEE Trans. Nucl. Sci. 34 (1987)

GUSSENHOVEN, M.S., MULLEN, E.G., OBERHARDT, M.R., AND BRAUTIGAM, D.H.
DMSP/F7 Dosimeter Measurements During the Solar Particle Events of 16 February and 24-28 April 1984
NOAA UAG Report 96 (1987)

GUSSENHOVEN, M.S., MULLEN, E.G., FILZ, R. C., BRAUTIGAM, D.H. (AFGL); and HANSER, F. A.
(Panametrics, Inc., Waltham, MA)
New Low Altitude Dose Measurements
IEEE Trans. Nucl. Sci. 34 (1987)

HARDY, D.A., GUSSENHOVEN, M.S., RAISTRICK, R. (AFGL); AND MCNEIL, W.J. (Radex Inc., Carlisle, MA)
Statistical and Functional Representation of the Pattern of Auroral Energy Flux, Number Flux, and Conductivity
J. Geophys. Res. 92 (1987)

HEPPNER, J.P. (GSFC); AND MAYNARD,

N.C. (AFGL)
Empirical High Latitude Electric Field Models
J. Geophys. Res. 92 (1987)

HOFFMAN, R.A. (NASA Goddard Space Flt. Ctr., Greenbelt, MD); SIGIURA, M. (Kyoto Univ., Kyoto, Japan); CANDEY, R.M. (ORI, Inc., Rockville, MD); CRAVEN, J.D., FRANK, L.A. (Univ. of Iowa, Iowa City, IA) and Maynard, N.C. (AFGL)
Electrodynamic Patterns in the Polar Region During Periods of Extreme Magnetic Quiescence
J. Geophys. Res. 93 (1988)

KAHLER, S.W. (Emmanuel Coll., Boston, MA); and CLIVER, E. (AFGL)
Solar Cycle Variation of Long Duration 10 Cm and Soft X-Ray Bursts
Solar Phys. 115 (1988)

KATZ, I., MANDELL, M., JONGEWARD, G. (S-Cubed, LaJolla, CA); and GUSSENHOVEN, M. S. (AFGL)
The Importance of Accurate Secondary Electron Yields in Modeling Spacecraft Charging
J. Geophys. Res. 91 (1986)

KOUTCHMY, O. (Univ. of Paris, Paris, France); KOUTCHMY, S. (AFGL); NITSCHHELM, C., SYKORA, J. (Astron. Inst. Tatranski, Lomnica, Czechoslovakia); and SMARTT, R. N. (Natl. Solar Obs., Sunspot, NM)
Image Processing of Coronal Pictures
Proc. Solar and Stellar Coronal Structure and Dynamics (June 1988)
ed. R.C. Altrock

KOUTCHMY, S.
Small Scale Coronal Structures
Proc. Solar and Stellar Coronal Structure and Dynamics (June 1988)
Space-Borne Coronagraphy
Space Sci. Reviews 47 (1988)

- KOUTCHMY, S. (AFGL); and BELMAHDI, M. (Inst. d'Astrophys., Paris, France)
Improved Measurements of Scattered Light Level Behind Occulting System
J. Optics **18** (1987)
- KOUTCHMY, S. (AFGL); and LEBECQ, C. (Institut d'Astrophysique, Paris, France)
The Solar Granulation II. Photographic and Photoelectric Analysis of Photospheric Intensity Fluctuations at the Meso-granulation Scale
Astron. Astrophys. **169** (1986)
- KOUTCHMY, S. (AFGL); and NITCHELM, C. (Paris Inst. d'Astrophysique, Paris, France)
Optical Detection of Space Debris Using a Large Achromatic Coronagraph
Astrophys. and Space Sci. **143** (1988)
- KOUTCHMY, S. (AFGL); and STELLMACHER, G. (Paris Inst. d'Astrophysique, Paris, France)
Properties of a Concentrated Magnetic Field Region
Proc. Role of Fine-Scale Magnetic Structure of the Solar Atmosphere (June 1988)
- LAI, S.T. (AFGL); MCNEIL, W.J. (Radex Inc., Lexington, MA); and MURAD, E. (AFGL)
Parametric Study in the Quenching of Critical Velocity Ionization
Proc. Am. Phys. Soc. Conf. on Numerical Simulation of Plasmas (1987)
The Role of Metastable States in Critical Ionization Velocity Discharges
J. Geophys. Res. **93** (1988)
- LAI, S.T., COHEN, H.A. (AFGL); AGGSON, T.L. (NASA Goddard Space Flight Ctr., Greenbelt, MD); and MCNEIL, W.J. (Radex, Inc., Lexington, MA)
The Effect of Photoelectrons on Boom-Satellite Potential Differences During Electron Beam Ejections
J. Geophys. Res. **92** (1987)
- LAI, S., DENIG, W.F., MURAD, E. (AFGL); and McNeil, W.J. (Radex, Inc., Bedford, MA)
The Role of Plasma Processes in the Space Shuttle Environment
Planetary and Space Sci. **36** (1988)
- VON DER LUHE, O. 1988, in *The Role of Fine-Scale Magnetic Fields in the Structure of the Solar Atmosphere: Workshop Proceedings*, Tenerife (Canary Islands), 6-12 October, 1986: 156-161: Photospheric Fine Structure Close to a Sunspot
- MACHADO, M.E. (NASA Marshall Space Flight Ctr., AL); AVRETT, E.H. (Harvard-Smithsonian Ctr. for Astrophysics, Cambridge, MA); FALCIANI, R. (Osservatorio Astrofisico di Arcetri, Firenze, Italy); FANG, C. (Naging Univ., Naging, China); GESZTELYI, L. (Heliophysical Obs., Debrecen, Hungary); HENOUX, L.C. (DASOP, Obs. de Muedon, France); HIEI, E. (Tokyo Astronomical Obs., Tokyo, Japan); NEIDIG, D.F. (AFGL); RUST, D.M. (JHU Applied Physics Lab., Laurel, MD); SOTIROVSKI, P. (DASOP, Obs., de Muedon, France); SVESTKA, Z. (Lab. for Space Res., Utrecht, The Netherlands); and ZIRIN, H. (California Inst. of Tech., Pasadena, CA)
White Light Flares and Atmospheric Modeling
The Lower Atmosphere of Solar Flares ed. D.F. Neidig (1986)
- MAKAROV, V.I., MAKAROVA, V.V. (Pulkovo Obs., Kislovodsk, USSR); KOUTCHMY, S. (AFGL); SIVARAMAN, K.R. (Indian Inst. of Astrophys., Bangalore, India)
Solar Cycle Variations of Coronal Neutral Lines and Polar Regions Activity
Proc. Solar and Stellar Coronal Structure and Dynamics (June 1988)
ed. R.C. Altrock
- MARKLUND, G.T., BLOMBERG, L.G. (Royal Inst. of Tech., Stockholm, Sweden);

- HARDY, D.A., AND RICH, F.J. (AFGL); et al
Snapshots of High-Latitude Electrodynamics Using Viking and DMSP/F7 Observations
J. Geophys. Res. 93 (1988)
- MARMOLINO, C.
Effects of Acoustic and Gravity Waves on the Curve of Growth
Solar Phys. 112 (1987)
- MARMOLINO, C. (AFGL); ROBERTI, G. (Univ. of Naples, Italy) and SEVERINO, G. (Capodimonte Obs., Naples)
Line Asymmetries and Shifts in the Presence of Granulation and Oscillations: The CLV of K I 7699 Resonance Line
Solar Phys. 108 (1986)
Fe II in the Presence of Photospheric Motions
Proc. of the IAU Colloquium on Physics of the Formation of Fe II Lines Outside LTE (June 1988) ed. R. Viotti, et. al.
On the Difference between Line Bisectors in Quiet and Active Sun
The Role of Fine-Scale Magnetic Fields in the Structure of the Solar Atmosphere
Cambridge Univ. Press (1988)
- MAYNARD, N.C. (AFGL); AGGSON, T.L., HERRERO, F.A. (NASA/Goddard Space Flight Center, Greenbelt, MD); and LIEBRECHT, M.C. (Science Applications Research, Inc., Lanham, MD)
Average Low Latitude Meridional Electric Fields from DE-2 During Solar Maximum
J. Geophys. Res. 93 (1988)
- MULLEN, E.G., GUSSENHOVEN, M.S., LYNCH, K.A., AND BRAUTIGAM, D.
A Space Measurement and Mapping of Upset Causing Phenomena
IEEE Trans. on Nucl. Sci. 34 (1987)
- MURAD, E.
Glow of Spacecraft in Low Earth Orbit
SPIE Conf. Proc. and Reprint Series 6 (1987)
The Role of Atomic and Molecular Processes in the Critical Ionization Velocity Theory
Proc. of Symp. on Atomic and Molecular Processes (1986) in *The Recent Studies in Atomic and Molecular Processes*
ed. A. E. Kingston, pub. Plenum Corp. (1987)
- MURAD, E. (AFGL); and BOCHSLER, P. (Univ. of Bern, Bern, Switzerland)
Speculation About the Origin of H_3O^+ Seen in Cometary Mass Spectra
Nature 326 (1987)
- NEIDIG, D.F.
Limitations in the Use of Ha Filament and Fibril Activity as a Short-Term (30-Minute) Predictor of Flares and Flare-Like Events
Solar-Terrestrial Predictions
ed. P.A. Simon et al AFGL/NASA/U.S. Department of Commerce (1986)
Energy Transport MAX '91: Flare Research at the Next Solar Maximum
ed. R.C. Canfield and B. R. Dennis
AFGL/NASA/U.S. -Department of Commerce (1988)
- NEIDIG, D.F. (AFGL); SMITH, JR., J.B. (NOAA, Boulder, CO); HAGYARD, M.J., and MACHADO, M.E. (NASA/Marshall Flight Ctr., Huntsville, AL)
Flare Activity, Sunspot Motions, and the Evolution of Vector Magnetic Fields in Hale Region 17244
Adv. Space Res. 6 (1987)
- NEIDIG, D.F., WIBORG, P.H. (AFGL); SEAGRAVES, P.H. (High Altitude Obs., Boulder, CO); HIRMAN, J.W., and FLOWERS, W.E. (NOAA, Boulder, CO)
Objective Forecasts for Solar Flares Using Multivariate Discriminant Analysis
Solar Terrestrial Predictions
ed. P. A. Simon et al AFGL/NASA/U.S. Department of Commerce (1986)
- PORTER, J.G. (NASA Marshall Space Flight Ctr., Huntsville, AL); GEBBIE, K.B. (National Bureau of Standards, Boulder, CO); and NOVEMBER, L.J. (AFGL)
The Excitation of Helium Resonance Lines in

Solar Flares

The Lower Atmosphere of Solar Flares
ed. D. F. Neidig (1986)

RADICK, R.R. (AFGL) and BALIUNGS, S.
*The Solar-Stellar Connection at Low
Spectral Resolution*
Proc. of The SHIRSOG Wkshp., Natl. Solar
Obs., Tucson, AZ (1987)
ed. M.S. Giampapa

RADICK, R.R. (AFGL); AND BALIUNAS, S.L.
(Harvard-Smithsonian Center for
Astrophysics, Cambridge, MA)
*Stellar Activity and the Rotation of Hyades
Stars*
Proc. Cool Stars, Stellar Systems, and the
Sun (January 1988)

RADICK, R.R. (AFGL); THOMPSON, D.T.,
LOCKWOOD, G.W. (Lowell Obs., Flagstaff,
AZ); DUNCAN, D.K. and BAGGETT, W.E.
(Mt. Wilson and Las Campanas Obs.,
Pasadena, CA); and BAGGETT, W. E. (New
Mexico State Univ., Albuquerque, NM)
*The Activity, Variability, and Rotation of
Lower Main-Sequence Hyades Stars*
Astrophys. J. **321** (1987)

RICH, F.J., AND GUSSENHOVEN, M.S.
*A Search for Region 1/Region 2 Field-
Aligned Currents During Quiet Times*
Geophys. Res. Lett. **14** (1987)

RICH, F.J., GUSSENHOVEN, M.S. (AFGL),
AND GREENSPAN, M. (Regis Coll., Weston,
MA)
*Observations by DMSP Satellites of the
Energy Flow Into the High Latitude
Ionosphere*
Ann. Geophys. **5** (1987)

ROBINSON, R.M., VONDRAK, R.R.
(Lockheed, Palo Alto, CA); MILLER, K.
(Utah State Univ., Logan, UT); DABBS, T.
(SRA Intl., Menlo Park, CA); and HARDY,
D. (AFGL)
On Calculating Ionospheric Conductances

From the Flux and Energy of Precipitating Electrons

J. Geophys. Res. **92** (1987)

ROBINSON, R.M., VONDRAK, R.R.
(Lockheed, Palo Alto, CA); HARDY, D.,
GUSSENHOVEN, M.S. (AFGL); POTEIRA,
T.A., AND BYTHROW, P.F. (The Johns
Hopkins Univ., Laurel, MD)
*Electrodynamics of Very High Latitude Arcs
in the Morning Sector Auroral Zone*
J. Geophys. Res. **93** (1988)

ROTHWELL, P.L. (AFGL); SILEVITCH, M.B.
(Northeastern Univ., Boston, MA); and
BLOCK, L. P. (Royal Inst. of Tech.,
Stockholm, Sweden)
*A Unified Model for the WTS and the
Generation of Pi 2 Pulsations*
Proc. 21st ESLAB Conf., Bolkesjo,
Norway (22-25 June 1987)
*The Motion of the WIS as a Function of
Electron Temperature Anisotropy in the
Plasma Sheet In Modeling Magnetosphere
Plasma*
ed. T.E. Moore and J.H. Waite, Jr., AGU
Monograph **44** (1988)

ROTHWELL, P.L. (AFGL); BLOCK, L.P.,
FALTHAMMAR, C. G. (Royal Inst. of Tech.,
Stockholm, Sweden); and SILEVITCH,
M.B. (Northeastern Univ., Boston, MA)
*A New Model for Substorm Onsets: The Pre-
Breakup and Triggering Regimes*
Geophys. Res. Lett. **15** (1988)

ROTHWELL, P.L. (AFGL); SILEVITCH, M.B.
(Northeastern Univ., Boston, MA);
BLOCK, L.P. (Royal Inst. of Tech.,
Stockholm, Sweden); and TANSKANEN, P.
(Univ. of Oulu, Oulu, Finland)
*A Model of the WTS and their Generation of
Pi 2 Pulsations*
J. Geophys. Res. **93** (1988)

SEVERINO, G. (Capodimonte Obs., Naples,
Italy); Roberti, G. (Univ. of Naples,
Naples, Italy);

- MARMALINO, C. (AFGL); AND GOMEZ, M.T. (Capodimonte Obs., Naples, Italy)
The Effects of Acoustic-Gravity Waves on the K 1 7699 Line
 Solar Phys. **104** (1986)
- SHEA, M.A.
Overview of Cosmic Ray, Solar, and Interplanetary Research (1983-1986)
 Rev. Geophys. **25** (1987)
Overview of Solar-Terrestrial Physics Phenomena for STIP Interval XV (12-21 Feb 1984) and STIP Interval XVI (20 April - 4 May 1984); Summary of the Cosmic Ray Intensity During the Solar-Terrestrial Events of 16 February and 24-28 April 1984
 UAG Solar-Terr. Phys. Report (1987)
- SHEA, M.A., SMART, D.F. (AFGL); and FLUCKIGER, E.O. (Univ. of Bern, Switzerland)
Possible Neutron Monitor Responses to Solar Neutrons in April 1984
 20th Internat. Cosmic Ray Conf. Papers 3 (1987)
- SHEA, M.A., SMART, D.F. (AFGL); and GENTILE, L.C. (Emmanuel Coll., Boston, MA)
Asymptotic Directions for Selected Cosmic Ray Stations Calculated Using the International Geomagnetic Reference Field for 1980
 UAG Solar-Terr. Phys. Report (1987)
Estimating Cosmic Ray Vertical Cutoff Rigidities as a Function of the McIlwain L-Parameter for Different Epochs of the Geomagnetic Field
 Phys. Earth Planet. Inter. **48** (1987)
- SMART, D.F., SHEA, M.A. (AFGL); and FLUCKIGER, E.O. (Univ. of Bern, Bern, Switzerland)
Unusual Aspects of the Ground-Level Cosmic Ray Event of 7/8 December 1982
 20th Internat. Cosmic Ray Conf. Papers 3 (1987)
- SMITH, JR., J.B. (NOAA, Boulder, CO); and NEIDIG, D.F. (AFGL)
Working Group C Report on Short-Term Solar Predictions
 Solar-Terrestrial Predictions
 ed. P.A. Simon et al, AFGL/NASA/U.S. Department of Commerce (1986)
- SVESTKA, Z.F. (Laboratory for Space Research, Utrecht, The Netherlands); FONTELA, J.M. (IAFE, Buenos Aires, Argentina); Machado, M.E. (NASA, Huntsville, AL); MARTIN, S.F. (California Inst. of Tech., Pasadena, CA); NEIDIG, D.F. (AFGL); and POLETO, G. (Osservatorio Astrofisico di Arcetri, Firenze, Italy)
A Dynamic Flare With Anomalous Dense Flare Loops
 Adv. Space Res. **6** (1987)
Multi-Thermal Observations of Newly Formed Loops in a Dynamic Flare
 Solar Phys. **108** (1987)
- SWIDER, W.
Electron Loss and the Determination of Electron Concentrations in the D-Region
 Pure & Applied Geophys. **127** (1988)
- TITLE, A.M., TARBELL, T.D., SIMON, G.W., (nine other authors), HARVEY, J.W., LEIBACHER, J.W., LIVINGSTON, W.C., AND NOVEMBER, L.J. 1987, Adv. Space Res. **6**, no. 8, 253-262: *White-Light Movies of the Solar Photosphere from the SOUP Instrument on Spacelab 2*
- VON DER LUHE, O.
Application of the Knox-Thompson Method to Solar Observations; Calibration Problems in Solar Speckle Interferometry; Study of Sizes, Brightnesses and Dynamics of Solar Facular Points
 Interferometric Imaging in Astronomy
 ed. J.W. Goad, European Southern Obs./National Optical Astron. Obs. (1987)
Signal Transfer Function of the Knox Thompson Speckle Imaging Technique

J. Opt. Soc. Am. **5** (1987)

*Photon Noise Analysis for a LEST
Multidither Adaptive Optical System*
LEST Technical Reports 28 (January 1988)
*A Wavefront Error Measurement Technique
Using Extended, Incoherent Light Sources*
Opt. Eng. **27** (1988)

VON DER LUHE, O., and DUNN, R.B.
*Solar Granulation Power Spectra From
Speckle Interferometry*
Astron. Astrophys. **177** (1987)

WILSON, P.R. (Univ. of Sydney, Sydney,
Australia); ALTROCK, R.C. (AFGL);
HARVEY, K.L. (Solar Phys. Res. Corp.,
Tucson, AZ); MARTIN, S.F. (Calif. Inst.
Tech. Pasadena, CA); and SNODGRASS,
H.B.
(Lewis and Clark Coll. Portland, OR)
The Extended Solar Activity
Nature **333** (April 1988)

YEH, H.C., HEINEMANN, N. C. (Boston
Coll., Chestnut Hill, MA); GUSSENHOVEN,
M. S., HARDY, D.A., and REDUS, R.H.
(AFGL)
*Precipitating Polar Cap Particles during
Northward IMF*
SPIE Conf. Proc. and Reprint Series 7 (1988)

PRESENTATIONS 1987-1988

ALTROCK, R.C.
*Overlapping Solar Cycles as Discovered in
Coronal Fe XIV Emission*
169th Mtg. Am. Astron. Soc., Pasadena, CA
(5-9 January 1987)
The Extended Solar Cycle
NSO Mini-Symp. on Solar Cycle Processes,
Tucson,
AZ (6-7 April 1987)
Solar Cycle Coronal Variations
2nd Internat. Solar Cycle Wkshp., Fallen

Leaf Lake, CA (11-14 May 1987)

*The Relationship of Low Coronal Transients
to Chromospheric Phenomena; Variation of
5303A Emission during Solar Cycle 21*

9th Sac Peak Wkshp. on Solar and Stellar
Coronal Structure and Dynamics, Sunspot,
NM (17-21 August 1987)

*Evidence for an Extended Solar Cycle from
Fe XIV and Other Observations* NSO/HAO
Inter-Obs. Mtg., Santa Fe, NM (7-9 October
1987)

*Ground-Based Solar Coronal Observations
as a Possible Input to Atmospheric Models*
Wkshp. on Atmospheric Density and
Aerodynamic Drag Models for AF Oper.,
Hanscom AFB, MA (20-22 October 1987)
*Further Evidence for an Extended Solar
Cycle*

172nd Mtg. Am. Astron. Soc., Kansas City,
MO (5-9 June 1988)

*Results of Systematic Observations of the
Sun in Coronal Green Line Emission: Solar
Fe XIV 5303A Observations: Evidence for a
20-Year Solar Cycle*

IAU Mtg., Baltimore, MD (3-10 August 1988)

ALTROCK, R.C. (AFGL); and SIME, D.G.
(High Altitude Obs., Boulder, CO)
*Transient Events in Coronal Fe XIV and K-
Coronal Observations*
AGU Mtg., San Francisco, CA (5-9 December
1988)

ALTROCK, C. (AFGL); SMITH, R.C., and
Williams, D.A. (Natl. Solar Obs.,
Sunspot, NM)

*A Study of FeXIV Transients in the Low
Solar Corona and Their Relationship to
Other Forms of Solar Activity*
AGU Mtg., San Francisco, CA (6-11
December 1987)

BASINSKA, E.M., AND BURKE, W.J.
*Ionospheric Signatures of the FTE in the S3-
2 Data?*
AGU Mtg., Baltimore, MD (16-20 May 1988)

BLOCK, L.P. (Royal Inst. of Tech.,

Stockholm, Sweden); ROTHWELL, P.L. (AFGL); SILEVITCH, M.B. (Northeastern Univ., Boston, MA); and TANSKANEN, P. (Univ. of Oulu, Oulu, Finland)
Experimental Verification of Westward Traveling Surge Model
 AGU Mtg, San Francisco, CA (6-11 December 1987)

BRAUTIGAM, D.H., GUSSENHOVEN, M.S., and HARDY, D.A.
A Statistical Study on the Effects of IMF Bz and Solar Wind Speed on Auroral Ion Precipitation
 AGU Mtg, San Francisco, CA (6-11 December 1987)
Variation in Boundary Layer Spectra as a Variation of IMF Bz and Solar Wind Speed
 AGU Mtg., Baltimore, MD (16-20 May 1988)
The Effects of IMF Bz, By, and Solar Wind Speed on Precipitating Ion Global and Cusp Morphology
 XXVII COSPAR Mtg., Espoo, Finland (18-29 July 1988)
Response of Precipitating Ion and Electron Equatorward Boundary to Extended Periods of IMF Bz North
 AGU Mtg., San Francisco, CA (5-9 December 1988)

BRAUTIGAM, D.H., GUSSENHOVEN, M.S., MULLEN, E.G., and OBERHARDT, M.R.
Low Altitude Flux and Dose Measurements During Two Solar Flare Events
 STIP Symp., Huntsville, AL (12-14 May 1987)

BRAUTIGAM, D.H., MULLEN, E.G., GUSSENHOVEN, M. S., and FILZ, R.C.
A Comparison of Measured Dose in Polar Orbit with NASA Model Predictions
 AGU Mtg, Baltimore, MD (6-11 May 1987)

BROADFOOT, A.L., SANDEL, B.R. (Univ. of Arizona, Tuscon, AZ); and Knecht, D.J. (AFGL);
Interaction Analysis by Remote Sensing
 Proc. Ionospheric Effects Symp. 87,

Springfield, VA (6 May 1987)

BURKE, W.J.
Particle Acceleration by Obliquely Propagating Electromagnetic Fields
 Wkshp. on Active Experiments in Space, Kyoto, Japan (18-21 October 1987)

BURKE, W.J., and HEINEMANN, M.
Small Cross Section Plasma Beam Propagation Across Magnetic Fields in Space
 AGU Mtg., San Francisco, CA (6-11 December 1987)

BURKE, W.J., MALCOLM, P.R., and MURPHY, G.P.
A Beam-Induced Upset During the Flight of the Echo-7 Rocket
 AGU Mtg., San Francisco, CA (5-9 December 1988)

CAROVILLANO, R.L., HEINEMAN, N. C. (Boston Coll., Chestnut Hill, MA); Yeh, H.C. (MIT Haystack Obs., Westford, MA); Gussenhoven, M. S., and Hardy, D.A. (AFGL)
Dispersion at the Poleward Auroral Boundary
 Chapman Centenary Conf. on Auroral Physics, Cambridge, England (11-15 July 1988)

CLIVER, E.W.
Was the Eclipse Comet of 1893 a Disconnected Coronal Transient?
 STIP Symp., Huntsville, AL (12-15 May 1987)

CLIVER, E.W. (AFGL); and WEBB, D.F. (Emmanuel Coll, Boston, MA)
Are All Metric Type II Bursts Piston-Driven by Coronal Mass Ejections?
 Am. Astron. Soc. Mtg., Kansas City MO (5-9 June 1988)

CLIVER, E.W. (AFGL); CASE, H.V. (NASA/Goddard, Greenbelt, MD); and FORREST, D.J. (Univ. of NH, Durham,

NH)

Coronal Type II Shocks and Gamma Ray Line Emission From Solar Flares
172nd Am. Astron. Soc. Mtg., Kansas City, MO (5-9 June 1988)

CLIVER, E.W. (AFGL); FORREST, D.J. (Univ. of New Hampshire, Durham, NH); MCGUIRE, R.E., VON ROSENGINGE, T.T., REAMES, D.V., CASE, H. V. (NASA Goddard Space Flight Ctr., Greenbelt, MD); and KANE, S.R. (Univ. of California, Berkeley, CA);

Solar Flare Nuclear Gamma-Rays and Interplanetary Proton Events
20th Intl. Cosmic Ray Conf., Moscow, USSR (2-15 August 1987)

COOKE, D.L.

Double Layers in Contact Plasmas
AGU Mtg., San Francisco, CA (6-11 December 1987)
Computer Models of Steady State Electron Collection by SPEAR I
AIAA Aerospace Sci. Mtg., Reno, NV (January 1988)

COOKE, D.L. (AFGL); and Tautz, M. (Radex, Inc., Carlisle, MA)
Steady State Computer Simulation of Wake-Electron Temperature Enhancement
AGU Mtg., San Francisco, CA (5-9 December 1988)

COOKE, D.L., (AFGL); TAUTZ, M.F. (Radex, Inc., Carlisle, MA); and RUBIN, A.G. (AFGL)
The Sheath of a Positive Probe in a Flowing Plasma
12th Conf. on the Numerical Simulation of Plasma, San Francisco, CA (20-23 September 1987)

DENIG, W.F. (AFGL); and FOSTER, J.C. (MIT Haystack Obs., Westford, MA)
The Z5-27 -APR Gismos Campaign
AGU Mtg., San Francisco, CA (5-9 December 1988)

DENIG, W.F., MAYNARD, N.C., BURKE, W.J. (AFGL); and MAEHLUM, B.N. (Norwegian Defense Res. Est., Kjeller, Norway)
E-Field Measurements During Electron Beam Emissions on Maimik
AGU Mtg., San Francisco, CA (6-11 December 1987)
Electric Field Measurements During Pulsed Electron Beam Operations on the Maimik Rocket
XXVII COSPAR Mtg., Espoo, Finland (18-29 July 1988)

DENIG, W.F. (AFGL); MENDE, S.B., SWENSON, G.R. (Lockheed, Palo Alto, CA); KENDALL, D.J.W., GATTINGER, R.L. (Natl. Res. Council, Ottawa, Canada); and LLEWELLYN, E.J. (Univ. of Saskatchewan, Saskatoon, Canada)
Measurements of Shuttle Glow on Mission 41-G
Fifth Intl. Ionospheric Effects Symp., Springfield, VA (5-7 May 1987)

DENIG, W.F., MAYNARD, N.C. (AFGL); MAEHLUM, B.N., SVENES, K., TROIM, J. (Norwegian Def. Res. Est., Kjeller, Norway); FRIEDRICH, M. (Tech. Univ., Graz, Austria); TORKAR, K. (Austrian Acad. of Sci. Graz, Austria); and HOLMGREN, G. (Swedish Inst. of Space Phys., Sweden)
MAIMIK, A Tethered Mother-Daughter Electron Accelerator Rocket
Second Intl. Conf. on Tethers in Space, Venice, Italy (6-8 October 1987)
Plasma Phenomena Observed Several Hundred Meters Away from a Charged Space Vehicle in the Ionosphere
XXVII COSPAR Meeting, Espoo, Finland (18-29 July 1988)

DOBSON-HOCKEY, A.K. (Natl. Solar Obs., Sunspot, NM); and RADICK, R.R. (AFGL)
Coronal Activity and Rotation of Late-Type Stars
169th Mtg. Am. Astron. Soc., Pasadena, CA (5-9 January 1987)

DONATELLI, D.E.

Indeed Perturbations in Space Plasma

Third Intl. School for Space Simulation, La
Londe-Les-Maures and Beaulieu, France (15-
27 June 1987)

DONATELLI, D.E., and ERNSTMEYER, J.

*Virtual Cathode Formation During Electron
Beam Experiments*

AGU Mtg., San Francisco, CA (6-11
December 1987)

DONATELLI, D.E., ERNSTMEYER, J.

(AFGL); and COHEN, H.A. (W.J. Schaefer
Assoc., Arlington, VA)

*Plasma Beam Emissions at Geosynchronous
Altitudes*

AGU Mtg., Baltimore, MD (18-22 May 1987)

DRESSLER, R.

*Laser Probing of Ion Velocity Distributions in
Drift Fields: Doppler Profile Measurements
of Ba+ in He*

MOLEC VII, 7th European Conf. on
Dynamics of Molecular Collisions, Assisi, Italy
(5-9 September 1988)

DUBS, C.W., and COOKE, D.L.

*Kinetic Interactions and Ion Heating in and
Around an Orbiting Polarized Plasma Cloud*
AGU Mtg., San Francisco, CA (5-9 December
1988)

ERICKSON, G.M., and HEINEMANN, M.

*Physical Stability Limit on Sunward-
Convection Models*

AGU Mtg., San Francisco, CA (5-9 December
1988)

ERNSTMEYER, J.

*Simple Two Fluid Modeling of a Virtual
Cathode*

AGU Mtg., San Francisco, CA (6-11
December 1987)

ERNSTMEYER, J., and GINET, G.

*Electromagnetic Waves in the Wake of the
Echo-7 Electron Beam*

AGU Mtg., San Francisco, CA (5-9 December
1988)

ERNSTMEYER, J., DONATELLI, D.E.,

MURPHY, G. (AFGL); and COHEN, H.A.
(W.J. Schaefer Assoc., Arlington, VA)

*Spacecraft Charging and Wave Emission
During Electron Gun Operations*

AGU Mtg., Baltimore, MD (18-22 May 1987)

FILZ, R.C.

*A New Measurement of 20 MeV Trapped
Protons at Low L-Values —*

Evidence for a Leveling in Long Term Decay

AGU Mtg., San Francisco, CA (8-12
December 1987)

FLUCKIGER, E.O. (Univ. of Bern,

Switzerland); SHEA, M.A., and SMART,
D.F. (AFGL)

*On the Latitude Dependence of Cosmic Ray
Cutoff Rigidity Variations During the Initial
Phase of a Geomagnetic Storm*

20th Intl. Cosmic Ray Conf., Moscow, USSR
(2-15 August 1987)

FOSTER, J.C. (MIT Haystack Obs.,

Westford, MA); BYTHROW, P. F. (The
Johns Hopkins Univ., Laurel, MD);

Maynard, N. C. (AFGL); and

WINNINGHAM, J. D. (SRI, San Antonio,
TX)

Equipotential Contours and Charged

Particle Boundaries in the Pre-Midnight

*Sector: A Composite from DE and Millstone
Hill*

AGU Mtg., San Francisco, CA (6-11
December 1987)

FREDERICKSON, A.R.

*Partial Discharge Phenomena in Space
Applications*

Centre D'Etudes et de Recherches De
Toulouse, Toulouse, France (1988)

FRUSHON, C.J., 1Lt, and GAUDET, J.A., LT
COL

Large Space Systems Environmental

Entanglements

AIAA 26th Aerospace Sci. Mtg., Reno, NV
(11-14 January 1988)

FUJII, R., HOFFMAN, R.A. (NASA/Goddard
Space Flight Center, Greenbelt, MD);
SUGIURA, M. (Kyoto Univ., Kyoto, Japan);
Craven, J.D., Frank, L.A. (Iowa Univ.,
Iowa City, IA); and MAYNARD, N.C.
(AFGL)

*The Field-Aligned Current System
Associated with Bulge-Type Auroral
Expansion*

AGU Mtg., Baltimore, MD (16-20 May 1988)

GREEN, B.D., LINTZ, A., CALEDONIA, G.E.,
PERSON, J., JOSHI, P., STAIR, A.T., MURAD,
E., AHMADJIAN, M., and HASTINGS, D.

*Shuttle Experiments to Measure the Optical
Environments Surrounding Large Space
Structures*

AIAA 26th Aerospace Mtg., Reno, NV (13
January 1988)

GUSSENHOVEN, M.S.

Recent Space Environment Measurements

Fifth Annual Symp. on Single Event Upsets
Los Angeles, CA (7-8 April 1987)

*Quiet-Time Convection and Precipitation in
the Polar Caps*

XIX General Assembly, IUGG, Vancouver,
Canada (9-22 August 1987)

*New Radiation Measurements at Low-
Altitudes*

Conf. on the High Energy Radiation
Background in Space, Sanibel Island, FL (3-5
November 1987)

*Particle Access to the Polar Caps During
IMF Bz Northward*

AGU Mtg., San Francisco, CA (5-9 December
1988)

*Polar Rain and the Question of Direct
Particle Access*

NATO Wkshp. on Electromagnetic Coupling
in the Polar Clefts and Caps, Lillehammer,
Norway (20-24 September 1988)

GUSSENHOVEN, M.S. (AFGL); and BASS,

J.N. (RADEX, Inc., Bedford, MA)

*The Baseline Magnetosphere in the Near-
Geosynchronous Region Derived from
SCATHA Data*

AGU Mtg., Baltimore, MD (16-20 May 1988)

GUSSENHOVEN, M.S. (AFGL); and
MADDEN, D. (Boston Coll., Chestnut Hill,
MA)

A Polar Rain Index

AGU Mtg., San Francisco, CA (6-11
December 1987)

GUSSENHOVEN, M.S., BRAUTIGAM, D.H.,
and MULLEN, E.G.

*Characterizing Solar Flare High Energy
Particles in Near-Earth Orbits*

1988 IEEE Annual Conf., Portland, OR (11-
15 July 1988)

GUSSENHOVEN, M.S., HARDY, D.A., and
MULLEN, E.G.

*Comparison of DMSP Precipitating Ion
Maps and SCATHA Atlas Ion Maps*

AGU Mtg., Baltimore, MD (18-22 May 1987)

GUSSENHOVEN, M.S., RICH, F.J., EVANS,
D.S. (AFGL); HEINEMANN, N.C. (Boston
Coll., Chestnut Hill, MA); CRAVEN, J.D.,
FRANK, L.A. (Univ. of Iowa, Iowa City,
IA); and HEELIS, R. A. (Univ. of Texas,
Richardson, TX)

*Satellite Data Overview of the ETS/GTMS
Period: 17-24 September 1984*

AGU Mtg., San Francisco, CA (5-9 December
1988)

HALL, W.N.

Space System Electrostatic Discharge Testing

10th Aerospace Testing Seminar, Los
Angeles, CA (10-12 March 1987)

*Large Space System Environmental
Entanglements*

26th AIAA Aerospace Sciences Mtg., Reno,
NV (11-14 January 1988)

HARDY, D.A.

New Measurements of the Low Altitude

Space Radiation Environment

NATO Advance Inst. on Terrestrial Radiation and Its Radiobiological Effects, Corfu, Greece (11-24 October 1987)

Overview of Global Auroral Electron and Ion Precipitation

Auroral Physics International Conf., Cambridge, England (11-15 July 1988)

HARDY, D.A., and BURKE, W.J.

Observation of Auroral Electron Precipitation Produced by VLF Waves

AGU Mtg., San Francisco, CA (6-11 December 1987)

HARDY, D.A., and GUSSENHOVEN, M.S.

Statistical Modeling of Auroral Particle Fluxes and Conductivities

Intl. Symp. on Quantitative Modeling of Magnetosphere-Ionosphere Coupling Processes, Kyoto, Japan (9-13 March 1987)

HARDY, D.A., GUSSENHOVEN, M.S., and BRAUTIGAM, D.H.

Magnetospheric Dynamics Leading to Average Patterns of Precipitating Ions in the Auroral Regions

AGU Mtg., Baltimore, MD (18-22 May 1987)

HARDY, D.A., GUSSENHOVEN, M.S., REDUS, R. (AFGL); HEINEMANN, N., and CAROVILLANO, R.L. (Boston Coll., Chestnut Hill, MA)

Particle Precipitation Patterns During the Small, Isolated Substorm: 18 January 1984

AGU Mtg., San Francisco, CA (5-9 December 1988)

HEINEMANN, M.

MHD Stability of the Magnetosphere

AGU Mtg., San Francisco, CA (7-11 December 1987)

Representations of Currents and Magnetic Fields in Anisotropic Magnetohydrostatic Plasma

AGU Mtg., San Francisco, CA (5-9 December 1988)

HEINEMANN, M., and YATES, G.K.

Equilibrium MHD Magnetosphere

AGU Mtg., Baltimore, MD (18-21 May 1987)

HEINEMANN, M., GUSSENHOVEN, M.S., and HARDY, D.A.

Dependence of the Low-Altitude Precipitating Electron Equatorward Auroral Boundary on Dst_e

AGU Mtg., San Francisco, CA (6-11 December 1987)

HEINEMANN, N.C. (Boston Coll., Chestnut Hill, MA); GUSSENHOVEN, M.S., HARDY, D.A., and RICH, F.J. (AFGL)

Electron/Ion Precipitation Difference in Relation to Region 2 Field-Aligned Currents

AGU Mtg., Baltimore, MD (16-20 May 1988)

HEINEMANN, N. C. (Boston Coll., Chestnut Hill, MA); GUSSENHOVEN, M.S. (AFGL); CRAVEN, L., FRANK, A. (Univ. of Iowa, Iowa City, IW); EVANS, D.S. (NOAA, Boulder, CO); and HEELIS, R.A. (Univ. of Texas at Dallas, Richardson, TX)

Satellite Data Overview of the ETS/GTMS Period: 17-24 September 1984

AGU Mtg., San Francisco, CA (5-9 December 1988)

HOFFMAN, R.A., SLAVIN, J.A. (NASA Goddard Space Flight Ctr., Wallops Island, VA); HANSON, W.B., HEELIS, R.A. (Univ. Texas at Dallas, Richardson, TX); MAYNARD, N.C. (AFGL); and SUGIURA, M. (Kyoto Univ., Kyoto, Japan)

Divergence of the Electric Field Associated with Electron Precipitation Structures

AGU Mtg., San Francisco, CA (5-9 December 1988)

KAHLER, S.W. (Emmanuel Coll., Boston, MA); and CLIVER, E.W. (AFGL)

Solar Energetic Proton Events and Coronal Mass Ejection Near Solar Minimum

Intl. Cosmic Ray Conf., Moscow, USSR (2-14 August 1987)

KEIL, S.L.

A Stabilized Spectral Time Sequence of High-Frequency Propagating Waves in the Solar Atmosphere

169th Mtg. Am. Astron. Soc., Pasadena, CA (5-9 January 1987)

The Effects of Magnetic Structures in the Solar Photosphere on Energy Transport Mechanisms

Am. Astron. Soc., Honolulu, HI (13-15 July 1987)

Granulation and Magnetic Concentrations
Wkshp. on Solar and Stellar Granulation,
Faraglioni, Italy (21-25 June 1988)

KEIL, S.L. (AFGL); and MOSSMAN, A.
(Wellesley Coll., Wellesley, MA)

Observations of High Frequency Waves in the Solar Atmosphere

Wkshp. on Solar and Stellar Granulation,
Faraglioni, Italy (21-25 June 1988)

KEIL, S.L. (AFGL); and ROUMELIOTIS, G.
(Natl. Solar Obs., Sunspot, NM)

Observations of High Frequency Oscillations Using the Agile Mirror

10th Sac Peak Wkshp. on High Spatial
Resolution Solar Obs., Sunspot, NM (22-26
August -1988)

KOUTCHMY, S. (AFGL); and LOUCIF, M.
(IAP, France)

The Coronal Solar Cycle as Revealed by the Large-Scale Coronal Features

Solar Cycle Wkshp., Fallen Leaf Lake, CA
(11-14 May 1987)

KOUTCHMY, S. (AFGL); and NOENS, J.C.
(OPMT, Bagneres de Bigorre, France)

About the Coronal Activity Cycles of the Sun
Fifth European Mtg. on Solar Physics,
Titisee, FRG (27-30 April 1987)

LAI, S.T.

Theory and Observation of Triple-Root Jump in Spacecraft Charging

AGU Mtg., Baltimore, MD (18 May 1987)

Triple-Root Jump in Spacecraft Charging:

Theory and Observation

Fourth Intl. Symp.: Spacecraft Materials in
Space Environment, Toulouse, France (6-9
September 1988)

Effect of Ion Beam Ionization on Spacecraft Charging

AGU Mtg., San Francisco, CA (5-9 December
1988)

LAI, S.T., and MURAD, E.

Comments on CIV Experiments in Space

AGU Mtg., San Francisco, CA (6-11
December 1987)

Feasibility and Consequences of Critical Velocity Ionization in Space Plumes

AIAA Aerospace Science Mtg., Reno, NV
(11-14 January 1988)

LAI, S.T. (AFGL); MCNEIL, W.J. (REX
Inc., Lexington, MA); and MURAD, E.
(AFGL)

Time Evolution of Critical Ionization Velocity Process in a Spacecraft Environment

Third Intl. School for Space Simulations, La-Londe-les-Maures and Beaulieu, France (15-27 June 1987)

Competing Processes Following Onset of CIV Discharges

AGU Mtg., Baltimore, MD (16-20 May 1988)

LAI, S.T., MURAD, E. (AFGL); and
MCNEIL, W. J. (REX, Inc., Bedford, MA)

An Overview of Atomic and Molecular Processes in Critical Velocity Ionization

Fifteenth IEEE Intl. Conf. on Plasma
Science, Seattle, WA (6-8 June 1988)

LUDLOW, G.R., HUGHES, W.J., and
CORNILLEAU-WEHLIN, N. (Boston Univ.,
Boston, MA); and Singer, H.J. (AFGL)

Observations of PC1 Events Using Ground-Based and Satellite Measurements

Intl. Union of Geodesy and Geophysics,
Vancouver, Canada (9-22 August 1987)

LUDLOW, G.R., HUGHES, W.J. (Boston
Univ., Boston, MA); CORNILLEAU-
WEHLIN, N. (CRPE/CNET, Molineaux,

FR); ARNOLDY, R.L. (Univ. of New Hampshire, Durham, NH); and SINGER, H.J. (AFGL)

Observations of PC1 Events Using Ground-Based and Satellite Measurements
Chapman Conf. on Plasma Waves and Instabilities in Planetary Magnetospheres and at Comets, Sendai, Japan (12-16 October 1987)

LUDLOW, G.G., HUGHES, W.J. (Boston Univ., Boston, MA); ENGEBRETSON, M.J. (Augsburg Coll., MN); Slavin, J.A. (NASA Goddard Space Flight Ctr., Greenbelt, MD); SUGIURA, M. (Kyoto, Univ., Kyoto, Japan); and SINGER, H.J. (AFGL)

Ground-Satellite Correlations of PC1 Events Near the Plasmasphere
AGU Mtg., Baltimore, MD (16-20 May 1988)
PC1 Waves Observed During Conjunctions of DE 1 and the AFGL Magnetometer Network
AGU Mtg., San Francisco, CA (5-9 December 1988)

VON DER LUHE, O. 1987, EsoNOAD Workshop on High-Angular-Resolution Imaging from The Ground Using Interferometric Techniques; Tucson, AZ, 12-15 Jan 87: *Application of the Knox-Thompson Method to Solar Observations*

VON DER LUHE, O. 1987, Eso-NOAD Workshop on High-Angular-Resolution Imaging from The Ground Using Interferometric Techniques; Tucson, AZ, 12-15 Jan 87: *Calibration Problems in Speckle Interferometry*

VON DER LUHE, O. 1987, Eso-NOAD Workshop on High-Angular-Resolution Imaging from The Ground Using Interferometric Techniques; Tucson, AZ, 12-15 Jan 87: *Study of Sizes, Brightnesses and Dynamics of Solar Facular Points*

MCNEIL, W.J. (RADEX, Bedford, MA); LAI, S.T., and MURAD, E. (AFGL)

Effect of Metastable States in Critical Velocity Ionization Processes
AGU Mtg., Baltimore, MD (18 May 1987)
Simulation of Collisional Processes in a Critical Ionization Discharge
AGU Mtg., San Francisco, CA (5-9 December 1988)

MAEHLUM, B., SVENES, K., TROIM, J. (Norwegian Defense Research Est., Kjeller, Norway); DENIG, W., MAYNARD, N. (AFGL); HANSEN, T. (Univ. of Tromsø, Norway); EGELAND, A., MASEIDE, K. (Univ. of Norway, Norway); WINNINGHAM, J. (SRI, San Antonio, TX); FRIEDRICH, M. (Tech. Univ., Norway); and HOLMGREN, G. (Uppsala Ionospheric Obs., Sweden)
MAIMIK — A High Current Electron Beam Experiment on Sounding Rocket from Andoya Rocket Range
ESA Symposium on Rockets, Sunne, Sweden (22 May 1987)

MAYNARD, N.C.
Large Scale Polar Cap Convection
1988 Cambridge Workshop, Cambridge, MA (13-17 June 1988)
High Latitude Convection Patterns
NATO Advanced Res. Wkshp. on Electromagnetic Coupling in the Polar Clefts and Caps (20-24 September 1988)

MAYNARD, N.C. (AFGL); and AIKIN, A.C. (NASA Goddard Space Flight Ctr., Greenbelt, MD)
A Van de Graf Source Mechanism for Anomalous Middle Atmospheric Electric Fields
AGU Mtg., San Francisco, CA (5-9 December 1988)

MAYNARD, N.C. (AFGL); SCHUNK, R.W., SOJKA, J.J. (Utah State Univ., Salt Lake City, UT); HEPPNER, J.P., and BRACE, L.A. (NASA/Goddard Space Flight Center, Greenbelt, MD)
A Test of the Applicability of Magnetospheric Convection Models for Northward IMF

Conditions

AGU Mtg., Baltimore, MD (16-20 May 1988)

MULLEN, E.G.

SPACERAD: A Comprehensive Space Radiation Effects Measurement Program
Conf. on High Energy Radiation Background in Space, Sanibel Island, FL (3-5 November 1987)

MULLEN, E.G., GUSSENHOVEN, M.S., and BRAUTIGAM, D.H.

Star Counts in Low Altitude Polar Orbit
AGU Mtg., Baltimore, MD (18-22 May 1987)

MULLEN, E.G., GUSSENHOVEN, M.S., and HARDY, D.A.

Satellite Charging from Electron Beam Emission on the SCATHA Satellite
AGU Mtg., San Francisco, CA (6-11 December 1987)

MULLEN, E.G., GUSSENHOVEN, M.S., BRAUTIGAM, D.H., and HOLEMAN, E.
Another Look at Low Altitude Cosmic Ray Cutoffs

AGU Mtg., San Francisco, CA (5-9 December 1988)

MURAD, E.

Applications of High Temperature Chemistry to Space Research
172nd Mtg. of the Electrochemical Society, Honolulu, HI (17-23 October 1987)

MURAD, E. (AFGL); and BOCHSLER, P. (Univ. of Bern, Bern, Switzerland)

The Role of Vaporization Processes in Cometary Atmospheres
AGU Mtg., Baltimore, MD (16-20 May 1988)

NEIDIG, D.F.

New Views of Solar White-Light Flares
New Mexico Symp. on New Astronomical Results/National Radio Astronomy Obs., Socorro, NM (10 November 1988)

NEIDIG, D.F. (AFGL); GROSSER, H. (Univ.

Sternwarte, Gottingen, FRG); and KIPLINGER, A.L. (NASA Goddard Space Flight Ctr., Greenbelt, MD)

The Largest White Light Flare Ever

Observed: 25 April 1984

STIP Symp. on Physical Interpretation of Solar/Interplanetary and Cometary Intervals, Huntsville, AL (12-15 May 1987)

The Spectrum and Energetics of the 25 April 1984 White Light Flare

Am. Astron. Soc. Mtg., Honolulu, HI (13 July 1987)

OBERHARDT, M.R., GUSSENHOVEN, M.S., MULLEN, E.G., and BRAUTIGAM, D.N.

Monitoring Magnetospheric Solar Particle Events with the DMSP/F7 Dosimeter
AGU Mtg., Baltimore, MD (18-22 May 1987)

OKSMAN, J., ROSENBERG, T.J., LANZEROTTI, L.J., MACLENNAN, C.G. (Univ. of Maryland, College Park, MD); and SINGER, H. J. (AFGL)

Study of Conjugate Pc 5-6 Magnetic and Absorption Pulsation Event at Sub-Auroral Latitudes in the Morning Sector
Intl. Union of Geodesy and Geophysics XIX - General Assembly, Vancouver, Canada (9-22 August 1987)

ORIENT, O.J., CHUTJIAN, A. (JPL, Pasadena, CA); and MURAD, E. (AFGL)
Generation of Fast, High-Flux Ground-State Oxygen Atom Beam

Intl. Conf. on the Physics of Electronic and Atomic Collisions, Brighton, UK (22-28 July 1987)

ORRALL, F.Q., LINDSEY, C.A., MICKEY, D.L. (Univ. of Hawaii, Honolulu, HI); DULK, G., ROTTMAN, G. (Univ. of Colorado, Boulder, CO); ALTROCK, R.C. (AFGL); FISHER, R. R. and SIME, D.G. (High Altitude Obs., Boulder, CO)

Observations of the Sun and Corona for the 1988 March 18 Total Solar Eclipse
Am. Astron. Soc. Mtg., Kansas City, MO 5-9 June 1988)

PFAFF, R.F., GOLDBERG, R.A. (NASA Goddard Space Flight Ctr., Greenbelt, MD); WITT, G., HALE, L. (Penn State Univ., University Park, PA); and MAYNARD N.C. (AFGL)

Electric Field Measurements in a Noctilucent Cloud

AGU Mtg., San Francisco, CA (5-9 December 1988)

PFAFF, R.F., HEPPNER, J., HOEGY, W., SLAVIN, J. (NASA Goddard Space Flight Ctr., Greenbelt, MD); Liebrecht, M.C. (SAR, Inc., Lanham, MD); and MAYNARD, N.C. (AFGL)

A Survey of Enhanced Sub-Auroral Electric Fields Observed by Dynamics Explorer-2

AGU Mtg., San Francisco, CA (5-9 December 1988)

RADICK, R.R., LOCKWOOD, G.W., THOMPSON, D.T., and SKIFF, B.A.

Long-Term Variability Characteristics of Lower Main-Sequence Hyades Stars

Am. Astron. Soc. Mtg., Pasadena, CA (5-9 January 1987)

Is Stellar Activity Responsible for the Hyades Anomaly?

Am. Astron. Soc. Mtg., Kansas City, MO (5-9 June 1988)

In Pursuit of Higher Photometric Precision

9th Annual Fairborn Obs./Smithsonian Astrophys. Obs. Symp., Tucson, AZ (February 1988)

RADICK, R.R., LOCKWOOD, G.W., THOMPSON, D.T., AND SKIFF, B.A. 1987, Am. Astron. Soc. Mtg. No 169, Pasadena CA, 5-9 Jan 87, Bull. Am. Astron. Soc. 18, 982, 1986 (Abstract Only). [Presented by R.R. Radick]: *Long-Term Variability Characteristics of Lower Main-Sequence Hyades Stars*

REDUS, R.H., GUSSENHOVEN, M.S., HARDY, D.A., and BRAUTIGAM, D.H.

Deviations from the Average Patterns of Auroral Ion Precipitation

AGU Mtg., Baltimore, MD (18-22 May 1987)

Quiet Time Deviations from Average Auroral Ion Precipitation Patterns

Cambridge Wkshp. on Theoretical Geoplasma Physics, Cambridge, MA (28 July - 1 August 1987)

REDUS, R.H., GUSSENHOVEN, M.S., HARDY, D.A. (AFGL); and HEINEMANN, N.

(Boston Coll., Chestnut Hill, MA)

Patterns of Electron and Ion Precipitation during IMF Bz North

AGU Mtg., San Francisco, CA (5-9 December 1988)

REDUS, R.H., GUSSENHOVEN, M.S., HARDY, D.A., and RICH, F.J.

A Polar Cap Arc Interval During the February 1986 Magnetic Storm: Part I, Particle and Current Morphology

AGU Mtg., Baltimore, MD (16-20 May 1988)

RICH, F.J., and MAYNARD, N.C.

Consequences of Using Simple Analytical Functions for the High-Latitude Convection Electric Field

AGU Mtg., Baltimore, MD (16-20 May 1988)

RICH, F., HARDY, D.A., GUSSENHOVEN, M.S., and BRAUTIGAM, D.H.

Variations of Cusp Ion Precipitation with Solar Wind Velocity and IMF Bz

AGU Mtg., San Francisco, CA (6-11 December 1987)

ROTHWELL, P.L.

A Unified Model for the WTS and the Generation of Pi 2 Pulsations

ULF Wave Mtg., New York, NY (22-23 October 1987)

ROTHWELL, P.L. (AFGL); BLOCK, L.P. (The Royal Inst. of Tech., Stockholm, Sweden); and SILEVITCH, M.B. (Northeastern Univ., Boston, MA)

Steady State Solutions for Auroral Arc Foundation during Substorm Breakup and Multi point Measurements

Intl. Conf. on Auroral Phys., Cambridge, UK
(11-15 July 1988)
COSPAR XXVII Plenary Mtg., Helsinki,
Finland (18-29 July 1988)

ROTHWELL, P.L. (AFGL); SILEVITCH, M.
(Northeastern Univ., Boston, MA); and
BLOCK, L. P. (Royal Inst. of Tech.,
Stockholm, Sweden)

*The Dynamics of the Westward Traveling
Surge and the Temperature Anisotropy of
Plasma Sheet Electrons*

21st ESLAB Symp., Bolkesjo, Norway (22-25
June 1987)

*The Motion of the Westward Traveling Surge
and Electron Temperature Anisotropy in the
Plasma Sheet*

IAGA Conf., Vancouver, Canada (9-22 August
1987)

*Multipoint Experimental Verification of
Westward Traveling Surge Model*

Intl. Conf. on Auroral Physics, Cambridge,
England (11-15 July 1988)

COSPAR XXVII Plenary Mtg., Helsinki,
Finland (18-29 July 1988)

ROTHWELL, P.L. (AFGL); SILEVITCH, M.
(Northeastern Univ., Boston, MA); Block,
L.P., and Falthammer, C.G. (Royal Inst.
of Tech., Stockholm, Sweden)

*Stability of Auroral Arc Formation During
Substorm Breakup*

AGU Mtg., San Francisco, CA (5-9 December
1988)

ROTHWELL, P.L. (AFGL); SILEVITCH, M.B.
(Northeastern Univ., Boston, MA);
BLOCK, L.P. (Royal Inst. of Tech.,
Stockholm, Sweden); and Tanskanen, P.
(Univ. of Oulu, Oulu, Finland)

*Solutions for Auroral Arc Formation During
Substorm Breakup*

AGU Mtg., San Francisco, CA (6-11
December 1987)

RUBIN, A.G., and BESSE, A.L.

*Effect of Spacecraft Size on Charging to High
Negative Potentials during Passage thru the*

Aurora

AGU Mtg., Baltimore, MD (18-21 May 1987)

SHEA, M.A.

Heliospheric Environment

Intl. Union of Geodesy and Geophysics, XIX
General Assembly, Vancouver, Canada (9-22
August 1987)

SHEA, M.A. (AFGL); and DRYER, M.
(NOAA, Boulder, CO)

Overview of STIP Intervals XV-XIX

STIP Symp. on Physical Interpretation of
Solar/Interplanetary and Cometary Intervals,
Huntsville, AL (12-14 May 1987)

SHEA, M.A., and SMART, D.F.

*Summary of New Results Relating to the
Solar and Galactic Cosmic Ray Environment
(1983-1986)*

Single Event Effects Symp., Los Angeles, CA
(7-8 April 1987)

SHEA, M.A., SMART, D.F. (AFGL); and
FLUCKIGER, E.O. (Univ. Bern,
Switzerland)

*Probable Detection of Solar Neutrons by
Ground-Level Neutron Monitors During
STIP Interval XVI*

STIP Symp. on Physical Interpretation of
Solar/Interplanetary and Cometary Intervals,
Huntsville, AL (12-14 May 1987)

SHEA, M.A., SMART, D.F., and LAL, D.
*Calculated Change in the Flux of Galactic
Cosmic Radiation Incident on the Earth's
Atmosphere Due to Changes in the
Geomagnetic Field Over a Period of 25 Years*
Intl. Union of Geodesy and Geophysics,
Vancouver, Canada (9-22 August 1987)

SHEA, M.A., SMART, D.F. (AFGL);
FLUCKIGER, E.O. (Univ. Bern,
Switzerland); and HUMBLE, J.E.
(Emmanuel Coll., Boston, MA)

*Difficulties Associated with the Ground-Level
Detection of Solar Neutrons on 25 April 1984*
2nd NASA Wkshp. on Impulsive Solar Flares,

(26-28 September 1988)

SHEA, M.A., SMART, D.F. (AFGL);
MCKINNON, J.A. and ABSTON, C.C.
(NOAA, Boulder, CO)

*Solar Activity Asymmetries During the Last
Three Solar Cycles*

AGU Mtg., San Francisco, CA (7-11
December 1987)

SHEA, M.A., SMART, D.F. (AFGL);
HUMBLE, J. E. (Emmanuel Coll., Boston,
MA); FLUCKIGER, E.O. (Univ. Bern,
Switzerland); GENTILE, L.C., and NICHOL,
M. (Emmanuel Coll., Boston, MA)

*A Revised Standard Format for Cosmic Ray
Ground-Level Event Data*

20th Int. Cosmic Ray Conf., Moscow, USSR
(2-15 August 1987)

*Difficulties in Acquiring a Standardized Set
of Cosmic Radiation Data for Solar Ground-
Level Cosmic Ray Events*

Intl. Union of Geodesy and Geophysics,
Vancouver, Canada (9-22 August 1987)

*Problems Associated with Assembling
Neutron Monitor Data for Ground-Level
Solar Cosmic Ray Events*

11th European Cosmic Ray Symp.,
Balatonfured, Hungary (21-27 August 1988)

SHEA, M.A., SMART, D.F. (AFGL);
MCKINNON, J.A., ABSTON, C.C. (NOAA,
Boulder, CO); COFFEY, H.E., SWINSON,
D.B., and HUMBLE, J.E. (Emmanuel
Coll., Boston, MA)

*Anomalous Episodes of Solar Activity Since
the IGY*

11th European Cosmic Symp., Balatonfured,
Hungary (21-27 August 1988)

SHEA, M.A., SMART, D.F. (AFGL);
STO.ZHKOV, Y.I., SVIRZHEVSKY, N.S.,
SVIRZHEVSKAYA, A.K., BAZILEVSKAYA, G.A.
(Lebedev Physical Inst., Moscow, USSR);
CHARACKCHYAN, T. N. (Moscow State
Univ., Moscow, USSR);

*Cosmic Ray Latitude Surveys in the Atlantic
Ocean Area*

20th Intl. Cosmic Ray Conf., Moscow, USSR
(2-15 August 1987)

SIME, D.G., FISHER, R.R., (HAO, Boulder,
CO), and ALTROCK, R.C.

*Rotation Characteristics of the Fe XIV
(5303A) Corona*

Internat. Solar Cycle Wkshp., Fallen Leaf,
CA (11-14 May 1987)

SIMON, G.W.

Magnetoconvection on the Solar Surface

MIT Symp. on Phys. of Space Plasmas,
Boston, MA (26 January 1988)

*Observations of the Size and Spacing of
Mesogranules*

Sac Peak Wkshp., Sunspot, NM (22-26
August 1988)

SIMON, G.W. (AFGL); and WEISS, N.O.
(Cambridge Univ., Cambridge, UK)

*Simulation of Surface Flows in
Supergranulation*

Am. Astron. Soc. Mtg., Pasadena, CA (5-8
January 1987)

*A Simple Model of Mesogranular and
Supergranular Flows*

NATO Advanced Res. Wkshp., Faraglioni,
Italy (21-25 June 1988)

*Simulating Plumes and Sinks Observed at
the Solar Surface*

Sac Peak Wkshp., Sunspot, NM (22-26
August 1988)

SIMON, G.W. (AFGL); FERGUSON, S.,
TARBELL, T., TITLE, A.M., TOPKA, K.
(Lockheed, Palo Alto, CA); November, L.
(Natl. Solar Obs., Sunspot NM); and
ZIRIN, H. (Calif. Inst. Tech., Pasadena,
CA)

*On the Relation Between Large-Scale
Granular Flow and Supergranules and
Mesogranules*

Am. Astron. Soc. Mtg., Honolulu, HI (13-15
July 1987)

SIMON, G.W. (AFGL); TITLE, A.M., TOPKA,
K.P., TARBELL, T.D., SHINE, R.A.,

FERGUSON, S.H. (Lockheed, Palo Alto, CA); and Zirin, H. (Calif. Inst. Tech., Pasadena, CA)

The Relation between Convection Flows and Magnetic Structure at the Solar Surface
XXVII COSPAR, Espoo, Finland, (18-29 July 1988)

SIMON, G.W. (AFGL); NOVEMBER, L.J. (Natl. Solar Obs., Sunspot, NM); Zirin, H. (Calif. Inst. Tech., Pasadena, CA); TITLE, A.M., TOPKA, K.P., TARBELL, T.D., SHINE, R.A., and FERGUSON, S.H. (Lockheed, Palo Alto, CA)

Variability of Solar Mesogranulation
XXVII COSPAR Mtg., Espoo, Finland, (18-29 July 1988)

SIMON, G.W., et. al.
Symposium on Outstanding Problems in Solar System Plasma Physics: Theory and Instrumentation, Yosemite, CA, 2-5 Feb. 1988. [Presented by G.W. Simon]: *Magnetoconvection on the Solar Surface*

SIMON, G.W., et. al.
Workshop on Solar and Stellar Granulation (NATO Advanced Research Workshop), Faraglioni, Italy, 21-25 June 88 [Presented by G.W. Simon]: *Details of Large Scale Solar Motions Revealed by Granulation Test Particles*

SINGER, H.J. (AFGL); and HUGHES, W.J. (Boston Univ., Boston, MA)

Development of a Pi 2 Wave Index for Substorm Detection and It's Comparison with the AL Index
AGU Mtg., San Francisco, CA (5-9 December 1988)

SINGER, H.J., and ROTHWELL, P.L.
Ring Current Effects on Magnetospheric Magnetic Field Geometry and Standing Alfvén Wave Eigen-Frequencies
Intl. Union of Geodesy and Geophysics, Vancouver, Canada (9-22 August 1987)

SINGER, H.J. (AFGL); HONES, JR., E.W. (Los Alamos National Lab., Los Alamos, NM); and ROSENBERG, T.J. (Univ. of Maryland, College Park, MD)

The Relation Between Magnetic Pulsations Observed During Substorms at Mid Latitudes and Plasma Sheet Thickening in the Near Magnetotail

AGU Mtg., San Francisco, CA (7-11 December 1987)

Multipoint Measurements from Substorm Expansion Onset to Recovery: The Relation between Magnetic Pulsations and Plasma Sheet Thickening
XXVII COSPAR Mtg., Espoo, Finland (18-29 July 1988)

SINGER, H.J. (AFGL); HUGHES, W.J. (Boston Univ., Boston, MA); CRAVEN, J.D., and FRANK, L.A. (Univ. of Iowa, Iowa City, IA)

DE-I Auroral Images and Ground-Based Magnetic Observations at Substorm Onset: CDAW-8
AGU Mtg., Baltimore, MD (18-21 May 1987)

SMART, D.F., and SHEA, M.A.
Advanced Solar Proton Prediction Model (PPS-87)

Single Event Effects, Sixth Annual Mtg., Los Angeles, CA (5-6 April 1988)
PPS-87: A New Event Oriented Solar Proton Prediction Model

XXVII COSPAR Mtg., Espoo, Finland (18-29 July 1988)

The Concept of "Flagship" Stations for Neutron Monitor Detection of Ground-Level Solar Cosmic Ray Events
11th European Cosmic Ray Symp., Balatonfüred, Hungary (21-27 August 1988)
AGU Mtg., San Francisco, CA (5-9 December 1988)

SMART, D.F., SHEA, M.A. (AFGL); and GENTILE, L.C. (Emmanuel Coll., Boston, MA)
Vertical Cutoff Rigidities Calculated Using the Estimated 1985 Geomagnetic Field

Coefficients

20th Intl. Cosmic Ray Conf., Moscow, USSR
(2-15 August 1987)

SMITHSON, R.C., ACTON, D.S., PERI, M.L.,
SHARBAUGH, R.J. (Lockheed, Palo Alto,
CA); DUNN, R.B. (Natl. Solar Obs.,
Sunspot, NM); VON DER LUHE, O., and
KEIL, S.L. (AFGL)

*Observational Results in Solar Astronomy
with the Improved Lockheed Active Mirror
System*

Am. Astron. Soc. Mtg., Kansas City, MO (5-9
June 1988)

SMITHSON, R.C., SHARBAUGH, R.J.,
RAMSEY, H.E., ACTON, D.S., PARI, M.,
KEIL, S.L., RADIC, R.R., SIMON, G.W., VON
DER LUHE, O., AND ZIRKER, J.B. 1987, Am.
Astron. Soc. Mtg. No. 169, Pasadena CA,
5-9 Jan. 87, Bull. Am. Astron. Soc. 18,
933, 1986 (Abstract Only). [Presented by
R.C. Smithson]: *Initial Solar Observations
at Sacramento Peak Using The Lockheed
Active Optics System*

SPRUETT, H.C. (Natl. Solar Obs., Sunspot,
NM); and SIMON, G.W. (AFGL)
*What Determines the Temperature of a
Sunspot?*
Am. Astron. Soc. Mtg., Honolulu, HI (13-15
July 1987)

SWIDER, W., GUSSENHOVEN, M.S., REDUS,
R.H., HARDY, D.A. (AFGL); and MADDEN,
D. (Boston Coll., Chestnut Hill, MA)
*Low Energy Ion Precipitation during the
February 6-10, 1986, Magnetic Storm*
AGU Mtg., San Francisco, CA (5-9 December
1988)

TOPKA, K., FERGUSON, S., TITLE, A.,
TARBELL, T. (Lockheed, Palo Alto, CA);
Zirin, H. (Calif. Inst. Tech., Pasadena,
CA); SIMON, G. (AFGL); and NOVEMBER,
L. (National Solar Obs., Sunspot, NM)
*Simultaneous Observations of Emerging
Flux from the Big Bear Solar Observatory*

and the SOUP Instrument on Spacelab 2
Am. Astron. Soc. Mtg., Honolulu, HI (13-15
July 1987)

VON DER LUEHE, O.
Solar Image Stabilization
169th Mtg. Am. Astron. Soc., Pasadena, CA
(5-9 January 1987)

WEIMER, D.R. (Regis College, Weston,
MA); and MAYNARD, N.C., BURKE, W.J.
(AFGL)
Auroral Current Oscillations
AGU Mtg., San Francisco, CA (7-11
December 1987)

WEIMER, D.R. (Regis Coll., Weston, MA);
RICH, F.J. (AFGL); and BASU, S.
(Emmanuel Coll., Boston, MA)
*Large-Scale Fluctuations in the Density of
the High-Latitude Plasma at 830 km
Altitude*
AGU Mtg., Baltimore, MD (18-22 May 1987)

WODARCZYK, F.J. (AFOSR, Washington,
DC); SALTER, R.H., and MURAD, E.
(AFGL)
*The Reaction of N_2^+ with H_2O , D_2O , and
 D_2O^{18}*
40th Annual Gaseous Electronics Conf.,
Atlanta, GA (13-16 October 1987)

YASUKAWA, E.A. (High Altitude Obs.,
Boulder, CO); ALTROCK, R.C. (AFGL);
FISHER, R.R., and SIME, D.G. (High
Altitude Obs., Boulder, CO)
*Long Term Variations in the Integrated Fe
XIV Green Line Flux*
Am. Astron. Soc. Mtg., Honolulu, HI (13-15
July 1987)

YEH, H.C., FOSTER, J.C., HOLT, J.M. (MIT
Haystack Obs., Westford, MA); REDUS,
R.H., and RICH, F.J. (AFGL)
*Radar and Satellite Observations in the
Dayside Cusp for the February, 1986
Magnetic Storm*
AGU Mtg., Baltimore, MD (16-20 May 1988)

TECHNICAL REPORTS **1987-1988**

DUBS, C.W.
Theoretical Analysis of Charging Data from Rocket with Charged Beam Emission
AFGL-TR-86-0209 (2 October 1986),
ADA183853

DUBS, C.W., and COOKE, D.L.
Particle Trajectories and Potentials in a Plane Sheath Moving in a Magnetoplasma
AFGL-TR-87-0225 (15 July 1987),
ADA196228

HEINEMANN, N. (Boston Coll., Chestnut Hill, MA)
The Equatorward Boundary of Auroral Ion Precipitation
AFGL-TR-87-0141 (6 May 1987), ADA180295

HEINEMANN, M., RUBIN, A. (AFGL);
TAUTZ, M., and COOKE, D. (Radex Corp., Carlisle, MA)
Computer Models of the Spacecraft Wake
AFGL-TR-86-0160 (24 July 1986),
ADA176881

SHUMAN, B.M., and COHEN, H.A.
An Automatic Charge Control System for Satellites
AFGL-TR-88-0245 (26 September 1988),
ADA201452

TAUTZ, M.F. (Radex Inc., Carlisle, MA);
and COOKE, D.L. (AFGL)
Preliminary Documentation for the MACH Code
AFGL-TR-88-0035 (January 1988),
ADA198956

CONTRACTOR PUBLICATIONS **1987-1988**

AN, C.H., BAO, J.J., AND WU, S.T. (U. Alabama, Huntsville) 1987, "Foundation of Active Region and Quiescent Prominence Magnetic Field Configurations, Coronal and Prominence Plasmas," (A. Poland, editor) NASA Publication 2442, 47-50.

AN, C.H., BAO, J.J., AND WU, S.T. (U. Alabama, Huntsville) 1988, "Numerical Simulation of Mass Injection for the Formation of Prominence Magnetic Field Configurations, I. Asymmetric Injection," *Solar Physics* 115, 81-92.

AN, C.H., BAO, J.J., WU, S.T., AND SEUSS, S.T. (U. Alabama, Huntsville) 1988, "Numerical Simulation of Mass Injection for the Formation of Prominence Magnetic Field Configurations II. Symmetric Injection," *Solar Physics* 115, 93-106.

AN, C.H., BAO, J.J., WU, S.T., AND SEUSS, S.T., (U. Alabama, Huntsville) 1988, "MHD Simulations for Quiescent Prominence Formation by Photospheric Shearing or Converging Motions," Dynamics and Structure of Solar Prominences, Proc. of a workshop held at Palma de Mallorca, Nov. 18-29 (J.L. Ballester and E.R. Priest, eds.).

BASINSKA, E.M. (Regis Coll., Weston, MA); BURKE, W.J. (AFGL); BASU, S. (Emmanuel Coll., Boston, MA); RICH, F.J., and Fougere, P.F. (AFCL)
Low Frequency Modulation of Plasma and Soft Electron Precipitation Near the Dayside Cusp
J. Geophys. Res. 92 (1987)

CODONA, J.L. (U. of Calif., San Diego), "The Scintillation Theory of Eclipse Shadow Bands," *Astron. & Astrophys.*, 164, 415.

DING, Y.J., HAGYARD, M.J., DELOACH, A.C., HONG, Q.F., AND LIE, X.P.

- (NASA/MSFC) 1987, "Explorations of Electric Current Systems in Solar Active Region. I. Empirical Inferences of the Current Flows," *Solar Phys.*, 109, 307.
- DRYER, M., SMITH, Z.K., AND WU, S.T. (U. Alabama, Huntsville) 1988, "The Role of Magnetohydrodynamics in Heliospheric Space Plasma Physics Research," *Astrophysics & Space Sciences* 114, 407-425.
- GARY, G.A., MOORE, R.L., HAGYARD, M.J., AND HAISCH, B.M. (NASA/MSFC) 1987, "Non-Potential Features Observed in the Magnetic Field of an Active Region," *Ap. J.*, 314, 786.
- GOLUB, L., and KALUTA, K. (Smithsonian Astrophys. Obs., Cambridge, MA) *High Resolution Imaging Detector for Use with a Soft X-Ray Telescope* Proc. of SPIE 733 (1986)
- HAGYARD, M.J. (NASA/MSFC) 1987, "Changes in Measured Vector Magnetic Fields When Transformed into Heliographic Coordinates," *Solar Phys.*, 107, 239.
- HAGYARD, M.J. (NASA/MSFC) 1987, "The Relation of Sheared Magnetic Fields to the Occurrence of Flares," *Artificial Satellites*, 22, 69.
- HAGYARD, M.J. (NASA/MSFC) 1988, "Observed Nonpotential Magnetic Fields and the Inferred Flow of Electric Currents at a Location of Repeated Flaring," *Solar Phys.* 115, 107.
- HAGYARD, M.J. AND RABIN, D.M. (NASA/MSFC) 1986, "The Measurement and Interpretation of Magnetic Shear in Solar Active Regions," *Advanced Space Res.*, 6, 7.
- HAGYARD, M.J., GARY, G.A. AND WEST, E.A. (NASA/MSFC) 1988, "The SAMEX Vector Magnetograph," NASA Technical Memorandum 4048, Marshall Space Flight Center.
- HAIRSTON, M.R., and HEELIS, R.A. (Univ. of Texas, Richardson, TX) *Determination of the Ionospheric Convection Pattern from DMSP DATA* 1988 Cambridge Wkshp. Conf. Proc. 8 (1988)
- HAISCH, B.M., WHITEMORE, T.E., JOKI, E.G., BROOKOVER, W. J. (Lockheed Missile and Space Co.), "A Multilayer X-ray Mirror for Solar Photometric Imaging Flown on a Secondary Rocket," Proc. SPIE 982.
- JACKSON, B.V. (Univ. of California, La Jolla, CA) *Helios Photometer Measurements of In-Situ Density Enhancements* Adv. Space Res. 6 (1986)
- JACKSON, B.V. (University of California, San Diego), ROMPOLT, B. (High Altitude Observatory), and SVESTKA, Z. (University of California, San Diego), "Solar and Interplanetary Observations of the Mass Ejection on 7 May 1979," *Sol. Phys.* 115, 327-343 (1988).
- KAHLER, S.W., MOORE, R.L., KANE, S.R., AND ZIRIN, H. (NASA/MSFC) 1988, "Filament Eruptions and the Impulsive phase of Solar Flares," *Ap. J.* 328, 824.
- KALUTA, K., GOLUB, L. (Smithsonian Astrophys. Obs.) 1988, "Design Considerations for Soft X-ray Television Imaging Detectors," Proc. SPIE 982. X-ray Instrumentation in Astronomy (L. Golub, ed.)
- LOCKWOOD, G.W., AND SKIFF, B.A. (Lowell Obs.) 1988, "Luminosity Variations of Stars Similar to the Sun," GL-TR-88-0221.
- LOCKWOOD, G.W., AND SKIFF, B.A. (Lowell Obs.) 1988, "Some Stars with Solar-Like Brightness Variations," *Solar Radiative*

Output Variations (P. Foukal, ed.).

LOCKWOOD, G.W., AND SKIFF, B.A. (Lowell Obs.) 1987, "Monitoring Solar Type Stars for Luminosity Variations" in Second NASA/NBS Workshop in Improvements to Photometry, NASA CP-10015.

MACHADO, M.E., GARY, G.A., HAGYARD, M.J., SMITH, J.B., HERNANDEZ, A. AND ROVIRA, M.G. (NASA/MSFC) 1986, "Characteristics, Location and Origin of Flare Activity in a Complex Active Region," *Adv. Space Res.*, 6, 33.

MACHADO, M.E., AND MOORE, R.L. (NASA/MSFC) 1986, "Observed Form and Action of the Magnetic Energy Release in Flares," *Adv. Space Res.*, 6, 217.

MACHADO, M.E., MOORE, R.L., HERNANDEZ, A.M., ROVIRA, M.G., HAGYARD, M.J. AND SMITH, J.B. (NASA/MSFC) 1988, "The Observed Characteristics of Flare Energy Release. I. Magnetic Structure at the Energy Release Site," *Ap. J.* 326, 425.

MACHADO, M.E., XIAO, Y.C., WU, S.T., PROKAKIS, TH., AND DIALETIS, D. (NASA/MSFC) 1988, "The Observed Characteristics of Flare Energy Release. I. High Speed Soft X-ray Fronts," *The Astrophysical Journal* 326, 451-461.

MOORE, R.L. (NASA/MSFC) 1987, "Observed Form and Action of the Magnetic Field in Flares," *Solar Phys.* 113, 121.

MOORE, R.L. (NASA/MSFC) 1988, "Evidence that Coronal Mass Ejections are Magnetically Self-Propelled," in R.C. Altrock (ed.), *Solar and Stellar Coronal Structure and Dynamics*, National Solar Observatory, p. 520.

MOORE, R.L. (NASA/MSFC) 1988, "Evidence that Magnetic Energy Shedding in

Solar Filament Eruptions is the Drive in Accompanying Flares and Coronal Mass Ejections," *Ap. J.* 324, 1132.

MOORE, R.L., HAGYARD, M.J. AND DAVIS, J.M. (NASA/MSFC) 1987, "Flare Research with the NASA/MSFC Vector Magnetograph: Observed Characteristics of Sheared Fields that Produce Flare," *Solar Phys.* 113, 347.

NAKAGAWA, Y., HU, Y.Q., AND WU, S.T. (U. Alabama, Huntsville) 1987, "The Method of Projected Characteristics for Evolution of Magnetic Arches," *Astron. & Ap.*, 179, 354-370.

PORTER, J.G. AND MOORE, R.L. (NASA/MSFC) 1988, "Coronal Heating by Microflares," in R.C. Altrock (ed.), *Solar and Stellar Coronal Structure Dynamics*, National Observatory, p. 125.

PORTER, J.G., MOORE, R.L., REICHMANN, E.J., ENGVOLD, O., AND HARVEY, K.L. 1987, "Microflares in the Solar Magnetic Network," *Ap. J.*, 323.

SONG, M.T., WU, S.T., AND DRYER, M. (U. Alabama, Huntsville) 1987, "A Linear MHD Instability Analysis of Solar Mass Ejection with Gravitation," *Solar Phys.*, 108, 347-382.

STEINOLFSON, R.S. AND TAJIMA, T. (Inst. for Fusion Studies, Univ. Texas) 1987, "Energy Buildup in Coronal Magnetic Fields," *Astrophys. J.* 322, 503.

UNDERWOOD, J.H., BRUNER, M.E., HAISCH, B.M., BRUN, W.A., ACTON, L.W., "X-ray Photographs of a Solar Active Region with a Multilayer Telescope at Normal Incidence," *Science*, p. 61 (20 Oct 1987).

VENKATAKRISHNAN, P., HAGYARD, M.J. AND HATHAWAY, D.H. (NASA/MSFC) 1988, "Elimination of Projection Effects from Vector Magnetograms: The Pre-Flare Configuration

of Active Region AR4474," *Solar Phys.* 115, 125.

WEBB, D.F. (Emmanuel College), and B.V. JACKSON (University of California, San Diego), "Detection of CME's in the Interplanetary Medium from 1976-1979 Using HELIOS-2 Photometer Data," Proc. of the 6th Solar Wind Conference. 267-271 (1987).

WILSON, R.M. (NASA/MSFC) 1987. "Geomagnetic Response to Magnetic Clouds," *Planet Space Sci.*, 35, 329.

WILSON, R.M. (NASA/MSFC) 1987, "On Bimodality of the Solar Cycle and the Duration of Cycle 21," *Solar Phys.*, 108, 195.

WILSON, R.M. (NASA/MSFC), "Statistical Aspects of Solar Flares," *NASA Technical Paper 2714*, (April 1987).

WILSON, R.M. (NASA/MSFC) 1988, "Bimodality and the Hale Cycle," *Solar Phys.* 117, 269.

WILSON, R.M. (NASA/MSFC) 1988, "On the Long-Term Secular Increase in Sunspot Number," *Solar Phys.* 115, 379.

WILSON, R.M. (NASA/MSFC) 1988, "Predicting the Maximum Amplitude for the Sunspot Cycle from the Rate of Rise in Sunspot Number," *Solar Phys.* 117, 179.

WU, S.T. (U. Alabama, Huntsville), "Magnetohydrodynamic (MHD) Modeling of Solar Active Phenomena Via Numerical Methods," *Developments in Theoretical and Applied Mechanics XIV*, (S.Y. Wang, R.M. Hackett, S.L. Deleeuw and A.M. Smith, eds.), Univ. of Mississippi Press, Proceedings of SECTAM XIV (1988).

WU, S.T., BAO, J.J., AN, C.H., AND TANDBERG-HANSEN, E. (U. Alabama, Huntsville) 1988, "A Numerical

Magnetohydrodynamic (MHD) Simulation of Prominence Formation with Condensation and Thermal Conduction," *Dynamics and Structure of Solar Prominences*, Proc. of a workshop held at Palma de Mallorca, Nov. 18-29 (J.L. Ballester and E.R. Priest, eds.)

WU, S.T., BAO, J.J., AND WANG, J.F. (U. Alabama, Huntsville) 1987, "Numerical Simulation of Flare Energy Buildup and Release via Joule Dissipation," *Journal of Adv. Space Research*, 6, 53-56.

WU, S.T., DRYER, M., AND HAN, S.M. (U. Alabama, Huntsville) 1988, "Computational Mechanics '88 Theory and Applications," *Proceedings of the International Conference on Computational Engineering Science, ICE88-Atlanta, GA*, April, 10-14, 1988, Vol. 2 (S.N. Atluri, G. Yagawa, eds.), Springer-Variag, New York.

WU, S.T., AND WANG, J.F. (U. Alabama, Huntsville) 1987, "Numerical Tests of a Modified Full Implicit Continuous Eulerian (FICE) Scheme with Projected Normal Characteristic Boundary Conditions for MHD Flows," *Computer Methods in Applied Mechanics and Engineering* 64, No. 1-3.

WU, S.T., AND XIAO, Y.C. (U. Alabama, Huntsville) 1987, "Filament Formation Due to Photospheric Shear," *Coronal and Prominence Plasmas*, (A. Poland, editor) NASA Publication 2442, 51-56.

CONTRACTOR TECHNICAL REPORTS 1987-1988

ACTON, D.S., SMITHSON, R.C., ROEHIG, J.R., and SHARBAUGH, R.J. (Lockheed, Palo Alto, CA)
Study of Fine Scale Solar Dynamics
AFGL-TR-88-0304 (23 October 1988),

ADA205182

BARKER, T.G. (5-Cubed, La Jolla, CA)
*Analytic and Observational Approaches to
 Spacecraft Auroral Charging*
 AFGL-TR-87-0021 (November 1986),
 ADA181456

BASINSKA, E.M. (Regis Coll., Weston, MA)
*Development of Software for the Analysis of
 Plasma Measurements Using the Retarding
 Potential Analyzer*
 AFGL-TR-84-0327 (20 December 1984),
 ADA176890

BATES, D.R. (Queen's Univ., Belfast, UK)
*Theoretical Studies of Atomic and Molecular
 Processes Important in Space Experiments*
 AFGL-TR-88-0158 (June 1988), ADA200699

CARPENTER, D.L., and CLAUER, C.R.
 (Stanford, Univ., Stanford, CA)
*Analysis of Coordinated Observations in the
 Region of the Day Side Polar Cleft*
 AFGL-TR-88-0120 (April 1988), ADA200627

DICHTER, B.K., and HANSER, F.A.
 (Panametrics, Inc., Waltham, MA)
*Demonstrate the Feasibility of a Detection
 Method to Separate Neutral Particles from
 Charged Particles in the MeV/Nucleon
 Energy Range*
 AFGL-TR-88-0202 (October 1988),
 ADA201114

DICKE, R.H., and KUHN, J.R. (Princeton
 Univ., Princeton, NJ)
Solar Distortion Measurements
 AFGL-TR-87-0098 (15 April 1987),
 ADA181116

DYER, G. (Kimball Physics, Inc., Wilton,
 NH)
High-Current Electron Gun for Space Flight
 AFGL-TR-86-0217 (31 August 1986),
 ADA179287

ELGIN, J.B., and SUNDBERG, R.L.

(Spectral Sciences, Inc., Burlington, MA)
*Model Description for the SOCRATES
 Contamination Code*
 AFGL-TR-88-0303 (21 October 1988),
 ADA205181

GARY, D.E., and HURFORD, G.J.
 (California Inst. of Tech., Pasadena, CA)
*Microwave Spectroscopy of a Solar Active
 Region Observed during a Partial Eclipse*
 AFGL-TR-87-0123 (April 1986), ADA181468

GENTILE, L., HOLEMAN, E., HUBER, A.,
 KAHLER, S., PANTAZIS, J., WEBB, D., and
 HAGAN, M.P. (Emmanuel Coll., Boston,
 MA)
*Satellite Instrument Development and Data
 Analysis*
 AFGL-TR-88-0041 (30 September 1987),
 ADA198921

GREEN, B.D., RAWLINS, W.T., CALEDONIA,
 G.E., MARINEIII, W.J., WHITE, C., SIMONS,
 G.A. (Physical Sciences, Inc., Andover,
 MA); GOLD, B., (EKTRON Applied
 Imaging); and MIRANDA, H. (Miranda
 Laboratories, Bedford, MA)
*The Determination of the Spacecraft
 Contamination Environment*
 AFGL-TR-87-0303 (October 1987),
 ADA196435

GREENSPAN, M.E., ANDERSON, P.B., and
 PELAGATTI, J.M. (Regis Coll., Weston,
 MA)
*Characteristics of the Thermal Plasma
 Monitor (SSIES) for the Defense
 Meteorological Satellite Program (DMSP)
 Spacecraft S8 Through D10*
 AFGL-TR-86-0227 (30 October 1986),
 ADA176924

HASTINGS, D.E., GATSONIS, N.A., and
 MOGSTAD, T. (Massachusetts Inst. of
 Technology, Cambridge, MA)
*A Simple Model for the Initial Phase of a
 Water Plasma Cloud about a Large Structure
 in Space*

AFGL-TR-87-0140 (4 May 1987), ADA187686

HEELIS, R.A. (Univ. of Texas at Dallas,
Richardson, TX)

*A Collaborative Study of Plasma
Irregularities from the HILAT Satellite*
AFGL-TR-87-0036 (January 1987),
ADA182597

HEGE, E.K. (Univ. of Arizona, Tucson,
AZ)

*Investigations of High Resolution Imaging
through the Earth's Atmosphere Using
Speckle Interferometry*
AFGL-TR-87-0097 (15 March 1987),
ADA189295

HORENSTEIN, M.N., and FREEMAN, G.
(Boston Univ., Boston, MA)

*A Projectile Probe for Measuring the Electric
Field Inside a Spacecraft Plasma Sheath*
AFGL-TR-87-0094 (3 March 1987),
ADA200957

HUGHES, W.J. (Boston Univ., Boston, MA)
*Geomagnetic Pulsation Studies Using the
AFGL Magnetometer Network*
AFGL-TR-87-0191 (June 1987), ADA183748

HUNERWADEL, J.L., SELLERS, B., and
HANSER, F.A. (Panametrics, Inc.,
Waltham, MA)

*Design, Fabricate, Calibrate, Test and
Deliver Two Satellite Electron Flux Detectors*
AFGL-TR-87-0205 (June 1987), ADA190799

JACKSON, B.V. (Univ. of California at San
Diego, La Jolla, CA)

*Scientific Background and Design
Specifications for a Near-Earth Heliospheric
Imager*
AFGL-TR-88-0195 (9 August 1988),
ADA205194

JONGEWARD, G.A., KATZ, I., MANDELL,
M.J., and LILLEY, J.R., JR. (S-Cubed, La
Jolla, CA)

Charging of a Man in the Wake of the Shuttle

AFGL-TR-86-0139 (July 1986), ADA182789
*Polar 2.0 Validation and Preflight SPEAR I
Calculations*
AFGL-TR-88-0056 (February 1988),
ADA201094

KALMAN, G.J., and LI, T. (Boston Coll.,
Chestnut Hill, MA)

*Neutral Beam Propagation through the
Atmosphere*
AFGL-TR-87-0267 (15 June 1987),
ADA188984

KAN, J.R. (Univ. of Alaska, Fairbanks,
AK)

*Pi2 Pulsations and the Westward Travelling
Surge in the Magnetosphere - Ionosphere
Coupling*
AFGL-TR-86-0244 (November 1986),
ADA180270

KATZ, I., JONGEWARD, G.A., LILLEY, J.R.,
and MANDELL, M.J. (S-Cubed, La Jolla,
CA)

*POLAR Code Calculations of the Shuttle
Orbiter Plasma Wake and Direct
Comparisons with Space-lab II
Measurements*
AFGL-TR-87-0041 (November 1986),
ADA181160

KATZ, I., MANDELL, M.J., PARKS, D.E.,
WRIGHT, K., STONE, N.H., and SAMIR,
U. (S-Cubed, La Jolla, CA)

*The Effect of Object Potentials on the Wake of
a Flowing Plasma*
AFGL-TR-87-0023 (December 1986),
ADA184038

LAFRAMBOISE, J.G. (York Univ., Ontario,
Canada); and Parker, L.W. (Lee W.
Parker, Inc., Concord, MA)

*Progress toward Predicting High-Voltage
Charging of Spacecraft in Low Polar Orbit*
AFGL-TR-86-0261 (28 October 1986),
ADA176939

LI, T., KALMAN, G., and PULSIFER, P.

(Boston Coll., Chestnut Hill, MA)
*Neutral Beam Propagation Effects in the
 Upper Atmosphere II*
 AFGL-TR-86-0192 (1 March 1986),
 ADA182601

LIN, C.C. (Univ. of Wisconsin, Madison,
 WI)
*Production of Atomic and Molecular
 Radiation by Electron Impact*
 AFGL-TR-88-0155 (8 September 1988),
 ADA200620

MOREL, P.R., HANSER, F.A., SELLERS, B.,
 COHEN, R., and KANE, B.D. (Panametrics,
 Inc., Waltham, MA)
*Fabricate, Calibrate and Test a Dosimeter for
 Integration into the CRRES Satellite*
 AFGL-TR-87-0232 (June 1987), ADA185439

PETERKA, D., and KATZ, I.(S-Cubed, La
 Jolla, CA)
*Documentation for the SHADO Particle Wake
 Routine*
 AFGL-TR-87-0042 (January 1987),
 ADA181531

RABALAIS, J.W. (Univ. of Houston,
 Houston, TX)
Inelastic Ion-Surface Collisions
 AFGL-TR-87-0206 (15 May 1987),
 ADA183167
*Inelastic Ion-Surface Collisions: Ion
 Neutralization on Intermetallic Surfaces*
 AFGL-TR-88-0137 (1 June 1988),
 ADA196500

RAITT, W.J. (Utah State Univ., Logan,
 UT)
*Modeling the F-Region of the High Latitude
 Ionosphere*
 AFGL-TR-86-0238 (7 November 1986),
 ADA178383

RAMSEY, L.W. (Pennsylvania State Univ.,
 University Park, PA)
*Development of High Stability Fiber Optic
 Spectrophotometric Systems for Study of*

Solar Stellar Magnetic Activity
 AFGL-TR-87-0218 (17 February 1987),
 ADA189327

ROBSON, R.R., WILLIAMSON, W.S., and
 SANTORU, J. (Hughes Research Labs.,
 Malibu, CA)
Flight Model Discharge System
 AFGL-TR-87-0143 (April 1987), ADA185657

ROELOF, E.C. (Johns Hopkins Univ.,
 Laurel, MD)
*Evidence for Regions of Negligible Cosmic-
 Ray Modulation in the Inner Heliosphere
 (<10 AU) AFGL-TR-88-0211 (14 September
 1988), ADA200018*
*Three-Dimensional Gradients of Solar
 Particles Inside 5 AU*
 AFGL-TR-88-0214 (14 September 1988),
 ADA200020

SASS, C.S., and RABALAIS J.W. (Univ. of
 Houston, Houston, TX)
*Ion Beam Induced Decomposition of
 Transition Metal Fluoroanions*
 AFGL-TR-88-0136 (9 June 1988),
 ADA197025

SECAN, J.A. (Physical Dynamics, Inc.,
 Bellevue, WA)
*Development of Techniques for the Use of
 DMSP SSIE Data in the AWS 4D Ionosphere
 Model*
 AFGL-TR-85-0107(I) (20 April 1985);
 ADA176412

STEVENS, N.J., and KIRKPATRICK, M.E.
 (TRW Space and Technology, Redondo
 Beach, CA)
*Spacecraft Environment Interaction
 Investigation*
 AFGL-TR-86-0214 (October 1986)
 ADA179183

THAYER, J.S., NANEVICZ, J.E., and DANA,
 D.R. (SRI Intl., Menlo Park, CA)
Transient Pulse Monitor
 AFGL-TR-88-0147 (20 May 1988),

ADA201211

TOOMRE, J., and GEBBIE, K.B. (Univ. of Colorado, Boulder, CO)

Solar Oscillations and Convective Flows as Probes of Structure in the Subphotosphere
AFGL-TR-87-0132 (15 April 1987),
ADA183687

ULWICK, J.C., ALLRED, G.D., BAKER, K.D., and HOWLETT, L.C. (Univ. of Utah, Logan, UT)

Rocketborne and Ground Based Measurements in Support of the Field-Widened Interferometer Experiment
AFGL-TR-85-0115 (28 May 1985),
ADA189105

WEIMER, D.R. (Regis Coll., Weston, MA)
Large-Scale Plasma Density Fluctuations Measured with the HILAT Satellite at 830 km Altitude

AFGL-TR-87-0110 (1 April 1987),
ADA183043

WEIMER, D.R., ANDERSON, P.B., GREENSPAN, M.E., BASINSKA-LEWIN, E.M., JAMES, J.H., and PELAGATTI, J.M. (Regis Coll., Weston, MA)

A Study of Plasma Irregularities in the High-Latitude Region
AFGL-TR-86-0233 (27 October 1986),
ADA179910

WU, S.T. (Univ. of Alabama in Huntsville, Huntsville, AL); and SMITH,

J.B., JR. (NOAA, Boulder, Co)

MHD Modeling of Energy Build-up Due to Photospheric Shearing Motion and Its Relation to Flare Prediction Criteria
AFGL-TR-87-0029 (23 September 1987),
ADA198208

FREEMAN, J.W., JR., et al (Rice Univ., Houston, TX)

An Operational Magnetospheric Specification Model
Ionospheric Effects Symp., Springfield, VA (5-7 May 1987)

GREENSPAN, M.E. (Regis Coll., Weston, MA)

Joint Radar and Satellite Observations of Large Subauroral Ion Drifts
AGU Mtg., San Francisco, CA (5-9 December 1988)

WEBB, D.F. (Emmanuel Coll., Boston, MA); and MOSES, J.D. (American Science & Engineering, Cambridge, MA)

The Correspondence Between Small-Scale Coronal Structure and the Evolving Solar Magnetic Field
XXVII COSPAR Mtg., Espoo, Finland (18-29 July 1988)

WEIMER, D.R. (Regis Coll., Weston, MA)
Auroral E-Fields from DE-1 and -2 at Magnetically Conjugate Points
XXVII COSPAR Mtg., Espoo, Finland (18-29 July 1988)



Adjusting Laser Transmitter of High-Altitude Lidar.

III IONOSPHERIC PHYSICS DIVISION

The ionosphere, that portion of the atmosphere and/or space that extends roughly from 50 above the earth to 1000 km is an extremely important region for the Air Force. Approximately 80 percent of all Air Force satellites operate in these altitudes. Virtually all vlf, lf, hf, vhf, uhf communications and radar systems, as well as UV and IR surveillance systems, are critically dependent upon the ionosphere for effective operation. In the future, this same region will continue to be important for such emerging systems as the National Aerospace Plane (NASP).

The ionosphere, however, is highly variable, changing the path of all radio signals propagating through it. The basic physical processes that govern the production, loss, and transport of ionization in the atmosphere must be understood, so that outages in Air Force communications and surveillance systems can be predicted.

During this reporting period the Ionospheric Physics Division of GL has been especially successful in advancing the fundamental level of understanding that drives many extremely complex ionospheric processes, as well as providing crucial and timely support to several Air Force systems designers and operators. It is with great pride that we present in the following pages a summary of some of this Division's recent progress in

ionospheric physics, specifically in ionospheric effects, ionospheric scintillations, ionospheric modeling, atmospheric density and satellite drag, ionospheric interactions, atmospheric ion chemistry, artificial plasma technology, and the ultraviolet spectrum.

IONOSPHERIC EFFECTS

Large-scale processes affect the overall structure and dynamics of the ionosphere in the polar cap, auroral oval, F-layer trough, and equatorial regions and produce variations within these regions on time scales ranging from minutes to years. Within these quasi-global regions, density fluctuations, or ionospheric irregularities, are caused by the complex interaction of neutral winds and ionospheric plasma, plasma drifts driven by electric fields, ion chemistry, and particle precipitation. Medium and small-scale processes lead to the formation of irregularities extending from tens of kilometers to centimeters as observed, for example, in equatorial plasma depletions, in the auroral oval, and in polar-cap F-layer auroras and patches. These medium and small-scale irregularities result from various plasma instabilities and, on some occasions, from localized strong particle precipitation as, for example, in discrete auroras.

The temporal variabilities and spatial irregularities affect radio propagation in the frequency range from hf through shf and are therefore of importance to Air Force systems from the high-frequency Over-The-Horizon-Backscatter (OTH-B) Radar to the satellite communications systems (AFSATCOM, MILSATCOM) operating over the entire uhf and part of the ehf band. The same physical processes are believed to drive similar effects through ehf frequencies in the nuclear-disturbed ionosphere.

Theoretical efforts during this reporting period have been concerned with

studies of: the generation of ionospheric scintillation, relating ultraviolet images to ionospheric densities for mapping the global ionosphere; the modeling of large-scale ionospheric dynamics with special emphasis on the equatorial and polar ionosphere; and the global modeling of thermospheric neutral density, composition, and dynamics. The theoretical and semi-empirical ionospheric and neutral atmospheric models developed by GL are being transitioned to Air Weather Service for operational use by the Space Forecasting Center.

Experimental efforts in the reporting period focused on the determination of the variability of the neutral atmosphere, the structure of, and transport within, the polar cap ionosphere, the generation of ionospheric irregularities at high latitudes, and the effects of large-scale disturbances and irregularities on Air Force systems. A complement of ground-based, airborne, rocket, and satellite diagnostics are used to perform these experiments.

Research efforts related to the ionospheric effects program, and of special interest to the OTH system and to the Air Weather Service, have been pursued in the areas of natural and man-made ionospheric disturbances, including the development of the daytime and nighttime F-layer troughs, improvement in forecasting geomagnetic, auroral, and ionospheric activity and storms, and assessment of the disturbed equatorial region as a potential source for ionospheric scatter (clutter) relevant to the OTH system.

Polar Cap Sounding: For decades the polar cap ionosphere eluded any systematic ordering because of its extreme variability. Its phenomena could not be organized using data obtained from standard observing techniques and applying standard geophysical parameters. GL in the early 1980's brought new ionospheric

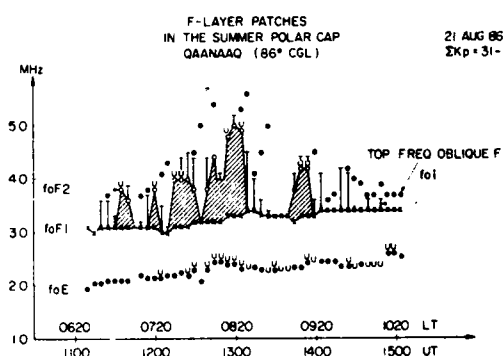
sounding and optical imaging techniques to bear on the problem. The discovery of auroral F-layer arcs populating the polar cap (in darkness) under magnetically quiet conditions and of fast-moving polar-cap F-layer patches were a major step forward in the ordering of polar-cap F-layer phenomenology. The F-layer arcs result from soft (~ 100 eV) auroral precipitation occurring along shearlines of a complex convection pattern (quiet magnetic conditions). The patches originate under disturbed conditions in the sub-cusp F-region illuminated by the sun. They are driven by the polar-cap potential generated by the solar wind at high velocities in a predominantly antisunward direction. Recent efforts have shown that the direction of the polar-cap plasma convection measured by modern digital ionosondes is well correlated with the Interplanetary Magnetic Field (IMF) B_z component.

Improved understanding of this highly irregular region will lead to a descriptive model of this regime. To systematically approach the description of the polar cap ionosphere, GL cooperated with the Danish Meteorological Institute (DMI) and the University of Lowell Center for Atmospheric Research to expand GL's ionospheric sounder chain. A Digisonde 256 was deployed at the DMI Qanaq Geophysical Observatory (86° corrected geomagnetic latitude, CGL). This supplements GL's subauroral chain at Argentia, Newfoundland (57° CGL) and the auroral chain at Goose Bay, Newfoundland (65° CGL). The Qanaq station provides a continuous database for the description of polar-cap ionospheric structure and ionospheric plasma convection.

Previous ionosonde and optical imaging observations under full darkness have shown large plasma patches typically 500-1000 km in diameter, with densities of up to 10^6 electrons per cm^3 .

These observations suggest that the patches originate in the solar-illuminated ionosphere south of the cusp.

High time-resolution measurements of the polar cap ionosphere under sunlit disturbed magnetic conditions have shown that patch occurrence is not limited to darkness. Even during summer under conditions of constant solar illumination, patches dominate the F-layer when the magnetic field is disturbed. The figure shows an example of a sequence of F2-layer patches with maximum density of 3×10^5 el cm^{-3} (foF2 ~ 5 MHz) above a background F1-layer maximum density of 1×10^5 el cm^{-3} (foF1 ~ 3 MHz). With typical summer drift velocities of 500 m/sec^{-1} , the patches have dimensions of 300 to 900 km diameter, comparable to the winter measurements.



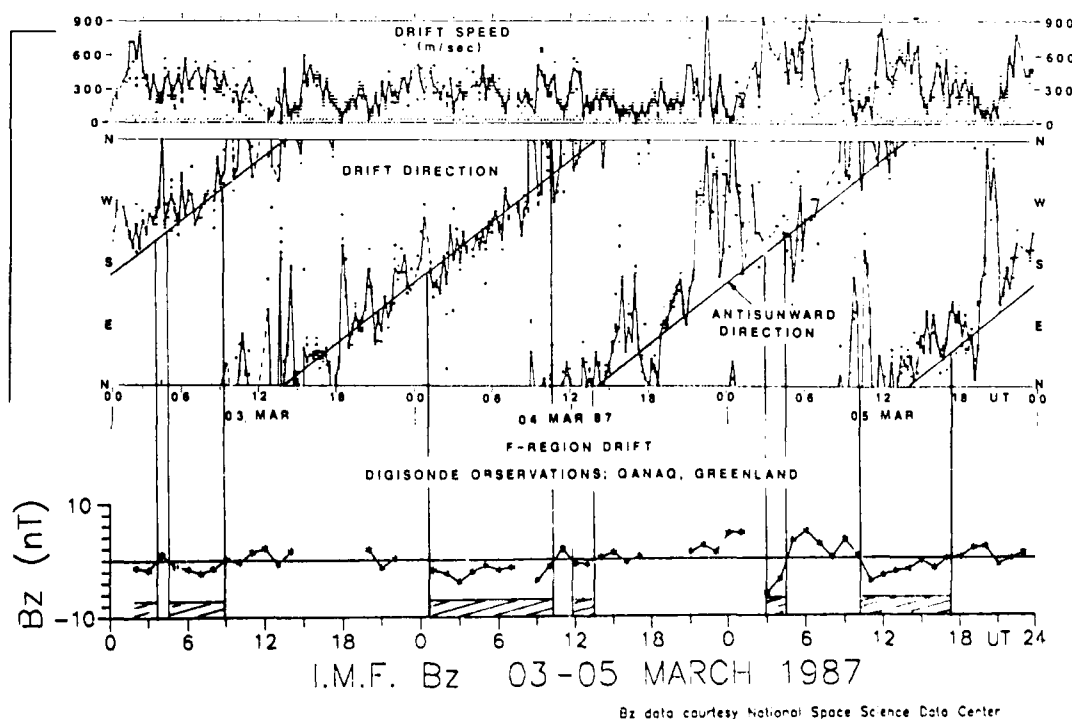
F-Layer Patches Observed in Polar Cap under Sunlit Conditions and Increased Magnetic Activity.

The patches of solar-produced plasma observed under magnetically active conditions are imbedded in a steady anti-sunward flow of polar-cap background plasma. The maximum densities observed in these patches vary by almost one order of magnitude over a solar cycle. Of importance to the modeling of the polar ionosphere is the relation of the observed ionospheric densities to the morphology of polar plasma convection,

which is controlled by the solar wind. A newly developed technique, automated plasma-drift measurements made with the Digisonde 256, has been deployed in the central polar cap at Qanaq. Drift data taken in 1987 and 1988 on the three world days of each month have been analyzed in the context of the IMF data obtained by the NASA IMP 8 satellite. The figure gives as an example the drift direction and magnitude measured over the three world days of March 1987 (March 3 -- 5) together with the B_z component of the IMF. The antisunward direction, rotating 360° over 24 hours, is indicated as a straight line in the center panel, which shows the horizontal drift direction as a function of CGL direction

the plasma flow varies widely or becomes sunward (March 4 -- 5 1987, 21-02 UT). The observed convection velocities range from 100 to 900 m/sec⁻¹.

The steady antisunward flow is the result of the known well-organized structure of polar convection under the $B_z < 0$ condition, while the rapidly changing direction is indicative of plasma flow shears associated with the occurrence of polar cap arcs under $B_z > 0$ conditions. These latter conditions, especially when following strong $B_z < 0$ conditions, have also been correlated with short periods of steady sunward flow. These examples and the full 1987 -- 1988 drift database corroborate the current understanding of the dynamic morphology of the convec-



Drift Direction and Speed of Polar Cap Plasma Convection Measured at Qanaq, Greenland (86-CGL) with Digisonde 256 and IMF B_z Component. (The straight slanted lines in the graph indicate the antisunward direction as a reference.)

and UT. The data reveal clearly ordered antisunward drift during periods of $B_z < 0$, indicated as cross-hatched time bands. During periods of $B_z > 0$, the direction of

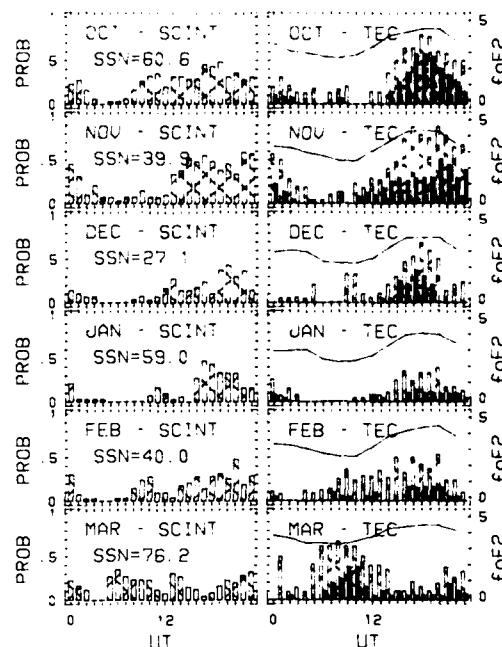
tion pattern and its control by the IMF B_z component. The effects of the B_x and B_y components are under study. This technique of plasma drift measurements

is expected to allow continuous monitoring of the polar convection.

An expansion of the observing network is planned with the establishment of a Digisonde station at Sondrestrom, Greenland (75° CGL), where measurements under the cusp region of the auroral oval/magnetosphere system will be made in daytime. The goal is a set of measuring stations to define in real time the configuration of the convection geometry as a driver for ionospheric specification and prediction models of the polar ionosphere.

Polar-Cap Total Electron Content: The first full winter-season observations of Total Electron Content (TEC) in the northern polar-cap ionosphere were made from October, 1987, to March, 1988. Observations of relative TEC variations were made at Thule, Greenland, by measuring the differential carrier phase of dual-frequency L-band signals transmitted from the GPS satellites. Relative TEC variations, measured from satellite signals at high elevation angles, show many enhancements from background levels of 5 to 10 TEC units (one TEC unit is 10^{16} el/m² column) and enhancements of 15 or 20 units are occasionally seen. Many of these enhancements occur in as little as 10 min.

For each month of the period a comparison was made of the hourly occurrence of TEC enhancements and amplitude scintillations recorded from 250 MHz signals from quasigeostationary communications satellites. The occurrence of amplitude-intensity fade levels of > 5 dB with TEC enhancements of > 1 TEC unit in 5 min was strikingly good. The figure shows the diurnal occurrence of significant TEC enhancements as well as the occurrence of amplitude scintillation for the 6 month period studied. Also shown is the predicted foF2 curve at Thule, Greenland. Note that there is excellent agreement of the occurrence of



Diurnal Occurrence of Significant TEC Enhancements Showing General Linkage with Occurrence of Significant 250 MHz Amplitude Scintillation and Predicted foF2 Curve at Thule, Greenland, October, 1987, to March, 1988.

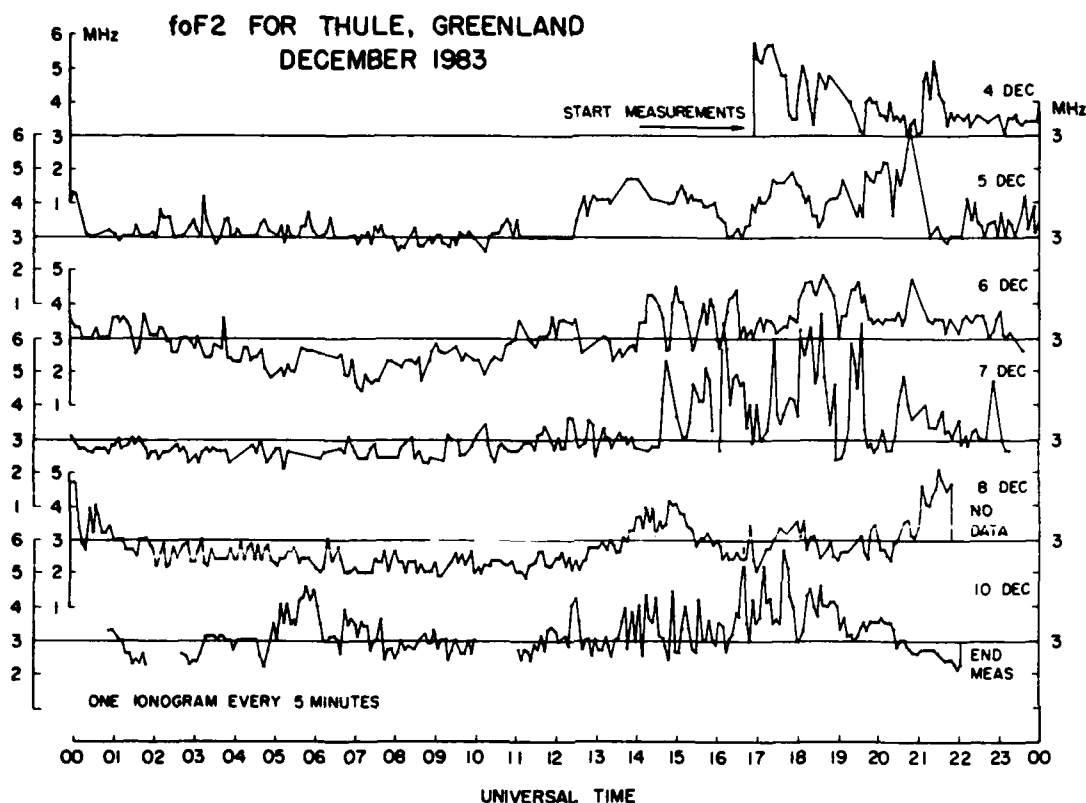
scintillation and TEC enhancements. The values of predicted foF2 also agree, in general, with the times of enhancements of TEC.

Density Enhancements in Winter Polar Cap:

As a result of a number of winter campaigns in the polar-cap region carried out by GL scientists at Thule and Sondrestrom, Greenland, substantial evidence exists, both observational and theoretical, which suggests that enhanced "patches" of ionization, 200-

1000 km in horizontal extent, are associated with a southward directed interplanetary magnetic field orientation ($B_z < 0$).

The figure presents observed foF2 values as a function of universal time at Thule (86° CGL) for the period December 4-10, 1983. The patches of ionization are evidenced as ionization enhancements



Observed foF2 Values as Function of Universal Time at Thule (86° CGL) December 4-10, 1983.

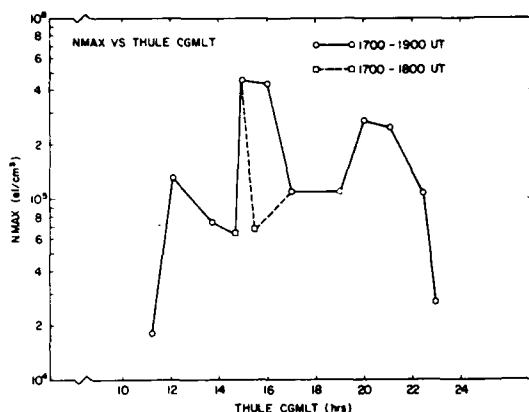
normally observed between 1400 and 2200 UT and may be broad patches on December 5 or "spiky" patches as on December 7 and 10.

A number of different studies have demonstrated that the plasma within the enhanced region is produced by solar ultraviolet radiation in flux tubes located equatorward of the subcusp region before convecting over Thule. Quantitative arguments by scientists at GL have demonstrated that the observed variation in N_{max} at Thule in December cannot be accounted for by local production due to precipitating energetic electrons and quantitatively showed that the source of plasma is equatorward of the cusp region.

The problem of what causes the "patchiness" in ionization has been stud-

ied by solving the time-dependent plasma continuity equation, including production by solar ultraviolet radiation, loss through charge exchange, and transport by diffusion and convection $E \times B$ drift. Time and spatially varying horizontal $E \times B$ drift patterns are imposed and subsequent ionospheric responses are calculated to determine how enhanced plasma densities in the dark polar cap could result from the extended exposure of relevant flux tubes to significant solar production.

The next figure presents two trajectories followed by the plasma for two different $E \times B$ convection patterns, one specified by a polar cap radius of 12° and a cross tail potential of 80 kV and the other by a radius of 15° and potential of 100 kV.

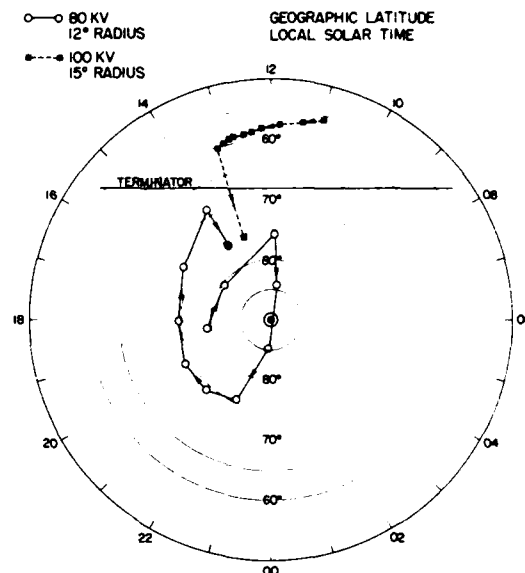


Calculated Nmax Values at Thule as Function of Corrected Geomagnetic Local Time for a Time-Varying Convection Pattern. (At 1700 UT, the convection model was changed from 80 kV, 12° to 100 kV, 15° and maintained for either 2 hours or 1 hour.)

Both trajectories cross Thule at 1400 LT but one spends most of its time in the sunlit region (. . .) while other is predominantly in darkness (0----0). The former trajectory produces a daytime density $N_{max} = 5 \times 10^5 \text{ el/cm}^3$ at 1400LT.

"Patches" of enhanced ionization are formed when a time-varying convection pattern is introduced into the simulation. The next figure presents calculated Nmax values at Thule as function of corrected geomagnetic local time when an initial convection pattern characterized by an 80 kV cross tail potential and a 12° polar cap radius is abruptly changed to a 100 kV potential and a 15° polar cap radius. The horizontal extent of the patch is related to the length of time the new convection pattern is "turned on." The patch is formed simply by allowing plasma, normally found in the sunlit, subcusp region, access to the polar cap regions for short periods of time.

Polar Arcs: To investigate the acceleration processes associated with polar cap arcs, as well as the horizontal structure and motion, the Polar Acceleration Regions and Convection Study (Polar

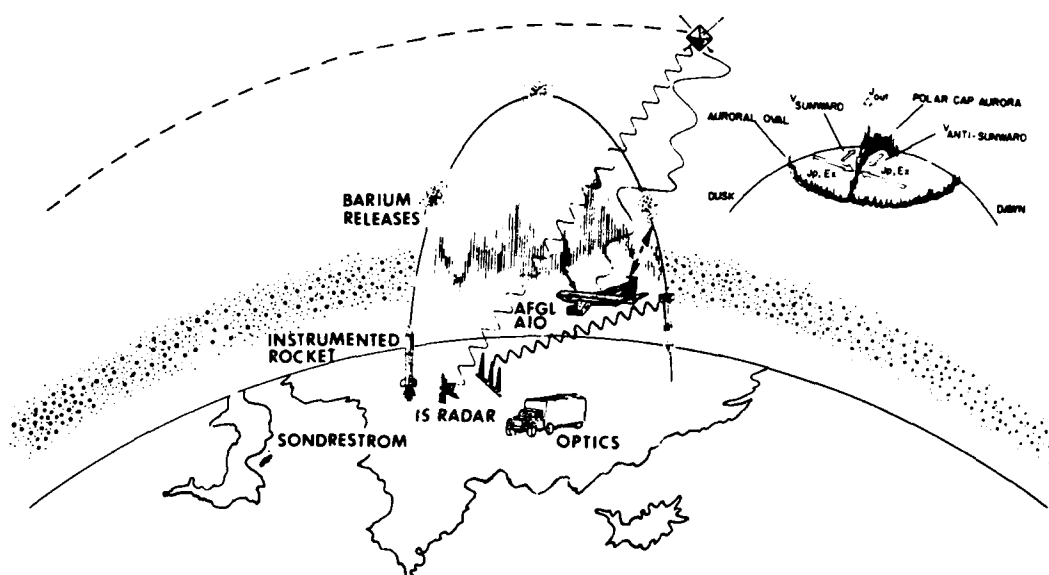


Plasma Trajectories in a Geographic Latitude, Local Solar Time Coordinate System for Two Heelis Convection Patterns Characterized by Respective Cross-Tail Potential and Polar Cap Radius Values of 80 kV, 12° and 100 kV, 15°. (The time between the points on each curve represents one half-hour elapsed time.)

ARCS) rocket experiment was conducted from Sondrestrom, Greenland, on February 27, 1987. (For launch details, see "Cope/Polar ARCS" in Chapter VII below.) The objectives of Polar ARCS were: to inject multiple barium shaped-charge chemical releases near, and within, a polar cap aurora to investigate acceleration processes aligned with the magnetic field; to fly a fully instrumented rocket payload through the same aurora to measure the plasma, particle, and field parameters; and to measure the plasma density, temperature, and velocities with the Sondrestrom Incoherent Scatter Radar.

Real-time All Sky Imaging Photometer measurements conducted from the GL Airborne Ionospheric Observatory were used to locate a polar cap arc within the rocket trajectory. The first rocket with three barium shaped-charges was

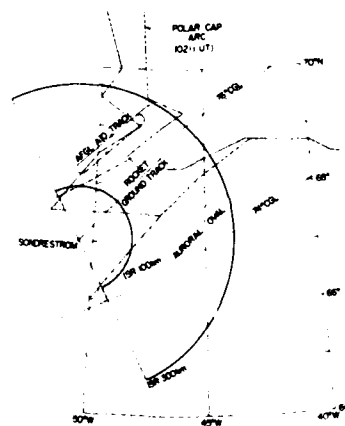
POLAR ARCS



Polar cap auroras represent regions of C^3 outage and are optical signatures of flow reversal boundaries. The Polar Acceleration Regions and Convected Studies (POLAR ARCS), using barium release, instrumented rockets, incoherent scatter radar, and the GL Ionospheric Observatory, were conducted to measure the three dimensional structure and dynamics of these auroras. Electric circuit parameters of the arcs were a major objective of the experiment.

launched into the aurora, followed within 5 min by the instrumented payload. All releases and instruments performed as planned. One barium jet was released within the arc, and sensors on the instrumented payload showed clear signatures that the payload crossed the arc. Analysis is continuing to compare horizontal arc drift with the motion of the barium clouds and electric fields measured by the rocket and incoherent scatter radar. A second area of interest is the field-aligned acceleration processes along the arc magnetic flux tube, while a third involves electrodynamic circuitry within the arc.

Advanced knowledge of irregularities, which produce scintillation constraints on communications and surveillance systems, stems from studies of naturally occurring irregularities (especially at



Configuration of Aurora During POLAR CAP Rocket Flight. (The rocket trajectory successfully traversed a polar cap arc, extending from the poleward boundary of the auroral oval to the north. Also shown are the flight track of the GL Airborne Ionospheric Observatory and the extent of the azimuth scan of the Sondrestrom Incoherent Scatter Radar.)

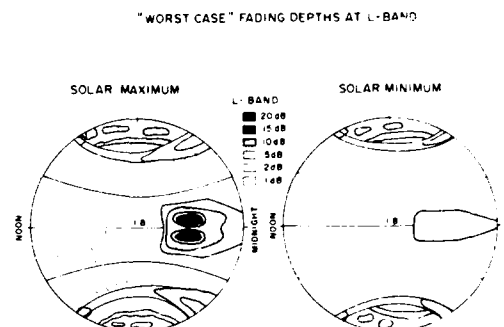
high latitudes), as well as those produced by chemical releases and high-power hf transmitters, as we shall see below.

IONOSPHERIC SCINTILLATIONS

Variation: An extensive vhf/uhf scintillation database covering the frequency range of a few hundred megahertz to a few gigahertz has been utilized to determine the drastic variation of the magnitude of phase and intensity scintillations and their temporal and spatial structures with sunspot number. The results of this study influence the choice of frequency and the type of radar and communication system to be deployed in the future. GL acquired this database by performing continuous scintillation measurements with stationary and orbiting satellites at crucial locations in the equatorial, auroral, and polar cap regions.

The most disturbed scintillation environment was located at dip latitudes of $\pm 15^\circ$, corresponding to the position of the crest of the equatorial anomaly. During solar maximum at this location, amplitude scintillation fades of 20 dB at 1.5 GHz were obtained 30 percent of the time in the post-sunset hours. At such times, decorrelation distances as small as 15 m were measured at 1.5 GHz. These magnitudes provide guidelines for the choice of L-band frequencies in space-based radars. At a reduced phase of solar activity during 1982, a similar percent occurrence of scintillations was obtained at the much reduced level of 5 dB. During the sunspot maximum period, at the crest of the equatorial anomaly, the median value of phase scintillation at 250 MHz was 5 rad for a detrend interval of 100 sec.

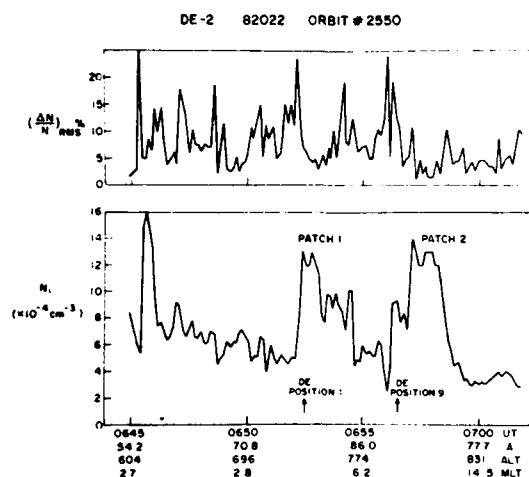
At high latitudes, the winter polar-cap region has been observed to provide the most disturbed scintillation environment. At Thule, Greenland, deep within the polar cap, the median values of scintillation fades and phase deviation at



Global Variation of Scintillation Fades During Solar Maximum and Solar Minimum.

250 MHz are as large as 20 dB and 4 rads during the sunspot maximum period. In 1986 with sunspot numbers in the vicinity of 10, fade levels as low as 5 dB were recorded. Based on these studies, a global schematic diagram of worst case L-band scintillation activity during the sunspot maximum and minimum periods is shown in the figure.

Polar Cap Patches: Polar cap patches have been successfully modeled to yield phase and amplitude scintillations by utilizing high-resolution plasma density measurements from the Dynamics Explorer-2 (DE-2) satellite orbiting at an altitude of 800 km in combination with digisonde measurements of peak F-region density and irregularity layer thickness. During high sunspot conditions, the patches even at an altitude of 800 km were found to show a twofold to threefold increase in density as compared to the background. Irregularity amplitudes as large as 20 percent were observed at the edges of patches as shown in the figure. Such spatially discrete density structures were found to correspond to temporally discrete scintillation patches, with saturated amplitude scintillations and phase scintillations as high as 20 rad (with an 82 sec detrend interval) at 250 MHz. The success of this endeavor makes it feasible to utilize the so-called "scintillation meter" (which is

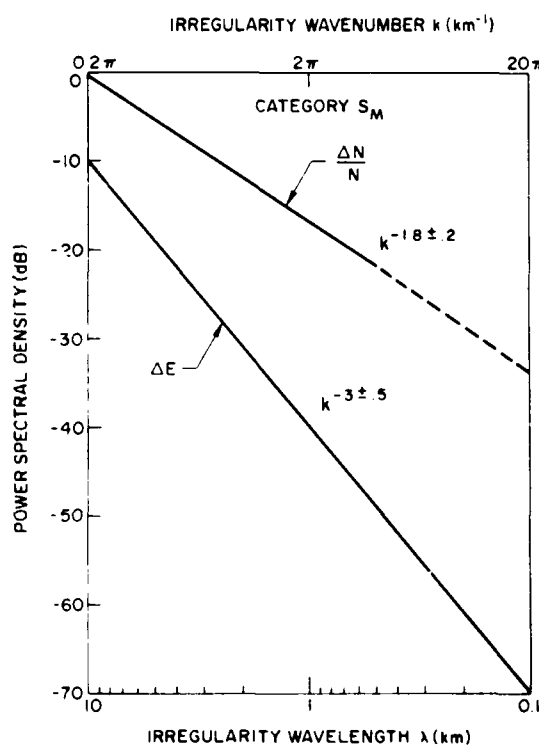
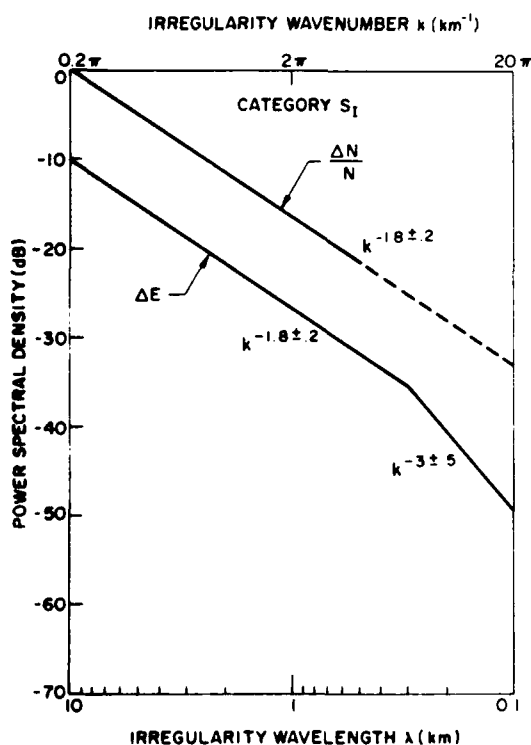


Ion Density N_i and Irregularity Amplitude ($\Delta N/N$) Seen on DE2 Orbit 2550 on January 22, 1982. (Note that DE2 passed closest to Thule at 0654:37 UT and provided evidence for two patches of ionization even though it was at an altitude of ~800 km.)

actually an irregularity meter) on the DMSP F-8 satellite at similar altitudes for providing real-time inputs to operational Air Weather Service scintillation models.

Nightside Auroral Oval Instabilities:

Simultaneous satellite in-situ measurements of density ($\Delta N/N$) and electric-field fluctuation (ΔE) spectra in the high-latitude ionosphere were studied using Dynamics Explorer-2 (DE-2) data. The spectral study was primarily confined to large structured velocity regions in the auroral oval. By means of the very complete set of energetic particle, dc and ac electric field, field-aligned current, thermal plasma density and temperature measurements available from DE-2, we identified two categories of spectra asso-

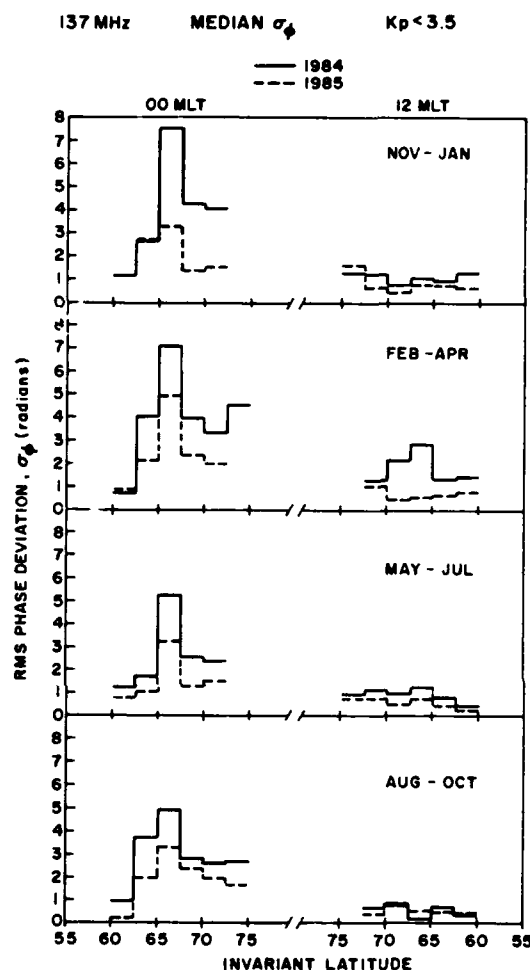


Idealized Representation of the Two Categories of $\Delta N/N$ and ΔE Spectra Observed in Association with Velocity Shears in the Auroral Oval: Category S_I for Intense Shears (~10Hz) and Category S_M for Moderate Shears (~1Hz). (The ΔN and ΔE spectra have been arbitrarily separated. The short scale-length ends of the $\Delta N/N$ spectra are shown dashed because of uncertainty in psd estimates.)

ciated with velocity shears, as shown in the figure. The first category (S_I) was observed in very intense velocity shear regions having shear frequencies ~ 10 Hz in conjunction with large field-aligned current densities. The second category (S_M) was observed in more moderate velocity shear regions having shear frequencies ~ 1 Hz in conjunction with weak field-aligned currents.

The observations of $(\Delta N/N)$ and ΔE spectral behavior in the presence of shear flows have stimulated a lot of theoretical/simulation efforts by NRL, GL, and MIT scientists on: (1) collisional Kelvin-Helmholtz instability driven by velocity shears perpendicular to the magnetic field; (2) an instability driven by shears parallel to the magnetic field; and (3) an instability driven by a combination of transverse shears and field-aligned currents.

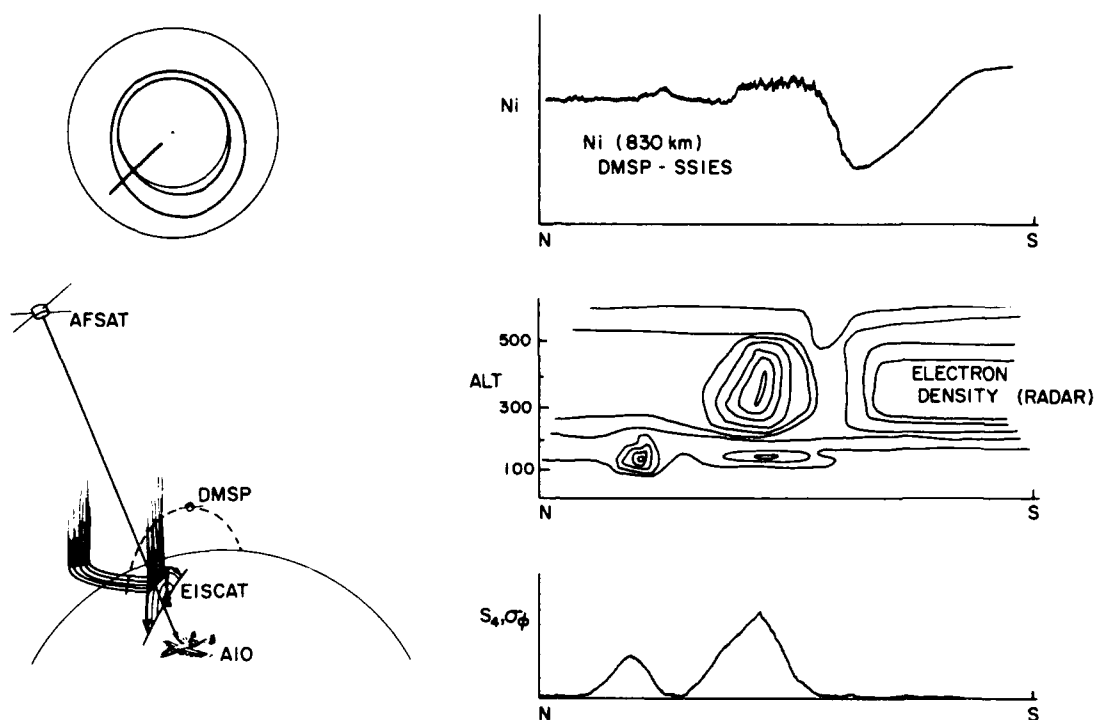
Coordinated measurements of the nightside auroral oval were also conducted by using the HILAT satellite data obtained by the Tromso, Norway, Telemetry Station. Particular emphasis was placed on determining the sunspot cycle/seasonal variation of scintillations and the anisotropy of auroral irregularities. The figure shows the seasonal variation of median phase scintillation (σ_ϕ) obtained with a 20 sec detrend interval for noon and midnight magnetic local times as a function of invariant latitude during 1984 and 1985. Two major effects were noticeable: (1) the geometrical enhancement caused by the alignment of the propagation vector with the local L-shell and (2) the solar-cycle variation of scintillations, the latter providing more scintillations in 1984 than in 1985. The geometrical enhancement caused by the anisotropy of auroral irregularities was further investigated by using the spaced-receiver technique at Tromso. Moderate-to-small sheets were found in the geometrical enhancement region, with small



Seasonal Variation of Median rms Phase Deviation, σ_ϕ (137 MHz), with Invariant Latitude Along the Midnight-Noon Meridian Under Quiet Conditions in 1984 and 1985.

rod-like, and even isotropic, irregularities being detected north of Tromso.

Calibration of DMSP SSIES Sensor: During this period, a new program was initiated to determine the relationship between thermal plasma parameters measured at 850 km altitude by the DMSP satellite and the same parameters mapped along the earth's magnetic field to the altitude of the peak density in the F-layer (300 km). A prime mission of the SSIES sensor on DMSP is to specify regions where



Schematic Diagram of DMSP SSIES Calibration Experiments. (Simultaneous radar, DMSP, and Airborne Ionospheric Observatory measurements are used to compare actual measured scintillation with scintillation computed from DMSP SSIES in-situ data.)

amplitude and phase scintillation (regions of C3 outage) will occur. Scintillation is a radio-propagation effect which depends on the total integrated effect of the ionosphere. A series of experiments were devised to measure the amplitude and phase scintillation at uhf in the auroral oval using the GL Airborne Ionospheric Observatory (AIO). These measurements were coordinated with direct overpasses of the DMSP F-8 satellite. In addition, an incoherent scatter radar simultaneously measured the actual (and variable) electron density profile over a large range of latitudes traversed by DMSP. The combined set of measurements allows calculation of the expected scintillation for comparison with actually measured scintillation.

The experiments were performed in January, 1988, in northern Norway.

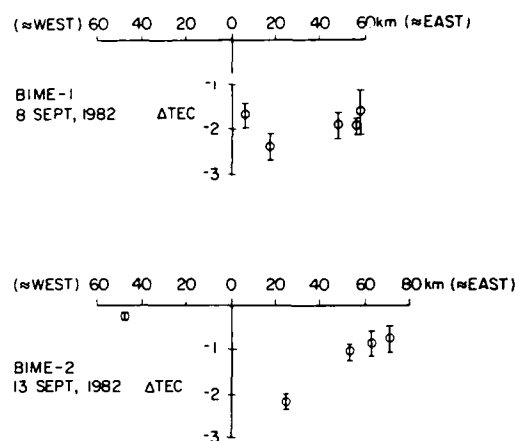
Several coordinated AIO flights and DMSP overpasses were obtained. Preliminary results show excellent correlation between the large-scale features (plasma blobs and F-layer trough) measured by the radar and by the DMSP satellite. Small-scale (1 km) structure, which produces scintillation, is in qualitative agreement. Detailed calculations are currently being performed to assess the quantitative ability of SSIES to specify C3 outages on satellite communication links.

CRRES Program: As a part of the NASA Combined Release and Radiation Effects Satellite (CRRES) program, Ionospheric Effects Branch scientists will conduct two chemical-release experiments to investigate the evolution of artificially generated ionospheric irregularities and their altitude extent.

Two 50 kg barium releases will be conducted from a launch site in Puerto Rico. These will be placed within the beam of the Arecibo Incoherent Scatter Radar, so that background conditions, as well as the chemical-induced high-density plasma, may be measured. Simultaneous amplitude and phase scintillation measurements conducted from the GL Airborne Ionospheric Observatory will determine the spatial extent, amplitude, and spectrum of the resulting ionospheric irregularities in the F-region. The experiment will be conducted at dawn so that the effects of the solar-produced E-layer can be observed during sunrise. (For other GL CRRES experiments, see Chapter II.)

Irregularities Injection: On two separate evenings in September, 1982, rockets BIME-1 and BIME-2 were launched into the *bottomside equatorial F2-region* off the coast of Natal, Brazil, to inject chemicals, consisting of mainly H_2O and CO_2 , to create a hole in ionization. The chemicals were injected near the height where the density gradient was steepest, and at a time when the F2-region was rising rapidly, to see whether plasma bubble irregularities could be generated from instabilities triggered by the ionization hole. On both occasions, hole-induced depletions in Total Electron Content (TEC) of more than 10^{16} el/m² were observed over horizontal distances of at least 670 km from the chemical injection point. The figure illustrates the TEC depletions observed from stations at distances east or west of the chemical release point.

A further analysis of the BIME data was done recently to ascertain the eastward drifts of these artificial depletions. These were determined by the time difference in the TEC features observed at various TEC monitoring stations, and from the changing range of oblique ionosonde echoes observed by an



Change in Total Electron Content (TEC) (units of 10^{16} el/m²) as a Function of Distance (East or West) of Chemical Release Point.

ionosonde located 300 km magnetically east of the chemical release point. The subsequent evolution of artificial depletions into plasma bubble irregularities was demonstrated from the observations of spread-F echoes, strong amplitude scintillation, and TEC depletion at distances from 300 to 500 km eastward of the release points.

The fact that similar behavior of the ionosphere was observed during the evenings of both rocket chemical releases, and on no other nights of the campaign, is strong evidence of successful artificial generation of bubble irregularities by chemical injection into the bottomside F2-region.

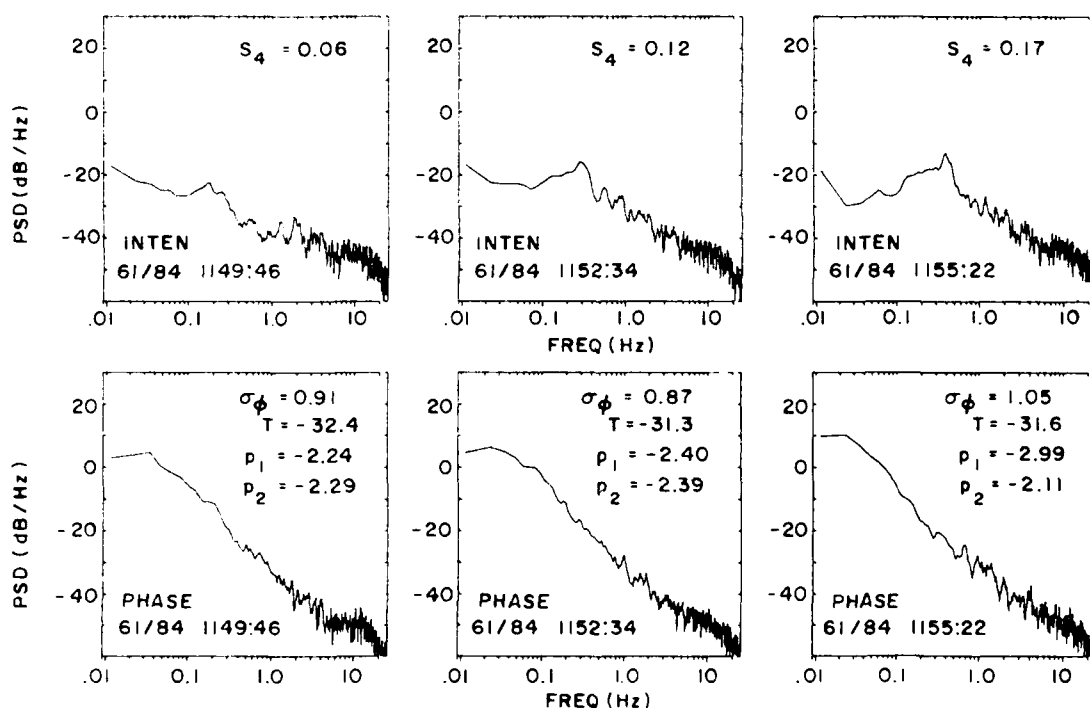
Structuring Modification by High-Power Radio Waves: The effects of high-power, high-frequency heating on uhf communication links operating through the high-latitude ionosphere were assessed. The hf heating facility of the Max Planck Institut fur Aeronomie located at Ramfjordmoen, Norway, in the auroral zone was used to develop an incident power density of 0.3 mW/m^2 at 225 km altitude. The 250 MHz transmissions from Air Force satellites propagating

through this heated volume were received by GL at the Tromso satellite station. To avoid the effects of strong natural disturbances that routinely occur during nighttime hours in the auroral zone, the experiments were performed during the daytime.

Everytime the heater was turned on, irregularities of electron density developed in the high-latitude ionosphere, which caused scintillations on the 250 MHz communication link established between the ground station at Tromso and the Air Force satellites. The intensity scintillation spectra revealed that a narrow band spectral feature was generated during the period of heating. The growth of the spectral feature due to heating over a 10 min period, commencing at 1150 UT, is shown in the figure. It displays successive intensity and phase

spectra obtained from 1.5 min data segments at intervals of approximately 2.5 min. By utilizing the information on the background ionosphere obtained by the European Incoherent Scatter Radar (EISCAT) located near Tromso, agreement between the predictions of the self-focusing instability theory and the observed results was obtained.

Electron Flux Modification by High Power Heating: An ionospheric heating experiment was performed at the Arecibo Observatory, Puerto Rico, in March and April, 1988. The experiment addressed electron acceleration processes, for which mechanisms are unknown and thresholds are not identified. The experiment focused explicitly on proving or disproving the following hypothesis: When hf power densities in the ionosphere deposit energy in excess of those which can be



Power Spectra of Intensity (top) and Phase Scintillation (bottom) of 250 MHz Signals from the Polar Beacon Satellite Acquired over 82-s Data Intervals.

dissipated by processes identified at the 100 kW ERP (effective radiated power) level, there is a "runaway" condition to the next limiting process, which involves substantial electron acceleration. Verification of this hypothesis would have a profound implication to plasma physics, and would be a powerful argument for building a gigawatt facility to pursue both Air Force applications and basic research in optical, ionospheric, and aeronomic physics. The initial experiments documented clear initial linear growth of the electron acceleration process, and identified the source altitude of accelerated electrons. Variable ambient ionospheric conditions were such that only weak electron acceleration was achieved with hf power available at Arecibo. The experiment will have to be repeated to observe the nature of the conversion to strong electron-acceleration conditions.

Extensive modeling activity, summarized below, provides a framework for assessing our understanding of the ionosphere and a vehicle for applying our ability to specify and predict.

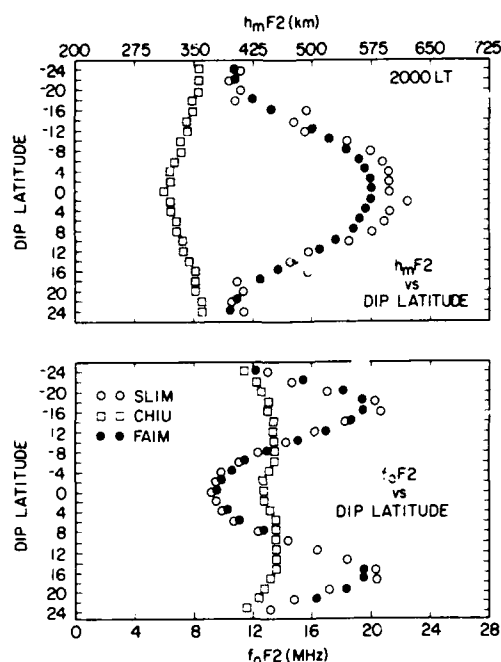
IONOSPHERIC MODELING

FAIM: The development at GL of a Fully Analytic Ionospheric Model (FAIM) has followed naturally from recent work in generating a Semi-empirical, Low-latitude Ionospheric Model (SLIM). Since current empirical models specifying low-latitude electron density profiles severely underestimated the daytime density-scale height and Total Electron Content (TEC), SLIM was developed. It is not only computationally fast but also more realistic than previous models. Very briefly, SLIM consists of functions and coefficients which reproduce nine sets of theoretically calculated low-latitude electron-density profiles corresponding to the three seasons (equinox, June solstice, and December solstice) for three levels of

solar activity: solar minimum ($F10.7 = 70$), moderate solar activity ($F10.7 = 125$), and solar maximum ($F10.7 = 185$). A separate set of six coefficients exists for each 2° interval in latitude (24°S to 24°N dip latitude) and each half hour in local time (over the 24 h day).

While electron density profiles are easily generated from the various sets of coefficients given in tabular form, a more convenient approach would be to specify the coefficients as analytic functions of local time and latitude, as in the Chiu empirical model. Furthermore, because the Chiu ionospheric model has been so extensively used to specify the low and middle latitude ionospheric region, it was decided to recast the coefficients in an analytic form so that present users of the Chiu model would have access to the new, improved formulation without having to modify any of the input or output parameters.

A graphic comparison of both SLIM and FAIM with the Chiu model is given in Figure 69. It illustrates the magnitude of the improvement in $h_m F2$ and $foF2$ at 2000 LT as a function of latitude. This is a comparison at only one local time but is indicative of the differences which provided the impetus to develop SLIM initially. An unrealistically low F-layer peak height is provided by the Chiu model, which can have significant consequences if it is used in neutral dynamics calculations. In particular, after sunset when the two main horizontal forces on the neutrals are the pressure gradient and ion drag forces, low $h_m F2$'s and hence unrealistically large plasma densities, result in significant underestimating of the zonal wind speed. When the eastward neutral wind velocity is calculated incorporating the Chiu ionospheric model, a peak zonal wind of 120 m/sec is reached at 2000 LT. When FAIM is assumed to be the ionospheric model, peak wind speeds of 180 m/sec are



Comparison of $h_m F_2$ (top) and $f_o F_2$ values (bottom) as Function of Dip Latitude at 2000 LT Given by SLIM, CHIU, and FAIM for Solar Cycle Maximum Equinoctial Conditions.

obtained, in much better agreement with measured wind velocity at these local times. The cause of the increase is the greater layer height in FAIM, which reduces the electron density and, hence, the ion-drag term at 300 km and below.

FAIM has recently been merged with the Air Weather Service (AWS) operational ionospheric specification model (Ionospheric Conductivity and Electron Density - ICED) to extend its capability from the mid-latitude to the equatorial ionospheric region.

Electron Density Profiles (EDP) from Satellite UV and In Situ Data: For a number of years there has been substantial interest in using satellite measurements for the remote sensing of ionospheric properties. Recently, work in the Ionospheric Physics Division has been aimed at assessing the utility of satellite ultraviolet (UV) emission measurements and in-situ plasma measurements in deducing the daytime mid-latitude Electron

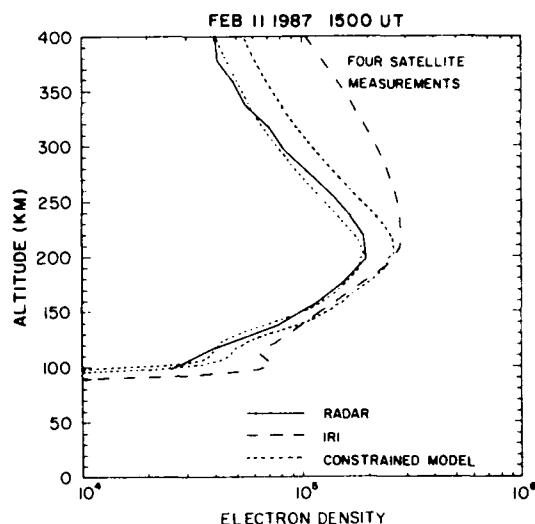
Density Profile (EDP). The starting point for this work was the development of a theoretical airglow/EDP model based on first principles. In such a model a number of geophysical input parameters are required. If these parameters are poorly specified, the results of the model will have large uncertainties due to the natural variation of the parameters. Thus, if such a model is to calculate an accurate EDP, the geophysical inputs must be accurately specified. The remote sensing concept that GL scientists have been studying involves using real-time satellite measurements to constrain the geophysical input parameters and in turn reduce the uncertainty in a calculated EDP. In particular, four measurements were considered: two in-situ measurements in the top side ionosphere (the plasma density and temperature) and two measurements of ultraviolet emission features (one or more features on the N_2 Lyman-Birge-Hopfield band system and the atomic oxygen line at 1356 Å).

A theoretical simulation was conducted to establish how well, in principle, this four-measurement concept could work. The study showed that using the four measurements to constrain the GL airglow/EDP model reduced the uncertainty in the predicted EDP compared to that of an ab initio calculation of the EDP. The uncertainty in the EDP that remained was comparable to the assumed error in the four measurements.

While the simulation demonstrated the degree of certainty possible in a determination of the EDP, questions remained concerning the accuracy of the GL airglow/EDP model. To answer such questions, a ground-truth data-gathering campaign was conducted and comparisons were made between the model and actual EDP data. To use satellite measurements to help constrain the model in

these tests, coincident satellite and EDP measurements were needed. The November 1986 launch of the AIRS (Auroral Ionospheric Remote Sensor) instrument on the Polar BEAR satellite made it possible to arrange two campaigns to collect such data. (See "UV Remote Sensing" below.) The electron density data were collected using the Millstone Hill uhf incoherent scatter radar during periods when ultraviolet images recorded by the AIRS instrument overlapped the radar's field of view.

The Polar BEAR satellite did not make in-situ measurements of plasma density and temperature, but radar measurements of these quantities at a predetermined altitude were used to simulate these required in-situ satellite measurements. The two required ultraviolet emission measurements were available from the AIRS images at 1356 Å and 1596 Å wavelengths. By using these data to constrain the geophysical parameters, a most likely EDP and its standard deviation were calculated. The calculated EDP and its uncertainty were then compared with the radar-measured EDP as well as with the EDP predicted by the International Reference Ionosphere (IRI) empirical model. An example of this analysis is shown on the following figure. The solid curve is the radar-measured EDP, the long dashed curve is the IRI EDP, and the short dashed curves are the calculated EDP plus and minus its uncertainty. Much of the uncertainty in the expected EDP, especially in the topside, comes from an assumed 20 percent random error in the measurements. The relative performances of the IRI empirical model and the constrained airglow/EDP model in fitting the radar data illustrate the advantage of using a model that can incorporate real-time information as compared to an empirical (or average) model like the IRI, which incorporates no real-time data.



Comparison of GL Constrained EDP Model, Radar Ground-Truth EDP Measurement, and IRI Empirical EDP Model.

Kinetic Model for Diffuse Aurora: One of the most important sources of magnetospheric-ionospheric coupling is the precipitation of energetic electrons from the plasma sheet of the magnetosphere into the high-latitude ionosphere in the diffuse aurora zone. In turn, modern models of the inner magnetosphere require an accurate treatment of ionospheric precipitation and backscatter to properly describe the population of the plasma sheet. The strong-diffusion treatment of precipitation, which is commonly used, will not always satisfy the requirements of these models. The Ionospheric Physics Division has developed a detailed, but still efficient, kinetic model of plasma sheet convection and precipitation. The trapped particle-velocity distributions are described by a numerical solution of the bounce-averaged, pitch-angle diffusion equation, including the advective terms necessary to describe the effects of plasma-sheet convection. The precipitating flux is determined by a boundary-layer analysis of the loss cone in velocity space, while its interaction with the

atmosphere is modeled using a transport code. The output of the model includes the pitch-angle and energy distributions of the particles as functions of latitude, both in the trapped distribution and at low altitude. Profiles in latitude or trapped-population temperatures, precipitating energy fluxes, ionospheric conductivities, and other quantities have been calculated and compared with the observations of polar orbiting satellites.

When the pitch-angle diffusion rate falls with energy (as many theoretical models predict and observations confirm), the precipitative loss rate peaks near the energy marking the transition from the strong-diffusion regime. When this transition energy falls near or below the characteristic energy of the diffuse auroral electron population, the detailed kinetic model shows that the energy flux into the diffuse aurora is controlled by the strength of the pitch-angle scattering, rather than the simple geometric considerations of strong pitch-angle diffusion. In these circumstances, precipitation generally does not occur rapidly enough to deplete the trapped population. Some other phenomena, such as the effect of limits on convection motion, are required to explain the equatorward edge of the diffuse aurora. Large-scale statistical studies of auroral precipitation have previously suggested this interpretation of the equatorward edge, but the Ionospheric Physics Division's detailed kinetic model is the first theoretical model capable of describing it.

Collision Effects: Discrete interactions (collisions) between charged particles and between charged and neutral particles play important roles in determining the properties of ionospheric, as well as some laboratory, plasmas. Collisions are important not only in establishing the equilibrium state, but they also affect the waves that are excited when the plasma is perturbed from its equilibrium

state. Unless collisional effects are treated by using rigorous collision operators, the calculated results are often dubious and, sometimes, may even be erroneous.

A few years ago, physicists at the GL Ionospheric Physics Division developed a method for solving the problem using the Balescu-Lenard collision operator in the plasma kinetic equation. This collision operator is rigorous and is derived from first principles. The solutions obtained using the GL method have provided several new and interesting results.

Electron-ion collisions have recently been found to have a destabilizing effect on ion-acoustic waves in a weakly collisional plasma. This destabilizing effect manifests itself in the form of enhanced ion-acoustic fluctuation levels in a thermal plasma ($T_e = T_i$), and, also, in the form of marginally stable ion-acoustic waves that can be sustained in a non-thermal plasma ($T_e \gg T_i$). It is interesting to recall that in the absence of collisions ion-acoustic waves are always damped.

An analytic expression for the marginal stability condition that relates the electron-ion collision frequency to the wavelengths of the modes and to other pertinent plasma parameters has been derived. This predicts that when the collision frequency exceeds the threshold value given by the condition, a collision-driven ion-acoustic instability may be expected in a plasma with $T_e \gg T_i$, even though there is no current. A laboratory experiment is currently in progress in order to check this prediction. Preliminary results indicate that, indeed, such an instability may be excited.

Daytime F-Layer Trough: A study using an extensive network of ground-based ionospheric sounders in the Northern Hemisphere has observed the daytime F-layer trough and described its properties under conditions of solar maximum near

winter solstice. This work has found the trough to be a fundamental but previously unrecognized feature of the high-latitude ionosphere which can present a barrier to hf communication and radar. The trough is seen as a region in which electron density is depleted, often by an order of magnitude. It occurs in sectors of the magnetospheric-ionospheric convection pattern where sunward convection displaces high-density daytime plasma with low-density nighttime plasma, a morning trough corresponding to the dawn cell and an afternoon trough corresponding to the dusk cell.

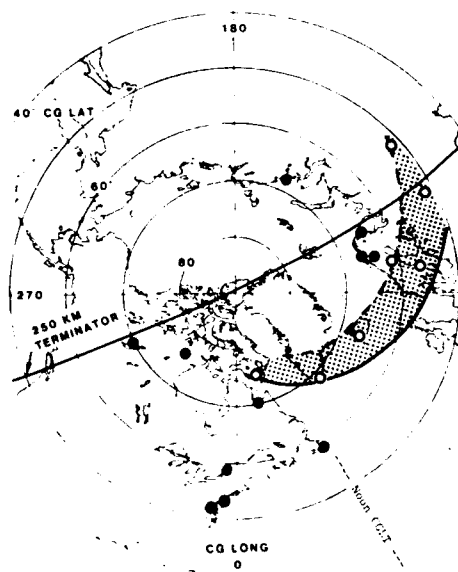
Although highly variable from day to day, the trough is a permanent feature at high latitudes during the thirty-one day period of continuous observation and is apparent in the diurnal distributions of the monthly medians of F-layer electron density measured by stations in this network. The afternoon trough, which is detected independently by at least 5, and as many as 18, stations on each day, is generally continuous and stationary for many hours in the reference frame of magnetic latitude/magnetic local time.

The trough contracts during quiet conditions to lie above 70° magnetic latitude but expands during disturbed conditions to extend from 75° to 52° magnetic latitude. The trough has a pronounced dependence on longitude, appearing principally in the afternoon in eastern magnetic longitudes but in the morning in western magnetic longitudes. This longitude effect is so prevalent that the diurnal maxima of the median F-layer electron densities are displaced relative to one another to earlier local time in the east and to later local time in the west. The longitudinal dependence occurs because the convection pattern, which produces the trough, resides in solar geomagnetic coordinates, but the undisturbed daytime F-layer resides in solar terrestrial coordinates. The two coordi-

nate systems vary systematically with respect to one another with longitude, and this variation accounts for the observed variation of the trough with respect to the daytime F-layer.

Like the auroral oval, the convection pattern-trough system exists on a global scale. Unlike the oval, the trough emits no radiation by which it can be imaged remotely by satellite on such scale. However the world-wide extent and high density of stations available to this study have made it possible for the first time to map the instantaneous location of the daytime trough and to show its global conformation.

The best example of such an image occurred on a disturbed mid-December day at 1430 UT when an array of stations simultaneously observed the



"Snapshot" of the Daytime Trough: An image of the instantaneous extent of the trough in the afternoon daytime F layer and, in effect, of sunward plasma flow in the dusk cell of magnetospheric-ionospheric convection. (Constructed from the simultaneous observations by 7 ionospheric sounding stations--open circles. The shaded area spans depletions of a factor of 4 in solar-produced electron density. Solid circles locate the additional 11 stations which observed the trough at other times on this day.)

trough and mapped its nearly total daytime extent in the afternoon sector. This case is shown in a plot of the Northern Hemisphere in Corrected Geomagnetic Latitude and corrected Geomagnetic Longitude in which the trough is shown as the shaded region and the 7 observing stations are shown as open circles (see the figure). The dashed line at the lower right hand side of the figure locates the noon CGLT meridian, and the F-layer is illuminated by the sun for all points up to the terminator at 250 km. The solid curve is the equatorward boundary of the trough, and the dashed curve marks the location where the daytime electron density has decreased by a factor of approximately 4 below its undisturbed level.

Altogether 18 stations observed the trough on this day, 7 at the time of the image (open circles) and 11 at other times (solid circles). The first observation was at 0730 UT at Dixon Island near the northern coast of Asia and the last at 2200 UT at Yellowknife on Great Slave Lake in the Northwest Territory of Canada. The trough pattern shown in the figure remained stationary in relation to the noon CGLT meridian as the rotation of the earth carried the stations under it. The afternoon trough was observed to exist continuously for a duration of 14.5 hours UT, corresponding to a longitudinal span of 220 degrees of Corrected Geomagnetic Longitude.

The portion of the trough defined by these stations in the figure extends 6000 km from Frobisher Bay on Baffin Island, across Greenland, Iceland, Scandinavia, European USSR to Sverdrup in western Asia, and occupies an area of 4 million sq km.

This is the first such image of the daytime trough and is therefore the first direct evidence that it is an integral, spatially continuous entity on a macroscopic, global scale. Because the daytime

trough is a product of the convection pattern, these properties can therefore also be attributed to the convection pattern of which the figure provides an indirect image.

ATMOSPHERIC DENSITY AND SATELLITE DRAG

Neutral atmospheric research in the 90-1500 km altitude region is directed toward development of a global-scale dynamic model that accurately specifies and predicts neutral densities, winds, temperatures, and composition. The model is needed to support design and operation of aerospace vehicles (including the National Aerospace Plane), satellite tracking and control, reentry prediction, decoy discrimination, and point density specification.

Empirical models have not been able to meet the accuracy requirements for these operations. Recently developed physical models, called thermosphere-ionosphere general circulation models (TGCM), will be used to circumvent limitations of the empirical models (see "Thermospheric Model Development" below). They will provide neutral-atmosphere absolute values and variability as a function of such parameters as latitude, longitude, local time, day of year, solar flux, and geomagnetic activity.

The observational database required to upgrade dynamic models is acquired through development of a high-altitude lidar capability and new satellite-based remote and direct techniques to sense density. Particular emphasis is placed on the 90-250 km region, where there have been relatively few measurements because the region is above that accessible to most rockets and below that of most satellites. As the required accuracy of dynamic models is achieved through theoretical interpretations of data, the models will be transitioned for operational use to support Hq AWS, US Space

Command, Air Force Satellite Control Facility, the Air Force Space Forecast Center, and Special Strategic Programs.

High-Latitude Lidars: The development of laser remote-sensing techniques for measurement of atmospheric properties in the middle atmosphere and lower ionosphere has received continual support by the Ionospheric Physics Division. Measurements of density up to 90 km are crucial to the modeling of the 90-250 km region with accuracies less than 5 percent error. Measurements of the Rayleigh scattering produced by the exposure of the atmosphere's neutral constituents to the beam from a pulsed high-intensity laser may be analyzed to generate height profiles of basic properties such as neutral density and temperature. The GL effort is based on two high-altitude lidar systems: the laboratory facility (GLEAM-Ground-based Lidar Experiment for Atmospheric Measurements) and the mobile unit (GLINT-Ground-based Lidar Investigation-Transportable).

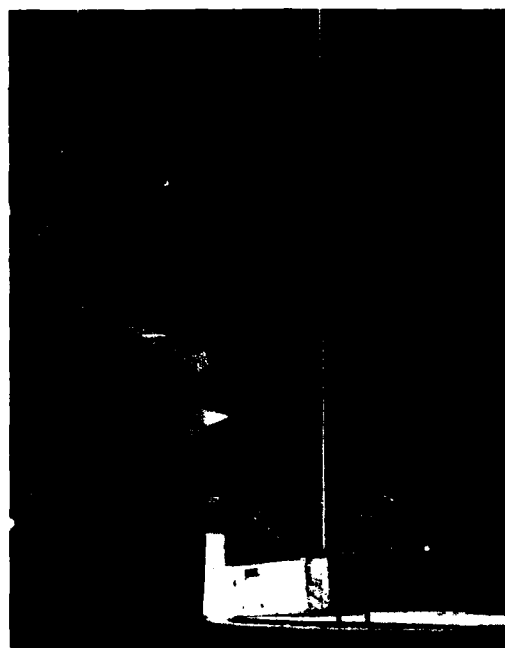
With commercially available high-power lasers and improved electronic detection systems, Rayleigh lidar has become a reliable tool in determining neutral density. This opens up the possi-

bility of quantifying short time-scale density perturbations such as those caused by acoustic gravity waves. New capabilities were added to the systems in 1988. Lidar measurements with an excimer laser operating at 351 nm demonstrate the applicability of this type of high-power laser in Rayleigh lidar technology. The addition of the new excimer laser increases the GLINT performance factor by 4. The second implementation is a Fabry-Perot filter which allows measurements under the conditions of the very bright daytime sky-radiance background. (Normally, the lidar is operated at night.) A Raman lidar has also been developed and implemented to improve the absolute density calibration in the low-altitude region.

A long-term campaign was initiated in August, 1988, to collect a comprehensive database of density profiles for comparison with the modeling efforts. Data are



Excimer Laser Transmitter (xenon fluoride, 351 nm) in GLINT Trailer.



GLEAM and GLINT Lidars Operating with Green Radiation.

collected at the rate of 150 altitude profiles per month. In addition, planning for a field campaign with GLINT has resulted in an invitation to collaborate with the Air Force Wright Aeronautical Laboratory to use their 100 in. optical receiver. An exploration of a possible collaboration with NASA and NATO colleagues has been initiated to quantify the consequences of high-altitude clouds (known as polar mesospheric and noctilucent clouds) to Air Force orbital vehicles, particularly during the re-entry phase. This work relates to the specification of density for the engineering design of the NASP vehicles now envisioned for the late 1990's.

Satellite Density Remote Sensor: The University of Michigan evaluated the feasibility of measuring atmospheric density in the upper mesosphere and lower thermosphere by using passive satellite remote-sensing techniques. A spectrometric technique based upon daytime resonance fluorescence measurements of the molecular oxygen atmospheric-band emissions was determined capable of providing density and temperature data in the 60-120 km region with an accuracy of 5 percent at a resolution of 2-3 km in the vertical and about 200 km in the horizontal direction. The estimated power, weight, data analysis complexity, and costs were determined to be compatible with typical research probes. Such an instrument provides the capability to routinely monitor global density in an altitude region where measurements presently consist of only a few rocket flights. A prototype satellite sensor, based on results of this study, is being designed and fabricated.

Thermospheric Model Development: GL satellite accelerometer measurements of density from nine satellites during the period 1974-1984 have led to the development of our most extensive database of density in the 150-250 km altitude

region. These data were used to evaluate the accuracy of atmospheric models developed from 1960 to the recent 1986 MSIS (Mass Spectrometer and Incoherent Scatter) model. The study showed a lack of significant progress in error reduction even in the most recent models. Models typically have a one sigma standard deviation of 15 percent, with larger errors occurring at high latitudes and at higher geomagnetic activity. To achieve the higher accuracies required for Air Force systems, new physical concepts and new dynamics parameters have been incorporated into models. The basis for these improvements is the new Thermosphere General Circulation Model (TGCM) developed at the National Center for Atmospheric Research (NCAR). This model considers the dynamic, energetic, and chemical processes as part of the coupling between the neutral atmosphere, the ionosphere and the magnetosphere. The *Report on Research* for 1985-1986 (AFGL-TR-87-0188) described preliminary results comparing predictions of general circulation and empirical models with accelerometer measurements of density and winds. Initial results demonstrated the feasibility of using dynamic models to develop a more accurate capability for forecasting density and drag. The completed study shows that the TGCM predicted several features of the measured data not described by empirical models: a localized hot spot of enhanced density (60 percent) in the high-latitude dayside thermosphere, wavelike structures with horizontal scales of 1500 km and phases propagating toward the equator in the night sector, polar winds with velocities of 250 -- 600 m/s consistent with antisunward convection and return flows characteristic of a two-cell ion-convection pattern but rotated several hours later in local time.

In conjunction with Hq AWS, GL initi-

ated an effort to deliver a more accurate operational model based on the TGCM to specify and predict neutral density, temperature, winds, and composition from 90-1500 km. This is a four-year effort to upgrade modeling capability in three phases: 250-1500 km (FY90), 140-250 km (FY91), and 90-140 km (FY91). The TGCM simulations of atmospheric variability over a wide range of variables will be run on a CRAY computer. The information will be converted to a computationally efficient format accessible to the DoD and scientific community by using a vector spherical harmonic truncation technique that regenerates time-dependent neutral variable fields from sets of pre-stored coefficients. The advantage of this model is its ability to quickly and accurately reconstruct neutral variable fields that were created by the original NCAR TGCM, with all the thermospheric dynamics included, in only a fraction of the time.

To quantify the occurrences of wave structure and obtain a preliminary assessment of their magnitude and dependence on magnetic activity, GL satellite accelerometer density measurements for typical quiet and active days in July, 1983, were spectrally analyzed using the Maximum Entropy Method. Wave motions were found to contribute to the observed variability of density during both quiet and active conditions, and to become increasingly important as magnetic disturbances become more intense. Evidence exists for enhanced wave activity at high latitudes and during nighttime, and for a significantly higher probability of finding waves with horizontal wavelengths between 1250-2000 km and 150-500 km, than waves with wavelengths between 500 and 1250 km, especially during geomagnetically disturbed conditions. The larger scale waves are known to be capable of propagating large distances with little attenu-

ation. The relatively frequent occurrence of the shorter scale waves, even at low latitudes, was tentatively concluded to be attributable to ducting in the lower thermosphere, which allows the waves to travel large distances.

Absolute Density Mass Spectrometer: The measurement of the absolute neutral-gas density and composition to high accuracy has proved to be a difficult task. Among the problems to be overcome in the in-situ measurement of these parameters are: performing the measurements aboard a spacecraft moving at nearly 8 km/sec, measuring ambient gases that interact with the physical surfaces of the instrumentation, calibrating the instrumentation to very high accuracies, and ensuring low short-term and long-term drifts in instrument sensitivity.

GL has begun development of a new mass spectrometer intended to provide high accuracy measurements of neutral gas density and composition. This instrument combines many of the improvements and concepts developed over the last twenty years, along with state-of-the-art microprocessor-controlled electronics to provide for operation in a wide variety of orbital conditions. The culmination of this program will be a mass spectrometer capable of measuring absolute neutral density and composition to within 5 percent absolute accuracy.

This instrument addresses the measurement problems using a variety of techniques. Key to the high-accuracy measurement of non-reactive gases is the accommodation sphere at the front of the instrument. This converts, in a well-defined manner, the gas molecule striking the spacecraft at orbital velocities to a thermalized gas at a known temperature which can be very accurately measured. Reactive gases such as atomic oxygen are measured by moving the flag aside to allow direct access to the gas beam. The instrument has two modes of

operation, a fly-through mode and a retarding potential analyzer mode, that directly use the energy of the incoming gas beam to reject molecules that have undergone surface interactions. It can, therefore, measure unperturbed reactive gases. A calibration source is included on-board to permit continuous monitoring of any short-term or long-term changes in instrument calibration.

The instrument has been tested at the Los Alamos high-velocity atomic-oxygen beam facility and the University of Minnesota high-velocity molecular-beam facility to simulate the effects of orbital operations. Initial results show confirmation of the validity of the basic mass spectrometer design and its ability to measure both absolute density and composition. The data also showed that the fly-through mode of operation has a 40,000 to 1 rejection ratio against molecules that have undergone surface interactions, which will provide the necessary tool to measure reactive gases. Work is continuing to improve the accuracy of reactive gas measurement and to construct a static calibration facility having a very high accuracy.

IONOSPHERIC INTERACTIONS

In the ionosphere, the many ion and neutral species undergo a wide variety of encounters which affect radio propagation in this region. Such effects can be particularly acute at high latitudes. They also influence the environment of spacecraft in orbit and during re-entry. A comprehensive network of polar ionospheric monitoring experiments has been assembled to conduct radio-wave propagation studies within the polar cap. Topics such as meteor scatter were studied with the aid of installations in Greenland. A new technique was introduced to determine the very low electron density and electrical conductivity of the lower ionosphere where propagation of

elf/vlf waves under stressed conditions is effectively controlled by the conductivity. In addition, both the ion and neutral chemistry of the ionosphere have been studied theoretically as well as in laboratory and field experiments.

Research in ion chemistry centered on measurements of rate constants, cross sections, bond dissociation energies, and electron affinities for the reactions of ions in the gas phase with neutral molecules, electrons, photons, and other ions. These reactions cause, among other things, radio blackout during atmospheric reentry of spacecraft. The measured rate constants serve as input to computer codes developed to model the blackout conditions. Also, several chemicals have been investigated for their ability to react with free electrons in the gas phase to produce negative ions. A good electron quenchant is one that attaches electrons rapidly and for which the energy to detach the electron from the resulting negative ion is large. Such species have long been used to produce effective and long-lasting perturbations of the local ionospheric electron densities, but improved chemicals are required.

Research programs have also been initiated to assess the potential of greatly enhancing Air Force Command, Control, and Communications (C3) capabilities by exploiting both ground- and space-based techniques to control the properties of selected (small) regions of the ionosphere. In the ground-based arena, theoretical and experimental investigations were initiated on the use of high-power radio waves to alter the refractive properties of the existing ionosphere as well as to create new plasma regions where none existed before. Space-based rocket and satellite platform techniques, studied theoretically, included the use of electron, ion, and plasma beams, x-ray and extreme ultraviolet beams, and neutral gas releases to change the ionization in

designated regions.

Survivable Propagation: Communication survivability across the frequency spectrum from extremely low frequencies (elf, 30 3000 Hz) through very high frequencies (vhf 30 -- 300 MHz) is controlled by absorption in the lower (D-region) ionosphere. A research program was undertaken to examine techniques for measuring and predicting the electron density in this region and to assess the effects of ionospheric disturbances on those propagation modes which provide the best potential for meeting the survivable communication requirements of the Air Force. A key feature of this program is the simultaneous measurement of ionospheric and propagation parameters during polar ionospheric disturbances, which simulate the effects of certain high-altitude nuclear events. Because of the current DoD interest, the program emphasizes ionospheric effects in two areas: vhf meteor-scatter propagation and long-range, low-frequency propagation. Meteorscatter performance is being examined through the development of theoretical models and high-latitude measurements. Low-frequency (lf) propagation is being evaluated by determining the electron density profile between 40 -- 65 km, a parameter which has previously been unavailable for this region which controls the survivability of elf/vlf/lf propagation.

The meteor-scatter program is characterizing the performance of vhf meteor-scatter propagation, under both normal and disturbed ionospheric conditions. Present emphasis is centered on acquiring experimental data in the polar cap at six frequencies over the 35 -- 150 MHz band, using a meteor-scatter diagnostic link between Sondrestrom Air Base and Thule Air Base, Greenland. This diagnostic link is providing critical data on propagation survivability, including absorption and polarization rotation, as

a function of frequency, time, path length, and disturbance severity. Additional diagnostic links are used in occasional campaigns to study auroral, directional, and latitude effects.

The If program to measure the electron density profile of the lower ionosphere is based on a new, and very promising, technique which combines a chemical release and mass spectrometer measurement. This program was initiated to develop a technique for measuring the electrical conductivity of the ionosphere over the 40 -- 65 km altitude range. Although the conductivity in this range effectively controls the propagation of elf/vhf waves under stressed conditions, it has heretofore been impossible to acquire experimental data to characterize it. The problem has been the difficulty in measuring the very low electron densities in that relatively dense region of the atmosphere. GL's novel approach to the problem consists of seeding the region with a chemical (sulfur hexafluoride [SF_6]) so that a reaction occurs rapidly, resulting in the formation of negative ions equal in number to the original number of free electrons. The density of the newly formed ions can then be measured using a mass spectrometer developed and routinely used in space by GL. A proof-of-concept rocket-borne experiment was conducted from Wallops Island, VA, in August, 1987. The experiment demonstrated that the concept was valid, as the data showed good qualitative agreement with theoretical models of the collection process.

The follow-on to the initial, proof-of-concept experiment will be actual measurements of the conductivity of the lower ionosphere. Rocket launches have been scheduled in FY89 from Wallops Island which will include the SF_6 -mass spectrometer as well as supporting Gerdien condenser and ringed electrode probe measurements. Successful comple-

tion of these flights will be followed by flights from Thule Air Base, Greenland, in FY92 during, and immediately after, a polar-cap absorption event.

Atmospheric Ion Chemistry: The primary objective of the program in atmospheric ion chemistry is to obtain information on the reactions of ions in the gas phase with neutral molecules, electrons, photons, and other ions. These kinds of reactions are important in the stratosphere, mesosphere, and thermosphere, and under other conditions in which weak plasmas are generated, as in combustion and some gas-phase laser chemistry. Such phenomena as antenna breakdown, radio blackout during atmospheric reentry, and radio and radar blackout following nuclear detonations are in part the result of these reactions. The computer codes which have been developed to model these phenomena require as input rate constants, cross sections, bond dissociation energies, and electron affinities.

Our studies on reactions between ions and neutral molecules are performed using a selected ion flow tube (SIFT). A diagram of the apparatus is shown in the 1985-1986 *Report on Research* (AFGL-TR-87-0188, p. 88). In the SIFT, reactant ions are generated either by electron bombardment or as the result of ion-neutral reactions. These ions are mass-analyzed, and the desired ion species is injected into a fast-flowing (10^4 cm s⁻¹) stream of inert carrier gas, usually helium. Further downstream, after the ions have reached the same temperature as that of the carrier gas, reactant neutral gas is injected into the flow tube at a known flow rate. Ion neutral reactions may then occur, causing depletion of the reactant ions and formation of product ion species. The ion composition of the gas stream is monitored with a second mass spectrometer at the downstream end of the flow tube. Reaction rate con-

stants are determined by measuring the loss of reactant ions as the flow rate of the reactant neutral gas is varied. The temperature range available in these studies is from 85°K to about 600°K. Possible reactant neutral species include atomic hydrogen and atomic oxygen, in addition to more stable species. As a result of the addition of a drift tube to the apparatus, converting the SIFT to a Variable Temperature Selected Ion Flow Drift Tube (VT-SIFDT), a longitudinal electric field can be generated in the reaction region of the flow tube, allowing the average ion kinetic energy to be varied. By this means, translational energies corresponding to temperatures up to several thousand degrees Kelvin can be obtained. However, the internal energies of the ions and neutral molecules are not equilibrated with the translational energy of the ions, and the effects of very high temperature on reaction kinetics are only incompletely simulated.

The VT-SIFDT is an extremely versatile instrument and allows for the determination of many types of temperature or energy dependences by the appropriate choice of conditions. This allows us to extend our past work on the temperature dependence of ion-molecule rate constants to include more specific types of energy effects. Knowledge of various types of energy dependences is important in that many of the plasmas we are interested in, such as those involved in radio blackout, occur at high temperatures outside the range of the VT-SIFDT. By understanding how various types of energy affect the rate constants of interest, better extrapolations of the data taken at moderate temperatures can be made.

Of special interest are two recent studies. The first of these involves the determination of the dependence of the rate constant for an ion-molecule reaction on the rotational temperature of the reac-

tant neutral. Rate constants are measured as a function of ion kinetic energy at several temperatures. In general, comparisons between data taken at different temperatures are difficult because more than one type of energy has been changed. However, for monatomic ions, the situation simplifies. Comparing data at the same center of mass kinetic energy at different temperatures gives the dependence of the data on the internal temperature of the reactant neutral. Further simplification arises if the vibrational frequencies of the reactant neutral are large. In this case the comparison refers only to the rotational temperature dependence. To date we have seen no large effects due to rotation, but this in itself has proven interesting.

The other study on specific aspects of energy is a study of the collisional vibrational quenching of NO^+ . These quenching rates are important to understanding the chemistry of the ionosphere, where NO^+ is an important species. The use of a monitor ion inlet just before the sampling orifice allows us to detect vibrational excitation in the ions. In this manner we have managed to study the quenching rates for a number of species. The rate constants we have measured at 300°K are shown Table 3. The quenching rate constants vary dramatically from less than 10^{-13} to $10^{-9} \text{ cm}^3 \text{ s}^{-1}$. Also shown in the table are the collision rate constants (k_c) and the average number of collisions before quenching occurs (Z). The results are explained by a vibrational predissociation model in which the quenching rate is strongly dependent on the lifetime of the collision complex. This results in a correlation between quenching rate constant and polarizability of the neutral. We have also been able to measure the temperature dependence of

these rates for the first time and have even been able to measure energy dependences as a function of temperature. We have found the quenching rate constants to have slight, or negative, temperature dependences varying between T^0 and $T^{-2.3}$. These results are in accord with the theory mentioned above.

The ion composition of the lower atmosphere is now known to be dominated by complex solvated ion species derived from such neutral molecules as water, acetonitrile, acetone, ammonia, sulfuric acid, hydrochloric acid, and nitric acid. The abundances of these species as neutrals in the atmosphere are vanishingly small (with the exception of water), and it is apparent that the processes which convert the minor neutral species into the dominant ionic species must be very efficient. Information on the relative ion abundances, together with the rate constants for the production and loss of the solvated ion species, can be used to derive the concentrations of the minor neutral species in the stratosphere. Following the application of this technique to the derivation of nitric acid and acetonitrile concentrations, as reported in the 1983-1984 *Report on Research* (AFGL-TR-85-0113, p. 21) and 1985-1986 report (AFGL-TR-87-0188, p. 88), we have recently measured the rate constants for the reactions of mixed water and ammonia ions, i.e., $\text{H}^+(\text{NH}_3)_m(\text{H}_2\text{O})_n$ for $n + m \leq 6$, with pyridine and picoline. These ions are the predominant ion species at ground level. We have used these data to derive the concentration of pyridine and picoline at the ground in conjunction with the ion composition data measured by F.L. Eisele. A concentration on the order of 10 parts per trillion is derived for pyridine.

TABLE 3
QUENCHING RATE CONSTANTS (k_q)
for VARIOUS NEUTRALS with NO^+ at 300°K
 (Also shown are the collision rate constants (k_c) and the average number of collisions before quenching occurs. (Z))

Neutral	k_q (cm^3s^{-1})	k_c (cm^2s^{-1})	Z ($=k_c/k_q$)
Kr	<1(-13) _a	7.8(-10)	>7800
Xe	2.8(-13)	9.5(-10)	3400
H ₂	6.0(-14)	1.5(-9)	25000
D ₂	5.6(-14)	1.1(-9)	20000
N ₂	2.6(-12)	8.1(-10)	310
O ₂	2.4(-13)	7.5(-10)	3000
CO	4.9(-12)	8.9(-10)	8.6
CO ₂	1.1(-10)	9.5(-10)	180
NO ₂	8.3(-11)	1.05(-9)	13
SO ₂	6.1(-11)	2.0(-9)	33
CH ₄	5.0(-11)	1.2(-9)	24
CH ₃ F	1.7(-10)	2.4(-9)	14
CH ₃ CL	5.7(-10)	2.4(-9)	4.2
CH ₃ Br	6.5(-10)	2.2(-9)	3.4
C ₂ H ₆	6.6(-10)	1.3(-9)	2.0
C ₃ H ₈	1.0(-9)	1.4(-9)	1.4
SF ₆	2.2(-12)	1.2(-9)	545

^a 1(-13) means 1×10^{-13}

ARTIFICIAL PLASMA TECHNOLOGY

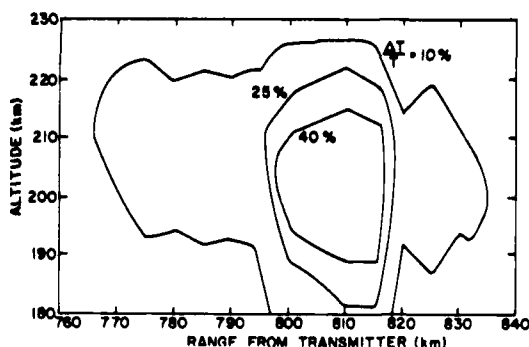
As a direct result of impetus provided by System Command's Project Forecast II, research programs have been initiated to assess the potential of exploiting techniques to control the properties of selected (small) regions of the ionosphere to greatly enhance Air Force Command, Control, and Communication (C3) capabilities. The research involves revolutionary technologies and includes both ground-based and space-based approaches. Rather than working within the limitations imposed on conventional systems by the natural ionosphere, our revolutionary concepts envision seizing control of aspects of the propagation environment to insure that it has the radio-wave reflection properties required to achieve a desired C3 capability. The research has opened up the possibility for new classes of innovative and pioneering experiments

to be conducted in the future.

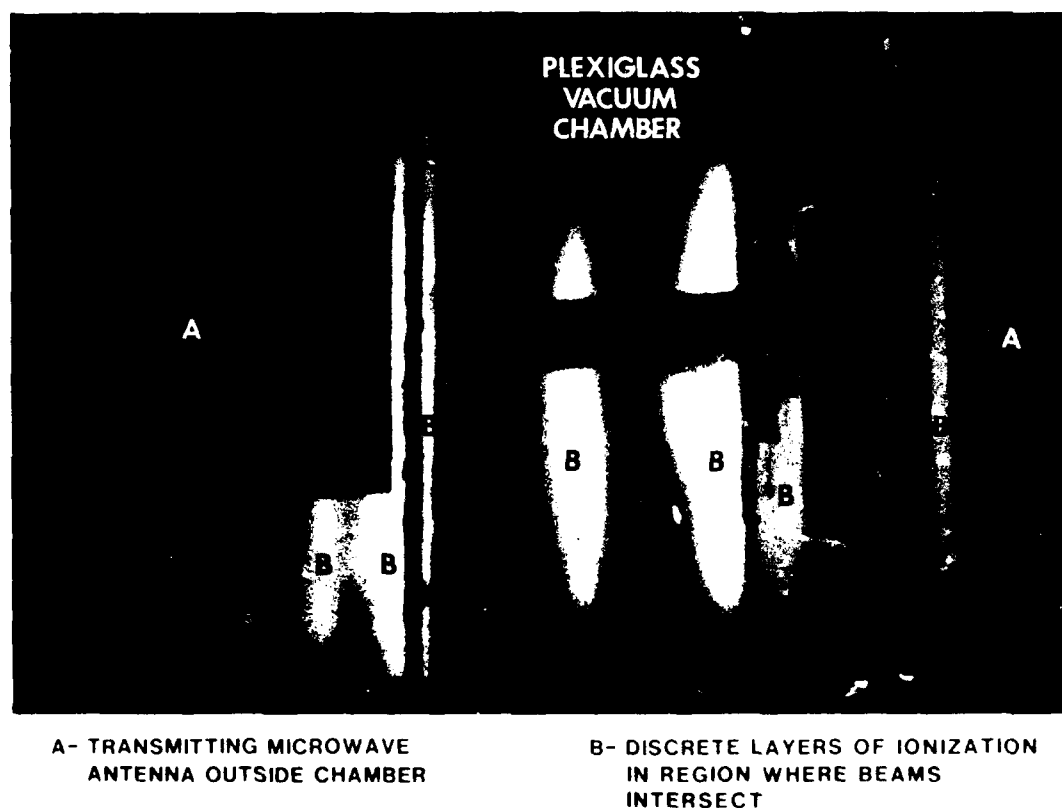
Ground-Based Concepts: Significant theoretical and experimental investigations were begun in FY87 on the use of ground-based, high-power radio waves to alter the refractive properties of the ionosphere. A number of ground-based approaches have been identified but, to date, the research has focused on the heating effects produced in the ionosphere by obliquely propagating, high-frequency (hf) waves, and the use of high-power microwaves to produce, in effect, an Artificial Ionospheric Mirror (AIM) in the atmosphere.

The ability of high-power hf radio waves to modify the ionosphere, to produce self-limiting perturbations, or to interfere with other signals, has been observed using vertically incident hf "heaters." However, because vertical heaters only alter the ionosphere directly overhead, their potential for military purposes is very limited. The potential exploitation of oblique hf heating to modify the ionosphere at great distances from a "heater" is much more applicable to Air Force interests.

Recent theoretical research indicates that, although obliquely propagating high-power hf waves cannot excite the same parametric decay instabilities produced by vertical heaters, and although such waves suffer greater free-space



Percent Increase in Electron Temperature over Daytime Ambient Conditions Caused by an Oblique, High-Power (85 dBW), HF (15 MHz) Transmitter.



Air Breakdown in a Laboratory Chamber Using High Power Crossed Microwave Beams

spreading losses as well, they may produce substantial effects near caustics (regions where strongly focused fields occur). Electric fields in such caustics can reach strengths sufficient to produce substantial heating of F-region electrons (see the figure), resulting in changes in electron-loss rates in the ionosphere as well as diffusion of electrons away from the heated region. Both phenomena result in changes in the refractive properties of the heated region.

The degree to which these changes can affect other radio waves passing through such heated regions is a focus of ongoing research. A numerical model based on linear theory has been developed which, for a given high-power hf transmitter, defines the caustic surfaces for a normal

ionosphere, uses a full-wave calculation to estimate field strengths in the caustic region, calculates the temperature changes due to the electric fields, estimates the electron density changes due to both the temperature changes and diffusion, and evaluates the effect of the changed refractive properties on signals propagating through the disturbed region. The model has been used successfully to predict changes in ground field strength observed during an oblique heating experiment. Near-term plans consist of expanding the theory to include non-linear effects, and conducting a series of field experiments using very high power hf transmissions (of the order of 90 dBW), beginning in FY89.

The concept of the Artificial

Ionospheric Mirror (AIM) involves the use of a ground-based radio frequency heater to create patches of ionization ("mirrors") in the atmosphere (nominally 70-80 km altitude) which could be used to reflect and/or scatter radio waves. In FY87 a number of research programs were initiated to assess the viability of the AIM concept, including the development of theoretical models and numerical simulation codes, and laboratory chamber experiments. Studies have been conducted on the use of crossed-microwave beams (see the figure) and single (focused) microwave beams to create, maintain, and control the patches of ionization. Critical issues investigated include: the heater power requirements and how they vary with heater frequency and the desired altitude of the ionization patches; the resultant electron densities, including structures; the obtainable patch sizes; the time required to make a patch; the patch lifetimes; and the radio-wave reflection properties of the patches. A Fokker-Planck equation was formulated to model the breakdown processes and for numerical simulations.

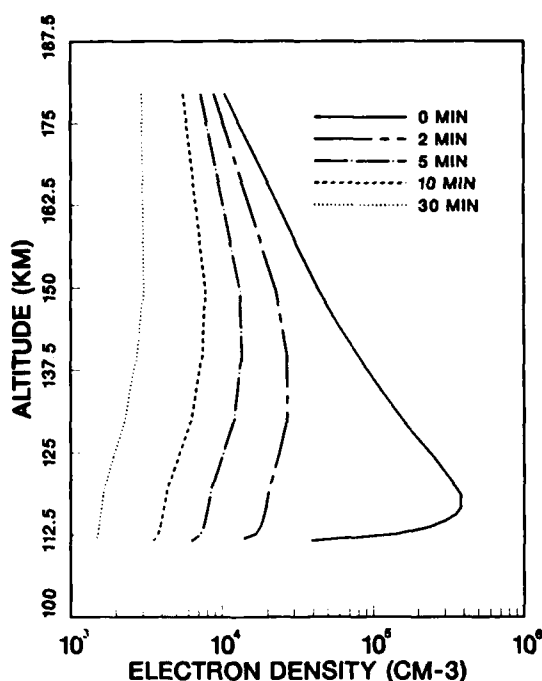
Recent research results include the determination that a 400 MHz heater, focused at 75 km and having an effective radiated power of about 140 dBW, could produce ionization patches which could be exploited to greatly enhance long-range hf/vhf systems. A candidate heater to achieve this was also developed, consisting of a 1 km-square antenna array having 60 dB gain and producing 100 MW peak power. Only 1-2 MW average power would be required, however, since the ionization patches could be formed by pulsing the heater.

In addition, preliminary studies have been conducted on potential Air Force system applications for the AIM concept. The research shows that there are a large number, and a wide variety, of complex interrelated physical and system

parameters that must be understood and quantified in order to properly assess the technical feasibility and potential system desirability of the AIM concept. An overall simulation model called MOTHS (Mirror Over-The-Horizon Simulation) has been partially completed. It will be useful as a quantitative tool to examine the performance sensitivity of the numerous interrelated parameters that control patch-ionization characteristics, including whether (ultimately) "mirrors" can be created that will have the necessary spatial and temporal coherence for specific Air Force applications.

Space-Based Concepts: Theoretical investigations were conducted of a number of space-based techniques for altering the refractive properties of the ionosphere. These included the use of low and moderate energy (below 500 keV) electron beams, relativistic electron beams, ion beams, x-ray and extreme ultraviolet (EUV) beams, and neutral gas releases from rapidly moving space vehicles.

Recent rocket and space shuttle experiments have shown that it is possible to launch electron beams into the earth's ionosphere and magnetosphere. The research indicates that, through proper selection of beam-related parameters, a variety of plasma density variations can be created. As illustrated in the figure, it should be possible to create significant and comparatively persistent ionization enhancements in the E- and lower F-regions of the ionosphere. By directing repetitive pulses of an electron beam downwards along the geomagnetic field, a structure consisting of a regularly-spaced series of ionized columns would be produced that could be observed from the ground by suitably located radars. Observations of the striated plasma screen, or "picket fence," would provide information about some properties of the local ionospheric plasma as well as the ionization produced by the electron gun.



Temporal Variation of Ionization Densities Produced in a Uniform Plasma Sheet by a 1A, 5 kV Electron Beam from a Platform Moving at 140 m/s.

It could also conceivably be used as a diffraction screen for hf/vhf radio transmissions.

Highly energetic (relativistic) electron beams (greater than 500 keV) penetrate down into the lowest regions of the ionosphere, and even into the comparatively un-ionized middle atmosphere. They therefore offer a new capability for altering the properties of the ionosphere. The research shows that a single pulse from a moderately powerful (5 MW) relativistic (5 MeV) electron accelerator on a rocket or satellite platform can penetrate to the lower mesosphere and upper stratosphere, creating a dense column of free electrons and positive ions as it does so. The ionized column can scatter electromagnetic radiation. Preliminary computations indicate that it may also have a most unusual property: it may initiate an intense upward traveling electrical

discharge similar to lightning. The research has shown that a rocketborne relativistic electron beam experiment is feasible with current technology.

Ion and plasma beams have been shown to produce artificial plasma-density structures in the ionosphere in the same manner as electron beams, but at higher altitudes. Likewise x-ray/EUV beam generators, with characteristics similar to ones already in use in laboratories, have been found to produce columns of substantially enhanced ionization in the ionosphere. Unlike beams of charged particles, such photon beams propagate through the ionosphere with little or no dependence on the geomagnetic field. Thus, the columns of ionization that are produced do not have to be aligned with the geomagnetic field. Further, x-ray/EUV beams would avoid the potential difficulties with vehicle charging that charged particle beams on space platforms normally entail.

A study of neutral gas releases in the ionosphere drew attention to a new process which is independent of the better known Critical Ionization Velocity (CIV) effect and which could lead to the generation of elf/vlf waves and to electron density fluctuations that could disturb the local ionosphere. The key to the initiation of the process, which involves charge exchange, is release of the neutral gas from a rapidly moving vehicle such as the space shuttle. It is also important that the neutral particles should be relatively heavy (compared with O^+). The study provided several recommendations of additional theoretical and experimental work that could be done to test the viability of the technique, including a possible shuttle experiment to test the concepts involved in the new process.

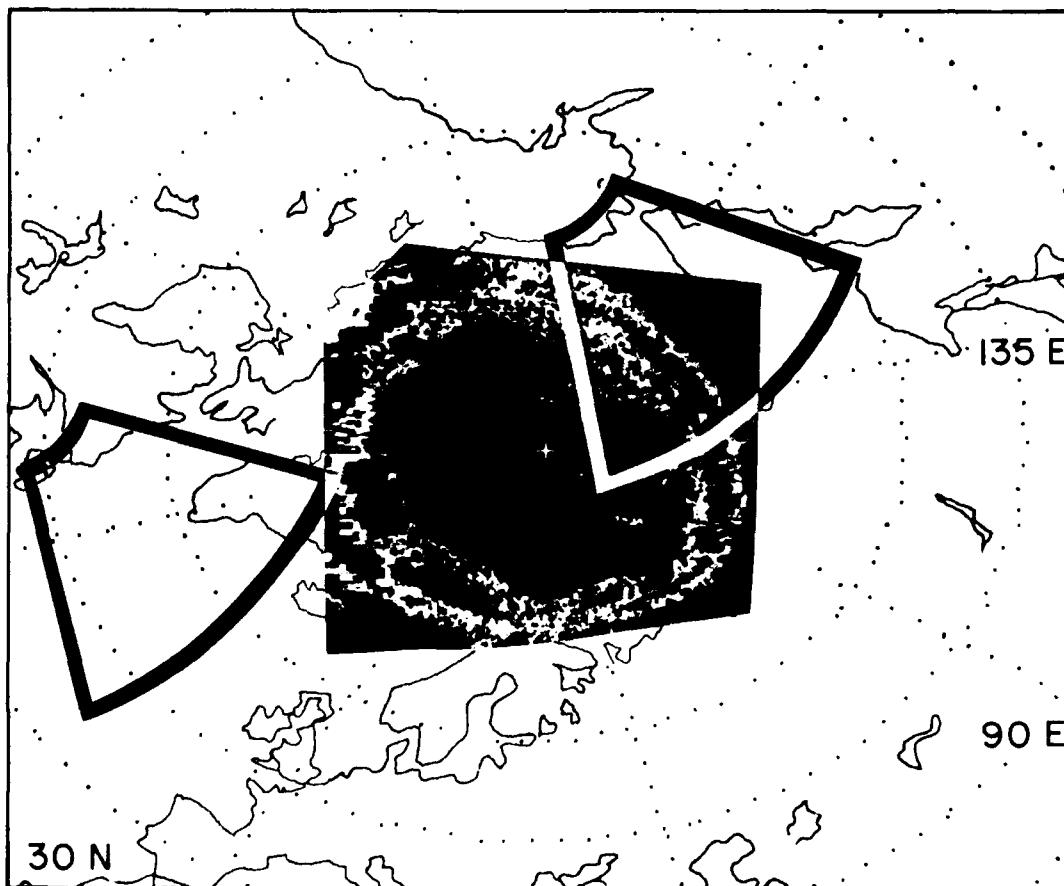
UV REMOTE SENSING

Ultraviolet radiation from the Earth's

atmosphere is being used to develop remote-sensing methods for determining the electron density structure of the ionosphere, for locating the auroral disturbance region including auroral and polar cap structures, and for characterizing the energy spectrum of incident particles producing the aurora. These improved methods will enhance the operation of Air Force radar and communications systems by enabling near real-time specifications of ionospheric conditions over a large fraction of the globe.

Following its launch in November, 1986, aboard the Polar BEAR (Polar Beacon and Auroral Research) satellite,

the Auroral/Ionospheric Remote Sensor (AIRS) has provided many thousand images of atmospheric radiation at far ultraviolet and visible wavelengths, as shown in the accompanying figure. Polar BEAR is in a polar orbit at 1000 km altitude; with an earth-facing, movable mirror making repetitive cross-track scans. The resulting raw strip images extend nearly 5000 km, horizon-to-horizon. To display the images and aid in their analysis, geometric corrections are applied, and the often weak signals are processed with an adaptive spatial filter to preserve as much as possible of the structural detail of auroral zone features.



AIRS/Polar BEAR UV Auroral Image Showing Overlap with OTH Radar Coverage.



AIRS Polar BEAR UV Auroral Image at Higher Spatial Resolution in a Region with Polar Cap Arcs and Radio Wave Scintillation.

Final, calibrated images are rendered in false color displays at a microcomputer-based work station.

One interesting example of the studies carried out with these data is shown in the accompanying figure. Here an AIRS image is annotated to show the presence of auroral structures (bright, arc-like features of atomic oxygen radiation) along the propagation path of a radiowave known to have experienced phase scintillation in traversing the ionosphere from Polar BEAR to a receiver at Sondrestrom, Greenland.

In another of its modes of operation, the AIRS scanning mirror is held at nadir position and the far ultraviolet

spectrum of the atmosphere is scanned from 1100 Å to 1900 Å. During the summer of 1987, coordinated measurements were carried out between the Millstone Hill incoherent scatter radar in Westford, MA, and Polar BEAR as it passed overhead, with AIRS operating in the spectrometer mode. That small program has produced a well-documented set of spectrally resolved far ultraviolet dayglow measurements obtained while a ground-based radar simultaneously measured the electron density structure and temperature of the same ionospheric volume. This experiment makes available the means to test and validate models which predict the electron density profile

of the ionosphere based on knowledge of passively sensed ultraviolet atmospheric emission (see "EDP Profiles from Satellite UV and In-Situ Data" above). A sensor utilizing this technology may find future application as a component of the Defense Meteorological Satellite Program.

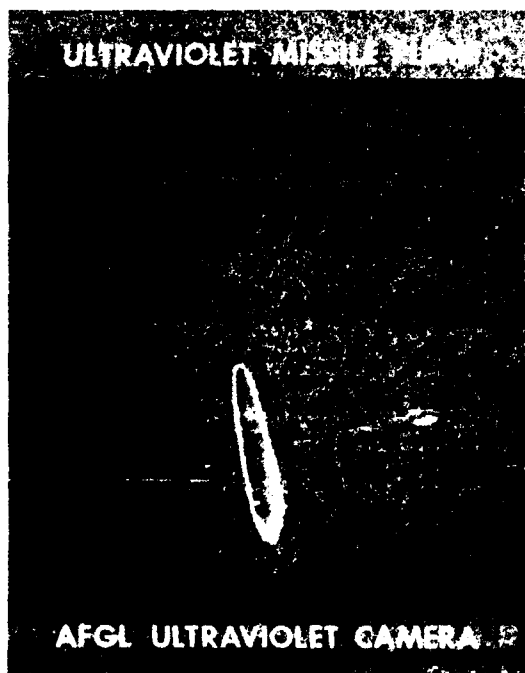
Planning based on insights gained from the AIRS experience and continuing analysis of high-resolution spectral data from the earlier S3-4 satellite is now well underway for the Atmospheric Ultraviolet Radiance Analyzer (AURA) satellite payload. It will provide ultraviolet data with improved sensitivity, spectral resolution, and spatial resolution.

UV Targets and Backgrounds: Plume measurements in the ultraviolet from a Scout rocket were measured during the launch of Polar BEAR at Vandenberg Air Force Base in 1986. The sensors consisted of solar-blind ultraviolet photometers

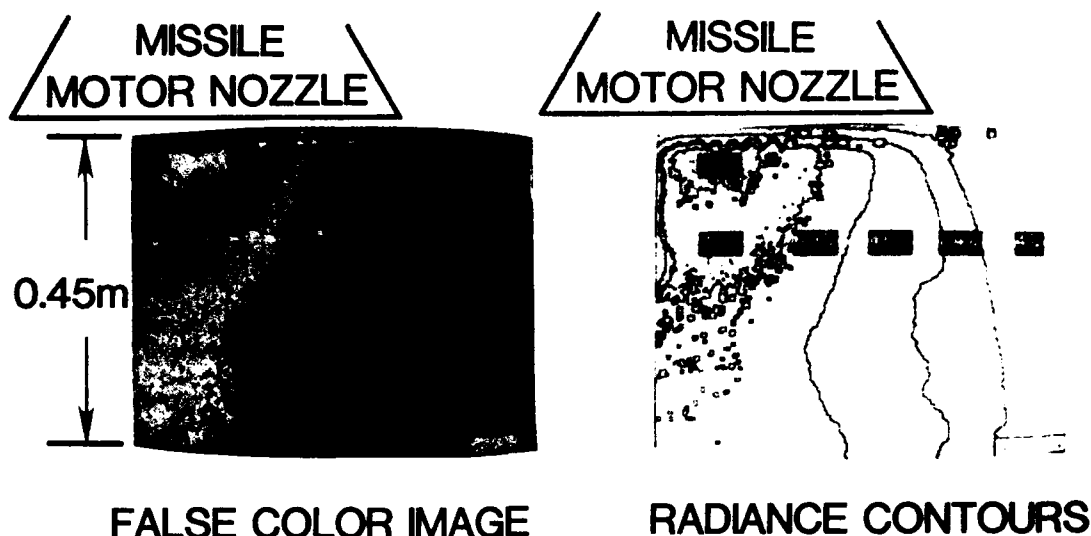
with peak response at four different wavelengths in the region from 200 to 300 nm. In addition, an ultraviolet imager observed the rocket-exhaust plume throughout the first stage and through a portion of the second stage of the rocket ascent. The size of the plume and its variation with altitude were determined. With GL's LOWTRAN 6 code (for a description, see Chapter V, "Computer Codes and Databases"), the transmission of the atmosphere was calculated and the radiance values of the plume were determined.

To measure the ultraviolet radiations at longer distances and, hence, into the upper stages of a rocket's trajectory, an 18 in. telescope at Vandenberg AFB was refurbished and recoated for use in the ultraviolet region of the spectrum. A special imager was developed for this telescope, including special filters for detecting the near ultraviolet radiation from rocket plumes. The telescope and imager have been assembled on a Cine-Sextant tracker and tested. The unit is now ready for making ultraviolet observations, and preliminary data were acquired in 1988.

The ultraviolet radiations from a series of four Super BATES motors were measured as they were fired in a test cell at Arnold Engineering Development Center. The purpose of these tests was to determine the radiation characteristics of this motor as a function of the aluminum loading of the propellant. The motors were fired at a simulated altitude of approximately 30 km. The ultraviolet radiations were measured with an ultraviolet imager consisting of an ultraviolet telescope, filter wheel with five filters having center wavelengths from 200 nm to 325 nm, a cesium telluride photocathode, a microchannel plate, a phosphor, a relay lens, a CCD video camera, and a tape recorder. The images were digitized and analyzed to obtain the spatial char-



UV Plume Image of Launch of Scout Missile from Vandenberg, AFB CA.



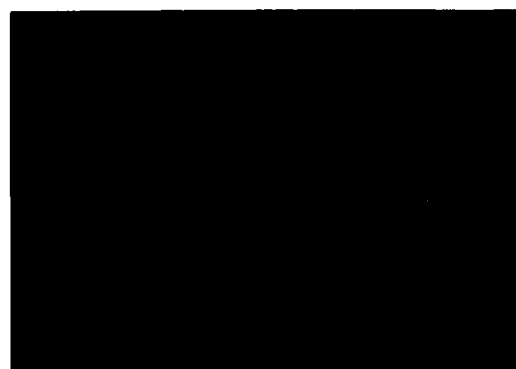
UV Plume Radiance Contours Obtained by the GL Imager During Missile Test Firings at AEDC.

acteristics of the radiation in terms of radiance values and how these values vary with wavelength and aluminum loading. A very strong variation in the radiance with aluminum loading was found at all wavelengths measured. A report has been completed.

The objectives of the Horizon Ultraviolet Program (HUP) include measurements of the airglow (particularly toward the horizon), auroras, and the shuttle environment in the far ultraviolet (1100 -- 1900 Å) wavelength range. The principal sensor is a scanning spectrometer with a spectral resolution of 5 Å. The spectrometer consists of an Ebert-Fastie monochromator with a photon-counting photomultiplier detector and a light collecting telescope which is mounted on a single-axis scan platform. This allows the HUP sensor to view a range of angles vertically from the payload bay and out to 20 degrees forward. With the orbiter oriented with its nose toward earth center (gravity-gradient stabilized mode), view directions ranging from horizontal to 20 degrees below horizontal are available, allowing scans of airglow

emission over a range of altitudes relative to the earth limb. The HUP sensor has been completed, tested, and calibrated and is ready for integration into the shuttle for a flight in 1990.

Ultraviolet models are needed because the usefulness of ultraviolet sensors for missile defense depends on an accurate knowledge of the radiative environment or background within which such sensors may be used. Theoretical work on



Horizon Ultraviolet Sensor (HUP) Scan of the Horizon from the Shuttle to Measure UV Limb Radiance.

this background effort concentrated on models for the dayglow and Rayleigh scattering of sunlight. The wavelength range for dayglow is from 800 to 10,000 Å and for Rayleigh scattering from 2010 to 8000 Å. Limb profiles in 100 Å bands from 1400 to 3000 Å were determined. These profiles combine dayglow and Rayleigh scattering and show how the brightness varies with tangent altitude.

The spatial clutter characteristics of the background have been obtained from photometer measurements of the ultraviolet earth background from the Polar BEAR satellite. The data were processed into normalized Power Spectral Density (PSD) curves. Integration of these PSD's yielded curves of rms clutter as a function of spatial scale. The PSD's were analyzed to derive a phenomenological basis for clutter estimation at spatial scales that were finer than the footprint of the sensor. Fine-scale clutter estimates were generated at five wavelengths: 1304 Å, 2250 Å, 3371 Å, 3914 Å and 6300 Å. The slope of the PSD's at the lower spatial frequencies are characteristic of fractal spatial structure, consistent with turbulence control of the radiance spatial patterns. The fractal character permits the clutter characteristics to be extrapolated to fine scales, even as low as 1 to 10 m if the sensitivity of the sensor is great enough. By choice of wavelength and bandwidth, rms clutter was controlled and clutter levels were found to be lower than those predicted by turbulence models alone. Volume scattering is proposed as the origin of suppressed clutter.

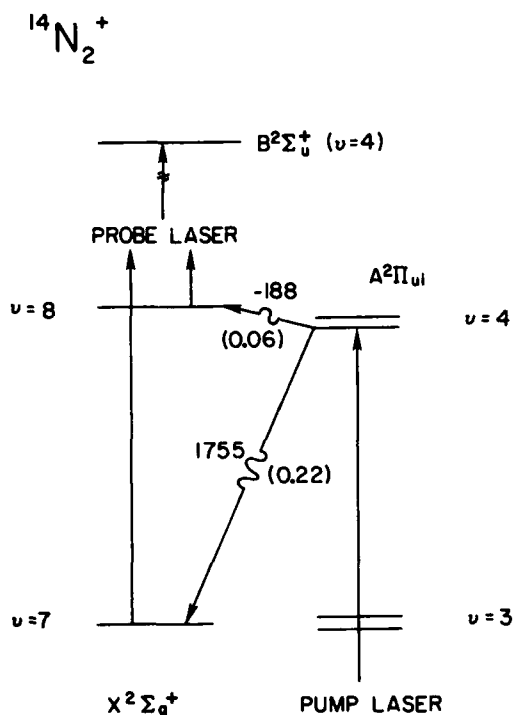
GL has been actively involved in several satellite programs in which one of the aims is to obtain ultraviolet measurements of targets and backgrounds. Among such programs are STARLAB, IBSS, LACE, the Delta Programs, and the S262 Program. This effort has involved recommendations on sensors

and wavelength bands, membership in science committees, preparation of the experiments to be conducted on the satellites, and development of the techniques for the analysis of the satellite data when it is obtained.

UV Laser Spectroscopy: Knowledge of electronic excitation and collisional quenching processes of atmospheric molecules and ions are necessary to characterize ultraviolet emissions in complicated environments such as auroras and nuclear-perturbed atmospheres. Laser double-resonance experiments have been conducted to obtain information on collisional deactivation paths and state-specific quenching rates of electronically excited molecules. In addition, a new kinetics facility has been set up to measure rate constants of reactions important in the production of ultraviolet emissions from plumes and the upper atmosphere.

State-specific electronic quenching rates in a diatomic molecule have not been reported previously. We have succeeded in measuring state-specific electronic quenching rates of the molecular nitrogen ion by using a two-laser double-resonance technique. A schematic diagram of the experiment is shown in the figure. The pump laser selectively excites a level of the $A(v = 4)$ rotational manifold, and the collision-induced electronic transfer to the $X(v = 8)$ and $X(v = 7)$ levels is monitored by the pump laser. The collisional branching ratio to these two levels is determined from the laser-induced fluorescence of the probe laser. This branching ratio is used in an electronic relaxation model whose equation is fit to observed radiative-decay curves from the $A(v = 4)$ level as a function of helium pressure. The state-specific electronic quenching rates are deduced from these fits.

Besides these experiments, a multisection flow tube with various injection



Schematic Diagram of the Double Resonance Experiment for the Nitrogen Molecular Ion. (The energy gaps are in reciprocal centimeters and the numbers in parentheses are Franck-Condon factors.)

ports has been built and a computer-controlled electronic detection system has been set up for chemical kinetic experiments. A preliminary experiment to observe the ultraviolet emissions from the reaction of electronically excited nitrogen with NO was conducted using a 2.2 m ultraviolet spectrograph. The resulting rotationally resolved spectra show the NO gamma bands to be rotationally "hot."

The results of these laboratory measurements find application in various computer models and codes describing the ultraviolet emission from rocket engine plumes and the radiance expected from the ambient ultraviolet airglow and auroral emission.

PUBLICATIONS 1987-1988

AIKIN, A.C. (NASA Goddard Space Flight Center, Greenbelt, MD); GALLAGHER, C.C. (AFGL); SPICER, C.W., and HOLDREN, M. W. (Battelle Columbus Laboratories, Columbus, OH)

Measurement of Methane and Other Light Hydrocarbons in the Troposphere and Lower Stratosphere

J. Geophys. Res. 92 (1987)

ANDERSON, D.N. (AFGL); HEELIS, R.A., and MCCLURE, J.P. (Univ. of Texas at Dallas, Richardson, TX)

Calculated Nighttime Eastward Plasma Drift Velocities and Their Solar Cycle Dependence

Ann. Geophys. 5A (1987)

BASU, B. (AFGL); and COPPI, B. (Massachusetts Inst. of Tech., Cambridge, MA)

Fluctuations Associated with Sheared Velocity Regions Near Auroral Arcs

Geophys. Res. Lett. 15 (1988)

BASIN, B., and JASPERSE, J.R.

Marginal Stability of Ion-Acoustic Waves in a Weakly Collisional Two-Temperature Plasma Without a Current

Phys. Rev. A 38 (1988)

BASU, S. (AFGL); BASU, S.U. (Emmanuel Coll., Boston, MA); STUBBE, P. (Max Planck Inst fur Aeronomie, Lindau, FRG); and WAARAMAA, J. (AFGL)

Daytime Scintillation Induced by High Power HF Waves at Tromso, Norway

J. Geophys. Res. 92 (1987)

BASU, S.U., MCKENZIE, E. (Emmanuel Coll., Boston, MA); BASU, S., MAYNARD, N., FOUGERE, P.F. (AFGL); COLEY, W.R., HANSON, W.B. (Univ. of Texas at Dallas, Richardson, TX); SUGIURA, M. (Kyoto Univ., Kyoto, Japan); WINNINGHAM, J.D.

(Southwest Res. Inst., San Antonio, TX); and HOEGY, W.R. (NASA Goddard Space Flight Ctr., Greenbelt, MD)

Simultaneous Density and Electric Field Fluctuation Spectra Associated with Velocity Shears in the Auroral Oval
J. Geophys. Res. 93 (1988)

CARLSON, H.C., WEBER, E.J. (AFGL); HEELIS, R.A. (Univ. of Texas at Dallas, Richardson, TX); and SHARBER, J.R. (Southwest Res. Inst., San Antonio, TX)
Coherent Mesoscale Convection Patterns During Northward IMF
J. Geophys. Res. 93 (1988)

COSTA, E., and FOUGERE, P.F.
Cross-Spectral Analysis of Spaced Receiver of Spaced-Receiver Measurements
Radio Sci. 23 (1987)

COSTA, E., FOUGERE, P.F., and BASU, S.
Cross Correlation Analysis and Interpretation of Spaced-Receiver Measurements
Radio Sci. 23 (1987)

DANIELL, R.E., JR., BROWN, L.D. (Computational Physics, Inc., Newton, MA); ANDERSON, D. N. (AFGL); SOJRA, J.J., and SCHUNK, R.W. (Utah St. Univ., Logan, UT)
A Real-Time High Latitude Ionospheric Specification Model
Proc. 1988 MIT Wkshp. on Theoretical Geoplasma
Phys., Cambridge, MA (1988)

GALLAGHER, C.C.
Inorganic Bromine in the Lower Stratosphere
J. Atmos. Terr. Phys. 49 (1987)

HALL, L. A., and ANDERSON, G.P.
Instrumental Effects on a Proposed Mg II Index of Solar Activity
Ann. Geophys. A. 6 (1988)

HENCHMAN, M. (Brandeis Univ.,

Waltham, MA); and PAULSON, J.F. (AFGL)

The Gas-Phase and Solution Mechanism of the Isotope Exchange Reaction
 $OH + D_2 = DO + HD$: Beam
Study of the Solvated-Ion Reaction
 $OH.H_2O + D_2$ in the Collision Energy Range 0-2eV
Radiat. Phys. Chem. 32 (1988)

HIERL, P.M., AHRENS, A.F. (Univ. of Kansas, Lawrence, KS); HENCHMAN, M.J. (Brandeis Univ., Waltham, MA); VIGGIANO, A. A., and PAULSON, J. F. (AFGL)
Rate Constants and Product Distributions as Functions of Temperature for the Reaction of OH (H_2O) 0, 1, 2 with CH_3CN
Internat. J. Mass Spectrometry and Ion Processes 81 (1987)

JASPERSE, J.R., and BASU, B.
Collisional Enhancement of Low Frequency Density Fluctuations in a Weakly Collisional Electron-Ion Plasma
Phys. Rev. Lett. 58 (1987)

KATAYAMA, D.H.
Comment on: "Observation of Strong Rydberg-Valence Mixing in the E^3u State of O_2 by 3 + 1 MPI Photoelectron Spectroscopy
J. Chem. Phys. 89 (1988)

KATAYAMA, D.H. (AFGL); DENTAMARO, A.V. (SCEEE, St. Cloud, FL); and WELSH, J.A. (AFGL)
State Specific Electronic Quenching Rates for $^{14}N^+_2$ and $^{15}N^+_2$
J. Chem. Phys. 87 (1987)

KLOBUCHAR, J.A.
Ionospheric Time-Delay Algorithm for Single-Frequency GPS Users
IEEE Trans. on Aerospace and Electric Systems, AES-23 (1987)

MENDILLO, M., BAUMGARDNER, J., AARONS, J. (Boston Univ., Boston, MA);

FOSTER, J. HAYSTACK (Obs., Westford, MA); and KLOBUCHAR, J. (AFGL)
Coordinated Optical and Radio Studies of Ionospheric Disturbances: Initial Results from Millstone Hill
 Ann. Geophys. 5 (1987)

MORRIS, R.A., VIGGIANO, A.A., DALE, F., and PAULSON, J.F.
Collisional Vibrational Quenching of $\text{NO}^+(v)$ Ions
 J. Chem. Phys. 88 (1988)

PAULSON, J.F. (AFGL); and HENCHMAN, M. J. (Brandeis Univ., Waltham, MA)
The Gas-Phase and Solution Mechanism of the Isotope Exchange Reaction $\text{OH} + \text{D}_2 = \text{DO} + \text{HD}$: Beam Study of the Solvated-Ion Reaction $\text{OH} \cdot \text{H}_2\text{O} + \text{D}_2$ in the Collision Energy Range 0-2eV
 Radiat. Phys. and Chem. 32 (1988)

REITERER, J.M., DECKER, D.T. (Boston Coll., Chestnut Hill, MA); and JASPERSE, J. R. (AFGL)
A Kinetic Model for the Diffuse Aurora
 EOS 69 (1988)

SWIDER, W.
Electron Loss and the Determination of Electron Concentrations in the D-Region
 Pure and Applied Geophys. 127 (1988)
Ionic Mobility, Mean Mass and Conductivity in the Middle Atmosphere from Near Ground Level to 70 Km
 Radio Sci. 23 (1988)

VIGGIANO, A.A. (Systems Integration Engineering, Lexington, MA); DALE, F., and PAULSON, J. F. (AFGL)
Proton Transfer Reactions of $\text{H}^+(\text{H}_2\text{O})_{n=2-11}$ with Methanol, Ammonia, Pyridine, Acetonitrile and Acetone
 J. Chem. Phys. 88 (1987)

VIGGIANO, A. A. (Systems Integration Engineering, Lexington, MA); MORRIS,

R.A., and PAULSON, J.F. (AFGL)
Rotational Temperature Dependences of Gas Phase Ion - Molecule Reactions
 J. Chem. Phys. 89 (1988)

VIGGIANO, A.A. (Systems Integration Engineering, Lexington, MA); DEAKYNE, C.A. (Wentworth Inst. of Technology, Boston, MA); DALE, F., and PAULSON, J. F. (AFGL)
Neutral Reactions in the Presence of Alkali Ions
 J. Chem. Phys. 87 (1988)

VIGGIANO, A.A. (Systems Integration Engineering, Lexington, MA); MORRIS, R.A., DALE, F., and PAULSON, J.R. (AFGL)
Tropospheric Reactions of $\text{H}^+(\text{NH}_3)_m(\text{H}_2\text{O})_n$ with Pyridine and Picoline
 J. Geophys. Res. 93 (1988)

VIGGIANO, A.A. (Systems Integration Engineering, Lexington, MA); MORRIS, R.A., DALE, F., and PAULSON, J.R. (AFGL); and FERGUSON, E.E. (Univ. Paris, France)
Deuterated Methyl Cation Reactions with Atomic Oxygen
 Chem. Phys. Lett. 148 (1988)

WHALEN, J.A.
Daytime F-Layer Trough Observed on a Macroscopic Scale
 J. Geophys. Res. 92 (1987)

PRESENTATIONS 1987-1988

ANDERSON, D.N. (AFGL); and FORBES, J.M. (Boston Univ., Boston, MA)
Development of a Modified Chiu Ionospheric Model
 IUGG, XIX General Assembly, Vancouver, Canada

(9-22 August 1987)

A Fully Analytic, Low and Mid Latitude Ionospheric Model

Ionospheric Structure and Variability on a Global Scale and Interaction with Atmosphere, Magnetosphere, Munich, Germany (16-2+0 May 1988)

ANDERSON, D.N., and KLOBUCHAR, J. A.
Modeling the Low latitude Response to the Sept. 19, 1984, Geomagnetic Storm
AGU Mtg., San Francisco, CA (-5-9 December 1988)

ANDERSON, D.N., BUCHAU, J. (AFGL); and HEELIS, R. A. (Univ. of Texas at Dallas, Richardson, TX)

Origin of Density Enhancements in the Wintertime Polar Cap Ionosphere

IUGG, XIX General Assembly, Vancouver, Canada (9-22 August 1987)

On the Generation Mechanism of Ionization Patches

AGU Mtg., San Francisco, CA (6-11 December 1987)

BASU, B., and JASPERSE, J.R.
Ion-Acoustic Instability in a Weakly Collisional Two-Temperature Plasma Without a Current

AGU Mtg., San Francisco, CA (6-11 December 1987)

BASU, S. (AFGL); and BASU, SU. (Emmanuel Coll., Boston, MA)
High Latitude Scintillations: A Review
XXII Gen. Assbly. of the Internat. Union of Radio Science, Tel Aviv, Israel (24 August - 2 September 1987)

High Latitude Scintillations
SPIE 1988 Internat. Beacon Satellite Symp., Beijing, China (18-21 1988)

BASU, S. (AFGL); MACKENZIE, E., BASU, SU. (Emmanuel Coll., Boston MA)
Ionospheric Constraints on VHF/UHF Communication Links During Solar Maximum and Minimum Periods

Ionospheric Effects Symp., Springfield, VA (5-7 May 1987)

BASU, S. (AFGL); BASU, SU., MACKENZIE, E. (Emmanuel Coll., Boston, MA), and WEIMER, D. (Regis Coll., Weston, MA)

Ionospheric Scintillations and In-Situ Measurements at an Auroral Location in the European Sector

AGARD Electromagnetic Wave Propagation Panel Specialists Mtg., Rome, Italy (18-22 May 1987)

BASU, S. (AFGL); BASU, SU. (Emmanuel Coll., Boston, MA); STUBBE, P. (Max Planck Institut fur Aeronomie, Lindau, FRG); and CARLSON, H.C. (AFGL)

Artificial Irregularities Induced by High Power HF Waves at Tromso, Norway

XNII Gen. Assbly. of the Internat. Union of Radio Science, Tel Aviv, Israel (24 August - 2 September 1987)

BASU, S., EASTES, R.W., DEL GRECO, F.P., HUFFMAN, R.E. (AFGL); and BASU, SU. (Emmanuel Coll., Boston, MA)

Nightside UV Auroral Images and VHF/UHF Scintillation

U.S. National URSI Mtg., Boulder CO (5-8 January 1988)

BASU, S. (AFGL); BASU, SU. (Emmanuel Coll., Boston, MA); WEBER, E.J. (AFGL); VALLADARES C. (Emmanuel Coll., Boston, MA); G.J. BISHOP, and J. BUCHAU (AFGL)
Coordinated Observations of High Latitude Ionospheric Turbulence

Wkshp. on Polar Cap Dynamics, and High Latitude Turbulence, Cambridge, MA (13-17 June 1988)

BASU, SU. (Emmanuel Coll., Boston, MA); and BASU, S. (AFGL)

Density and Electric Field Turbulence in Arcs and Patches at High Latitudes

AGU Mtg., Baltimore, MD (16-20 May 1988)
Irregularities in Blobs, Arcs and Patches
Wkshp. on Polar Cap Dynamics and High

Latitude Ionospheric Turbulence, Cambridge, MA (13-17 June 1988)

BASU, SU. (Emmanuel Coll., Boston, MA); and CARLSON, H.C., JR. (AFGL)
First CEDAR/WITS High Latitude Campaign: Objectives and Initial Results
AGU Mtg., Baltimore, MD (16-20 May 1988)

BASU, SU. (Emmanuel Coll., Boston, MA); BASU, S. (AFGL); COLEY, W.R. (Univ. of Texas at Dallas, Richardson, TX); and MAYNARD, N.C. (AFGL)
Structures of Density and Velocity Fluctuations in the Auroral and Their Impact on Communication and Radar System
AGARD Electromagnetic Wave Propagation Panel Specialists Mtg., Rome, Italy (18-22 May 1987)
DE-2 Measurements of Density and Electric Field Turbulence Associated with the Theta Aurora
AGU Mtg., San Francisco, CA (7-11 December 1987)

BASU, SU. (Emmanuel Coll., Boston, MA); BASIN, S., WEBER, E.J. (AFGL); and COLEY, W. R. (Univ of Texas at Dallas, Richardson, TX)
Case Study of Polar Cap Scintillation Modeling Using DE-2 Irregularity Measurements at 800 km
Ionospheric Effects Symp., Springfield, VA (5-7 May 1987)

BISHOP, G.J., KLOBUCHAR, J.A. (AFGL); and BLOOD, D.W. (Raytheon, Wayland, MA)
Recent Observations of Polar Cap Total Electron Content Variations
Wkshp. on Polar Cap Dynamics and High Latitude Ionospheric Turbulence, Cambridge, MA (13-17 June 1988)

BISHOP, G.J., KLOBUCHAR, J.A., JACAVANCO, D.J., 1 LT (AFGL); and COKER, C. (Univ. of Texas at Dallas,

Richardson, TX)
Some Observations and Mitigation of Multipath Effects on GPS Differential Group Delay
AGU Mtg., San Francisco, CA (7-11 December 1987)

BUCHAU, J.
Field Reports: Polar Cap and Auroral Ionosphere Dynamics;
Field Reports: Satellite Observations in the Polar Region
Review of U. S. Programs in Greenland by Danish Commission for Scientific Res. in Greenland, Copenhagen, Denmark (6 April 1988)

BUCHAU, J. (AFGL); REINISCH, B.W., BIBL, K., and SALES, G.S. (Univ. of Lowell, Lowell, MA)
Multistation / Multiparameter Observations with a Network of Digital Ionosondes
Electromagnetic Wave Propagation Panel, Munich, Germany (16-20 May 1988)

BUCHAU, J. (AFGL); REINISCH, B. W. (Univ. of Lowell, Lowell MA); ANDERSON, D.N., WEBER, E. (AFGL); and DOZOIS, C. (Univ. of Lowell, Lowell, MA)
Polar Cap Plasma Convection Measurements and Their Relevance to the Real-Time Modeling of the High Latitude Ionosphere
Fifth Internat. Ionospheric Effects Symp., Springfield, VA (5-7 May 1987)

BYTHROW, P.F., MENG, C.I., POTEMRA, T.A., ZANETTI, L.J., ERLANDSON, E.R. (The Johns Hopkins Univ., Laurel, MD); and HUFFMAN, R.E. (AFGL)
Intense Auroral Emissions Near 1400 MLT: A Relationship to Structure in the Region 1 Current
AGU Mtg., San Francisco, CA (6-22 December 1987)

CARLSON, H.C.
Sun Aligned Arcs in the Polar Cap
Wkshp. on Ionosphere-Magnetosphere-Solar

Wind Coupling Processes, Cambridge, MA
(13-17 June 1987)

*Auroral and Polar Cap Ionospheric
Phenomenology*

Fifth Internat. Symp., Washington, DC
(1987)

*Arctic Upper Atmosphere: Perturbations and
Their Effects*

AGU Mtg., San Francisco, CA (5-9 December
1988)

CARLSON, H.C., and ANDERSON, D.N.
*The Effect of the Ionosphere on Air Force
Systems*

Ionospheric Structure and Variability on a
Global Scale and Interaction with
Atmosphere, Magnetosphere, Munich,
Germany (16-20 May 1988)

CARLSON, H.C. (AFGL); BLOCK, L. (Royal
Inst. of Tech., Stockholm, Sweden);
WEBER, E.J., BUCHAU, J. (AFGL);
EGELAND, A. (Univ. Oslo, Oslo, Norway);
ILLANSSON, L., MURPHREE, I. S.,
MARKLAND, G., POTEIRA, T.A., and
ZANETTI, L.J. (VIKING Team)
*VIKING - Airborne Observatory
Magnetically Conjugate Observations of
Aurora*
AGU Mtg., San Francisco, CA (7-11
December 1987)

CARLSON, H.C., HUFFMAN, R., WEBER, E.
(AFGL); MENDE, S.B., SWENSON, G.
(Lockheed, Palo Alto, CA); JONES, A.V.
(Natl. Res. Council, Ottawa, Canada);
MERIWETHER, J., JR., NICIEJEWSKI, R.
(Univ. of Michigan, Ann Arbor, MI);
VALLADARES, C. (Emmanuel College,
Boston, MA); CHRISTENSEN, A.B., HECHT,
I. H. (Aerospace Corp., El Segundo, CA);
and SIVJEE, G. G. (Embry Riddle
Aeronautical Univ., Daytona Beach, FL)
*Sondrestrom 87 CEDAR Campaign:
Observations of E Region Sun Aligned Arcs*
AGU Mtg., San Francisco, CA (7-11
December 1987)

COPPI, B. (Massachusetts Inst. of Tech.,
Cambridge, MA); and BASU, B. (AFGL)
*Fluctuations Associated with Sheared
Velocity Regions Near Auroral Arcs*
Wkshp. on Polar Cap Dynamics and High
Latitude Ionospheric Turbulence, Cambridge,
MA (13-17 June 1988)

DECKER, D.T. (Boston Coll., Chestnut
Hill, MA); JASPERSE, J.R. (AFGL); and
WINNINGHAM, I.D. (Southwest Res. Inst.,
San Antonio, TX)
Energetic Ionospheric Photoelectrons
Wkshp. on Ionosphere-Magnetosphere-Solar
Wind Coupling Processes, Cambridge, MA (28
July -2 August 1987)
*Energetic Photoelectrons Due to Solar Soft X-
Ray and Auger Production*
Wkshp. on Polar Cap Dynamics and High
Latitude Ionospheric Turbulence, Cambridge,
MA (13-17 June 1989)
Energetic Photoelectrons and the Polar Rain
AGU Mtg., San Francisco, CA (5-9 December
1988)

DECKER, D.T. (Boston Coll., Chestnut
Hill, MA); DANIELL, R.E. (Computational
Phys. Inc., Annandale, VA); JASPERSE, J.
R. (AFGL); and STRICKLAND, D.J.
(Computational Phys. Inc., Annandale,
VA)
*Determination of Ionospheric Electron
Density Profiles from Satellite UV Emission
Measurements*
Fifth Internat. Ionospheric Effects Symp.,
Springfield, VA (5-7 May 1987)

DECKER, D.T., RETTERER, J.M. (Boston
Coll., Chestnut Hill, MA); JASPERSE, J.
R., ANDERSON, D.N., EASTES, R.W., DEL
GRECO, F. P., HUFFMAN, R.E. (AFGL); and
FOSTER, J.C. (Haystack Obs., Westford,
MA)
*A Study of Coincident Satellite UV Emission
and Incoherent Scatter Radar Electron
Density Profiles from Satellite UV and In-
Situ Data*
SPIE 1988 Tech Symp. on Optics, Electro-

Optics and Sensors, Orlando, FL (4-8 April 1988)

DEL GRECO, F.P., HUFFMAN, R.E., EASTES, R.W. (AFGL); MENDILLO, M., and BAUMGARDNER, J. (Boston Univ., Boston, MA)

Comparisons of Ground-Based and Satellite Imaging of Auroral Emissions
AGU Mtg., Baltimore, MD (18-22 May 1987)

DEL GRECO, F.P., HUFFMAN, R.E., EASTES, R. W. (AFGL); ROMICK, G.J. (NSF, Washington, DC); STRICKLAND, D.J., and DANIELL, R.E. (Computational Phys. Inc., Annandale, VA)

Multiple Wavelength Imagery of the Ultraviolet and Visible Aurora from the Polar BEAR Satellite
AGU Mtg., San Francisco, CA (5-9 December 1988)

DEL GRECO, F.P., HUFFMAN, R. E., LARRABEE, J.C., EASTES, R.W. (AFGL); LEBLANC, F.J. (Northwest Res. Assoc., Bellevue, WA); and MENG, C.J. (The Johns Hopkins Univ., Laurel, MD)

Organizing and Utilizing Imaging and Spectral Data from the Polar Bear UV Sensor
SPIE 1988 Tech. Symp. on Optics, Electro-Optics and Sensors, Orlando, FL (4-8 April 1988)

DENTAMARO, A.V. (SCEEE, St. Cloud, FL); STERGIS, C.G., and BAISLEY, V.C. (AFGL)

Spatial Dependence of Transmission of Ultra-Violet Radiation through the Atmosphere
SPIE 1988 Tech. Symp. on Optics, Electro-Optics and Sensors, Orlando, FL (4-8 April 1988)

EASTES, R.W., HUFFMAN, R.E., LARRABEE, J.C. (AFGL); LEBLANC, F.J. (NWRA, Bellevue, WA)

High Resolution Ultraviolet Nightglow

Observations (1600-2900Å) from the S3-4 Satellite

AGU Mtg., San Francisco, CA (12-16 December 1988)

DEWAN, E., and FOUGERE, P.F.

Gravity Waves and the Maximum Entropy Method (MEM) of Power Spectral Analyses
Wkshp. on Gravity Waves and Turbulence in the Middle Atmosphere, Adelaide, Australia (21-23 May 1987)

FOUGERE, P.F.

On the Extreme Accuracy of Maximum Entropy Spectrum Estimation from an Error Free Autocorrelation Function

IEEE Internat. Conf. on Acoustics Speech and Signal Proc., Dallas, TX (April 1987)

Maximum Entropy Calculations on a Discrete Probability Space

Seventh Annual Wkshp. on Maximum Entropy and Bayesian Methods on Applied Statistics, Seattle, WA (August 1987)

On Maximum Entropy

MAXENT Wkshp., Cambridge Univ., Cambridge, England (1-7 August 1988)

Why Maximize Entropy?

Boston Chapter of Acoustics, Speech, and Signal Proc. Soc. of IEEE, Lincoln Lab (13 September 1988)

FUKUI, K.

Unique Increase of Solar Lyman Alpha Flux Observed by AE-E Satellite During Cycle 21
AGU Mtg., Baltimore, MD (16-20 May 1988)

HENCHMAN, M. (Brandeis Univ., Waltham, MA); PAULSON, J. F. (AFGL); LINDINGER, W. (Univ. of Innsbruck, Innsbruck, Austria); SMITH, D., and ADAMS, N. (Univ. of Birmingham, Birmingham, UK)

Energy Barriers in Exothermic Ion-Molecule Reactions: Isotope Exchange and the Fractionation of Deuterium in Interstellar Molecules

Tenth Internat. Symp. on Gas Kinetics, Univ. Coll. of Swansea, UK (24-29 July 1988)

HIERL, P.M., AHRENS, A.F. (Univ. of Kansas, Lawrence, KS); HENCHMAN, M. (Brandeis Univ., Waltham, MA); PAULSON, J. F. (AFGL); and CLARY, D. C. (Univ. Chemical Lab., Cambridge, MA)
Gas-Phase Ionic Clusters: Reactivity as a Function of Temperature and Cluster Size. Comparison with Solution
 Faraday Discussion on Solvation, Univ. of Durham, England (28-30 March 1988)

HIERL, P.M., AHRENS, A.F. (Univ. of Kansas, Lawrence, KS); HENCHMAN, M. J. (Brandeis Univ., Waltham, MA); VIGGIANO, A.A., and PAULSON, J.F.
Chemistry as a Function of Solvation Number: Solvated-Ion Reactions in the Gas Phase and Comparison with Solution
 Faraday Discussion on Solvation, Univ. of Durham, England (28-30 March 1988)

HUFFMAN, R.E.
The Polar Bear Imager: Results from the July 87 Polar Bear-Radar Interactive Experiments
 Auroral Dynamics Wkshp., Univ. of Saskatchewan, Saskatoon, Canada (24-26 August 1987)
Ultraviolet Atmospheric Backgrounds for Aerospace Surveillance
 AIAA 26th Aerospace Sciences Mtg., Reno, NV
 (11-14 January 1988)

HUFFMAN, R.E., LARRABEE, J.C. (AFGL); and EASTES, R. W. (SCEEE, St. Cloud, FL)
Observations of Ultraviolet Nightglow Emissions in the O₂ Herzberg and NO Bands from the S3-4 Satellite
 AGU Mtg., Baltimore, MD (18-22 May 1987)

HUFFMAN, R.E. (AFGL); MEJER, R.R., and CONWAY, R.R. (Hulbert Center for Space Res., Washington, DC)
Satellite Observations of Atomic Oxygen Depletions at High Latitudes under Geomagnetically Disturbed Conditions

XXVII COSPAR Mtg., Espoo, Finland (18-29 July 1988)

HUFFMAN, R.E., DEL GRECO, F.P., EASTES, R.W., and LARRABEE, J.C.
Polar Bear Satellite Multispectral Auroral and Polar Cap Images
 Auroral Phys. Internat. Conf., St. Johns Coll., Cambridge, England (11-15 July 1988)

HUFFMAN, R.E., DEL GRECO, F.P., LARRABEE, J.C., EASTES, R. W. (AFGL); MENG, C.I. (The Johns Hopkins Univ., Laurel, MD); and ROSENBERG, N.W. (Northwest Res. Assoc., Bellevue, WA)
Multispectral Ultraviolet Imaging of Aurora from the Polar Bear Satellite
 IUGC XIX Gen. Assbly., Vancouver, Canada (9-22 August 1987)

HUFFMAN, R.E., DEL GRECO, F.P., EASTES, R.W., LARRABEE, J.C. (AFGL); ROSENBERG, N.W., LEBLANC, F.J. (Northwest Res. Assoc., Bellevue, WA); and MENG, C.W. (The Johns Hopkins Univ., Laurel, MD)
Polar Bear Satellite Multispectral Aurora and Polar Cap Images and Spectra
 Auroral Phys. Internat. Conf., St. Johns Coll., Cambridge, England (11-15 July 1988)

HUNTON, D.E.
Mass Spectrometer Measurements in the Largest Vacuum of All: Space
 American Vacuum Society, St. Paul, MN (7 May 1987)

ISHIMOTO, M., MENG, C.I. (The Johns Hopkins Univ., Laurel, MD); ROMICK, G.J. (Univ. of Alaska, Fairbanks, Ak); and HUFFMAN, R. E. (AFGL)
Anomalous UV Spectra in the Diffuse Auroral Region (Apparently?) Due to KeV Heavy Particles
 AGU Mtg., San Francisco, CA (7-11 December 1987)

ISHIMOTO, M., MENG, C.I. (The Johns

Hopkins Univ., Laurel, MD); ROMICK, C.J., DEGEN, V. (Univ. of Alaska, Fairbanks, AK); and HUFFMAN, R. E. (AFGL)
NI(1745A) and NII(2143A) Auroral Emissions Observed from S3-4 Satellite
 AGU Mtg., Baltimore, MD (18-22 May 1987)

JASPERSE, J.R. and BASU, B.
Collisional Enhancement of Electron Density Fluctuations Near the Ion-Acoustic Frequency in the F-Region Ionosphere
 1988 Cambridge Wkshp. on Polar Cap Dynamics and High Latitude Ionospheric Turbulence, Cambridge, MA (13-18 June 1988)

KATAYAMA, D.H. (AFGL); and Dentamaro, A.V. (SCEEE, St Cloud, FL)
Collision Complex Model Predictions for Electronic Transitions in a Diatomic Molecule
 1987 Conf. on the Dynamics of Molecular Collisions, Wheeling, VA (12-17 July 1987)
Electronic Energy Transfer Between the $A_2\Pi$ ($v=0$) and $X^2\Sigma+(v=10)$ States of CO^+
 American Phys. Soc. Mtg., Baltimore, MD (18-21 April 1988)

KATAYAMA, D.H., DENTAMARO, A.V., and WELSH J.A.
Collisional Deactivation of Selectively Excited $^{14}N_2^+$ and $^{15}N_2^+$
 XVth Internat. Conf. on the Physics of Electronic and Atomic Collisions, Brighton, England (22-28 July 1987)

KLOBUCHAR, J.A.
Effects of High Latitude Ionosphere on Transionospheric Systems
 DoD Symp. and Wkshp. on Arctic and Arctic-Related Environmental Sciences, Hampton, VA (28-30 January 1987)
Ionospheric Corrections for Timing Applications
 PTTI Applications and Planning Mtg., Tyson's Corner, VA (December 1988)

KLOBUCHAR, J.A. (AFGL); and HICKS, P.A. (ALCOA Defense Systems, Inc., San Diego, CA)
A Proposed New Generation Satellite Beacon System for Geophysical Measurements
 Internat. Beacon Satellite Symp., Beijing, China (18-21 April 1988)

KLOBUCHAR, J.A. (AFGL); and KERSLEY, L. (Univ. Coll. of Wales, Aberystwth, Wales)
Optimum Longitudes for Geostationary Satellites for Protonospheric Electron Content Measurements
 Internat. Beacon Satellite Symp., Beijing, China (18-21 April 1988)

KOSSEY, P.A., and RASMUSSEN, J.E.
ULF/VLF Radiowave Studies of the Structure of the Equatorial, Mid-Latitude, and Polar Ionosphere below 100 Km
 AGARD Electromagnetic Wave Propagation Panel
 Specialists Mtg., Munich, Germany (16-20 May 1988)

LEE, M.C. (Massachusetts Inst. of Tech., Cambridge, MA); and KLOBUCHAR, J. A. (AFGL)
Faraday Polarization Fluctuations of Satellite Beacon Signals; Evidence of Precursors for Exciting Plumes of Equatorial Ionospheric Irregularities
 SPIE 1988 Internat. Beacon Satellite Symp., Beijing, China (18-21 April 1988)

LOWRANCE, J.L., COPE, A.D. (Princeton Sci. Inst., Princeton, NJ); and STERGIS, C.G. (AFGL)
Spatial Frequency Response of Proximity Focused Image Tubes in the Near Ultraviolet
 Tech. Symp. on Optics and Sensors, Orlando, FL (4-8 April 1988)

MARCOS, F.A.
Accuracy of Satellite Drag Models
 AIAA Astrodynamics Conf., Kalispell, MT (10-13 August 1987)

Accuracy of Atmospheric Drag Models at Low Satellite Altitudes;
Comparison of Satellite Accelerometer Density Measurements with CIRA 86;
Thermospheric Density Structure from Satellite Accelerometer Data at Low Solar Cycle, Equinox Conditions
 XXVII COSPAR Mtg., Espoo, Finland (18-29 July 1988)

MARCOS, F.A. (AFGL); WHITTEN, R.C. (NASA, Houston, TX); BAUGHAN, W.W. (Univ. of Alabama, Huntsville, AL); and PRASAD, S. S. (Aerojet ElectroSystems)
A Guide to Reference and Standard Atmospheres
 XXVII COSPAR Mtg., Espoo, Finland (18-29 July 1988)

MENG, C.I. (The Johns Hopkins Univ., Laurel, MD); HUFFMAN, R.E., DEL GRECO, F. P., and EASTES, R. W. (AFGL)
UV Images of Dayside Auroral Oval
 AGU Mtg., Baltimore, MD (18-22 May 1987)

MERIWETHER, J.W. (AFGL); BIONDI, M.A. (Univ. of Pittsburgh, Pittsburgh, PA); and ROBLE, R. G. (Natl. Ctr. of Atmos. Res., Boulder, CO)
Theoretical and Experimental Comparison of Equatorial Thermospheric Neutral Winds and Temperatures for Fabry-Perot Observations Obtained from Arequipa, Peru
 AGU Mtg., San Francisco, CA (5-9 December 1988)

MIKKELSEN, I. S. (Division of Geophysics, Copenhagen, Denmark); CARLSON, H.C., WEBER, E., and VICKERY, K. (AFGL)
The Motion of Six Barium Clouds and a Samarium Cloud in the Dawn Auroral Oval and Polar Cap
 AGU Mtg., San Francisco, CA (7-11 December 1987)

MORRIS, R.A., VIGGIANO, A.A. (Systems Integration Engineering, Lexington, MA); and PAULSON, J.F. (AFGL)

Translational Energy Dependence of Rate Constants for Ion-Molecule Reactions as a Function of Temperature
 Tenth Internat. Symp. on Gas Kinetics, Univ. Coll. of Swansea, UK (24-29 July 1988)

MORRIS, R.A. (AFGL); VIGGIANO, A.A. (Systems Integration Engineering, Lexington, MA); DALE, F., and PAULSON, J. F. (AFGL)

Collisional Vibrational Quenching of $\text{NO}^+(v)$ Ions

40th Annual Gaseous Electronics Conf., Atlanta, GA (13-16 October 1987)

MORRIS, R.A. (AFGL); VIGGIANO, A.A. (Systems Integration Engineering, Lexington, MA); Su, T. Southeastern Mass. Univ., N. Dartmouth, MA); and PAULSON, J.F. (AFGL)

Rate Constants for the Reaction $^{22}\text{Ne}^+ + ^{20}\text{Ne}$ as a Function of Collision Energy at Several Temperatures

41st Annual Gaseous Electronics Conf., Minneapolis, MN (18-21 October 1988)

MOSKOWITZ, W.P., DAVIDSON, G. (Photometrics, Inc., Woburn, MA); Philbrick, C. R., Sipler, D., Phan, Dao (AFGL)

Raman Augmentation for Rayleigh Lidar
 Internat. Laser Radar Conf., Innichen, San Candido, Italy (20-24 June 1988)

PAULSON, J.F., MORRIS, R.A., DALE, F. (AFGL); and VIGGIANO, A. A. (Sys. Integration Eng. Inc., Lexington, MA)
Energy Transfer in Collisions of $\text{NO}^+(v>0)$ with Quenching Species

Symp. on Atomic and Surface Phys., LaPlagne, France (17-23 January 1988)

PHILBRICK, C.R., and SIPLER, D.P.
Lidar Measurements of Atmospheric Structure

1987 Mtg. of the Internat. Assoc. of Geomagnetism and Aeronomy, Vancouver, Canada (9-22 August 1987)

PHILBRICK, C.R., SIPLER, D.P. (AFGL);
DAVIDSON, G., and MOSKOWITZ, W.P.
(Photometrics, Woburn, MA)
*Remote Sensing of Structure Properties in
the Middle Atmosphere Using Lidar*
1987 Laser and Optical Remote Sensing
Topical Mtg. of OSA, North Falmouth, MA
(28 September -1 October 1987)

RASMUSSEN, J.E., KOSSEY, P.A. (AFGL);
SOWA, M.J., QUINN, J.M. (RADC);
OSTERGAARD, J.C. (ElektronikCentralen,
Horsholm, Denmark)
*A Statistical Analysis of Polar Meteor Scatter
Propagation in the 45-104 Mhz Band*
AGARD Specialists Mtg. on Scattering and
Propagation in Random Media, Rome, Italy
(18-22 May 1987)

RETTNER, J.M., DECKER, D.T. (Boston
Coll., Chestnut Hill, MA); and JASPERSE,
J.R. (AFGL)
A Kinetic Model for the Diffuse Aurora
Cambridge Wkshp. on Ionosphere-
Magnetosphere Solar Wind Coupling
Processes, Cambridge, MA
(27 July - 1 August 1987)

RETTNER, J.M., DECKER, D.T. (Boston
Coll., MA); CHANG, T. Massachusetts
Inst. of Tech., Cambridge, MA); and
JASPERSE, J.R. (AFGL)
*Two-D Simulation of Ion and Electron
Acceleration by VLF Turbulence in the
Supraauroral Region*
AGU Mtg., San Francisco, CA (7-11
December 1987)
*Plasma Simulation of Intense VLF
Turbulence and Particle Heating in the
Supraauroral Region*
Internat. Conf. on Auroral Physics,
Cambridge, England (11 July 1988)

ROSENBERG, N.W. (Tel Aviv Univ., Tel
Aviv, Israel); and QUESADA, A. F. (AFGL)
Satellite UV Image Processing
SPIEE 1988 Tech. Symp. on Optics, Electro-
Optics and Sensors, Orlando, FL (4-8 April

1988)

SALES, G.S., REINISCH, B.W. (Univ. of
Lowell, Lowell, MA); BUCHAU, J. (AFGL);
and FOSTER, J.C. (MIT Haystack Obs.,
Westford, MA)
*Modification of the Ionosphere Using a High
Power HF Transmitter*
2nd Susdal URSI Symp. on Ionospheric
Modification by Powerful Radio Waves,
Tromsø, Norway (19-23 September 1988)

SWIDER, W.
The D-Region: Electron Loss and Pollution
AGU Mtg., Baltimore, MD (18-21 May 1987)
*Mean Ion Masses and Reduced Mobilities
from the Tropopause to the Mid-Mesosphere*
AGU Mtg., San Francisco, CA (6-11 December
1987)

THOMAS, J. M., DENTAMARO, A. V. (SCEE,
St. Cloud, FL); and KATAYAMA, D.H.
(AFGL)
*Energy Transfer from Electronically Excited
States of Nitrogen*
AFOSR Molecular Dynamics Conf., Los
Angeles, CA (30 October - 2 November 1988)

VALLADARES, C. (Emmanuel Coll., Boston,
MA); and CARLSON, H. C. (AFGL)
*Sondrestrom Observations of Sun-Aligned
Arc Electrodynamics*
AGU Mtg., San Francisco, CA (7-11
December 1987)

VIGGIANO, A.A. (Systems Integration
Engineering, Lexington, MA); PAULSON,
J. F., and DALE, F. (AFGL)
*The Effect of Temperature and Kinetic
Energy on Ion-Molecule Reactions;
Predicting the Temperature Dependence of
Non-Dissociative Electron Attachment*
5th Internat. Swarm seminar, Univ. of
Birmingham, Birmingham, England (29 - 31
July 1987)

VIGGIANO, A.A. (Systems Integration
Engineering, Lexington, MA); MORRIS, R.

A., PAULSON, J.F., and DALE, F. (AFGL)
*Pyridine and Picoline in the Troposphere -
Ion Chemistry and Concentration
Measurements*

AGU Mtg., San Francisco, CA (7-11
December 1987)

*The Kinetic Energy Dependences of the Rate
Constants for the Reactions of O⁻ With CH₄,
N₂O, and SO₂ at Several Temperatures*
36th ASMS Conf. on Mass Spectrometry and
Allied Topics, San Francisco, CA (5-10 June
1988)

*Deriving Rotational Energy Dependences for
Ion-Molecule Reactions: The Kinetic Energy
Dependence of the Rate Constants for the
Reactions of O⁻ with CH₄, N₂O, and SO₂ at
Several Temperatures*
AFOSR Molecular Dynamics Contractors
Conf. Newport Beach, CA (30 October 2
November 1988)

VIGGIANO, A.A. (Systems Integration
Engineering, Lexington, MA); MORRIS,
R.A., PAULSON, J.F. (AFGL); and
MICHELS, H.H. (United Technologies Res.
Corp., East Hartford, CT)

*Rate Constants for the Reactions of O⁻ With
CH₄ and CD₄, and CH₂D₂ as a Function of
Energy at Different Temperatures*
11th Internat. Mass Spectrometry Conf.,
Bordeaux, France (29 August - 2 September
1988)

WEBER, E. J.

*Field Report: Polar Acceleration Regions and
Convection Study, Polar Arcs*
Review of U.S. Programs in Greenland by
Danish Commission for Scientific Research in
Greenland, Copenhagen, Denmark (6 April
1988)

WEBER, E.J., BUCHAU, J., and CARLSON,
H.C.

*Polar Cap Structure and Dynamics: A
Review of Ground Based and Airborne
Experiments*

1988 Cambridge Wkshp. on Polar Cap
Dynamics and High Latitude Ionospheric

Turbulence, Cambridge, MA (13-17 June
1988)

WEBER, E.J., BUCHAU, J., CARLSON, H.C.,
BASU, S., MAYNARD, N., HARDY, D.,
BALLETHIN, J., SMIDDY, M. (AFCL);
RODRIGUEZ, P. (Naval Res. Lab.,
Washington, DC); and KELLEY, M.C.
(Cornell Univ., Ithaca, NY)

*Rocket Measurements of a Polar Cap Arc:
Plasma, Particle, and Electric Circuit
Parameters*

AGU Mtg., San Francisco, CA (7-11
December 1987)

WHALEN, J.A.

*The Relation Between the Reference Frames
of Magnetic Local Time and Local Time as
Observed in the Longitude Dependence of the
Daytime F-Layer Trough*

AGU Mtg., San Francisco, CA (7-11
December 1987)

Daytime and Nighttime F Layer Troughs
1988 Cambridge Wkshp. on Polar Cap
Dynamics and High Latitude Ionospheric
Turbulence, Cambridge, MA (13-17 June
1988)

TECHNICAL REPORTS

1987-1988

BASU, B., and JASPERSE, J.R.

*Marginal Stability of Ion-Acoustic Waves in
a Weakly Collisional Two-Temperature
Plasma Without a Current*
AFGL-TR-87-0242 (6 August 1987),
ADA195840

BISHOP, G.J., JACAVANCO, D.J. (AFGL);
COCO, D.S., COKER, C.E. (Univ. of Texas,
Austin, TX); KLOBUCHAR, J.A., WEBER,
E.J. (AFGL); and DOHERTY, P.H.
(Emmanuel Coll., Boston, MA)

*An Advanced System for Measurement of
Transionospheric Radio Propagation Effects*

Using GPS Signals

AFGL-TR-87-0319 (13 November 1987),
ADA205046

FORBES, J.M., MARCOS, F.A., and
FOUGERE, P.F.

*Wave Structures in Thermosphere Density
from Satellite Electrostatic Triaxial
Accelerometer Measurements*
AFGL-TR-87-0189 (June 1987), ADA194134

KLOBUCHAR, J.A., ANDERSON, D.N.,
BISHOP, G.J. (AFGL); and DOHERTY, G.J.
(Emmanuel Coll., Boston, MA)
*Measurements of Trans-Ionospheric
Propagation Parameters in the Polar Cap
Ionosphere*
AFGL-TR-87-0121 (3 April 1987),
ADA189446

MACKENZIE, E. (Emmanuel Coll., Boston,
MA); BASU, S. (AFGL); and BASU, S.U.
(Emmanuel Coll., Boston, MA)
*Ionospheric Scintillation / TEC and In-Situ
Density Measurements at an Auroral
Location in the European Sector*
AFGL-TR-87-0245 (14 August 1987),
ADA205543

MCMAMARA, L.F., REINISCH, B.W. (Univ. of
Lowell, Lowell, MA); and BUCHAU, J.
(AFGL)
*Ionosonde Studies of Field-Aligned
Irregularities During High-Power HF
Heating at Arecibo*
AFGL-TR-86-0168 (February 1988),
ADA195848

METCALF, J.I.
*Interpretation of the Autocovariances and
Cross-Covariance from a Polarization
Diversity Radar*
AFGL-TR-87-0062 (4 March 1987),
ADA177983

REINISCH, B.W. (Univ. of Lowell, Lowell,
MA); BUCHAU, J., WEBER, E.J. (AFGL)
DOZOIS, C.G., and BIBL, K. (Univ. of

Lowell, Lowell, MA)

High Latitude F-Region Drift Studies
AFGL-TR-87-0154 (December 1986),
ADA184466

SHERMAN, C.

*Scaling Laws for Geomagnetic Tail Current
Sheet Acceleration*
AFGL-TR-87-0235 (22 July 1987),
ADA193379

SWIDER, W.

On Formulating a Simple D-Region Model
AFGL-TR-87-0308 (28 October 1987),
ADA195841

TURTLE, J. (RADC); HECKSCHER, J., and
KOSSEY, P. (AFGL)

*TE/TM Height Profile Measurement of
Transpolar VLF Signals*
RADC-TR-87-207 (October 1987), ADA194503

CONTRACTOR PUBLICATIONS 1987-1988

DEAKYNE, C.A. (Wentworth Inst. of
Technology, Boston, MA)
*Ionic Hydrogen Bonds, Part II. Theoretical
Calculations in Molecular Structure and
Energetics: Biophysical Aspects*
ed. by J.F. Liebman and A. Greenberg, VCH
Pub. Co. (1987)

MCCORMAC, F.G., KILLEEN, T.L., BURNS,
A.G., MERIWETHER, J.W. (Univ. of
Michigan, Ann Arbor, MI); ROBLE, R. G.
(Natl. Ctr. for Atmos. Res., Boulder, Co);
WHARTON, L. E., and SPENCER, N. W.
(Goddard Space Flight Ctr., Greenbelt,
MD)

*Polar Cap Diurnal Temperature Variations:
Observations and Modeling*
J. Geophys. Res. 93 (1988)

CONTRACTOR PRESENTATIONS 1987-1988

BLOCK, L. (Royal Inst. of Tech., Stockholm, Sweden)
Satellite-Airborne and Radar Observations of Auroral Arcs
XXVII COSPAR Mtg., Espoo, Finland (18-29 July 1988)

COLLINS, D.F. (Warren Wilson College, Swannanoa, N.C.)
Quantitative Image Analysis of UV Rocket Plumes and Laboratory Images
SPIE 1988 Symp. on Optics, Electro-Optics and Sensors, Orlando, FL (4-8 April 1988)

DEAKYNE, C.A. (Wentworth Inst. of Technology, Boston, MA)
A Molecular Orbital Study of FSO₃SO₃H
195th Natl. Mtg. of the American Chemical Society, Toronto, Canada (5-11 June 1988)

DEAKYNE, C.A. (Wentworth Inst. of Technology, Boston, MA) and MEOT-NER, M. (Natl. Bureau of Standards, Gaithersburg, MD)
Methyl Cation Affinities of N, O, and C Lone-Pair Donors
194th Natl. Mtg. of the American Chemical Society, New Orleans, LA (30 August - 4 September 1987)

KOLB, C.E., RYALI, S.B., and WORMHOUDT, J. C. (Aerodyne Research, Billerica, MA)
The Chemical Physics of Ultraviolet Rocket Plume Signatures
SPIE 1988 Symp. on Optics, Electro-Optics and Sensors, Orlando, FL (4-8 April 1988)

PAPADOPOULOS, D. (Univ. of Maryland, College Park, MD)
The Physics of RF Breakdown of the Lower Ionosphere
2nd Susdal URSI Symp. on Ionospheric Modification by Powerful Radio Waves, Tromso, Norway
(19-23 September 1988)

STEWART, C., SHORT, R., SHANNY, R. (ARCO Power Technologies, Inc., Washington, DC); PAPADOPOULOS, D. (Univ. of Maryland, College Park, MD)
Artificial Ionospheric Mirrors Applied to Over the Horizon Radar
34th Tri-Service Radar Symp., Peterson AFB, CO (21-23 June 1988)

VIGGIANO, A.A. (Systems Integration Engineering, Lexington, MA)
Atmospheric Ion Chemistry - The Use of Laboratory and In-Situ Experiments in Deriving Trace Neutral Concentrations
Tohoka Univ., Sendai, Japan (30 September 1987)
Energy Effects on Rate Constants as Measured in Flow Drift Tubes
Max Planck Institut fur Kernphysik, Heidelberg, FGR (24 August 1988)

CONTRACTOR TECHNICAL REPORTS 1987-1988

BANKS, P.M., FRASER-SMITH, A.C., GILCHRIST, B.E., HARKER, K. J., STOREY, L. R. O., and WILLIAMSON, P. R. (Star Lab. Stanford, CA)
Ionospheric Modification
AFGL-TR-88-0133 (April 1987), ADA100181

BASU, SU., DOHERTY, P., MACKENZIE, E., and HAGAN, M. P. (Emmanuel Coll., Boston, MA)
Multi Technique Study of Ionospheric Structures Causing Degradation in Trans-Ionospheric Communications Systems
AFGL-TR-87-0148 (20 April 1987), ADA183542

BIONDI, M.A., and JOHNSEN, R. (Univ. of Pittsburgh, Pittsburgh, PA)
Atomic Collisions and Plasma Physics
AFGL-TR-86-0188 (31 August 1986), ADA175727

- BLAKE, A.J. (Univ. of Adelaide, Adelaide, Australia)
Oxygen Photoabsorption
 AFGL-TR-84-0025 (14 October 1983),
 ADA176896
- CHANG, T. (Massachusetts Inst. Tech., Cambridge, MA)
Ionospheric Plasma Study
 AFGL-TR-86-0206 (15 September 1986),
 ADA175695
- FORBES, J.M. (Boston Univ., Boston, MA)
Global Density Specification in the Lower Thermosphere
 AFGL-TR-88-0220 (31 August 1988)
 ADA204699
- GAMACHE, R.R., KERSEY, W.T., and REINISCH, B. W. (Univ. of Lowell, Lowell, MA)
Electron Density Profiles from Automatically Scaled Digital Ionograms. The ARTIST's Valley Solution
 AFGL-TR-85-0181 (July 1985), ADA180990
- HEELIS, R.A. (Univ. of Texas at Dallas, Richardson, TX)
Global Convection Patterns in the High Latitude
 AFGL-TR-87-0131 (February 1987),
 ADA185794
- KERSLEY, L., PRYSE, S.E., and WHEADON, N. S. (Univ. College of Wales, Aberystwyth, UK)
Radiowave Scintillation and Ionospheric Irregularities at High Latitudes
 AFGL-TR-87-0247 (30 May 1987),
 ADA192140
- LASINGER, J.M. (Northwest Research Associates, Bellevue, WA)
Support for FY87 Midlatitude Electron-density Calibration Campaign
 AFGL-TR-87-0299 (15 October 1987),
 ADA190174
- LIVINGSTON, R.C. (SRI Intl., Menlo Park, CA)
Ionospheric Scintillation Studies
 AFGL-TR-88-0148 (1 May 1988), ADA205210
- LUCAS, R.D., and ROBINS, R.E. (Northwest Research Associates, Bellevue, WA)
Geometric Restoration of Satellite Image Data
 AFGL-TR-87-0270 (15 October 1987),
 ADA190462
- MENDILLO, M. and HERNITER, B. (Boston Univ., Boston, MA)
A Model for the Low Latitude Ionosphere with Coefficients for Different Seasonal and Solar Cycle Conditions
 AFGL-TR-86-0260 (1 November 1986),
 ADA178207
- MERIWETHER, J.W., JR. and KILLEEN, T.L. (Univ. of Michigan, Ann Arbor, MI)
Collaborative Studies of Polar Cap Ionospheric Dynamics
 AFGL-TR-87-0012 (12 October 1987),
 ADA187888
- REINISCH, B.W., BIBL, K., DOZOIS, C.G., GAMACHE, R.R., KITROSSER, D.T., LI, S. W., SALES, G.S., and TANG, S.H. (Univ. of Lowell, Lowell, MA)
High Latitude Ionospheric Radio Studies
 AFGL-TR-87-0056 (February 1988),
 ADA192270
- ROSENBERG, N. (Northwest Research Assoc., Bellevue, WA)
Satellite UV Image Processing
 AFGL-TR-87-0271 (9 November 1987),
 ADA190466
- SECAN, J.A. (Northwest Research Assoc., Inc., Bellevue, WA)
An Assessment of the Application of In Situ Ion-Density Data from DMSP to Modeling of Transionospheric Scintillation
 AFGL-TR-87-0269 (I) (14 September 1987),

ADA188919

SECAN, J.A., and BUSSEY, R.M.
(Northwest Research Assoc., Inc.,
Belleve, WA)
*An Assessment of the Application of In Situ
Ion-Density Data from DMSP to Modeling of
Transionospheric Scintillation*
AFGL-TR-88-0280 (II) (15 September 1988),
ADA202415

SHEEHAN, R.E. (Trustees of Boston Coll.,
Chestnut Hill, MA)
Model Results with PIIE Rocket Data
AFGL-TR-86-0196 (26 September 1986),
ADA176999
*Rocket Measurements Within a Polar Cap
Arc: Ionospheric Modelling*
AFGL-TR-87-0326 (19 November 1987),
ADA192381

SIMONS, J.C. (MicroCoatings, Div. of
Optical Corp. of America, Westford, MA)
*High Resolution Ultraviolet Filter
Development*
AFGL-TR-87-0090 (7 February 1987),
ADA184183

SMITH, D., and ADAMS, N.G. (Univ. of
Birmingham, Birmingham, UK)
*Ion and Electron Interactions of Atmospheric
Importance*
AFGL-TR-88-0021 (31 December 1987),
ADA192255

SMITH, D., ADAMS, N. G., and HERD, C. R.
(Univ. of Birmingham, Birmingham, UK)
*Ion and Electron Interactions at Thermal
and Suprathermal Energies*
AFGL-TR-88-0295 (30 September 1988),
ADA201418

STOKES, C.S., and MURPHY, W.J.

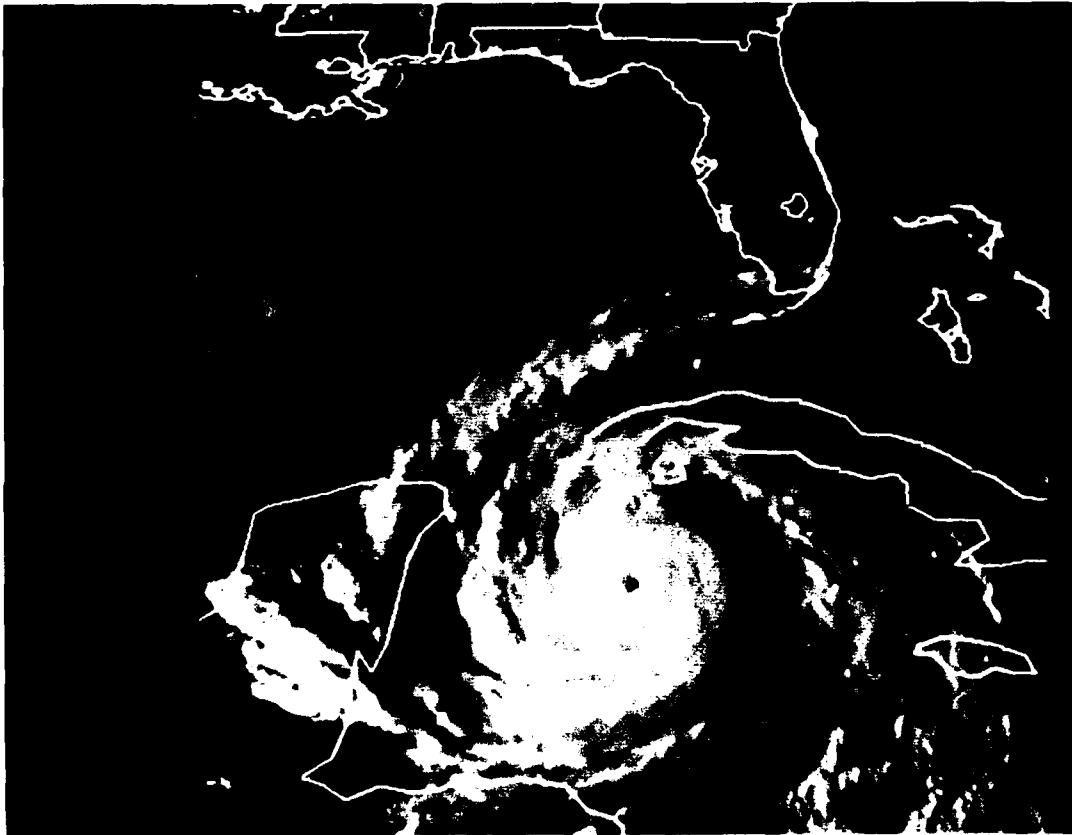
(Franklin Research Center, Elverson
Test Facility, Elverson, PA)
*High Altitude Chemical Release Systems for
Project BIME (Brazilian Ionospheric
Modification Experiments) Project IMS
(Ionospheric Modification Studies) Project
PIIE (Polar Ionospheric Irregularities
Experiment) Project Polar Arcs*
AFGL-TR-87-0231 (30 June 1987),
ADA188299

STRICKLAND, D.J., BARNES, R.P.
(Computational Physics, Inc.,
Annandale, VA), and Anderson, D.E., Jr.
(Naval Res. Lab., Washington, DC)
*UV Background Calculations: Rayleigh
Scattering and Dayglow Backgrounds from
1200 to 3000A*
AFGL-TR-88-0200 (24 August 1988),
ADA201118

SUCHY, K., and RAWER, K. (Univ. of
Dusseldorf, Dusseldorf, FRG)
*Improvements in Empirical Modelling of the
World-Wide Ionosphere*
AFGL-TR-87-0109 (3 November 1987),
ADA187051

THOMAS, J.M. (Univ. of Pittsburgh,
Pittsburgh, PA)
*Energy Transfer Processes of Important
Atmospheric Species*
AFGL-TR-87-0117 (11 February 1987),
ADA183042

THOMAS, T.F. (Univ. of Missouri, Kansas
City, MO)
*Kinetic, Thermochemical, and
Photodissociation Studies of Sulfur-
Containing Atmospheric Ions*
AFGL-TR-88-0187 (29 August 1988),
ADA200740



Hurricane Gilbert, as Viewed by GOES East, on September 13, 1988 at 1730 Eastern Daylight Time, as It Buffeted Grand Cayman Island. (Satellite imagery is used for tracking and classification of hurricanes and other tropical storms.)

IV ATMOSPHERIC SCIENCES DIVISION

Research in atmospheric sciences continues to be an important component of present-day military operations. Air Force systems and operations attempt to seek "all-weather" systems but find instead at least a continued dependence on weather due to atmospheric effects which impose limits on sensing devices. The Atmospheric Sciences Division investigates atmospheric effects on Air Force systems and operations. This research in developing better methods of observing and predicting meteorological conditions is likely to continue to be a vital part of the geophysical research program of the Air Force as we move into the next century.

During the period 1987-1988, projects in the Atmospheric Sciences Division have included: The development of improved satellite image-processing techniques; the retrieval of atmospheric temperature and water-vapor profiles from passive satellite sensors and the measurement of several other atmospheric parameters from active satellite sensors; the use of weather satellites to aid in specifying conditions occurring in tropical storms; the use of differential inversion techniques to obtain remote temperature retrieval from satellite radiances; research in atmospheric dynamic modeling and mesoscale prediction techniques; research in automated Doppler

weather radar techniques; the use of ultra high frequency radar to measure wind profiles; the development of climatological techniques for the design and operation of Air Force systems and the development of prediction techniques for toxic chemical spills; the development of techniques to better predict triggered and natural lightning; and research in upper atmosphere specification.

SATELLITE METEOROLOGY

Research in satellite meteorology is focused on a broad range of remote-sensing areas in an effort to provide the Air Force with new and improved capabilities of acquiring and analyzing real-time environmental satellite data. Recent projects include the development of improved satellite image-processing techniques for the automated analysis of clouds, the investigation of infrared and microwave spectral regions for retrieving atmospheric-temperature and water-vapor profiles, and the assessment of active sensors for the measurement of several atmospheric parameters. Most of the data for this research comes from the primary sensors onboard meteorological satellites, including polar-orbiting Defense Meteorological Satellite Program (DMSP) and National Oceanic and Atmospheric Administration (NOAA) spacecraft and from the NOAA Geostationary Operational Environmental Satellite (GOES). Data from the satellite systems are often used for different purposes, but all the meteorological satellites yield information indispensable for assessing the state of clouds and weather within the atmosphere.

GOES Data Ingest and Applications: An important tool used by the Satellite Meteorology Branch is the AF Interactive Meteorological System (AIMS). AIMS is a networked system of minicomputers and image-processing workstations designed to acquire,

process, manage, and display satellite imagery along with conventional meteorological surface and upper-air weather data in real time. The interactive capabilities of AIMS allow GL scientists to display research results on a color monitor and readily compare those results with the supporting data used to generate them. Limitations to research algorithms are identified and corrected using such interactive capabilities.

As part of a planned ground-station upgrade and in anticipation of enhanced capabilities for GOES-NEXT, NOAA changed the format of data transmission from the GOES satellites in 1987. This new transmission format, called Mode-AAA, required the purchase of new equipment, and a complete rewrite of the acquisition software. The hardware acquisition included redundant demodulators, bit synchronizers and frame synchronizers, as well as computer interface hardware. The new software ingests a large sector of the visible imagery and three infrared images at sensor resolution. This imagery exists on rotating mass storage on the ingest computer for only one-half hour before it is overwritten. A scheduling program on the display computer extracts predefined images from this large sector and places them in specified areas in the AIMS cluster. These predefined images exist for twenty-four hours before they are overwritten. A utility program was written which allows an inexperienced user to display, animate, and interact with these images with only a few keystrokes. A more experienced user can easily extract images other than the default imagery from the raw data sector, and save any imagery for later analysis.

Since the GOES satellite takes simultaneous images in the visible and three infrared bands, it is a simple procedure to produce multispectral imagery on the AIMS workstations. One example of

multispectral imagery uses the visible band to drive the red gun of the full color display, the thermal infrared band to drive the green, and water vapor (6.7 micrometer) imagery to drive the blue gun. In this multispectral imagery, low clouds appear red, high clouds appear yellow, and mid-level clouds appear green. Regions without clouds which are relatively moist have a blue tint, whereas drier regions have a dark tint.

A technique was developed to depict cloud motion without image animation. This technique also makes use of the AIMS full-color display device. Three co-registered images from three consecutive times are loaded into the display device such that the earlier image drives the red gun, the next image drives the green gun, and the last image drives the blue gun. In the resulting time-composited image, advancing edges of cloud systems appear blue and the trailing edge appears red. Regions which have the cloud in all three images appear white.

Improved Cloud-Analysis Models: Visible and infrared satellite imagery data are the primary source of global cloud observations. Visible channels measure reflected solar energy and are used to detect clouds and snow. Infrared channels measure emitted thermal energy and, consequently, the brightness temperatures of clouds and the earth's surface both day and night. Computer processing of such imagery is sometimes difficult because of varying conditions encountered on global scales. Snow cover is often confused with clouds in visible imagery because each surface reflects sunlight well. Low clouds are frequently confused with cloud-free land and oceans in infrared imagery because their temperatures can be nearly equal.

Many of these limitations in cloud imagery analysis can be overcome by using additional channels of multispectral meteorological sensor data. More

confident discriminations can be performed between clouds, snow, and the earth's surface when coincident data from the DMSP Operational Linescan System (OLS), DMSP Special Sensor Microwave Imager (SSM/I), NOAA Advanced Very High Resolution Radiometer (AVHRR), or Nimbus Scanning Multifrequency Microwave Radiometer (SMMR) are used for the same scenes. Multispectral image-display techniques have been developed that simultaneously combine the most desirable characteristics of images from several spectral channels into one image, clearly revealing features of meteorological interest.

Discrimination between low clouds/fogs and cloud-free land/oceans, along with improved detection of thin cirrus, can be performed more confidently when using multispectral infrared color-composite imagery. Combining infrared and microwave imagery reveals that discrimination between opaque cirrus and nimbostratus can be performed successfully over oceans. The presence of snow cover and ice can also be detected more confidently using visible and near-infrared data. Studies are ongoing at GL to make more efficient use of coincident multispectral data to improve Air Force real-time operational global-cloud analyses.

The Air Force Global Weather Central (AFGWC) at Offutt AFB, Nebraska, operates and maintains a global cloud analysis model known as the Real-time Nephanalysis (RTNEPH). The model generates analyses of the extent, location, and vertical structure of global cloud cover. Much of the analysis is derived using satellite imagery from the DMSP OLS sensor. GL is developing alternate methods of satellite data-processing including AVHRR multispectral models with the intent of improving the quality and reliability of the RTNEPH

cloud analysis.

Several problem areas exist with the RTNEPH satellite-data processor. The accuracy of the infrared cloud-detection algorithm has long been a source of concern. Since it is based upon empirical relationships, it is difficult and time-consuming for the AFGWC to maintain operationally. The RTNEPH infrared-processor algorithms frequently fail to detect a cloud in situations when thermal contrast between the cloud and the underlying surface is weak, especially low stratus over cold ocean and fog over land. In addition to multispectral techniques, GL is investigating potential improvements in cloud detection using physically-based infrared radiative-transfer techniques designed to improve the detection of low clouds, thin cirrus, and even some precipitating clouds. A new cloudlayer analysis algorithm has been developed at GL. Known as CLUSTER, it is being tested and evaluated against the current RTNEPH layer analysis algorithm. Initial results indicate that the GL layer-analysis scheme will provide improvements over the RTNEPH scheme, and further transition activities are scheduled.

Special Sensor Microwave/Imager (SSM/I): A new passive microwave imaging sensor, the SSM/I, was launched by the Defense Meteorological Satellite Program in June, 1987. The SSM/I instrument is working well, with system noise, gain, physical temperatures, and absolute calibration all operating within specifications. GL was the initiator and technical leader in the early specification for the SSM/I. The SSM/I is a scanning radiometer which measures upwelling energy from the earth-atmosphere system at four frequencies from 19.35 GHz to 85.5 GHz with an earth swath width of 1394 km. Three of the four frequencies employ both vertically and horizontally polarized channels for a total of seven

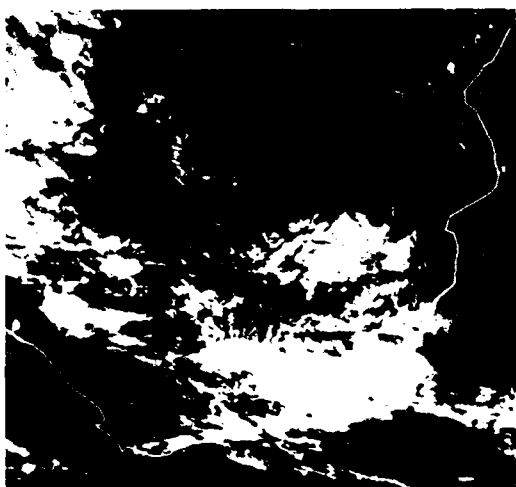
channels. Relationships among the brightness temperatures from the various channels provide a means to determine several geophysical parameters. Hughes Aircraft Company was the instrument manufacturer and, with a subcontract to Environmental Research and Technology, Inc., developed the geophysical parameter-extraction algorithms.

An SSM/I geophysical parameter-extraction algorithm validation effort, managed by the Naval Research Laboratory (NRL), was completed on December 1, 1988. GL was a member of the validation team and was responsible for analysis of output from the two Hughes algorithms for estimating cloud amounts (percent cloud coverage). One is applicable over snow backgrounds; the other over land backgrounds. Hughes has not been tasked to develop cloud-amount estimation algorithms for ocean backgrounds.

Results from the SSM/I cloud algorithms were evaluated by statistical comparison to an optical cloud cover analysis. Comparison data were obtained from computer-aided manual analyses of coincident visible and infrared imagery from the Operational Linescan System (OLS) on the same DMSP spacecraft as the SSM/I. The image processing and display capabilities of the AIMS were used extensively to aid the analyst. It was concluded that the Hughes SSM/I cloud-amount algorithms over land and snow backgrounds do not work and that it is not possible to devise working SSM/I cloud amount algorithms over these backgrounds because of a lack of discernible cloud signature.

However, the case of well-developed convective clouds which contain a thick layer of ice particles is an exception. These clouds have a strong cold signature at 85 GHz over all surface types. Over oceanic backgrounds, all other

cloud types, except for cirrus which are transparent, have a warm cloud signature at 37 and 85 GHz. An example of an 85 GHz horizontally polarized bright-



a. 85GHz Horizontally Polarized Brightness Image of Southern African Land Mass and Adjacent Ocean, January 14, 1988. (Areas of warm brightness temperatures are black and areas of cold brightness temperatures are white.)



b. Coincident Operational Linescan System Visible Image. (The black areas are cloud-free and the white areas are cloudy. Arrows point to lakes which have cold brightness temperatures similar to those of an ocean.)

ness-temperature image is given in the figure. This image shows the southern African land mass, as well as a bit of the ocean south of the land, for January 14, 1988. Areas of warm brightness temperatures are dark grayshades (black) in this image and areas of cold brightness temperatures are bright grayshades (white). Note the strong contrast between land and ocean; land areas have warm brightness temperatures while ocean areas have cold. Also shown is the coincident OLS visible image. In this image, the dark grayshades (black) areas are cloud-free (low visible reflectivity) and the bright grayshade (white) areas are cloudy (high visible reflectivity). Comparison of the OLS and SSM/I images shows that the microwave image discerns the strong convective cells within the cloudy regions seen in the visible image. Note that there are two small white areas, one at the top center and the other below and slightly to the left of it, in the SSM/I image which are not within the cloudy areas depicted in the OLS image. These two areas are lakes which have cold brightness temperatures similar to those of an ocean background.

Tropical Cyclones: The Air Weather Service (AWS) provides observational information on Tropical Disturbances. This mission was significantly affected when reconnaissance aircraft in the western Pacific were deactivated in October, 1987. These aircraft provided direct information on storm location, maximum surface and flight level winds, the horizontal extent of specified wind speeds, and other parameters relating to storm intensity. This information was used by the AFGWC and the Joint Typhoon Warning Center (JTWC) in Guam. With the loss of these direct observations, GL initiated a research program having the goal of using satellite sensor data to infer the information previously obtained by aircraft.

Microwave imagery from the SSM/I Sensor and infrared imagery from the OLS, both available on a DMSP satellite, are being used to study the structure and environment around tropical cyclones. Valuable meteorological information on the distribution of water vapor, rain-rate, and wind speed can be obtained from analysis of microwave data collected over oceans. The goal of the current research is to use this information combined with infrared derived cloud-height data to develop operationally useful techniques for specifying conditions occurring in tropical storms.

Active and Passive Sensors: A contractual study of a satellite meteorological radar has recently been completed for GL. The prime goal of the study was to determine the capability of satellite radars to detect the height of the cloud base for non-precipitating clouds. Other parameters which could be measured included the cloud top, cloud amount, vertical and horizontal extent of precipitation, winds in clouds and rain, winds over ocean surfaces, cloud phase (ice or water), and the ocean state. The proposed system includes a radar operating at a frequency of 36 GHz and passive radiometers operating at 19 and 37 GHz. The system was shown to be capable of detecting cloud layers, and it could provide cloud bases and cloud tops to an accuracy of 300 m for most clouds which have bases higher than 1 km.

A computer transmission code for microwave and millimeter waves for clear, cloudy, and rainy atmospheres has been written. The code, called RADTRAN, allows both ground-based and satellite-based instruments to be modeled using realistic atmospheric parameters. The code is extremely fast yet it treats the primary absorbers of electromagnetic energy in the microwave spectrum such as oxygen, water vapor, and liquid water drops. The code is currently

being upgraded in FORTRAN-77 language for transportability and will include improved models for scattering from solid surfaces and ice particles.

RADTRAN was the code used to simulate the new DMSP microwave water vapor sounder, the SSM/T-2. The Atmospheric Sciences Division of GL has proposed to undertake the calibration/validation of this new sensor which is scheduled for launch in the early 1990's. The calibration/validation will include ground-truth experiments world wide and will incorporate radiosonde and aircraft measurements as well as lidar measurements of water vapor profiles from the ground and aircraft.

In partial preparation for the validation of the SSM/T-2, a Raman lidar which was designed for water-vapor profile measurements was tested at the GL Otis Weather Test Facility on Cape Cod during September and October, 1987. Water-vapor profiles were measured every 2.5 min from sunset to sunrise. This experiment recorded the temporal behavior of water vapor and demonstrated that large changes can occur in the vertical structure of water vapor over relatively short periods of 1-3 hours. Future research will use lidars for measuring both the temporal and spatial structure of water vapor from the ground and from aircraft. These measurements will provide the needed input to validate the profiles measured from the SSM/T-2.

Remote Temperature Sounding by Satellite: Years of intensive theoretical effort in the area of remote temperature retrieval from satellite radiances have borne fruit in the development and data application of Differential Inversion. Concomitant with this new method, the current operational retrieval techniques have been shown to be gravely flawed, to the point of questioning their utility and capability of improving on the (required) first-guess

profile (see J. King, Publications, in Bibliography). Their difficulties arise from the ill-posed character of matrix inversion which, unless severely constrained, leads to unacceptable temperature instabilities.

In contrast, the Differential Equation format insures a properly posed problem, with the accuracy of the inferred profile limited only by how well the higher derivatives of the radiance profile are known. Since these derivatives are obtained from numerical differentiation of observed radiance data points, this imposes a requirement for numerous, accurate radiance observations.

The first application of Differential Inversion to TOVS (Tiros Operational Vertical Sounder) satellite data (May 1988) is shown in the accompanying table. This represents the first remote temperature inference based on satellite radiances alone, i.e., from any a priori database input. (Further applications to 9 point TOVS data are given in the paper "Application and Evaluation of a Differential Inversion Technique for Remote Temperature Sensing" by King, Hohfeld, and Kiliam, which has been accepted for publication in the *Journal of Meteorology and Atmospheric Physics*.)

TABLE 4
DIFFERENTIAL INVERSION RESULTS FOR TOVS.
(The value of p is 400 millibars.)

Latitude	Longitude	Time	Inferred Temperature	Raob Temperature	ΔT
27.2	-82.6	13:30:22	253.27	252.75	+1.52
24.3	123.8	11:12:19	255.53	256.25	-0.72
29.1	122.1	11:13:51	254.83	255.25	-0.42
14.7	120.8	23:41:12	256.00	257.16	-1.16
-14.8	-171.4	18:46:07	255.04	257.20	-2.16
-29.6	32.6	17:42:47	247.87	245.19	+2.68
-20.0	139.4	22:09:22	253.57	254.25	-0.68
27.7	-82.6	00:44:30	254.40	252.05	+2.35
23.7	154.2	09:09:21	257.02	258.86	-1.84
26.3	-79.7	13:08:17	253.61	250.55	+3.06
23.3	-106.9	14:50:41	253.63	255.69	-1.06
24.3	153.4	21:35:20	256.88	258.45	-1.57
28.3	129.1	23:15:31	253.62	252.95	+0.67
14.9	104.9	12:29:12	256.79	258.25	-1.46

ATMOSPHERIC PREDICTION

Basic research studies in atmospheric prediction have concentrated on improving the representation of moist physical processes in global and regional scale atmospheric models. Concurrently, exploratory development programs have focused on the development and evaluation of global and regional layered cloud-forecast techniques and computer-compatible mesoscale techniques and models

which will provide point and area forecasts of surface wind and sensible weather (clouds, visibility, precipitation) for time periods out to 12 hours. Techniques and models under development are expected to have the potential of operational application in the Air Weather Service (AWS) at either the Global Weather Central (AFGWC) or at the nearly 200 base weather stations which AWS mans around the world.

Consideration is given to the capabilities and/or limitations of current and future systems in the formulation of models (techniques). Other studies examine the benefits that could accrue to operations if the system capabilities were expanded beyond present operational limits, particularly as regards additional data sources.

Global Dynamic Modeling: Much of the progress attained during the past two to three decades in weather forecasting accuracy can be attributed to advances in numerical simulation models of broad-scale weather-circulation patterns. The accuracy of the numerical models depends on three factors: (1) the accuracy or completeness of the physical laws governing atmospheric interactions, (2) the accuracy with which the mathematical statements expressing the physical laws are carried out computationally, and (3) the adequacy of databases used to initialize the models. The global numerical weather prediction (NWP) program at GL uses a research-grade spectral model of the global atmosphere which follows closely the structure of many other multi-layer spectral models. With global spectral models (GSM), horizontal variations are represented by values in discrete layers. The basic equation set includes the equations of motion in sigma coordinates, momentum (represented by absolute vorticity and divergence), continuity, and hydrostatic and thermodynamic equations (the last two in forms suited to Arakawa vertical differencing).

Certain subgrid-scale physical processes must be accommodated within larger scale numerical simulation models through procedures known as parameterization. In establishing a baseline model at GL, we adopted the global spectral model implemented operationally at AFGWC as a point of departure. The parameterized physical processes in it

fall into three broad categories: boundary layer processes; moisture physics, including convective adjustment and large-scale saturation effects; and sub-grid-scale diffusion.

Research and development with the GSM involves a substantial amount of computer simulation running with large, global databases. Two computer systems are being used for these purposes: (1) a CYBER 860 at GL for the preliminary testing of new procedures in the model's software and for the analysis and evaluation, after the fact, of model performance data and (2) a CRAY-2 computer at the Weapons Laboratory for the actual model simulation experiments. Two five-day periods that are part of the First Global GARP Experiment (FGGE) database are being used to test the performance of the GSM in generating predictions of geopotential height, wind, temperature, and water vapor for time periods out to 96 hours.

FGGE was designated as a period of intense international cooperation in 1979 during which atmospheric and oceanographic observational field programs were undertaken to provide a "state-of-the-science" database of operational and research-grade measurements to support a wide-range of global and regional research and development purposes. The FGGE database has become the basis for major numerical weather prediction (NWP) modeling research and development efforts world-wide. For studies concentrating on cloud and moisture processes and prediction globally, it is particularly ideal when augmented by the highly-detailed 3D cloud (neph) analysis fields of AFGWC.

Earlier studies with the baseline GSM had demonstrated that moisture forecasts are the least skillful aspect of the model, exhibiting only minimal skill at all forecast intervals from 12 to 96 hours. This problem was attributed, in part, to

the poor quality of the analyzed FGGE moisture fields, to the moisture physics parameterization schemes, and/or to the vertical advection and interpolation schemes for the model's moisture variable, specific humidity.

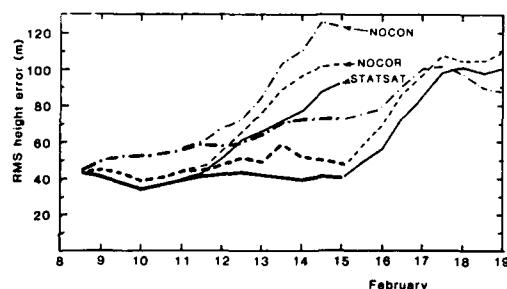
Objective Analysis and Data Assimilation: The accurate global depiction of atmospheric variables (height, wind, temperature, humidity, and clouds) is crucial to the initialization of global NWP models. During the period of this report, considerable attention was paid to investigating the impact of satellite observations (imagery and soundings) on NWP model performance and accuracy. This was done through a series of Observing System Experiments (OSE) using various combinations of real data in four-dimensional data assimilations and another series of Observing System Experiments (OSSE) using combinations of real and simulated data. The simulated data were added to represent data sources potentially available from one or more future satellite sensor options. The OSSE series considered new sensor designs for satellites (1) in the microwave portion of the spectrum to provide vertical profiles of atmospheric moisture and (2) lidar-based (CO_2 wavelength) wind soundings. With the GL GSM and its associated global analysis procedure, based on the widely-used optimal interpolation (OI) method, it was demonstrated that simulated lidar winds provide a positive impact on the model's wind and geophysical height forecasts. This improvement was determined by comparing model performance to an analogous model initialized without the simulated lidar winds. In conducting OSSE experiments, one has to make certain assumptions about the distribution and quality of the simulated winds. Plans are underway now to conduct a series of follow-on experiments in which these assumptions are varied in order to

evaluate the sensitivity of the model's performance to the "quality and measures" assigned to the simulated winds.

The OSE's experiments have been performed using the GL global data assimilation system (GDAS) (GSM and OI) and data from two special observing periods of the Global Weather Experiment of 1979. The first experiment, called STATSAT, used all available conventional and satellite data and it provided a basis for comparison of the other experiments. The second experiment, called NOSAT, removed all the available satellite data from the input set. These included TOVS temperature soundings from polar-orbiting satellites and cloud-tracked winds from geosynchronous satellites. The third experiment, called GLASAT, used a physically based, rather than a statistically based, procedure to retrieve temperature profiles from the radiances measured by the satellite sensors. The fourth experiment, called NOCON, was designed to test degradation when all conventional data were denied globally and only satellite data were used in the assimilation. The last experiment, called NOCOR, used only satellite data over a particular region (Europe and Asian Russia) and the full set of data over the rest of the globe.

The differences between the baseline experiment (STATSAT) and the others provide measures of observing system impacts. The differences between NOSAT and STATSAT analyses are found mainly over the oceans, where available satellite data is known to make its greatest contribution. There are substantial differences throughout the Southern Hemisphere and smaller differences along the western edges of Northern Hemisphere land masses. The GLASAT experiment suggests only small sensitivity (using the GL GDAS system) to physically vs. statistically based temperature retrievals. Forecasts in the NOCON experiment depart rapidly from the baseline forecasts, especially in

the Northern Hemisphere, where the differences became very obvious by 48 hs. In the Southern Hemisphere, the difference starts to become substantial after 72 hs. Finally, in the limited area data-denial experiment (NOCOR), differences between forecasts were noted first over the western Pacific (i.e., downstream from the data-denied area). The spread of the differences across the Pacific was noted to be faster in winter. The relative degradation of forecast skill in the two data-denied experiments as a function of the baseline experiment is illustrated in the figure.



Time Evolution of the rms Difference Between Analyses and Forecasts and Radiosonde Observations of 500 mb Height for the February, 1979, period. (The analysis phase of the experiments (indicated by the thick lines) are presented for STATSAT (solid), NOCOR (dashes), and NOCON (dash/dots). Four-day global prediction experiments are illustrated (with thin lines) for two periods starting at February 11 and 15. Forecast degradation is shown to be greater for the data-denied experiments (NOCON and NOCOR.)

Planetary Boundary Layer Processes: For simplicity, most global circulation models neglect the influence of surface moisture flux over land because they are mainly concerned with the prediction of mass and motion fields and, perhaps, precipitation. In the quest for global models tailored for moisture and cloud forecasting, surface moisture flux can have important influences on the diurnal development of the planetary boundary layer, related low cloud fields, and mass and

motion patterns in general. Considerable research has been concentrated, therefore, on the development of models for stability-dependent potential evaporation, for transpiration, and the canopy water budget in the atmospheric boundary layer. In accounting for surface heat and moisture fluxes over land, snow, and ice (as well as over water, as is commonly done in operational models), the boundary layer model (BLM) includes a diurnal cycle and a surface energy budget calculation. It has been structured to account for surface albedo, soil type, snow/ice characteristics, and vegetation type. As such, it explicitly predicts hour-by-hour the depth of the boundary layer, the ground surface (or skin) temperature, air temperature just above the ground, soil temperature and moisture, and boundary layer winds, stability, and cloud amount.

An important procedure added to the boundary layer model, in order to facilitate its being coupled with the GSM, is the parameterization of subgrid-scale surface fluxes of heat, moisture, and momentum. These procedures seek to account for (1) transport by motions larger than the turbulent scale, (2) surface inhomogeneities within a "grid box", and (3) lack of equilibrium between turbulence and the local surface. While the established formulation for this procedure has been found to be adequate in regions of neutrally stable and unstable temperature lapse rates, the dependence of the exchange coefficient on the Richardson number had to be reformulated for application in stable lapse-rate regimes.

Because of an incomplete understanding of the nature of turbulence in stable conditions, special attention has had to be paid to the parameterization of the very stable boundary layer. Nocturnal cooling can be seriously over-predicted if one inadequately accounts for sensible

heat transfer. The approach studied consisted of (1) a determination of the boundary layer height under stable conditions, (2) the reformulated calculation of the exchange coefficient mentioned above, and (3) a reformulation for eddy diffusivity in the boundary layer to account for increased mixing in the boundary layer. These changes have the positive effect of decreasing the extent of predicted surface cooling under very stable lapse-rate conditions. This situation has been particularly troublesome in the past over regions of extensive snow cover under nighttime conditions. Lastly, methods to incorporate the effect of shallow convection (and clouds) into the transport of heat and moisture from the boundary layer into the free atmosphere have been established for the GSM. Without accounting for these processes, moisture will accumulate in the boundary layer, thereby leading to reduced latent and sensible heat fluxes from the surface. While this consideration is deemed to be warranted over large regions of the globe, it is of particular importance over trade-wind regions where shallow cumulus play a dominant role in the real atmospheric process.

Cloud-Radiation Interactions: Another factor neglected in many global circulation models, but one that has greater importance when the model's purpose is moisture and cloud forecasts, is radiation effects. A broadband emissivity and absorptivity approach was used to develop a computationally reasonable parameterization model to account for the transfer of thermal (infrared) and solar radiation in clear and cloudy atmospheres. The emissivity for the individual absorption bands was derived either from band models (water vapor and ozone) or line-by-line data (carbon dioxide). High clouds in the atmosphere were treated as non-black and their emissivity, transmissivity, and reflectivity were parameter-

ized in terms of their vertical ice content. Solar radiation was accounted for by developing broad-band absorptivity for water vapor, carbon dioxide, and ozone. Cloud reflection and transmission properties were parameterized in terms of liquid water content and solar zenith angle. These properties were then used to compute upward and downward radiative fluxes for clear and cloudy atmospheres having one or two layers.

In research pursued during this period, the radiation scheme was extended to compute fluxes in cloudy atmospheres with up to three cloud layers. It defines cloud layers using an empirically based relationship to relative humidity and assigns low, middle, and high cloud bases and tops based on the height of specific model layers uniformly at all locations globally. An alternative cloud-height assignment procedure was tested wherein the model-generated relative humidity profile was used to define cloud bases and tops more directly. This approach would yield a more representative heating/cooling profile if clouds were being properly accounted for. The present empirical scheme, which is based only on relative humidity, is judged to be most deficient with regard to defining high (cirrus) cloud layers. Research into alternative cloud schemes that consider additional parameters, including contributions due to the convective parameterization scheme, will lead to a series of tests during the next reporting period that will more properly evaluate the alternative cloud-height assignment procedure. Another modification made to the radiation calculations was to separate and collect the terms dealing with solar radiation from those dealing with terrestrial radiation. By so doing, the less computationally demanding solar calculations could be invoked on an hourly cycle while retaining a three-hourly cycle for the time-demanding terrestrial calcula-

tions. At a very modest increase in model computational needs, this change yielded surface-temperature and boundary-layer moisture flux profiles (temporal) that were much improved representations of the smoothly varying transitions observed in nature.

Cumulus Convection: Moist physical processes in the atmosphere typically occur on spatial scales smaller than the scale that can be resolved by a global prediction model. Thus their effects are simulated via a parameterization process that seeks to account for the sub-grid scale events on the spatial scale of the model. The third area that such research has been focusing on is the treatment of cumulus convection where the effects of condensation, evaporation, and the vertical transport of heat and moisture by cumulus clouds is accounted for on the model grid. The objective of the modifications made to the existing procedures was to design a procedure better suited to cloud and moisture prediction and less focused on convective precipitation. To that end, an alternative partitioning of calculation of the vertical (convective) advection, of potential temperature (heat), and specific humidity was developed. In addition, the procedure now incorporates cloud-top height based on convective strength and environmental stability and more completely accounts for the effects of dry-air entrainment on the cloud's heating and moistening profiles.

Initial testing of the new convection scheme revealed some encouraging results, though not totally resolving the problem. One of the major deficiencies noted in the operational global numerical weather-prediction model at AFGWC was its inability to predict precipitation, especially convective precipitation. The new scheme substantially overcomes that deficiency, to the point of generating too much precipitation globally. A more

detailed examination of its performance revealed the unrealistic generation of copious amounts of precipitation in certain tropical land mass areas. Because the model was "raining out" so much precipitation, the atmosphere was being dried out too fast and clouds were being lost.

Assessment of the separate attributes that contribute to (or should contribute to) convective precipitation in the procedure led to several modifications to the method that have adjusted its precipitation generation to more appropriate levels. These modifications included the following: (1) including the entrainment of environmental air into the cloud column from the lowest layer of convective instability to the calculated cloud top, (2) allowing for evaporation in lower, unsaturated portions of the vertical column, (3) calculating, rather than arbitrarily assigning, the lifted condensation level of the air parcel and using the moist adiabatic term, at its level in the subsequent heating and moistening calculations, and (4) using a centered differencing (leap frog) scheme rather than a forward differencing scheme to calculate the moisture-tendency term needed to determine the amount of water available (via moisture convergence) for heating and moistening of the convective column. Besides their generally positive effects on precipitation generation, these modifications yield mixed effects on the model's thermal and moisture fields. Our current emphasis is to "tune" the convection scheme such that it generates the most representative temperature, water vapor, and precipitation forecasts globally. A similar process is ongoing independently with the boundary layer model and with the cloud-radiation scheme, after which the "tuned" versions will be incorporated into an advanced version of the GSM and "returned" in an integrated sense.

Regional NWP Models: The operational Air Force requires cloud forecasts on horizontal scales (50-100 km) that can only be obtained, computationally, through the use of limited-area or regional NWP models. Because there has been substantial interest internationally in forecasting mass, motion, and precipitation on these scales, there is ample evidence that regional models can indeed deliver useful and more detailed forecasts of these variables out to 48-60 h. Here, again, the main USAF interest is for cloud and moisture forecasts, where little emphasis has been placed up to now.

We undertook the development of a research-grade relocatable limited area NWP model (called RLAM), structured in a flexible modular fashion to accommodate testing and experimentation. As with the GSM, the principal research and development focus will be on the impact of alternative moist physics processes on model performance. In view of the likely sensitivity of the cloud and moisture forecasts to numerical and dynamic factors, as well as moist physics, a modular structure has also been used for those aspects. The RLAM would, in an operational forecast setting, be executed in a nested framework using initial and boundary conditions from a GSM. Two or more options exist for solving each of the following components of the RLAM: vertical discretization, lateral boundary conditions, and filtering. The initial version of the model contains separate routines to activate a simple moist-convection scheme, a dry convective adjustment, and a simple boundary-layer flux of momentum and temperature over water.

One particular area of research into numerical schemes sought to incorporate the so-called semi-implicit time-integration scheme, which offers the advantage of using larger time steps but requires more computations per time step. In this

procedure, the linear terms in the equations are treated implicitly and the nonlinear terms are treated explicitly. Our attempts to include this procedure have not been totally successful. The scheme has been found to be quite sensitive to the model's vertical configuration and does not tolerate large time steps in areas with rugged topography or variations in underlying surface (e.g., land-sea boundaries). We've concluded that the linear stability criteria of semi-implicit schemes do not guarantee stability in nonlinear systems, especially when physical parameterizations are included as part of the tendency calculations. In the experiments conducted; adjusting the time step interval to smaller values (thereby increasing the model's computational load) allowed stable solutions for longer forecast periods. However, applying these adjusted values to other synoptic situations and geographic areas did, in some cases, result in unstable solutions. Clearly, this condition is not desirable in any NWP model being considered for eventual operational use.

Mesoscale NWP Models: A research program is underway to develop generic mesoscale NWP models for cloud and precipitation forecasting applications at both AFGWC and in base weather stations. The basis of these studies are three-dimensional hydrostatic and non-hydrostatic moist primitive-equation models which, in their first form for testing, were initialized with a single radiosonde and modified by underlying terrain variation. The hydrostatic model structure consists of 16 terrain-following surfaces and a square domain spanning 500 km with a grid resolution of 20 km. An alternative to the single-sounding initialization approach was studied wherein a network of relatively dense surface observations was used in conjunction with the single sounding to initialize

model fields through the boundary layer. While this simple blending approach yielded improvements for potential temperature and mixing ratios, the initialized wind fields were, in fact, degraded.

In addition, two modifications to the prognostic model were tested. The first introduced a time-dependent lower boundary condition via a so-called slab model to compute ground potential temperature through the surface energy-budget equation, which balanced net radiation-heat flux (short and long wave) with heat flow into the substrate, heat flux into the atmosphere, and latent heat flux. The second modification added a time-dependent sponge boundary condition which assimilated at the lateral boundaries the conditions provided by the larger-scale observation data set. The first modification led to a modestly improved precipitation forecast by the model but with some degradation of the boundary-layer temperature forecasts. The modified lateral-boundary treatment improved both the amplitude and positioning of the precipitation pattern.

Lastly, research has concentrated on the formulation of methods of accounting for diurnal variations of ground surface temperature in order to more properly model the fluxes of energy from the surface into the boundary layer of a mesoscale NWP model. To this end, a soil-slab model was formulated using the so-called force-restore method. It explicitly specifies the diurnal variation of ground surface temperature which in turn drives the calculation of soil heat flux. This study demonstrated that the soil heat-flux term in a soil model's upper boundary condition can be approximated by an analytical expression and that the upper boundary condition itself can be solved numerically as a time-dependent problem for the given nonlinear heating function.

The nonhydrostatic (cloud-scale) model

has been used primarily to study (simulate) cumulonimbus cloud processes as a means of increasing our understanding of precipitation processes. Typically, the model is used in a 2-D framework (X-Z) where spatial grid resolutions of the order of 200-250 (domains of 24 km horizontally and 16 k vertically) can accommodate a full simulation of vigorous cumulus. The model accounts for precipitation growth via both warm rain and ice processes. The focus of recent simulation experiments has been to determine how the parameterized microphysical processes react, within the model, to varying initial concentrations of cloud droplets above cloud base and to the assumed critical radius of cloud droplets above which conversion to precipitation droplets is assumed. Two experiments were completed during this period, one involving a large thunderstorm observed and measured during a major field program in Montana (dry, high plains environment) and the other involving a comparably sized storm in Alabama (humid, Gulf coast environment). In both cases, the model represented rather well the cloud top height, peak vertical velocities, and the precipitation growth stages in the development of the storm in those simulations in which the environmental factors (e.g., cloud droplet concentration) were set at values appropriate for the geographical region in question.

Mesoscale Prediction Techniques:

Improvements in mesoscale (or short-range) weather prediction can be tied to a more complete description of the atmosphere at observation time and changes in its recent past. The extent of spatial and temporal detail incorporated into this capability, generally referred to as "nowcasting," is largely dependent on the basic data sources used in the analysis. At this point of technology development, the potential of combining conventional surface and radiosonde observations

with digital satellite (imagery and sounding) and radar imagery (Doppler and conventional) offers promise of substantial improvement in our ability to more completely describe the state of the atmosphere (nowcast). That potential is greatest in mesoscale meteorology with geosynchronous satellite (GOES-type) data (which provides practically continuous views of the same geographical area at half-hour intervals), with the use of minicomputer-based interactive graphics systems, and with the viable emergence of meso-scale and cloud-scale NWP models.

A research and development program was started during this period in response to the need for an information-processing methodology to deal with the wealth of data to be generated by new weather-observing systems coming into operational use at base weather stations over the next several years. These include: NEXRAD Doppler weather radar, DMSP and GOES satellite imagery and soundings, conventional data through AWDS (Automated Weather Distribution System), ground-based wind and thermodynamic vertical profilers, and automated continuous observation at one or more locations on an airbase. The program, called AMPS (Advanced Meteorological Processing System), has the objective to develop, test, and evaluate both numerically-based and expert system procedures for the assessment, analysis, and short-range prediction of weather events critical to safe and efficient aviation activities on and around individual air bases.

There are three areas of emphasis during this period: (1) objectively based extrapolation procedures to nowcast/forecast NEXRAD and/or GOES imagery through the use of small but powerful image-processing work stations, (2) numerically based prediction models, suited for real-time execution in a micro-

computer environment, that are designed to specifically deal with the processes of convective initiation and with nonconvective cloud and precipitation systems, and (3) artificial intelligence (expert system) approaches to specific short-range aviation weather data-processing and forecast problems. Toward this end, an AMPS Experimental Facility is being established at GL to support both the technique development phases and subsequent test and evaluation experiments.

GROUND-BASED REMOTE SENSING

Knowledge of the environment is essential to the operation of nearly all weapon, surveillance, and communication systems in the Air Force. The Atmospheric Sciences Division develops techniques for the remote sensing of environmental conditions and the use of the derived information in weather advisories and forecasts for times up to several hours. The ground-based remote-sensing program relies primarily on the 10-cm wavelength Doppler radar and other radars at the Remote Sensing Facility in Sudbury, MA. Significant accomplishments during 1987 and 1988 included (1) the first measurement of the differential reflectivity of lightning, (2) observations of precipitation by means of a 3.2-mm Doppler radar, and (3) continued development of automated techniques for detection and warning of atmospheric hazards based on Doppler weather radar observations. From December 1988 through February 1989 the 10-cm Doppler radar is being operated in cooperation with the Experiment on Rapidly Intensifying Cyclones over the Atlantic (ERICA), which is sponsored by the Office of Naval Research and other agencies, to document the structure of precipitation and winds in coastal cyclonic storms.

Automated Doppler Weather Radar

Analyses: The Next Generation Weather Radar (NEXRAD) is now in the first stage of production, and operational deployment is scheduled to begin in 1990. Doppler radar weather research at GL provided much of the scientific foundation for the NEXRAD Program, in which GL has been deeply involved from its beginning. Activities at GL during the past two years have continued to focus on the development and testing of algorithms for the detection, identification, and prediction of severe weather hazards at the ground and in the lowest few kilometers of the atmosphere. The topics addressed in these studies during 1987 and 1988 included evaluation of the intensity of large cyclonic storms, the initiation of thunderstorms, and the correction of ambiguous velocity measurements.

A substantial effort has been directed to the analysis of curved wind fields, such as are encountered in tropical cyclones and in mid-latitude (extra-tropical) cyclonic storms, with the goals of specifying and predicting the intensity of these storms. Although tropical cyclones (hurricanes or typhoons) are commonly considered the most dangerous, large mid-latitude winter storms can develop to comparable intensity. GL scientists are developing techniques to predict the intensification and decay of these storms, using the wind-field derivatives (divergence, curvature, crosswind shear, and downwind shear) from Doppler radar measurements. The data acquired by GL during the passage of Hurricane Gloria in 1985 have been augmented by observations of several winter storms derived from the GL Doppler radar during the past two years. The analysis of these data led to the formulation of a Storm Strength Index (SSI). When applied to the data from Hurricane Gloria, the SSI accurately described the reduction in strength of the storm when

the eye was more than 200 km from the radar and the surface wind at the radar site was still increasing. This index appears to be useful in the estimation of wind speeds toward the center of the storm and in the definition of warning areas for high wind speeds. A better indicator of the overall vitality of circulation and of trends in storm severity is the Potential Vortex Fit (PVF), which is a measure of the Degree to which the storm circulation matches that of a model vortex. Values near unity outside the eyewall of a hurricane imply a well-developed potential vortex circulation. Values less than unity imply that the storm is weakening.

Spacecraft launch and recovery operations require accurate predictions of the occurrence of thunderstorms near the flight corridor. GL personnel conducted Doppler radar observations of the clear atmosphere at NASA Kennedy Space Center, FL, during August and September 1987, with the goal of defining regions of convergence in the clear atmospheric boundary layer. The resulting data are being analyzed at GL as part of the effort to develop improved cloud and precipitation forecasts for use by NEXRAD.

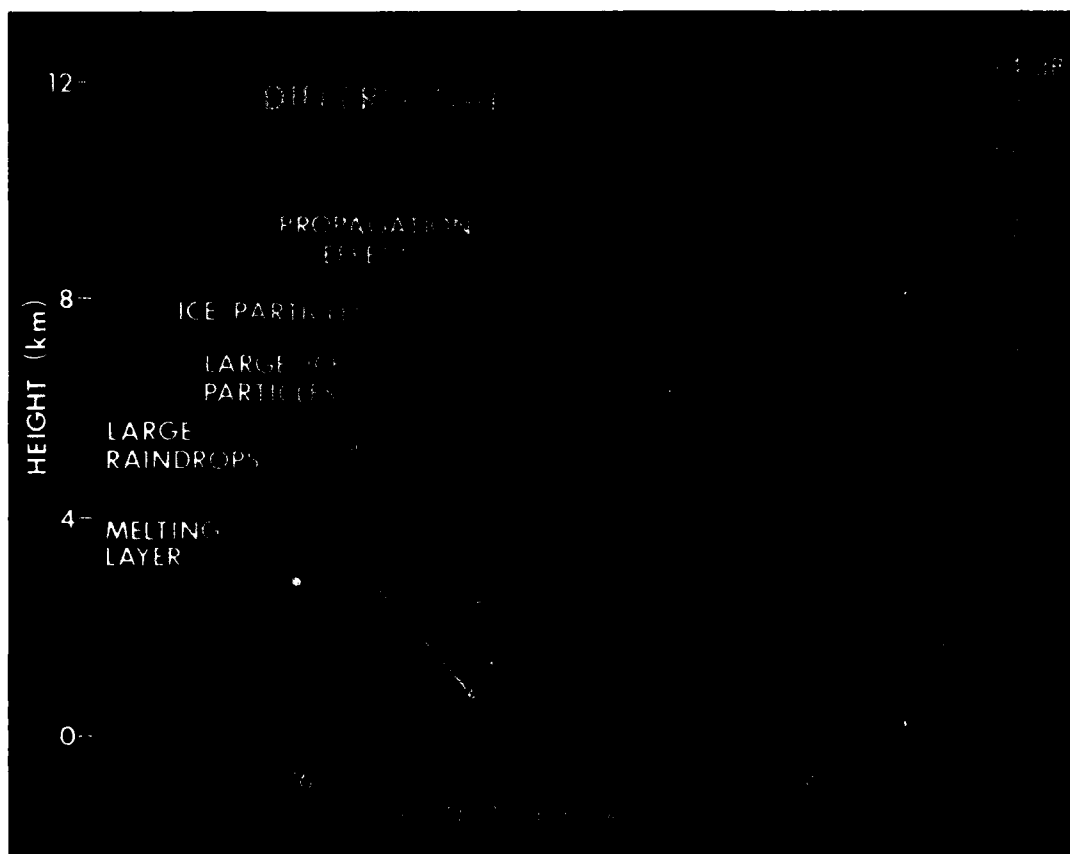
A fundamental problem in the analysis of data from a pulsed Doppler radar is aliasing of the Doppler mean velocity. The domain of measurable velocity is proportional to the pulse repetition rate of the radar, and actual velocities outside this domain are aliased by a multiple of the domain width. It is generally easy for a radar meteorologist to identify aliased velocity measurements on a display, but the automated analysis of wind fields requires that aliased velocities be identified and corrected automatically. During the past two years a new algorithm for velocity de-aliasing has been developed. This algorithm is more reliable than earlier algorithms developed elsewhere,

including the de-aliasing algorithm presently incorporated in NEXRAD. The accurate wind fields produced by this algorithm are to be used in several algorithms that identify and evaluate particular features of the wind field, such as mesocyclones, gust fronts, and layers of strong shear.

Precipitation Characteristics: The characteristics of water drops and ice particles that constitute clouds and precipitation are of significant practical concern to the Air Force because of their effects on (1) the depolarization and attenuation of terrestrial and satellite communication

systems, (2) the safe performance and even the survivability of airframes in regions of hail or heavy icing, and (3) the erosion of reentry vehicles. The water drops and ice particles are known to be affected by electric fields in clouds and thus may provide clues to the electrification of clouds, even those that are not producing lightning.

GL has developed techniques for deriving information on the sizes, shapes, number concentrations, and thermodynamic phases of cloud and precipitation particles from measurements with polarization diversity radars. These tech-



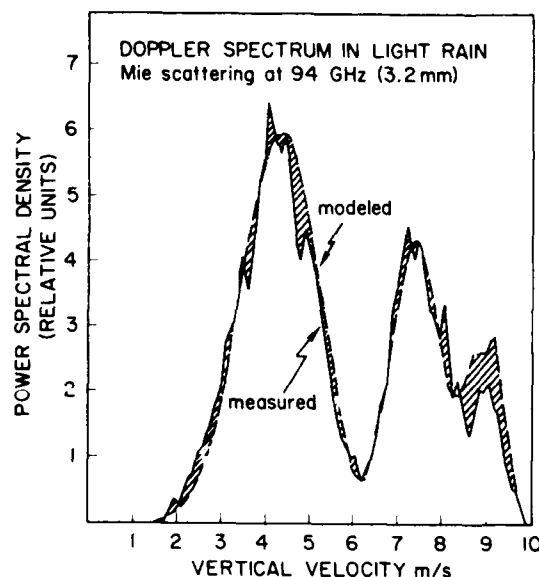
Polarization Differential Reflectivity of a Thunderstorm. (Vertical cross section through the core of a thunderstorm reveals the different types of particles present. Values near zero decibels are characteristic of ice particles. Persistence of this value below the height of the melting level, coincident with high values of absolute reflectivity (not shown), indicates large ice particles, i.e., hail. Large water drops are present in heavy rain at low altitude between 25 and 30 km range and in the updraft region near 37 km range.)

niques rely on the fact that many types of hydrometeors are non-spherical and tend to orient themselves in a preferred way in response to aerodynamic or electrical forces. The hydrometeors thus constitute an anisotropic scattering and propagation medium. This characteristic of the medium has implications for the performance of surveillance, guidance, and communication systems in clouds and precipitation. It also makes it possible to use the relative amplitude and relative electromagnetic phase of received signals of opposite polarizations to derive microphysical information. The polarization-dependent quantities, together with the conventional reflectivity and Doppler mean velocity and spectrum variance, enable the most comprehensive possible description of the scattering and propagation media from a single radar.

During 1987 a high-power microwave switch was installed in the GL 10-cm Doppler radar to enable the measurement of the differential reflectivity between horizontally and vertically polarized signals with an accuracy of 0.1-0.2 dB. The radar observed both convective and stratiform storms throughout the period. Of particular significance were the first observations ever made of the differential reflectivity of lightning and the observation of a developing hailstorm. The observations of lightning channels have shown that the differential reflectivity lies between -2 and +2 dB, indicating that the channels have only slight tendencies toward orientation in the vertical and horizontal, contrary to the expectation of magnitudes up to 8 dB that would have indicated predominant horizontal or vertical orientation of the channels. Observations of a storm that produced 3/4-inch hailstones in Dedham, MA, about 35 km from the radar site, revealed the downward progression of small values of the differential reflectivity in a region of high abso-

lute reflectivity, a combination indicative of hail, about 10 minutes before hail was observed at the surface.

The first measurements of rain at vertical incidence with a Doppler radar of 3.2 mm wavelength were made in Sudbury, MA, in 1987. At this wavelength the backscatter cross-section of raindrops lies in the resonance region, or Mie scattering region, because the diameters of the raindrops are similar to the radar wavelength. The resulting multi-peaked power spectra permit a more detailed view of the raindrop-size distribution than is possible with radars of



Doppler Spectrum Measured by 94 GHz Radar at Vertical Incidence in Light Rain. (Measured spectrum, solid line, is fitted to a modeled spectrum, broken line, to determine the radial component of air velocity, i.e., the vertical component, with an accuracy of a few centimeters per second. Multiple peaks in the spectra are due to resonances in the backscatter from raindrops, which have sizes comparable to the radar wavelength of 3.2 mm.)

longer wavelengths and the derivation of the vertical air velocity with great accuracy. Although the analysis is not yet complete, it is evident that such measurements will provide deeper understanding of turbulence and mixing pro-

cesses and of the development of precipitation in clouds.

Wind Profiling: The detailed structure and temporal variability of winds aloft are of particular concern in the launch of spacecraft. A new program was initiated in 1987 to use an ultra high frequency radar to measure wind profiles in the troposphere and lower stratosphere. GL plans to install its profiler at the Remote Sensing Facility in Sudbury, MA, in 1989. In preparation, GL is acquiring the necessary data-acquisition equipment and making detailed plans for the use of the profiler, in close coordination with the National Oceanic and Atmospheric Administration (NOAA) and other operators of wind profilers. To aid this process, GL is acquiring data from a wind profiler installed at Otis ANGB, MA, on Cape Cod by Pennsylvania State University in conjunction with ERICA. The GL profiler will be operated in coordination with the nation-wide network of profilers operated by NOAA.

ATMOSPHERIC CHARACTERIZATION

Air Force systems and material must be designed to operate in, and withstand the total range of, atmospheric conditions from the normal to the extremes. These conditions have a vital effect on the successful accomplishment of the Air Force mission. Over-design may be uneconomical or even ineffective, whereas under-design can result in failure, with possible loss of life and equipment. As a result, material and systems design require careful consideration of various atmospheric elements, including their variability and duration. Limitations of current meteorological data make it necessary to develop theoretical and empirical models, or algorithms, and to improve the utility of available climatic information as well as to provide more accurate estimates of the structure and variability of the atmosphere.

Consequently, climatological research is continuing in order to better describe the atmosphere and its effect on Air Force plans and the design and operation of equipment.

Environmental Simulation and Statistical Modeling: The requirements for the Strategic Defense Initiative Organization continued to be the primary focus for our cloud simulation research. SDIO needs to know the effect of clouds on the ability of a ground-based laser system to operate effectively. Since there is insufficient empirical data to characterize cloud size and spacing, GL has chosen to simulate various sky conditions and perform statistical analyses on the resultant simulated data.

Toward that end, modeling of areal cloud cover was advanced from three-dimensional space to include the dimension of time. Cloud cover was simulated from the aspects of both a ground observer and a satellite. Generalized formulas were obtained for spatial correlations. Other aspects of the temporal and spatial extent of weather conditions were investigated, such as fractal structure.

A report was published on the probabilities of spatial and lineal coverages in three dimensions. Another report is in review on parameter determinations. Still another report is in preparation on the probabilities of cloud-free-lines-of-sight (CFLOS) and cloud-free intervals (CFI). The modeling of temporal duration is under revision.

A major field effort was mounted to gather data to verify these CFLOS models. Whole Sky Imager systems were built, tested, and deployed at six CONUS sites, where they'll operate for about two years. These systems take high-resolution (spatial and temporal) digitized images of the celestial dome during daylight hours. Concurrently, a dedicated database was initiated which will allow the resultant data (about a gigabyte a

week) to be organized for efficient retrieval in the outyear. Output from these systems will be compared to output from the GL Cloud-Free Arc (CFARC) model, in the hope that the statistics of cloud-freeness will be roughly similar. If so, it can be argued that CFARC is an accurate model of the reality assumed to reside in the whole sky images.

Cloud-Impacts Assessment Research: Various analytical studies are underway which allow for more quantitative assessments of the impacts of clouds on planned or existing DoD systems. Two general research areas summarize these studies. A cirrus cloud initiative was undertaken to analyze existing lidar data, both airborne (ER-2 research aircraft) and ground-based. One objective is an improved vertical profile of the extinction coefficient within various cirrus-cloud conditions. Another is the development of a spatial correlation function for cirrus attenuation.

It has become evident that existing cirrus-cloud climatologies are seriously flawed in that they systematically underestimate the occurrence of cirrus cloud, especially thin cirrus, and underestimate the height of cirrus within the troposphere. Another ongoing cirrus-cloud initiative is the production of an improved global cirrus climatology using multiple infrared sensors onboard meteorological satellites.

View-angle research was continued using space-based cloud-viewing platforms and ground-based scanning lidar. Cloud imagery taken during an experiment onboard the orbiting space shuttle is being used to develop models for the apparent increase in cloud amount with increasing view angle, i.e., increasing angle, off-nadir. A second shuttle experiment is being designed which will measure the radiance from specific cloud scenes as a function of the viewing angle. In the meantime, quantitative lidar data

having high vertical resolution and considerable extent in space or time is being employed to specify the change in cloud optical effects, in a statistical sense, as a function of the view angle.

In addition to conducting cloud research, the Atmospheric Sciences Division annually conducts the tri-service Cloud Impacts on DoD Operations and Systems (CIDOS) Conference where current cloud-impacts problems are posed and the results of the latest cloud research are given.

Rainfall Rate Modeling: The Air Force requires frequency distributions of 1-minute precipitation rates at locations throughout the world to determine design and operational requirements for many types of equipment. Precipitation, especially at heavier intensities, attenuates microwave signals used by Air Force systems in satellite detection and tracking, communications, air traffic control, reconnaissance, and weaponry. Erosion due to rain affects helicopter rotor blades, leading edges of aircraft and missiles, and fuses on airborne ordnance. Intense rainfall can cause jet engines to malfunction and can penetrate protective coverings on exposed electronic and mechanical material.

Attenuation due to rain is the major environmental cause of outages to extra-high-frequency satellite communication systems. Because of the paucity of data on 1-minute rain rates needed to estimate outages, a method was developed for extracting and digitizing 1-minute rain rates from original analog rain gauge recordings. The method employs modern digitizing and filtering techniques to obtain the 1-minute data that are ordinarily unreadable by eye. This was used to extract 1-minute rain rates over a 10-year period of record at forty-two locations in the United States chosen to represent worldwide rainfall regimes. The data were used to estimate potential out-

ages for satellite communication systems depending on radio frequency, power levels, and other considerations. Results can be used to design satellite communications to minimize the impact of rain attenuation.

Atmospheric Transport and Diffusion: The atmospheric transport and diffusion of toxic chemicals is of significant practical concern to the Air Force. Accidental chemical spills can occur anytime when storing or transporting chemicals. For emergency-response planning and operations, models are needed for predicting the hazard area resulting from a chemical spill. Several computer models were developed to handle gas and liquid releases over smooth and complex terrain. These models include AFTOX, a Gaussian puff-dispersion model; WADOCT, a complex terrain dispersion model; and ADAM, a heavy gas model.

AFTOX handles continuous and instantaneous releases, liquid and gas, elevated and surface, from a point or area source. This model and its documentation have been turned over to the Air Weather Service (AWS). The AWS has accepted the model as a replacement to its 25-year-old Ocean Breeze/Dry Gulch diffusion model. The WADOCT (Wind and Diffusion over Complex Terrain) model is a combination of AFTOX and a surface-layer wind flow model (AFWIND). In this model, the concentration contours are distorted by the wind field defined by the wind flow model. The ADAM (Air Force Dispersion Assessment Model) model was recently developed under contract. This model takes into account the various physical, chemical reaction, and thermodynamic phenomena that take place when the chemical is suddenly released to the atmosphere. The model is designed specifically for nitrogen tetroxide, chlorine, hydrogen sulfide, ammonia, sulfur dioxide, and phosgene. Both WADOCT

and ADAM are undergoing extensive testing and evaluation.

BATTLEFIELD WEATHER

The Battlefield Weather Observation and Forecast System (BWOFS) is an advanced development program that, when fielded, will eliminate critical shortfalls in tactical weather support to Air Force and Army operations. The objective of BWOFS is to develop methods to gather vital weather information and process it for use by battle staff planners and aircrews. It provides a key to optimizing force effectiveness during varying weather conditions. To meet this objective, GL divided the BWOFS into two components. The first component does the target-area data acquisition. The second component, called Tactical Decision Aids (TDA), applies the data using a series of algorithms which combine environmental data with target intelligence and weapon system characteristics to provide an electro-optical effects forecast.

Weather Data Within Battle Areas: As defined by the Military Airlift Command's Statement of Need (MAC SON 508-78 for Pre-Strike Surveillance/Reconnaissance System, or PRESSURS), the Air Force critically needs the ability to observe and collect weather data at points within uncontrolled or enemy-controlled battle areas and airspace. Data must be processed and transmitted for use in Tactical Air Force decision assistance at in-theatre weather facilities. Weather is a major factor in determining the success or failure of tactical air missions. Timely weather data, plus a knowledge of its effect on Air Force systems, is vital to the battle director in making tactical decisions. To accomplish this, these data must be provided to the in-theatre weather facilities in near real-time.

MAC SON 508-78 requires measure-

ments of cloud areal coverage (and the altitude of tops and bases), wind, temperature, pressure, humidity, path transmission, and contrast transmission. GL has developed a concept which involves the use of an enhanced satellite system complemented by unmanned air vehicles (UAVs). Weather satellite enhancements include improved ground-data processing, distribution, and display using new Mark IVB vans scheduled to support TAC/TAF field operations. The UAV will provide weather observations that cannot be obtained from a satellite, while the satellite will continue to provide critical gridded information which will be used to support TDA operation.

Full verification of the UAV concept began in 1987. A meteorological sensor package was developed and integrated, with processing equipment, into a pod for aircraft tests. Software was developed for transmitting the weather data to a ground receiving station and displaying it in a standard weather message format. Test results show the effect of increased speed on sensor performance, and the utility of a "roller-coaster" profile for reliable meteorological measurements.

Tactical Decision Aid Development: Air Weather Service Geophysical Requirement 9-73 (Forecasting Aids for Precision Guided Munitions) states a need for forecaster aids which will allow an estimate of maximum target detection and lock-on range based on known sensor target and environmental parameters. These aids, called Tactical Decision Aids (TDA), are being developed for use by battle staff planners and air crews to insure effective employment of precision-guided munitions (using infrared, television, laser, and millimeter wave-guidance systems) under battle-field conditions. Tactical Decision Aids were developed which can be used to predict the performance of 1.06 μm laser

designator, television, low-light-level television, and 8-12 μm infrared precision-guided munitions and target acquisition systems under a wide variety of environmental conditions.

A microcomputer version of these TDAs is now used by weather forecasters and decision makers in the field. The TDA has been successfully employed at a number of locations worldwide. It continues to be used for test and operational support on infrared systems. This version was developed specifically for the Zenith series of microcomputers which are used at base weather stations around the world. Updates of TDA capability are provided to Air Weather Service annually. The next update will include a physically correct Thermal Contrast Model, replacing the empirical model currently in use. This will allow the infrared TDA to be used to predict the appearance of complex high-value targets, and allow the user to "build" his or her own target by entering physical target specifications.

CLOUD PHYSICS

During the last two years there was a change in emphasis of the cloud modeling work within the division towards mesoscale forecasting, and with the transfer of key personnel, the cloud-microphysics modeling effort has all but terminated. In response to newly emerging requirements from the Air Force and NASA we have shifted our research into the prediction of both triggered and natural lightning as it pertains to aircraft and missiles.

Cloud Microphysics Modeling: The cloud microphysical model was improved by incorporating our empirically determined doubly truncated particle-size spectra. This gave better agreement between model results and data obtained from field studies. We participated in the second World Meteorological

Organization (WMO) workshop on cloud microphysical models. Our results on the blind cases were an improvement over the results of the previous workshop, and our model was one of the best performers in specifying and predicting the microphysics.

This model was successfully applied to some Air Force problems. In particular, it was used to define the small-scale wind regimes for two separate aircraft accidents, and was employed to investigate the deposition of soot in the atmosphere due to fire-storms created by nuclear bombs. This latter study focused on the effects of singular nuclear events and helped to point out the need to include intermediate scale interactions in the on-going debate on "nuclear winter."

The absorption and scattering of electromagnetic waves propagating through the atmosphere, aircraft icing, and nosecone erosion are each very dependent on the concentration and sizes of hydrometeors in the earth's atmosphere. The Smith-Feddis model was developed over two decades ago to provide information on hydrometeor type and particle size distributions using surface-based observations and satellite data. The model has been applied with mixed results over the years. We recognized that there were some deficiencies in the microphysical aspects of the model, but in our investigation into the model we found that the major difficulty was the large footprint of the satellite data which averaged or smoothed the data over hundreds of square kilometers. This smoothing makes the results not appropriate for many of the intended Air Force applications. On the other hand, high-resolution visual and infrared satellite data plus the addition in the future of weather radar data from satellites will provide the necessary resolution to satisfy Air Force needs through a complete revamp-

ing of the model when these data become routinely available in the future.

Mountain Thunderstorm Initiation: Our modeling efforts have shown that the lee side of mountain ranges is a fertile region for the initiation of thunderstorms, and that moisture, upper level winds, and the intensity of surface heating by the sun strongly control the ability of these regions to produce clouds. Satellite data over the Rocky Mountains were used to investigate thunderstorm initiation sites and to investigate thunderstorm prediction techniques. This was also done for an Air Force application to a Central American area, and it has possible application to other mountainous areas anywhere in the world.

Instrumentation and Techniques: To incorporate the distribution of hydrometeor particle size and concentrations in cloud microphysical models, it has been the practice to use simple mathematical approximations such as the Marshall-Palmer distribution. As the data became better and more accurate, we found that the aircraft data did not fit the radar data. Closer inspection revealed that there were fewer particles at both the large and the small ends of the size range in the aircraft data, so doubly truncated distributions were developed which were then successfully incorporated into the cloud microphysical models mentioned above.

A large amount of the meteorological microphysical data contains noise and needs to be smoothed. A technique for smoothing the data was developed by Berthel (1987). It has been used by others to smooth radar data and has been submitted through the Air Force for a patent.

A patent was allowed for the M-Meter, which is designed to measure the particulate mass content of hydrometeors, dust, and atomic debris that might be present in the atmosphere. Flight

tests showed it to be more sensitive than expected, and that it operates as a spectrometer since the mass of individual particles may be determined.

Measurement Support: Fast-response rain and snow-rate meters developed by the division were employed at the Otis ANGB site in the testing of equipment to be used in the Automatic Observing System (AOS), which is being designed by GL for Air Weather Service (AWS) for world-wide use.

Prediction of Triggered and Natural Lightning: The Air Force and NASA have become more interested in the prediction of both triggered and natural lightning since the loss of Atlas-Centaur 67 on March 26, 1987, due to lightning. GL hosted a joint GL/AWS/NASA Workshop on Triggered Lightning at Cape Canaveral AFS on February 17-19, 1988, to develop recommendations for the improvement of the forecasting of triggered lightning at the ranges and to develop an airborne field-mill test plan. A joint Air Force/NASA Steering Committee was set up which directed the utilization of the New Mexico instrumented aircraft in the collection of airborne field-mill data in September, October, and November, 1988, over Cape Canaveral. NASA is dedicating one of its Learjets to obtain airborne field-mill data in the future so as to reduce the hazards of lightning to missile operations at Cape Canaveral/Kennedy Space Center.

In an effort to improve the prediction of lightning, neural network back-propagation techniques are being applied to meteorological and lightning data from Cape Canaveral.

UPPER ATMOSPHERE SPECIFICATION (50-90 km)

Many Air Force systems operate in or through the upper atmosphere. These systems include high-altitude reconnais-

sance aircraft, missiles, military satellites, optical and infrared surveillance systems, radars and communications. Atmospheric conditions are particularly important for the launch and reentry of missiles, the launch of all satellites, the reentry of satellites such as the space shuttle, and the operation and reentry of the National Aerospace Plane. A number of technologies and systems in Project Forecast II, such as Hypersonic Aerothermodynamics, Hypersonic Vehicles and Weapons, and Full Spectrum Sensors, critically need precise specification of atmospheric properties for efficient design and effective operation. This requires investigating the phenomenology and developing climatologies and empirical and theoretical models. These products must specify mean values, systematic variations, and ranges of variability.

Models and Data: The Proceedings of the Workshop on Reference Atmospheres and Thermospheric Models (held as part of the COSPAR Meeting at Toulouse, France, in July, 1986) were edited and published in 1987 as part of a volume in the Journal *Advances in Space Research* entitled "The Earth's Middle and Upper Atmosphere." This publication contains data and empirical models of the middle atmosphere and thermosphere and theoretical thermosphere models. There is a discussion of the contribution of satellite temperature data to the development of middle atmosphere models and a determination of the variability of atmospheric properties obtained from analysis of rocketsonde data. Analysis of the Meteorological Rocket Network temperature and wind data yielded the amplitudes and phases of their annual and semiannual variations. A new set of reference ozone models is included, and one paper showed a 6K temperature increase at an altitude of 24 km as a result of increased heating due to dust injected

into the atmosphere by the El Chicon volcanic eruption.

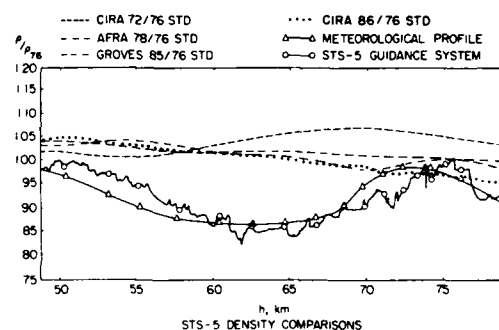
A unique set of data obtained from instruments on-board space shuttles was analyzed and compared with models developed by GL. In a number of flights, large density changes and fluctuations were observed above 70 km altitude. Analysis of wind data from the Global Radar Network yielded mean zonal and meridional winds for altitudes from 75 to 110 km. Important differences were found between these winds and geostrophic winds derived from rocket and satellite data. There are two probable causes of the differences: one is due to differences in the sampling times and the other is a geostrophic component, such as that due to gravity-wave momentum deposition.

The final section of the publication covers thermospheric models and data. A comprehensive theoretical general circulation thermospheric model is included, followed by an empirical model (MSIS) based on analysis of satellite mass spectrometer and radar incoherent-scatter data. A number of papers present results of measurements of thermospheric temperatures and winds using different techniques, including satellite in-situ measurements, satellite optical remote sensing and ground-based optical and incoherent scatter measurements. Other papers include effects in the thermosphere due to turbopause height variations and magnetic storms.

GL contractor G. Groves continued his development of middle atmosphere models with a new report entitled "Modeling of Atmospheric Structure, 70-130 km." In this report a formulation is presented for modeling neutral atmosphere structure in an intermediate height region between given lower and upper models of temperature, pressure, density, and composition to maintain continuity in the second derivative of temperature and the

other properties with respect to altitude. The method is well suited to linking lower and upper atmospheric models that have analytical representations. The parameters given in the report match the Groves 1985 models at 70 km and the MSIS 86 models at 130 km. Tables are presented for diurnal and zonal mean properties for mid-month dates and two values each of solar and geomagnetic activity. The agreement between models and data is, in general, good but mid-latitude incoherent scatter temperature data are, on average, higher than the models. This discrepancy may be due to limitations in the models or to the temperature values being anomalously high due to heating by precipitating particles.

An extensive analysis was made of density data derived from on-board accelerometers during the reentry of twelve space shuttles. The data were compared with several models (see the figure) and were analyzed to investigate



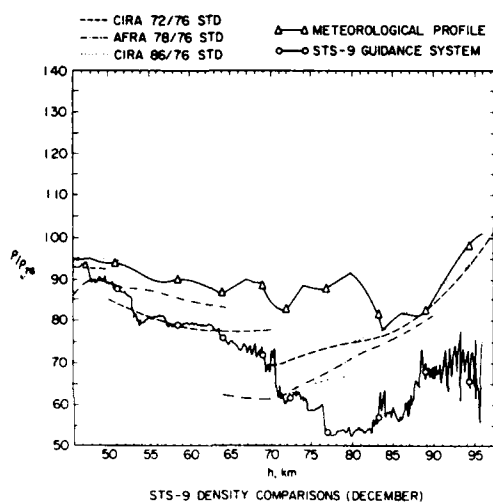
Ratio of Density from Drag on STS-5 During Reentry to the U.S. Standard 76, the Meteorological Profile and the CIRA 72, AF Reference Atmospheres (AFRA) 78, Groves 85, and Tentative CIRA 86 Models.

systematic variations with season and latitude. The orbital inclinations of all the flights except one were low- to mid-latitude. The one exception was STS9 with an orbital inclination of 57°. The

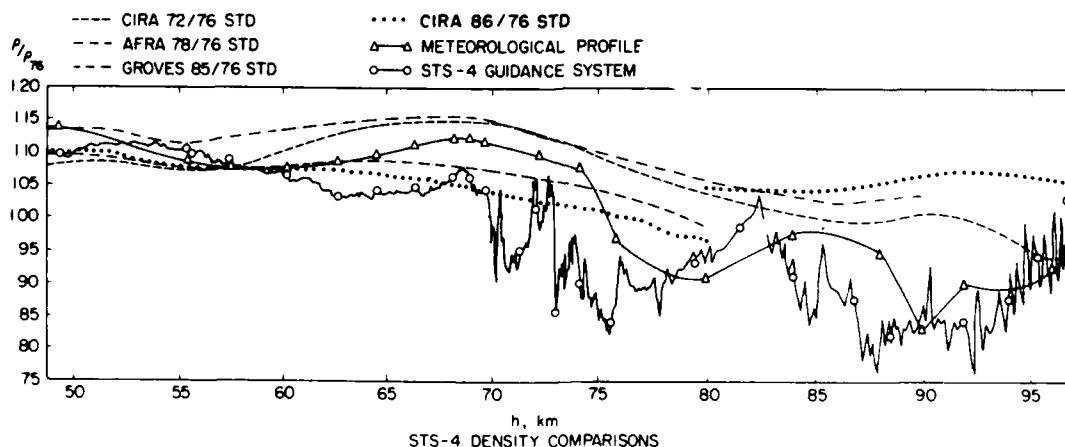
data from this flight in the altitude range 46-73 km agree well with model predictions of variation with latitude (40° - 60°) for December, as shown in the accompanying figure. At higher altitudes near Alaska the data are 12 to 24 percent below the models. The reason for this could be that the data show the

effects of high-latitude particle precipitation, auroral activity, or a high-latitude low atmosphere storm. The low- to mid-latitude flights provide information at altitudes near 70-90 km that can be used to improve the summer/winter models given in the U.S. Standard Atmosphere Supplements 1966 and also develop separate models for spring and autumn.

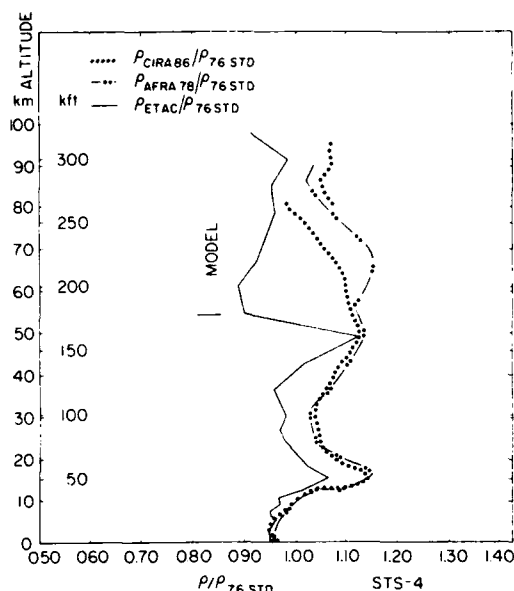
The data from STS4 exhibit unusual properties (see the figure). This spacecraft reentered at low latitudes over the central Pacific Ocean on July 4, 1982. They exhibit large-scale fluctuations from the highest altitude of the data (97 km) down to below 70 km. This is unique among the data sets considered. Satellite cloud photographs over the Pacific Ocean at the time of reentry show extensive areas of heavy cumulus underneath and near the satellite trajectory. A vertical profile of density in the accompanying figure (derived from analysis fields and remote temperature soundings), cloud layers, and atmospheric moisture obtained from NOAA and ETAC confirm the conclusion of heavy convective activity producing gravity waves in the upper atmosphere. The effect of shuttle flights through the upper mesosphere is much



Ratios of Density for the Reentry of STS-9. (The models, starting from the left of the figure, are, with increasing altitude, for latitudes of 40° , 50° , and 60° .)



Ratios of Density for the Reentry of STS-4 Showing Large Scale Fluctuations at All Altitudes above 70 km.



Synthetic Density Profile and Models for the Time of STS-4 Over-pass at 27°N, 170°W. (Above this location, the satellite was at an altitude of 76 km. Note the minimum in the density at this altitude in the preceding figure.)

more marked than had been expected.

Erosion During Reentry: Erosion due to hydrometeors (water droplets, snow, ice) and excessive dust in the lower and middle atmosphere is a major problem to all vehicles that pass through these regions of the atmosphere with hypervelocity. The vehicles include reentry vehicles from missiles and space vehicles, such as the National Aerospace Plane. Research has been done to develop a more comprehensive and accurate algorithm to compute the amount of erosion of the surface of particular vehicles traveling with specified trajectories through atmospheric regions containing particles. The performance of the new algorithm has been compared with that of existing algorithms by computing the erosion produced by each algorithm for a number of specified hydrometeor profiles. There is a wide spread of results predicted by the various algorithms. Research will contin-

ue to further improve the algorithms and compare the predictions with actual data where they are available.

PUBLICATIONS 1987-1988

CHAMPION, K.S.W. (AFGL); and ROEMER, M. (Univ. of Bonn, FRG), editors
Chapter 2 - Reference Atmospheres and Thermosphere Models
Adv. Space Res. 7 (1987)

D'ENTREMONT, R.P., and THOMASON, L.W.
Interpreting Meteorological Satellite Images Using a Color-Composite Technique
Bull. Am. Meteor. Soc. 68 (1987)

D'ENTREMONT, R.P., THOMASON, L.W., and BUNTING, J.T.
Color-Composite Image Processing for Multispectral Meteorological Satellite Data
Proc. SPIE Digital Image Processing and Visual Communications Tech. in Meteor. (27-28 October 1987)

DYER, R.
Expert Systems in Weather Forecasting and Other Meteorological Applications
AI Applications in Natural Resource Management Winter (1987)
Summary Report on the Second Workshop on Artificial Intelligence in the Environmental Sciences (AIRIES) 15-17 September 1987, Boulder, CO
Bull. Am. Meteor. Soc. 69 (1988)

MCCLATCHY, R.A.
A Review of Statistical Models of the Temperature and Gaseous Components
Bull. Am. Meteor. Soc. 69 (1988)

METCALF, J.I.

A New Slant on the Distribution and Measurement of Hydrometeor Canting Angles

J. Atmos. and Oceanic Tech. 5 (1988)

Panel Report on Technology of Polarization Diversity Radars for Meteorology

Proc. 40th An. Conf. on Radar Meteor. (1988)

The "Middle Ages" of Polarization Diversity Research

Proc. of Battan Mem. and 40th An. Conf. on Radar Meteor. (1988)

NORQUIST, D.C.

Alternate Forms of Humidity Information in Global Data Assimilation

Monthly Weather Review 116 (1988)

SCHAAF, C.B., BANTA, R.M. (AFGL); and WURMAN, J. (Ophir Corp., Denver, CO)

Thunderstorm-Producing Terrain Features

Bull. Am. Meteor. Soc. 69 (1988)

SNOW, J.W. (AFGL); and TOMLINSON, E.M. (Air Weather Service, Los Angeles AFS, CA)

Cloud Population Measurements Using Photographs Taken From the Space Shuttle

Proc. Sixth Symp. on Meteorological Observations and Instrumentation (12-16 January 1987)

TATTELMAN, P.

Analyses of One-Min Rainfall Rates Extracted From Weighing Raingage Recordings

J. Applied Meteor. 27 (1988)

TATTELMAN, P., KANTOR, A.J. (AFGL); and WILLAND, J.H. (Systems and Applied Sciences Corp., Lexington, MA)

Model Profiles of Temperature and Density Based on Extremes at Selected Altitudes

AIAA J. 26 (1988)

YANG, C.H.

Global NWP Modeling for 1-4 Day Cloud Forecasting

Res. Activities in Atmos. and Oceanic Modeling (1987)

YEE, S.Y.K.

The Force-Restore Method Revisited

Boundary-Layer Meteor. 43 (1988)

PRESENTATIONS

1987-1988

ANGUS, P.J.

Short-Term Prediction of Thunderstorm Probability and Intensity by Screening

Observation and Derived Predictors

15th Conf. on Severe Local Storms, Baltimore, MD (22-26 February 1988)

BANTA, R.M.

Cumulus and Thunderstorm Initiation by Mountains

Symp. on Mesoscale Analysis and

Forecasting Incorporating Nowcasting, 19th

Gen. Assembly, IUGG, Vancouver, BC (17-19 August 1987)

BANTA, R.M., and PANTLEY, K.C., CAPT

Simulations of Daytime Mountain Upslope Circulations as Precursors to Cumulus Development

4th Conf. on Mountain Meteorology, Seattle, WA (25-28 August 1987)

Simulations of the Daytime Mountain Boundary Layer with Cumulus Cloud Initiation

8th Symp. on Turbulence and Diffusion, Monterey, CA (April 1988)

Numerical Simulations of the 20 July, 1986 MIST Cumulonimbus

Second Internat. Cloud Modelling Wkshp., Toulouse, France (8-12 August 1988)

BANTA, R.M., PANTLEY, K.C., GAPT

(AFGL); and Cannon, P.T., Sr. (Lyndon State Coll., Lyndonville, VT)

Soil Moisture and Ridge Height Effects on

Katabatic Flow Simulations

4th Conf. on Mountain Meteorology, Seattle, WA (25-28 August 1987)

BANTA, R.M., PANTLEY, K.C., CAPT, BERTHEL, R.O., and PLANK, V.G.

Parameterized Microphysics Based on a Truncated Exponential Distribution: Warm-Rain Simulations

10th Internat. Cloud Physics Conf., Bad Homburg, FRG (15-20 August 1988)

BARNES, A.A., JR.

The AFGL Weather Attenuation Program
Natl. Radio Sci. Mtg., Boulder, CO (12-15 January 1987)

EHF Attenuation Through the Melting Layer

10th Internat. Cloud Physics Conf., Bad Homburg, FRG (15-20 August 1988)

BOHNE, A.R.

Extrapolative Forecasting of Precipitation and Cloud Fields

Conf. on Mesoscale Precipitation: Analysis, Simulation, Forecasting, Boston, MA (14-16 September 1988)

BROWN, H.A.

Lightning Detection for An Air Force Automated Observation System

AGU Mtg., Baltimore, MD (18-22 May, 1987)

CHAMPION, K.S.W.

Middle Atmosphere Density Data and CIRA 1986;

AIAA Aerospace Sci. Mtg., Reno, NV (15 January 1987)

Middle Atmosphere Density Data and Comparison with Models

COSPAR Mtg., Espoo, Finland (18-29 July 1988)

CHISHOLM, D.A.

Arctic Meteorology Working Group Report; Atmospheric Models

Wkshp. on Arctic Environmental Sciences, The John Hopkins Univ., Laurel, MD (27-30 January 1987)

D'ENTREMONT, R.P.

Color-Composite Meteorological Satellite Image Processing

SPIE Digital Image Processing and Visual Communications Technologies in Meteorology, Cambridge, MA (25-30 October 1987).

D'ENTREMONT, R.P., BUNTING, J.T., FELDE, G.W., and THOMASON, L.W.

Improved Cloud Analysis Using Visible, Near-Infrared, and Microwave Imagery

Internat. Geoscience and Remote Sensing Symp., Ann Arbor, MI (18-21 May 1987)

DYER, R.M.

The Adaptability of Expert Systems in Meteorology

4th Internat. Conf. on Interactive Information and Processing Systems for Meteorology, Oceanography and Hydrology, Anaheim, CA

(31 January - 5 February 1988)

Enhancing the Adaptability of Expert Systems

Resource Technology 88, Fort Collins, CO (20-23 June 1988)

Between Phototype and Deployment: Lessons Learned Field-Testing an Expert System

Symp. on Artificial. Intelligence Research for Exploitation of the Battleground Environment, El Paso, TX (14-18 November 1988)

FALCONE, V.J., JR.

The DMSP Microwave Suite

Passive Microwave Observing from Environmental Satellites, Williamsburg, VA (1-4 June 1987)

FALCONE, V.J., JR., MORRISSEY, J.F., JACOBS, L.P., and HOAR, R.C.

Ground Based Infrared Temperature Profiling

Internat. Wkshp. on Remote Sensing Retrieval Methods, Williamsburg, VA (15-18 December 1987)

FELDE, G.W., and CONANT, R.W. JR.
*Status Report On the Special Sensor
 Microwave Imager Cloud Amount
 Validation*
 Natl. Radio Sci. Mtg., Boulder, CO (5-8
 January 1988)

FELDE, G.W., BUNTING, J.T., and HARDY,
 K.R.
*Atmospheric Remote Sensing in Arctic
 Regions*
 DoD Symp. and Wkshp. on Arctic and Arctic-
 Related Environmental Sciences., The John
 Hopkins Univ., Laurel, MD (27-30 January
 1987)

GRIFFIN, M.K. (AFGL); and LIU, J.-N.
 (Univ. of Utah, Salt Lake City, UT)
Clouds and the Surface Radiation Budget
 Internat. Radiation Symp., Lille, France (18-
 24 August 1988)

HARDY, K.R.
*Some Atmospheric Features Observed by
 Radars and Satellites*
 Symp. on Meteorology and Oceanography,
 Ann Arbor, MI (20-21 May 1988)

HARDY, K.R. (AFGL); and Gage, K.S.
 (NOAA, Boulder, CO)
*The History of Radar Studies of the Clear
 Atmosphere*
 40th An. Conf. on Radar Meteorology, Boston,
 MA (9-13 November 1987)

KING, J.I.F.
*The Remote Inference of Temperature and
 Transmittance from Space: The Exact
 Solution*
 Internat. Wkshp. on Remote Sensing
 Retrieval Methods, Williamsburg, VA (15-18
 November 1987)

KLEESPIES, T.J.
*Temporal Display of Meteorological Satellite
 Imagery of a Static Full Color Display
 System*
 Digital Image Processing and Visual

Communications Technologies in
 Meteorology, Cambridge, MA (25-30 October
 1987)

4th Internat. Conf. on Interactive
 Information and Processing Systems for
 Meteor. and Hydrology, Anaheim, CA (31
 January-5 February 1988)
*Multispectral Image Display Techniques
 Applied to Meteorological Satellite Imagery*
 3rd Internat. Satellite Direct Broadcast
 Services User's Conf., Baltimore, MD (20-24
 June 1988)

KLEESPIES, T.J. (AFGL); and McMILLAN,
 L.M. (NOAA/NESDIS, Washington, DC)
*An Extension of the Split Window Technique
 for the Retrieval of Precipitable Water:
 Experimental Verification*
 Internat. Wkshp. on Remote Sensing
 Retrieval Methods, Williamsburg, VA (15-18
 December 1987);
 3rd Internat. Satellite Meteor. and
 Oceanography Conf., Anaheim, CA (31
 January-5 February 1988)
*Determination of Precipitable Water with the
 AVHRR*
 4th Internat. TOVS Study Conf., Igls, Austria
 (16-22 March 1988)

KLEESPIES, T.J. (AFGL); and POPHAM,
 R.W. (NOAA/NESDIS, Washington, DC)
*Status Report On the NOAA/NESDIS
 Electronic Bulletin Board*
 4th Internat. TOVS Study Conf., Igls, Austria
 (16-22 March 1988)

KLEESPIES, T.J., D'ENTREMONT, R.P.,
 FELDE, G.W., HARDY, K.R., THOMASON,
 L.W. (AFGL), GUSTAFSON, G.B., and
 IVALDI, C.F., JR. (AER, Cambridge, MA)
*Application of the AFGL Interactive
 Meteorological System to Atmospheric
 Research*

3rd Internat. Conf. on Interactive
 Information and Processing Systems for
 Meteorology, Oceanography and Hydrology,
 New Orleans, LA (12-16 January 1987)

KUNKEL, B.A.

Evaluation of the AFGL Toxic Chemical Dispersion Model (AFTOX)

5th Annual Chemical Modeling Conf.,
Aberdeen Proving Ground, MD (25-26 August 1987)

A Review and Current Status of the USAF Toxic Chemical Dispersion Model (AFTOX)

JANNAF Safety and Environmental
Protection Subcommittee Mtg., Monterey, CA
(23-27 May 1988)

MCCLATCHEY R.A.

The Air Force Perspective in Remote Sensing of Meteorological Parameters

Internat. Wkshp. on Remote Sensing
Retrieval Methods' Williamsburg, VA (15-18
December 1987)

METCALF, J.I.

Meteorological Applications of Radar

IEEE Lecture Series Microwave Remote
Sensing, Weston, MA (2-3 June 1988)

Design Considerations for Polarimetric Radars to Measure Backscatter from Hydrometeors

1988 Polarimetric Technology Wkshp., Red-
stone Arsenal, AL (16-18 August 1988)

Polarization Differential Reflectivity of Lightning

24th Conf. on Radar Meteorology,
Tallahassee, FL (27-31 March 1989)

METCALF, J.I., and GLOVER, K.M.

A History of Weather Radar Research in the U.S. Air Force

40th Anniversary Conf. on Radar
Meteorology, Boston, MA (9-13 November
1987)

MITCHELL, K.E.

Low-Level Systematic Cooling Tendencies Due to the Nonuniform Vertical Resolution Used With Modern PBL Parametrizations

8th Conf. on Numerical Weather Prediction,
Baltimore, MD (February 1988)

MODICA, G.D.

The Impact on Short-Term Precipitation Forecast Skill of Time-Dependent Lateral and Lower Boundary Conditions Within A Meso-Beta Numerical Prediction Model

Symp. on Mesoscale Analysis and
Forecasting Incorporating Nowcasting, 19th
Gen. Assembly, IUGG, Vancouver, BC (17-19
August 1987)

NORQUIST, D.C. (AFGL); and NEHRKORN,
T. (Atmospheric and Environmental
Research, Cambridge, MA)

Exploring the Use of Cloud Analyses to Infer Humidity Profiles for Use in Data Assimilation

National Storm Program Tech. Wkshp. on
Regional Data Assimilation, Arlington, VA (5-
9 October 1987)

NORQUIST, D.C., YANG, CHIEN-HSUNG,
and MITCHELL, K.E.

Interaction Between the Deep Convection and Boundary Layer Schemes in the AFGL Global Spectral Model and its Impact on the Long-term Heat and Moisture Budgets
CAS/JSC Working Group on Numerical
Experimentation, Toronto, Canada (19-23
September 1988)

PLANK, V.G.

The M-Meter (Particulate Mass Sensor and Spectrometer)

2nd Airborne Sci. Wkshp., Miami, FL (3-6
February 1987)

An Airborne Instrument for Measuring the Mass Content and Mass Distribution of Atmospheric Dust Particles

Dust Symp. III, The Johns Hopkins Univ.,
Laurel, MD (23-25 June 1987)

RAJ, P.K., MORRIS, J.A. (Technology and
Management Systems, Inc., Burlington,
MA); and KUNKEL, B.A. (AFGL)

A Propellant and Chemical Spill and Dispersion Model

JANNAF Safety and Environmental
Protection Subcommittee Mtg., Monterey, CA
(23-27 May 1988)

RUGGIERO, F.H. (AFGL); and DONALDSON, R.J. (STX, Lexington, MA)

Wind Field Derivatives: A New Diagnostic Tool for Analyses of Hurricanes by a Single Doppler Radar

17th Conf. on Hurricanes and Tropical Meteorology
Miami, FL (7-10 April 1987)

SADOSKI, P.A., LT, BOHNE, A.R. (AFGL), and HARRIS, F.I. (STX, Lexington, MA)

The AFGL Remote Atmospheric Processing and Interactive Display (RAPID) System

4th Conf. on Interactive Information and Processing Systems for Meteorology, and Hydrology, Anaheim, CA (31 January - 5 February 1988)

TATTELMAN, P.

How To Use MIL-STD-210C To Determine Climatic Design Requirements

33rd Annual Mtg. of the Institute of Environmental Sciences, San Jose, CA (4-8 May 1987)

Interpreting Climatic Information for Designing Military Equipment

26th (AIAA) Aerospace Sciences Mtg., Reno, NV (11-14 January 1988)

Rainfall Rates and Drop-Size Distributions for Environmental Testing

34th Annual Tech Mtg., of the Institute of Environmental Sciences, King of Prussia, PA (2-6 May 1988)

THOMASON, L.W.

Temperature Retrieval By Maximum Entropy Estimation

Internat. Geoscience and Remote Sensing Symp., Ann Arbor, MI (18-21 May 1987)

YANG, C.H., et al

The Impact of New Physical Parameterization Schemes of A Global NWP Model

8th Conf. on Numerical Weather Prediction, Baltimore, MD (February 1988)

YEE, S.Y.K., and MODICA, G.D.

An Analytical Soil Thermodynamic Model for the Diurnal Variation of Ground Surface Temperature

3rd Conf. on Mesoscale Processes, Vancouver, BC (21-26 August 1987)

TECHNICAL REPORTS 1987-1988

BERTHEL, R.O.

A Computer Decision-Making Process for the Elimination of Noise From Data

AFGL-TR-87-0118 (27 March 1987).
ADA185745

BERTHEL, R.O., BANTA, R.M., and PLANK, V.G.

The Application of Doubly-Truncated Hydrometeor Distributions to Numerical Cloud Models

AFGL-TR-87-0050 (9 February 1987).
ADA185273

D'ENTREMONT, R.P., and KLEEPSIES, T.J.
Possible Measurement Errors in Calibrated AVHRR Data

AFGL-TR-88-0105 (1 April 1988).
ADA198342

FELDE, G.W.

Capabilities and Limitations of Estimating Cloud Amount From the Special Sensor Microwave Imager

AFGL-TR-87-0249 (16 April 1987).
ADA195842

KUNKEL, B.A.

User's Guide for the Air Force Toxic Chemical Dispersion Model (AFTOX)

AFGL-TR-88-0009 (4 January 1988).
ADA199096

LANICCI, J.M., CAPT (AFGL); and WARD, J.M. (SASC Technologies, Inc., Lexington, MA)

A Prototype Windflow Modeling System for Tactical Weather Support Operations
AFGL-TR-87-0159 (7 May 1987), ADA189362

METCALF, J.I., ARMSTRONG, G.M., and BISHOP, A.W.
A Polarization Diversity Meteorological Radar System
AFGL-TR-87-0105 (19 March 1987),
ADA189291

MORRISEY, J.F., IZUMI, Y., and COTE, O.R.
Microwave Refractive Index Structure Function Profiles (C_n^2) Measured From A Small Aircraft
AFGL-TR-87-0080 (5 March 1987),
ADA184343

SADOSKI, P.A. (AFGL); EGERTON, D., HARRIS, F.I. (ST Systems Corp., Lexington, MA); and BOHNE, A.R. (AFGL)
The Remote Atmosphere Probing Information Display (RAPID) System
AFGL-TR-88-0036 (15 January 1988),
ADA196314

TATTELMAN, P.
MIL-STD-210C, Climatic Information to Determine Design and Test Requirements for Military Systems and Equipment
AMSC F2302 (9 January 1987)

TATTELMAN, P. (AFGL); KNIGHT, R.W. (National Climatic Data Center, Asheville, NC); and SCHARR, K.G. (Bedford Research Associates, Bedford, MA)
Estimates of Satellite EHF Communication Outages Due to Attenuation by Rain
AFGL-TR-87-0081 (5 March 1987),
ADA183969

YEE, S.Y.K., and JACKSON, A.J.
Blending of Surface and Rawinsonde Data in Mesoscale Objective Analysis
AFGL-TR-88-0144 (14 June 1988),
ADA203984

CONTRACTOR TECHNICAL REPORTS 1987-1988

BISWAS, K.R., and HOBBS, P.V. (Univ. of Washington, Seattle, WA)
Preliminary Evaluations of the Use of a 35 GHz Radar for Measuring Cloud Base and Cloud Top Heights
AFGL-TR-88-0098 (6 June 1988),
ADA199133

COTTON, W.R., and TRIPOLI, G.J. (Colorado State Univ., Collins, CO)
Cloud/Mesoscale Model Development and Application Studies
AFGL-TR-87-0219 (30 September 1987),
ADA199592

DAVIS, L.G., and LAWSON, R.P. (Colorado Intl. Corp., Boulder, CO)
Research and Development to Acquire and Reduce Melting Layer Cloud Physics and Evaluate a Prototype M-Meter
AFGL-TR-87-0161 (May 1987), ADA188390

GERLACH, A.M. (SASC Technologies, Inc., Lexington, MA)
Objective Analysis and Prediction Techniques - Final Report
AFGL-TR-87-0013 (30 November 1986),
ADA183450
Objective Nephology
AFGL-TR-88-0109 (15 April 1988),
ADA200500

GRIFFIN, M.K., LIOU, K.N., and KOENIG, G. (Univ. of Utah, Salt Lake City, UT)
Cloud Climatology Derived from AFGWC 3D-Nephanalysis for January and July 1979
AFGL-TR-87-0122 (15 January 1987),
ADA183086

GROVES, G.V. (Univ. of London, UK)
Modeling of Atmospheric Structure, 70-130 km
AFGL-TR-87-0226 (July 1987), ADA201077

HOFFMAN, R.N. (Atmospheric and Environmental Research, Inc., Cambridge, MA)

Documentation of the AFGL Statistical Analysis Program (ASAP) for the Global Multivariate Analysis of Heights and Winds
AFGL-TR-87-0155 (December 1986),
ADA182600

HOFFMAN, R.N., ISAACS, R.G., and GRASSOTTI, C. (Atmospheric and Environmental Research, Inc., Cambridge, MA)

A Study of Satellite Emission Computed Tomography
AFGL-TR-87-0321 (15 September 1987),
ADA189567

HOHLFELD, R.G. (Creative Optics, Inc., Bedford, MA); WACHTMANN, R. F. (ST Systems Corp., Lexington, MA); and KILIAN J.C. (Creative Optics, Inc., Bedford, MA)

Application and Evaluation of a Differential Inversion Technique for Remote Temperature Sensing
AFGL-TR-88-0138 (30 June 1988),
ADA199155

ISAACS, R.G. (Atmospheric and Environmental Research, Inc., Cambridge, MA)

Review of 183 GHz Moisture Profile Retrieval Studies
AFGL-TR-87-0127 (15 April 1987),
ADA182417

JASPERSON, W.H., and VENNE, D.E. (Control Data Corp., Minneapolis, MN)
A Single-Station Weather Forecasting Expert System
AFGL-TR-87-0194 (August 1987),
ADA184889

LEIBOVICH, S., LUMLEY, J.L., and HUNT, J.C.R. (Flow Analysis Assoc., Ithaca, NY)
Heat and Moisture Transport in the Atmospheric Boundary Layer

AFGL-TR-87-0011 (5 January 1987),
ADA184222

LIU, K.-N., and OU, S.-C. (Univ. of Utah, Salt Lake City, UT)

Remote Sounding of Atmospheric Temperature Profiles Using the Differential Inversion Method
AFGL-TR-88-0152 (15 June 1988),
ADA199896

LORENZ, E.N. (Massachusetts Inst. of Tech., Cambridge, MA)

Climate Sensitivity and Long-Period Temperature Fluctuations
AFGL-TR-87-0124 (March 1987), ADA183540

LOUIS, J.F., HOFFMAN, R.N., NEHRKORN, T., BALDWIN, T., and MIKELSON, M. (Atmospheric and Environmental Research, Inc., Cambridge, MA)

Baseline Observing System Experiments Using the AFGL Global Data Assimilation System
AFGL-TR-87-0327 (18 November 1987),
ADA188861

MAHRT, L.J., PAN, H.L., RUSCHER, P.H., and CHU, C.T. (Oregon St. Univ., Corvallis, OR)

Boundary Layer Parameterization for a Global Spectral Model
AFGL-TR-87-0246 (17 August 1987),
ADA199440

RAJ, P.K., and MORRIS, J.A. (Technology & Management Systems, Inc., Burlington, MA)

Source Characterization and Heavy Gas Dispersion Models for Reactive Chemicals
AFGL-TR-88-0003 (I) (18 December 1987),
ADA200121

A Users Manual for ADAM (Air Force Dispersion Assessment Model)
AFGL-TR-88-0003 (II) (18 December 1987)
ADA192209

RASMUSSEN, G., JANOTA, P. (The Analytic Sciences Corp., Reading, MA); FERRARO, R. (Research and Data Systems Corp., Lanham, MD)

Evaluation of the AFGL Cloud Simulation Model

AFGL-TR-88-0116 (October 1987),
ADA203542

RAYMOND, W.H., and STULL, R.B. (Univ. of Wisconsin, Madison, WI)

CAT Forecasting Using Transient Turbulence Theory

AFGL-TR-88-0106 (20 February 1988),
ADA198768

SCHWARTZ, D., and BURNHAM, D. (U.S. Dept of Transportation, Cambridge, MA)

Otis ANGB Visibility Sensor Field Test Study

AFGL-TR-86-0011 (February 1987),
ADA179176

SEITTER, K.L. (Univ. of Lowell, Lowell, MA)

The Specification of Lateral Boundary Conditions in Three-Dimensional Mesoscale

Numerical Models

AFGL-TR-87-0015 (21 January 1987),
ADA179185

SELLERS, A.H., and HUGHES, N.A. (Univ. of Liverpool, UK)

Cloud Archiving Strategies

AFGL-TR-84-0166 (2 April 1984),
ADA180269

STUNDER, M.J., KOCH, R.C., SLETTEN, T.N. and LEE, S.M. (GEOMET Technologies, Inc., Germantown, MD)

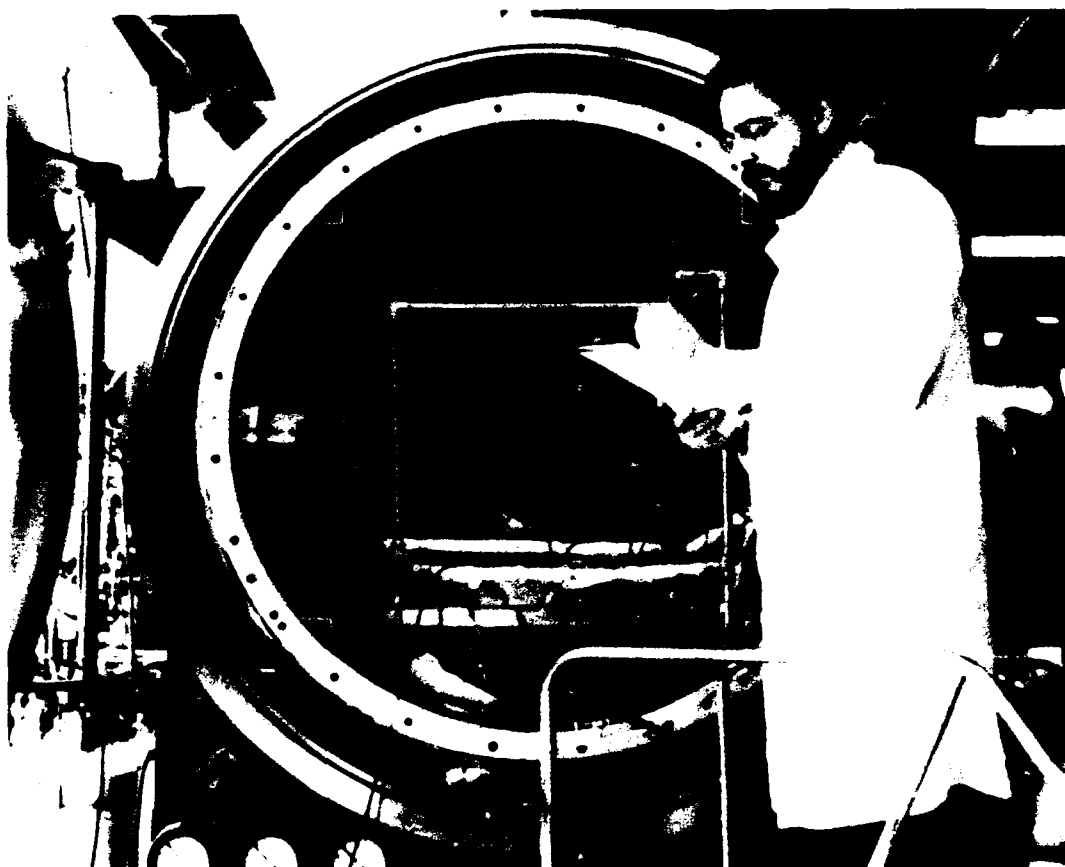
ZEUS: A Knowledge-Based Expert System that Assists in Predicting Visibility at Airbases

AFGL-TR-87-0019 (15 January 1987),
ADA184137

VOLFSON, L.B., PEET, C., and GAUTIER, C. (Chase Consulting, Inc., San Diego, CA)

Initial Processing of Space Shuttle Cloud Photographs

AFGL-TR-87-0181 (28 March 1987),
ADA183543



COCHISE (Cold Chemi-Excited Infrared Simulation Experiment) at GL. COCHISE is a unique, cryogenic, ultra-sensitive simulation chamber used to characterize atomic and molecular processes which produce IR backgrounds in the upper atmosphere. The data from COCHISE evaluates how well IR surveillance and tracking systems will perform their missions.

V OPTICS AND INFRARED TECHNOLOGY DIVISION

The Optics and Infrared Technology Division conducts basic and advanced research in all the regimes which impact the performance of Air Force electro-optical systems. A blending of field tests, laboratory studies, and theory supports the goal of developing "tools" to be used directly in the design, testing, and operation of Air Force and DoD electro-optical systems. These tools include various databases, models, and computer codes which enable system developers to fully understand the environment in which their sensors must operate.

A large number of Air Force programs rely on electro-optical sensors operating in the spectral region between the ultraviolet and long wave infrared (LWIR) bands. No matter where these sensors are based (ground, air, or space), they rely on electromagnetic radiation propagating from the target through the intervening atmosphere to the sensors which collect both the desired radiation and unwanted background radiation. Improving the ratio of the signal to the noise is a constant challenge to system designers.

Ground and airborne sensors and laser systems are particularly influenced by the transmission characteristics of the atmosphere. Propagation can be degraded by the absorption and scattering of

radiation by aerosols and molecules, which reduce the intensity of radiation and target contrast and by turbulence and scattering, which cause distortion, false movement, and blurring of either the image or a transmitted laser beam.

The ultimate performance of all sensors may be dictated by the reception of unwanted radiation. This may be naturally occurring phenomena, such as the scattering of solar radiation and the excitation of molecules with subsequent emission of radiation, leading to earth-limb and celestial background radiation, or it may be man-made such as excitation of molecules due to a nuclear detonation.

Radiation from a target also plays a critical role in signal-to-background ratios. A primary emphasis in the Division has been on infrared signatures of aircraft in flight. However, work is also being done on missile and rocket plumes and some satellite emissions.

The high performance demands on emerging Air Force systems require a thorough understanding of the propagation path, the target emissions, and the nature of the extraneous radiation in the sensor field of view. The mission of this Division is to understand the optical phenomena and to make the information available to system users in a straightforward and timely manner.

Because transmission, emission, and background radiation are often interrelated, the following discussion is organized by the methods of investigation rather than by discipline: ground and airborne experiments, rocket and satellite experiments, laboratory research, and computer codes and databases.

GROUND AND AIRBORNE EXPERIMENTS

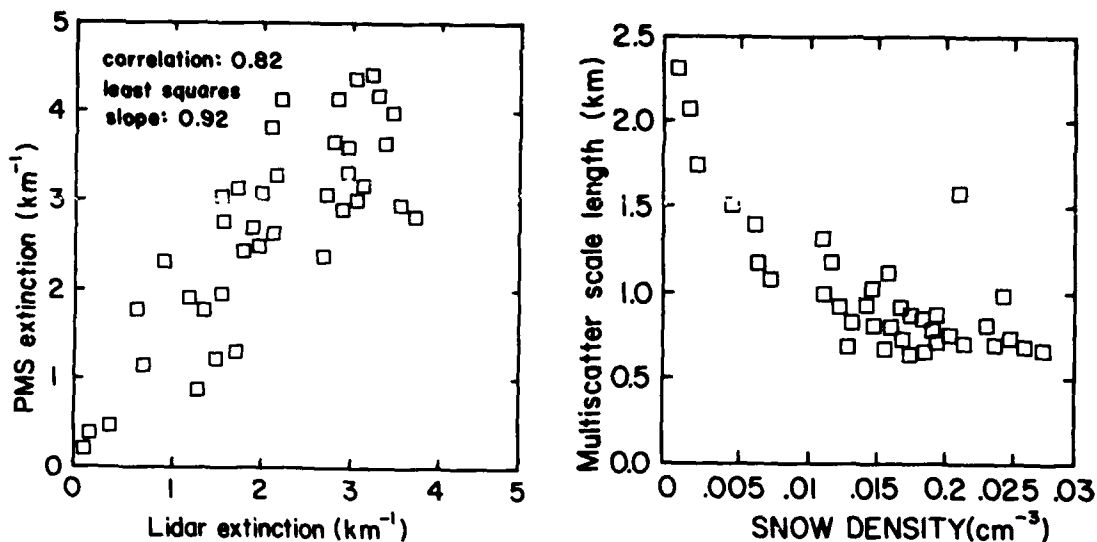
Lidar Measurement of Aerosols: Currently there is considerable concern about the influence of large temporal increases in the concentration of aerosols from indus-

trial activity and slash-and-burn agriculture on the earth's radiative balance and climate. Volcanic aerosols, which spread globally in the lower stratosphere, also influence the general radiative balance and introduce additional optical extinction at these altitudes. To investigate these problems and, at the same time, to provide a flexible mechanism for responding quickly to unplanned data needs, a mobile optical/infrared laboratory has been constructed which consists of two trailers housing a variety of optical instrumentation controlled by microcomputer systems.

High-resolution spatial and temporal profiles of aerosol and cloud backscatter and the intensities of the polarization components are measured at a wavelength of 0.532 μm using a Neodymium:YAG laser radar system mounted in the roof of one trailer. The laser radar, or lidar, backscatter profiles are analytically inverted using the far boundary solution of the lidar equation to yield range-resolved information on the optical extinction coefficient. Measurements of the polarization components can be used to determine the Stokes parameters and differentiate degrees of beam depolarization associated with single or with multiple scattering.

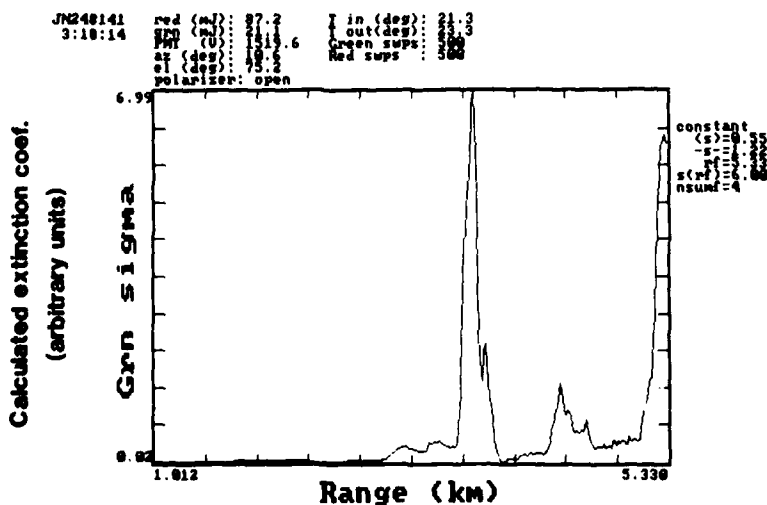
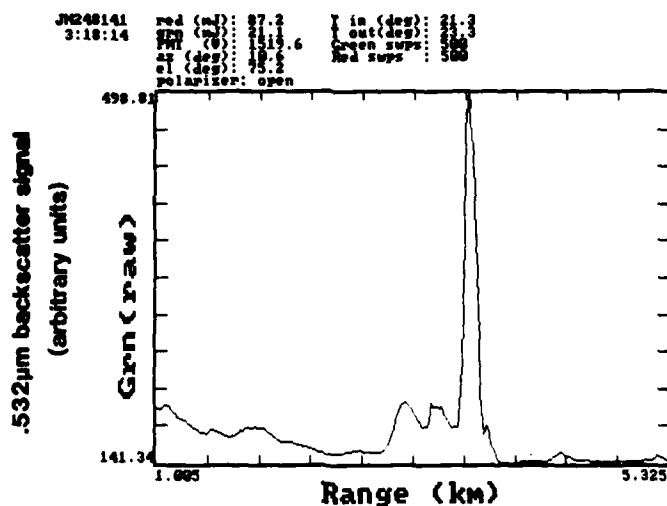
Aerosol, raindrop, and snow-flake particle-size distributions and total concentrations are determined with particle-sensing probes and size spectrometers. Angular scattering properties of these particulates are measured with nephelometers operating at both visible and infrared wavelengths. GL has also developed optical transmissometers having a relative spectral resolution of 6 percent in the 0.55 μm , 3 to 5 μm and 8 to 14 μm ranges.

A series of snow measurements were made in the winter of 1987/88 using the lidar system, a visible transmissometer, a snow nephelometer, and a raindrop



Extinction Coefficient for Snow Calculated from Size Distributions and Concentrations. (Particle Measurement System). (It correlated well with the extinction coefficient determined from lidar measurements.)

Multi-Scatter Scale Length Obtained from Lidar Depolarization as Function of Snow Density. (Multi-scatter scale length information is usable to remotely determine snow density.)

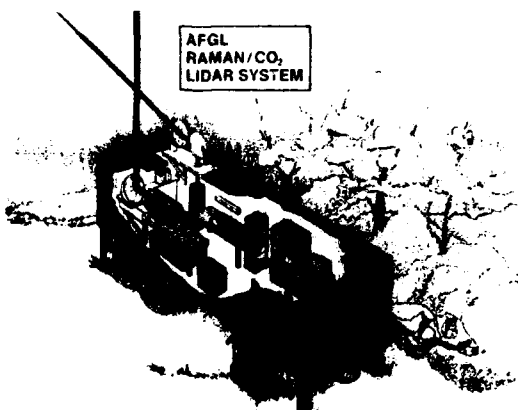


Typical 0.532 μm Lidar Backscatter from a Cloud and the Derived Extinction Coefficient.

spectrometer. The optical extinction coefficient, averaged over a 1 km path, resulting from the inversion of the lidar data correlated well with the extinction coefficient obtained from the raindrop spectrometer. In addition, the multiple scatter scale length obtained from the lidar depolarization information was found to be a function of snow density. From this result it appears that the scale length information can be used to determine the particulate density of snow by remote means.

During the early summer of 1988, the trailer was moved to Dripping Spring, NM, to participate in the CONUS II field program, where numerous clear-air and cloud backscatter returns were obtained with the Nd:YAG lidar.

An important problem of recent interest relates to the optical properties of thin and subvisual cirrus clouds and their effects on such sensor systems as the Infrared Search and Track System.



New Mobile Lidar System Containing CO₂ Coherent Lidar and Raman Lidar using an Excimer Lidar.

Recent up-grades to the trailer instrumentation which improve detection sensitivity will lead to a better understanding of these thin clouds with unusual optical properties.

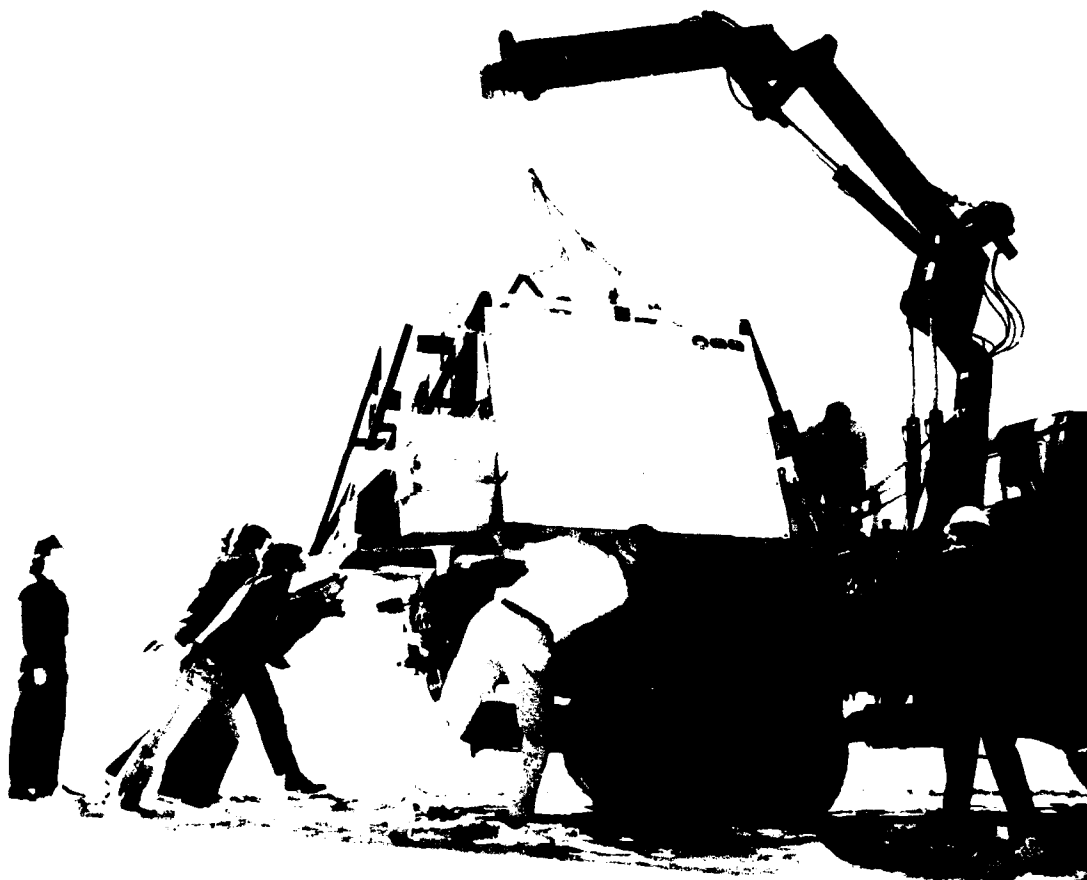
Airborne Lidar: The GL program also includes the use of lidar instrumentation sited in aircraft and balloons with a long-term goal of placing equivalent systems in space. The straightforward approach of measuring backscattered radiation, and the more complex variants of this approach using molecular absorption, or the spectral shifts introduced by particle motions, provide information on: aerosol concentrations and optical extinction; the presence and concentration of minor species such as water vapor, carbon dioxide, and ozone; and the magnitude and direction of atmospheric wind fields. From lidar systems positioned in space, all these optical and meteorological parameters become available on a global scale, with spatial resolution and accuracy superior to present methods.

The presence of particulates in the atmosphere is key to the lidar technique, most particularly at the longer wavelengths where molecular scattering is insignificant. With a goal of developing space-based systems for global sampling of atmospheric properties, it becomes important to know how aerosols are distributed worldwide and whether their concentrations in unpopulated or non-industrialized areas are sufficient to provide the necessary scattering medium required for the lidar measurements. To investigate this issue, GL has undertaken a measurement program to determine aerosol scattering profiles as a function of altitude and geographic location, using airborne and balloonborne lidar sensors and the previously discussed ground-based system.

The use of high-altitude balloons is a relatively inexpensive way to carry instrumentation to altitudes in the lower stratosphere and simulate, at least in part, operation in a spacelike environment. For lidar, this gives the investigator the opportunity to look down at the earth from a point outside the major por-

tion of the scattering atmosphere with a lidar orientation much like that to be experienced in space. The laboratory's ABLE (Atmospheric Balloonborne Lidar

and which radiates at $1.064\text{ }\mu\text{m}$, $0.532\text{ }\mu\text{m}$, and $0.3547\text{ }\mu\text{m}$. On the first two flights, only direct backscatter signals were measured, which allowed separa-



GL Balloonborne Lidar Recovery Operations at White Sands Missile Range.

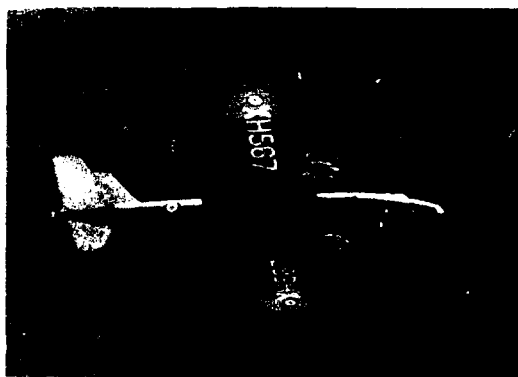
Experiment) payload has been flown three times: August, 1984; September, 1987; and September, 1988: it reached altitudes between 75,000 and 110,000 ft for several hours on each occasion.

The ABLE lidar is based on a Neodymium:YAG laser transmitter which operates at the fundamental, and at the doubled and tripled frequencies,

tion of the molecular and aerosol contributions to the total backscatter signal. On the third flight, additional detectors were added for three wavelengths appropriate for Raman-shifted emissions of water vapor, carbon dioxide, and nitrogen. The latter provided an accurate route to overall calibration of the lidar system. Auxiliary instrumentation has

consisted of dropsondes, low-light level television cameras, and magnetic heading sensors. The data from the fall of 1988 are now in analysis. All three balloon flights were carried out in the vicinity of White Sands Missile Range in southern New Mexico.

In October and November, 1988, a series of measurements were made at Ascension Island, an isolated region of the South Atlantic eight degrees south of the equator. This experimental program was a joint venture with the Royal

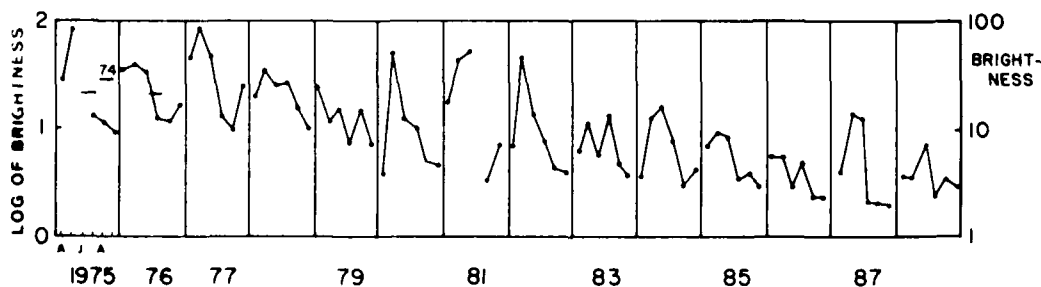


Canberra B-57 Bomber Used in Ascension Island Measurement Program.

Signals and Radar Establishment (RSRE) of the United Kingdom. A Canberra B-57 bomber supplied by RSRE was used to measure particulate backscatter at $10.6 \mu\text{m}$ with a CO_2 lidar

mounted in the bomb bay of the aircraft in a forward-looking orientation. The aircraft flew a number of sorties to altitudes of 50,000 ft and over ranges out to 600 mi. The data indicated a highly variable backscatter profile at altitudes above the marine boundary layer up to approximately 45,000 ft, where very strong backscatter returns were occasionally observed from regions where no cirrus clouds were seen or identified in satellite-derived imagery. During the three-week field campaign, distinct differences were noted in the scattering properties of the air masses which moved over the island from different points of the compass. Additional field operations are planned, combining extensive ground-based instrumentation and other atmospheric probes to augment the aircraft measurements.

Aerosol Particles: The presence of large aerosol particles (5 to over $100 \mu\text{m}$) is important in the production of rain by warm clouds, in the propagation of high-power laser beams, and in the measurement of wind by Doppler-shifted lidar returns. Local observations of the strong scattering of solar radiation at small angles by large aerosols have been made since 1975. Typically, the monthly averages show a maximum in the springtime caused by abundant tree pollen, which, due to preferred particle size, is recognizable by colored aureoles. However, dur-



Monthly Averages (April to September) of the Logarithm of the Brightness of the Solar Aureole due to Giant Aerosol Particles Since 1975. (The usual spring maximum is mainly caused by tree pollen.)

ing the last 10 years there has been a significant decrease in the average column load by large particles. The column load detected by the aureole measurements is now about an order of magnitude lower than it used to be. The most likely reason for the change is a reduction in the number and size of giant dust particles available for dispersion in the atmosphere, and efforts are now underway to obtain insights into the nature, origin, and concentration of these big particles near the ground.

Turbulence: The most important parameter used in the description of atmospheric optical turbulence is the index of refraction structure constant, C_n^2 . System design criteria are in turn defined by parameters deduced from C_n^2 . Some of the limitations imposed by C_n^2 can be partially or fully overcome by compensating imaging techniques and adaptive optics. The work at GL has been in the areas of measurement, modeling, and analysis of atmospheric C_n^2 , its derivative parameters, and the resulting effects on systems.

The thermosonde provides unique capabilities for making in situ turbulence measurements from the ground to altitudes of 30 km with high spatial resolution. The relatively low cost thermosonde consists of micro-thermal, fine-wire thermometry instrumentation packaged with a standard radiosonde and carried aloft by a balloon. It has provided most of our turbulence data. As the 6 ft diameter balloon ascends, the atmospheric temperature is sampled simultaneously at two points 1 m apart. The difference in temperature is detected, filtered, and amplified by a sensitive Wheatstone bridge and synchronous detector circuit. Radio transmission of the differential temperature measurement, along with other meteorological variables, is broadcast by the sonde. A ground-based computer converts the sig-

nals into C_n^2 and stores the data as a function of altitude.

Measurements have been performed for a range of goals, including site characterization, field support for other groups and agencies, and basic atmospheric research. Collaborative efforts have been undertaken with the Army Atmospheric Sciences Laboratory, NASA, NOAA, the Air Force Weapons Laboratory, and a number of universities. Two joint efforts recently took place: one at Cape Cod with NASA using the Goddard Space Flight Center's ground-based Raman lidar system and the second with GL's ABLE balloonborne lidar. The high-resolution lidar measurements of water vapor and aerosols were compared with the thermosonde turbulence and meteorological data, shedding some light on the turbulence induced mixing and layering of the atmosphere and on the temporal behavior of such layers.

Further site characterization work has been done at the Air Force Malabar Optical Station in Florida in collaboration with personnel from the Weapons Laboratory to generate the primary database for optical turbulence at this site.

An experimental program to compare turbulence, radar, and optical measurements at a site far from mountains and general orographic features was carried out at Flatlands, IL, with NOAA, university, and Army personnel. The specific purpose was to characterize the narrow layers, or pancakes, of large horizontal extent in which turbulence is found to occur in the free atmosphere. (For applications, see "Computer Codes and Databases" below.)

Horizontal scintillometers have been used to characterize turbulence along a fixed path near the ground. Using two, orthogonally arrayed scintillometers, together with anemometers and ground-based thermosonde units, we have

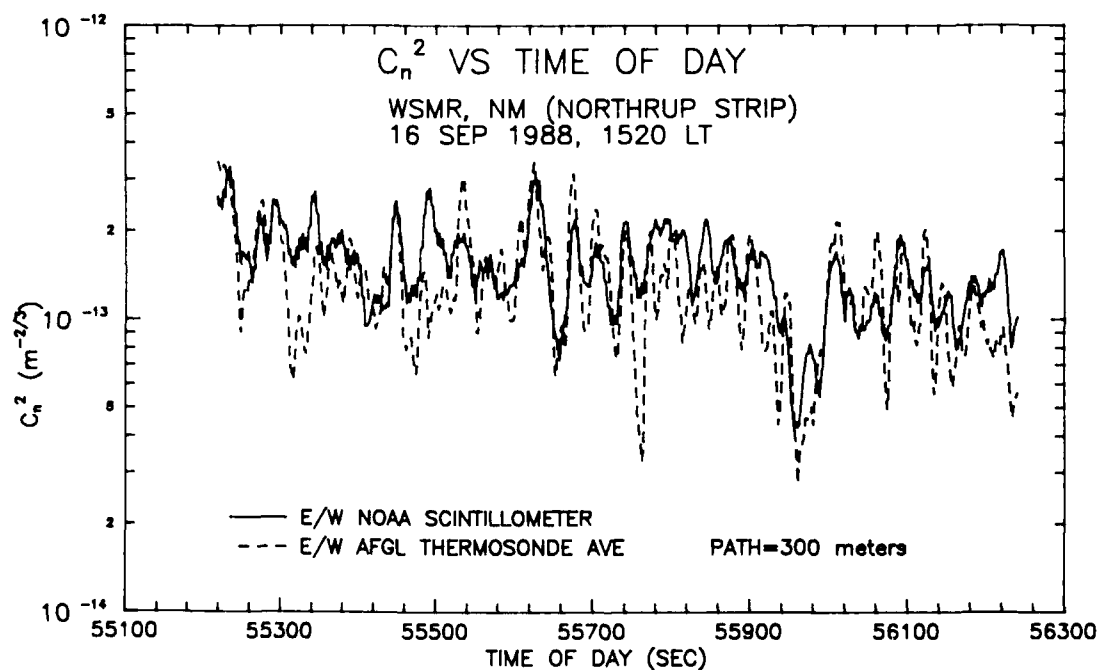


Instrumentation for Horizontal Turbulence Measurements at White Sands Missile Range.

defined the horizontal homogeneity of the turbulence and assessed the time and spatial scales over which turbulence persists. Data of this type were acquired over a two-week period in September, 1988, at White Sands Missile Range.

MAPSTAR: The mesosphere contains airglow layers at 85 km, 90 km, and 95 km composed of emitting species. The thicknesses of these layers vary and are on the order of several kilometers each. These airglow layers have structures which exhibit large ranges of temporal and spatial frequencies. They are usually undetectable by the unaided eye but can easily be detected by optical sensors. Such structures can represent sources of optical clutter, which impose operational constraints on infrared and other optical surveillance systems.

The purpose of the MAPSTAR program (Middle Atmosphere Periodic Structure Associated Radiance) is to obtain an



Typical Index of Refraction Structure Constant Agreement Between Two Different Measurement Techniques; One Direct, One Indirect.



Periodic Variations in Mesospheric Airglow Layers Observed in Summer, 1988, in Colorado. (The most probable cause of these variations appears to be atmospheric acoustic gravity waves.)

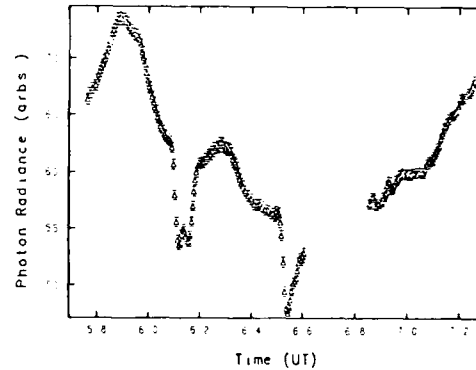
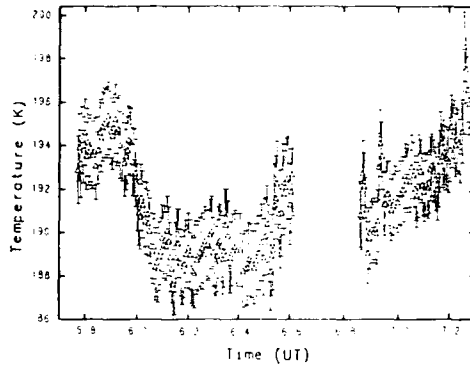
enhanced theoretical and experimental understanding of these periodic structures and to arrive at predictive models and codes for the presence of such clutter.

The most probable cause of periodic variations in the mesospheric layers presently appears to be atmospheric acoustic gravity waves (AGW's) and possibly "billow turbulence" events created by the breakdown of AGW's. These waves have periods ranging from over 8 h to as short as 4-5 min. Turbulent eddies could theoretically have durations as short as 3 sec and wavelengths of about 1 m. The most likely sources of AGW's (away from auroral latitudes) are tropospheric weather phenomena such as thunderstorms, weather-front effects (e.g., jet streams and associated shear-induced turbulence structures) and "mountain waves" generated by winds going over mountains. Less likely sources include earthquakes, nuclear

explosions, ocean waves (tsunamis), atmospheric tidal interactions, and auroral heating effects.

Acoustic gravity waves can affect the temperature of the airglow-emitting species by compressions and expansions due to induced changes in altitude and by direct wave-compression effects. These temperature changes, in turn, affect the rate of the chemical reactions responsible for the radiance. At the same time, the AGW induces changes in density (i.e., number of emitters per unit volume), which also contributes to changes in brightness. Although infrared radiance from OH Meinel bands, which are responsible for the chemical reactions $H + O_3 \rightarrow OH^* + O_2$ and $O + H_2O \rightarrow OH^* + O_2$, occurs at wavelengths that are absorbed in the lower atmosphere, overtone OH emissions at shorter wavelengths are very easily measured by ground-based optical instruments.

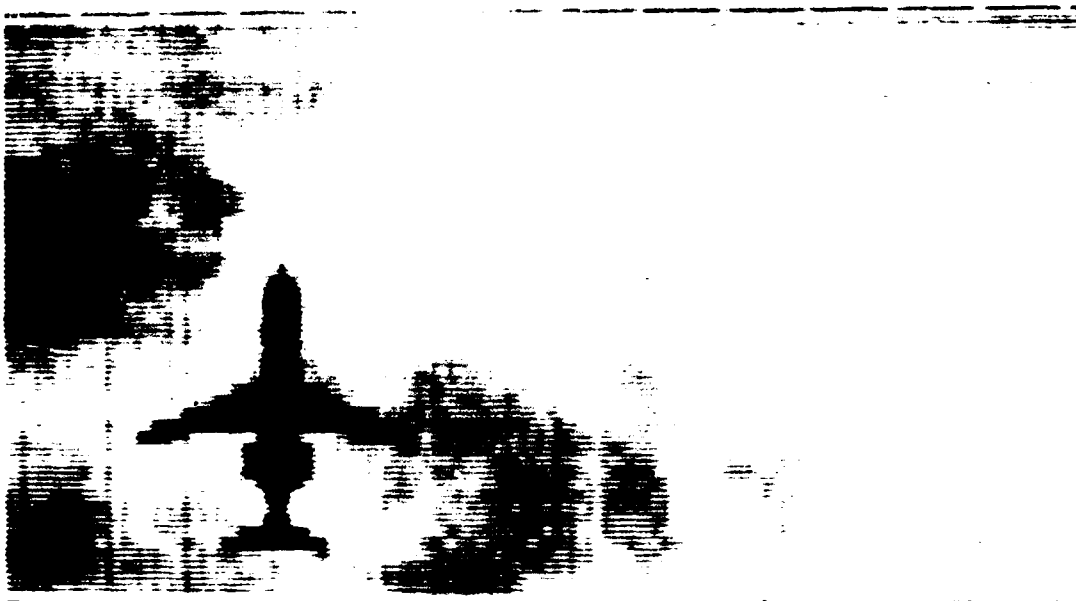
The MAPSTAR program office com-



Temperature and Intensity for OH Radiation Airglow. (Major decreases in radiation are attributed to intervening clouds which would decrease the radiance but not the measured temperature.)

pleted a field campaign in the summer (May, June, July) of 1988 in Colorado. The two mountain-based imaging observatories at Estes Park and the INSTITUTE for Arctic and Alpine Research (INSTAAR) (altitudes of approximately 10,000 ft) were oriented to produce stereo images of airglow located over the Eastern Colorado Agricultural Research

Center station. This gave an elevation angle of $20^\circ - 30^\circ$ for 85 km airglow as seen from these mountain observatories. The resulting images benefited from the contrast-enhancing van Rhijn effect. The INSTAAR site included the infrared field-widened interferometer boresighted to a fixed point in the video imager's field of view. Temperatures and intensi-



Infrared Image of Cold Aircraft at High Altitude Viewed Against Warm Earth Background.

ties from the OH radiation obtained from the interferometer indicate that the temperature profile is generally followed by the intensity.

The experimental information from the Colorado field campaign will be applied to broad scientific questions about AGW's, including: the "universal power spectrum theory" of AGW's, AGW source locations, the presence of mountain waves in airglow, and possibly the explanation of why there are relatively rare occasions when the airglow structures can be perceived directly by the unaided human eye (i.e., "bright nights"). This occurred near the end of the campaign and seemed to be associated with the large numbers of thunderstorms in the region.

Infrared Aircraft (FISTA): The Flying Infrared Signatures Technology Aircraft (FISTA) is a comprehensive laboratory for inflight research and measurement on the infrared phenomenology of targets and backgrounds. Radiometers, interferometers, spectrometers, and a variety of spatial mappers that produce TV-like images of infrared emissions collect spectral intensities and thermal images.

The aircraft's range of more than 5000 mi permits worldwide deployment. Its ability to fly at altitudes above 40,000 ft allows infrared scientists to study the environment from near sea level to well above obscuring clouds and above nearly all atmospheric water vapor. This aircraft is a reliable platform for the study of geographic, seasonal, and diurnal variations of the sky, clouds, and earth. The flights are frequently associated with rocket launches and other test aircraft flights from which infrared properties are measured. In recent years, a large part of the measurement capability has been employed to understand the inflight infrared characteristics of aircraft. Unique measurements of the infrared radiation of the boost phase of missile

launches have also been obtained from the FISTA. The important role that the surrounding environment of the land, sea, and atmosphere plays in influencing target infrared behavior, or "signature," is determined in detail. The data obtained are used to develop new models that can simulate infrared behavior and to validate and test specific theoretical and laboratory-based models.

As infrared technology has made large advances in recent years, the need for understanding the behavior and appearance of targets at high spatial resolutions and from long measurement ranges has become important. New complex infrared mosaic and scanning sensors introduce a whole new class of problems to be solved so that these instruments can be used successfully in weapon seekers, surveillance systems, and for intelligence gathering by remote sensing. The FISTA provides an important platform from which to test new sensor concepts and to obtain detailed infrared images of targets and backgrounds so that new systems can achieve their development goals.

The aircraft has a variety of unique instrumentation. Five Michelson interferometers provide high-resolution spectral data. These instruments, when



Tracking an Aircraft in the Infrared on Board the FISTA Aircraft with a Schottky Barrier Array Imager.

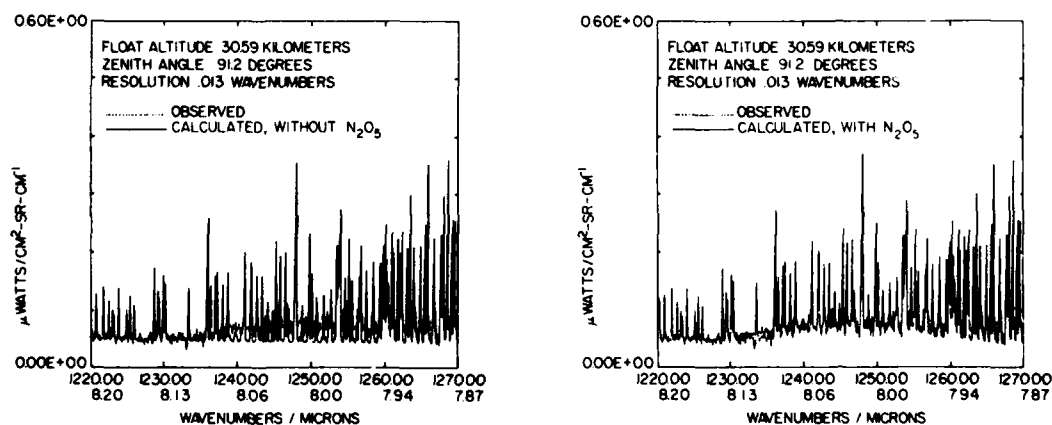
mounted in a special "eyeball" window, can look out the side of the aircraft over a wide range of angles. A gold-coated periscope mirror can be inserted through the eyeball into the ambient airstream, allowing viewing in any direction simply by rotation of the periscope. This combination of mounts permits a target to be viewed anywhere in the hemisphere to the right side of the aircraft.

Two different kinds of thermal-imaging scanners are available to be operated simultaneously with the spectral-measuring interferometers. The imaging systems produce TV-like images from the infrared radiation in the 2.5 to 14 μm spectral region. One system uses an array of 18 HgCdTe detectors to provide spatial data in a scene and to resolve temperature differentials of less than 0.1 $^{\circ}\text{C}$. When mounted behind 7 in. aperture optics, the sidelooking system has a spatial resolution of better than 0.3 mrad. This system will soon be replaced with a new system cooled to low temperatures and with a linear array of 180 HgCdTe detectors. The second system uses a Schottky barrier PtSi mosaic array with more than 30,000 detector elements that has been specially developed for the aircraft. It is sensitive in the 2.5 to 5.0 μm region and will be extended to cover the

1.4 to 5.5 μm region. These systems provide absolutely calibrated radiometric imagery in the infrared.

The airborne infrared measurements program collects large amounts of data from a variety of backgrounds and targets. Spectral and spatial data have been collected from desert, urban, cultivated, forested, mountain, snow, cloud and water backgrounds. Special flights have been used to measure the scattering and transmission of clouds when viewed from above, below, and through a variety of cloud types. Flights have been made over selected terrain throughout the day to determine the diurnal variation of its infrared characteristics. A wide variety of targets has also been measured. More than thirty types of aircraft have been measured over power settings from idle to maximum thrust and between altitudes from 500 ft to 40,000 ft. Industrial sites, tanks, and ships have also been measured from various flight altitudes.

SCRIBE: The SCRIBE (Stratospheric CRYogenic Interferometer Balloon Experiment) instrument is a balloon-launched, Michelson interferometer cooled by liquid nitrogen. It can remain at float altitude in the stratosphere for up to 12 h. The instrument is particularly suited for the study of the diurnal



Spectral Data from SCRIBE Flight Compared with Calculation.

variation of atmospheric molecules. The instrument has had several successful engineering and scientific flights prior to the 1987-1988 time period.

The SCRIBE interferometer is presently configured specifically to determine the presence and diurnal variation of the trace molecule dinitrogen pentoxide. This molecule is of great interest as a daytime source and nighttime sink for nitrogen dioxide and nitrogen trioxide, which participate in atmospheric ozone chemistry. Preliminary analysis of flight data revealed the broad-band spectral signature of dinitrogen pentoxide. This discovery is particularly significant because the data were collected at mid-morning, a time when theoretical calculations suggest that most of the nitrogen pentoxide should have been photodissociated. Another SCRIBE flight is planned for June, 1989, to confirm the findings and to determine a vertical profile.

Solar Flux: Analysis of balloonborne direct observations of solar ultraviolet irradiance has continued in conjunction with the Ionospheric Physics Division. A "top of the atmosphere" solar flux at 0.1 nm resolution has been derived and compared with atmospherically uncontaminated rocket and satellite measurements. The agreement was generally excellent, within 5 to 12 percent over the wavelength range from 200.0 - 310.0 nm. This comparison established the ability to correctly extrapolate from within the atmosphere through both the strongly absorbing ozone layer and the large amounts of molecular oxygen. At 40 km, ozone absorbs almost 97 percent of the solar energy at 255.0 nm while O₂ and O₃ combine equally to deplete over 50 percent at 200.0 nm. This physical description has been incorporated into both LOWTRAN7 and FASCOD3 (discussed below), validating their extension to 200.0 nm.

ROCKET AND SATELLITE EXPERIMENTS

SPIRIT I: The SPIRIT I (SPatial/SPectral Infrared Rocketborne Interferometric Telescope) experiment, launched on April 8, 1986, was a rocketborne probe designed to measure the long-wavelength infrared emission spectra from a bright (IBC class III) aurora above the earth's limb. The primary instrument was a cryogenically cooled, five-detector Michelson interferometer mated to a cooled telescope with high off-axis-rejection capabilities. Approximately 140 spectral scans (covering 450 - 2500 wavenumbers, 4 to 22 μm), were recorded for tangent heights ranging from 40 to 225 km. Most of the scans were rapid scans with resolution on the order of 10 wavenumbers, but there were 17 slower scans with resolution of 1 wavenumber. The spectra provide a comprehensive database on a number of molecular emission features in the nighttime sky, including CO₂ (15 μm), O₃ (9.6 μm) and NO (5.3 μm).

The primary observations from analysis of the spectral limb radiance data for the CO₂, O₃, and NO emissions obtained in the SPIRIT I rocket experiment are:

1. The CO₂ radiance agrees with previous experiments to within a factor of two.
2. The O₃ radiance below 95 km also agrees with other previous nighttime measurements to within a factor of two. However, above 95 km tangent height, the O₃ radiance measured by SPIRIT I is significantly lower than previous observations and the current earthlimb radiance model.
3. No aurorally produced effects are apparent in either the CO₂ or the O₃ bands. This result is in sharp contrast to the observations made during the HIRIS experiment (flown in 1976 from the same launch site) in which dramatic auroral enhancements were reported for both bands. This result has led to a recent

reexamination of the HIRIS observations, which yields an alternative interpretation attributing the high radiance values observed during the HIRIS earth-limb scans to off-axis-leakage effects. This explanation brings the HIRIS results into close agreement with SPIRIT I and other previous measurements.

4. SPIRIT I data on ozone hot bands ($10 - 12.5 \mu\text{m}$) represents a significant improvement over previous data. The observed spectral structure due to partially resolved bands has resulted in important revisions to the spectroscopic and kinetic parameters of ozone, which in turn has led to a significant update to the atmospheric radiance model in the $10 - 12.5 \mu\text{m}$ window region, where previous versions were seriously underpredicting the radiance in the long-wavelength side ($11 - 12.5 \mu\text{m}$) of the window. The fraction of energy in these hot bands (that due to the $\text{O}_2 + \text{O} + \text{M}=\text{O}_3 + \text{M}$ mechanism) relative to the fundamental band ($9.6 \mu\text{m}$) is a factor of two lower than that measured by the SPIRE (non-auroral) experiment. This may reflect a lower concentration of atomic oxygen relative to the atmosphere measured by SPIRE.

5. SPIRIT I measured significantly less radiance from nitric oxide ($5.3 \mu\text{m}$) than previous high-latitude observations; for example, a factor of 3 to 7 smaller than SPIRE observations.

6. Nitric oxide hot bands associated with the auroral $\text{N}(^2\text{D}) + \text{O}_2$ mechanism are somewhat difficult to discern. It is estimated that they comprise at most 10 percent of the total $5.3 \mu\text{m}$ NO emission seen by SPIRIT I above 120 km. This estimate is within the range of previous auroral observations.

SPIRIT II: SPIRIT II (SPatial/SPectral Infrared Rocketborne Interferometric Telescope) is a high-resolution infrared experiment which will measure the spatial and spectral structure of the high-

latitude atmosphere during intense geomagnetic storm conditions.

The SPIRIT II payload will be launched to an apogee of approximately 260 km on an Aries booster from Poker Flat Research Range, Alaska, during the October 1991-April, 1992, launch window. The prime infrared sensors, a Michelson interferometer covering the spectral region from 4 to $25 \mu\text{m}$ with a spectral resolution of 1-2 wavenumbers and a filtered radiometer having six spectral bands, will simultaneously collect spectral and spatial data on the upper atmosphere at tangent heights from 60 to 160 km. Both sensors share the field of view of a cryogenically cooled, high off-axis-rejection telescope necessary to allow measurement of the upper atmosphere in the presence of upwelling radiation from the lower atmosphere and the earth. The interferometer will sample fields of view a few kilometers square at the 100 km tangent point (at a range of 1500 km), while the radiometer will simultaneously measure atmospheric clutter with a spatial resolution of 100 m by 240 m. The interferometer focal plane consists of six detectors and four filters. The radiometer focal plane consists of six arrays of fifty detectors, each of which has been filtered for nitric oxide ($5.3 \mu\text{m}$), ozone ($9.6 \mu\text{m}$), carbon dioxide ($15 \mu\text{m}$) and three atmospheric window bands. Secondary sensors provide real-time information on the pointing of the payload, and a joystick uplink will permit the program scientist to update the orientation of the payload in flight.

SPIRIT II will collect approximately 390 seconds of data that will provide infrared databases on the spatial and spectral characteristics of long wavelength infrared clutter, altitude profiles of infrared radiation species, and definition of atmospheric infrared windows. Analyses of these databases will be used to refine predictive infrared atmospheric



Drop Body Being Prepared for Test of SPIRIT II Recovery System at Air Force Flight Test Center, Edwards AFB, CA, by Parachute Test Branch. (The drop body was released three times at an altitude of 15,000 ft from an MC-130 aircraft. The tests simulated conditions much worse than anticipated. All tests were successful.)

radiance codes.

CIRRIS 1A: CIRRIS 1A (Cryogenic InfraRed Radiance Instrumentation for Shuttle) is a high-sensitivity, shuttle-borne infrared sensor system consisting of a Michelson interferometer for high-spectral-resolution measurements (one wavenumber) of the earth's atmosphere from 2.5 to 25 μm and a dual focal-plane radiometer with selectable bandpass filters for spatial measurements. The interferometer and radiometer share the collection optics of a high off-axis rejection telescope necessary to prevent spurious radiation from the lower atmosphere and



CIRRIS 1A, a shuttle-borne infrared sensor system to collect data on the Earth's climate.

the earth from interfering with the experimental measurements. The optics, detectors, and detector preamplifiers are cooled to a few degrees Kelvin to maximize the sensitivity of the sensor system to the faint infrared emissions in the earthlimb.

Earthlimb data collection is executed by means of several measurement modes, including vertical and horizontal scans and staring modes in conjunction with various interferometer, radiometer, and filter combinations. A mid-latitude earthlimb scan, for example, may consist of a pre-programmed sequence during which the sensor gimbals will step the sensor system through a sequence of tangent heights to provide atmospheric radiance profiles. Observation of auroral events will be performed as opportunities permit. For these measurements, the on-board payload specialist will interrupt the pre-programmed measurement program to focus on the auroral region of interest.

During the week-long shuttle mission, the CIRRI IA sensor system will accumulate a global database on the spatial and spectral characteristics of the earth's atmosphere which will allow atmospheric modelers to validate and upgrade the codes currently used to predict infrared atmospheric radiance and variability.

IBSS: The Infrared Background Signature Survey (IBSS) is an SDIO Program with major objectives of measuring plumes as well as clutter in the infrared background of both the hard earth and the earth limb. The system and the plume measurements have been described in Chapter II above.

The objective of the IBSS earthlimb mission is to measure spatial clutter in the earthlimb at tangent altitudes ranging from 30 to 140 km for both day and night conditions. Measurements are also planned across the terminator, and auroral measurements will be made if the

opportunity arises. Measurements in the vicinity of the solar specular point are the prime objective of the hard-earth experiment. These will be done in two bandwidths around 4.3 μm .

EXCEDE III: EXCEDE III (EXCitation by Electron DEposition) is a rocketborne experiment which uses a high-power (60 kW) electron beam to excite a small volume of the atmosphere to produce infrared emissions similar to those occurring in a highly disturbed atmosphere. Two payloads, the electron source and the detectors, will be carried to 120 km by a single Aries booster. The payloads will separate from the booster at 71 km, and from each other at 83 km, with a separation velocity of 3.3 m/sec. The sensor module will be oriented so the instruments look at the electron beam, which is fired up along the field lines. After the dosing period, the irradiated volume of the atmosphere continues to undergo reactions as the excited molecules interact with other molecules. This time period is referred to as the "afterglow," and the emissions are due to either long-lived metastable states or radiance from an excited state formed by the reaction between excited molecules and either ambient or other excited molecules. Quenching of the various excited states will also occur and will be a reaction channel competing with the radiation channels.

Four spectrometers on the sensor module will be aimed at the electron beam path. They are an infrared circularly variable filter (CVF) spectrometer (2.5 - 23 μm , 2 percent spectral resolution), a dual optical channel interferometer (2.2 - 24 μm , 1 wavenumber resolution), an ultraviolet grating spectrometer (0.13 - 0.30 μm 0.0006 μm resolution), and a visible grating spectrometer (0.3 - 0.8 μm , 0.001 μm resolution). These will provide data that will identify emitting states, vibrational levels, and emission

rates as a function of altitude and dose. Two other similar CVF spectrometers will be looking into the afterglow at displacement angles of 80 and 200 degrees. These instruments will measure the decay in emission intensity of various infrared emitters. A four-channel scanning filter photometer will determine the spatial distribution of the primary (391.4 nm) and secondary (380.5 nm) beams, as well as excitation efficiency and quenching for Vegard-Kaplan metastable nitrogen emission (276.1 nm) and for the green line of atomic oxygen (557.7 nm). An additional filter photometer will measure the intensity of the doublet D state of atomic nitrogen in the afterglow region. There are also experiments to determine the density of atomic oxygen and the mean beam energy at the observation site. A set of film cameras, two video systems, and an intravehicle ranging system are also on board. Although the attitudes of both modules are preprogrammed, a backup groundbased system will be available to make corrections in the sensor module pointing program if the real-time video display indicates a misalignment.

The accelerator module has two sections: an accelerator and a sensor. The accelerator section consists of eight accelerators rated at 3 kV, 2.5 A each, for a total output of 60 kW; four dc-dc converters and nearly 500 NiCad cells. The sensor section contains another CVF spectrometer, 7 photometers, 2 film cameras to obtain near-field radiance data, a Retarding Potential Analyzer, which measures the flux of electrons with energies in the range from 0 to 100 eV, and an Electrostatic Analyzer, which measures the flux of electrons with energies in the range from 100 to 6000 eV. These instruments provide diagnostic information on the performance of the accelerators and data for correlation with previ-

ous experiments in the series.

Visual Photometric Experiment: The visual photometers used for aspect determination on probe rocketborne experiments flown in the early 1980's consistently measured the diffuse visual zodiacal background at lower levels than earlier ground-based observations. A new visual photometric experiment, configured as a shuttle "get-away special" experiment, is designed to measure the large-scale diffuse background in the visual spectral regions. The experiment includes the traditional B, V, and R astronomical filters in addition to an H alpha filter. The instrumentation has been constructed and qualified and awaits a shuttle flight.

DIGBE: The Diffuse Galactic Background Experiment (DIGBE) is a rocketborne experiment designed to obtain the spectral energy distributions of extended infrared celestial sources. The intent is to search for the spectral features in interstellar dust. The "polycyclic aromatic hydrocarbons" believed to be responsible for this dust have an 8 to 14 μm photometric intensity, many orders of magnitude greater than that predicted based on equilibrium with the interstellar radiation field. During this period the sensor flown on the Zodiacal Infrared Projects (ZIP) was modified and the ZIP payload refurbished. A circular variable filter replaced the field chopper at the first focus. This filter covers the 5 to 17 μm region at 2 percent spectral resolution. The focal plane is a state-of-the-art device: a 6 x 6 element array of infrared solid-state photomultipliers which achieve nearly the theoretical limit in sensitivity.

LABORATORY RESEARCH

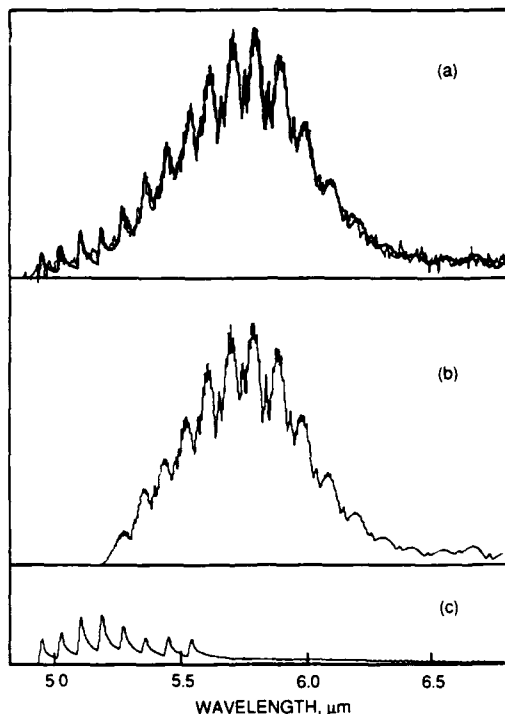
Specific atomic and molecular processes which produce infrared radiation in the quiescent, as well as the auroral and nuclear disturbed, atmosphere are inves-

tigated using a variety of laboratory facilities. Laboratory investigations offer the unique opportunity to study specific physical and chemical excitation processes under controlled conditions so infrared emission processes can be identified and characterized. Reaction parameters, including excitation cross sections, initial vibrational population distributions, rate constants for collisional relaxation and quenching, and radiative lifetimes are measured for specific vibrational and electronic states of a given radiating species. These data support the theoretical models of atmospheric radiance which are used to predict and assess the impact of spatially and temporally structured infrared backgrounds on infrared surveillance and tracking systems. Results from the laboratory program are also used to interpret field measurements of the airglow and aurora, which validate the significance of the various infrared emission processes. This approach has made major contributions to the understanding of infrared emission processes in the upper atmosphere. The laboratory facilities used to make these measurements include COCHISE, LABCEDE, FACELIF, FTMS, and LINUS.

COCHISE: The production of infrared radiation by thermochemical processes is investigated in the unique, cryogenic COCHISE (Cold Chemi-excited Infrared Simulation Experiment) program. The internal walls of the system are cooled to 20°K, which produces an enormous reduction in the thermal infrared background and permits the detection of infrared emissions with unparalleled sensitivity. Molecular infrared spectra are dispersed with a grating monochromator and detected with a solid state photomultiplier detector capable of detecting single infrared photons. Thermochemical reactions are initiated by four microwave discharges. "Active"

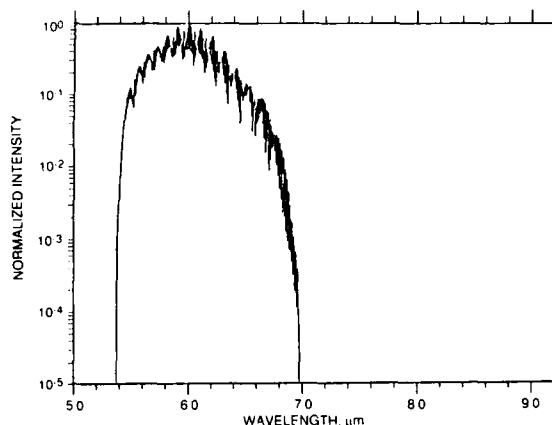
gas samples excited by the microwave discharges flow into a reaction cell in which the excited gas reacts with a counterflow of gas.

The first laboratory observations of

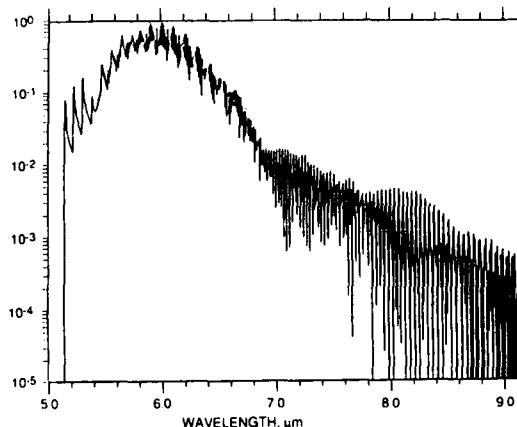


Spectrum of NO Chemiluminescence in COCHISE. (a. The light curve is the data. The dark curve is a synthetic spectral fit to the data. The fit consists of two NO components. b. Synthetic spectrum of the rotationally cold (120°K) component of the fit. c. Synthetic spectrum of the rotationally hot (10,000°K) component of the fit.)

very highly rotationally excited NO and CO have been made using this apparatus, and the findings supported data from the auroral rocket-probe observations of the Field Widened Interferometer. The observed spectrum is found to consist of two components: one is highly vibrationally excited but is rotationally cold, the other component is also vibrationally excited but is rotationally very hot (10,000°K). Emissions from



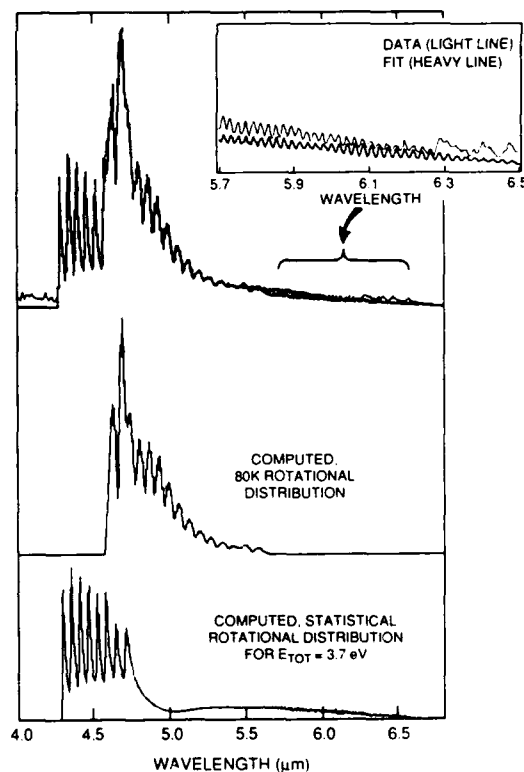
a. Synthetic Spectrum of NO Chemiluminescence Computed Using 1978 Initial Vibrational Population Distribution Observed in COCHISE.



b. Synthetic Spectrum of NO Chemiluminescence Computed Using the New Initial Vibrational Population Distributions for the Rotationally Cold and Hot Components of NO Observed in COCHISE. (Emission from the hot component now fills the 7-9 μ radiance window.)

the rotational levels responsible for the hot component extend across and fill the atmospheric 7 to 9 μ m radiance window. Analysis of the possible chemical reactions responsible for the production of the rotationally cold and hot NO indicates that the cold component is produced by the $N(^2D) + O_2$ reaction and the hot component is produced by the $N(^2P) + O_2$ reaction. This production of rotationally hot NO is the first example of a new class of infrared emission processes which must be included in models of atmospheric radiance: processes producing radiators which are not in rotational equilibrium at relatively low altitudes. As a result, the chemical dynamics of individual rotational, as well as vibrational, levels must be treated in the models.

The second example of a highly rotationally excited atmospheric radiator which has been investigated in COCHISE is CO. As was the case with NO, the observed spectrum is a composite of the spectra of rotationally cold CO and rotationally ultra-hot CO. In this case the emissions from rotationally hot



Comparison of Experimental and Computed Spectra of CO Excited by Active Nitrogen in COCHISE.

CO extend down in wavelength to the 4.3 μm region. Analysis of the possible chemical reactions which could excite the rotationally hot CO indicates that the rotationally hot CO is excited by the quenching of the $\text{N}_2(\text{a}')$ state by CO. Again, as with the case of NO, these results are significant because they suggest that rotational excitation and relatively slow deexcitation may be important in the atmosphere at surprisingly low altitudes (100 - 150 km). The question arises whether rotationally hot NO is also excited by the interaction of cold NO with active nitrogen in a fashion analogous to the excitation of CO. Preliminary data indicate that, in fact, bright emissions from rotationally hot NO are observed when NO is excited by active nitrogen. These results are currently being investigated further.

LABCEDE: In the LABCEDE (LABoratory Cryogenic Electron Dependent Emissions) program, the production of infrared radiation by the interaction of electrons with atmospheric species is investigated. Two particularly important sources of bright, structured infrared background radiation in the upper atmosphere are the aurora and nuclear explosions. In both cases, collisions between electrons (emitted by the decay of fission debris or produced by ionization caused by absorption of x-rays in the nuclear case) and constituents of the atmosphere (atomic and molecular constituents) results in infrared radiation.

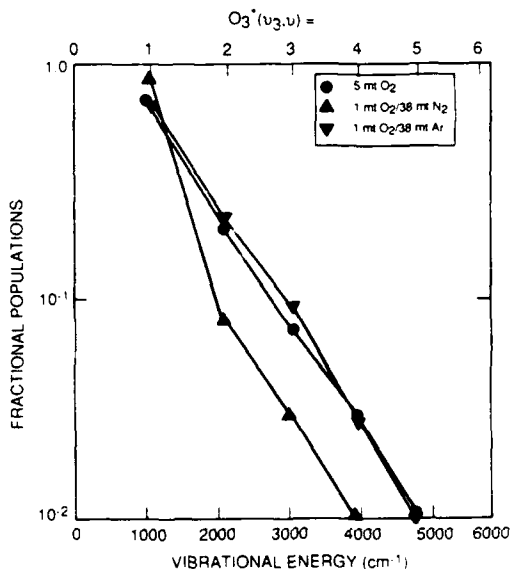
The cryogenic LABCEDE facility is used to measure and characterize infrared emissions from electron-irradiated gases. The internal walls of the system are cooled to 80°K to reduce the thermal infrared background (by four orders of magnitude at 10 μm). As a result of the low thermal background and the large volume of the observation region, weak infrared emissions can be

detected from samples at low pressure corresponding to the altitude range of 60 to 110 km. (This altitude range includes the region where x-rays from high-altitude nuclear explosions are absorbed by the atmosphere.) Gas samples are irradiated by up to 20 mA currents of 2-6 keV electrons. This maximum available flux exceeds auroral fluxes by several orders of magnitude and is comparable to some nuclear environments. A magnetic field can be applied to independently control the density of primary electrons and the density of secondary electrons produced by ionization. The gas pressure and flow rate in the LABCEDE chamber can be varied independently to investigate the effects of electron impact on atoms and molecules created by the electron bombardment.

Another capability of LABCEDE is the illumination of electron-irradiated gases by light from a solar simulator to simulate the daylit aurora and laser beams to perturb or probe populations of irradiated molecules in particular vibrational and electronic states. Fluorescence and chemiluminescence excited by electron bombardment can be observed from the ultraviolet to the long-wavelength infrared by using grating spectrometers in the ultraviolet and visible spectral regions, circular variable filters, and both warm and cryogenic interferometers in the 2 to 22 μm region. In addition, a spatially scanning 391.4 nm photometer is used to monitor the spatial distribution of energy deposited by the electron beam and to normalize the intensity of fluorescence observed in the production of electron-ion pairs in the beam.

A number of investigations of potentially important infrared emission processes have been performed recently. The anomalously efficient production of vibrationally excited O_3 by electron-irradiated O_2 has been observed and characterized. In the atmosphere at low alti-

tude (below 100 km), the familiar three-body mechanism ($O + O_2 + \text{third body}$) is the major source of O_3 . However, a key LABCEDE result is the observation of

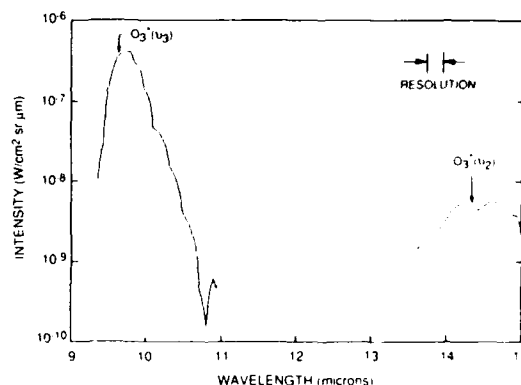


O_3 Vibrational Distributions Observed in LABCEDE at Beam Termination for Three Different Gas Mixtures. (The distributions are collisionally unrelaxed and much colder than the COCHISE three body distribution.)

much more O_3 from irradiated O_2 than can possibly be accounted for by using the three-body mechanism. This increase is potentially important because the process responsible could produce high-altitude O_3 radiance in an electron-disturbed atmosphere which is significantly higher than predicted by current models of infrared backgrounds. The dependence of the O_3 emissions on gas mixture, flow and pressure, and on the intensity and duration of the pulses of electrons used to produce the O_3 emission has been investigated. On the basis of these measurements, the O_3 emissions appear to result from the interaction of a short-lived and a long-lived precursor. Possible O_3 production processes are currently

being investigated to identify the specific process responsible.

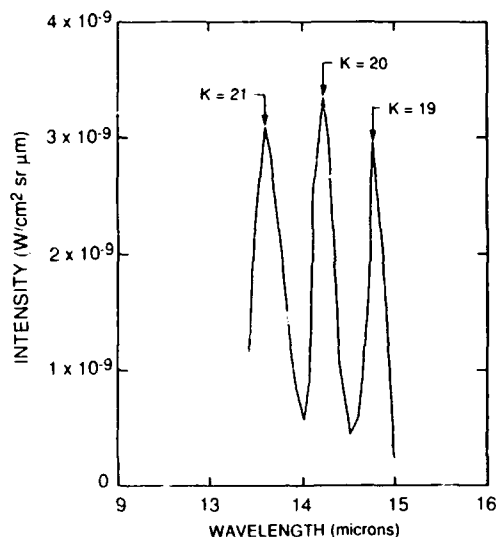
In a related investigation, O_3 fluorescence was excited by bombarding externally-generated O_3 with electrons. A number of O_3 bands were observed, including the v_3 band, which radiates at



O_3 Fluorescence Excited by Electron Bombardment of Trace Quantities of O_3 in Ar at 36 mT Observed in LABCEDE Using a Circular Variable Filter.

9.6 μm , the $v_1 + v_3$ combination band, which radiates at 4.8 μm and the v_2 band which radiates at 14 μm and which has not previously been observed in emission. Relative efficiencies for exciting these bands by electron bombardment were obtained. In addition, the efficiency for producing vibrationally excited O_3 per electron-ion pair formed in the gas by electron bombardment was determined. These results are required to model O_3 fluorescence in the 9 to 11 μm region in the electron-disturbed atmosphere.

The excitation of long wavelength infrared (LWIR) emission from highly rotationally excited OH has been observed in electron-bombardment of $O_2/H_2/Ar$ and $O_3/H_2/Ar$ mixtures. These results are important because the process responsible for these LWIR emissions is a potential source of unexpected



Spectrum of Chemiluminescence from High Rotational Levels of OH Produced in Electron-Bombarded 36 mT Ar/1% O₂/1% H₂ Observed in LABCEDE Using a Circular Variable Filter.

LWIR background in the electron-disturbed atmosphere. The emissions originate from low vibrational, highly excited rotational levels (up to level 21) of OH. These observed OH emissions cannot be associated with the familiar H + O₃ reaction since only low vibrational levels of OH are produced, and the 2.8 μm fundamental vibrational band emissions are not observed. Possible OH production processes are being investigated.

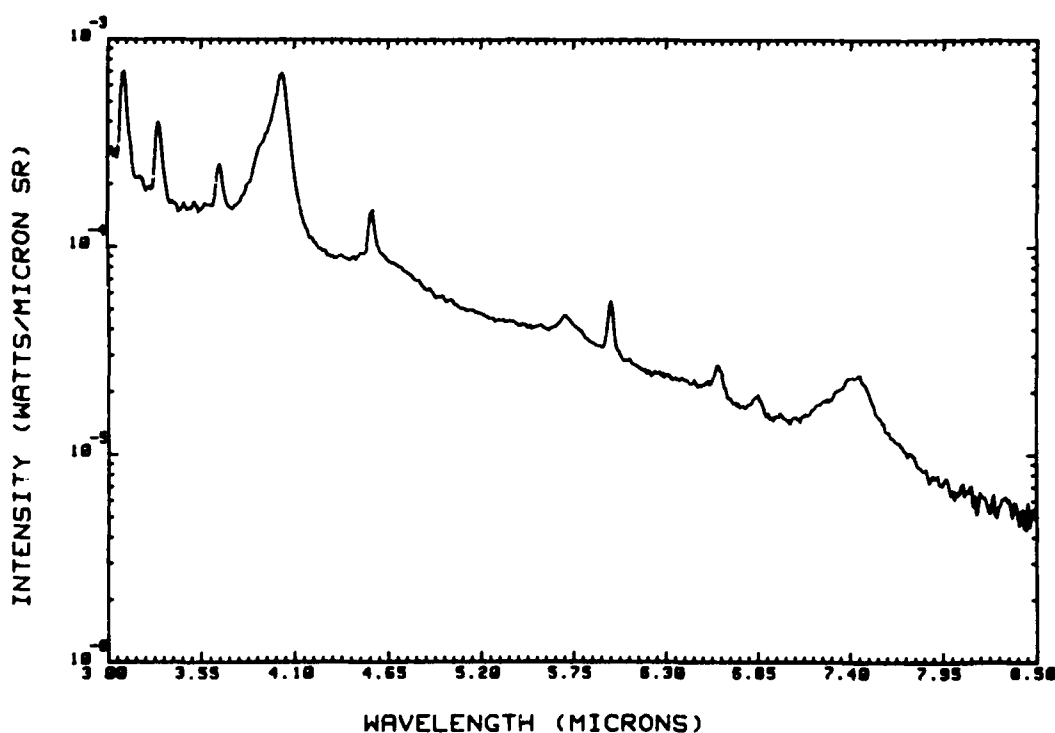
FACELIF: Chemical rate constants are measured using the FACELIF (Flowing Atmospheric Chemistry Experiment with Laser-Induced Fluorescence) facility. Laser-based spectroscopic techniques are used with a standard flow-tube kinetics apparatus to investigate reaction rate constants. The populations of species undergoing reaction are monitored using the highly sensitive technique of multiphoton ionization in which light from a tunable, pulsed dye laser is mixed in a nonlinear crystal to produce

tunable ultraviolet light, which then is used to ionize the species being monitored. The ions can then be detected with high efficiency.

Two investigations have recently been completed which have provided important inputs to theoretical models of NO radiance at 2.7 and 5.3 μm in the electron-disturbed atmosphere. The rate constant for the N(²P) + O₂ reaction has been remeasured. This measurement is important because the N(²P) + O₂ reaction produces rotationally hot NO. The N(²P) atoms were produced in a microwave discharge and then introduced into the FACELIF flow tube. The depletion of N(²P) by reaction with O₂ was monitored by multiphoton ionization.

The rate constant for the N(²D) + O reaction has also been measured. This rate is important because the N(²D) + O reaction destroys N(²D), which would otherwise be available for the production of NO. Several old measurements of the rate constant for the reaction provided values which were consistent with aeronomomic models used to interpret field data on NO in the upper atmosphere.

LINUS: Infrared backgrounds from high-altitude nuclear plasma plumes are being investigated using the LINUS (Laser Induced Nuclear Simulation) facility. An important source of bright line emissions in the upper atmosphere is a nuclear explosion. The data obtained during the atmospheric nuclear weapons test series, however, cover a limited spectral range and are insufficient to meet current mission requirements. The LINUS facility is used to make measurements of the emissions of highly excited atoms formed by electron-ion recombination processes in a laser-produced oxygen plasma. Emissions are observed from 0.3 to 8.5 μm in order to characterize the spectral signature of high-altitude nuclear plas-



SWIR-MWIR Emission Spectrum of Laser-Produced Oxygen Plasma.

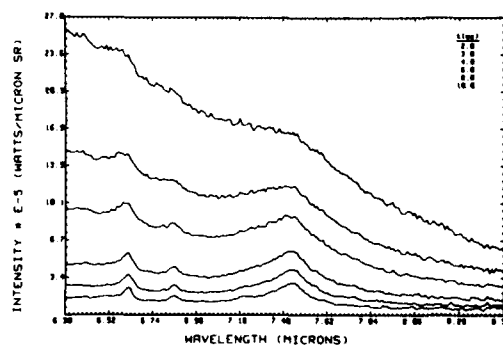
ma plumes. These laboratory measurements provide data to validate/improve nuclear plasma emission models and to interpret/extend the atmospheric nuclear test database.

The experimental approach consists of focusing a high-powered, pulsed Nd:YAG laser into a target gas cell containing oxygen. A power intensity approaching $1\text{gW}/\text{cm}^2$ can be achieved in the focal volume, resulting in temperatures in excess of $100,000^\circ\text{K}$.

Two classes of oxygen-atom line-emission features are observed for the same laser-produced oxygen plasma conditions, one narrow (e.g. 4.56 and $5.98\ \mu\text{m}$) and one broad (e.g. 4.0 and $7.45\ \mu\text{m}$). The ultra-broad, medium-wavelength infrared lineshapes are due to the effects of electric fields in the plasma which spectrally shift and broaden the emission

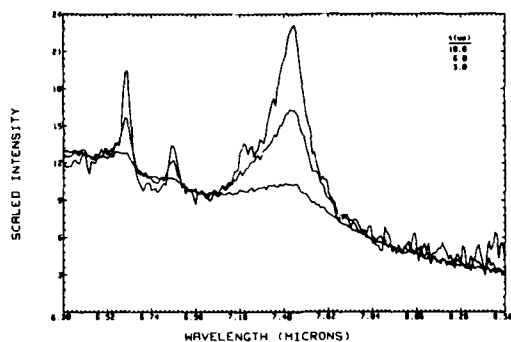
lines.

The $7.45\ \mu\text{m}$ oxygen atom emission feature is assigned to transitions between high-lying atomic Rydberg lev-



Temporal Dependence of MWIR Oxygen Atom Emissions. (Experimental data for five different delay times, $2.0\ \mu\text{sec}$ to $10\ \mu\text{sec}$, top to bottom.)

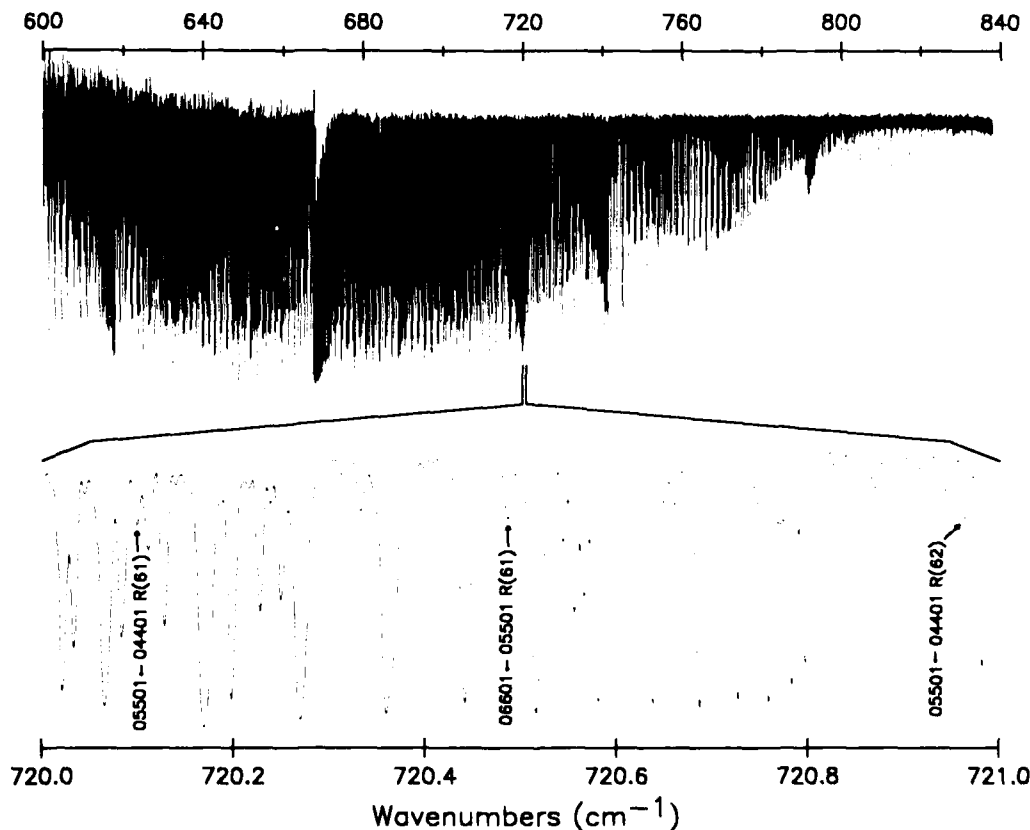
els. Since this cluster of lines radiates in the important 7 to 9 μm radiance win-



Temporal Dependence of MWIR Oxygen Atom Emissions. (Normalized intensities for three different delay times and the greater line broadening, full width, half maximum, for the shorter delay time, lower curve.)

dow, the systematics of this emission feature and the 6.62 and 6.68 μm lines have been investigated. These data indicate more line broadening at shorter delay times and higher pressures. The observed line-broadening systematics are significant because they indicate the importance of electric field effects on emissions in major infrared radiance windows.

The infrared emission spectra shown are also used to determine the wavelength dependence of the underlying continuum intensity. Possible sources of this emission are blackbody radiation and bremsstrahlung. These LINUS measurements provide important experimental benchmark data for nuclear plasma emission models.



Absorption Spectra of 5 Torr of CO_2 at 800 K over an Optical Path of 1.75 m.

High Temperature Absorption Cell: The GL high-resolution Fourier-transform spectrometer and high-temperature absorption cell provide a unique capability for the study of atmospheric gases. Research with this instrument has focused primarily on the estimation of spectral line positions and, from these, the determination of molecular rotational constants. These results are used to enhance the GL HITRAN and HITEMP databases. The measured line positions have also been used to validate and refine theoretical calculations of line positions from a model of molecular potential.

Extensive studies of water vapor, NO, and CO₂ have been undertaken. Previous studies have concentrated on the 2 to 6 μm region. In the past year and a half, however, instrument changes have been made to permit data collection in the 12 to 17 μm region, which includes fundamental vibrational-rotational absorption bands of both nitrous oxide and CO₂.

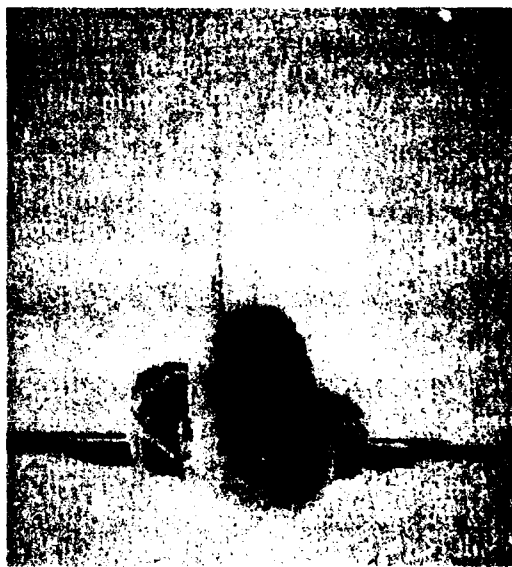
Spectra of CO₂ have been collected. Low-pressure samples (1 to 5 Torr) of naturally occurring CO₂ have been used to minimize collision broadening. At these pressures and with maximum resolution (0.005 wavenumber) the spectral data are limited by instrument broadening. Sample temperatures of 800°K were used to populate high rotational and vibrational energy levels not observed at room temperature. The spectrum resulting from these high temperatures is dramatic. The results show at least 10 times as many spectral lines belonging to dozens of vibration-rotation bands as would be observed at room temperature--some of which have not been measured before.

To analyze spectra as densely populated with spectral lines as shown in the figure requires automated computer programs. These have been under development for some time and development is continuing. Recent theoretical calcula-

tions, using the method of direct numerical diagonalization for vibration-rotation bandline positions of CO₂, have been found to be in such good agreement with the preliminary measurements (in the 15 μm region) that a new computer data-analysis technique is being programmed. Based on a modification of the Loomis-Wood graphical technique, the new scheme allows the display and visualization of a large amount of spectral data in such a way that a particular band can easily be identified. The technique will speed the data analyses process and has already been used to identify spectral lines of vibration-rotation bands which could not otherwise have been found.

COMPUTER CODES AND DATABASES

Infrared Models: Two infrared models, SPIRITS and NIRATAM, are being jointly sponsored with several DoD agencies to allow the infrared image of an aircraft to be completely modeled on a computer and the output to closely agree with validation data recorded by the FISTA. The



Infrared Image of T-38 Generated with the SPIRITS Code.

SPIRITS code can generate an infrared image of an aircraft from any viewing direction. The NIRATAM code is being developed by seven NATO nations (with which GL participates) to give an infrared modeling capability which can be used by many nations.

To enhance the ability to process data, two MS-DOS 386 systems have been developed for processing and calibration of spatial infrared images and for data reduction and analysis of spectral data. These new data-reduction and analysis tools will improve the amount and quantity of data that can be processed.

LOWTRAN and FASCODE: The atmospheric transmittance and background radiance modeling program focuses on the absorption and scattering properties of the molecular and aerosol constituents of the earth's atmosphere and their effects on radiation propagating through it. In addition, adverse weather effects, such as fogs, clouds, rain, and snow are included in the programs. Two different models for predicting the transmission and radiative properties of the atmosphere for low and high spectral-resolution applications have been developed: LOWTRAN (LOW resolution TRANsmission) and FASCODE (Fast Atmospheric Signature CODE). Each model uses similar representative model atmospheres, aerosol models, slant-path refractive geometry, and both diffuse and continuum absorption models. The models differ in their spectral resolution, spectral range, and computational speed of calculation.

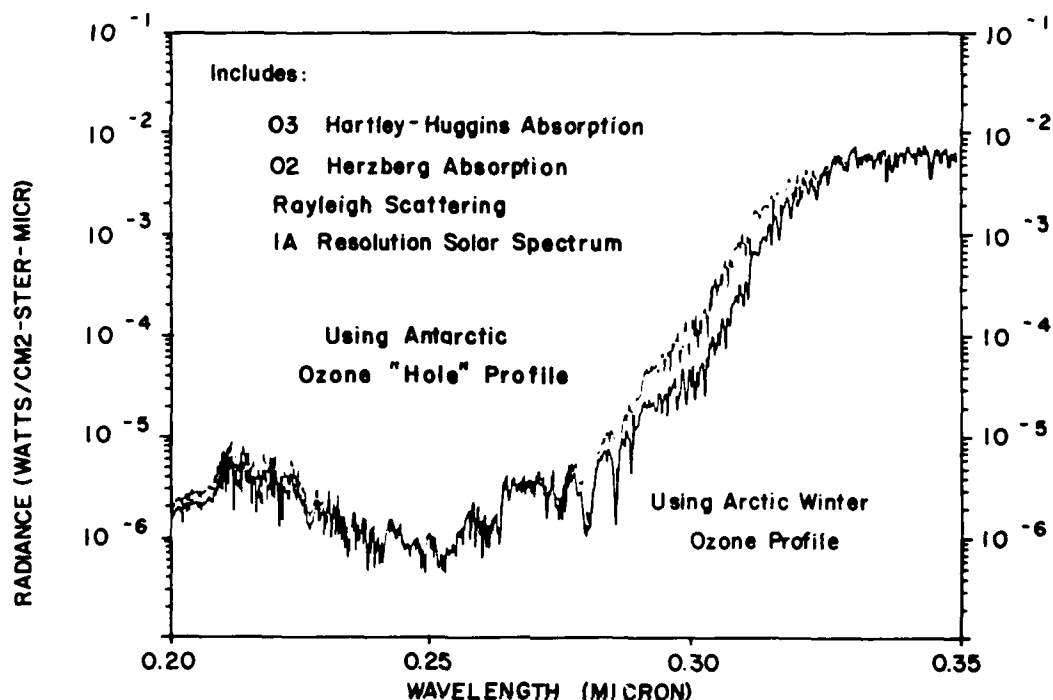
LOWTRAN predicts atmospheric transmittance, background radiance, and scattered solar radiation at a fixed spectral resolution (20 cm^{-1}) and covers the spectral region from the ultraviolet through the infrared. It provides a simple and computationally rapid means of estimating the atmospheric effects on broadband radiation with an accuracy

adequate for many applications.

The LOWTRAN code calculates atmospheric transmittance, atmospheric background radiance, single scattered solar and lunar radiance, direct solar irradiance, and multiple scattered solar and thermal radiance. The spectral resolution of the model is 20 cm^{-1} (full width at half-maximum) in steps of 5 cm^{-1} from 0 to $50,000\text{ cm}^{-1}$ ($0.2\text{ }\mu\text{m}$ to infinity). A single-parameter band model is used for molecular line absorption, and the effects of molecular continuum-type absorption, molecular scattering, aerosol and hydrometer absorption and scattering are included. Refraction and earth curvature are considered in the calculation of the atmospheric slant path and attenuation amounts along the path. Representative atmospheric, aerosol, cloud, and rain models are provided in the code with options to replace them with user-provided theoretical or measured values.

The LOWTRAN code has recently been upgraded as LOWTRAN7 (AFGL-TR-88-0177), which incorporates the following:

1. A new atmospheric database consisting of separate molecular profiles (0 to 100 km) for 13 minor and trace gases.
2. Separate band models and band-model absorption parameters.
3. A decrease of about 20 percent in the self-density continuum absorption values of water vapor at $10\text{ }\mu\text{m}$.
4. New ultraviolet absorption parameters for molecular oxygen (Schumann-Runge bands, Herzberg continuum).
5. Update of ozone absorption data (Hartley and Huggins bands), including the addition of temperature-dependent absorption coefficients.
6. An improved extraterrestrial solar-source function covering the spectral region from 0 to $57,470\text{ cm}^{-1}$.
7. An efficient and accurate multiple scattering parameterization routine
8. An extension of existing aerosol



Nadir View (Space to Ground) of Backscattered UV Radiation as Calculated by LOWTRAN. (The upper curve incorporates the Antarctic ozone "hole" profile, and the lower curve assumes the Arctic winter ozone profile.)

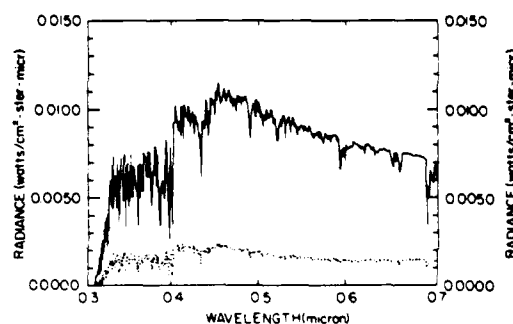
models and the rain model through the millimeter wavelength region.

9. Addition of water cloud models from FASCOD2.

10. Two new cirrus cloud models, as well as a new aerosol model for desert conditions with a wind-speed dependence.

The FASCOD3 (Fast Atmospheric Signature Code - Version 3) algorithm for accelerated line-by-line spectral transmittance and radiance calculations is designed for both atmospheric and laboratory simulations. As with FASCOD2 (released in 1985), the program is applicable to the spectral region from the middle ultraviolet to the microwave and employs standard spectroscopic parameters usually supplied from external line atlases such as HITRAN. New FASCOD3 capabilities include multiple scattering

of thermal radiation, CO_2 and O_2 temperature-dependent line coupling, enhanced non-local thermal dynamic equilibrium (NLTE) calculations, ultravi-



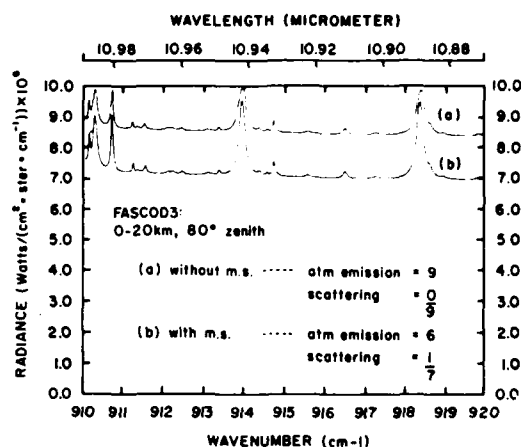
Single and Multiple Scattered Solar Radiance. (The path for this case is 20 km to 0 km, the surface albedo is 0.4 and the solar zenith angle is 60° . The solid line is the multiple scattered radiance and the dotted line is the single scattered solar radiance.)

olet diffuse absorption (O_2 and O_3), and improved weighting function options. Flexibility and utility of the general FASCOD3 algorithm has been established by successful participation in the International Radiation Commission's Intercomparison of Transmittance and Radiance Algorithms.

In addition to efficient line-by-line calculations, FASCOD3 provides auxiliary capabilities which facilitate spectral synthesis under a variety of geophysical conditions. Full access to the LOWTRAN7 20 cm^{-1} band model particulate scattering and absorption processes is available, including several new or modified aerosol and cloud models. The embedded molecular constituent profiles (AFGL-TR-86-0110) remain unchanged. They include six climatological choices for temperature and density, along with H_2O , O_3 , CH_4 , CO , and NO_2 mixing ratios. Single mixing-ratio profiles are available for 20 other gases. The default profile for CO_2 has, however, been increased from 330 ppmv to a more current estimate of 345 ppmv.

Some of the secondary FASCOD3 features include HITRAN82/86 database compatibility, filter and scanning capability for the weighting-function options, a user-defined spectrally variable ground-reflection term, and a simplified output array for generic post-processing.

Both FASCOD2 and FASCOD3 without multiple scattering assume conservative scattering: that is, scattering extinction is equivalent to absorption, which is all subsequently re-emitted. When the multiple scattering option is not implemented, radiance calculations required only a single pass through the atmosphere, appropriately merging the layer radiances. FASCOD3 with multiple scattering must do both an upward and downward pass of the layers, deriving boundary fluxes, single scattering albedos, and backscatter fractions for each



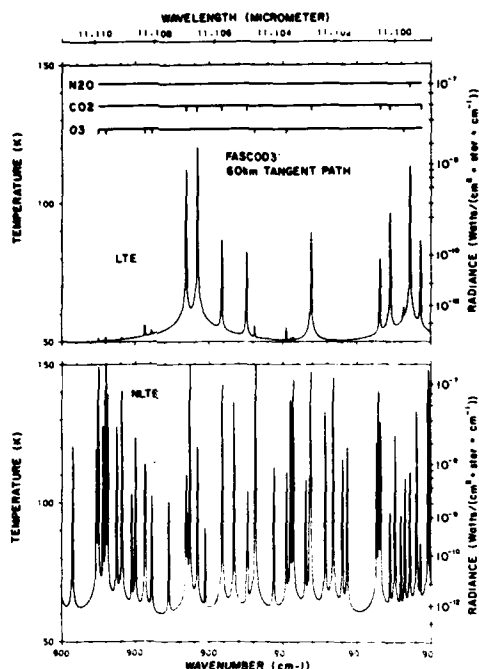
FASCOD3 Calculations for Line-of-Sight from 0 to 20 km at Zenith Angle of 80° through Relatively Hazy Atmosphere (5 km visibility). (Multiple scattering effects are included in the lower curve, b, while the upper curve, a, includes scattering as an absorption and re-emission process. The fractional contributions of emission as a function of scattering for each curve are approximated within the figure.)

layer before combining source functions for the final radiance calculation.

FASCOD3 collates the populated NLTE levels according to the specified statistics, while maintaining detailed balance within the total energy distribution, and combines the NLTE contributions with the standard local thermal equilibrium (LTE) components. The results clearly show a large degree of potential contamination for a reasonable estimate of NLTE pumping. It should be emphasized that FASCOD3 does not calculate NLTE line positions, strengths, or populations explicitly, but rather uses values provided from external data files.

These applications of FASCOD3 are only a preliminary set of validation exercises. When testing is finished in 1989, the code and documentation will be available for public release through both GL and the National Climatic Data Center, Asheville, NC.

ARC and AARC: The main "first-principles" scientific models dealing with the emission from the natural non-equilibri-



Comparison of FASCOD3 Calculations for LTE and NLTE Conditions. (The assumption of LTE is now thought to be incorrect.)

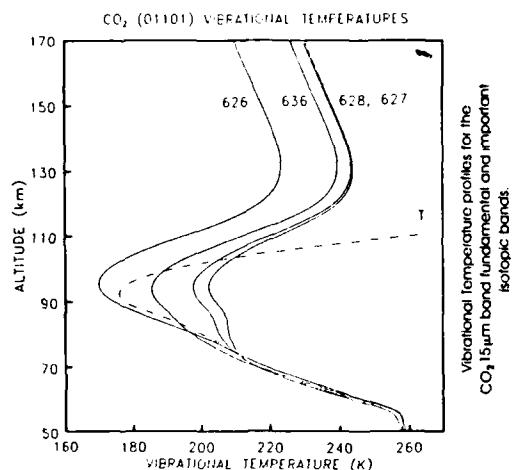
um atmosphere are ARC (Atmospheric Radiance Code) and AARC (Auroral Atmospheric Radiance Code). ARC deals with the emission from the quiescent atmosphere, while AARC is concerned with emissions following atmospheric dosing by electrons during an aurora.

ARC is composed of two main modules. The first, known as RAD, deals with the calculation of the populations of excited molecular states which radiate photons in infrared/visible light and is the first code to include an explicit line-by-line radiative transfer formulation of the radiative excitation terms. The second, known as NLTE, takes these excited-state populations and calculates the emission of light from them and its subsequent transport.

The main emphasis during 1987 and

1988 for ARC/AARC has been improvement in the RAD program module. In a non-LTE atmosphere, the major complication in calculating the radiative contribution to the excitation rate is that the source function (thus the vibrational temperature) must be known at all levels that contribute to the excitation. Thus, all these levels are coupled together. An iterative technique is used in RAD to solve this nonlinear-coupled level problem. By using an initial guess at the vibrational temperature, the radiative intensity is calculated, followed by the excitation rates and then a new profile for the vibrational temperature. This procedure is repeated until the vibrational temperature has converged. In optically thick cases (most notably the 4.3 μm band of CO_2), convergence can be slow. An accelerated convergence algorithm has been developed which does not redo the entire radiative transmission calculation at each iteration, but only rescales the excitation rates to take account of the current iteration's recalculated vibrational temperatures (source functions). This approximation compares favorably with the full iteration and is sound, since only a very small fraction of the population is in the upper (radiating) state. Even large relative changes in the upper state population reflect very small relative changes in the lower (absorbing) state population. The validity of a fully linearized approximation is also being investigated since it can replace all iterations with a set of coupled linear equations. Investigations are ongoing as to which method is most computationally efficient and accurate.

For CO_2 , radiative excitation from the warmer upper stratosphere and lower mesosphere is an important process for the less abundant isotopes, since the smaller optical depth allows radiation from further away to excite these molecules in the upper mesosphere.

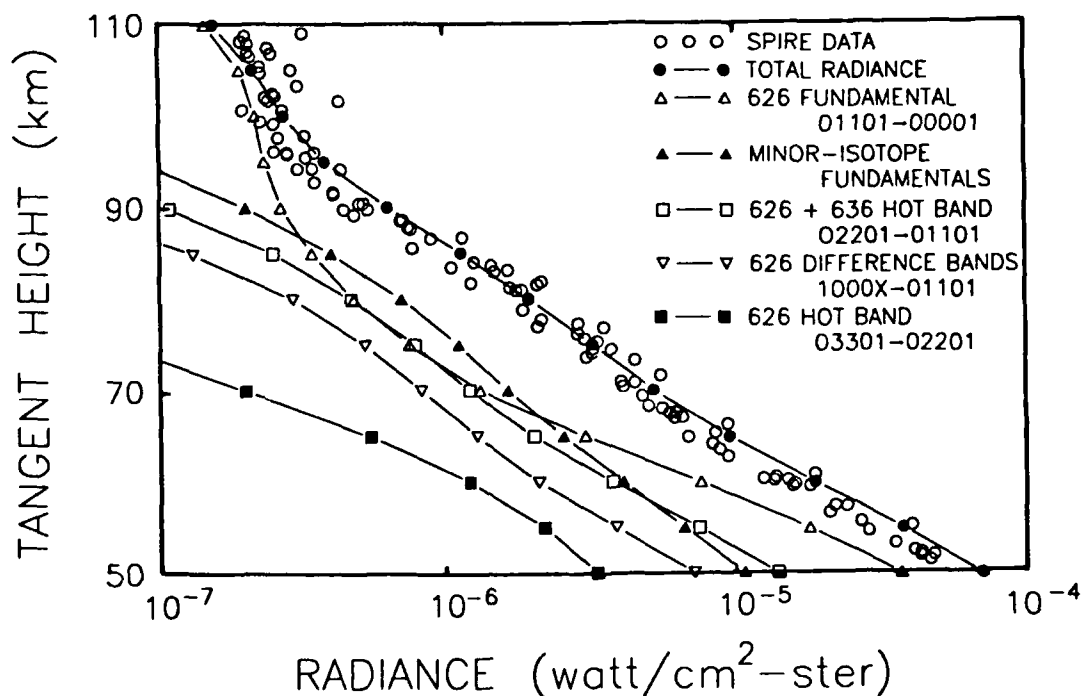


The major isotope of CO_2 (626) is in local thermal equilibrium up to about 90 km. The lesser isotopes deviate significantly because they are excited by radiation originating over a significantly larger volume.

Thus the weakest bands, which are most optically thin, have the highest vibrational temperatures. The major isotope, 626, remains nearly in LTE up to around 80 km and does not deviate very far until above 90 km. At that point, it falls below the rising kinetic temperature because the collision rate, which is decreasing, cannot keep pace with the loss of radiation to space.

In the 80 km region, the 626 fundamental is not even the major contributor to the limb radiance. Therefore, an accurate radiance model must include isotopes and weak bands along with the major isotope. Furthermore, an accurate radiative transfer algorithm that includes all the important lines in a band and considers their changing populations and lineshapes as functions of

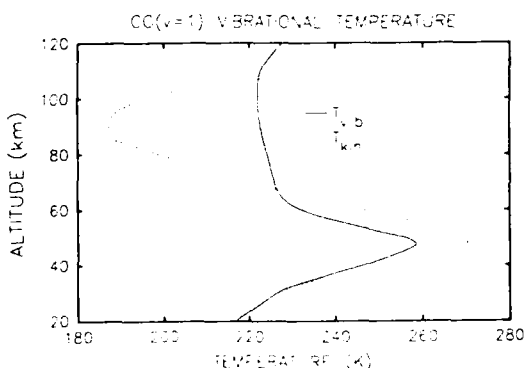
SPIRE BAND RADIANCE, 13–16.5 μm



Comparison of ARC Model Radiances with Those Measured by SPIRE (Spectral Infrared Rocket Experiment) Showing the Importance of Including Isotopes and First Hot Bands.

altitude is needed to obtain accurate results.

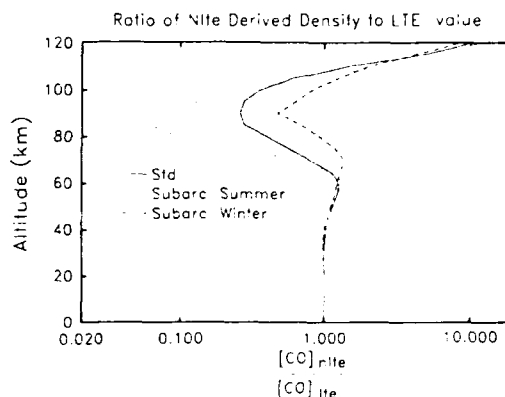
A third application of RAD has been to the nightglow radiance from CO at 4.8 μm . RAD has been used to extensively study the non-LTE behavior of CO, which is produced in the thermosphere by solar dissociation of CO_2 and by the ion molecule reaction of $\text{CO}_2^+ + \text{O}$ and in the stratosphere from oxidation of CH_4 .



CO starts to depart from local thermal equilibrium at an altitude of only 45 km.

The profile in the mesosphere is determined by the rate of transport from above and below coupled with a chemical sink via the reaction $\text{CO} + \text{OH}$, since there are very few sources for CO in the mesosphere. Investigation has shown that CO starts to depart from LTE as low as 45 km. At 70 km and above, CO ($v = 1$) is very close to radiative equilibrium, where the population is determined by the absorption of radiation from the warmer regions below and radiative loss to space. If the non-LTE effects are not correctly taken into account, large errors in the densities can occur, leading to incorrect conclusions about the dynamics of the upper mesosphere and lower thermosphere.

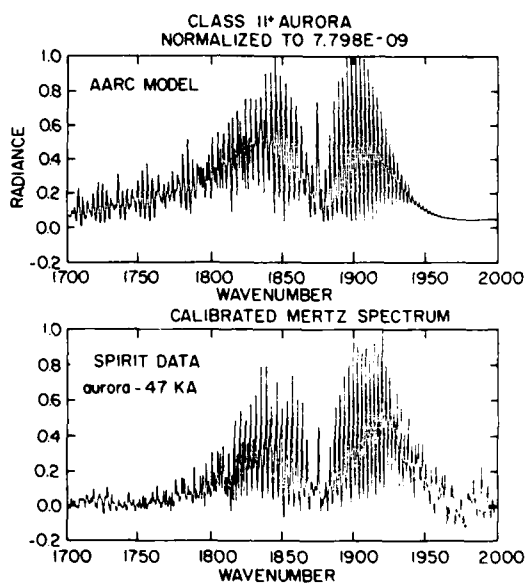
Investigations have also begun on describing the response of atmospheric airglow to structure induced by acoustic-



Relative Error in Calculated Density if CO Is Assumed in Local Equilibrium with the Kinetic Temperature.

gravity waves. The importance of gravity waves as sources of structure has been ascertained in a number of observational programs, including MAPSTAR (see above).

The first-principles auroral radiance model, AARC, includes a user-oriented, menu-driven code based on scientifically



Comparison of SPIRIT NO Spectra with AARC Model.

well-founded production and loss mechanisms. The model calculates the transport of the line-of-sight radiance, where necessary, by very accurate line-by-line methods adapted from the NLTE algorithm of the ARC model. The model includes the main emission bands from NO, NO⁺, and CO₂ in the 2 to 7 μ m region of the spectrum. A report describing the scientific basis and use of the AARC model was written in 1987 and is available.

At present, ARC/AARC together form a spectral model describing the mean behavior of the atmospheric emission spectra. It assumes the atmospheric emissions are spatially and temporally smooth and devoid of structure. ARC assumes that the state of the quiescent, non-auroral atmosphere and its local emissions depend only on altitude. In contrast, the real atmosphere has spatio-temporal structure on all scales which result in structured atmospheric radiance. Although there is a great deal of work remaining to be done in spectral modeling of the mean behavior of the atmosphere, attention is turning to the question of atmospheric radiance structure, and future research will include attempts to formulate a first-principles atmospheric radiance-structure model.

SHARC: The Strategic High-Altitude Radiation Code (SHARC) is being developed to support the analysis of data obtained by the various field programs as well as other systems requirements. SHARC presently calculates the infrared radiance and transmittance for high-altitude paths through quiescent atmospheres. This code, which has been developed over the past two years, calculates radiation on a line-by-line basis for lines of sight that pass no lower than 60 km with a spectral resolution of 0.5 wavenumber. The initial version includes the five most important molecules for high-altitude, NLTE radiance: carbon

dioxide, ozone, nitric oxide, water, and carbon monoxide.

SHARC is user-interactive and employs a modular architecture so that new results from field and laboratory experiments can be easily incorporated. SHARC can determine populations for highly excited vibrational levels by iterating between production rates from a general kinetics module and energy transfer between vibrational bands. SHARC uses a Monte Carlo process for radiative excitation and also determines energy transfer between atmospheric layers. Calculation of radiation transport is based on an equivalent width formulation that incorporates Voigt lineshapes. SHARC is not yet a mature code and is currently being validated against field measurements. Additional work will be done to incorporate additional radiators, and auroral, diurnal, dawn/dusk, latitudinal, and seasonal effects.

HITRAN: The HITRAN molecular absorption database is the archival compilation which forms the basis for spectral modeling codes from visible to infrared wavelengths. Research on the database is directed to several areas. The fundamental parameters have been expanded to provide more detailed physics that enable accurate simulations of atmospheric paths, especially for problems involving remote sensing and inversion techniques. During this research period, a substantial amount of highly accurate photometric data have become available from Fourier transform spectrometers. The impact of these improvements will be especially noticed in satellite programs viewing the nadir, or earthlimb, in the far infrared.

Application of a direct numerical diagonalization technique has been implemented to provide intensities as well as line positions of molecular transitions where observed data are unavailable. This theoretical program relies on uti-

lization of current computer technology and is becoming internationally recognized as a superior means of solving Hamiltonian systems for simple molecules. In the case of CO_2 , there are over 600 bands that must be considered for HITRAN (including the significant isotopic variants), and even though the available laboratory observations have greatly expanded during this period, many weak bands must still be calculated. In addition, the development of a high-temperature version of HITRAN relies heavily on such calculations. The predictive capability of this program has been validated in a recent effort where high vibrational bands of CO_2 were observed using the GL 2 meter interferometer and hot gas absorption cell.

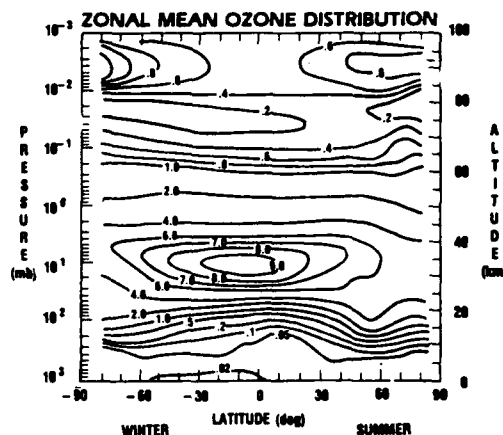
Another theoretical effort that has provided HITRAN with improved parameters has been the development of a cut-off-free theory based on the Anderson-Tsao-Cornutte approach to molecular collisions. This theory was used in the calculation of halfwidth parameters for ozone and water vapor. In addition, the theory has provided information on the pressure shifts of lines.

The present edition of HITRAN contains over a third of a million transitions as well as a supplemental file of molecular species such as the chlorofluorocarbons and some oxides of nitrogen that are not yet amenable to line-by-line representation.

Significant progress has been made towards the establishment of a high-temperature database, HITEMP. The initial version will contain parameters for species such as water vapor, CO_2 , and CO , with a temperature standard relevant to 1000 °K. This database is essential for accurately modeling aircraft and missile exhaust plumes.

Ozone Profile: A new ozone (O_3) profile climatology has been developed for use with LOWTRAN and FASCODE. This

climatology provides vertical profiles of ozone mixing ratios at altitudes up to 100 km over 10° latitude intervals for each month. The climatology is based primarily on satellite remote soundings of the stratosphere, coupled with in situ and photochemical estimates in the tro-



Typical Zonal Mean Contour Plot of Ozone for January. (The high mixing ratios of up to 9.0 ppmv at about 35 km are due to efficient photochemical production of ozone.)

posphere and mesosphere, respectively. The profiles represent zonally averaged conditions with preliminary diurnal variability estimates. Subsequent efforts will extend the climatologies to include water vapor and other trace constituents.

Ozone is a highly variable atmospheric constituent, subject to both photochemical and dynamic influences. In the troposphere (0 to 12 km) it is considered a pollutant, with average mixing ratios between 0.02 and 0.1 ppmv. Much larger concentrations of ozone occur higher in the atmosphere because of efficient photochemical production of ozone. In the middle to upper stratosphere (35 to 50 km), maximum mixing ratios of 8 to 10 ppmv occur. The dominant production mechanism in the stratosphere is:

photolytic destruction of O_2
 $O_2 + h\nu \rightarrow O + O$
 coupled with collisional recombination
 of O with O_2 :
 $O + O_2 + [M] \rightarrow O_3 + [M]$
 with this constant daytime source bal-
 anced by:

$O_3 + h\nu \rightarrow O_2 + O$
 where $h\nu$ represents the ultraviolet
 solar energy available for photodissocia-
 tion and [M] is a third body, usually O_2
 or N_2 , required for energy balance in
 three-body reactions.

Weather, photochemistry, and pollu-
 tion-related variability influence the dis-
 tribution of ozone, suggesting that a sim-
 ple set of 6 default profiles (as available
 in LOWTRAN and FASCODE) may be
 insufficient for some purposes. To further
 improve these programs, GL has pro-
 duced a new, zonally averaged ozone cli-
 matology. The climatology consists of 12
 monthly averages of ozone mixing ratio
 described on a grid between 0 and 100
 km at 10° latitude intervals. The prima-
 ry source data is a NASA/Goddard com-
 pilation proposed for the COSPAR
 International Reference Atmospheres
 (CIR) in 1986. These data were derived
 from publicly available satellite data
 sets. The tropospheric analysis encom-
 passed in this climatology is derived
 from work done at NASA Langley, using
 in situ, aircraft, balloon, and ground-
 based measurements. The higher lati-
 tude tropospheric profiles provided in
 the climatology have been inferred from
 assorted individual measurements cou-
 pled with dynamic constraints and may
 not be truly representative of climatolog-
 ical means.

The change in the ozone mixing ratio
 at the tropopause is very large. The gra-
 dient between 12 and 25 km has pur-
 posely been smoothed out by using loga-
 rithmic interpolation in mixing ratio
 against linear altitude and/or low pres-
 sure. This provides a cleaner estimate of

the ozone ledge, but may not realistically
 represent the profile. Information on the
 height of the tropopause as determined
 by radiosonde data would provide a bet-
 ter estimate of the O_3 vertical structure
 at the tropopause. If the current simula-
 tion proves inadequate, more appropri-
 ate mathematical schemes will have to
 be determined and adopted.

A further variant on tropospheric O_3
 centers on large-scale plumes originating
 from mid-latitude industrial and tropical
 biomass burning. The zonal mean nature
 of the climatology loses this detail, but
 the NASA community is now gathering
 techniques to derive real-time tropo-
 spheric estimates of these sources from
 combined satellite data sets.

The upper atmosphere presents a dif-
 ferent set of limitations on the climatolo-
 gy. At and above the mesopause (80 km),
 ozone measurements are not readily
 available. This imposes a uniformity of
 ozone in our model which is not repre-
 sentative of the atmosphere. However,
 until more confidence is established in
 photochemical theories through addition-
 al validation, it is difficult to adopt new
 standards.

Photochemistry has, however, been
 used to derive a first-order estimate of
 the diurnal cycle of O_3 . Based on these
 calculations and measurements, ozone is
 invariant from day to night below about
 45 km; however, above this level the
 nighttime values increase dramatically.
 Nighttime ozone rapidly accretes the
 available O atoms, reaching a steady-
 state value which is the sum of daylight
 O plus O_3 . At 50 km the nighttime val-
 ues are approximately 20 percent larger
 than the day, while at 60 km the factor
 increases to two. The maximum varia-
 tion occurs near 75 km, where the factor
 is between five and seven, depending
 upon season.

Near 80 km, i.e., at the mesopause, the
 chemical interactions become very com-

plex, with diurnal dissociative processes becoming secondary to the dominating influence of temperature dependence of the HO_x and NO_x reactions plus the influx of thermospherically produced atomic oxygen. Initial estimates of the diurnal ratio show a sharp decrease, with night values equaling those in the day over a very narrow altitude range (80 \pm 2 km). This trend is rapidly reversed above 85 km, with the night values again exceeding the day by a factor of 10 at 100 km. Because these theoretical predictions have been calculated

only for mid-latitudes and have not been substantiated by measurements, the day/night ratios as provided in this climatology are preliminary. Caution should be employed if the results at and above 75 km are to be used for system design purposes.

Celestial Background: The existing database on the infrared celestial background is being analyzed in order to develop physical and phenomenological models of the specified background components. These models are being incorporated into a scene generator capable of



Gray Scale Image from 12 to 100 μ m of the Sky Centered on the Ecliptic Plane as Measured by the Infrared Astronomical Satellite (IRAS). (The wide diagonal band occupying most of the image is the emission from the warm zodiacal dust in the solar system. Faintly visible within this broad band are dust bands of lower contrast. The linear streak nearly parallel to the zodiacal band is the dust trail from comet Temple 2. The patchy structure above the zodiacal band (top center) is infrared emission from galactic dust. This so-called "galactic cirrus" is observed with varying degrees of intensity over the entire sky. The structure is highly detailed, having a wispy appearance and filaments with scale lengths from many degrees down to the smallest detector (0.22 mrad) used by IRAS.)

accurately describing the long-wavelength infrared (LWIR) celestial background at a spatial resolution of 2 arc seconds ($10 \mu\text{rad}$) and a flux level of 2 milli-jansky ($5 \times 10^{-21} \text{ w/cm}^2/\mu\text{m}$) with a spectral definition of less than $0.1 \mu\text{m}$ over a range of 2 to $30 \mu\text{m}$.

A multi-component model of the LWIR celestial background was developed. A physical description of the galaxy and the large-scale structure of the universe was adopted based on observations at a variety of wavelengths. An artificial intelligence program divided the low-resolution spectra obtained by the InfraRed Astronomy Satellite (IRAS) on bright infrared point sources in the celestial background into 77 distinct classes grouped into 9 separate categories. Each of these components is characterized by an individual spatial, spectral, and intrinsic brightness distribution. The distribution parameters were determined from the IRAS point source catalog and by constraining the model to fit the observations from sensitive high-resolution near-infrared surveys.

A model of diffuse zodiacal emission had been constructed based on the physics of thermal re-emission of absorbed sunlight by interplanetary dust. The model parameters are derived from the current database of visible observations, polarization measurements, and rocket-probe and satellite-based infrared measurements. The model includes the variation of volume emissivity and/or albedo with heliocentric distance, global irregularities such as possible warping of the plane of maximum brightness, and annual variations of brightness at the ecliptic poles. A number of zodiacal dust bands have been discovered and modeled. About one hundred small-scale features such as cometary dust trails and asteroidal debris have been identified in the IRAS observations and will be analyzed as to

the clutter problem they pose. A detailed statistical analysis of the suspected solar system objects is currently underway, and a statistical description of the number density as a function of brightness and position will be derived.

The emission mechanism for the structured infrared galactic background is being analyzed based on physical principles and correlation of the LWIR emission with observations at other wavelengths taken at higher resolution and/or sensitivities. The frequency content of this structured emission will be determined. Power spectral densities on these wispy features have significantly shallower spectral indices than that predicted by turbulent cascade; that is, the intensity of the phenomenon is brighter than predicted at small spatial scales. A point-source detection scheme was run over several test fields and the number of occurrences beyond 3 sigma was an order of magnitude greater than predicted by the stellar model.

The phenomenological and physical models defined above are to be integrated into a single computer code which will accurately describe all components of the LWIR celestial background. This code will generate either an intensity map with pixels sized to the required resolution and total field of view, or user-specified output such as two-dimensional power spectral density as a function of position. This is an independent product which can be combined with other background descriptors such as models for the earthlimb. The NASA point source model has already been combined with the GL zodiacal model to create a preliminary scene descriptor. Additionally, selected IRAS infrared images of the sky have been Fourier-edited to remove striping and baseline drift and are to be included in the scene descriptor as an option.

Notable progress has been made to

super-resolve the IRAS observations. The IRAS observations are a unique database which presents interesting challenges for super-resolution. For reference, the IRAS focal plane consists of eight arrays which contain 62 detectors arranged for redundant coverage in four spectral bands centered at 12 μm , 25 μm , 60 μm , and 100 μm . The 59 operational detectors have different responses. Low-pass filtering in the signal-processing electronics and low-frequency detector effects (memory) produce "tails" in the in-scan response profiles, particularly in the 12 μm and 25 μm bands. This asymmetric response makes scan direction an important parameter. Furthermore, the cross-scan response is complex, giving double peaks for most of the 12 μm and 25 μm bands.

The survey in-scan sampling is band-limited, but is critically sampled in the Nyquist sense in cross-scan. The potential for super-resolution arises from the fact that the in-scan data are strongly band-limited (being nominally sampled at twice the survey rate) and the field is raster-scanned, with adjacent tracks offset by a fraction of a detector length. Super-resolving the survey data and improving the results rely on multiple scans over a given area. This, however, adds the additional complication of field rotation and the fact that the sequential offsets are not uniformly spaced.

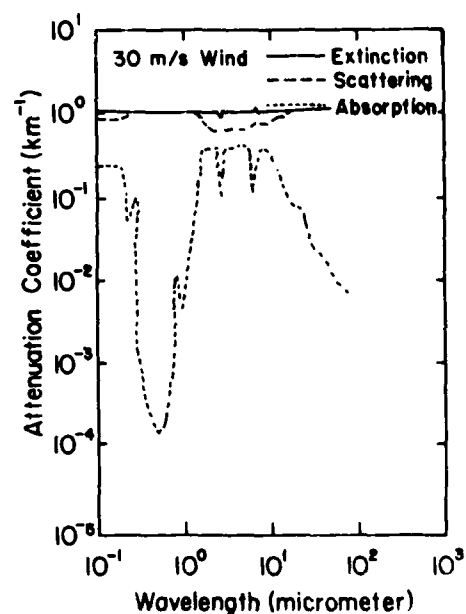
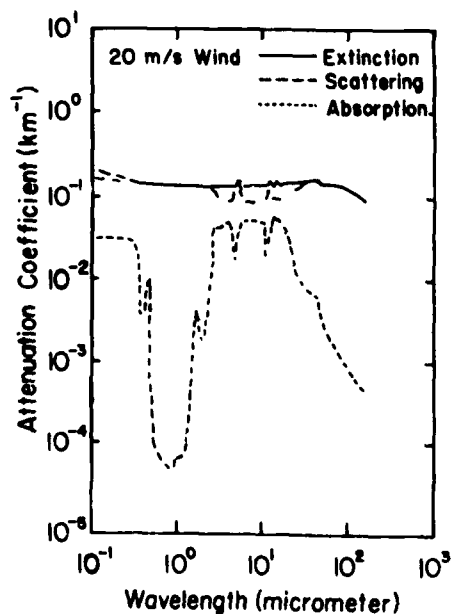
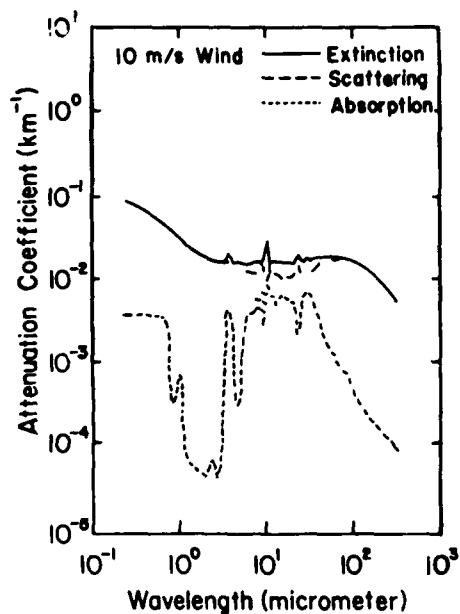
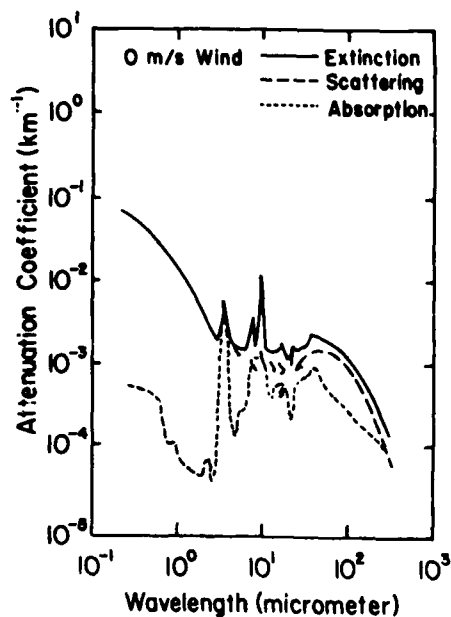
A robust flat-fielding routine with an iterated weighted least-squares routine is used to eliminate baseline drifts and large-scale background variations. The observations are regridded with a minimum mean-square error procedure. A detailing routine was also developed which corrects the detector memory to better than 5 percent.

Aerosols and Particulates: A major result of theoretical studies of atmospheric aerosols and particulates is the formulation of models to describe their proper-

ties. Such models are based on laboratory and field measurements of the type described and results are available in the general scientific literature. The models for the boundary layer (which represent rural, urban, and maritime environments) are dependent on the relative humidity. The desert aerosol model depends on the prevailing wind speed. Models for the stratosphere allow for the effects of recent volcanic eruptions which can inject significant quantities of dust and gases into stratospheric regions. The stratospheric model was recently modified to take into account new observational data on size distributions and temperature dependence resulting from volcanic activity. Models have also been generated for various water and ice clouds and for fogs and precipitation.

One of the primary applications of the aerosol and particulate models is in the atmospheric transmittance/radiance codes, LOWTRAN and FASCODE. These models are also used in such applications as lidar simulation and inversion. Some of these GL aerosol models have served as the basis of models incorporated in the "Standard Atmosphere for Radiation Computation" developed by the International Association for Meteorology and Atmospheric Physics. Recent studies have led to the development of scaling laws which relate the scattering properties at one wavelength to the scattering or extinction at another. Currently, research is underway to develop a global climatology of the atmospheric aerosols to aid in determining which model best represents the existing conditions at a given time and place.

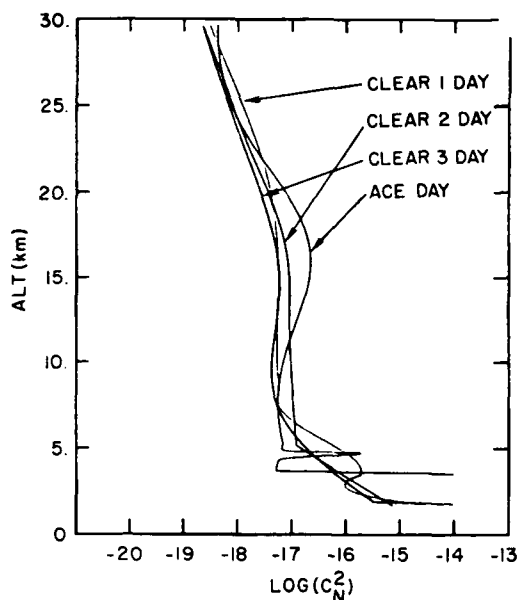
Turbulence: The turbulence database established by GL now includes measurements from Massachusetts, Pennsylvania, Colorado, Hawaii, Florida, Illinois, and New Mexico. These data have permitted the construction of site-specific empirical models which have



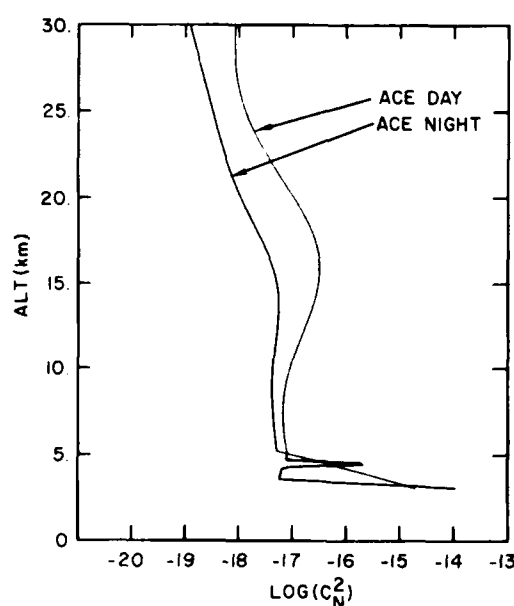
Attenuation Coefficients for the Desert Aerosol Model as a Function of Wavelength for Wind Speeds from 0 m/s to 30 m/s.

been useful in comparing turbulence results from different locations and

under different meteorological conditions. The next level of modeling involves



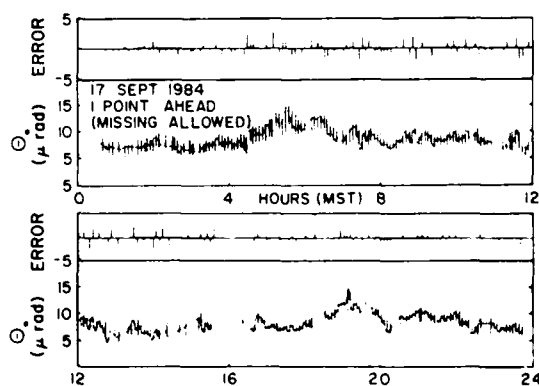
Empirical Models for Four Experimental Turbulence Campaigns. ("Clear" refers to three models developed for New Mexico and "Ace" refers to a model for Hawaii. Note the variation in the turbulence levels at the tropopause, 17 km, and in the boundary layer, 3-5 km.)



Empirical Day and Night Turbulence Models for Hawaii. (Note the large diurnal variation above the boundary layer and the effect of the inversion height on the daytime profile.)

development, testing, and validation of models which directly incorporate meteorological data. Models such as the Hufnagel, NOAA, Kaimal and others are regularly examined against simultaneous meteorological data provided by the thermosonde for both accuracy and limits of applicability. GL has also developed its own models which are similarly tested and compared to others for further refinement.

The modeling of optical turbulence closely resembles that of optical propagation. In this context, the analysis and modeling of optical turbulence for application to laser beam propagation has been carried out in terms of the various moments of the refractive index structure constant, C_n^2 . These moments include coherence length, isoplanatic angle, scintillation variance, and Greenwood frequency. Work at GL has included calculation of Strehl ratios, the ratios of peak beam intensity with and without a particular turbulence effect. These parameters are used in adaptive optics and systems design applications and generally to characterize laser-beam propagation effects. These analytic efforts have resulted in a high-energy laser, wave optic propagation code capa-



Autoregressive Linear Prediction of the Isoplanatic Angle. (The solid line represents actual sample data, while the vertical hash lines are predicted values. The short-term prediction is based on a knowledge of past data and its autocovariance function.)

ble of incorporating GL atmospheric data codes and of modeling the propagation of a laser beam from the ground to space.

A pilot project is now underway to examine the potential of chaos dynamic theory and fractals for application to problems in optical turbulence. This effort has a phenomenological goal of devising new computational modeling techniques capable of describing the fine structure and stratification of C_n^2 and a more basic research goal of understanding the intermittency of turbulence, the mixing of atmospheric quantities, and the interrelations of the various characteristic scale factors.

NEW INSTRUMENTATION

FAST: FAST is a basic research program that is studying and comparing different methods of producing a non-scanning optical spectrometer suitable for capturing spectra of randomly occurring pulsed-emission sources. During the last two years, two different configurations of photodiode array Fourier interferometers were studied. These interferometers produce an interferogram in space instead of scanning with time. Detailed analyses of these instruments showed that they do not provide the expected increase in the signal-to-noise ratio over a conventional grating spectrograph fitted with the same photodiode array. Investigation is now focused on a concept which uses a Hadamard mask in place of a single slit at the entrance plane of a conventional photodiode-array spectrograph. Computer simulation of a preliminary design indicates that this technique will produce significant increases in sensitivity compared to that realized by a conventional grating-array spectrograph. A prototype instrument will be fabricated for laboratory testing.

TDI (FALCON): An on-going instrumental development project, previously known as FALCON, is now called the Target

Discrimination Imager (TDI). The objective is to build and test a system which will pass high spatial frequencies and block low frequencies to improve detection of targets in clutter. The system is based on standard TV technology and uses a platinum silicide integrating detector array (244 X 160 pixels) operating at 30 Hz. The foreoptics are a Cassegrain telescope (150 mm focal length, 50 mm aperture) with a steerable secondary mirror. On alternate frames, the secondary mirror is programmed to (1) be centered to provide a well-focused image followed by (2) a nutation such that the image is swept circularly around its original position by a radius of roughly one pixel.

Recent tests with the TDI system using helicopter targets flying against a cloud background were recorded on analog tape using a standard VCR. Simple frame-to-frame subtraction without mirror nutation achieved good results when the target moved rapidly across the field of view (signal-to-noise ratio = 20 for target velocity of 2 pixels per frame), but was virtually useless for a target more or less stationary in the field of view. However, the TDI process, subtracting a slightly smeared frame from a sharp frame, performs best for the stationary target (signal-to-noise ratio = 5 to 15) and loses efficiency with increasing speed of the target across the field of view. Thus, the two techniques are complementary. From the standpoint of target detection, the results are highly significant, since a system that includes the nutating mirror can raise low signal-to-noise ratio values for a stationary target to a value of 5 or more and lead to a markedly higher probability of detection than can be obtained by simple frame-to-frame subtraction.

Imaging Spectrometer: The GL imaging spectrometer became operational during this period. The heart of this instrument

is a 58 x 62 pixel mosaic array which, when used with the prism spectrometer, will produce either two-dimensional images in a narrow spectral band or a full 8 to 14 μm spectrum in one dimension and spatial coverage in the other. Preliminary observing runs at the University of Wyoming produced infrared spectra of bright infrared sources, including spatially resolved spectra of the circumstellar shell source +10420. Future plans are to replace the array with a more sensitive device and to extend the observations to obtain the spatial dependence of the spectra on extended and bright infrared sources.

Eye-Safe Lasers: Space-based lidar systems clearly have unique requirements, the most constraining of which are associated with the laser transmitter. System demands include long unattended lifetime, high efficiency (corresponding to low electrical power), light weight, reasonable size, and a high level of stability. Current lasers most often considered are CO_2 and Nd:YAG. Both have problems associated with their use in space for unconstrained global sampling. CO_2 lasers of current design are large, heavy, and power-demanding and require a constantly renewed supply of gas. The most often considered YAG emission is at the doubled frequency, or a wavelength of 0.532 μm . This wavelength is at the peak of the hazardous response curve for the human eye and consequently there are serious limitations on how such a laser may be used. To address such problems, GL has been sponsoring research in lasers which emit close to the lower edge of, but within, the eye-safe region of the spectrum, which begins at about 1.4 μm . Specifically, by using rare earth dopants such as Holmium, Thulium, and Erbium in various host crystals, solid-state lasers can be made to operate at wavelengths from 1.6 to 2.1 μm , which are considered eye-safe. Diode-pumping of

these laser materials is possible and will yield conversion efficiencies which are much higher than those for flashlamp-pumped systems. This development program will explore such issues as the optimal dopant concentration and host crystal combination as well as cavity design, stability, and diode-pumping techniques.

PUBLICATIONS

1987-1988

BENSON, P.J. (Wellesley Coll., Wellesley, MA); and LITTLE-MARENIN, I.R. (AFGL)

A Water Maser Associated with EU and A Carbon Star near an Oxygen-Rich Circumstellar Shell

Astrophys. J. Lett. 316 (1987)

EATON, F.D., PETERSON, W.A., HINES, J.R., PETERMAN, K.R. (US Army ASL); GOOD, R.E., BELAND, R.R. and BROWN, J.H.

(AFGL)

Comparisons of VHF Radar, Optical and Temperature Fluctuation Measurements of C_n^2 , r_o , and Θ_o

Theor. Appl. Climatol 39 (1988)

FRASER, M.E., RAWLINS, W.T. (Physical Sciences, Inc., Andover, MA); and

MILLER, S.M. (AFGL)

Infrared (2 to 8 m) Fluorescence of the $W^3 \Delta u$ to $\rightarrow B^3 \Pi g$ and $w^1 \Delta u \rightarrow \alpha^1 \Pi g$ Systems of Nitrogen

J. Chem. Phys. 88 (1988)

GAMACHE, R.R. (Univ. of Lowell, Lowell, MA); and Rothman, L.S. (AFGL)

Temperature Dependence of N_2 - Broadened Halfwidths of Water Vapor: The Pure Rotation and ν_2 Bands

J. Mol. Spectrosc. 128 (1988)

HOWARD, S.J.

Fast Algorithm for Implementing the Minimum-Negativity Constraint for Fourier Spectrum Extrapolation II. Part 2
Appl. Opt. 27 (1988)

LEVAN, P.D. and PRICE, S.D.

IRAS Large and Ground Based Small Beam Measurements of the Unidentified 11.3 and [NeII] 12.8 Microm Line Fluxes in the Starburst Galaxy H82
Astrophys. J., 312 (1987)

LITTLE, S.J. (Bentley Coll., Waltham, MA); LITTLE-MARENIN, I.R. (AFGL); and BAUER, W.H. (Wellesley Coll., Wellesley, MA)

Additional Late-Type Stars with Technetium
Astron. J. 94 (1987)

LITTLE-MARENIN, I.R. (AFGL); and LITTLE, S.J. (Bentley Coll., Waltham, MA)

Search for Technetium II in Barium Stars
Astron. J. 93 (1987)
Emission Features in IRAS LRS Spectra of MS, S and SC Stars
Astrophys. J. 333 (1988)

LITTLE-MARENIN, I.R. (AFGL); BENSON, P.S. (Wellesley Coll., Wellesley, MA); and DICKINSON, D.F. (Lockheed, Palo Alto, CA)

Masers Associated with Two Carbon Stars: V778 CYGNI and EU Andromedae
Astrophys. J. 330 (1988)

LITTLE-MARENIN, I.R. (AFGL); RAMSAY, M.E., STEPHENSON, C.B., LITTLE, S.J. (Bentley Coll., Waltham, MA); and Price, S.D. (AFGL)

New Carbon Stars Identified from Low Resolution IRAS Spectra
Astron. J. 93 (1987)

MARINELLI, W.J., GREEN, B.D., DEFACCIO, M.A. (Physical Sciences, Inc., Andover, MA); and BLUMBERG, W.A.M. (AFGL)

Vibrational Relaxation and Intersystem Crossing in $N_2(a' \Pi_g)$

J. Phys. Chem. 192 (1988)

PHILLIPS, C.M., STEINFELD, J.I. (Massachusetts Inst. of Tech., Cambridge, MA); and MILLER, S.M. (AFGL)

Remeasurement of $N(^2P) + O_2$ Reaction Rate Using Multiphoton Ionization Detection of Nitrogen Atoms
J. Phys. Chem. 91 (1987)

PRICE, S.D.

Structures of the Extended Emission in the Infrared Celestial Background
Opt. Eng., 27 (1988)

PRICE, S.D.

Extraneous Radiation on Space Borne Infrared Sensors
IR Technology, Proc. of SPIE 972 (1988)

PRICE, S.D.

The Infrared Sky: A Survey of Surveys
Astron. Soc. Proc. 100 (1988)

RAWLINS, W.T. (Physical Sciences, Inc., Andover, MA); and ARMSTRONG, R.A. (AFGL)

Dynamics of Vibrationally Excited Ozone Formed by Three-Body Recombination I. Spectroscopy; II. Kinetics and Mechanisms
J. Chem. Phys. 87 (1987)

ROTHMAN, L.S. (AFGL); GAMACHE, R.R. (Univ. of Lowell, Lowell, MA); GOLDMAN, A. (Univ of Denver, Denver, CO); BROWN, L.R., TOTH, R.A., PICKETT, H.M., POYNTER, R.L., FLAUD, J.M., CAMY-PEYRET, C. (Univ. of Paris, France); BARBE, A., HUSSON, N., RINSLAND, C.P., and SMITH, M.A.H. (NASA)

The HITRAN Database: 1986 Edition
Appl. Opt. 26 (1987)

SMITH, D.R.

Evidence for Off-Axis Leakage Radiance in

High Altitude IR Rocketborne Measurements
Proc. of SPIE (November 1988)

TOMIYAMA, K. (Pennsylvania State Univ., University Park, PA); CLOUGH, S.A., AND KNEIZYS, F.X. (AFGL)

Complex Susceptibility for Collisional Broadening
Appl. Opt. 26 (1987)

TRAKHOVSKY, E. (Technion-Israel Inst. of Tech., Haifa, Israel); and SHETTLE, E.P. (AFGL)

Wavelength Scaling of Atmospheric Aerosol Scattering and Extinction
Appl. Opt. 26 (1987)

VAN TASSEL, R.A. (AFGL); and WONG, W.K. (SSG, Inc., Waltham, MA)

Signal-to-Noise Characteristics of Photodiode Array Fourier Transform Spectrometers
Microchimica Acta. (1988 II)

PRESENTATIONS 1987-1988

ALEJANDRO, S.B.

Lidar Research at the Air Force Geophysics Laboratory
11th Internat. Conf. on Lasers 88, Lake Tahoe, NV (4 December 1988)

ALEJANDRO, S.B., and ESTES, M.J.
Compact Pulsed CO₂ Heterodyne Lidar System for Ground Based and High Altitude Balloon Borne Measurements
14th Internat. Laser Radar Conf., Innichen-San Candido, Italy (20-24 June 1988)

ANDERSON, G.P., HALL, L.A., and SHETTLE, E.P.
High Resolution Solar Irradiance Measurements: 200-319 nm

IUGG, Vancouver, Canada (21 August 1987)

ANDERSON, G.P. (AFGL); GILLE, J.C. (NCAR, Boulder, CO); HERMAN, J.R. (NASA Goddard Space Flight Center, Greenbelt, MD); and CLOUGH, S.A. (Atmospheric and Environmental Research, Inc., Cambridge, MA)
Presunset Variation in the 9.6 μO_3 Signature
Quadrennial Ozone Symp., Gottingen, FRG (8-13 August 1988)

ANDERSON, G.P., HOKE, M.L., KNEIZYS, F.X. (AFGL); CLOUGH, S.A., and WORSHAM, R.D. (Atmospheric and Environmental Research, Inc., Cambridge, MA)
Validation of FASCODE Calculations with HIS Spectral Radiance Measurements
Internat. Radiation Symp., Lille, France (18-24 August 1988)

ANDERSON, G.P. (AFGL); CLOUGH, S.A. (Atmospheric and Environmental Research, Inc., Cambridge, MA); Kneizys, F.X., Shettle, E.P., Chetwynd, J.H., Abreu, L.W., Hall, L.A. (AFGL); and WORSHAM, R.D. (Atmospheric and Environmental Research, Inc., Cambridge, MA)
FASCODE: Spectral Simulation
Internat. Radiation Symp., Lille, France (18-24 August 1988)

BAROWY, W.M., ESPLIN, M.P., HUPPI, R.J. (Stewart Radiance Laboratory, Bedford, MA); and VANASSE, G.A. (AFGL)
High Resolution Fourier Spectroscopy of N₂O at Elevated Temperatures
6th Internat. Conf. on Fourier Transform Spectroscopy, Vienna, Austria (24-28 August 1987)

BEDO, D.E.
Development of Space Based Lidar at the Defense Meteorological Satellite Program and at the Air Force Geophysics Laboratory
Conf. on Lasers and Electro-Optics, Baltimore, MD (27 April 1- May 1988)

BELAND, R.R., MURPHY, E.A., KOENIG, G.G., and THOMAS, P.J.

Comparison of Horizontal Scintillation Measurements and Models

SPIE 1988 Tech. Symp. on Optics, Electro-Optics and Sensors, Orlando, FL (7 April 1988)

BLUMBERG, W.A.M. (AFGL); and GREEN, B.D. (Physical Sciences, Inc., Andover, MA)

Relative Cross Sections for IR Emissions from Highly Excited O in Irradiated O₂

18th Annual Mtg. of the Division of Atomic, Molecular, and Optical Physics of the American Physical Society, Cambridge, MA (18-20 May 1987)

BLUMBERG, W.A.M., WALKER, K. (AFGL); and GREEN, B.D. (Physical Sciences, Inc., Andover, MA)

IR Emission Dynamics of Highly-Excited O in Irradiated O₂

AGU Mtg., San Francisco, CA (7-11 December 1987)

BLUMBERG, W.A.M., IP, P.C.F. (AFGL); GREEN, B.D., MARINELLI, W.J., and PERSON, J. (Physical Sciences, Inc., Andover, MA)

Electron Beam Growth in N₂

40th Annual Gaseous Electronics Conf., Atlanta, GA (13-16 October 1987)

BLUMBERG, W.A.M., LIPSON, S.J. (AFGL); UPSCHULTE, B.J., HOLTZCLAW, K.W., and GREEN, B.D. (Physical Sciences, Inc., Andover, MA)

LWIR Emissions from OH in Irradiated O₂/H₂ and O₃/H₂

AGU Mtg., San Francisco, CA (5-9 December 1988)

BLUMBERG, W.A.M., MILLER, S.M., LIPSON, S.J. (AFGL); GREEN, B.D., RAWLINS, W.T., FRASER, M.E., HOLTZCLAW, K.W., MARINELLI, W.J., and Upschulte, B.I. (Physical Sciences,

Inc., Andover, MA)

Collisional Excitation and Quenching of Atmospheric Species

AFOSR Molecular Dynamics Conf. Newport Beach, CA (31 Oct-2 Nov 1988)

BROWN, J.H. (AFGL); and GROSSEBARD, N.J. (Boston Coll., Boston, MA)

Short Term Prediction of Optical Turbulence Parameters

SPIE 1988 Tech. Symp. on Optics, Electro-Optics, and Sensors, Orlando, FL (7 April 1988)

DANA, V., VALENTIN, A., HENRY, A., MARGOTTIN-MACLOU, M. (Univ. of Paris, Paris, France); and ROTHMAN, L.S. (AFGL)

Line Intensities and Linewidths of Carbon Dioxide in the 13 μ m Region

High Resolution Molecular Spectroscopy Conf., Univ. of Burgundy, Dijon, France (13-18 September 1987)

DEWAN, E.M.

New Results Concerning the Saturation Explanation of the "Universal" Gravity Wave Spectral Model

Internat. Wkshp. on Gravity Waves and Turbulence in the Middle Atmosphere (GRATMAP), Univ. of Adelaide, Adelaide, Australia (21-23 May 1987)

Statistical Tests for Casual Correlations between Time Series Having Large Autocorrelations: Are Sunspot-Weather Correlations Real?

CEDAR, Boulder, CO (6-10 June 1988)

DEWAN, E.M., and FOUGERE, P.F.

Gravity Waves and the Maximum Entropy Method (MEM) of Power Spectral Analysis

Internat. Wkshp. on Gravity Waves and Turbulence in the Middle Atmosphere (GRATMAP), Univ. of Adelaide, Adelaide, Australia (21-23 May 1987)

DEWAN, E.M., and TUAN, T.F.

On Hydrostatic and Non-Hydrostatic

Changes of Pressure Caused by Atmospheric Gravity Waves

AGU Mtg., San Francisco, CA (5-9 December 1988)

FRASER, M.E., RAWLINS, W.T. (Physical Sciences, Inc., Andover, MA); and MILLER, S.M. (AFGL)

Auroral Chemiexcitation and Infrared Branching Ratios for the Fundamental and First Overtone Vibrational Transitions of NO ($X^2\Pi$, $V < 12$)

AGU Mtg., Baltimore, MD (16-20 May 1988)

FRASER, M.E., RAWLINS, W.T., PIPER, L.G. (Physical Sciences, Inc., Andover, MA); MILLER, S.M., and BLUMBERG, W.A.M. (AFGL)

Dynamics of $E \rightarrow V$, R Energy Transfer: Excitation of $CO(v,J)$ by Metastable Nitrogen
AFOSR Molecular Dynamics Conf., Newport Beach, CA (31 October-2 November 1988)

GAMACHE, R.R. (Univ. of Lowell, Lowell, MA); and ROTHMAN, L.S. (AFGL)

Temperature Dependence of Linewidths and Line Shifts

High Resolution Molecular Spectroscopy Conf., Univ. of Burgundy, Dijon, France (13-18 September 1987)

GARNER, R.C., TROWBRIDGE, C.A., DAVIDSON, G. (Photometrics Inc., Woburn, MA); and Koenig, G.G. (AFGL)

Polarization Studies of Backscattered 532 nm Radiation from Snow Using a Nd:YAG Based LIDAR

14th Internat. Laser Radar Conf., Innichen-San Candido, Italy (20-24 June 1988)

GELB, A., and RAWLINS, W.T. (Physical Sciences, Inc., Andover, MA); and BLUMBERG, W.A.M. (AFGL)

Molecular Dynamics of the $O+O_2$ Interaction: O_3 Formation, Atom Exchanges, and Vibrational Deactivation

AGU Mtg., Baltimore, MD (16-20 May 1988)

GOOD, R.E., MURPHY, E.A., BELAND, R.R., and BROWN, J.H.

A Review of Atmospheric Turbulence Models
SPIE 1988 Tech. Symp. on Optics, Electro-Optics and Sensors, Orlando, FL (4-8 April 1988)

GREEN, B.D., RAWLINS, W.T. (Physical Sciences, Inc., Andover, MA); and MURPHY, R.E. (AFGL)

Mechanisms for Excitation of IR Emission in Strong Aurorae

Symp. on Spectroscopic Emissions Resulting from Energetic Particle Precipitation, Vancouver, Canada (10-21 August 1987)

GREEN, B.D., MARINELLI, W.J., PIPER, L.G. (Physical Sciences, Inc., Andover, MA); and BLUMBERG, W.A.M. (AFGL)

Pressure Dependence of N_2B ($v=0-12$)

Populations

AGU Mtg., Baltimore, MD (16-20 May 1988)

GREEN, B.D., UPSCHULTE, B.L., HOITZCLAW, K.W. (Physical Sciences, Inc., Andover, MA); and BLUMBERG, W.A.M. (AFGL)

Laboratory Studies of the Electron Excitation of Singlet and Triplet Electronic States of N_2
40th Annual Gaseous Electronics Conf., Atlanta, GA (13-16 October 1987)

Spectral Measurements of N_2 Electronic Emission Between 0.8 to 7 Microns

AGU Mtg., San Francisco, CA (6-11 December 1987)

GREEN, B.D., UPSCHULTE, B.L., RAWLINS, W.T. (Physical Sciences, Inc., Andover, MA); and BLUMBERG, W.A.M. (AFGL)

Observation of Infrared Fluorescence from O_3 Created by a Two-Body Process

Symp. on Spectroscopic Emissions Resulting from Energetic Particle Precipitation, Vancouver, Canada (10-21 August 1987)

GREEN, B.D., UPSCHULTE, B.J., HOLTZCLAW, K.W. (Physical Sciences, Inc., Andover, MA); LIPSON, S.J., and

BLUMBERG, W.A.M. (AFGL)

Ozone Infrared Emissions Upon Electron Impact

AGU Mtg., San Francisco, CA (5-9 December 1988)

GROSSBARD, N. (Boston Coll., Chestnut Hill, MA); and RATKOWSKI, A. (AFGL)

Filtering Method for Estimating Amplitudes of Sinusoids of Known Frequency and Phase
4th Wkshp. on Spectrum Estimation and Modeling, Univ. of Minnesota, Minneapolis, MN (3-5 August 1988)

HOKE, M.L. (AFGL); CLOUGH, S.A.

(Atmospheric and Environmental Research, Inc., Cambridge, MA); Lafferty, W., and Olson, B.W. (Natl. Bureau of Standards, Gaithersburg, MD)
Line Coupling in Oxygen and Carbon Dioxide

Internat. Radiation Symp., Lille, France (18-24 August 1988)

HOWARD, S.J.

Minimum-Negativity Constraint Applied to Large Data Sets

1987 Optical Society of America Annual Mtg., Rochester, NY (18-23 October 1987)

HUMMEL, J.R. (Optimetrix, Inc., Burlington, MA); SHETTLE, E.P. (AFGL); and LONGTIN, D.R. (Optimetrix, Inc., Burlington, MA)

A New Background Stratospheric Aerosol Formulation for Use in Modeling the Radiative Characteristics of the Atmosphere
AGU Mtg., San Francisco, CA (5-9 December 1988)

HUPPI, E.R.

Cryogenic Instrumentation and Detector Limits in FTS

6th Internat. Conf. on Fourier Transform Spectroscopy, Vienna, Austria (24-18 August 1987)

HUSAR, R.B., HUSAR, J.D., GOLENKO, F. (Washington Univ., St. Louis, MO);

Shettle, E.P. (AFGL); and WILSON, W.E. (U.S. Environmental Protection Agency, Washington, DC)

Aerosol Climate of North America and Europe

12th Internat. Conf. on Atmospheric Aerosols and Nucleation, Vienna, Austria (22-27 August 1988)

ISLER, J., TUAN, T.F. (Univ. of Cincinnati, Cincinnati, OH); PICARD, R.H. (AFGL); LIN, P.L. (National Central Univ., Taiwan, China); and MAKHIOUF, U. (Univ. of Cincinnati, Cincinnati, OH)

Perturbation Treatment of Nonlinear Airglow Response to a Linear Gravity Wave

AGU Mtg., San Francisco, CA (5-9 December 1988)

LEVAN, P. D. (AFGL); and SLOAN, G. (Univ. of Wyoming, Laramie, WY)

Calibration and Data Reduction Techniques for AFGL Astronomical IR Array Spectrometer

SPIE 1987 Tech. Symp. on Optics, Electro-Optics, and Sensors, San Diego, CA (19 August 1987)

LEVAN, P.D., and TANDY, P.C.

AFGL Ten Micron Array Spectrometer

Ground-Based Astronomical Observations with Infrared Arrays, Univ. of Hawaii, Hilo, HI (24-26 March 1987)

AFGL Mosaic Array Spectrometer

172nd Mtg. of American Astronomical Society, Kansas City, MO (5-9 June 1988)

LITTLE, S.J. (Bentley Coll., Waltham, MA); LITTLE-MARENIN, I.R., and PRICE, S.D. (AFGL)

Emission Features in IRAS LRS Spectra of MS, S and CS Stars

5th Cambridge Wkshp. on Cool Stars, Stellar Systems and the Sun, Boulder, CO (8-11 July 1987)

LITTLE-MARENIN, I.R. (AFGL); BENSON, P.J. (Wellesley Coll., Wellesley, MA); and

DICKINSON, D.F. (Lockheed Palo Alto Research Laboratory, Palo Alto, CA)
Water Masers Around Two Short Period Miras: R CETI and RZ SCORPII
 Haystack Observatory, Westford, MA (10-13 June 1987)

LITTLE-MARENIN, I.R. (AFGL); BENSON, P.J. (Wellesley Coll., Wellesley, MA); and LITTLE, S.J. (Bentley Coll., Waltham, MA)
Water Masers Associated with Two Carbon Stars: EU Andromedae and V778 CYGNI
 5th Cambridge Wkshp. on Cool Stars, Stellar Systems and the Sun, Boulder, CO (8-11 July 1987)

LONGTIN, D.R. (Optimetrix, Inc., Burlington, MA); SHETTLE, E.P. (AFGL); HUMMEL, J.R. and PRYCE, J.D. (Optimetrix, Inc., Burlington, MA)
A Desert Aerosol Model for Radiative Transfer Studies
 XIX IUGG Gen. Assbly. Vancouver, Canada (9-22 August 1987)

MARINELLI, W.J., GREEN, B.D. (Physical Sciences, Inc., Andover, MA); and BLUMBERG, W. A. M. (AFGL)
Electron Excitation and Intersystem Quenching of $N_2(a^1 \Pi_g)$ by N_2
 18th Annual Mtg. of the Division of Atomic, Molecular, and Optical Physics of the American Physical Society, Cambridge, MA (18-20 May 1987)

MARINELLI, W.J., KESSLER, W.J., GREEN, B.D. (Physical Sciences, Inc., Andover, MA); and BLUMBERG, W.A.M. (AFGL)
Quenching of $N_2(a^1 \Pi_g, v = 0)$
 AGU Mtg., San Francisco, CA (7-11 December 1987)

MILLER, S.M., BLUMBERG, W.A.M. (AFGL); FELL, C.P., and STEINFELD, J.I. (MIT, Cambridge, MA)
Rate Constants for the Quenching of N^ by $O(^3P)$*

AGU Mtg., San Francisco, CA (5-9 December 1988)

MURCRAY, F.J., MURCRAY, F.H., MURCRAY, D.G., KOSTERS, J., WILLIAMS, J. (Univ. of Denver, Denver, CO); and VANASSE, G.A. (AFGL)

Observation of Upwelling Radiation by SCRIBE
 6th Internat. Conf. on Fourier Transform Spectroscopy, Vienna, Austria (24-28 August 1987)

MURPHY, E.A., BELAND, R.R., BROWN, J.H., and THOMAS, P.J.
Scintillation and Turbulence Measurements over a Range of Meteorological Conditions
 SPIE 1988 Tech. Symp. on Optics, Electro-Optics, and Sensors, Orlando, FL (4-8 April 1988)

NEBEL, H. (Alfred Univ., Alfred, NY); SHARMA, R.D. (AFGL); and WINTERSTEINER, P.P. (Arcon Corp., Waltham, MA)
Night-Time $CO_2(OO1)$ Vibrational Temperatures in the 50 to 150 km Altitude Range
 AGU Mtg., San Francisco, CA (6-11 December 1987)

NEBEL, H., SHARMA, R.D., WINICK, J.R., PICARD, R.H. (AFGL); WINTERSTEINER, P.P., and JOSEPH, R.A. (Arcon Corp., Waltham, MA)
 $CO_2(OO1)$ Vibrational Temperatures and Limb-View Infrared Radiances Under Terminator Conditions in the 60-120 km Altitude Range
 AGU Mtg., San Francisco, CA (5-9 December 1988)

PICARD, R.H., and SHARMA, R.D.
Nonequilibrium IR Emissions from the Mesosphere and Thermosphere
 SPIE 1988 Tech. Symp. on Optics, Electro-Optics, and Sensors, Orlando, FL (4-8 April 1988)

PICARD, R.H., WINICK, J.R. (AFGL);
JOSEPH, R.A., and WINTERSTEINER, P.P.
(Arcon Corp., Waltham, MA)

*Infrared 4.3 μm Radiance from the Auroral
Thermosphere*

AGU Mtg., San Francisco, CA (7-11
December 1987)

PIPER, L.G., HOLTZCLAW, K.W., GREEN,
B.D. (Physical Sciences, Inc., Andover,
MA); and BLUMBERG, W.A.M. (AFGL)

*Experimental Characterization of the
Einstein Coefficients for the $N_2(B-A)$
Transition*

40th Annual Gaseous Electronics Conf
Atlanta, GA (13-16 October 1987)

*Re-Evaluation of the Radiative Lifetimes for
 $N_2(B)$ and $N_2(A)$*

AGU Mtg., Baltimore, MD (16-20 May 1988)

PRICE, S.D., LEVAN, P.D. (AFGL);
KENNEALY, J. and KORTE, R. (Mission
Research Corp., Nashua, NH);
GONSALVES, R., and LYONS, T. (Tufts
Univ., Medford, MA)

IRAS Image Reconstruction and Restoration

4th Internat. Symp. on Optical and
Optoelectronic Applied Science and
Engineering, The Hague, Netherlands (30
March-3 April 1987)

RAWLINS, W T., FRASER, M.E. (Physical
Sciences, Inc., Andover, MA); BLUMBERG,
W.A.M., and MILLER, S.M. (AFGL)

*Observation of Aurorally Excited Infrared
Emission from Molecular Nitrogen*

AGU Mtg., Baltimore, MD (16-20 May 1988)

ROTHMAN, L.S.

*The Evolution of the Spectroscopic Database
for High Resolution Modeling*

Internat. Radiation Symp., Lille, France (18-
24 August 1988)

*The Spectroscopic Database for High
Resolution Atmospheric Modeling*

10th Internat. Conf. on High Resolution
Infrared Spectroscopy, Prague,
Czechoslovakia (5-9 September 1988)

SPIE 1988 Tech. Symp. on Optics, Electro
Optics, and Sensors, Orlando, FL (4-8 April
1988)

ROTHMAN, L.S., HAWKINS, R. (AFGL); and
GAMACHE, R.R. (Univ. of Lowell, Lowell,
MA)

*Simplified Expression for the Total Internal
Partition Sum as a Function of Temperature*

43rd Symp. of Molecular Spectroscopy, Ohio
State Univ., Columbus, OH (13-17 June 1988)

ROTHMAN, L.S., HAWKINS, R. (AFGL); and
WATTSON, R.B. (Visidyne, Inc.,
Burlington, MA)

*CO_2 Spectroscopic Constants Determined by
Global Least-Square Fitting and Direct
Numerical Diagonalization*

43rd Symp. of Molecular Spectroscopy, Ohio
State Univ., Columbus, OH (13-17 June 1988)

ROTHMAN, L.S. (AFGL); WATTSON, R.B.,
NEWBURGH, A., PAVELLE, R. (Visidyne,
Inc., Burlington, MA)

*Calculations of Energies and Intensities for
the Asymmetric Species of CO_2*

43rd Symp. of Molecular Spectroscopy, Ohio
State Univ., Columbus, OH (13-17 June 1988)

SHARMA, R.D.

Filling of the Atmospheric Transmission

*Window Due to Emission from Very High
Rotational Levels of NO and O_3*

Background Symp., Monterey, CA (February
1988)

SHARMA, R.D. (AFGL); BAKSHI, P.M.
(Boston College, Chestnut Hill, MA); and
SINDONI, J.M. (Yap Analytics, Inc.,
Lexington, MA)

*Impulse Approximation (Quantum
Mechanical Spectator Model) for Atom-
Molecule Collisions*

AFOSR Molecular Dynamics Contractors
Mtg., Newport Beach, CA (30 Oct-2 Nov
1988)

SHARMA, R.D., PICARD, R.H., WINICK, J.R.

(AFGL); WINTERSTEINER, P.P., PABOOJIAN, A. (Arcon Corp., Waltham, MA); and YAP, B.K. (Yap Analytics, Inc., Lexington, MA)
Modelling of Mesospheric Infrared Limb Emission Around 6 μ m Observed by SPIRE
 AGU Mtg., San Francisco, CA (7-11 December 1987)

SHEATTLE, E.P.

Impact of Atmospheric Aerosols in Air Force Operations and the Need for Satellite Based Measurements

NOAA/NESDIS Wkshp. on NOAA Satellite Aerosol Products, Camp Springs, MD (25-26 April 1988)

SHEATTLE, E.P. (AFGL); and TRAKHOVSKY, E. (Technion-Israel Inst. of Tech., Haifa, Israel)

On the Scaling of Atmospheric Aerosol Scattering and Extinction with Wavelengths
 IUGG 19th Gen. Assbly., Vancouver, Canada (9-22 August 1987)

SHEATTLE, E.P. (AFGL); and WARREN, S.G. (Univ. of Washington, Seattle, WA)

Radiative Properties of Cirrus Clouds and the Uncertainties in the Optical Constants of Ice

AGU Mtg. San Francisco, CA (5-9 December 1988)

TUAN, T.F., ISLER, J. (Univ. of Cincinnati, Cincinnati, OH); PICARD, R.H. (AFGL); and MAKHLOUF, U. (Univ. of Cincinnati, Cincinnati, OH)

On the Nonlinear Airglow Response to a Linear Gravity Wave

AGU Mtg., San Francisco, CA (5-9 December 1988)

TURNER, V.D., and KOENIG, G.G.

Atmospheric Scintillation Measurements with a Transmissometer

SPIE 1988 Tech. Symp. on Optics, Electro-Optics, and Sensors, Orlando, FL (4-8 April 1988)

UPSCHULTE, B.L., GREEN, B.D., WOLNIK, S.J., CLAWSON, M.J., CARINS, K., RAWLINS, W.T., CALEDONIA, G.E. (Physical Sciences, Inc., Andover, MA); and BLUMBERG, W.A.M. (AFGL)

Investigations of Ozone: Two Body Production and Vibrational Relaxation
 AGU Mtg., San Francisco, CA (7-11 December 1987)

VANTASSEL, R.A. (AFGL); and WONG, W.K. (SSG, Inc., Waltham, MA)

Signal-to-Noise Characteristics of Photodiode Array Fourier Transform Spectrometers

6th Internat. Conf. on Fourier Transform Spectroscopy, Vienna, Austria (24-28 August 1987)

VOLZ, F.E.

Optical Investigations of Forest Fire Smoke
 Annual Mtg. of Optical Society of America, Rochester, NY (18-23 October 1987)

VOLZ, F.E. (AFGL); and LONGTIN, D. (Optimetrix, Inc., Burlington, MA)

Neutral Points and Twilight Color Ratios after the El Chichon Eruption

Annual Mtg. of Optical Society of America, Rochester, NY (18-23 October 1987)

WARNOCK, J.M. (NOAA, Boulder, CO); BROWN, J.H. (AFGL); CLARK, W.L. (NOAA, Boulder, CO); EATON, F.D. (Atmospheric Sciences Laboratory, White Sands Missile Range, NM); GAGE, K.S., GREEN, J.L. (NOAA, Boulder, CO); HINES, J.R. (Atmospheric Sciences Laboratory, White Sands Missile Range, NM); MURPHY, E.A. (AFGL); NASTROM, G.D. (St. Cloud Univ., St. Cloud, FL); and VANZANDT, T.E. (NOAA, Boulder, CO)

Comparisons of C_n^2 Measurements Made with the Flatland VHF Radar with Other Measurement Techniques and Model Estimates

4th Mesosphere/Stratosphere/Thermosphere

Radar Wkshp., Kyoto, Japan (29 November-2 December 1988)

WATTSON, R.B. (Visidyne, Inc., Burlington, MA); and ROTHMAN, L.S. (AFGL)

The Extension of Direct Numerical Diagonalization for the Determination of the Infrared Properties of Hot Carbon Dioxide
High Resolution Molecular Spectroscopy Conf., Univ. of Burgundy, Dijon, France (13-18 September 1987)

WINICK, J.R., PICARD, R.H. and BLUMBERG, W.A.M.

Data Needs for Modeling the Infrared Radiance from the Upper Atmosphere
AFOSR Molecular Dynamics Contractors Conf., Newport Beach, CA (30 October-2 November 1988)

WINICK, J.R., PICARD, R.H. (AFGL); WINTERSTEINER, P.P. and PABOOJIAN, A.J. (Arcon Corp., Waltham, MA)

NLTE CO Infrared Emission in the Upper Mesosphere and Lower Thermosphere and its Effect on Remote Sensing
AGU Mtg., San Francisco, CA (5-9 December 1988)

WINICK, J.R., NEBEL, H. (Alfred Univ., Alfred, NY); SHARMA, R.D., PICARD, R.H. (AFGL); WINTERSTEINER, P.P., and JOSEPH, R.A. (Arcon Corp., Waltham, MA)

Modeling CO NLTE Infrared Radiation in the Upper Mesosphere and Lower Thermosphere
AGU Mtg., San Francisco, CA (7-11 December 1987)

WINTERSTEINER, P.P. (Arcon Corp., Waltham, MA); SHARMA, R.D., WINICK, J.R., and PICARD, R.H. (AFGL)
Determination of CO₂ ν₂ Vibrational Temperatures Using a New Algorithm for Line-by-Line Radiative Transfer
AGU Mtg., San Francisco, CA (5-9 December

1988)

ZACHOR, A.S. (Atmospheric Radiation Consultants, Inc., Acton, MA); and Sharma, R.D. (AFGL)

Simultaneous Retrieval of Atomic Oxygen and Temperature by an IR Limb Scanning Technique

Internat. Wkshp. on Remote Sensing Retrieval Methods, Williamsburg, VA (15-18 December 1987)

TECHNICAL REPORTS

1987-1988

BAROWY, W.M., ESPLIN, M.P. (Stewart Radiance Lab., Bedford, MA); VANASSE, G.A. (AFGL); and HUPPI, R.J. (Stewart Radiance Lab., Bedford, MA)

Medium- and Long-Wave Infrared Absorption Spectra of Carbon Dioxide and Nitrous Oxide at 800K

AFGL-TR-87-0016 (8 January 1987), ADA179430

ESPLIN, M.P., BAROWY, W.M., HUPPI, R.J. (Stewart Radiance Lab., Bedford, MA); ROTHMAN, L.S., and VANASSE, G.A. (AFGL)

High Resolution Infrared Spectroscopy of Carbon Dioxide and Nitrous Oxide at Elevated Temperatures

AFGL-TR-88-0067 (11 March 1988), ADA196317

LONGTIN, D.R. (Optimetrix, Inc., Burlington, MA); and VOLZ, F.E. (AFGL)
Sky Polarization Data for Volcanic and Nonvolcanic Periods

AFGL-TR-86-0223 (October 1986), A0A188862

SUNDBERG, R.L., ROBERTSON, D.C. (Spectral Sciences, Inc., Burlington,

MA); SHARMA, R.D., and RATKOWSKI, A.J. (AFGL)

HAIRM-87: A High Altitude Infrared Radiance Model

AFGL-TR-88-0014 (14 January 1988), A0A197673

WINICK, J.R., PICARD, R.H., JOSEPH, R.A., SHARMA, R.D. (AFGL); and WINTERSTEINER, P.P. (Arcon Corp., Waitham, MA)

An Infrared Spectral Radiance Code for the Auroral Thermosphere (AARC)

AFGL-TR-87-0334 (24 November 1987), ADA202432

CONTRACTOR PUBLICATIONS 1987-1988

ADAMS, G.W., BROSNAN, J.W., and HALDERMAN, T.D. (Utah State Univ., Logan, UT)

Direct Radar Observations of TID's in the D and E Regions

J. Atmos. Terr. Phys. 50 (1988)

ADAMS, G.W., PETERSON, A.W., BROSNAN, J.W., and NEUSCHAEFER, J.W. (Utah State Univ., Logan, UT)

Radar and Optical Observations of Mesospheric Wave Activity during the Eclipse of 6 July 1982

J. Atmos. Terr. Phys. 50 (1988)

FOX, J.L. (State Univ. of New York, Stonybrook, NY); and VICTOR, G.A. (Harvard-Smithsonian Ctr. for Astrophys., Cambridge, MA)

Electron Energy Deposition in N₂ Gas Planet. Space Sci. 36 (1988)

LI, L., LIPERT, R.J., LOBUE, J., CHUPKA, W.A., and COISON, S.D. (Yale Univ., New Haven, CT)

Adiabatic Dissociation of Photoexcited Chlorine Molecules

Chem. Phys. Lett. 151 (1988)

LI, L., LIPERT, R.J., PARK, H., CHUPKA, W.A., and COISON, S.D. (Yale Univ., New Haven, CT)

Dynamics and Spectroscopic Manifestations of Two-Photon Bound-Bound Absorption Through a Repulsive Intermediate State

J. Chem. Phys. 87 (1988)

Spectroscopy and Photophysics of ¹I_g and ³I_g Rydberg, Ion-Pair States of Cl₂

Revealed by Multiphoton Ionization

J. Chem. Phys. 88 (1988)

MILLER, P.J., LI, L., CHUPKA, W.A., and Colson, S.D. (Yale Univ., New Haven, CT)

Observation of Strong Rydberg-Valence

Mixing in the E³ E⁻u State of O₂ by 3+1 MPI Photoelectron Spectroscopy

J. Chem. Phys. 88 (1988)

Shape Resonance and Non-Franck-Condon Behavior in the Photoelectron Spectra of O₂ Produced by (2+1) MPI via 3s σ Rydberg States

J. Chem. Phys. 89 (1988)

MORRILL, J., CARRAGHER, B.A., and Benesch, W. (Univ. of Maryland, College Park, MD)

Population Development of Auroral Molecular Nitrogen Species in a Pulsed Electric Discharge

J. Geophys. Res. 93 (1988)

PARK, H., MILLER, P.J., CHUPKA, W.A., and COLSON, S.D. (Yale Univ., New Haven, CT)

Multiphoton Optical and Photoelectron Spectroscopy of the 4s-3d and 5s-4d Rydberg Complexes of O₂; Production of Vibrationally State-Selected O₂ via Newly Discovered 4s-3d and 5s-4d Rydberg States of O₂

J. Chem. Phys. 89 (1988)

PIPER, L.G. (Physical Sciences, Inc.,

Andover, MA)

State-to-State N₂ (A₃ Eu) Energy Pooling Reactions: II The Formation and Quenching of N₂ (B₃ Π g, $v'=1-12$)

J. Chem. Phys. 88 (1988)

PIPER, L.G., and MARINELLI, W.J.
(Physical Sciences, Inc., Andover, MA)

Determination of Non-Boltzmann Vibrational Distributions of N₂ (X,V'') in He/N₂ Microwave Discharge Afterglows

J. Chem. Phys. 89 (1988)

RALL, R.I., SHARPTON, F.A., and LIN, C.C.
(Univ. of Wisconsin, Madison, WI)

Excitation of Emission Lines of Atomic Nitrogen Ion by Electron-Impact Dissociative Ionization of

J. Chem. Phys. 89 (1988)

SCHAPPE, R.S., SCHULMAN, M.B.,
SHARPTON, F.A., LIN, C.C. (Univ. of Wisconsin Madison, WI)

Emission of the O₂+(A₂ Π_u -X² Π g) Second Negative System, Produced by Electron-Impact on O₂

Phys. Rev. A 38 (1988)

STEINFELD, J.I. (MIT, Cambridge, MA);
ADLER GOLDEN, S.M. (Spectral Sciences, Inc., Burlington, MA); and GALLAGHER, J.W. (Natl. Bur. Standards, Boulder, CO)

Critical Survey of Data on the Spectroscopy and Kinetics of Ozone in the Mesosphere and Thermosphere

J. Chem. Ref. Data 16 (1987)

TAYLOR, M.J., and HAPGOOD, M.A. (Univ. of Southampton, Southampton, UK)

Identification of a Thunderstorm as a Source of Short Period Gravity Waves in the Upper Atmospheric Nightglow Emissions

Planet. Space Sci. 36 (1988)

TAYLOR, M.J., HAPGOOD, M.A., and ROTHWELL, P. (Univ. of Southampton, Southampton, UK)

Observation of Gravity Wave Propagation in

the OI (557.7 nm), Na (589.2 nm) and the near Infrared OH Nightglow Emissions
Planet. Space Sci. 35 (1987)

THOMAS, J.M., KAUFMAN, F., and GOLDE, M.F. (Univ. of Pittsburgh, Pittsburgh, PA)

Rate Constants for Electronic Quenching of N₂(A³ Σ μ^+ , $v=0-6$) by O₂, NO, CO, N₂O, and C₂H₄

J. Chem. Phys. 86 (1987)

TURNBULL, D.N., and LOWE, R.P. (Univ. of Western Ontario, London, Ontario, Canada)

An Empirical Determination of the Dipole Moment Function of OH

J. Chem. Phys. 89 (1988)

WANG, D.Y., and TUAN, T.F. (Univ. of Cincinnati, Cincinnati, OH)

Brunt-Doppler Ducting of Small-Period Gravity Waves

J. Geophys. Res. 83 (1988)

CONTRACTOR PRESENTATIONS 1987-1988

BASHKIN, S. (Univ. of Arizona, Tucson, AZ)

Excitation of Nitrogen by Energetic Particles
Tenth Conf. on the Applications of Accelerators in Research and Industry, Denton, TX (7-9 November 1988)

BASHKIN, S., LI, M.L., LIN, P.C., THIEDE, D.A., and JENKINS, D.G. (Univ. of Arizona, Tucson, AZ)

Excitation of Oxygen by Ion Bombardment
1st Asia-Pacific Conf. on Atomic and Molecular Phys., Taipei, Taiwan (24-30 November 1988)

FRASER, M.E., TUCKER, T.R., PIPER, L.G.,

and RAWLINS, W.T. (Physical Sciences, Inc., Andover, MA)
Mechanisms of N_2O Formation
 AGU Mtg., San Francisco, CA (7-11 December 1987)

GONSALVES, R.A., KORTE, R.M., and KENNEALY, J.P. (Mission Research Corp., Nashua, NH)
Entropy-Based Image Restoration: Modifications and Additional Results
 31st Annual Internat. Tech. Symp. on Optical and Optoelectronic Applied Science and Engineering, San Diego, CA (16-21 August 1987)

KAM, A.W., LAWALL, J.R., LINDSAY, M.D., PIPKIN, F.M., and ZHAO, P. (Harvard Univ., Cambridge, MA)
Laser-Molecular Beam Study of the $c_4(3)^1 \Sigma_u^+$ Rydberg State of N_2
 APS An. Mtg. of the Div. of Atomic, Molecular, and Optical Phys., Baltimore, MD (18-20 April 1988)

KAM, A.W., LINDSAY, M.D., PIPKIN, F.M., SHORT, R.C., and ZHAO, P. (Harvard Univ., Cambridge, MA)
Molecular Beam Study of Singlet Rydberg States of N_2
 APS An. Mtg. of the Div. of Atomic, Molecular, and Optical Phys., Cambridge, MA (18-20 May 1987)

KANE, T.J., and WALLACE, R.W. (Lightwave Electronics Corp., Mountain View, CA)
Performance of Diode-Pumped TM:H0:YAG Laser at Temperatures Between -55 and +20 C
 Conf. on Lasers and Electro-Optics, Anaheim, CA (29 April 1988)

KENNEALY, J.P., KORTE, R.M. (Mission Research Corp., Nashua, NH); GONSALVES, R.A., LYONS, T.D. (Tufts Univ., Medford, MA); PRICE, J.D., LEVAN, P.D. (AFGL); and AUMANN, H.H. (Jet

Propulsion Lab., Pasadena, CA)
IRAS Image Reconstruction and Restoration, Advances in Image Processing, The Hague, The Netherlands (31 March- 3 April 1987)

MAKHLOUF, U., YANG, D.Y., LIN, J.J., and Tuan, T.F. (Univ. of Cincinnati, Cincinnati, OH)
The Effects of Different Gravity-Wave Models and Horizontal Winds on the Mesospheric Emissions
 AGU Mtg., San Francisco, CA (7-11 December 1987)

PIPER, L.G., CUMMINGS, W.P. (Physical Sciences, Inc., Andover, MA)
Characterization of Metastable Nitrogen in the Effluents of Ozonizer Type Discharge
 40th Annual Gaseous Electronics Conf., Atlanta, GA (13-16 October 1987)

PIPER, L.G., HOLTZCLAW, K.W., GREEN, B.D. (Physical Sciences, Inc., Andover, MA)
Experimental Characterization of the Einstein Coefficients for the $N_2(B-A)$ Transition
 40th Annual Gaseous Electronics Conf., Atlanta, GA (13-16 October 1987)

SAPPEY, A.D., CROSLEY, D.R., COPELAND, R.A. (SRI International, Menlo Park, CA)
Laser-Induced Fluorescence in the $B^2\Sigma^+ - x^2\Pi$ System of OH
 Fourth Internat. Laser Science Conf., Atlanta, GA (2-6 October 1988)

WATSON, R.B. (Visidyne, Inc., Burlington, MA)
Studies Concerning the Optimum Hamiltonian for Use In Large Amplitude, Direct Numerical Diagonalization Calculations
 43rd Symp of Molecular Spectroscopy, Ohio State Univ, Columbus, OH (13-17 June 1988)

CONTRACTOR TECHNICAL REPORTS 1987-1988

BERKOFISKY, L. (Ben-Gurion Univ., Beersheva, Israel); LEVIN, Z. (Tel-Aviv Univ., Tel Aviv, Israel); COHEN, A. (Hebrew Univ. of Jerusalem, Israel); OPPENHEIM, U. (Israel Inst. of Tech., Haifa, Israel); and KOPEIKA, N. (Ben-Gurion Univ., Beersheva, Israel)

The Effect of Meteorological Conditions on Transmission of Radiation and Imaging Through Natural Dusty Environments
AFGL-TR-87-0119 (31 July 1986),
ADA183539

BERNSTEIN, L.S. (Spectral Sciences, Inc., Burlington, MA)

Non-Equilibrium Molecular Emission and Scattering Intensity Subroutine (NEMESIS) Vol. 1
AFGL-TR-88-0124 (5 April 1988),
ADA199295

BIEN, F., ADLER-GOLDEN, S.M., and GOLDSTEIN, N.M. (Spectral Sciences, Inc., Burlington, MA)

Study of Polyatomic Dynamics in the Atmosphere
AFGL-TR-87-0223 (25 March 1987),
ADA190964

EVANS, J.E., KUMER, J.B., and SEARS, R.D. (Lockheed, Palo Alto, CA)

Models of Infrared Auroral Structures
AFGL-TR-86-0024 (1 October 1985),
ADA177406

FOX, J.L. (Utah State Univ., Logan UT)

Studies of Infrared Aurorae
AFGL-TR-87-0010 (3 November 1986),
ADA179539

GALLERY, W.O., FARMER, D.A., and LONGTIN, D.R. (Optimetrics, Inc., Burlington, MA)

Validation of the OPAQUE Data from the US/FRG Meppen Site: Sept. 1978 to March

1980

AFGL-TR-86-0112 (13 May 1986),
ADA180268

GALLERY, W.O., LONGTIN, D.L., and TUCKER, G. (Optimetrics, Inc., Burlington, MA)

SCRIBE Data Survey and Validation
AFGL-TR-87-0061 (16 February 1987),
ADA183538

GALLERY, W.O., MANNING, J.L., and TUCKER, D. (Optimetrics, Inc., Burlington, MA)

Enhancements to the Atmospheric Transmittance/Radiance Program FAS-CODE
AFGL-TR-87-0207 (16 February 1987),
ADA188863

GALLON, D.W., and HUMMEL, J.R. (Optimetrics, Inc., Burlington, MA)

Review of Inversion Techniques for Spaceborne Lidar System
AFGL-TR-86-0266 (December 1986),
ADA184164

GAMACHE, R.R. (Univ. of Lowell, Lowell, MA)

Calculation of Molecular Absorption Parameters and Updating the AFGL Atmospheric Line Parameter Compilation
AFGL-TR-88-0228 (15 September 1988),
ADA202113

GOLDE, M.F. (Optimetrics, Inc., Burlington, MA)

Effect of Vibrational Excitation on Rate Parameters of Atmospheric Reactions
AFGL-TR-87-0262 (23 September 1987),
ADA190464

HAYCOCK, R.H., THURGOOD, V.A., STEED, A.J., and HARRIS, C.R. (Utah State Univ., Logan UT)

Catalog of High Resolution Infrared Spectra: Field-Widened Interferometer Payload: Sergeant A30-276 - Launched 13 April 1983

AFGL-TR-85-0161 (26 June 1985),

ADA197181

*Catalog of Low Resolution Infrared Spectra:
Field-Widened Interferometer Payload:*

Sergeant A30-276 - Launched 13 April 1983

AFGL-TR-85-0162 (26 June 1985),

ADA181164

HERSCHBACH, D.R. (Harvard Univ.,
Cambridge, MA)

Crossed Molecular Beam Studies

AFGL-TR-87-0210 (April 1987), ADA183166

IP, P.C.F., ARMSTRONG, R.A. (Mission
Research Corp., Nashua, NH); and
BAIRD, J. C. (Brown Univ., Providence,
RI)

*Investigation of Laser-Induced Plasma
Processes*

AFGL-TR-87-0052 (30 December 1986),

ADA190463

KAPLAN, L.D., ISAACS, R.G., and
WORSHAM, R.D. (Atmospheric and
Environmental Research, Inc.,
Cambridge, MA)

*Spectroscopic and Retrieval Studies in
Support of SCRIBE*

AFGL-TR-87-0084 (8 March 1987),

ADA184037

KEBSCHULL, K.A., and HUMMEL, J.R.
(OptiMetrics, Inc., Burlington, MA)

*Analysis of the Scattering and Extinction
Properties of Atmospheric Particulates from
the FTD Field Measurement Program*

AFGL-TR-87-0324 (20 November 1987),

ADA202114

KOLB, C.E., ZAHNISER, M.S., and LYONS,
R.B. (Utah State Univ., Logan UT)
*Assessment of Excitation Mechanisms and
Temporal Dependencies of Infrared
Radiation from Vibrationally Excited Carbon
Monoxide and Ozone in EXCEDE
Experiments*

AFGL-TR-87-0129 (31 March 1987),

ADA182930

NEAL, P.C. (Utah State Univ., Logan UT)
*High-Resolution Measurements of OH
Infrared Airglow Structure*

AFGL-TR-85-0261 (18 October 1985),

ADA181247

PARKINSON, W.H., YOSHINO, K., and
FREEMAN, D.E. (Smithsonian Inst.,
Cambridge, MA)

*Absolute Absorption Cross Section
Measurements of Ozone and the Temperature
Dependence at Four Reference Wavelengths
Leading to Renormalization of the Cross
Section Between 240 and 350 nm*

AFGL-TR-88-0161 (March 1988) ADA199737

PIERLUISSI, J.H., and MARAGOUidakis,
C.E. (Univ. of Texas at El Paso, El Paso,
TX)

*Molecular Transmission Band Models for
LOWTRAN*

AFGL-TR-86-0272 (31 December 1986),

ADA180655

PIPKIN, F.M. (Harvard Univ., Cambridge,
MA)

*Study of Energy Levels and Decay
Mechanisms for Singlet Rydberg States of
Molecular Nitrogen*

AFGL-TR-87-0274 (15 September 1987),

ADA192505

REES, D. (Univ. Coll., London, UK)
Components of an Atmospheric Lidar System

AFGL-TR-88-0031 (30 November 1987),

ADA193366

REGAN, F.C., JR. (Systems Integration
Engin., Lexington, MA)

Technical Support for Optical Turbulence

AFGL-TR-88-0269 (26 September 1988),

ADA204776

RICHARDS, E.N., DELAY, S.H., and
GRIEDER, W.F. (Utah State Univ., Logan,
UT)

AR Methods for Spectral Estimation from

Interferograms

AFGL-TR-87-0008 (19 September 1986),
ADA183676

SHIVANANDAN, K. (Naval Res. Lab.,
Washington, DC)

*Far Infrared Imaging Spectrometer for Large
Aperture Infrared Telescope System* AFGL-
TR-88-0144 (December 1985), ADA201652

SHULER, M.P., JR. (HSS, Inc., Bedford,
MA)

*Operation Manual for the Multiwavelength
Abridged Nephelometer*
AFGL-TR-88-0002 (30 November 1987),
ADA204297

STEINFELD, J., WINKLER, I., PHILLIPS,
C.M., SCHWEITZER, E., STACHNIK, R., and
VANZOEREN, C. (Massachusetts Inst. of
Tech., Cambridge, MA)

*Formation and Deactivation of Vibrationally
Excited Atmospheric Molecules*
AFGL-TR-86-0116 (27 May 1986),
ADA177410

TUAN, T.F. (Univ. of Cincinnati,
Cincinnati, OH)

*An Investigation of Atmospheric Dynamics
Through Their Effects on Mesospheric
Optical Emission*
AFGL-TR-87-0263 (23 March 1987),
ADA193367

WOLF, E. (Univ. of Rochester, Rochester,
NY)

*Coherence Effects in Optical Physics With
Special Reference to Spectroscopy*
AFGL-TR-88-0006 (January 1988),
ADA189520

WORMHOUDT, J., and BROWN, R.C.
(Teledyne Research, Inc., Billerica, MA)

*Molecular Line Shape Effects on
Atmospheric Window Absorption*
AFGL-TR-88-0108 (March 1988), ADA196516

YAP, B.K. (Utah State Univ., Logan, UT)

Atmospheric Radiance Profile Codes

AFGL-TR-87-0009 (17 September 1987),
ADA179258

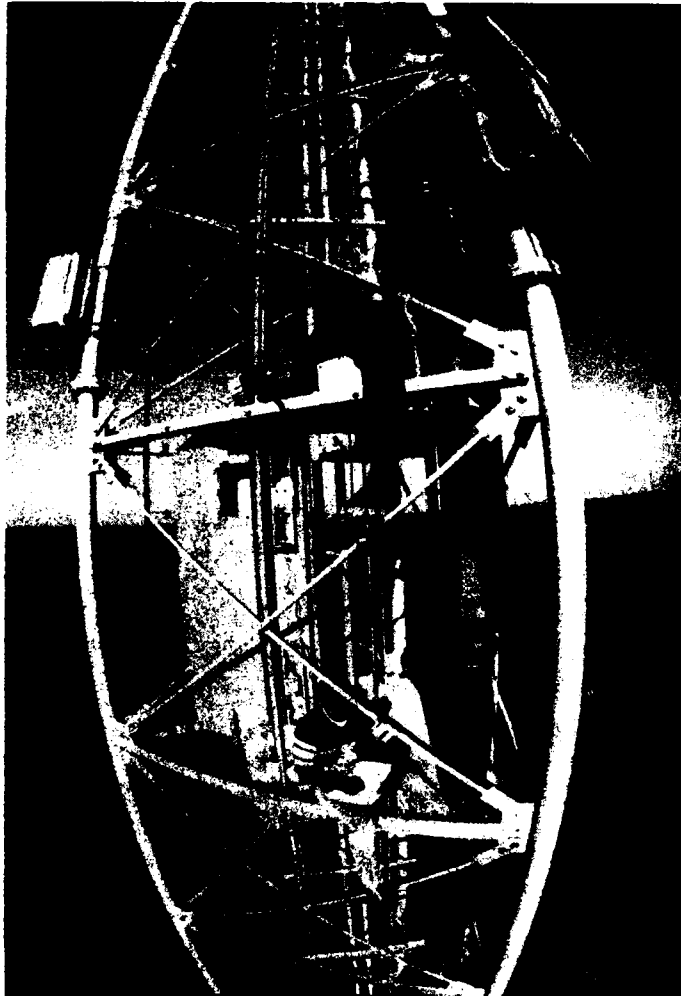
MEM Resolution of Line Spectra

AFGL-TR-87-0133 (23 March 1987),
ADA182860

ZACHOR, A.S., and SMITH, D.S. (Utah
State Univ., Logan, UT)

*A Study of the Maximum Entropy Method of
Power Spectrum Estimation as Applied to
Interferometer Data*

AFGL-TR-86-0162 (17 November 1986),
A0A179403



Laboratory researchers SMSgt Roger Sands and Mr. Anestis Romaides perform fifth-force gravity measurements on a 2000 ft TV tower near Raleigh, NC. (Courtesy of the National Geographic Society)

VI EARTH SCIENCES DIVISION

The Earth Sciences Division performs research in seismology, geodynamics, geology, geodesy, and gravity. This research supports the deployment, operations, and delivery of Air Force weapons with particular emphasis on strategic systems. It also supports the Air Force's mission to monitor compliance with nuclear test ban treaties. Instrumentation is designed and produced to measure geophysical phenomena worldwide at varying scales and accuracy levels to meet specific needs. Field work is conducted whenever and wherever necessary. Instrumentation is mounted on a variety of test beds designed to operate on land, in the air, or in space, and data are collected where the organization's experience and theory suggest the need. Theoretical models of geophysical phenomena are developed and cast into a quantitative form for comparisons with observations. Tested mathematical models of geophysical phenomena are produced in formats that are useful in various applications.

During the reporting period, work has been conducted on satellite interferometry with Global Positioning System (GPS) satellites, very long baseline interferometry, fundamental gravity theory, gravity gradiometry, geopotential modeling, and cryogenic inertial instrumentation. The structure and seismic propaga-

tion properties of the earth's crust have been investigated for areas of Air Force interest around the globe, specifically improved nuclear test-ban treaty monitoring and the forecasting of ground-motion effects of natural and man-made events, low-frequency transmission effects from jet engine suppressors (Hush Houses), and the seismo-acoustic detection of aircraft.

GEODESY AND GRAVITY

Geodesy is concerned with the size, shape, and mass distribution of the earth, and its orientation in inertial space. Geodetic information is a necessary foundation for the accurate determination of positions, distances, and directions for launch sites, tracking sensors, and targets. The geodetic and gravimetric parameters for the earth and geodetic information for positioning not only form the structural framework for mapping, charting, and navigational aids, but are also direct inputs for missile inertial guidance systems. Current geodetic information is inadequate to meet the requirements of future Air Force weapons systems.

The Geodesy and Gravity Branch conducts continuing research and development programs in geometric geodesy and in physical geodesy (gravity). These programs are directed toward improving the fundamental knowledge of the earth's size, shape, and gravity field and the techniques used for determining position, distance, and direction on the earth's surface in terrestrial and inertial three-dimensional coordinate systems.

In programs such as gravity gradiometry and GPS interferometry, GL cooperates with the Defense Mapping Agency, the Navy, the National Aeronautics and Space Administration, and the National Oceanic and Atmospheric Administration, as well as many other government agencies and universities.

GPS Geodesy: GL is continuing development of geodetic techniques for position and distance determination based on radio interferometric phase observations of the L-band carrier signals transmitted by the earth-orbiting NAVSTAR satellites of the GPS. GPS interferometry is a three-dimensional method by which the relative position vector (baseline vector) extending between two receivers is determined by analyzing data derived from simultaneous observations at the two ends of the baseline. To exploit this technique, GL developed a portable, dual-band (L1, L2) receiver for surveying over variable baselines using carrier signals. No knowledge of the coded GPS message is required, nor is mutual visibility between the ends of the baseline necessary. One goal of this research was to demonstrate that the components of a baseline vector between points on the earth can be determined to an accuracy better than first order geodetic survey accuracy (1 part in 500,000) determined by conventional instruments. A second goal was to establish that radio interferometry can also be utilized to determine GPS satellite orbits with unprecedented accuracy.

For GPS satellite-orbit determination, the most accurate observable available is carrier phase, differenced between observing stations and between satellites to cancel both transmitter and receiver-related errors. For maximum accuracy, the integer-cycle ambiguities of such observations must be resolved. To perform this ambiguity resolution, a bootstrapping strategy is effective. The tracking stations must have a wide-ranging progression of spacings. Then, by conventional "integrated Doppler" processing of the observations from the most widely spaced stations, the orbits can be determined well enough to permit resolution of the ambiguities of the observa-

tions from the most closely spaced stations. The resolution of these ambiguities reduces the uncertainty of the orbit determination enough to enable ambiguity resolution for more widely spaced stations, which reduces the orbital uncertainty further, and enables ambiguity resolution for still more widely spaced stations, and so on. In a test of this strategy with six tracking stations spaced from 71 km to 4000 km apart, both the formal and the actual errors of determining GPS orbits were reduced by a factor of 2.

Very Long Baseline Interferometry (VLBI):

Satellite radio interferometry was derived from techniques developed earlier from VLBI technology. In VLBI, a plane wave front from a distant quasar source arrives at two radio observatories at different times, depending on the direction of the sources, the orientation of the earth, and the locations of the observatories on the earth. The VLBI technique can precisely determine the time difference by the cross correlation of the signals recorded at the two observatories. As the earth rotates, the time difference changes, and the VLBI data can be used to determine the earth's rotation rate and its irregularities, polar motion, source directions, and the highly precise intercontinental distances between, and relative positions of, the radio observatories.

GL has studied the geophysical applications of VLBI, investigating the accuracies of the instrumentation used to obtain VLBI data and the models used to analyze the data, and evaluating the performance of water vapor radiometers as means of estimating the atmospheric propagation delay due to water vapor. In the final stages of this research, data from the Mark III VLBI system are used to study the relative motions of radio telescopes on the Pacific, North

American, and Eurasian plates, and the deformation zone between the North American and Pacific plates in the California region. The results are in accord with recent geologic plate-motion models, and a distributed deformation zone between the North American and Pacific plates. A number of studies on the accuracy of the results being obtained with VLBI have been carried out. The most notable of these studies includes the repeatability of the estimates of three-dimensional coordinates of the sites for long baselines (~4000 km), and the effects of calibrations of the "wet" tropospheric delays using water-vapor radiometers. The usefulness of observations made at very low elevation angles (~4°) for improving the accuracy of VLBI baseline determinations has also been studied, as well as the forced nutations of the earth. This has yielded results consistent with the flattening of the core-mantle boundary being about 5 percent greater than that predicted by the assumption of hydrostatic equilibrium within the earth. The effects of ocean tides and the anelasticity of the mantle on the forced nutations are not clearly evident.

Gravity Modeling: All Air Force inertial navigation systems (INS) rely on an accurate model of the earth's gravity field for precise point-to-point navigation. Precise positioning with respect to terrestrial and astronomic reference frames also requires knowledge of the local gravity vector, its direction and magnitude. As Air Force systems exploit the near-earth space environment, global gravity models become increasingly important in these respects since satellite orbital dynamics are also largely governed by the earth's gravity field. And, as the accuracy of INS increases, so does the demand for large amounts of short-wavelength gravity data. Therefore, the

Air Force has an interest in improving both global and local gravity models through new technology and enhanced data-acquisition systems and through advancements in theory and data processing.

A global gravity model is customarily expressed as spherical harmonic functions with coefficients that are determined from a global distribution of gravity data. Such a series is a function of latitude, longitude, and height and thus produces a functional description (with some error) of the gravity field everywhere on, or outside, the earth's surface. GL developed a new optimally estimated earth-gravity model consisting of a set of geopotential coefficients complete to degree and order 360 (a total of 130,321 coefficients), from a global set of 259,200 30'x30' surface mean gravity anomalies (gravity anomalies are residuals, of a sort, to a defined reference gravity field). The model is optimal in the sense that its derivation follows the principles of least-squares, resulting in the coefficients' errors being minimized. The global set of mean anomalies along with estimated accuracies was furnished by the Defense Mapping Agency (DMA). These anomalies were obtained from terrestrial observations and from predictions using satellite altimetry (GEOS-3, SEASAT, and GEOSAT data sets) and other geophysical data. Relative errors of the coefficients grow with degree and are estimated to have a value of 67 percent at degree 360.

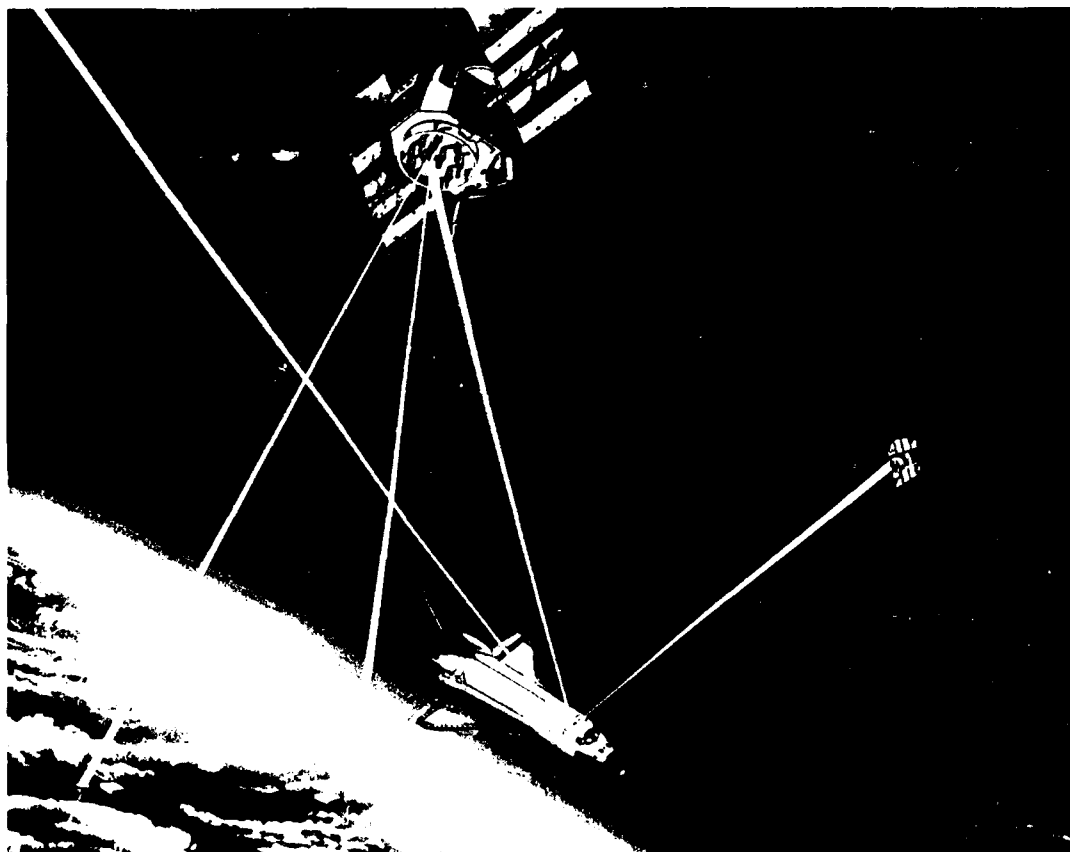
As the maximum degree of expansion increases, effects such as the nonsphericity of the earth's surface become significant. Transformation formulas were developed and implemented to relate spherical and ellipsoidal harmonic expansions since terrestrial gravity data reside on a surface resembling an ellipsoid more than a sphere. On the basis of simulation studies, a comparison of the

validity of spherical and ellipsoidal expansions showed that, with respect to a "true" field, a 70 percent relative error at degree 360 in the spherical expansion due to the neglected ellipticity was eliminated with the ellipsoidal expansion.

A second approach was developed in which gravity anomalies on the earth's surface were corrected for the fact that they are more nearly on an ellipsoid than a sphere. The resulting corrected anomalies can then be analyzed as if they were on a sphere to yield a spherical harmonic expansion of the field. Using a similar technique, we developed a procedure to account for the actual topography of the earth's surface, thus correcting surface-anomaly data not only for the nonsphericity of the surface on which they reside but also for its nonellipticity. This latter effect was found to be almost insignificant for expansions to degree 180. Results of this study have been incorporated into the DoD gravity library maintained by DMA to support gravity-data requirements for strategic weapons systems.

There are several ways of predicting, or estimating, local and global gravity field models from a given, limited, discrete gravity-data set. The Hardy method, a new approach to physical geodesy, was investigated using an extensive data set from the White Sands Test area. Both gravity anomalies and components of the deflection of the vertical were estimated using this method and compared to estimates obtained from other traditional techniques, such as least-squares collocation. It was found that the Hardy method is on a par with the other methods, which is a corollary to the main conclusion that improvement in gravity field models will not come from theoretical breakthroughs in data analysis, but from increased density and extent of gravity observations.

Although gravity data for global gravi-



Shuttle-Global Positioning System Tracking for Measuring the Earth's Gravity Field

ty models exist for most parts of the globe, some regions, including the polar caps and inaccessible continental areas, are largely devoid of adequate gravity surveys. Observing the motion of a near-earth, polar-orbiting satellite fills the gaps, provided the observing stations are also globally distributed. The most practical set of such stations is the constellation of Global Positioning System (GPS) satellites, which is designed to provide worldwide continuous positioning and navigation capabilities. The concept of satellite-to-satellite tracking is not new for global gravity surveying, but the existence of GPS offers for the first time the capability to determine the total (three-dimensional) vector of gravity uniformly

and consistently over the entire globe (see the figure). An analysis of such a mission using the shuttle as the low orbiter was performed.

A GPS receiver on board the shuttle would observe the carrier phases of at least four GPS satellites at all times. This yields the line-of-sight ranges to the satellites, and their second time derivatives yield the total acceleration of the shuttle with respect to GPS. Accelerometers on board the shuttle are needed to measure the nongravitational components of this observed acceleration. The accuracy of in situ gravitational measurements at shuttle altitude is estimated to be 0.56 mGal or better with improved processing of inertial instru-

mention data) for an integration time of 75 s ($1 \text{ mGal} = 1 \text{ milligal} = 10^{-5} \text{ m/s} \approx 1 \text{ micro-g}$, where g is the value of gravity at the earth's surface). The major error source in the measurement is the instability of the GPS clocks, from which comes the long integration time to keep the noise at a minimum. Although not as accurate as proposed dedicated gravity mapping missions (such as NASA's Geopotential Research Mission), satellite-to-satellite tracking using GPS was shown to contribute to an improvement of present models of the earth's gravity field at a relatively very low cost. Even the shuttle mission, to be viewed as a demonstration of the concept, would improve the model regionally, yielding estimates of 2° -mean gravity anomalies on the earth's surface to an accuracy of about 8 mGal. Global models in the form of spherical harmonic expansions would also benefit between degrees 20 and 60 from a single flight of the shuttle.

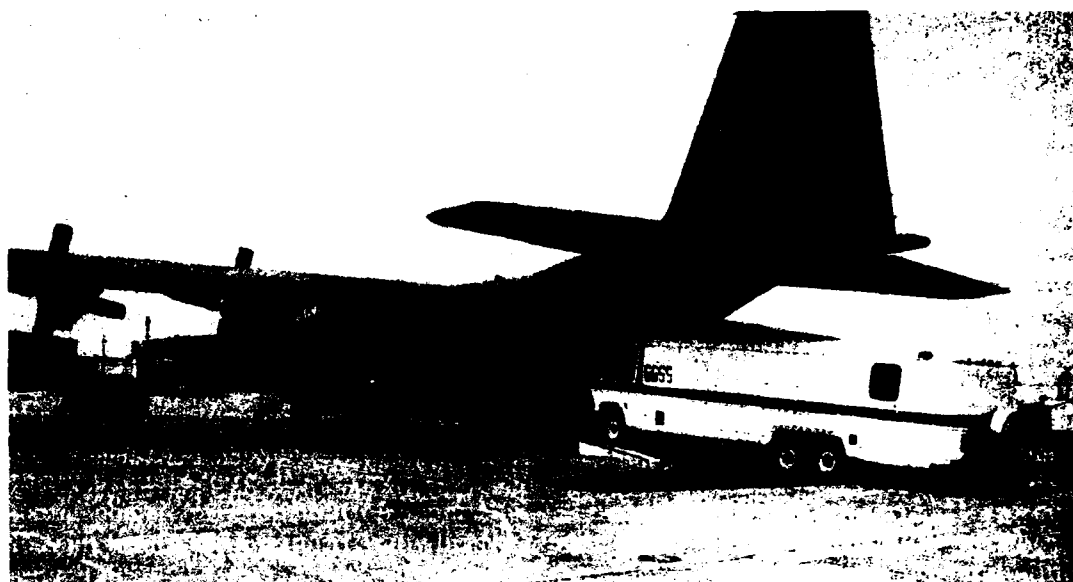
Geometric Geodesy: The techniques of tensor analysis and differential geometry were used to revisit a basic conjecture in differential geodesy regarding the possibility of employing the earth's gravity potential function as one member of a triply orthogonal coordinate system. In the 1960's, the famous geodesist Martin Hotine proposed this choice of natural coordinates (equipotential surface, latitude, and longitude) and conjectured that they must be triply orthogonal. Now, it has been shown with the new analysis that this conjecture is, in fact, invalid and finding such a system with the geopotential function as one of its members is a proposition with insurmountable mathematical difficulties.

Further work was performed using tensor analysis applied to torsion balance measurements which measure the curvature of the earth's gravity field. The inseparability of the curvature parameters in two orthogonal directions

was shown not to be a physical limitation of the measuring apparatus (e.g., the torsion balance), but a geometrical constraint. This means that the curvatures cannot be separated by refinements in instrument design.

Gravity Gradiometry: Local gravity modeling depends predominantly on point-by-point gravity observations which until now are obtained by labor-intensive and time-consuming procedures. In fact, in geographically harsh areas, conventional gravity surveys are nearly impossible to execute. The requirement for increased amounts of accurate gravimetric data has accelerated development of moving-base data-acquisition systems.

GL has been involved in the entire development of the mobile Gravity Gradiometer Survey System (GGSS), from the early basic research efforts more than two decades ago to the 1987-88 field testing of the fully operational system. This effort was pursued because of the great difficulties encountered with early mobile gravity systems, where the kinematic accelerations could not be separated from the measured gravitational accelerations. On an inertially stabilized platform, the gradiometer is insensitive to the linear kinematic accelerations. Furthermore, the gradiometer system comprises three (differently oriented) sensors which are sufficient to determine all the gradients. This permits the calculation of all three components of the gravity vector. The GGSS is installed in a dedicated van. It houses the gradiometer platform, various electronics racks, a data processor, and power and air-conditioning units. Surface navigation is performed by a fifth wheel attachment whose output is corrected for drift by waypoint calibrations (or with the aid of GPS). For gravity surveys over a larger area, the van is capable of being driven onto a cargo aircraft (like the C130; see the figure), where it is operated in flight



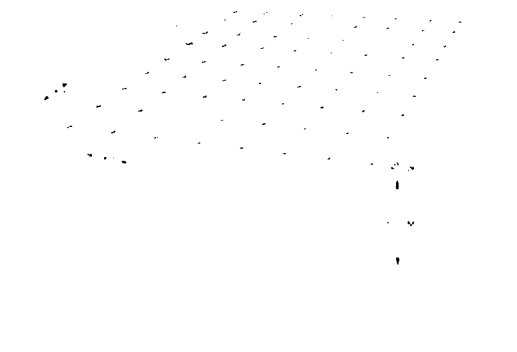
Gravity Gradiometer Survey System (GGSS) Driving onto a C-130 Cargo Aircraft

through an interface to the autopilot. The system in this configuration is able to fly predetermined survey patterns using positional information from the INS on the GGSS platform and with the aid of GPS.

The test program for the GGSS consisted of laboratory tests, road tests, and flight tests in the Texas-Oklahoma region. The airborne mode test covered

an area about 300 km square with parallel tracks running the full length at a spacing of about 5 km (see the figure). The altitude of the aircraft ranged between 600 m and 1000 m above ground, and with an aircraft speed of about 400 km/hr and a 10 s averaging time, the along-track resolution is about 1 km. The tests were performed in two phases. Phase I established the noise floor of the measured gradients by comparing data from repeat flights over the same track. Phase II comprised the actual areal survey over the test region.

Data processing is also divided into two stages. Stage I takes the raw gradiometer instrument outputs, applies the needed compensations and filters, and produces gradients as a function of position. Compensations include centripetal effects (due to rotation of the local-level platform in inertial space) and the self-gradients of the platform and the host vehicle(s). The self-gradients are determined using an elaborate calibration scheme, whereby the gradiometer instru-



Pattern of Tracks Flown by the GGSS During the Test Phase in the Texas-Oklahoma Region



Calibration of the Self-Gradients of the GGSS, the Van (inside the aircraft) and the Aircraft.

ments are maintained in a stationary mode (gravity gradients are constant) while the attitude of the vehicle is varied causing a varying gradient signal due to the platform and vehicle masses (see the figure).

Stage II processing begins with the numerical rotation of the gradients from the instrument frame to the local north-east-down coordinate frame, and proceeds with an integration relative to position to yield the three components of gravity. Any remaining instrument biases and drifts are removed through the use of ground-truth data and track-crossing adjustments. A number of uniquely appropriate analytical techniques were developed to perform the integration and downward continuation (in the airborne case). Some stressed minimization of estimation error, while others concentrated on reducing the computational load. All methods give approximately

equivalent results.

The conclusion of the tests (both airborne and land) determined that, although the amount of actually useful data obtained from the tests was modest, it was sufficient to demonstrate that the full gravity gradient tensor has been successfully measured using the GGSS. The airborne data were less noisy (± 9 E, typically, for 10 s averaging time; $1 \text{ E} = 1 \text{ Eotvos} = 10^{-9} \text{ s}^{-2}$) than GGSS measurements taken with the van driven on the earth's surface (± 22 E, typically, for 10 s averaging time). Single tracks of surface gravity recovered from airborne data were accurate to 3 to 4 mGal in each component when compared to true values of $5 \times 5'$ gravity means over a 90 km track. Multi-track processing yielded 2 to 3 mGal. Deflection of the vertical recovery over a distance of 150 km was accurate to about 1 arcsec. The GGSS was delivered to the Defense Mapping

Agency (DMA), the funding agency for the development program, in 1988. In December 1988, the GGSS was being operated on a platform to support navigation tests for Rail Garrison. Additional tests are being conducted by DMA with a goal to reduce these errors further.

Superconducting Gravity Tensor Gradiometer: The earth's gravity field can be described as: a geopotential field (scalar); a gravity field, the first derivative of the potential field (vector); or a gravity gradient field, the second derivative of the potential field (tensor). Although, in principle, each form contains all the gravity field information, the lower derivatives are more sensitive to longer wavelength components, while the higher derivatives are more sensitive to shorter wavelength components. The long wavelength components are due to large-scale or distant features, while the short wavelength components are due to small-scale or local features. The scalar field has no directional components, containing only a measure of the magnitude of the field. The vector has three orthogonal vector components, containing a measure of the magnitude and direction of the local field. The tensor has nine components (five are independent), containing a measure of the magnitude, direction, and curvature of the local field.

There are three components of acceleration at a single point: (1) linear acceleration, (2) rotational acceleration, and (3) gravitational acceleration. The acceleration field at a single point consists of three orthogonal linear and three orthogonal rotational components. Any measurement at a single point cannot distinguish between kinematic and gravitational acceleration (Einstein's Principle of Equivalence), whereas a full tensor field (requiring measurement at several points separated in space) can resolve all three components of acceleration, and

can thus separate kinematic from gravitational acceleration.

Resolving the three acceleration components is the task given to the Inertial Navigation Systems (INS), but as these components do not measure the full tensor (they measure a subset of the full tensor) the solution is ambiguous. This ambiguity is typically resolved by the introduction of additional information in the form of a gravity field model.

GL has approached the problem of measuring the full gravity tensor in two steps: (1) Develop an accelerometer measuring the three linear and three rotational acceleration components at a single point with the Superconducting Six-axis Accelerometer (SSA), and (2) Develop a tensor gravity gradiometer by placing several six-axis acceleration fields at points separated in three-dimensional space, thus forming the Superconducting Tensor Gravity Gradiometer (STGG).

The relevance of the two research efforts to the Air Force mission is in the development of ultra-resolution sensors. Highly sensitive, stable accelerometers and gravity gradiometers are required for inertial guidance, high-resolution gravity surveys, and precision gravity experiments. The SSA and the STGG will provide accurate, autonomous navigation and guidance of aircraft and missiles independently of pre-surveyed gravity. Furthermore, these efforts explore superconducting technologies needed to construct practical instruments for gravity survey and inertial guidance and navigation. Other applications include global mapping from satellites and Launch Region Gravity Model surveys from aircraft.

Non-Newtonian Studies: Since the early 1800's gravimetric experiments have been conducted to establish an accurate value for the least well-determined fun-

damental constant, the Newtonian gravitational constant G . These experiments were done in mines and boreholes, and most of the recent experiments have indicated that the gravitational constant was slightly larger than the accepted laboratory value. In 1986 a paper was published by Ephraim Fischbach, who reanalyzed the classic Eotvos torsion-balance experiment and claimed evidence for a compositional dependence to gravity, i.e., objects of different materials would fall at different rates. A flurry of experiments followed in an effort to establish the validity of Newtonian gravity. The experiments fell along two lines. One type of experiment involved the search for a compositional dependence to gravity. The other type attempted to determine the validity of the inverse-square law. The GL tower gravity experiment is the latter type experiment.

The experiment involves making an extensive surface-gravity survey in the vicinity of a tall tower, and merging these measurements with existing surface-gravity data extending to 200 km from the tower. These results are then used to analytically predict the value of gravity at various elevations on the tower if the inverse-square law is valid. Comparison between accurate gravimetric measurements at various elevations on the tower and predicted values serves as a test of the underlying theory.

The 610 m WTVD-TV television transmitting tower in Clayton, NC, was chosen for the experiment, in part because it is an extremely stable observing platform when wind speeds are light. Gravity measurements were taken at twelve elevations on the tower, with as many as five measurements at each particular level. All the measurements were made using a LaCoste-Romberg model G gravimeter whose past performance is well known and thoroughly tested. Least-squares reduction statistics indi-

cate the tower measurements are all accurate to better than 20 μGal . There were numerous other error sources that had to be accounted for, thus yielding final error estimates of about 30 μGal for the tower data. To achieve these kinds of accuracies, many problem areas had to be examined. The three major concerns were: tower motion, sensitivity of the instrument to magnetic fields, and radio-frequency interference from the tower. Careful examination insured these factors did not affect the results.

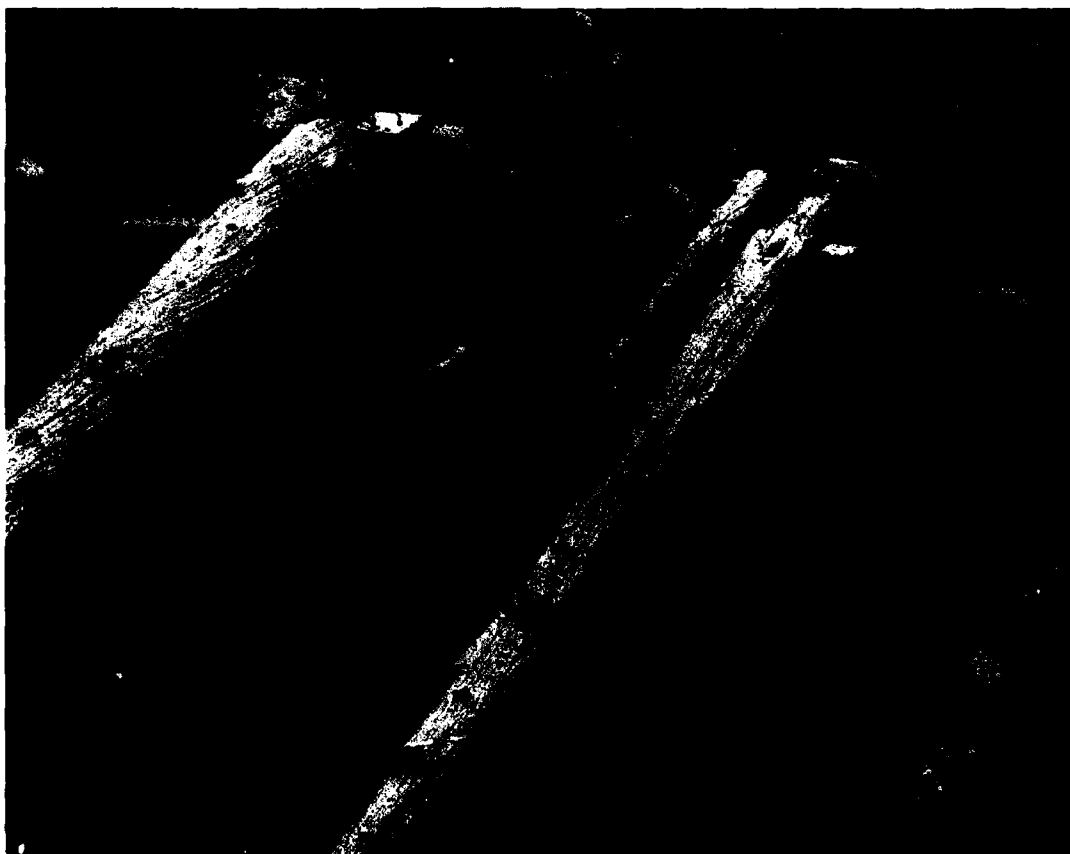
A total of 105 surface gravity measurements, contained in 11 roughly circular rings, were made in the tower vicinity out to a 5 km radius. The positions and elevations of the survey points were established by the Defense Mapping Agency's Geodetic Survey Squadron to accuracies of 1 m and 2 cm, respectively. The resultant surface-gravity data were accurate to better than 25 μGal . Previously measured surface data (accurate to better than 1 mGal) from the Defense Mapping Agency's Aerospace Center were merged to create a circularly symmetric data set about the tower out to 200 km. The merged data were analytically upward-continued using three independent computational techniques.

All three methods indicated a departure from the inverse-square law, asymptotically approaching 400 μGal at the top of the tower. The accuracy of the upward continuation is believed to be better than 75 μGal and indicative of an attractive non-Newtonian component to gravity. The majority of previous experiments done in mines and boreholes have indicated a repulsive effect about 1 percent of gravity. By some two-force theories, these findings are not necessarily in conflict. However, a more thorough model of fine gravity structure could negate these results, as well.

SOLID EARTH GEOPHYSICS

Solid earth geophysics, in particular seismology and the associated topic of geokinetics, plays a significant role in improving Air Force systems capabilities and performance. From the most obvious of applications, the evaluation of earthquake hazards and risks for Air Force facilities, to the more subtle, such as the study of vibration effects of low-flying aircraft on archaeological sites, the study of vibration-inducing sources and earth-transmission properties contributes to the successful completion of the Air Force mission. A seismic signal can contain information having intelligence

value, such as the signal for a nuclear test, or signals induced by lowflying aircraft or ground vehicles that must be extracted after the signal has been colored and masked by transmission effects and environmental noise factors. Similarly, the integrity of Air Force systems may require the suppression of such signals. As Air Force systems become technically sophisticated, they tend to become more susceptible to degradation from the natural and man-made seismic environment, and methods need to be developed to forecast, measure, suppress, or compensate for the geokinetic environment. Finally, Air



GL technician sets up seismometers and pressure transducers to monitor the effects of low aircraft overflights on a well-preserved kiva wall at Standing Fall House near Kayenta, AZ. This site was probably occupied around 1200 AD.

Force operations affect the geokinetic environment, and efforts should be taken to insure the minimum adverse effects on both nature and man.

The Solid Earth Geophysics Branch conducts continuing research on the topics of seismic and acoustic signal detection, source discrimination, propagation path effects, the structure of the crust and upper mantle of the earth, the statistical nature of the geokinetic environment, and the coupling of the air-earth interface. These programs are directed at increasing our knowledge of seismic sources and seismic and acoustic propagation characteristics for the purposes of improving our ability to forecast the geokinetic environment and its effect on Air Force systems, or to extract intelligence data from this environment.

Many of these efforts are conducted in cooperation with other agencies such as the Defense Advance Research Projects Agency, the Defense Nuclear Agency, the National Geodetic Survey, the United States Geological Survey, Oak Ridge National Laboratory, the Geological Survey of Canada, and other government agencies and universities.

Seismology: Seismology encompasses studies of earthquakes and related phenomena, the physics of explosions and other noise sources, and exploration of the earth's interior. Closely allied to seismology are the fields of geology and tectonics. The goal of seismological research is twofold: to understand the physics of seismic sources, and to understand how elastic (seismic) waves propagate through the earth, thereby elucidating the structure of the planet's interior.

The study of seismology is crucial to the Air Force in several respects. Foremost, seismology is the principal technique for monitoring underground nuclear test ban treaties. Secondly, seismological research is critical to predict-

ing ground-motion levels at Air Force facilities.

The Solid Earth Geophysics Branch maintains a strong program in observational seismology. During 1987-88, wide-ranging field efforts produced a wealth of unique data sets. Data were collected primarily using GL-owned digital seismic-recording systems in conjunction with other organizations such as the Weapons Laboratory, the Defense Nuclear Agency, the United States Geological Survey, and the National Geodetic Survey.

The Pacific Arizona Crustal Experiment is a long-term project by the United States Geological Survey (USGS) and various universities to study crustal structure on a 1000 km traverse from the Pacific Ocean to the interior of the continent. GL participated in the 1987 and 1989 phases of this experiment. A profile of 26 borehole explosions were recorded by GL and USGS seismographs between the Colorado River and Camp Wood, AZ. The GL data are diagnostic of the transition between the Basin and Range and Colorado Plateau tectonic provinces. This work has bearing on understanding ground motion at Air Force facilities as well as interpreting seismic measurements of nuclear tests conducted at the Nevada Test Site (NTS).

The MISTY PICTURE high-explosive test, conducted by the Defense Nuclear Agency at White Sands Missile Range, NM, added to the GL database of seismograms of above-ground explosions. The GL array was situated in such a way to record clear reflections from the crust-mantle boundary. Interpretation of these seismograms yielded a crustal thickness of 32 km in the Tularosa Valley, which is a part of the Rio Grande rift, a major continental extension feature.

A cooperative experiment to monitor quarry blasts was carried out by GL and

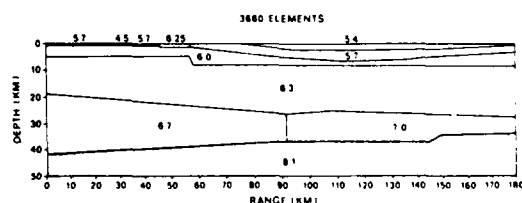
the Civil Engineering Test Division of the Weapons Laboratory (WL/NTESG) in July, 1987, at a quarry in eastern Massachusetts. GL and WL simultaneously recorded three 20,000-25,000 pound shots: WL at nearfield distances (0-1 km) and GL at far-field ranges (1-35 km). The goal of the experiment was to measure the source spectra of these blasts and then determine how the details of the spectra were preserved at long ranges.

The Joint Verification Experiment (JVE) between the United States and the Soviet Union involved monitoring nuclear tests in each country. It represented an unprecedented level of cooperation. GL recorded both JVE explosions. Regional-distance seismograms from the KEARSARGE test at NTS were recorded in eastern California to augment existing stations as well as to provide data on the Basin and Range - Sierra Nevada transition zone. Preliminary results showed that the crust thickens beneath the Sierra Nevada and Owens Valley. The Soviet test was recorded by portable instruments in the Adirondack Mountains, NY, as well as by a 16-element, high-frequency array at North Haverhill, NH. The high-frequency array was deployed in a cross pattern with 50-meter instrument spacing in order to measure signal coherence to test methods of signal detection, and to investigate the detailed structure of seismic phases. The array was in operation for the JVE as well as for the New York-New England Seismic Experiment.

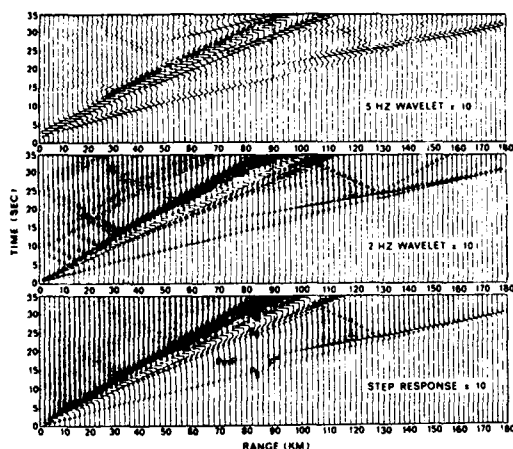
The New York-New England Seismic Experiment (NY-NEX) was a long-range seismic profile in the northeastern United States and southeastern Canada conducted by the United States Geological Survey (USGS), the Geophysics Laboratory (GL), and the Geological Survey of Canada (GSC). The profile began at Mamora, Ontario, con-

tinued to Long Lake, NY, crossed the states of Vermont and New Hampshire, and ended near Skowhegan, ME. Two diverse geological regions were sampled by the profile: the Precambrian North American shield of the Adirondacks and Southern Canada and the Paleozoic Appalachian orogenic zone. Specific objectives of the NY-NEX Seismic Experiment were the collection of detailed seismic data to aid geologic interpretations; intermediate length profiles to measure crustal properties; long-range observations to study the upper mantle; data on seismic-wave scattering, attenuation, and anisotropy; comparison of the profile explosions to local earthquakes, quarry blasts, and rockbursts; and strong ground-motion observations of known sources.

The experiment consisted of 34 bore-hole shots at 20 shot points distributed at approximately 30 km separation along the 650 km east-west main profile and 4 fan shots at 3 shot points in southern New Hampshire, Vermont, and Maine. Recording on the main profile was done by 250 USGS/GSC vertical seismographs in three deployments. Repeating major shot points for each deployment provided overlapping coverage of the subsurface. GL, in cooperation with WL, fielded 31 digital three-component stations on three profiles: Long Lake to Lorraine,



a. Geologic Model of the Earth's Crust and Upper Mantle on a Southwest Section across the State of Maine. (P-wave speeds are indicated in each homogeneous layer. Finer near-surface velocity structure and topography are included but are not apparent in the figure. (G.L. Wojcik et al. *Applied Numerical Mathematics*, 4, 1988, pp. 47-70.)



b. Suites of Magnified Vertical Velocity Seismograms at 2 km Station Spacing across the Maine Model. (The records clearly separate body and surface wave phases. The wavelet responses are obtained from the step response by convolution.)

NY; Addison, VT to Warner, NH, and Long Lake, NY, to Addison, VT. GL recorded all the shots on the high-frequency array at North Haverhill, NH.

Other significant research efforts included the study of PKP seismic-wave travel times, rockbursts, and super-computer modeling of seismic data. The PKP seismic wave travels through the earth's liquid iron core. PKP is observed to have a complicated travel-time curve caused by complexities of the structure within the core. This research is directed to associating travel-time observations with the correct PKP branch to allow accurate locations of small distant earthquakes.

Rockbursts are the sudden release of ambient stress at, or near, deep underground mines. These events can be large and have characteristics of coupled shear slip and explosion sources. This work seeks to define the seismic characteristics of rockbursts and to provide a means to discriminate between rockbursts and explosions at regional distances.

A large-scale finite-element model of USGS Maine seismic refraction data was

run on a Cray-2 supercomputer. The model consisted of a two-dimensional grid of 3660 x 1000 elements representing a 180 km (horizontal) x 50 km (vertical) slice through central Maine. Included were surface topography and a subsurface model inferred from USGS refraction data. Continuing research will be directed toward refining the model.

Two projects in conjunction with the National Geodetic Survey (NGS) were designed to understand long-term (days to years) deformation of the crust. A combined GPS/leveling survey in the Hegben Lake, MT, area was completed and the results were processed at NGS. Accurate timing of radio signals from GPS satellites allows millimeter-level baseline measurements between stations. Repeat measurements provide a measure of ground deformation between a suite of stations. The Hegben Lake area was selected because the crust was still deforming following an earthquake in 1959. These new measurements combined with earlier observations provided a record of the complete earthquake cycle. Another project involved construction of a continuously recording, superconducting gravity meter. This device allows high-precision gravity measurements at missile launch sites and equipment test facilities.

Underground Nuclear Test Ban Verification:

The Air Force is responsible for providing information for the verification of treaties dealing with the detonation of underground nuclear explosions. The primary treaties of concern are the Threshold Test Ban Treaty (TTBT) negotiated with the Soviet Union in 1974, and the Peaceful Nuclear Explosion Treaty (PNET), signed in 1976. While the TTBT has never been ratified, the signatory countries contend to abide by the 150 kt upper limit imposed for the yield of nuclear devices.

Resources for monitoring these treaties are seismic networks, surveillance satellites, sampling of radioactive debris and, potentially, on-site inspection and measurements. The Department of Defense conducts research in all these areas. Currently, seismological techniques are the primary means of detecting, discriminating, and determining the locations and yields of nuclear tests.

In support of the Air Force mission to provide information used to verify treaties, the Solid Earth Geophysics Branch manages the Defense Advanced Research Projects Agency (DARPA) Nuclear Test Ban Verification Basic Research Program. Two of DARPA's responsibilities are to supply scientific support to the arms control activities of the government and to support research efforts to improve the capability of the United States to monitor nuclear test-ban treaties. This charter complements the operational mission of the Air Force

to provide information to determine compliance with existing arms-control treaties. Any verification technique used by the Air Force or discussed by statesmen in the course of treaty negotiations must be based on well-understood and demonstrable physical principles. DARPA has, for the past 30 years, supported a program in basic research and exploratory development to improve existing seismic verification techniques and to develop new ones. GL management of the DARPA program allows the coordination of program objectives with Air Force requirements, and technology transition of research results into Air Force operations.

In general determining if a seismic event was generated by a nuclear explosion consists of three distinct problems: detection, discrimination, and yield determination (see the figure). The detection problem is simply determining that an event has been recorded. This



Variations in seismic shear wave velocity, at a depth of 100 km, are contoured. (These variations may be important in estimating the yields of nuclear devices exploded underground. Test sites used by various countries are also indicated in the figure.) (Courtesy of Dr. John Woodhouse, Harvard University)

can be difficult because of seismic noise generated by cultural and natural sources such as roadway traffic and weather fronts. Discrimination of the event involves deciding if it is an earthquake, rockburst, chemical blast, or nuclear explosion. This aspect of the problem can be difficult because a chemical explosion detonated in a rock quarry, for example, can look very similar to a local earthquake and may even resemble a small nuclear explosion. Determination of the yield of a nuclear event is the last step; it relies on the analyses of seismic wave amplitudes. This portion of the overall problem is not straightforward because the amplitudes of the seismic waves generated at one test site may differ substantially from those at another test site. Therefore, it is not always possible to use yield/magnitude relations interchangeably from one test site to another.

The technical basis for monitoring underground nuclear explosions has not changed significantly in the past few years. However, as a result of the research performed in the GL/DARPA program, a more complete understanding of the physics of seismic sources, the effects of path variations on seismic wave propagation, and anomalous shear-wave generation by underground nuclear explosions has been made possible.

The focus of research performed in 1987 and 1988 was to improve the capabilities of the United States to monitor underground explosions from long ranges (teleseismically). Teleseismic ranges are generally defined as greater than 2000 km. However, because of discussions between the Soviet Union and the United States, program research objectives shifted toward developing methods to monitor a reduced threshold treaty at regional distances (less than 2000 km). A reduced threshold treaty would involve a gradual lowering of the

150 kt associated with CTBT. While signals recorded at these shorter distances are extremely complicated, they can probably be used to detect explosions of very small magnitude. In a reduced threshold treaty scenario, seismic stations would be placed at regional distances from test sites. Therefore, the verification problem reduces to that of identification and discrimination at regional distances.

The focus of the GL/DARPA program was redirected to regional seismology in an effort to develop techniques for analyzing shorter period data and regional discrimination methods.

In broad terms, some of the most important research issues related to regional monitoring are seismic attenuation and detection capability, high frequency scattering and propagation effects, and source region coupling. All these topics were included in the program and substantial progress was accomplished. For example, seismic wave attenuation is crucial to understand as it determines the detectability level of an array. Research efforts were completed using regional data from the Norwegian Regional Seismic Array System (NORESS). These studies contributed to our understanding of attenuation. Realistic estimates of the attenuation from such studies were then used to estimate the detection capability of hypothetical networks proposed to be located in the Soviet Union.

Seismic wave scattering, while not as important to understand in a teleseismic monitoring situation, is believed to be critical for regional monitoring. Laboratory, field, and theoretical research efforts were completed that investigated the scattering of seismic waves. These studies indicated that scattering effects from surface (topographic) and near-surface inhomogeneities, including rough interfaces, may influ-

ence event magnitude and, hence, yield estimates. Results from these studies were applied to data recorded from explosions in the Soviet Union to evaluate the severity of the effects.

In the area of propagation effects, an analysis was completed using seismic data recorded inside the Soviet Union. Results from this study have given important insight into the propagation characteristics of the regions near the Soviet Union test site in Kazakh. Source-region phenomenology is particularly important to understand. Cooperative laboratory and computational research efforts were completed that contributed significantly to the better understanding of the salient physics in this area. It was shown that dilatancy, if properly accounted for, can have significant effects on the size of cavities produced by explosions and consequently, the seismic spectrum.

Efforts were begun to evaluate the usefulness of satellite image data to improve the accuracy of our yield estimates. Preliminary results indicated significant information can be obtained by combining different types of data such as multi-spectral images, elevation, and seismic data.

A number of technology transition events to Air Force users occurred in this time period, ranging from specifying the detection threshold of a hypothetical seismic network in Russia to procedures for combining various seismic magnitudes into a Unified Yield Estimate.

Seismo-Acoustic Studies: During 1987 and 1988, GL continued studies on the coupling of the atmospheric pressure field with the geokinetic environment. Three major efforts were undertaken by the Solid Earth Geophysics Branch in this area, including studies of the induced vibrations associated with jet engine ground run-up test facilities, or

Hush Houses; the effects of low-flying aircraft on archaeological structures; and the use of the air-coupled seismic phase for the detection and tracking of low-flying aircraft.

Continuing research initiated by a request for support from Logistics Command, GL conducted studies on the infrasonic emissions of jet-engine ground run-up test facilities and the adverse effects of these emissions on other structures. The goal of this work was to develop a methodology for forecasting the adverse vibration effects of Hush-House operation to aid in the site-selection process. During 1987, the primary effort was analysis of data taken during Hush-House operations at the Air National Guard facility at Fort Smith, AR. In 1988 a follow-up field program was carried out at Otis Air National Guard Base, MA.

Three basic findings resulted from the Fort Smith study. First, the pressure data recorded at Fort Smith were found to be similar to data taken at Luke AFB facility, supporting the concept that the infrasonic emissions are not particularly site-dependent. Second, the combined data from Luke AFB and from the Fort Smith tests allowed GL to hypothesize a theoretical model of the Hush-House infrasonic source to be tested at other sites. Finally, the data taken at Fort Smith demonstrated that existing siting procedures and guidelines for the T-10 Hush House were inadequate. The results of this work were used by Oak Ridge National Laboratory to update Hush-House siting guidance documents for Logistics Command.

Further testing for confirmation of the infrasonic source model was conducted during the summer of 1988 at the Massachusetts Air National Guard facility at Otis ANGB. Although the analysis of these data is not complete, it does appear to support previous work, with

one exception. The Otis data exhibited strong, periodic pressure pulses that had not been observed during previous studies. The cause and full significance of these pulses remains to be determined.

In 1987 the Strategic Air Command and the Noise and Sonic Boom Impact Technologies Office requested the support of GL to study the effects on archaeological sites of low-altitude flights on SAC training routes. Two field programs were conducted during 1987 to collect data on the vibration responses of ancient structures at Standing Fall House and Long House near Kayenta, AZ. During the Long House site study, measurements were made of the pressures and induced vibrations from low overflights of a B-52, RF-4C, and A-7 aircraft. In all cases, the overflights produced measurable vibrations in the Long House ruins. However, the vibrations were found to be well below criteria established to protect ancient structures. Even under the most severe pressure loading of the very high speed, very low altitude overflights of the A-7's measured vibrations were about a factor of five below these criteria. Because of the frequency-dependent nature of structural responses, the dominant pressure loading on the structures was most likely caused by either jet exhaust or airframe-generated noise. The major pressure signal appeared to be the turbulent wake of the aircraft. It was concluded from this study that subsonic overflights at or above 400 ft above ground level do not constitute a significant threat to ancient structures.

Finally, the Solid Earth Geophysics Branch pursued an in-house project to determine the feasibility of detecting and tracking low-flying aircraft using seismo-acoustic means. The goal of this project was to provide a passive detection and tracking system to be used against low-flying aircraft or missiles that, for various reasons, may be difficult to detect

with conventional means such as radar.

During 1987 a seismo-acoustic array was established under the SAC low-level training route at La Junta, CO. Using this array, we recorded the acoustic and seismic signatures of B-52 and B-1 overflights near the array. Analysis of the data indicated that the acoustic admittance of the site, the property governing seismo-acoustic coupling, was lower than might typically be expected based on previous experience. Even so, the nature of the air-coupled seismic wave allowed detection of low-flying aircraft at range far exceeding acoustic detection in the same frequency band. Further, the signal-to-noise ratio of the aircraft-generated seismic signal was not degraded by high wind, as was the case for the acoustic signal alone.

Analysis was also completed on the statistical attributes of the ambient noise environment at the La Junta site for the purpose of estimating aircraft signal-detection thresholds. This study examined the nature of the vertical and horizontal seismic noise and the atmospheric pressure field. Only weak correlations were found among these parameters. There were two major results from this study. First, Gumbel Extreme Value Type II distributions provided adequate statistical models for the observed data. Second, sufficient differences were found between the natures of the vertical and horizontal seismic noise to indicate that detection algorithms based on single-component vertical signals need to be very different from those based on multi-component signals.

During August 1988, an extensive survey was made of the spatial variation in seismo-acoustic coupling at the La Junta array. These data are being analyzed to provide information concerning the areal extent of the acoustic-coupling process and the spatial variability of acoustic admittance.

PUBLICATIONS 1987-1988

BRZEZOWSKI, S., GOLDSTEIN, J., HELLER, W., WHITE, J. (Analytic Sciences Corp., Reading, MA); GLEASON, D., and JEKELI, C. (AFGL)

Synopsis of Early Field Test Results from the Gravity Gradiometer Survey System
Proc. Chapman Conf. on Progress in Determining the Earth's Gravity Field (13-16 September 1988)

ECKHARDT, D.H., JEKELI, C., LAZAREWICZ, A.R., ROMAIDES, A.J., and SANDS, R.W.
A Tower Gravity Experiment: Evidence for Non-Newtonian Gravity
Phys. Rev. Lett. 60 (1988)

GLEASON, D.M.
Developing an Optimally Estimated Earth Gravity Model to Degree and Order 360 From A Global Set of 30' x 30' Mean Surface Gravity Anomalies
Manuscripta Geodaetica 12 (1987)
Comparing the Ellipsoidal Corrections to the Transformation between the Geopotential's Spherical and Ellipsoidal Spectrums
Manuscripta Geodaetica 13 (1988)
Computing Any Arbitrary Downward Continuation Kernel Function of An Integral Predictor Yielding Surface Gravity Disturbance Components From Airborne Gradient Data
Manuscripta Geodaetica 13 (1988)

JEKELI, C.
The Downward Continuation of Aerial Gravimetric Data Without Density Hypothesis
Bull. Geodesique 61 (1987)
New Instrumentation Techniques in Geodesy
Rev. of Geophys. 25 (1987)
The Exact Transformation between Ellipsoidal and Spherical Harmonic Expansions
Manuscripta Geodaetica 13 (1988)

Local Gravity Disturbance Estimation from Multiple-High-Single-Low Satellite-to-Satellite Tracking

Proc. Chapman Conf. on Progress in Determining the Earth's Gravity Field (13-16 September 1988)

MCCAFFREY, R.
Active Tectonics of the Eastern Sunda and Banda Arcs
J. Geophys. Res. 93 (1988)

MCCAFFREY, R. (AFGL); and FREDRICH, J. (Massachusetts Inst. of Tech., Cambridge, MA)
Source Parameters of Seven Large Australian Earthquakes Determined By Body Waveform Inversion
Geophys. J. 95 (1988)

ROMAIDES, A., and JEKELI, C.
Very Accurate Upward Continuation to Low Heights in a Test of Non-Newtonian Theory
Proc. Chapman Conf. on Progress in Determining the Earth's Gravity Field (13-16 September 1988)

ROMAIDES, A.J., and SANDS, R.W.
Gravity On A Tall Tower
Bull. D'Information 63 (1988)

UPADHYAY, T.N. (Mayflower Communications Co., Reading, MA); and JEKELI, C. (AFGL)
Satellite-to-Satellite Tracking Experiment for Global Gravity Field Mapping
Proc. Chapman Conf. on Progress in Determining the Earth's Gravity Field (13-16 September 1988)

VASCO, D.W.
Deriving Source-Time Functions Using Principal Component Analysis
Bull. Seismol. Soc. Am. 79 (1988)
Resolution and Variance Operators of Gravity and Gravity Gradiometer
Geophys. J. 93 (1988)

PRESENTATIONS

1987-1988

BARKA, A.A. (Massachusetts Inst. of Tech., Cambridge, MA); and KADINSKY-CADE, K. (AFGL)

Effects of Restraining Stepovers on Earthquake Rupture

U.S. Geological Survey Wkshp. on Fault Segmentation and Controls of Rupture Initiation and Termination, Palm Springs, CA (7-9 March, 1988)

BESSETTE, R.P.

Nonlinear Parametric Least Squares Adjustment - Example

AGU Mtg., San Francisco, CA (7-11 December 1987)

CIPAR, J.J.

Crustal Structure of the Tularosa Valley, Southern Rio Grande Rift, New Mexico

AGU Mtg., San Francisco, CA (7-11 December 1987)

Long Range Seismic Measurements of the Misty Picture Experiment, White Sands Missile Range New Mexico

Misty Picture Results Symp., Adelphi, MD (7-11 December 1987)

CIPAR, J.J. (AFGL); HUSSEY, V.K., and EBEL, J.E. (Boston Coll., Chestnut Hill, MA)

A Comparison of Shear Wave Velocity Structures of the Colorado Plateau and the Colorado Basin

AGU Mtg., Baltimore, MD (16-20 May 1987)

DUENNEBIER, T. (Hawaii Inst. of Geophysics, Honolulu HI); BESSETTE, R. (AFGL); KELLOGG, J. (Univ. of South Carolina, Columbia, SC); LAZAREWICZ, A. (AFGL); and KROENKE, L. (Hawaii Inst. of Geophysics, Honolulu, HI)

Micronesia Gravity and Geoid in Area of Postulated Incipient Trench

AGU Mtg., San Francisco, CA (7-11 December 1987)

ECKHARDT, D.H.

A Potential Function for the "Fifth Force"

AGU Mtg., San Francisco, CA (7-11 December 1987)

ECKHARDT, D.H., JEKELI, C., LAZAREWICZ, A.R., ROMAIDES, A., and SANDS, R.W.

Preliminary Results from a Tower Gravity Study

Neutrinos and Exotic Phenomena in Particle Physics and in Astrophysics, Les Arcs, Savoie, France (28-30 January 1988)

Results from a Tower Gravity Study

Fifth Marcel Grossmann Mtg., Univ. of Western Australia, Perth, Western Australia (8-13 August 1988)

Experimental Evidence for a Violation of Newton's Inverse-Square Law of Gravitation

AGU Mtg., San Francisco, CA (5-9 December 1988)

GLEASON, D.M.

Numerically Deriving the Kernels of an Integral Predictor Yielding Surface Gravity Disturbance Components from Airborne Gradient Data

Gravity Gradiometry Conf., Colorado Springs, CO (7-13 February 1987)

Developing an Optimally Estimated Earth Gravity Model to Degree and Order 360 from a Global Set of 30' x 30' Mean Surface Gravity Anomalies

AGU Mtg., Baltimore, MD (May 1987)

An Initial Look at 54 Tracks of Airborne Data from the Gravity Gradiometer Survey System

Gravity Gradiometry Conf., Colorado Springs, CO (10-11 February 1988)

GLEASON, D.M., and JEKELI, C.

Computing the Ellipsoidal Spectrum of the Earth's Geopotential and Transforming It to Any Desired Spherical Spectrum

AGU Mtg., San Francisco, CA (7-11 December 1987)

HELLER, W., BRZEWOSKI, S., GOLDSTEIN,

J., WHITE, J. (Analytic Sciences Corp., Reading, MA); GLEASON, D., and JEKELI, C. (AFGL)

The Gravity Gradiometer Survey System and Test Results

Chapman Conf. on Progress in the Determination of Earth's Gravity Field, Fort Lauderdale, FL (13-16 September 1988)

HSUI, A.T.

Determination of the Newtonian Gravitational Constant Based on a Borehole Gravity Measurement

AGU Mtg., Baltimore, MD (May 1987)

KADINSKY-CADE, K., and CIPAR, J.J.

Shear Wave Propagation in the Northwestern Basin and Range Province

AGU Mtg., Baltimore, MD (16-20 May 1988)

LAZAREWICZ, A.R. (AFGL); and EVANS, A.G. (Naval Surface Weapons Center, Dahlgren, VA)

GPS Differential Tracking and Gravimetry at 30 Km Altitude

AGU Mtg., San Francisco, CA (7-11 December 1987)

GPS-Aided Gravimetry at 30km Altitude from a Balloon-Borne Platform

Chapman Conf., Fort Lauderdale, FL (13-16 September 1988)

MCCAFFREY, ROBERT

Active Tectonics of the Banda Arc, Indonesia

AGU Mtg., Baltimore, MD (May 1987)

Earthquakes and Ophiolite Emplacement in the Molucca Sea Collision Zone, Indonesia

AGU Mtg., San Francisco, CA (7-11 December 1987)

MANGINO, S., and CIPAR, J.J.

Shear Wave Velocity Structure of Southwestern Maine

AGU Mtg., Baltimore, MD (16-20 May 1988)

ROMAIDES, A.J., and JEKELI, C.

A Detection of Non-Newtonian Gravity

Gravity Gradiometry Conf., Colorado

Springs, CO (10-11 February 1988)

Very Accurate Upward Continuation to Low Heights in a Test of Newtonian Theory

Chapman Conf. on Progress in the Determination of Earth's Gravity Field, Fort Lauderdale, FL (13-16 September 1988)

ROMAIDES, A.J., JEKELI, C., LAZAREWICZ, A.R., and SANDS, R.W.

Testing the Gravitational Inverse-Square Law Using Precise Measurements of Gravity Along a Tall Tower

AGU Mtg., San Francisco, CA (7-11 December 1987)

TAYLOR, C., and CIPAR, J.J.

Shallow Crustal Structure of Eastern Massachusetts

AGU Mtg., San Francisco, CA (7-11 December 1987)

UPADHYAY, T.N. (Mayflower Communications Co., Wakefield, MA); and JEKELI, C. (AFGL)

Satellite-to-Satellite Tracking Experiment for Global Gravity Field Mapping

Chapman Conf. on Progress in the Determination of Earth's Gravity Field, Fort Lauderdale, FL (13-16 September 1988)

UPADHYAY, T.N., COX, D.B., JR.

(Mayflower Communications Co., Wakefield, MA); and JEKELI, C. (AFGL)

STS-CPS Tracking Experiment for Gravity Anomaly Estimation

ION Natl. Technical Mtg., Santa Barbara, CA (26-28 January 1988)

STS-GPS Tracking for Anomalous Gravitational Estimation Stage Experiment

16th Gravity Gradiometry Conf., Colorado Springs, CO (10-11 February 1988)

UPADHYAY, T.N., COX, D.B., JR.

(Mayflower Communications Co., Wakefield, MA); MARTIN, C.F. (EG&G Washington Analytical Services Center, Inc., Lanham, MD); and JEKELI, C. (AFGL)

Gravity Anomaly Estimation Using GPS Measurements Onboard the STS
AGU Mtg., San Francisco, CA (6-11 December 1987)

VASCO, D.W.
Linear Inversion of Gravity and Gravity Gradiometry: A Tale of Two Operations
Gravity Gradiometry Conf., Colorado Springs, CO (10-11 February 1988)

VASCO, D.W. (AFGL); and JOHNSON, L.R. (Univ. of California, Berkeley, CA)
Inversion of Body-Waveforms for Extreme Source Models with an Application to the Isotropic Moment Tensor Component
AGU Mtg., San Francisco, CA (7-11 December 1987)

CONTRACTOR PRESENTATIONS 1987-1988

BLAHA, G. (Nova Univ., Dania, FL)
Non-Linear Parametric Least Squares Adjustment Theory
AGU Mtg., San Francisco, CA (7-11 December 1987)

COUNSELMAN, C.C. (Massachusetts Inst. of Tech., Cambridge, MA)
Demonstration of GPS Orbit-Determination Enhancement by Resolution of Carrier Phase Ambiguity: Resolving Carrier Phase Ambiguity in GPS Orbit Determination
AGU Mtg., San Francisco, CA (7-11 December 1987)

GRIERSON, A.D. (Bell Aerospace Textron, Buffalo, NY)
Suppression of Motion Sensitivity in Bell Aerospace Gravity Gradiometer Survey System
Gravity Gradiometry Conf., Colorado

Spring, CO (10-11 February 1988)

HELLER, W. (The Analytical Science Corp., Reading, MA)
GGSS Airborne Data Reduction Results
Gravity Gradiometry Conf., Colorado Springs, CO (10-11 February 1988)

MCLAUGHLIN, K.L., BARKER, T., STEVENS, J. (S-Cubed, La Jolla, CA); and DAY, S. (Univ. of California at San Diego, San Diego, CA)
An Analysis of 2-D Axisymmetric Nonlinear Finite Difference Explosion Simulations Using Moment Tensor Expansions
AGU Mtg., San Francisco, CA (5-9 December 1988)

PFOHL, L. (Bell Aerospace Textron, Buffalo, NY)
Program Review: Gravity Gradiometer Survey System
Gravity Gradiometry Conf., Colorado Springs, CO (10-11 February 1988)

CONTRACTOR TECHNICAL REPORTS 1987-1988

ALDEN, K.A., and HERRIN, E. (Southern Methodist Univ., Dallas, TX)
Automatic Detection and Recognition of the First Arrival Phase of Seismic Event Signals Contaminated by Noise: The Curious Case of the Missing Explosion
AFGL-TR-87-0230 (29 June 1987),
ADA196796

BAUMGARDT, D.R., and ZIEGLER, K.A. (Ensco, Inc., Springfield, VA)
Spectral Evidence for Source Multiplicity in Explosions
AFGL-TR-87-0045 (February 1987),
ADA187363

- BLAHA, G. (Nova Univ., Dania, FL)
Five-Diagonal Weighting Scheme for Geoidal Profiles
 AFGL-TR-87-0099 (March 1987), ADA188033
Resolution of a Rank-Deficient Adjustment Model via an Isomorphic Geometrical Setup with Tensor Structure
 AFGL-TR-87-0102 (March 1987), ADA184198
- BOSE, S.C. (Applied Science Analytics, Inc., Tiroga Park, CA)
Gravity Gradiometer Survey System (GGSS) Post-Mission Data Processing
 AFGL-TR-88-0008 (August 1987), ADA200739
- BRATT, S.R., and BACHE, T.C. (Science Applications Intl. Corp. San Diego, CA)
Location Estimation Using Regional Array Data
 AFGL-TR-87-0108 (31 December 1986), ADA181161
- BRZEZOWSKI, S.J., and HELLER, W.G. (The Analytic Sciences Corp., Reading, MA)
Independent Analysis of Gravity Gradiometer Survey System (GGSS) Development and Deployment: A Synopsis
 AFGL-TR-86-0173 (August 1986), ADA180-267
A Synopsis of Field Test Results from the Gravity Gradiometer Survey System
 AFGL-TR-88-0176 (11 August 1988), ADA200956
- CORMIER, V.F. (Massachusetts Inst. of Tech., Cambridge, MA)
Teleseismic Waveform Modeling Incorporating the Effects of Known Three-Dimensional Structure Beneath the Nevada Test Site
 AFGL-TR-87-0037 (2 January 1987), ADA179187
Teleseismic Waveform Modeling Incorporating the Effects of Known Three-Dimensional Structure Beneath the Nevada Test Site
 AFGL-TR-87-0192 (8 June 1987), ADA184203
- COUNSELMAN, C.C. (Massachusetts Inst. of Tech., Cambridge, MA)
Research in Geodesy Based Upon Radio Interferometric Observations of GPS Satellites
 AFGL-TR-87-0091 (31 December 1986), ADA184040
- COYNER, K.B., and MARTIN, R.J. (New England Research, Inc., White River Junction, VT)
Frequency Dependent Attenuation in Rocks
 AFGL-TR-88-0321 (3 October 1988), ADA205276
- CROWLEY, F.A., and BLANEY, J.I. (Weston Obs., Boston Coll., Weston, MA)
Surface Disturbances Produced by Low-Level, Subsonic B-1 Aircraft
 AFGL-TR-87-0325 (November 1987), ADA192257
- FERGUSON, J.F., and REAMER, S.K. (Univ. of Texas at Dallas, Richardson, TX)
Geophysical Investigations at Pahute Mesa, Nevada
 AFGL-TR-87-0242 (12 August 1987), ADA190478
- GIVEN, J.W., APSEL, R.J., MELLMAN, G.R., and WONG, P.C. (Sierra Geophysics, Inc., Kirtland, WA)
Approximation to the Boundary Integral Equation and Applications to Modeling Acoustics Waves in Three Dimensional Structures
 AFGL-TR-87-0147 (February 1987), ADA182598
- GOLDSTEIN, J.D., WHITE, J.V., COMER, R.P., and HELLER, W.G. (Analytic Sciences Corp., Reading, MA)
Estimation of Short-Wavelength Gravity on a Dense Grid Using Digital Terrain Elevation on Data
 AFGL-TR-87-0280 (15 October 1987),

ADA196325

HARVEY, D.J. (Univ. of Colorado, Boulder, CO)

A Spectral Method for Computing Complete Synthetic Seismograms

AFGL-TR-87-0238 (March 1987), ADA187663

HELMBERGER, D.V., HARKRIDER, D.G., and CLAYTON, R.W. (California Inst. of Tech., Pasadena, CA)

Path Effects in Strong Motion-Seismology

AFGL-TR-86-0050 (January 1986),

ADA181152

HERRING, T.A. (Harvard Coll. Obs., Cambridge, MA)

Research in Geodesy and Geophysics Based Upon Radio Interferometric Observations of Extragalactic Radio Sources

AFGL-TR-88-0204 (1 October 1988),

ADA200958

HERRMANN, R.B. (St. Louis Univ., St. Louis, MO)

Lg Wave Excitation and Propagation in Presence of One-, Two-, and Three-Dimensional Heterogeneities

AFGL-TR-87-0229 (15 July 1987),

ADA187364

HERRMANN, R.B. (St. Louis Univ., St. Louis, MO); MOKTITAR, T.A. (King Abdulaziz Univ., Jeddah, Saudi Arabia); and RUSSELL, D. R. (St. Louis Univ., St. Louis, MO)

Seismal Techniques in Regional Wave Studies

AFGL-TR-88-0149 (17 June 1988),

ADA201698

JONES, G.M., and MURPHY, V.J., (Weston Geographical Corp., Westboro, MA)

Tomographic Investigations at Landfill 4, Hill AFB, Layton, Utah

AFGL-TR-87-0055 (23 April 1987),

ADA181289

JORDAN, T.H. (Massachusetts Inst. of Tech., Cambridge, MA)

Investigations of Eurasian Seismic Sources and Upper Mantle

AFGL-TR-87-0101 (6 March 1987),

ADA165228

KENNETT, B.L.N. (Australian Natl. Univ., Canberra, Australia)

Lg-Wave Propagation in Heterogeneous Media

AFGL-TR-88-0141 (6 April 1988),

ADA198920

LANGSTON, C.A. (Pennsylvania St. Univ., Univ. Park, PA)

Calculation of Source and Structural Parameters at Regional and Teleseismic Distances

AFGL-TR-87-0066 (28 February 1987),

ADA183008

LANGSTON, C.A., and GREENFIELD, R. J. (Pennsylvania St. Univ., Univ. Park, PA)

Scattering Under Pasadena, CA

AFGL-TR-88-0100 (1 April 1988),

ADA196311

LEVINE, J. (Univ. of Colorado, Boulder, CO)

A Study of Secular and Tidal Tilt in Wyoming

AFGL-TR-86-0212 (1 November 1985),

ADA176416

McEVILLY, T.V., and JOHNSON, L.R. (Univ. of California, Berkeley, CA)

Regional Studies with Broadband Data

AFGL-TR-88-0131 (15 May 1988),

ADA199187

MCLAUGHLIN, K.L., and JIH, R.S. (Teledyne Geotech, Alexandria, VA)

Finite Difference Simulations of Rayleigh Wave Scattering by 2-D Rough Topography

AFGL-TR-86-0269 (November 1986)

ADA179190

- MCLAUGHLIN, K.L., ANDERSON, L.M., and LEES, A.C. (Teledyne Geotech, Alexandria, VA)
Effects of Local Geologic Structure for Yucca Flats, NTS, Explosion Waveforms: 2-Dimensional Linear Finite Difference Simulations
 AFGL-TR-86-0220 (October 1986), AOA179189
- MCLAUGHLIN, K.L., JIH, R.S., DER, Z.A., and LEES, A.C. (Teledyne Geotech, Alexandria, VA)
The Effects of Near-Source Topography on Explosion Waveforms: Teleseismic Observations and Linear Finite Difference Calculations
 AFGL-TR-86-0159 (July 1986), ADA183013
- MCLAUGHLIN, K.L., DER, Z.A., JIH, R.S., LEES, A.C., and ANDERSON, L.M. (Teledyne Geotech, Alexandria, VA)
Finite-Difference Modeling of Seismological Problems in Magnitude Estimation Using Body Waves, Surface Waves, and Seismic Source Imaging
 AFGL-TR-87-0106 (March 1987), ADA181455
- METZGER, E.H., AFFLECK, C.A., and RUSNAK, W. (Bell Aerospace Textron, Buffalo, NY)
Integrated Gravity Mapping System (IGMS) Study Program
 AFGL-TR-81-0355 (March 1982), ADA179188
- MURPHY, J.R., STEVENS, J.L., and RIMER, N. (S-Cubed, La Jolla, CA)
High Frequency Seismic Source Characteristics of Cavity Decoupled Underground Nuclear Explosions
 AFGL-TR-88-0130 (May 1988), ADA198121
- PETERS, J., and BEAUMONT, C. (Dalhousie Univ., Nova Scotia, Canada)
Report on Results of Borehole Tilt Measurements from the Charlevoix Observatory, Quebec
 AFGL-TR-87-0134 (31 November 1986), ADA201039
- PFOHL, L., RUSNAK, W., JIRCITANO, A., and GRIERSON, A. (Bell Aerospace Textron, Buffalo, NY)
Moving Base Gravity Gradiometer Survey System (GGSS) Program
 AFGL-TR-88-0126 (April 1988), ADA199335
- PRIOVOLOS, G.J. (The Ohio St. Univ., Columbus, OH)
Gravity Field Approximation Using the Predictors of Bjerhammar and Hardy
 AFGL-TR-88-0114 (March 1988), ADA200622
- RAPP, R.H., and CRUZ, J.Y. (The Ohio State Univ., Columbus, OH)
The Representation of the Earth's Gravitational Potential in a Spherical Harmonic Expansion Degree 250
 AFGL-TR-86-0191 (September 1986), ADA176479
- SAMMIS, C.G. (Univ. of Southern California, Los Angeles, CA); and ASHBY, M.F. (Cambridge Univ., Cambridge, UK)
The Damage Mechanics of Brittle Solids in Compression
 AFGL-TR-88-0160 (July 1988), ADA201653
- SERENO, T.J., and BRATT, S.R. (Science Applications Intl. Corp., San Diego, CA)
Attenuation and Detection Capability of Regional Phases Recorded at NORESS
 AFGL-TR-88-0095 (25 March 1988), ADA196508
- SERENO, T.J., BRATT, S.R., and BACHE, T.C. (Science Applications Intl. Corp., San Diego, CA)
Regional Wave Attenuation and Seismic Moment from the Inversion of NORESS Spectra
 AFGL-TR-87-0237 (31 July 1987), ADA187299
- SIMPSON, D.W., RICHARD, P.G., and LERNER-LAM, A. (Columbia Univ., New

York, NY)

Regional Network: Seismicity of Asia: And Frequency-Dependent Q

AFGL-TR-87-0049 (15 February 1987),
ADA181532

STEVENS, J.L., RIMER, N., and DAY, S.M.
(S-Cubed, La Jolla, CA)

Constraints on Modeling of Underground Explosions in Granite

AFGL-TR-86-0264 (October 1986),
ADA178288

TOKSOZ, M.N., and DAINITY, A.M.
(Massachusetts Inst. of Tech.,
Cambridge, MA)

Influence of Scattering on Seismic Waves
AFGL-TR-88-0170 (8 August 1988),
ADA201120

TOKSOZ, M.N., and PRANGE, M.
(Massachusetts Inst. of Tech.,
Cambridge, MA)

Analysis of Regional Phases Using Three-Component Data

AFGL-TR-88-0322 (28 November 1988),
ADA205480

TOKSOZ, M.N., REITER, E., and DAINITY,
A.M. (Massachusetts Inst. of Tech.,
Cambridge, MA)

Influence of Scattering on Seismic Waves: Velocity and Attenuation Structure of the Upper Crust in Southeast Maine

AFGL-TR-88-0094 (21 March 1988),
ADA199131

TOKSOZ, M.N., WU, R.S., and SCHMITT,

D.P. (Massachusetts Inst. of Tech.,
Cambridge, MA)

Influence of Scattering on Seismic Waves: Physical Mechanisms Contributing to Attenuation in the Crust

AFGL-TR-87-0276 (30 September 1987),
ADA191699

VASSILIOU, M.S., ABDEL-GAWAD, M., and
TITTMANN, B. R. (Rockwell International,
Thousand Oaks, CA)

Ultrasonic Physical Modeling of Seismic Wave Propagation from a Graben-Like Structure: A Preliminary Report

AFGL-TR-86-0228 (October 1986),
ADA178396

Ultrasonic Physical Modeling of Seismic Wave Propagation from a Graben-Like Structure

AFGL-TR-87-0256 (November 1987),
ADA189066

WANG, Y.M. (Ohio State Univ., Columbus,
OH)

Downward Continuation of the Free-Air Gravity Anomalies to the Ellipsoid Using the Gradient Solution, Poisson's Integral and Terrain Correction-Numerical Comparison and Computations

AFGL-TR-88-0199 (June 1988), ADA203739

ZUNE, J.D., and MOORE, W.A. (New
Mexico State Univ., Las Cruces, NM)
Conformal Geometry, Hotline's Conjecture, and Differential Geodesy

AFGL-TR-87-0233 (27 July 1987),
ADA189265



Inflating 11 Million Cubic Foot Balloon for Gamma Ray Advanced Detector (GRAD) Experiment at Williams Field, McMurdo Station, Antarctica

VII AEROSPACE ENGINEERING DIVISION

The Aerospace Engineering Division designs, builds, tests, and flies payloads for experiments aboard balloons, sounding rockets, the shuttle, and free-flying satellites. The experimenters are principally GL scientists and researchers at Air Force Systems Command and other agencies in the Department of Defense. We also support other United States government groups who need to obtain scientific measurements or to observe hardware performance in the atmosphere and space. The Division provides the ground and payload instrumentation for tracking and remote command-control of the experiments and vehicle, and the telemetry, onboard recorders, and television for data retrieval. Systems integration, electronics checkout, and environmental tests of the complete payload are conducted at the recently completed GL Payload Integration and Test Facility at Hanscom AFB, MA.

For GL scientists and large-scale projects — typically multi-agency, multi-probe satellite programs — the Division's Data Systems Branch designs, develops and implements coordinated data-management plans, generates databases and provides mathematical analysis services.

The Division also conducts an engineering technical-base development pro-

gram. This work supports our experimenters' on-going requirements for state-of-the-art, specialized instrumentation and computerized methods to record, display, and analyze the enormous data yields from our aerospace programs.

We regularly launch sounding rockets from the White Sands Missile Range, NM, and the Poker Flat Research Range, AK. Routinely, our balloonborne experiments are conducted from the permanent GL Balloon Flight Facility, GL Detachment 1 at Holloman AFB, NM, on the White Sands Missile Range. Increasingly, however, we are using our mobile equipment to launch sounding rockets and balloons from remote locations almost anywhere in the world.

BALLOON PROGRAM

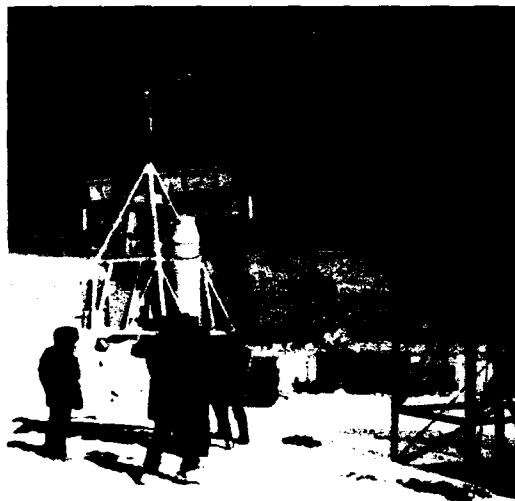
The Aerospace Engineering Division designs and develops completely instrumented balloon systems to carry heavy experimental payloads into the stratosphere. From the inception of a balloon program, our engineers work closely with the scientific investigators to ensure that all the individual payload components are environmentally suitable, and the balloon instrumentation and program plans do provide the appropriate data-handling capability, power budget, command-control and safety provisions, flight trajectory, and payload recovery operations to meet the experimental objectives.

Balloon experimenters have some options for data collection and payload design not available from the other aerospace vehicles. Balloons ascend slowly and can remain afloat for many hours, even days if so designed. Payload size and shape are restricted only by the handling capacity of the launch experiment. Instruments can be reeled down into the atmosphere thousands of feet below the balloon and up again, whenever

the experimenter commands.

Our operational flights during 1987-88 using Astrofilm E and Stratofilm-372 balloons with payloads up to 2600 lb have confirmed the fully successful performance record of our earlier tests of these new balloon films. With these very reliable vehicles and the versatility of micro-technology, the trend continues toward increasingly complex, large payloads with demanding flight plans. Of special interest is the somewhat belated recognition that it can be highly advantageous to fly an experiment intended for a satellite or the shuttle on a stratospheric balloon! Two such instances are among the balloon programs described below.

GRAD: For several reasons, the Gamma Ray Advanced Detector experiment,



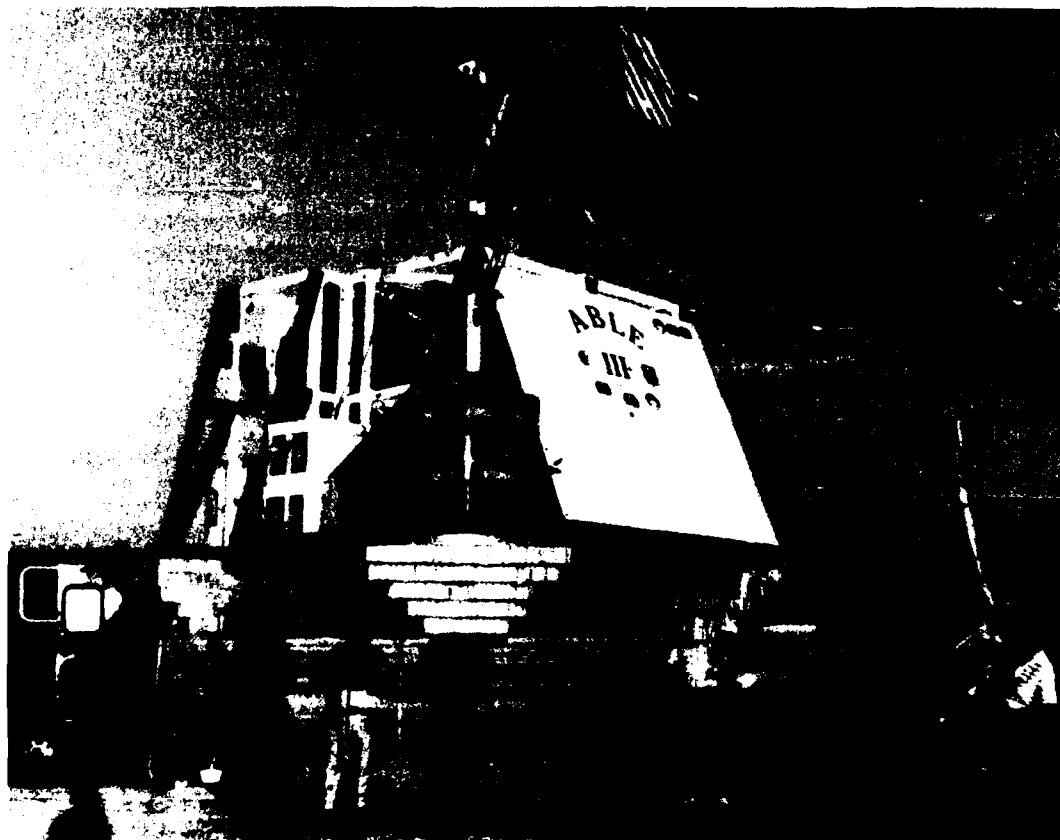
Attaching GRAD Payload to Launch Gantry at Williams Field, McMurdo Station, Antarctica.

GRAD, ranks among our most challenging balloon programs. Sponsored by the Nuclear Monitoring Office of the Defense Advanced Research Projects Agency and the DoD Space Test Program, GRAD involved working closely with fifteen dif-

ferent government and university groups, most of whom had no experience with balloon operations. Moreover, within 4 months the flight-ready payload, the 11.8 million cu ft balloon system, the helium supply, and all other equipment and spare parts had to be en route for launch of the first large stratospheric balloon from Antarctica. There would be no time for preliminary, dress rehearsal flights: the launch window was only a few days -- January 8-11, 1988, when the peak intensity of gamma rays from Supernova 1987A was expected. The supernova, visible only from the Southern Hemisphere, provided a unique target of opportunity to test the new type of gamma ray detector, originally intend-

ed for the space shuttle. The balloon was launched on the first scheduled day and flew near the 115,000 ft level until it was commanded down 3 days later. A ski-equipped United States Antarctic Program LC-130 aircraft recovered the payload on the East Antarctic ice shelf. This program produced invaluable information concerning the operational characteristics of the detector and also excellent, new data from Supernova 1987A itself.

ABLE: GL's Atmospheric Balloon-Borned Lidar Experiment, ABLE, simulates a future satellite lidar (light detection and ranging) mission at much lower cost. ABLE II, launched from Roswell



Pre-Launch Checkout of ABLE III, the Laboratory's Balloonborne Lidar Experiment.

NM, in August 1987, was a successful engineering test of a field-of-view monitor to measure aerosol scattering. The data will aid in establishing parameters for design of space-based lidar systems. ABLE III, launched from the White Sands Space Harbor, NM, in September 1988, collected data concerning atmospheric composition and optical properties that affect atmospheric transmission of radiation. This information will be used for design of Department of Defense electro-optical systems. (For more details, see "Airborne Lidar", Chapter V above.)

ASHCAN: GL maintains the air-sampling payload in flight-readiness status for the Department of Energy's project ASHCAN. In May, 1988, the 2700-lb payload was flown for several hours on a 2.9 million cu ft balloon. An additional objective was met when one of the new balloon materials, Stratofilm 372, performed flawlessly.

ALFAN: The Division flew the second Rome Air Development Center's Airborne Low Frequency Atmospheric Noise experiment, ALFAN, from Holloman AFB, NM, in May 1987, timed to float through sunrise. The experiment measured the levels of atmospheric low-frequency energy polarized in the transverse-electric and transverse-magnetic directions. The data are used to verify or modify computer codes that predict range and connectivity of essential airborne VLF/LF communications systems.

Tethered Aerostats: GL's working inventory of large tethered aerostats and our mobile capability enable us to respond quickly and efficiently to requests for help from other Air Force units, the Army, the Navy, and other branches of the Department of Defense. Tethered operations during 1987-88 included:

1. JTIDS: The Joint Tactical Information Data Systems (JTIDS) office, while conducting Intermediate Operational Test and Evaluation of the system at Eglin AFB, FL, had serious problems due to interference with transmissions caused by tall trees. Six days later GL tethered equipment and personnel were on site at Eglin with the remedy. On 12 hr shifts we flew a pair of 6000 cu ft tethered balloons, 18 miles apart, carrying antennas and transmission lines. Both systems transmitted and received data at alternate times. The balloons were reeled up from ground level to 200 ft in 6 ft increments to determine the minimum altitude where transmission capability was optimum. Jamming tests were also conducted during this mission.

2. EXDRONE: A GL tri-tethered aerostat served as a temporary, rapidly erected "tower" to test a tri-service battlefield drone called EXDRONE (EXpendable DRONE). Tri-tethered systems provide very stable positioning capability together with long duration testing -- days or weeks, as opposed to a few hours for self-powered flight test vehicles. Sponsored by the Army Intelligence and Security Board at Fort Huachuca, AZ, with technical support from the Navy Avionics Center and the Marine Corps, the test program involved our suspending a battlefield communications jamming drone beneath the tethered balloon flying 2500 ft above ground. Communications jamming tests and signal strength tests were conducted over a 3-week period at GL's Fair Site on the White Sands Missile Range.

3. TAAP: The tethered balloon system called TAAP (Tethered Aerostat Antenna Program), developed for the Defense Communications Agency, was successful-



Tethered Aerostat can be transported to a site, inflated, and reeled up to support the 3,000 ft antenna of the Tethered Aerostat Antenna Program (TAAP). It re-establishes vital LF communications in the event of a downed tower.

ly demonstrated to representatives of several branches of the Department of Defense in May, 1987. The system was designed to demonstrate the capability of a mobile, self-contained tethered aerostat system to reconstitute VLF/LF communications under wartime emergency conditions such as a post-nuclear attack. The 25,000 cu ft aerostat supports a 3000-ft long antenna that is an integral part of the aerostat cable. The same cable also conveys the power from the ground to operate the aerostat blowers, valves, and on-board telemetry. The entire system, contained in four trailers, can be inflated and launched by a trained crew in 5 to 6 hrs. For the demonstration exercise, the trailers were transported for 20 miles over roads in

various conditions and the aerostat was inflated and erected. The transmitter was connected to the antenna and messages transmitted world wide. The system has been accepted and is now in the GL tethered balloon inventory.

SOUNDING ROCKETS

With a history that includes the instrumenting and launching of over 1000 sounding rockets since 1946, our high success rate continues. In this time period, four sounding rockets were launched, two from NASA Wallops Flight Facility, VA, and two from our expeditionary site in Sondrestrom, Greenland. Four new payloads were started and are in various stages of design, fabrication, or test for upcoming launches. Three of these pro-

jects support the Strategic Defense Initiative Organization (SDIO).

As scientific requirements lead to the evolution of more sophisticated missions, both the size and complexity of our rocket payloads continue to increase. The EXCEDE III payload scheduled for launch early in 1990 weighs a record 5000 lb. The BEAR payload scheduled for launch in April, 1989, weighs 3500 lb and will radiate data from seven telemetry links, including two real-time video cameras, both firsts. The need continually to advance the state of the art of rockets and instrumentation has required a corresponding emphasis on our in-house engineering development. A new high-performance rocket-booster development was started in 1988 in cooperation with the Defense Nuclear Agency and the NASA Goddard Space Flight Center. In 1988, we also initiated research toward a guided parawing recovery system to improve recovery of balloon and rocket payloads, and development of a shuttle-qualified optical disc storage system.

COPE/POLAR ARCS: Project COPE, Cooperative Observations of Polar Electrodynamics, was a joint effort among GL, NASA, and the Danish Meteorological Institute. As part of this program, on February 27, 1987, GL and NASA launched a pair of rockets from Sondrestrom, Greenland, into a polar cap, F-layer arc. Commanded from the GL Airborne Ionospheric Observatory, a NASA Black Brant VIII rocket was launched carrying three barium-shaped charges that were ignited in the exo-atmosphere. Six minutes later, GL launched its 500-lb Polar Arcs payload on a Black Brant IX. As intended, the payload penetrated the auroral arc on the way to its 385-km apogee altitude. On March 21, 1987, GL launched its second rocket for the program on a Black Brant VIII, again as a pair with a NASA

rocket. This GL rocket discharged seven separate barium releases during its 10-min flight, reaching an apogee of 354 km. Both of these experiments were 100 percent successful. With the completion of this program, the launch site at Sondrestrom was dismantled and the site returned to its natural condition in accordance with our agreement with the Danish Government. (For more details, see "POLAR ARCS", Chapter III above.)

COLDR: For COLDR, CONductivity of the Lower D-Region, an unusual adaptation of a standard recovery system was



Launch of Nike Orion Rocket, August, 1987, Carrying the Conductivity of the Lower D-Region (COLDR) Experiment.

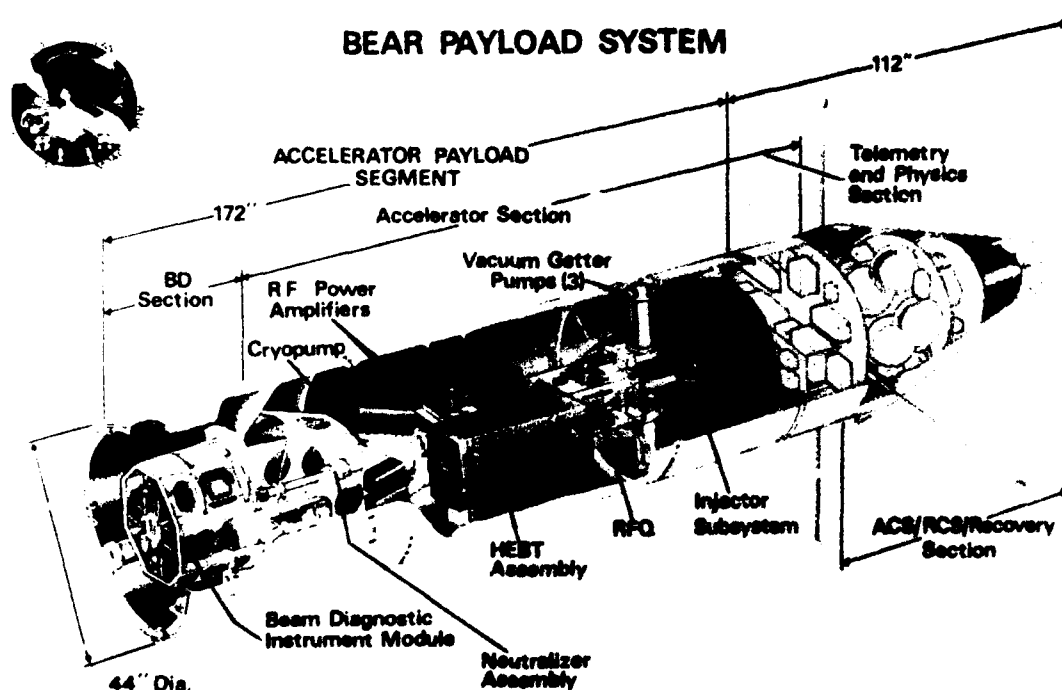
employed to measure positive and negative ions in the D-region (30-70 km), from a Nike-Orion rocket. The experiment required subsonic velocities, with the mass spectrometer oriented at less than a 15-degree angle of attack to the

velocity vector. To achieve these conditions, the rocket was ballasted to carry the 280-lb payload to an 85-km apogee, and a 63-ft diameter parachute normally used to recover 2000-lb payloads was deployed just before apogee. Upon reaching 70 km on the downleg, the parachute had trimmed the payload orientation to the velocity vector. The experiment functioned flawlessly, resulting in acquisition of 7.5 min of subsonic data between the 64- and 30-km altitude levels. A second COLDR mission is being prepared for launch from Wallops Island in 1989.

SPEAR: GL was the system integrator for the Space Power Experiment Aboard Rocket SDIO/DNA SPEAR 1 mission successfully launched from the NASA Wallops Flight Facility on December 13, 1987. The main experiment involved charging two spheres to high voltage (up to 44,000 V) to verify the insulating



Integration and Test of Space Power Experiment Aboard Rocket (SPEAR) Payload at GL Payload Test Facility.



Beam Experiment Aboard Rocket (BEAR) Payload.

properties of the near space environment. The launch vehicle was the Black Brant X, a three-stage unguided sounding rocket that carried the 823-lb payload to an apogee of 367 km. All systems performed as expected.

BEAR: Beam Experiments Aboard Rocket (BEAR) is an SDIO-sponsored mission that will fly the first linear accelerator in space. GL is the system integrator for this mission, working with the Los Alamos National Laboratory. The 3500-lb payload is scheduled to fly on an ARIES rocket from White Sands Missile Range in April 1989. GL is providing the vehicle, attitude control and recovery systems, and all payload support subsystems such as power, telemetry, video, and programming.

TM2: GL conceived the idea of employing a Navy surplus Talos booster under an Air Force surplus Minuteman I second stage to create a new, large rocket booster (TM2) with 40 percent more capability than our present largest system, the ARIES. This will be a joint development with the Defense Nuclear Agency and the NASA Wallops Flight Facility. We are providing the rocket motors, payload systems, and system integration. The Defense Nuclear Agency has contracted for the vehicle design and fabrication. NASA is providing a launch site and launch services. The first flight is scheduled from Wallops Island in June, 1989.

EXCEDE III: This GL program (Excitation by Electron Deposition) is supported by the Defense Nuclear Agency (for more details, see Chapter V above). It will use a single-stage ARIES rocket to carry the 5000-lb "mother/daughter" payload to an apogee of 120 km. A new launch site in the northwest corner of White Sands Missile Range is being developed for this

mission to satisfy the scientific requirement of flying north to south along a magnetic field line. The rocket, payload, and launch site are being readied for an April 1990 launch.

SPIRIT II: This SDIO-supported mission (Spatial Infrared Instrument Telescoped) will establish the infrared characteristics of a Class III aurora on the earth limb, using both radiometers and spectrometers. This payload is intended to be launched from Poker Flat Research Range, AK, in January, 1991. (For more details, see Chapter V above.)

SPACE SHUTTLE SYSTEMS

The Aerospace Engineering Division is carrying a heavy workload of payload integration and testing for space shuttle programs. Three payloads currently scheduled for the same shuttle launch during the third quarter of 1990 are described below.

CIRRIS 1A: The Cryogenic InfraRed Radiance Instrumentation for Shuttle (CIRRIS 1A) carries a 2-axis, gimbaled telescope with a radiometer and interferometer. During the recent shuttle downtime the program has completed a total rework of the detector and the engineering calibration. System baseline func-



Protected from ultraviolet radiation, technicians in the Jet Propulsion Laboratory Space Simulation Chamber measure "solar" flux incident on the CIRRIS 1A experiment system.

tional tests have been completed. In January, 1989, the system will undergo extensive space-simulation retesting at the Jet Propulsion Laboratory. (For more details, see Chapter V above.)

IBSS: The Division is also extensively engaged in supporting the Infrared Background Signature Survey program for Shuttle (IBSS). The IBSS payload is carried on a "free-flyer" that is deployed and recovered during the shuttle mission. We are providing low light level TV systems for the free-flying pointing system, including refinements such as time and reticle insertion into the video signal. We are also providing: radio frequency systems for transmitting the TV signal from the IBSS free flyer back to the shuttle over ranges exceeding 10 km; the digital data recording systems; and the experiment interface to the University of Arizona Imager Spectrograph, an experiment also carried on the free flyer. (For more details, see "Spacecraft Environmental Interactions," Chapter II above.)

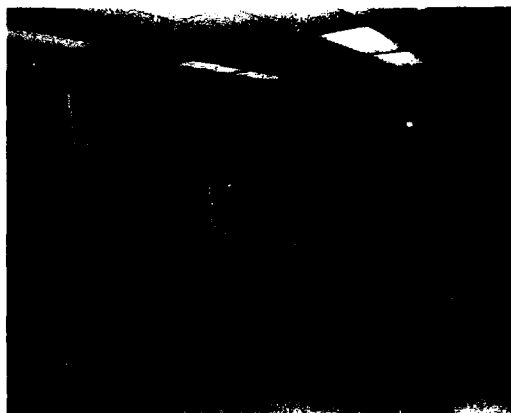
CIV: The Critical Ionization Velocity experiment (CIV), to be located in the shuttle bay, is being coordinated with the IBSS experiment. The Division is responsible for power distribution, sequencer control and data encoding and recording for this gas-release experiment. (For more details, see Chapter II above.) We are providing WORM (Write Once Read Many times) optical-disk recorders for this application. We are also adapting and qualifying WORM optical-disk recorders for our standard GAS (Get Away Special for Shuttle) payload support system.

VIPER (Visual Photometric Experiment), a GAS-type payload, is undergoing reintegration in preparation for its shuttle flight.

DATA SYSTEMS ANALYSIS

The Data Systems Branch designs, develops, and implements mathematical techniques and computational methods for processing and analyzing data recorded from ground and space probe experiments.

Telemetry Data Processing: The telemetry data-processing section converts data recorded during satellite, balloon, and rocket flights into computer-compatible formats. Data are converted from analog to digital formats, edited, time-correlated, and displayed. During the reporting



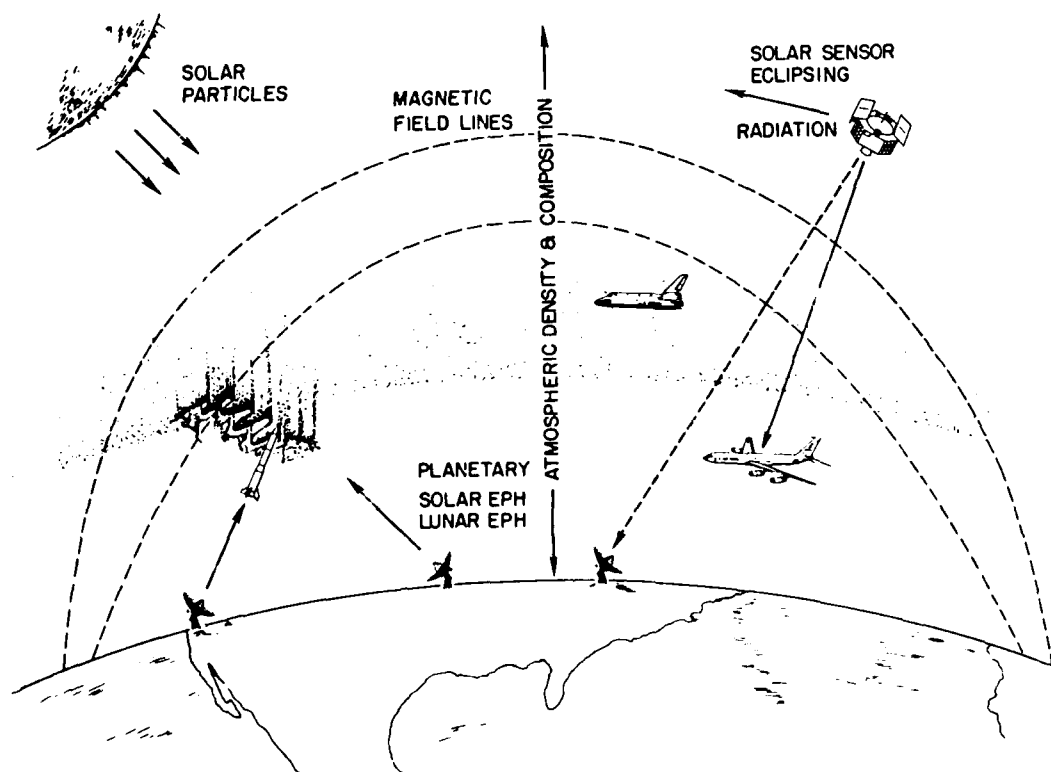
Telemetry Data Processing Facility.

period, the telemetry processing station was moved to a new facility which will enhance its ability to support GL space-flight projects. Additionally, the system was upgraded with state-of-the-art microprocessor-based telemetry demodulation hardware, which allows greater flexibility for processing high bit-rate and variable format telemetry. A major modification to the software operating system allows user-friendly interface to edit and quality-check data products. The detail design of the orbital data-processing system for the Chemical

Release Radiation Effects Satellite (CRRES) was also completed and documented during this time period.

Data Systems: The Data Systems section provides centralized support to large data-gathering space programs. Pre-launch support is normally a team effort, with project scientists and computer analysts working on plans to design an effective approach to processing large volumes of data to meet the program milestones. Post-launch support is mainly systematic implementation of developed data systems with recorded flight data to produce and maintain a database of geophysical parameters. The data systems analyst serves as data focal point for GL experiments. He interfaces with

outside agencies and data-processing facilities; designs and develops integrated data-management approaches and subsequent documentation in a data management plan; participates in data-analysis task groups with outside agencies to develop coordinated data-processing approaches for multi-agency, multi-probe satellite programs; develops data-support systems; generates compacted databases of geophysical units; and provides time-history displays of measured environmental parameters and archives of final history databases. The Data Systems section also maintains and upgrades interactive graphic display capabilities and develops special display techniques (contour, three-dimensional spectrogram, color).



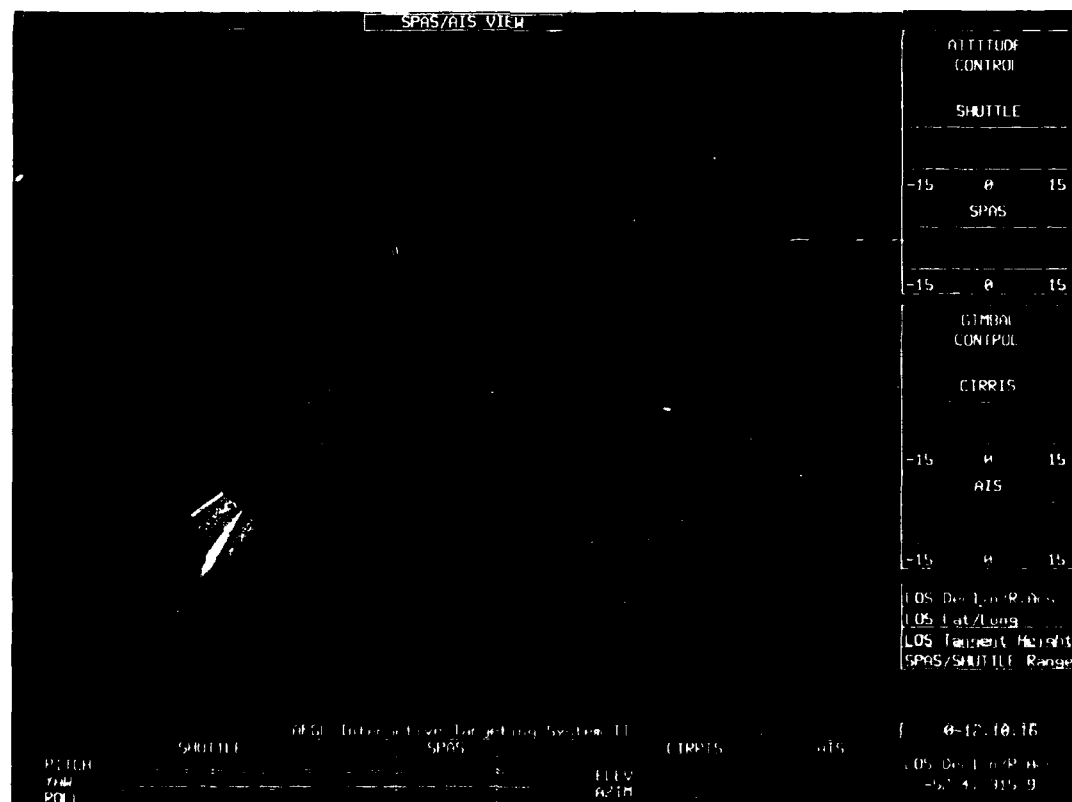
Space Vehicle Ephemerides and Model Calculations.

The GL Interactive Targeting System (AITS) was enhanced during this period to produce version II. The original version was designed to provide pre-mission and on-orbit planning support for the CIRRIS IA program. Version II has features which make the system useable by other projects. The major addition is a scene simulator which will depict an image in a sensor field of view with changing position and pointing parameters. A model of the airglow layer and simulated SPAS platform module was also added. Efforts were initiated to rehost the system from the VAX 750 to a Microvax III computer. This will make the system more portable.

AITS can be applied to any orbit sensor for which the pointing direction can be calculated. The system is specially

useful when the sensor-pointing direction can be controlled. AITS has been upgraded to display dynamic motion, allowing researchers to follow changes in sensor field-of-view during attitude maneuvers. For easier transport to field operations the AITS has been reconfigured to run on a scientific engineering workstation.

Orbital Analysis: The Orbital Analysis section supports researchers involved with interpreting flight-probe data. The analysts calculate vehicle trajectories and attitude; generate time-history databases of geophysical support parameters; and develop and maintain computational routines to calculate environmental and space-vehicle model parameters. They also develop analytical capa-



GL Interactive Targeting System II.

bilities for the Laboratory, including optimization methods, mathematical systems modeling, and spectral numerical and statistical analysis.

For the Chemical Release Radiation Effects Satellite (CRRES) program, for example, the specifications for generating ephemeris software have been developed. Magnetic field models have been evaluated and adopted, and methods devised for utilizing the fluxgate magnetometer data to despin the data and make inflight calibrations. Ephemeris and attitude routines were developed for the Polar BEAR (BEam and Auroral Research) program, using orbital data and solar magnetometer and horizon sensors. Lidar data from field campaigns for calculating atmospheric density and structure were processed and analyzed.

During 1987-88, models were developed for spacecraft charging and spacecraft contamination. Atmospheric density models were also evaluated using satellite accelerometer measurements, and auroral electron precipitation models were developed for DMSP satellite measurements. Systems have been evaluated for creating, displaying, and archiving databases with emphasis on the NSSDC Common Data Format.

CONTRACTOR TECHNICAL REPORTS JANUARY 1987-DECEMBER 1988

ALLISON, J., and BERTENSHAW, (Oklahoma State Univ., Stillwater, OK)
High Density Digital Data Recording System
AFGL-TR-87-0044 (28 January 1987),
ADA181115

BASS, J.N., BHAVNANI, K.H., BONITO, N.A., BRYANT, C. M., JR., HAHN, K.J., MCNEIL, W.J. (Radex, Inc., Carlisle, MA);

ROBERTS, F.R. (Logicon, Inc., Lexington, MA); SANNERUD, D.A., and KANTOR, A.J. (Radex, Inc., Carlisle, MA)

Integrated Systems with Applications to the Multi-phases of the Ephemerides, Physics, and Mathematics of the Upper Atmosphere
AFGL-TR-87-0064 (27 February 1987),
ADA185748

BASS, J.N., BHAVNANI, K.H., BONITO, N.A., COOKE, D.L., COTTRELL, K.G., ECKHARDT, R.J., HAHN, K.J., MCNEIL, W.J., TAUTZ, M.F. (Radex, Inc., Carlisle, MA); and Delorey, D.E. (Boston Coll., Chestnut Hill, MA)

Analysis of Geophysical Data Bases and Models for Spacecraft Interactions
AFGL-TR-86-0221 (31 October 1986),
ADA184869

BAWCOM, D., SHAW, H., CUNNINGHAM, L. (Physical Science Laboratory, Las Cruces, NM)

Engineering and Instrumentation Support of AFGL Rocket Research Program
AFGL-TR-86-0242 (7 November 1986),
ADA179257

BERTENSHAW, T.G., and HOLLOWAY, W.A. (Oklahoma State Univ. Stillwater, OK)
Inter-Vehicle Ranging System
AFGL-TR-87-0030 (1 January 1987),
ADA179492

DELOREY, D.E., SULLIVAN, B.F., and PRUNEAU, P.N. (Space Data Analysis Laboratory, Boston, MA)
Analysis Systems for Air Force Missions
AFGL-TR-87-0100 (28 February 1987),
ADA182S99

DONAHOO, R.D. (Oklahoma State Univ., Stillwater, OK)
Global Positioning System Adaptation for Balloon Payloads
AFGL-TR-88-0096 (7 May 1988), ADA199997

MORIN, R.L., and O'CONNOR, L.J.

(Northeastern Univ., Boston, MA)
Aerospace Payload Support Systems
AFGL-TR-88-0241 (July 1987), ADA199687

POIRIER, N.E., and WHEELER, T.P.
(Northeastern Univ., Boston, MA)
Programmable PCM Encoder
AFCL-TR-87-0067 (16 January 1985),
ADA183533

ROCHEFORT, J.S., O'CONNOR, L.J., SUKYS,
A., POIRIER, N.C., and WHEELER, T.P.
(Northeastern Univ., Boston, MA)

*Instrumentation and Communication
Systems for Sounding Rockets and Shuttle-
Borne Experiments*
AFGL-TR-87-0139 (27 April 1987),
ADA183541

SCHROEDER, C. (Space Data Corp.,
Tempe, AZ)
*Engineering Support of Space Shuttle
Experiment Integration*
AFGL-TR-87-0253 (11 November 1987),
ADA190135

APPENDIX A

Service On International Committees By GL Scientists

Committee on Space Research of the International Council of Scientific Unions (Space Studies of the Upper Atmosphere of the Earth and Planets, Including Reference Atmospheres, Program Committee, Executive Council URSI/COSPAR Task Group on the International Reference Ionosphere, Subcommission E-2 on Solar Physics, Interdisciplinary Scientific Commission E on Research in Astrophysics form Space, Commission on Magnetosphere Physics, Joint Working Group on Active Experiments, Scientific Program Committee, COSPAR Symposium on the International Heliospheric Study)

International Agency Coordinating Committee on Middle Atmosphere Programs

International Association for Meteorology and Atmospheric Physics (Working Group on Aerosols and Climate)

International Association of Geomagnetism and Aeronomy (committees on Magnetospheric Phenomena, Electrodynamics of the Middle Atmosphere, Pulsation, Quantitative Magnetospheric Models, and the US National Committee, International Association of Geodesy, President of Special Study Group on Gravimetric Tests of Newtonian Gravity Law; SSG3.111, President of Special Study Group)

International Radiation Commission (Remote Sensing Group, Commission on Cloud Physics Joint Working Group on the International Aerosol Climatology Project; Working Group on the Intercomparison of Radiation Codes for Climate Models)

International Scientific Radio Union (URSI) (US National Committee, Commission G; Chair, Working Group 12

"On Studies of the Ionosphere Using Beacon Satellites")

International Union of Geodesy and Geophysics

NATO Panel AC243, Panel IV (Chairman), RSG8, RSG14, NATO Advisory Group on Aerospace Research and Development (ElectroMagnetic Wave Panel)

Scientific Committee on Solar-Terrestrial Physics (SCOSTEP) (Monitoring Sun-Earth Environment Committee, Panel on World Data Centers

World Meteorological Organization (committees on Atmospheric Spectroscopy, Intercomparison of Transmittance Radiance Algorithms, Atmospheric Science)

APPENDIX B

Service On National Committees By GL Scientists

American Geophysical Union
(Committee on Atmospheric and Space
Electricity, Fleming Medal
Subcommittee of Committee of Fellows)

American Institute of Aeronautics and
Astronautics (National Technical
Committee of Plasma-dynamics and
Lasers, Atmospheric Environment Panel
Space Science and Astronomy
Environmental Committee on the
National Aerospace Plane, Standards
Committee, Technical Committee)

American Meteorological Society
(Committee on Satellite Meteorology and
Oceanography, Committee on
Atmospheric Environment)

Committee on TIROS Operational
Vertical Sounder

Department of Commerce (advisor to
National Geophysical Data Center)

Department of Defense (Chair,
Conference on Effects of Environment on
Systems Performance, Representative
Committee on Nuclear Phenomenology
Affecting Space Systems; National Storm
Program; OSD Aerospace Vehicle
Technology Working Group, SDIO
Sensors Office Working Group, SDIO
Natural and Nuclear Environments
Working Group, AFSC/NASA Spacecraft
Environmental Interactions Technology
Steering Committee, Co-Chair)

Department of State (Solar-Terrestrial
Physics Committee, Geophysics
Commission, Pan American Institute of
Geography and History, Organization of
American States)

Institute of Electrical and Electronic
Engineers, Acoustics, Speech, and Signal
Processing

Interagency Committee on Sensing
from Aircraft

Interdepartmental Committee for
Meteorological Services and Supporting
Research, Space Environmental

Forecasting (USAF technical advisor)

NASA Ozone Assessment Panel,
Management Operations Working Group

National Academy of Sciences
(Committee on Solar-Terrestrial Physics)

National Solar Observatory User's
Committee

National Research Council Geophysics
Research Board, Committee on
Geophysical Data, Chairman, Advisory
Panel for Solar-Terrestrial Physics

Office of Science Technology Policy of
the President (Interagency Coordinating
Committee on Solar Terrestrial
Relations)

Tri-Service Transmission Model
Workshop; Clouds Modeling Committee
MILSTD-210B Committee

APPENDIX C

GL PROJECTS BY PROGRAM ELEMENT
FY 1987

Program	Project Number and Title
61101F	<i>ILIR</i> In-House Laboratory Independent Research
61102F	<i>DEFENSE RESEARCH SCIENCES</i>
	2303G1 Upper Atmosphere Chemistry
	2303G2 Reactions of Fast Atoms and Ions with Surfaces
	2303G3 Atmospheric UV Processes
	2309G1 Geodesy and Gravity
	2309G2 Crustal Motion Studies
	2310G1 Molecular and Aerosol Properties of the Atmosphere
	2310G2 Infrared Atmospheric Background Measurements
	2310G3 Upper Atmosphere Composition
	2310G4 Infrared Atmospheric Processes
	2310G5 Infrared Airglow and Auroral Models
	2310G6 Local Ionospheric Processes
	2310G7 Atmospheric Prediction
	2310G8 Atmospheric Specification
	2310G9 Global Ionospheric Dynamics
	2311G3 Solar Environmental Disturbances
	2311G4 Solar Terrestrial Interactions
	2311G5 Magnetospheric Plasmas and Fields
	2311G6 Particle Beams in Space Plasmas
	2311G7 Infrared Astronomy
62101F	<i>GEOPHYSICS</i>
	760003 Geodesy and Gravity
	760006 Geodetic Instrumentation
	760009 Seismo-Acoustic Effects
	Magnetospheric Effects on AF Systems
	760118 Space Plasma Diagnostics
	760122 Space Particle Effects Characterizations
	760130 Spacecraft Environmental Interactions Technology
	760140 Interactions Diagnostics
	760150 Active Control of Space
	Aerospace Probe Technology
	765904 Sounding Rocket and Shuttle Payload Systems
	765912 Balloon Systems
	Optical/IR Properties of the Environment
	767006 Celestial and Earth Limb Background Measurements
	767009 Atmospheric Transmittance Modeling
	767015 Atmospheric Optical/IR Propagation Studies
	767016 Laser Sounding Technology
	Laboratory Operations
	Infrared Targets and Backgrounds

305401 Aurora/Airglow IR Backgrounds
 305402 Airborne Infrared Measurements
 Ionospheric Specification
 464307 Ionospheric Modelling
 464308 Ionospheric Dynamics
 464309 Ionospheric Scintillation
 464310 Ionospheric Effects on Communications and Optical Systems
 464311 Ultraviolet Technology
 464312 HF Targeting and Ionospheric Heating Technology
 Atmospheric Science and Technology
 667009 Climatological Techniques
 667010 Mesoscale Weather Forecasting
 667012 Cloud Physics
 667014 Boundary Layer Meteorology
 667017 Satellite Sounding Techniques
 667019 Ground-Based Remote Weather Detection

62410F *SPACE SYSTEMS ENVIRONMENTAL INTERACTIONS
TECHNOLOGY*

 Space Systems Design/Test Standards
 282101 Spacecraft Design Guidelines
 Interactions Measurement Payloads (IMPS)
 282201 Engineering Experiments for IMPS
 282202 Engineering Experiments for IMPS II
 282203 Astronaut EVA Equipment Test
 Charge Control System
 282301 Charge Control System Development
 63707F Weather Systems (Advanced Dev)
 Battlefield Weather Systems
 268801 Data Gathering Systems
 268802 Tactical Decision Aids
 268803 Automated Observation Systems
 268804 Technology Transition
 Next Generation Weather Radar
 278101 Storm Diagnosis

In addition to the continuing Air Force funded projects cited above, GL participates in joint programs supported by the following agencies:

- 1) U.S. Air Force
 - Space Systems Division
 - Ballistic Missile Systems Division
 - Weapons Laboratory
 - Air Weather Service
 - Electronic Systems Division
 - Rome Air Development Center
- 2) Defense Advanced Research Projects Agency

- 3) Defense Mapping Agency
- 4) Defense Nuclear Agency
- 5) Defense Communications Agency
- 6) Department of Energy
- 7) Strategic Defense Initiative Organization
- 8) National Aeronautics and Space Administration
- 9) Army
- 10) University of Denver

**GL PROJECTS BY PROGRAM ELEMENT
FY 1988**

Program	Project Number and Title
61101F	<i>ILIR</i> In-House Laboratory Independent Research
61102F	<i>DEFENSE RESEARCH SCIENCES</i>
	2302G2 Reactions of Fast Atoms and Ions with Surfaces
	2303G3 Atmospheric UV Processes
	2309G1 Geodesy and Gravity
	Seismic Sources and Wave Propagation
	2309G2 Crustal Motion Studies
	2310G1 Molecular and Aerosol Properties of the Atmosphere
	2310G2 Infrared Atmospheric Background Measurements
	2310G3 Upper Atmosphere Composition
	2310G4 Infrared Atmospheric Processes
	2310G5 Infrared Airglow and Auroral Models
	2310G6 Local Ionospheric Processes
	2310G7 Atmospheric Prediction
	2310G8 Atmospheric Specification
	2310G9 Global Ionospheric Dynamics
	2311G3 Solar Environmental Disturbances
	2311G4 Solar Terrestrial Interactions
	2311G5 Magnetospheric Plasmas and Fields
	2311G6 Particle Beams in Space Plasmas
	2311G7 Infrared Astronomy
62101F	<i>GEOPHYSICS</i>
	Infrared Targets and Backgrounds
	305401 Aurora/Airglow IR Backgrounds
	305402 Airborne Infrared Measurements
	Ionospheric Specification
	464307 Ionospheric Modeling
	464308 Ionospheric Dynamics
	464309 Ionospheric Scintillation
	464310 Ionospheric Defense Technology
	464311 Ultraviolet Technology Atmospheric Science and Technology
	667009 Climatological Techniques
	667010 Mesoscale Weather Forecasting
	667012 Cloud Physics
	667014 Boundary Layer Meteorology
	667017 Satellite Sounding Techniques
	667019 Ground-Based Remote Weather Detection
	760006 Gravity Modeling and Measurement
	760009 Seismo-Acoustic Analysis and Modeling
	Magnetospheric Effects on AF Systems
	760118 Space Plasma Diagnostics
	760122 Space Particle Effects Characterizations

760130 Spacecraft Environmental Interactions Technology
 760150 Active Control of Space
 Aerospace Probe Technology
 765904 Sounding Rocket and Shuttle Payload Systems
 765912 Balloon Systems
 Optical/IR Properties of the Environment
 767006 Celestial Backgrounds
 767009 Atmospheric Transmittance Modeling
 767015 Atmospheric Optical/IR Propagation Studies
 767016 Laser Sounding Technology

63410F *SPACE SYSTEMS ENVIRONMENTAL INTERACTIONS
 TECHNOLOGY*

 Space Systems Design/Test Standards

282101 Spacecraft Design Guidelines and Specifications
 Interactions Measurement Payload (IMPS)
 282201 Space Power Interaction Measurements
 282202 Environmental Interactions Measurement Investigations
 282203 Military Space Equipment Testing
 Charge Control System
 282301 Charge Control System Development

63707F *WEATHER SYSTEMS (ADVANCED DEV.) BATTLEFIELD WEATHER
 SYSTEMS*

268801 Data Gathering Systems
 268802 Tactical Decision Aids
 268803 Automated Observation Systems
 268804 Technology Transition
 Next Generation Weather Radar
 278101 Storm Diagnosis

65502F *SMALL BUSINESS INNOVATION RESEARCH*

In addition to the continuing Air Force funded projects cited above, GL participates in joint programs supported by the following agencies:

1) U.S. Air Force

Space Systems Division
 Ballistic Missile Systems Division
 Weapons Laboratory
 Air Weather Service
 Electronic Systems Division
 Rome Air Development Center

2) Defense Advanced Research Projects Agency

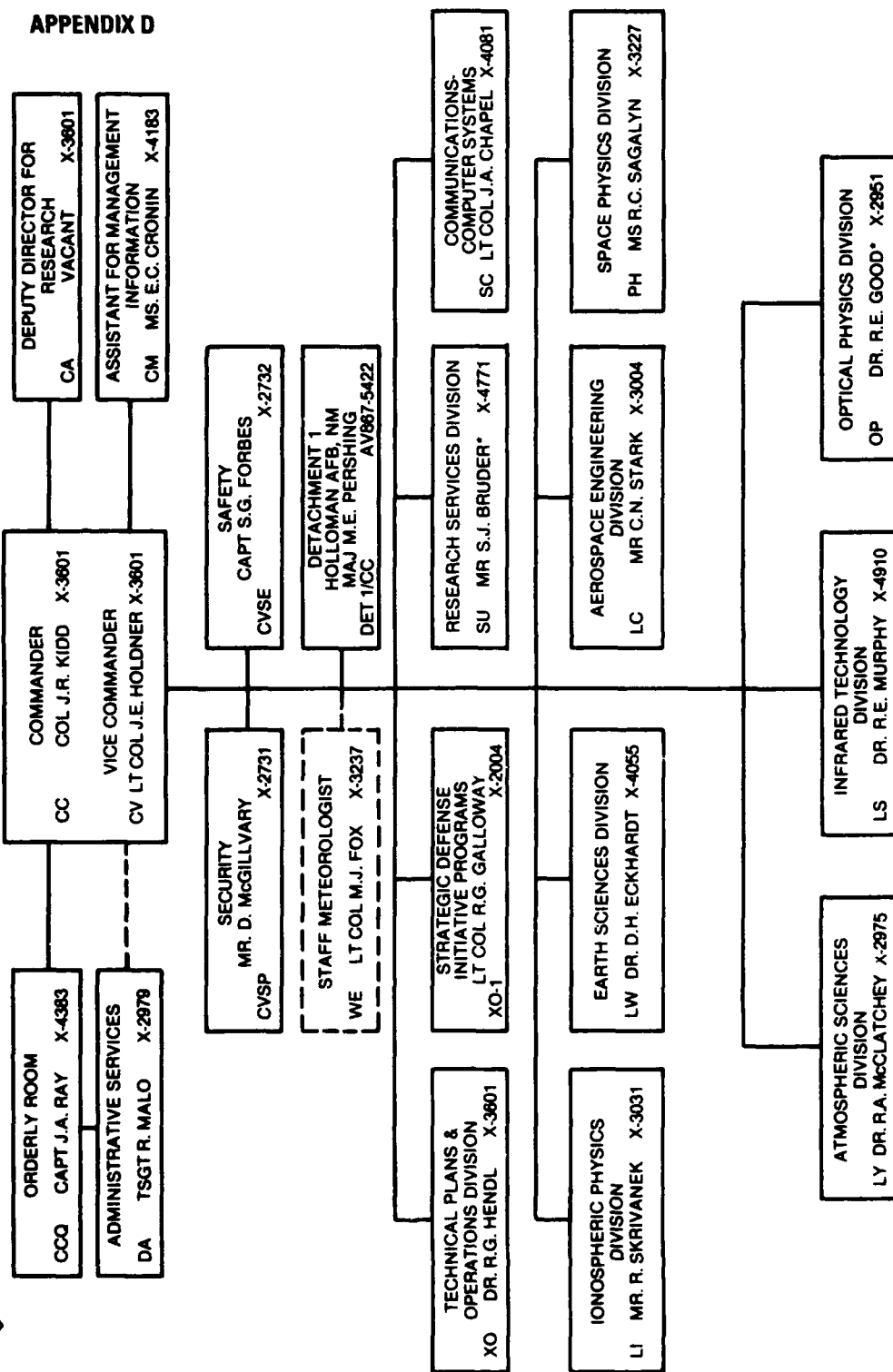
- 3) Defense Mapping Agency
- 4) Defense Nuclear Agency
- 5) Defense Communications Agency
- 6) Department of Energy
- 7) Strategic Defense Initiative organization
- 8) National Aeronautics and Space Administration
- 9) Army
- 10) University of Denver



Air Force Geophysics Laboratory

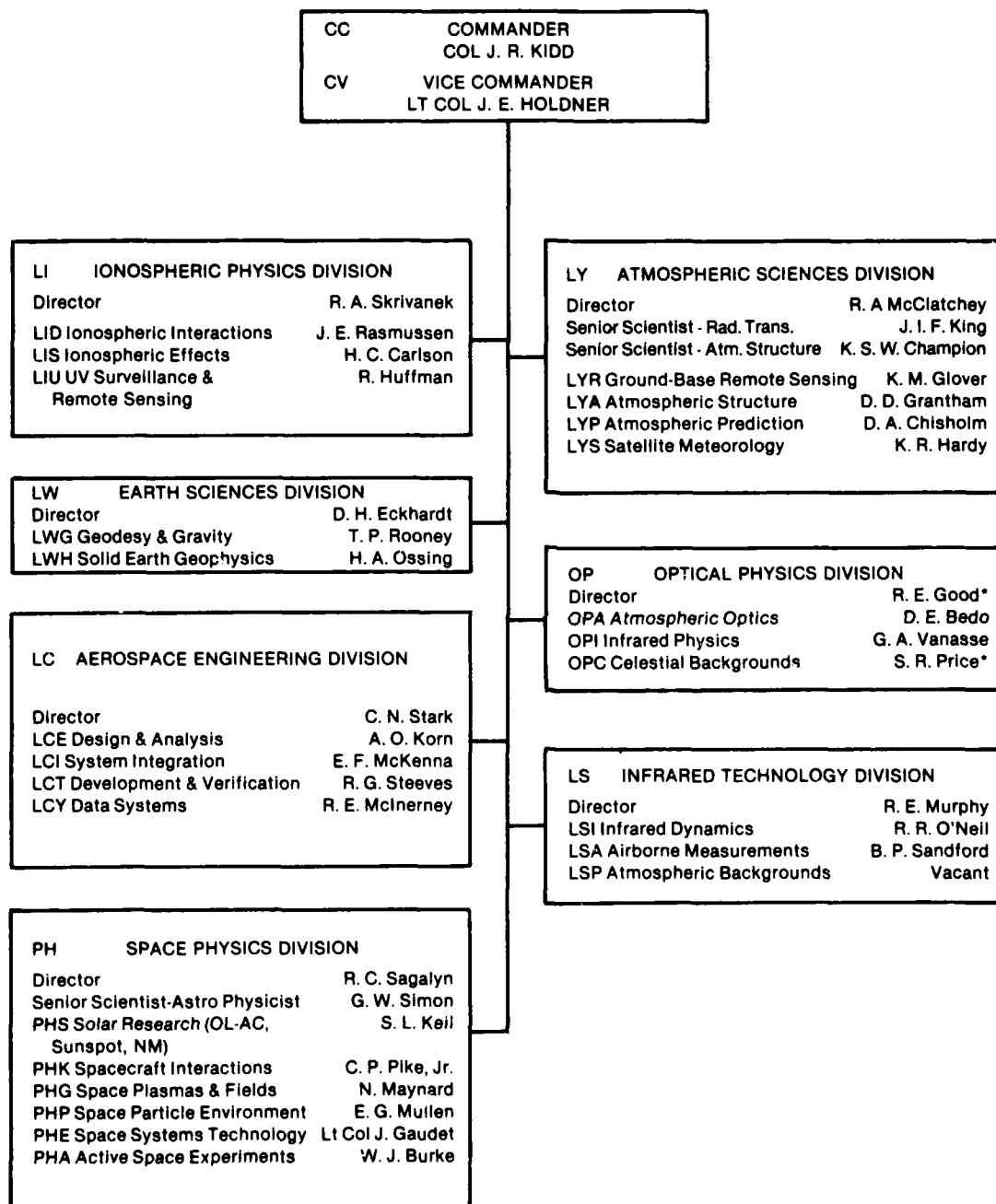
HANSCOM AIR FORCE BASE, BEDFORD, MASS.

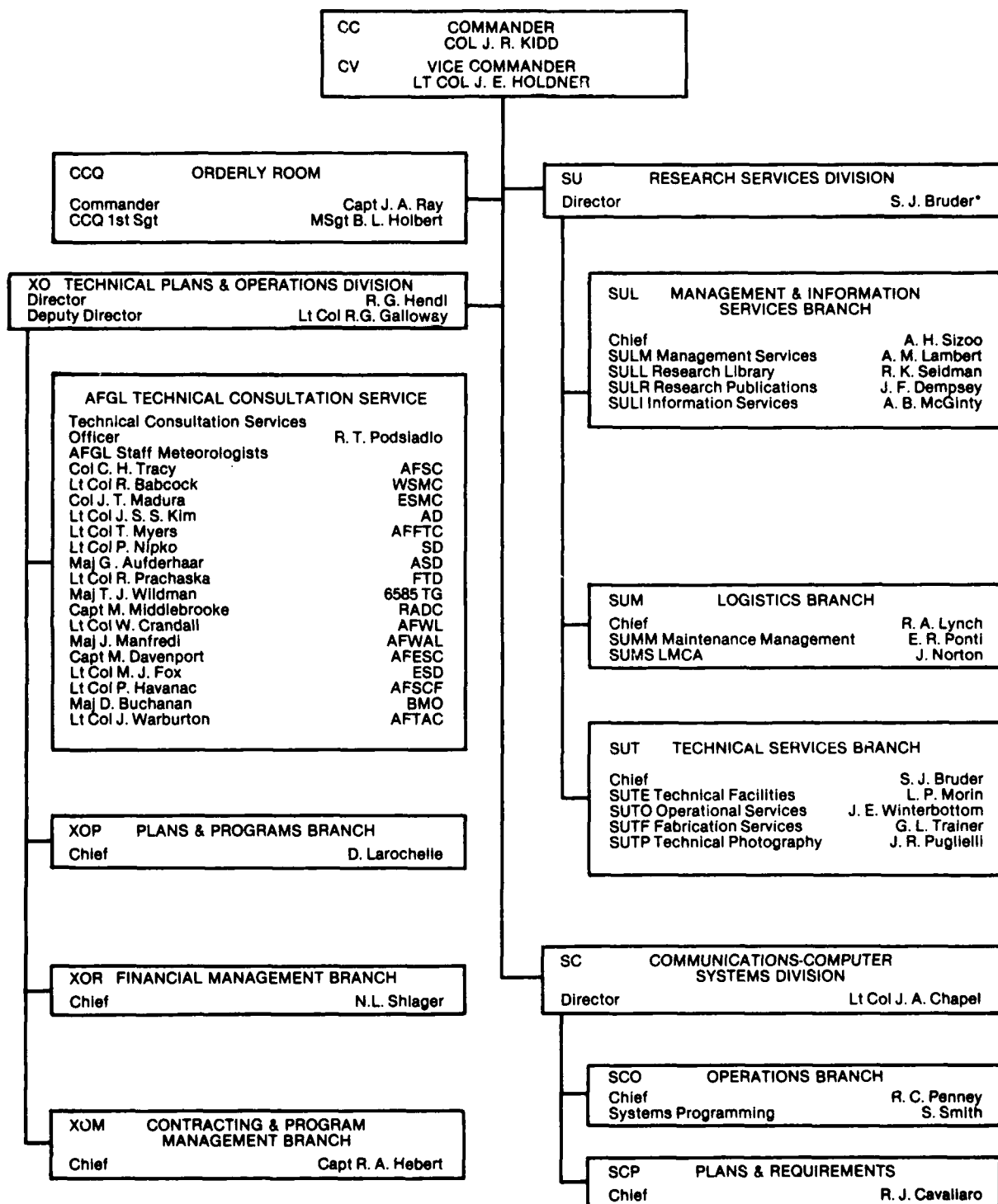
APPENDIX D



AUTOVON: 478-XXXX
Commercial - Area Code (617) 377-XXXX

As of 1 September 1987
*Acting

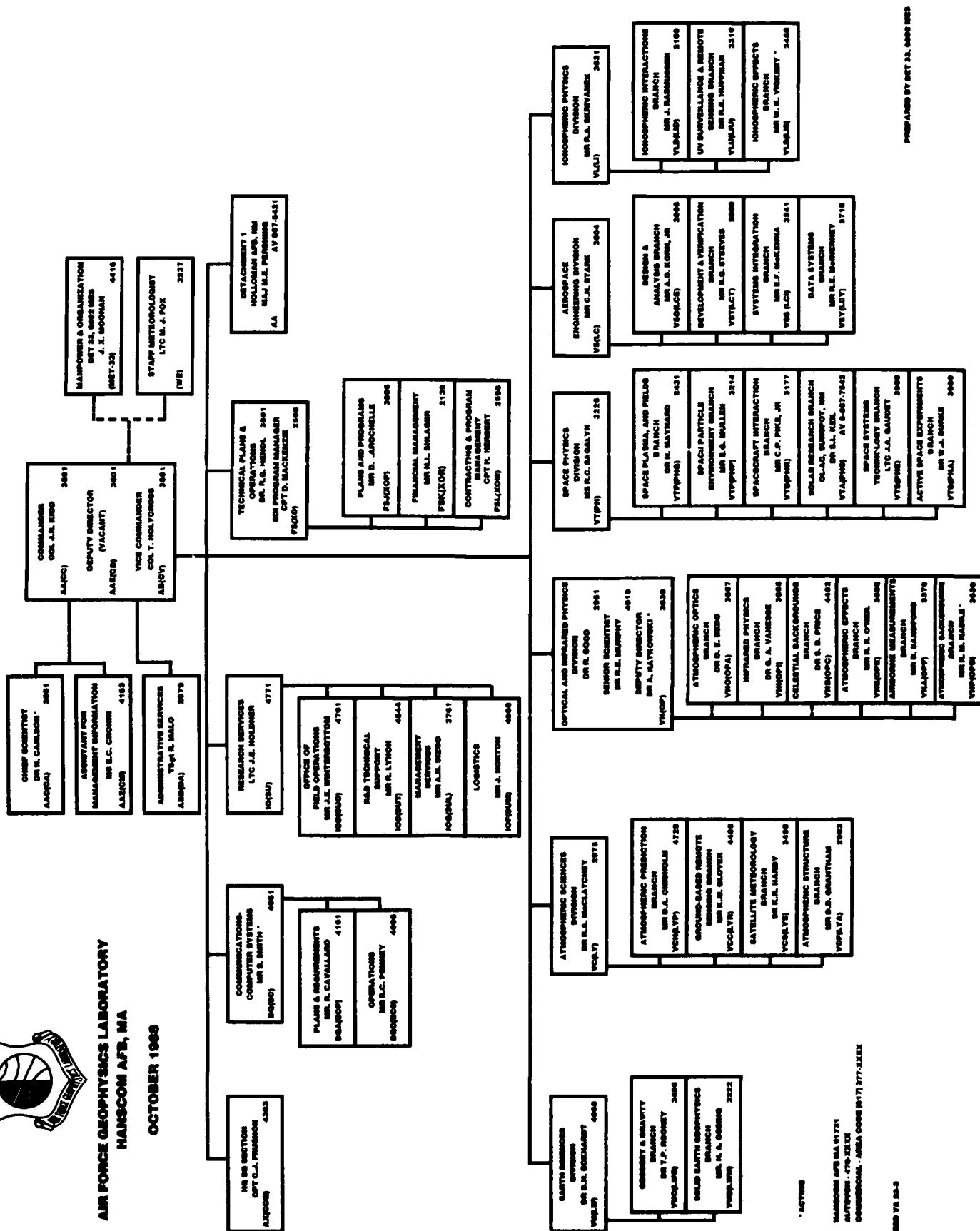






AIR FORCE GEOPHYSICS LABORATORY
HANSCOM AFB, MA

OCTOBER 1968



PREPARED BY DET 33, 6893 MED

END VA 20-5

HANSCOM AFB MA 01721
AUTOPHONE - 470-3232
COMMERCIAL - AREA CODE (617) 377-3232

* ACTIVE